frontiers | Research Topics

Dementia and neurodegenerative diseases – case report collection 2022

Edited by
Bruce Miller

Published in
Frontiers in Neurology

ISSN 1664-8714
ISBN 978-2-8325-3034-4
DOI 10.3389/978-2-8325-3034-4

About Frontiers

Frontiers is more than just an open access publisher of scholarly articles: it is a pioneering approach to the world of academia, radically improving the way scholarly research is managed. The grand vision of Frontiers is a world where all people have an equal opportunity to seek, share and generate knowledge. Frontiers provides immediate and permanent online open access to all its publications, but this alone is not enough to realize our grand goals.

Frontiers journal series

The Frontiers journal series is a multi-tier and interdisciplinary set of open-access, online journals, promising a paradigm shift from the current review, selection and dissemination processes in academic publishing. All Frontiers journals are driven by researchers for researchers; therefore, they constitute a service to the scholarly community. At the same time, the *Frontiers journal series* operates on a revolutionary invention, the tiered publishing system, initially addressing specific communities of scholars, and gradually climbing up to broader public understanding, thus serving the interests of the lay society, too.

Dedication to quality

Each Frontiers article is a landmark of the highest quality, thanks to genuinely collaborative interactions between authors and review editors, who include some of the world's best academicians. Research must be certified by peers before entering a stream of knowledge that may eventually reach the public - and shape society; therefore, Frontiers only applies the most rigorous and unbiased reviews. Frontiers revolutionizes research publishing by freely delivering the most outstanding research, evaluated with no bias from both the academic and social point of view. By applying the most advanced information technologies, Frontiers is catapulting scholarly publishing into a new generation.

What are Frontiers Research Topics?

Frontiers Research Topics are very popular trademarks of the *Frontiers journals series*: they are collections of at least ten articles, all centered on a particular subject. With their unique mix of varied contributions from Original Research to Review Articles, Frontiers Research Topics unify the most influential researchers, the latest key findings and historical advances in a hot research area.

Find out more on how to host your own Frontiers Research Topic or contribute to one as an author by contacting the Frontiers editorial office: frontiersin.org/about/contact

Dementia and neurodegenerative diseases – case report collection 2022

Topic editor
Bruce Miller — University of California, San Francisco, United States

Citation
Miller, B., ed. (2023). *Dementia and neurodegenerative diseases – case report collection 2022*. Lausanne: Frontiers Media SA. doi: 10.3389/978-2-8325-3034-4

Table of contents

frontiers | Frontiers in Neurology

CASE REPORT
published: 09 May 2022
doi: 10.3389/fneur.2022.875370

Atypical Case of VV1 Creutzfeldt–Jakob Disease Subtype: Case Report

Adrianna E. Carrasco[1], *Brian S. Appleby*[2], *Ignazio Cali*[3] *and Hamid R. Okhravi*[4]*

[1] School of Medicine, Eastern Virginia Medical School, Norfolk, VA, United States, [2] Department of Neurology, Case Western Reserve University, Cleveland, OH, United States, [3] Department of Pathology, Case Western Reserve University, Cleveland, OH, United States, [4] Department of Internal Medicine, Glennan Center for Geriatrics and Gerontology, Eastern Virginia Medical School, Norfolk, VA, United States

OPEN ACCESS

Edited by:
Bruce Miller, University of California, San Francisco, United States

Reviewed by:
Samir Abu-Rumeileh, Martin Luther University of Halle-Wittenberg, Germany
Adeline Ng, National Neuroscience Institute (NNI), Singapore

***Correspondence:**
Hamid R. Okhravi
okhravhr@evms.edu

Specialty section:
This article was submitted to Dementia and Neurodegenerative Diseases, a section of the journal Frontiers in Neurology

Received: *14 February 2022*
Accepted: *28 March 2022*
Published: *09 May 2022*

Citation:
Carrasco AE, Appleby BS, Cali I and Okhravi HR (2022) Atypical Case of VV1 Creutzfeldt–Jakob Disease Subtype: Case Report. Front. Neurol. 13:875370. doi: 10.3389/fneur.2022.875370

Creutzfeldt–Jakob disease (CJD) is a rare form of rapidly progressive, neurodegenerative disease that results from the misfolding and accumulation of an aberrant, disease-associated prion protein (PrPD). CJD affects 1–1.5 cases per million per year with the sporadic-type accounting for an estimated 85% of these cases. Sporadic CJD (sCJD) is further subdivided into five subtypes based on genetic polymorphisms; the rarest subtype, sCJDVV1, occurs at a rate of 1 case per one-hundredth million population per year. Clinical characteristics of the sCJDVV1 subtype have been reported to show, early age of onset (44 years), average disease duration of 21 months, absent PSWCs on electroencephalography (EEG), and MRI hyperintensities in the cerebral cortex with usual negative signal in the basal ganglia or thalamus. We present a case of the sCJDVV1 subtype with uncommon features. Contrary to current data on sCJDVV1, our patient presented with an unusual age at onset (61 years) and longer disease duration (32 months). The highly sensitive and specific real-time quaking-induced conversion (RT-QuIC) assay was negative. Presenting clinical symptoms included paranoid thoughts and agitation, rapidly progressive memory decline, prosopagnosia, and late development of myoclonus and mutism. Other findings showed positive antithyroid peroxidase antibodies (anti-TPO), and absent PSWCs on EEG. High-dose steroid therapy treatment was administered based on positive anti-TPO findings, which failed to elicit any improvement and the patient continued to decline. To our knowledge, only four cases with the sCJDVV1 subtype, including our patient, have been reported to have a negative result on RT-QuIC. This may suggest varied sensitivity across sCJD subtypes. However, given the rarity of our patient's subtype, and the relatively novel RT-QuIC, current data are based on a small number of cases and larger cohorts of confirmed VV1 cases with RT-QuIC testing need to be reported.

Keywords: Creutzfeldt-Jakob disease, VV1 type, real-time quaking-induced conversion, dementia, Hashimoto's thyroiditis

INTRODUCTION

Sporadic Creutzfeldt–Jakob disease (sCJD) is a rare, rapidly progressive, neurodegenerative disease that results from the misfolding and accumulation of an aberrant, disease-associated prion protein (PrP^D) (1).

The pathogenic PrP isoform or PrP^D is the abnormal isoform of the naturally occurring cellular prion protein (PrP^C). Compared to PrP^C, PrP^D is highly enriched with insoluble ß-sheet structure, which confers to its characteristic of being partially resistant to enzymatic digestion by proteases (e.g., proteinase K, PK). PrP^D is believed to induce conformational changes in the physiological PrP^C which is, in turn, converted into PrP^D at an exponential rate, thus making this an essentially uncontrollable process (2, 3). The accumulation of PrP^D insoluble aggregates interferes with neuronal function and ultimately leads to cell death (3).

In the 1920s, Spielmeyer used the term "Creutzfeldt–Jakob disease" for the first time to describe a series of six unusual degenerative neuropathological cases previously described by Creutzfeldt and Jakob (4).

Modern classification of sCJD into five phenotypically distinct subtypes is based on the combination of two modifiers of the disease phenotype: (1) the type of the PK-resistant PrP^D (termed type 1 or type 2), (2) three possible genotypes at codon 129 of the PrP gene (129 met/met or 129 val/val homozygous, and 129 met/val heterozygous) (5, 6). This modern classification of sCJD has proven to be important as it facilitates the diagnosis of this group of prion diseases.

CASE REPORT

A 63-year-old Caucasian woman presented to ER with a 1-year history of behavioral disturbance and memory loss with more recent (2 months) episodes of agitation, delusional thoughts, questionable visual and auditory hallucinations, and aggressive behavior. In the ER, she appeared with elevated affect and was overly cheerful, with poor judgment and insight. Her speech was fluent and spontaneous but slightly increased in rate, rhythm, and volume. The rest of her physical exam was within normal limits without any abnormal neurological findings. She was admitted to the psychiatric unit for further assessment and management and was started on olanzapine for agitation and disturbing delusions. The electroencephalogram (EEG), CT head, and pertinent blood work were unremarkable. She was screened for cognitive impairment with the Montreal Cognitive Assessment and scored 19/30. She was discharged home after a one-week stay at the psychiatric unit with a diagnosis of major neurocognitive disorder associated with psychosis. She was seen in our memory clinic 2 months after discharge with a rapidly progressive cognitive and functional decline. She was dependent on most activities of daily living, such as bathing, grooming, and dressing, and became socially withdrawn with reports of prosopagnosia in the last several months. Her neuropsychological testing assessment showed severe impairment in memory, attention, executive function, language, and visuospatial domains. She scored 7/30 on Mini-Mental State Examination. Her neurological examination remained unremarkable, except for motor apraxia. She underwent extensive workup for rapidly progressive dementia.

Laboratory tests performed at this time included paraneoplastic profile, serum, and urine heavy metals, infectious processes such as HIV, syphilis, and Lyme disease, which were found to be negative; however, she had both elevated antithyroid peroxidase (TPO-Ab) and antithyroglobulin (TG-Ab) antibodies indicative of Hashimoto's thyroiditis. An MRI of the brain with volumetric studies was performed. The MRI showed asymmetric (right>left) diffusion-weighted imaging (DWI) signal hyperintensities in the cortical ribbon of the parietal, frontal, and temporal lobes, hippocampi, caudate, and putamen (**Figures 1A,B**). There were no signal abnormalities in the perirolandic gyri, occipital cortex, thalami, and cerebellum. This pattern was highly suggestive of CJD. Volumetric studies showed mainly right-sided frontal, parietal, and temporal lobes atrophy. Hippocampal and medial temporal lobe volumes were within normal limits.

At her follow-up visit 2 weeks later, the husband reported the patient developed intermittent jerking movements in her extremities. The patient underwent a lumbar puncture and repeat EEG. The cerebrospinal fluid (CSF) analysis showed no RBCs, elevated 14-3-3 protein, elevated t-tau protein levels of 6,858 pg/ml (normal range <1,149), amyloid-beta 42 level of 185.85 pg/ml (normal range >1,026 pg/ml) and p-tau of 59.55 pg/ml (normal < 54 pg/ml). The t-tau/p-tau ratio was 115. Neuron-specific enolase (NSE) was also elevated at 62 ng/ml (normal range <15). Repeat EEG did not show periodic sharp wave complexes (PSWCs). A real-time quaking-induced conversion (RT-QuIC) test was negative. On her follow-up visit she had developed new symptoms; a resting tremor of the right hand, biceps tendon hyperreflexia, inappropriate laughter, urine and stool incontinence, and began eating nonfood items. Two months from her initial memory consultation visit, her exam was significant for myoclonic jerks and evolving mutism, highly suspicious for probable CJD. She also received 3 courses of high-dose steroid therapy followed by a tapering dose of prednisone for the possibility of Hashimoto's encephalopathy. The patient failed to elicit any improvement in steroid treatment, continued to decline, and was transitioned to hospice care. The patient's decline continued, requiring total care. She became bedbound and the patient expired 20 months after the CJD diagnosis, and her brain was sent to the National Prion Disease Pathology Surveillance Center (NPDPSC) for autopsy. The illness duration from symptom onset (neuropsychiatric symptoms) to death was 32 months (**Figure 2**). The long duration of the symptoms is consistent with the typically prolonged survival of VV1 (7).

The autopsy included histopathological and immunohistochemical analysis, western blot, and genetic testing. Western blot findings demonstrated PK-resistant PrP^D type 1, with the unglycosylated PrP^D isoform migrating to ∼ 20 kDa (data not shown) (7), and histopathological features of the VV1 subtype (**Figure 3**) (8). Genetic analyses did not detect pathogenic mutations of the prion protein gene (*PRNP*) and the patient was valine homozygous at codon 129 (129VV). The final diagnosis was sporadic CJD of the VV1 subtype (6, 7).

A B C

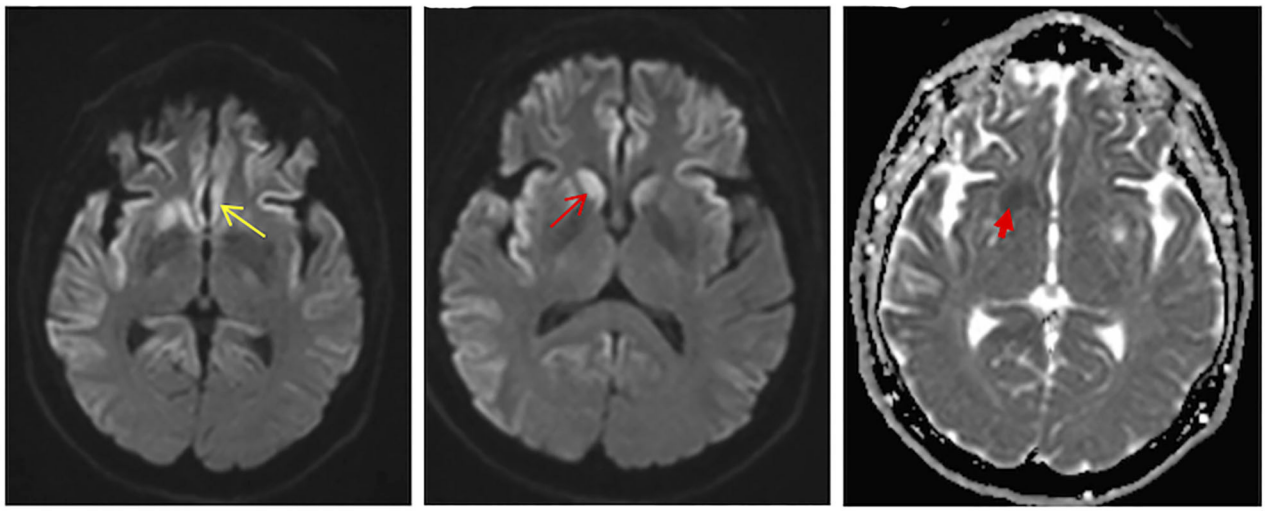

D

Intracranial Volume (ICV) (cm^3)	ICV Z-score	ICV Percentile
1395.51	-0.74	23

Brain Structure	LH Z-score	LH %	RH Z-score	RH %
Total Cerebral White Matter[1]	> 1.65	> 99	> 1.65	> 99
Total Cerebral Grey Matter[2]	-0.64	26	< -1.65	4
Total Ventricle[3]	-0.89	19	-0.65	26
Cerebellar White Matter	1.57	94	> 1.65	97
Cerebellar Gray Matter	-1.18	12	-1.19	12
Brainstem	-0.97	17	-0.64	26
Thalamus	1.23	89	1.26	90
Ventral Diencephalon	-0.62	27	0.04	51
Hippocampus	-0.04	48	-0.41	34
Amygdala	-0.99	16	-0.78	22
Basal Ganglia				
Putamen	1.11	87	1.14	87
Caudate	0.26	60	0.10	54
Nucleus Accumbens	1.45	93	> 1.65	> 99
Pallidum	-0.11	45	0.28	61

1] Total White Matter excludes Cerebellum
2] Total Grey Matter excludes Cerebellum
3] Total Ventricle includes Lateral Ventricle, 3rd Ventricle and 4th Ventricle
4] Medial Occipital includes Cuneus, Lingual, and Pericalcarine
** Normative values are for reference purposes.

Cortical Brain Regions	LH Z-score	LH %	RH Z-score	RH %
Frontal Lobe				
Precentral	< -1.65	2	-0.57	28
Premotor	-0.50	31	0.84	80
Superior Frontal	-0.61	27	< -1.65	< 1
Anterior Middle Frontal	0.35	64	-0.45	33
Parstriangularis	-1.22	11	< -1.65	< 1
Lateral Orbito Frontal	-1.19	12	< -1.65	< 1
Pars Orbitalis	-1.07	14	-1.63	5
Parietal Lobe				
Inferior Parietal	-0.25	40	> 1.65	> 99
Superior Parietal	0.79	79	< -1.65	2
Medial Parietal	1.30	90	> 1.65	99
Supra Marginal	0.77	78	1.28	90
Primary Sensory	-0.44	33	< -1.65	2
Primary Motor	-0.75	23	-1.45	7
Occipital Lobe				
Medial Occipital	1.06	86	0.75	77
Lateral Occipital	-0.48	31	-0.79	21
Temporal Lobe				
Fusiform	-0.65	26	-1.44	7
Anterior Medial Temporal	-0.09	47	-1.67	5
Posterior Medial Temporal	-0.05	48	-1.34	9
Temporal Pole	0.05	52	< -1.65	< 1
Transverse + Superior Temporal	-0.54	29	-1.60	5
Posterior Superior Temporal Sulcus	1.63	95	0.38	65
Middle Temporal	-1.27	10	< -1.65	< 1
Inferior Temporal	-1.17	12	< -1.65	< 1
Limbic Lobe				
Caudal + Rostral Ant Cingulate	0.90	81	-0.75	23
Isthmus + Post Cingulate	1.21	89	1.27	90

FIGURE 1 | Case report timeline.

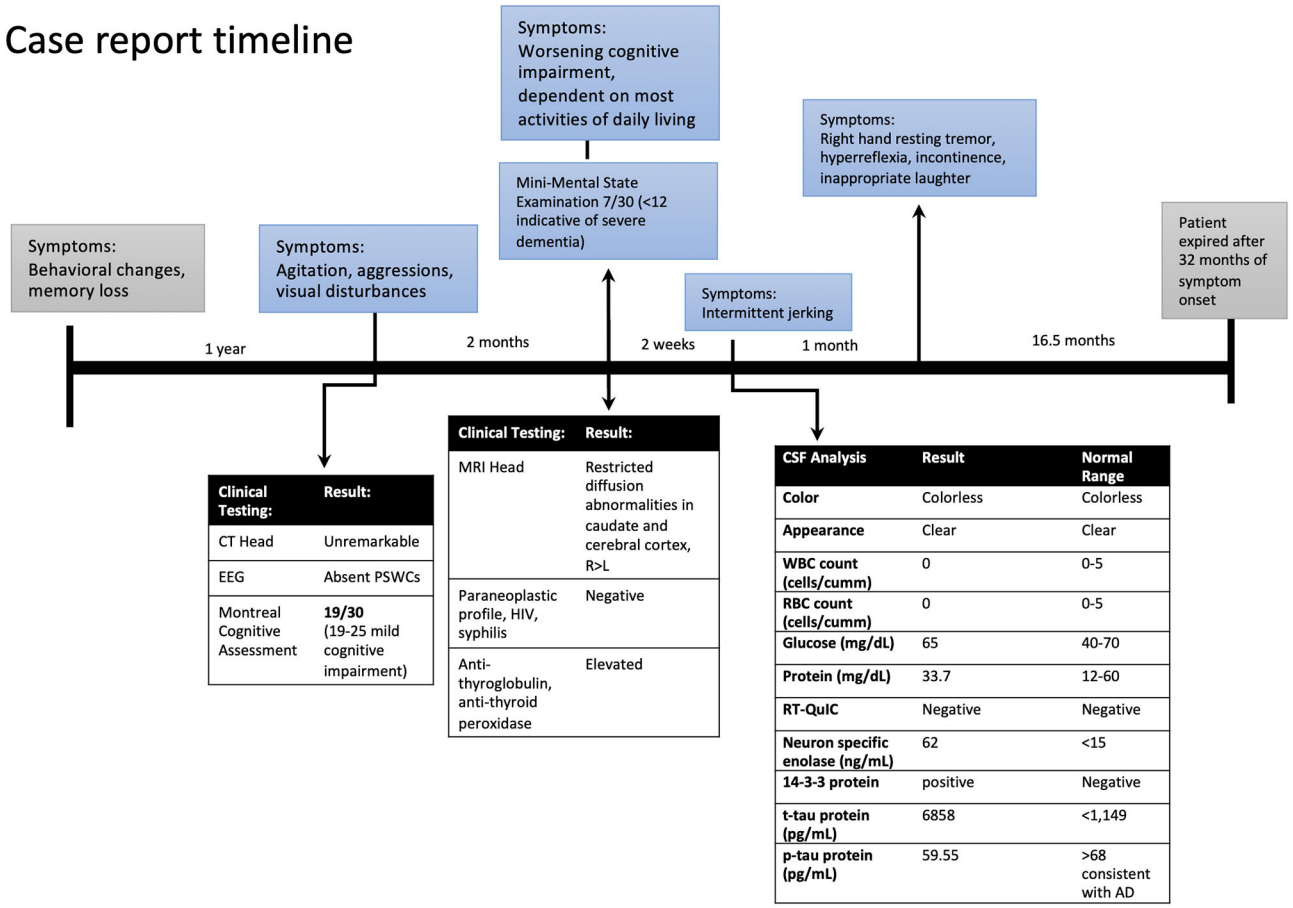

FIGURE 2 | Diffusion-weighted imaging (DWI) axial view, apparent diffusion coefficient (ADC) view, and regional volumetric studies. Asymmetric DWI increased signal intensity in the cortical ribbon of the parietal, frontal, and temporal lobes, hippocampi, caudate, and putamen. The signal hyperintensities are greater on the right. **(A)** Image shows increased signal intensity in the cingulate cortex (yellow *arrow).* **(B)** More superior image shows diffuse asymmetric involvement of parietal, frontal, and temporal lobes. There is notable involvement of the caudate head that is greater on the right (red *arrow*). **(C)** ADC sequence illustrating caudate changes (red *arrow*) consistent with the DWI hyperintensities. **(D)** Brain atrophy pattern (highlighted in red), mainly on the right frontal, temporal, and parietal lobes, consistent with areas of abnormal DWI in MRI.

BACKGROUND (ETIOLOGY, PATHOLOGY/PATHOPHYSIOLOGY)

Classification, Epidemiology, and Clinical Course

Creutzfeldt–Jakob disease (CJD) affects 1–1.5 cases per million per year and is classified into three types: sporadic (sCJD), genetic, or acquired (1). Acquired forms of the disease, which include kuru, iatrogenic, and variant CJD, account for < 1% of all cases (8). The genetic form, which accounts for 5–15% of cases, is due to an autosomal dominant mutation in the prion protein gene, *PRNP*.

Sporadic CJD (sCJD) is the most commonly occurring human prion disease, as it accounts for 85% of all cases. sCJD is further divided into five subtypes based on the type of PrP^D (types 1 and 2) and polymorphisms at codon 129 of the PrP gene (129 MM, MV, or VV) (9–11). Based on the combination of the aforementioned molecular features (PrP^D type and codon-129 genotype) sCJD includes the following subtypes: (1) MM/MV1; (2) VV1; (3) MM2; (4) MV2; and (5) VV2. The MM1 and MV1 groups were combined into one subtype (MM/MV1) because of the virtually identical phenotype. While sCJDMM1 is the most common human prion disease, the sCJDVV1 represents the rarest subtype, as it occurs at a rate of 1 case per one-hundredth million population per year (12). The mean age at onset of sCJDMM1 is 66 years, with a disease duration of 4 months. Unlike sCJDMM1, clinical characteristics of the rare VV1 subtype have been reported to show, early age of onset (44 years), disease duration of 21 months, elevated 14-3-3 and total tau in the CSF, absent PSWCs on electroencephalography (EEG), and magnetic resonance imaging (MRI) hyperintensities in the cerebral cortex with usual negative signal in the basal ganglia or thalamus (9–11). CSF RT-QuIC is typically negative in VV1 cases (13). The prodromal phase in VV1 cases also differs from typical sCJD in that it begins as slowly progressive dementia with behavioral symptoms for an extended time (7 months) in contrast

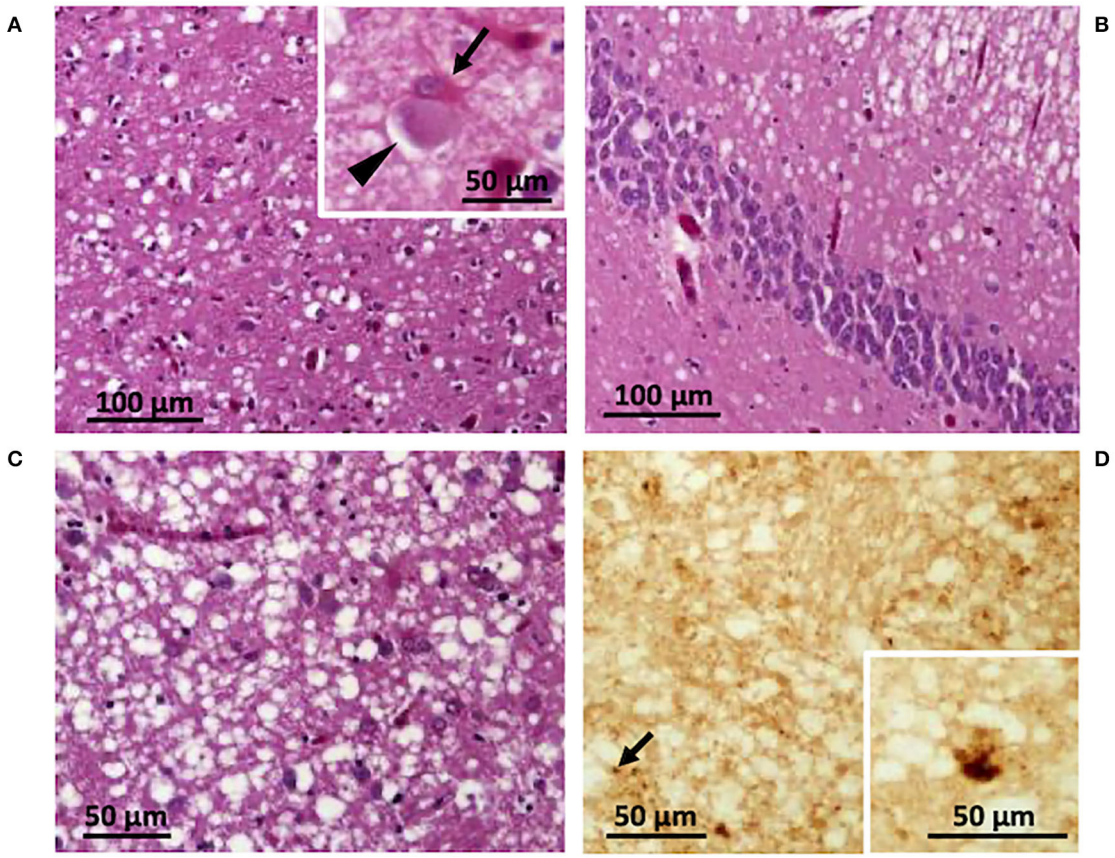

FIGURE 3 | Histological and immunohistochemical features. Spongiform degeneration with intermediate size vacuoles affecting cortical **(A,B)** and subcortical regions **(C)**; inset in **(A)** a ballooned neuron (*arrowhead*) and a reactive astrocyte (*arrow*). **(D)** Immunohistochemistry showing PrP granules (*arrow*) and dispersed deposits of larger PrP aggregates (inset). **(A)** Parietal cortex; **(B)** hippocampus; **(C,D)** putamen. Antibody: 3F4.

to initial cognitive decline followed by increased neurologic symptoms within weeks (12).

Diagnostic Criteria for CJD

The Centers for Disease Control (CDC) and WHO have established guidelines for the classification of probable, possible, and definite sCJD based on neuropathology or specific combinations of antemortem clinical testing and symptoms (1, 14, 15). Currently, it is only possible to make the definitive diagnosis of CJD through postmortem analyses of cerebral tissue. The diagnosis requires the presence of spongiform vacuolation, gliosis, neuronal loss, and PrP immunostaining (1). The well-known classical symptoms associated with sCJD include rapidly progressive dementia, ataxia, myoclonus/spasticity, and PSWCs on EEG (15). However, this combination of symptoms may not be present at every stage of the disease or at all in some cases (1, 8, 13). Thus, clinical testing and findings for probable sCJD must meet the subsequent conditions: PSWCs on EEG, one of the following imaging requirements; high signal in caudate/putamen on brain MRI, at least two cortical regions (frontal, temporal, parietal, and occipital) on either DWI or fluid-attenuated inversion recovery (FLAIR), and laboratory results showing increased levels of biomarkers in CSF and positive RT-QuIC results (1, 13, 15).

EEG and Imaging Findings

The presence of PSWCs on EEG is a highly recognized feature of CJD. This finding carries a 65% sensitivity and a specificity between 74 and 86%, however, PSWCs are not sufficient to make a CJD diagnosis (6, 13, 15–17). Furthermore, not all subtypes of CJD will demonstrate the same EEG abnormalities. For example, MM1 and MV1 display PSWCs' EEG waveforms while 42% of MM2 cases have PSWCs present, and VV1 does not (10, 12, 18). Advances in MRI techniques, such as FLAIR and DWI, have allowed physicians to improve the negative and positive predictive value in diagnosing CJD. Based on a recently published study, the sensitivity of MRI in aiding in the detection of sCJD is 90 and 95% with a specificity of 90 and 100% (19). Areas of gliosis and vacuole formation, associated with the disease process, have been found to correlate with high-intensity signal patterns on T2/Flair and DWI, respectively (20, 21). Our case underwent two separate EEG evaluations, both of which failed to demonstrate PSWCs. A study by Geschwind et al. (20) looked at the significance of tracking disease progression through

hippocampal volume and other regions of interest in sCJD cases *via* various imaging techniques. This study found a discordance among imaging assessments' regional involvement for sCJD cases, especially within the frontal and anterior and mid-limbic areas. Recent studies have described sCJD DWI hyperintensities to fluctuate based on disease stage, following a "J" or "U-shaped" curve (22, 23). According to this principle, diffusivity on MRI may be present in the early stages without any atrophy patterns among the same regions. Furthermore, as the disease process continued, DWI hyperintensities would fluctuate, yet brain atrophy would emerge and advance throughout the disease. This suggests the importance of correlating volumetric changes, which are progressive, with MRI findings for proper disease staging. Interestingly, our case had normal hippocampal volumes in volumetric studies and showed hyperintensity involvement in DWI, which may indicate an early time point in our patient's disease course. However, counter to the hippocampal comparisons, there were correlations in the cortical regions between DWI and volumetric studies (**Figures 1A–C**).

CSF Biomarkers

Cerebrospinal fluid (CSF) biomarkers that are commonly used to help establish a CJD diagnosis include, 14-3-3 protein and tau-protein. A systematic review showed that the 14-3-3 protein has a sensitivity and specificity of 83.3 and 78% in identifying sCJD respectively (24). The tau protein has sensitivity and specificity ranging from 75 to 100% and 49 to 100% (25, 26). However, these biomarkers demonstrate a varied sensitivity that is dependent on the 129 codon polymorphism with the VV1 carrying the highest sensitivity, approaching 100% (10, 16, 17). Emerging data on the diagnostic utility of neurofilament light chain (NfL), (a surrogate biomarker of neuroaxonal degeneration), have indicated a possible role as a highly sensitive, supportive third-level biomarker in prion disease cases with atypical clinical and laboratory findings (27–29). Compared to patients with Alzheimer's disease, CSF NfL has been reported to be significantly higher in patients with prion disease and may have characteristic subtype levels (27). There is currently limited data on CSF NfL levels for sCJDVV1, however, several studies have reported a handful of cases of this subtype to yield the highest levels among their study cohorts (27–29). Furthermore, given that these markers are released with neuronal damage and found in other neurodegenerative diseases, positive CSF results for NfL, 14-3-3, and/or tau protein are nonspecific for CJD.

Since its introduction in 2010, the RT-QuIC assay is quickly becoming the preferred method of detecting PrP^{Sc} in suspected CJD cases (30). RT-QuIC exploits the PrP^{Sc} self-replicating ability and aggregate formation, thus yielding a highly sensitive and specific test (30, 31). Modifications in the RT-QuIC assay have been made and improved its sensitivity. According to a recent analysis out of a large prion disease pathology surveillance center, RT-QuIC diagnostic sensitivity and specificity were found to be 90.3% and 98.5% for all prion disease types (13). The study also noted a decreased sensitivity in familial CJD (fatal familial insomnia, Gerstmann–Sraussler–Scheinker disease, and sporadic fatal insomnia) and the VV1 and MM2 sCJD subtypes. The latter findings are agreeable with our case's negative RT-QuIC.

DISCUSSION

Classical features of sporadic prion disease such as the age of onset, clinical presentation, diagnostic findings, progression, and average disease length, have largely been characterized but with less frequency in the rarer sCJDVV1 subtype (**Table 1**) (7). As stated earlier, this subtype has been described to have an average age of onset of 44 years and progressive dementia of the frontotemporal type which may develop for months without any other neurological findings (8, 11, 12, 32). Our patient was 61 years of age when they had first developed symptoms, which is an older age of onset for sCJDVV1. A notable discrepancy in our case was her length of the disease. The initial reported neuropsychiatric symptoms, namely, anxiety and mood disturbances, occurred one year before the first hospital admission, thus resulting in a total disease course of 32 months.

Given the combination of a relatively new test for a rare disease and an even rarer subtype, we found four cases of VV1, including ours with a negative RT-QuIC (33). In a recent large study in the United States which analyzed the diagnostic accuracy of RT-QuIC, all of the VV1 ($n = 3$) cases were shown to be negative (13). Another study by Lattanzio et al. (34) investigated the diagnostic value of prion RT-QuIC in pathologically confirmed cases and described a diverse sensitivity reliant on the codon 129 genotype. For example, they found RT-QuIC sensitivity to be higher in MM (84.2%) than in either MV (72.2%) or VV (79.5%) cases, with the more common VV2 type contributing to this percentage. Additional studies investigating similar parameters also indicated the RT-QuIC's varied sensitivity across sCJD subtypes, especially in the VV1, and MM2-C forms (35–37). These strongly suggest that the diagnostic advantage of RT-QuIC may be related to the type of prion strain present, thus demonstrating a possible concern in the CDC's updated guidelines for CJD. The RT-QuIC analysis was first used clinically in 2015 in the United States. Following extensive supportive research, it was included in the CDC's 2018 most recent updated clinical diagnostic criteria guidelines for a probable diagnosis of sCJD (1, 14). Although this relatively new clinical test has been proven to be highly sensitive for the common subtype, these recent findings indicate a disproportionate negative RT-QuIC result for the MM2 and especially the VV1 subtypes. Further investigations of pathologically confirmed VV1 cases combined with RT-QuIC testing need to be reported to establish this unique characteristic. In a different study, brain MRI and CSF RT-QuIC had a combined sensitivity of 100% for all sCJD subtypes (19).

Recently, MRI, FLAIR, and DWI have increased their utility in early CJD detection. For example, classical sCJD changes on MRI such as putamen and caudate head hyperintensities may present before anticipated EEG findings (38). In sCJD VV1 hyperintensities are found in the cerebral cortex, sometimes in the basal ganglia, and are commonly lacking within the thalamus (10, 12, 39). Our patient demonstrated asymmetric DWI signal

TABLE 1 | Comparison of typical VV1 characteristics and our case*.

Characteristic	Our case	Typical VV1
Subject demographic, disease course		
Sex	Female	Male predominance
Age of onset (years)	61	44 (19–55)
Disease duration (months)	32	21 (17–49)
Clinical features		
Cognitive problems[a]	Yes	Yes
Aphasia	Yes	Yes
Apraxia	Yes	Occasionally
Visual disturbances[b]	Yes, early	Occasionally
Limb or gait ataxia	No	Yes
Myoclonus	Yes	Yes
Pyramidal symptoms[c]	Yes, rigidity	Yes
Psychiatric symptoms[d]	Yes, early, agitation, aggressions	Yes, regression, fear, aggressions
EEG		
PSWCs[e]	No	No
MRI		
Widespread cortical signal involvement	Yes, right predominance	Yes
Basal ganglia signal increase	Yes, caudate and putamen	Sometimes
Laboratory findings		
14-3-3 positive	Yes	Yes
Tau	Yes, significantly elevated	Yes, significantly elevated
RT-QuIC	Negative	Unknown -mostly negative
Neuropathological features	Spongiform degeneration affecting cortical and subcortical regions	Severe spongiform changes in the cerebral cortex and striatum

Typical characteristics based on published findings from Meissner et al. (12).
[a]*Memory loss, dementia, and confusion.*
[b]*Visual loss, field defect, blindness, and distortion.*
[c]*Rigidity or spasticity.*
[d]*Anxiety, depression, aggression, psychosis, personality changes, and regression.*
[e]*PSWCs – periodic sharp wave complexes on electroencephalography.*

hyperintensities in the cortical ribbon of the parietal, frontal, and temporal lobes, basal ganglia, and hippocampi, which are consistent with VV1.

Pathological features of the VV1 include involvement of the corticostriatal regions and relative sparing of the occipital lobe compared to the frontal and temporal lobes (7, 10). Our case demonstrated these features. Furthermore, spongiform degeneration with intermediate size vacuoles affecting cortical and subcortical regions and ballooned neurons, two typical pathological features of the VV1 subtype, were present in our case (**Figures 3A–C**). Immunohistochemistry revealed a faint PrP staining and occasionally larger PrP aggregates (**Figure 3D**).

As anticipated, this pattern correlated with the signal hyperintensity findings on DWI. While CJD is currently an uncurable disease, these correlations may be useful in the antemortem setting for symptom management, disease pattern recognition, and insight into the disease microenvironment and cerebral region susceptibility.

TREATMENT CONSIDERATIONS

Despite numerous clinical trials, there are currently no effective treatments for CJD. Four drugs, flupirtine, quinacrine, pentosan polysulfate (PPS), and doxycycline have been studied on a large scale and are directed toward inhibiting the conversion of PrP^{c} to PrP^{sc} (40). Another emerging treatment approach for prion disease has been aimed at reducing the expression of PrP^{c} *via* antisense oligonucleotides (ASOs) (41). These PrP^{c} lowering therapies have yielded promising results in mice models across five different CJD subtypes (42). A recent study found that a CSF bolus of ASOs in prion-infected mice extended survival time by 61–98% (41). However, the effective dosing regimen and degree of adverse side effects of ASOs in human trials are currently unknown, and emerging clinical trials using this treatment modality are likely to take place in the near future.

At this time care for highly suspected cases is predominately aimed at symptom management and advanced care planning with families/next of kin. Regardless of ineffective clinical trials, it is important to identify potential sCJD cases early to provide adequate time for families to care for their loved ones and for those who wish to decide on study participation (40).

CONCLUSION

Our patient was a complex case in the sense that she demonstrated findings that differ from the other more commonly occurring forms of sCJD. The EEG findings and extended prodrome did not follow patterns of typical sCJD and the patient's age was older than most VV1 cases. Furthermore, studies indicate the probability of PSWCs on EEG increases with increasing age, and subtype, and is dependent on the disease stage (32). These unclear diagnostic findings paired with negative RT-QuIC results and elevated anti-TPO levels manifested a complex clinical judgment call for the care team and family. It is possible sCJDVV1 cases with a presentation similar to ours (older age, lengthy cognitive, and/or psychiatric prodrome without clear etiology) may go undiagnosed, especially if nonstandard diagnostic tests, such as CT, instead of MRI are performed. The presentation of rapidly progressive cognitive and functional decline, in conjunction with the late-adult onset of psychiatric disturbances in patients without any obvious infectious, malignant, or traumatic etiologies, should have sCJD included in their differential. Early suspicion of prion disease is important for proper management of tissue and specimens, adequate advanced care planning for the patient and loved ones, and to enable sufficient time to make an end of life decisions for their next of kin, or adequate time

to undergo clinical trials. Potential future therapies may also require subtype classification given the isoforms' theorized unique molecular interactions or their role in disrupting vital neuronal pathways and requiring different outcome measures given the clinical heterogeneity between sCJD subtypes. Furthermore, patients with a high suspicion of sCJD and negative RT-QuIC results should consider VV1, and other atypical prion diseases (e.g., sporadic fatal insomnia, variably protease-sensitive prionopathy, and some genetic forms of prion disease).

DATA AVAILABILITY STATEMENT

The original contributions presented in the study are included in the article/supplementary material, further inquiries can be directed to the corresponding author.

AUTHOR CONTRIBUTIONS

AC wrote the manuscript with support from HO, BA, and IC. AC and HO contributed to conception and design of the report. HO wrote the case report section. BA contributed to the background, discussion, treatment considerations, and conclusion sections of the manuscript. IC wrote the description of **Figure 1** and contributed to the background section of the manuscript. BA and IC provided immunohistochemistry sections. All authors contributed to manuscript revision, read and approved the submitted version.

FUNDING

This study was in part supported by the NIH NIA K99 AG068359 to IC.

REFERENCES

1. CentersforDiseaseControl. *Creutzfeldt-Jakob Disease, Classic: About CJD Center for Disease Control and Prevention.* (2021). Available online at: https://www.cdc.gov/prions/cjd/about.html.
2. Weissmann C, Enari M, Klohn PC, Rossi D, Flechsig E. Molecular biology of prions. *Acta Neurobiol Exp.* (2002) 62:153–66.
3. Prusiner SB. Prions. *Proc Natl Acad Sci U S A.* (1998) 95:13363–83. doi: 10.1073/pnas.95.23.13363
4. Spielmeyer W. Die histopathologische forschung in der psychiatrie. *Klin Wochenschr.* (1922) 1:1817–9. doi: 10.1007/BF01716575
5. Parchi P, Castellani R, Capellari S, Ghetti B, Young K, Chen SG, et al. Molecular basis of phenotypic variability in sporadic Creutzfeldt-Jakob disease. *Ann Neurol.* (1996) 39:767–78. doi: 10.1002/ana.410390613
6. Parchi P, Giese A, Capellari S, Brown P, Schulz-Schaeffer W, Windl O, et al. Classification of sporadic Creutzfeldt-Jakob disease based on molecular and phenotypic analysis of 300 subjects. *Ann Neurol.* (1999) 46:224–33
7. Cali I, Puoti G, Smucny J, Curtiss PM, Cracco L, Kitamoto T, et al. Co-existence of PrP(D) types 1 and 2 in sporadic Creutzfeldt-Jakob disease of the VV subgroup: phenotypic and prion protein characteristics. *Sci Rep.* (2020) 10:1503. doi: 10.1038/s41598-020-58446-0
8. Sitammagari KK, Masood W. Creutzfeldt Jakob Disease. StatPearls Treasure Island (FL) (2021).
9. Gambetti P, Kong Q, Zou W, Parchi P, Chen SG. Sporadic and familial CJD: classification and characterisation. *Br Med Bull.* (2003) 66:213–39. doi: 10.1093/bmb/66.1.213
10. Parchi P, Strammiello R, Giese A, Kretzschmar H. Phenotypic variability of sporadic human prion disease and its molecular basis: past, present, and future. *Acta Neuropathol.* (2011) 121:91–112. doi: 10.1007/s00401-010-0779-6
11. Puoti G, Bizzi A, Forloni G, Safar JG, Tagliavini F, Gambetti P. Sporadic human prion diseases: molecular insights and diagnosis. *Lancet Neurol.* (2012) 11:618–28. doi: 10.1016/S1474-4422(12)70063-7
12. Meissner B, Westner IM, Kallenberg K, Krasnianski A, Bartl M, Varges D, et al. Sporadic Creutzfeldt-Jakob disease: clinical and diagnostic characteristics of the rare VV1 type. *Neurology.* (2005) 65:1544–50. doi: 10.1212/01.wnl.0000184674.32924.c9
13. Rhoads DD, Wrona A, Foutz A, Blevins J, Glisic K, Person M, et al. Diagnosis of prion diseases by RT-QuIC results in improved surveillance. *Neurology.* (2020) 95:e1017–e26. doi: 10.1212/WNL.0000000000010086
14. WHO manual for surveillance of human transmissible spongiform encephalopathies, including variant Creutzfeldt-Jakob disease (2003).
15. Manix M, Kalakoti P, Henry M, Thakur J, Menger R, Guthikonda B, et al. Creutzfeldt-Jakob disease: updated diagnostic criteria, treatment algorithm, and the utility of brain biopsy. *Neurosurg Focus.* (2015) 39:E2. doi: 10.3171/2015.8.FOCUS15328
16. Tanev KS, Yilma M. An unusually presenting case of sCJD–the VV1 subtype. *Clin Neurol Neurosurg.* (2009) 111:282–91. doi: 10.1016/j.clineuro.2008.09.017
17. Figgie MP Jr, Appleby BS. Clinical use of improved diagnostic testing for detection of prion disease. *Viruses.* (2021) 13:789. doi: 10.3390/v13050789
18. Krasnianski A, Meissner B, Schulz-Schaeffer W, Kallenberg K, Bartl M, Heinemann U, et al. Clinical features and diagnosis of the MM2 cortical subtype of sporadic Creutzfeldt-Jakob disease. *Arch Neurol.* (2006) 63:876–80. doi: 10.1001/archneur.63.6.876
19. Bizzi A, Pascuzzo R, Blevins J, Grisoli M, Lodi R, Moscatelli MEM, et al. Evaluation of a New Criterion for Detecting Prion Disease With Diffusion Magnetic Resonance Imaging. *JAMA Neurol.* (2020) 77:1141–9. doi: 10.1001/jamaneurol.2020.1319
20. Geschwind MD, Potter CA, Sattavat M, Garcia PA, Rosen HJ, Miller BL, et al. Correlating DWI MRI with pathologic and other features of Jakob-Creutzfeldt disease. *Alzheimer Dis Assoc Disord.* (2009) 23:82–7. doi: 10.1097/WAD.0b013e31818323ef
21. Fragoso DC, Goncalves Filho AL, Pacheco FT, Barros BR, Aguiar Littig I, Nunes RH, et al. Imaging of Creutzfeldt-Jakob Disease: Imaging Patterns and Their Differential Diagnosis. *Radiographics.* (2017) 37:234–57. doi: 10.1148/rg.2017160075
22. Caverzasi E, Henry RG, Vitali P, Lobach IV, Kornak J, Bastianello S, et al. Application of quantitative DTI metrics in sporadic CJD. *Neuroimage Clin.* (2014) 4:426–35. doi: 10.1016/j.nicl.2014.01.011
23. Sacco S, Paoletti M, Staffaroni AM, Kang H, Rojas J, Marx G, et al. Multimodal MRI staging for tracking progression and clinical-imaging correlation in sporadic Creutzfeldt-Jakob disease. *Neuroimage Clin.* (2021) 30:102523. doi: 10.1016/j.nicl.2020.102523
24. Behaeghe O, Mangelschots E, De Vil B, Cras P. A systematic review comparing the diagnostic value of 14-3-3 protein in the cerebrospinal fluid, RT-QuIC and RT-QuIC on nasal brushing in sporadic Creutzfeldt-Jakob disease. *Acta Neurol Belg.* (2018) 118:395–403. doi: 10.1007/s13760-018-0995-8
25. Cohen OS, Chapman J, Korczyn AD, Warman-Alaluf N, Nitsan Z, Appel S, et al. CSF tau correlates with CJD disease severity and cognitive decline. *Acta Neurol Scand.* (2016) 133:119–23. doi: 10.1111/ane.12441
26. Ascari LM, Rocha SC, Goncalves PB, Vieira T, Cordeiro Y. Challenges and Advances in Antemortem Diagnosis of Human Transmissible Spongiform Encephalopathies. *Front Bioeng Biotechnol.* (2020) 8:585896. doi: 10.3389/fbioe.2020.585896
27. Abu-Rumeileh S, Capellari S, Stanzani-Maserati M, Polischi B, Martinelli P, Caroppo P, et al. The CSF neurofilament light signature in rapidly progressive neurodegenerative dementias. *Alzheimers Res Ther.* (2018) 10:3. doi: 10.1186/s13195-017-0331-1
28. Kovacs GG, Andreasson U, Liman V, Regelsberger G, Lutz MI, Danics K, et al. Plasma and cerebrospinal fluid tau and neurofilament concentrations in

rapidly progressive neurological syndromes: a neuropathology-based cohort. *Eur J Neurol.* (2017) 24:1326–e77. doi: 10.1111/ene.13389
29. Abu-Rumeileh S, Baiardi S, Ladogana A, Zenesini C, Bartoletti-Stella A, Poleggi A, et al. Comparison between plasma and cerebrospinal fluid biomarkers for the early diagnosis and association with survival in prion disease. *J Neurol Neurosurg Psychiatry.* (2020) 91:1181–8. doi: 10.1136/jnnp-2020-323826
30. Green AJE. RT-QuIC: a new test for sporadic CJD. *Pract Neurol.* (2019) 19:49–55. doi: 10.1136/practneurol-2018-001935
31. McGuire LI, Peden AH, Orru CD, Wilham JM, Appleford NE, Mallinson G, et al. Real time quaking-induced conversion analysis of cerebrospinal fluid in sporadic Creutzfeldt-Jakob disease. *Ann Neurol.* (2012) 72:278–85. doi: 10.1002/ana.23589
32. Collins SJ, Sanchez-Juan P, Masters CL, Klug GM, van Duijn C, Poleggi A, et al. Determinants of diagnostic investigation sensitivities across the clinical spectrum of sporadic Creutzfeldt-Jakob disease. *Brain.* (2006) 129:2278–87. doi: 10.1093/brain/awl159
33. Wiels WA, Du Four S, Seynaeve L, Flamez A, Tousseyn T, Thal D, et al. Early-Onset Creutzfeldt-Jakob Disease Mimicking Immune-Mediated Encephalitis. *Front Neurol.* (2018) 9:242. doi: 10.3389/fneur.2018.00242
34. Lattanzio F, Abu-Rumeileh S, Franceschini A, Kai H, Amore G, Poggiolini I, et al. Prion-specific and surrogate CSF biomarkers in Creutzfeldt-Jakob disease: diagnostic accuracy in relation to molecular subtypes and analysis of neuropathological correlates of p-tau and Abeta42 levels. *Acta Neuropathol.* (2017) 133:559–78. doi: 10.1007/s00401-017-1683-0
35. Foutz A, Appleby BS, Hamlin C, Liu X, Yang S, Cohen Y, et al. Diagnostic and prognostic value of human prion detection in cerebrospinal fluid. *Ann Neurol.* (2017) 81:79–92. doi: 10.1002/ana.24833
36. Connor A, Wang H, Appleby BS, Rhoads DD. Clinical laboratory tests used to aid in diagnosis of human prion disease. *J Clin Microbiol.* (2019) 57:e00769–19. doi: 10.1128/JCM.00769-19
37. Candelise N, Baiardi S, Franceschini A, Rossi M, Parchi P. Towards an improved early diagnosis of neurodegenerative diseases: the emerging role of in vitro conversion assays for protein amyloids. *Acta Neuropathol Commun.* (2020) 8:117. doi: 10.1186/s40478-020-00990-x
38. Collie DA, Sellar RJ, Zeidler M, Colchester AC, Knight R, Will RG, et al. of Creutzfeldt-Jakob disease: imaging features and recommended MRI protocol. *Clin Radiol.* (2001) 56:726–39. doi: 10.1053/crad.2001.0771
39. Bizzi A, Pascuzzo R, Blevins J, Moscatelli MEM, Grisoli M, Lodi R, et al. Subtype Diagnosis of Sporadic Creutzfeldt-Jakob Disease with Diffusion Magnetic Resonance Imaging. *Ann Neurol.* (2021) 89:560–72. doi: 10.1002/ana.25983
40. Appleby BS, Connor A, Wang H. Therapeutic strategies for prion disease: a practical perspective. *Curr Opin Pharmacol.* (2019) 44:15–9. doi: 10.1016/j.coph.2018.11.006
41. Raymond GJ, Zhao HT, Race B, Raymond LD, Williams K, Swayze EE, et al. Antisense oligonucleotides extend survival of prion-infected mice. *JCI Insight.* (2019) 5:e131175. doi: 10.1172/jci.insight.131175
42. Minikel EV, Zhao HT, Le J, O'Moore J, Pitstick R, Graffam S, et al. Prion protein lowering is a disease-modifying therapy across prion disease stages, strains and endpoints. *Nucleic Acids Res.* (2020) 48:10615–31. doi: 10.1093/nar/gkaa616

Conflict of Interest: The authors declare that the research was conducted in the absence of any commercial or financial relationships that could be construed as a potential conflict of interest.

Publisher's Note: All claims expressed in this article are solely those of the authors and do not necessarily represent those of their affiliated organizations, or those of the publisher, the editors and the reviewers. Any product that may be evaluated in this article, or claim that may be made by its manufacturer, is not guaranteed or endorsed by the publisher.

frontiers | Frontiers in Neurology

CASE REPORT
published: 16 June 2022
doi: 10.3389/fneur.2022.873735

Case Report: Semantic Variant Primary Progressive Aphasia With Impaired Verbal Word Discrimination

Nobuko Kawakami[1], Ayumi Morita[2], Shigenori Kanno[1], Nanayo Ogawa[1], Kazuo Kakinuma[1], Yumiko Saito[1], Erena Kobayashi[1,3], Wataru Narita[1] and Kyoko Suzuki[1]*

[1] Department of Behavioral Neurology and Cognitive Neuroscience, Tohoku University Graduate School of Medicine, Sendai, Japan, [2] Department of Rehabilitation, Tohoku University Hospital, Sendai, Japan, [3] Department of Neurology and Stroke Medicine, Yokohama City University, Yokohama, Japan

Some patients with primary progressive aphasia (PPA) present with various types of hearing deficits. Research on the auditory function and speech sounds in PPA, including temporal, phonemic, and prosodic processing, revealed impairment in some of these auditory processes. Many patients with PPA who present with impaired word recognition subsequently developed non-fluent variant PPA. Herein, we present a patient with semantic variant PPA (svPPA) who demonstrated impaired verbal word discrimination. Audiological examinations revealed normal auditory brainstem responses and slightly impaired pure-tone perception. By contrast, verbal word discrimination and monosyllable identification were impaired, and temporal auditory acuity deteriorated. Analyses of brain magnetic resonance images revealed a significant decrease in the gray matter volume in bilateral superior temporal areas, predominantly on the left, compared with those of patients with typical svPPA, which appeared to be associated with impaired word recognition in our patient.

Keywords: semantic variant, primary progressive aphasia, verbal word recognition, verbal word discrimination, word discrimination, auditory agnosia, nonverbal sound discrimination

OPEN ACCESS

Edited by:
Filippo Brighina, University of Palermo, Italy

Reviewed by:
Donna Clark Tippett, Johns Hopkins Medicine, United States
Vanessa Costa, Azienda Ospedaliera Universitaria Policlinico Paolo Giaccone, Italy

****Correspondence:***
Nobuko Kawakami
nobuko.kawakami.a2@tohoku.ac.jp

Specialty section:
This article was submitted to Dementia and Neurodegenerative Diseases, a section of the journal Frontiers in Neurology

Received: *11 February 2022*
Accepted: *23 May 2022*
Published: *16 June 2022*

Citation:
Kawakami N, Morita A, Kanno S, Ogawa N, Kakinuma K, Saito Y, Kobayashi E, Narita W and Suzuki K (2022) Case Report: Semantic Variant Primary Progressive Aphasia With Impaired Verbal Word Discrimination. Front. Neurol. 13:873735. doi: 10.3389/fneur.2022.873735

INTRODUCTION

Primary progressive aphasia (PPA) is a clinical syndrome characterized by progressive loss of language function and is associated with various neurodegenerative diseases. Based on its diagnostic criteria, PPA is classified into three variants: non-fluent/agrammatic variant PPA (nfvPPA), semantic variant PPA (svPPA), and logopenic variant PPA (lvPPA) (1). However, several patients do not meet the diagnostic criteria for PPA, which suggests the existence of atypical PPA (2–5). The previous studies have reported that some patients with PPA present with impaired recognition of auditory stimuli, including progressive word deafness (6–10), auditory agnosia in its broader sense (6–8, 11, 12), and pure auditory agnosia restricted to non-verbal sounds (13).

The neural bases of verbal and non-verbal sound processing in the patients with PPA were explored through neuroradiological examinations. Studies of voxel-based morphometry (VBM) on brain magnetic resonance images (MRI) have revealed that impairment in auditory phonemic discrimination in lvPPA was positively correlated with the gray matter volume in the left angular gyrus (14), and the phonetic spectral processing deficit was associated with the gray matter volume in the left supramarginal gyrus (SMG) in nfvPPA and svPPA (15). Activation fMRI study examined activated brain areas during listening to sequences of spoken syllables with manipulation of

temporal regularity, phonemic spectral structure, and pitch sequence entropy. Each variant of PPA exhibited a different distribution of abnormal activation in response to these auditory speech signal characteristics (16). Longitudinal fluorodeoxyglucose-positron emission tomography in a patient with PPA and environmental sound agnosia revealed increased hypometabolic areas in the left temporoparietal regions (13).

Some patients with svPPA demonstrated auditory agnosia for non-verbal sound (17–19), whereas impaired verbal word discrimination has not been reported in the patients with svPPA. Herein, we present a patient with svPPA who demonstrated impaired auditory word discrimination and recognition and temporal auditory acuity deficit. We performed neuroradiological studies to identify the brain regions associated with the auditory symptoms, which revealed marked atrophy in the perisylvian area, dominant on the left side, compared with our disease control patients with typical svPPA.

CASE REPORT

An 80-year-old, right-handed woman was referred to our hospital for a 3 year history of moderate amnesia and progressive difficulties in finding words and understanding conversations. She was a college graduate and had worked as a nurse until her mid-50 s. She was healthy except for bladder cancer surgery at the age of 60. At age 77, she demonstrated difficulty in finding words and diminished ability to recognize spoken words, which progressed in subsequent years. At age 78, in addition to the prominent aphasia, she demonstrated amnesia and slight behavioral change, such as compulsive washing of hands and dishes; however, they did not have a significant effect on her daily activities.

On admission to our hospital, she was alert and cooperative to the examination, but she was occasionally a little reluctant to, particularly memory tests. Sometimes, we had to repeat instructions because she could not understand the first time. However, she understood what should be done following repetitive instructions or written commands.

Frontal signs such as disinhibition were occasionally observed, but they were relatively mild. Neurological examination did not reveal motor or sensory disturbance and parkinsonian symptoms. She exhibited bilateral palmomental reflexes but no grasp reflex. Her autonomic functions were well preserved.

TABLE 1 | Performance on the neuropsychological tests.

Neuropsychological tests		Results	Normal range
Mini-Mental State Examination (30)		8	
Digit span (Forward, backward)		6, 3	
Tapping span (Forward, backward)		6, 2	
Rey–Osterrieth Complex Figure Test			
Copy (36)		36	
Delayed recall (36)		0	
Recognition (24)		18	
Wechsler Memory Scale-Revised			
Visual memory index		56	
Wechsler Adult Intelligent Scale III			
Performance IQ		76	
Raven's Colored Matrices (37)		21	
Birmingham Object Recognition Battery: Object decision task			
HARD A (32)		20	27.0 ± 2.2
EASY B (32)		6	30.5 ± 1.4
Semantic Memory Task (16)		10	16
Western Aphasia Battery (Japanese version)			
Aphasia quotient (100)		59.4	
Spontaneous speech	Information content (10)	5	
	Fluency (10)	8	
Auditory comprehension	Yes/No questions (60)	45	
	Auditory word recognition (60)	44	
	Sequential commands (80)	45	
Repetition (100)	Naming	91	
	Object naming (60)	0	
	Word fluency (20)	1	
	Sentence completion (10)	4	
	Responsive speech (10)	4	
Reading (10)		4.8	
Writing (10)		3.6	
Praxis (60)		50	
Drawing (30)		24	
Block design (9)		6	
Calculation (24)		14	
Test of Lexical Processing in Aphasia			
Naming (200)		31	191.80
Auditory comprehension (200)		137	199.50

Semantic Memory Task; The original task in which a participant is shown one target image and asked to choose the associated image from four others; similar to the Pyramid and Palm Trees test.

Neuropsychological Assessment

Neuropsychological assessments were performed between the second and 18th days of hospitalization. Some of her performance seemed to be affected by her impaired listening comprehension or non-serious attitude. For her best performance, clear and plain instructions were repeated until she could understand them. The results of the neuropsychological tests are presented in **Table 1**.

Test scores on WAIS-III and Raven's Colored Progressive Matrices were nearly at the lower limit of normal performance. The Wechsler Memory Scale-Revised and Rey–Osterrieth Complex Figure Test indicated severely impaired visual memory. Apraxia, visual agnosia, and prosopagnosia were not observed.

Her speech was fluent without distortion or agrammatism. She demonstrated difficulty in finding words and visual confrontation naming. Although auditory comprehension of sentences and words was impaired, they were due to the difficulty in phonological word processing. Written word comprehension was much better than spoken word comprehension. Results of

the Western Aphasia Battery Japanese version revealed anomia, poor spoken word comprehension, and poor writing, but speech production was relatively well preserved. The scores on the repetition task were good, but phonological errors in words were observed. She could read kana (phonogram) and regular kanji (morphogram) words, but she frequently made mistakes when reading irregular kanji words, indicating surface dyslexia (20). In addition, she demonstrated difficulty writing kanji but not kana. These features in Japanese suggested impairment of semantic memory for words (21) and were often observed in semantic dementia (22). On the standard tests in Japanese to examine naming and auditory comprehension of 100 high-frequency and 100 low-frequency words, she scored 31/200 on the naming task and 137/200 on the auditory comprehension task. We examined written comprehension for 61 of the 63 words that could not be understood on the auditory comprehension task. We excluded two words because we selected the word that she presented a two-way anomia. Accordingly, her written word comprehension was correct for 31 words (50%).

To evaluate her non-verbal semantic memory, we used the object decision task of the Birmingham Object Recognition Battery and an original semantic memory task, similar to the Pyramid and Palm Trees test. We used the original semantic task because some items in the Pyramid and Palm Trees test are unfamiliar to Japanese people. The results of these tests revealed that the patient also had non-verbal semantic memory impairment. Thus, the patient experienced prominent language deficits throughout the clinical course with verbal and non-verbal semantic memory impairment, which fulfilled the diagnostic criteria for svPPA (1).

By contrast, the patient demonstrated difficulty in repeating and dictating spoken words, which is not a common feature in svPPA. Listening errors were improved by the repetition of target words, and the ability to repeat long sentences was relatively preserved. Therefore, we hypothesized that impaired detection of each phoneme may affect her ability to comprehend and repeat spoken words. The context could also help estimate the words in long sentences.

Accordingly, we performed a comprehensive examination of the higher auditory functions of the patient and conducted neuroradiological analyses to reveal the areas associated with the auditory symptoms.

Elementary Auditory Functions

Auditory brainstem responses that were elicited with the standard protocol demonstrated normal waves. We used an adapted form of a standard clinical audiometry protocol in assessing frequencies of 500, 1,000, 2,000, and 4,000 Hz. The patient's pure-tone audiometry threshold was within the normal range for her age, with mean threshold values of 36.3 and 36.3 dB on the right and left, respectively.

Higher Auditory Functions

To examine the higher auditory functions, we performed: (1) temporal auditory acuity and; (2) verbal sound discrimination and recognition. The results are presented in **Table 2**. Her ability to identify non-verbal sounds and nursery songs was also examined (**Supplementary Table 1**). We did not analyze these data in detail because several factors including word-finding impairment and semantic memory loss made further analyses difficult.

TABLE 2 | Results of the examinations of auditory function.

	Right	Left	Normal range
Pure-tone audiometry threshold (dB)			
500 Hz	25	25	
1,000 Hz	35	35	
2,000 Hz	50	50	
4,000 Hz	45	35	
Auditory brain responses (ms)			
Wave I	1.58	2.00	<2.21
Wave II	3.73	3.79	<4.51
Wave V	5.69	5.93	<6.43
Temporal auditory acuity			
Click counting (counts/s)	5*	5*	9–11
Click fusion (ms)	8*	8*	1–3
Single mora recognition accuracy	75%*	80%**	80–100
2-mora word discrimination (36)	31*		35.82 (0.50)
2-mora non-word discrimination (36)	28*		35.14 (1.06)

**Impaired performance relative to normal controls; **lower limit of normal controls.*

Examinations of Temporal Auditory Acuity

Click counting and click fusion tests (23) were also performed. In the click counting test, the patient was asked to count the number of clicks per second. She was able to count five clicks per second in each ear, which was lower than the 9–11 clicks per second detected by normal controls (24). In the click fusion test, click sounds were delivered to each ear at various intervals between binaural pulses. The patient was requested to report whether one or two clicks were made. She exhibited binaural fusion at an interval of 8 ms, which was worse than the several milliseconds detected by normal controls (24).

Verbal Sound Recognition and Discrimination

In Japanese, the ultimate minimum unit of a verbal phoneme sound is expressed as a "mora." A mora was defined as one vowel or a unit of a consonant and a vowel, which corresponded to one kana letter. When measuring the speech recognition score in Japanese, the participants are requested to listen to a mora, a monosyllabic sound, produced verbally and to answer the corresponding kana letter by dictation (25). Because she was unable to write well enough, the test was performed by recitation. She recognizes 15/20 moras (75%) at 65 dB with the right ear and 16/20 moras (80%) at 65 dB with the left ear. The speech audiogram revealed significantly impaired speech recognition relative to the normal range advocated by the Japanese Audiological Society (25) (**Figure 1**). Her maximum recognition score in a phonetically balanced word list of the right ear was 75% (15/20 moras) at 65 dB and that of the left ear was 80% (16/20 moras) at 65 dB. Thus, a higher volume was

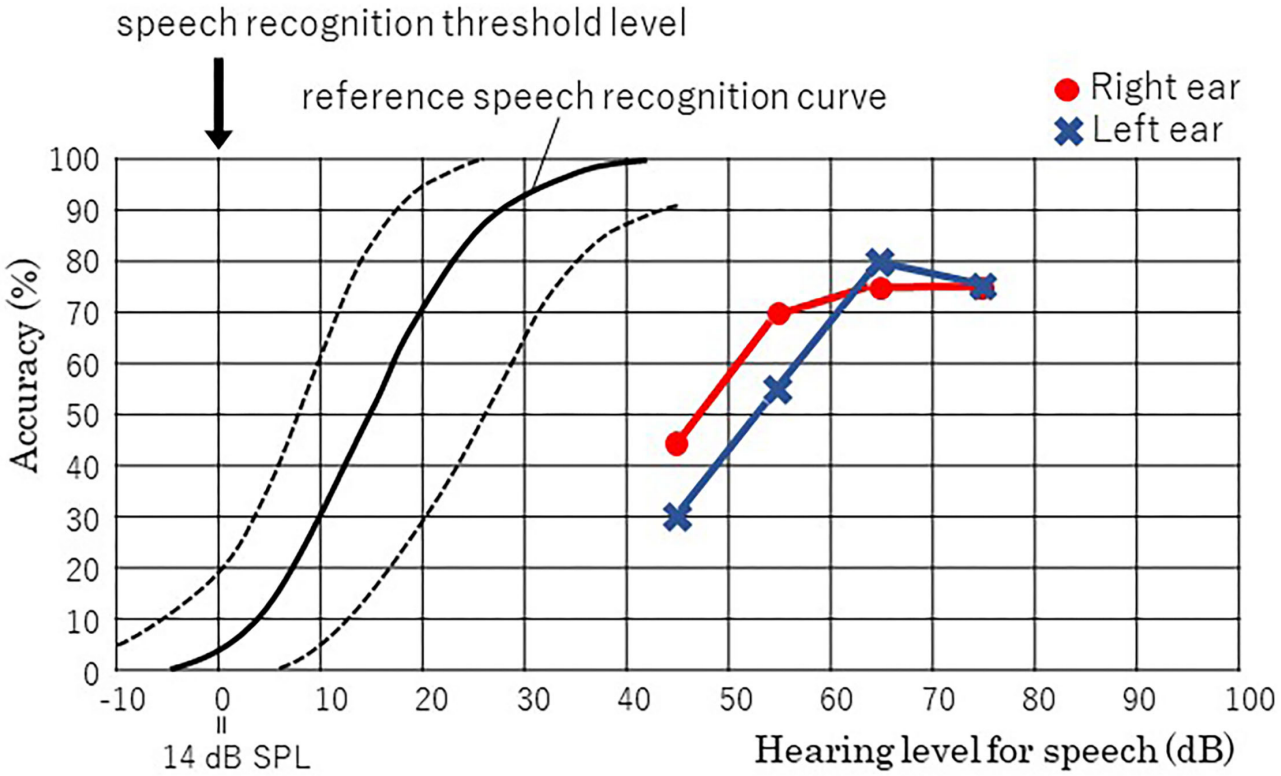

FIGURE 1 | Results of the speech audiogram. The curve marked with a solid black line is the reference speech recognition curve and that between the curves marked with black dashed lines on both sides of it represent the normal range. The speech recognition scores of the right ear are marked by red circles and those of the left ear are marked by a blue cross, and those are connected by solid lines of the same color with marks. Both are out of the normal range, and the maximum recognition score in the phonetically balanced word list of the right ear is 75% at 65 dB and that of the left ear is 80% at 65 dB.

needed to increase the accuracy, and speech recognition accuracy did not exceed 80% in either ear even at the suprathreshold level. The two-mora discrimination tasks using 36 words and 36 non-words were performed. She discriminated 31 of 36 words (normal range; 35.82 ± 0.50) and 28 of 36 non-words (normal range; 35.14 ± 1.06), which was worse than normal controls. These results support the hypothesis that the patient's ability to recognize phonemes was impaired, and she used the context of sentences to estimate the words.

Neuroradiological Investigations

The MRI scans and ^{123}I-iodoamphetamine single-photon emission computed tomography (^{123}I-IMP-SPECT) were performed.

Magnetic Resonance Imaging

Eight days after admission, we performed an MRI of the brain using a 3-Tesla MAGNETOM Trio (Siemens Medical Solutions United States, Inc., PA, United States). Three-dimensional magnetization-prepared rapid acquisition with gradient echo (3D-MPRAGE) images demonstrated diffuse cerebral atrophy, which was especially marked in the anterior and medial parts of the left temporal lobe (**Figure 2A**).

Voxel-Based Morphometry

To identify brain regions of the patient in which gray matter volumes were smaller than those in patients with typical svPPA, we performed VBM using statistical parametric mapping software (SPM), version 12 (http://www.fil.ion.ucl.ac.uk/spm/). Three-dimensional spoiled gradient echo or 3D-MPRAGE image data of 10 patients with typical svPPA as disease controls (mean age, 64 ± 8.0 years; 7 women and 3 men) were used for the analysis. The imaging parameters used for the acquisition of structural imaging data are presented in **Supplementary Table 2**. The disease controls were retrospectively recruited from the database for the study of dementing illnesses from June 2009 to April 2021 in Tohoku University Hospital and were diagnosed by board-certified neurologists based on the PPA criteria (1).

The protocol of the study was approved by the Ethics Committee of Tohoku University Hospital (approval nos. 2006–19, 2014–1–278, 2018–1–024, 2019–1–156, and 2020–1–285).

A Z-score map of the present patient was created using the mean and standard deviation of the gray matter volume (normalized by the total intracranial volume) of each voxel in the disease controls and the following equation: Z-score = [(Control mean) – (Present patient's value)]/(control standard deviation). Significance was defined as a Z-score above 3.29 ($\alpha < 0.0005$). The Z-score map is exhibited in **Figure 2B**. Compared

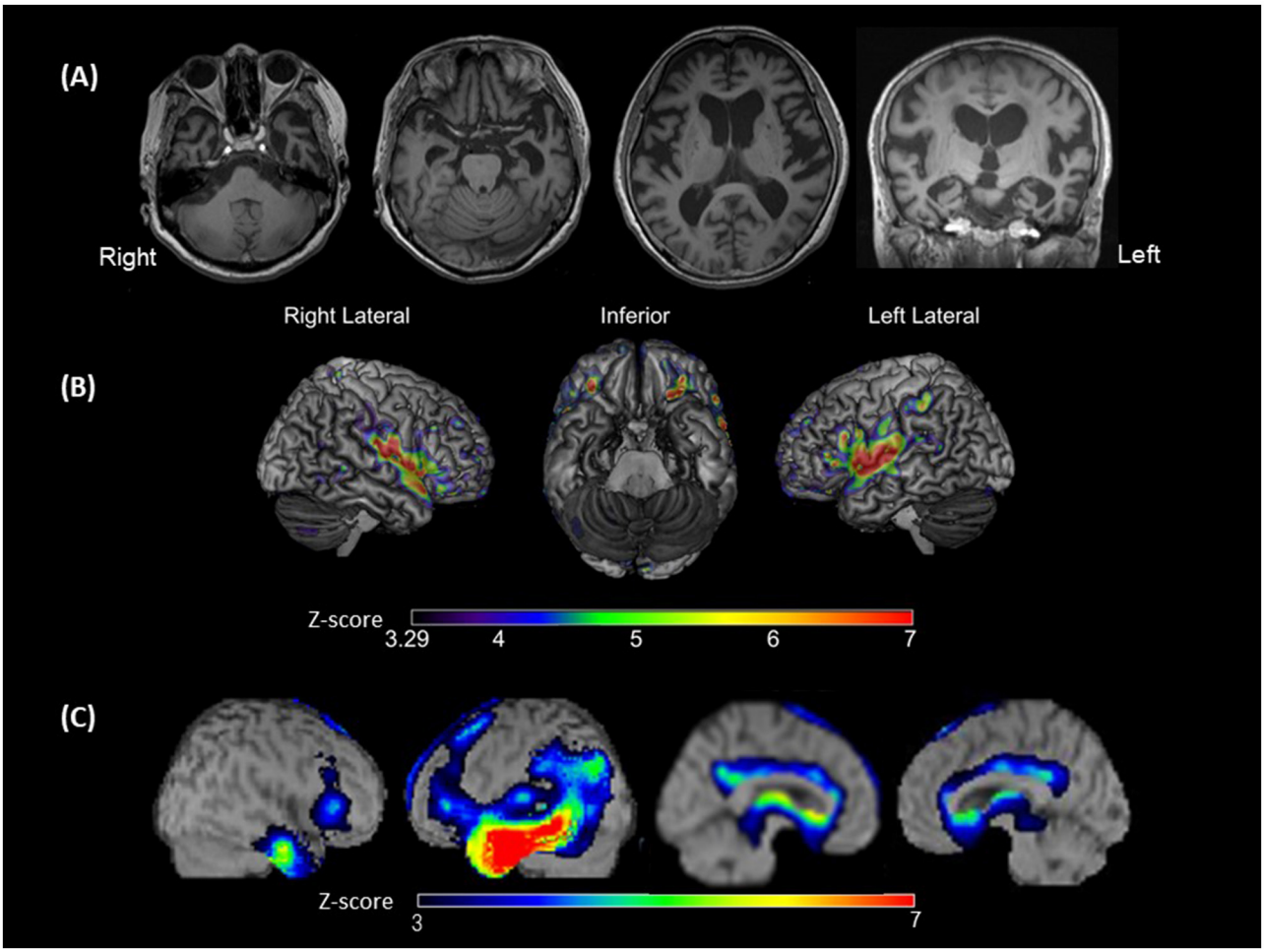

FIGURE 2 | Brain magnetic resonance imaging (MRI), voxel-based morphometry on brain MRI (VBM), and single-photon emission computed tomography (SPECT). **(A)** Brain MRI showing left-sided predominant atrophy, especially in Heschl's gyrus, superior temporal gyri (STG), and the anterior and medial temporal areas; **(B)** VBM showing the significantly smaller gray matter volume areas in the bilateral STG, plana temporale, Rolandic area and frontal inferior opercula, and the left supramarginal gyrus of the patient compared with those observed in patients with typical svPPA (disease controls). The colored bars indicate the *Z*-values; **(C)** SPECT data analyzed with three-dimensional stereotactic surface projections showing predominant hypoperfusion of the temporal lobe, especially at the anterior temporal area and middle and inferior temporal gyrus. Hypoperfusion is expanded to the temporoparietal junction in the left hemisphere. The colored bars indicate the *Z*-values.

with that of disease controls, in the present patient, gray matter volume was significantly smaller in the bilateral perisylvian areas, including the bilateral superior temporal gyri (STG), bilateral plana temporale (PT), bilateral Rolandic area and frontal inferior opercula, and left SMG.

Region of Interest-Based Analyses

We performed ROI-based analyses for gray matter volumes using the computational anatomy toolbox (CAT12, http://www.neuro.uni-jena.de/cat/) for SPM (26). The ROIs were defined based on the previous studies that have reported lesions that were associated with the manifestation of word deafness or auditory agnosia (12–16, 27–29). These ROIs were as follows: (i) left and right STG; (ii) left and right PT; (iii) left and right Heschl's gyri; (iv) left and right angular gyri; and (v) left and right SMG. A *Z*-score of each ROI was calculated by the same equation as that used for creating the *Z*-score map. Significance was defined as a *Z*-score above 2.81 ($\alpha < 0.025/10$). The results of the ROI-based analyses are presented in **Supplementary Table 3**. Compared with those of the disease controls, in the present patient, gray matter volumes were significantly smaller in the left STG (*Z*-score = 4.28), left PT (*Z*-score = 3.88), and bilateral SMG (left: *Z*-score = 4.21; right: *Z*-score = 3.35).

^{123}*I-Iodoamphetamine Single-Photon Emission Computed Tomography*

To assess the patterns of hypoperfusion, ^{123}I-IMP-SPECT data were analyzed with three-dimensional stereotactic surface

projections using the normal perfusion database for a Siemens e-cam. There was hypoperfusion from the temporal to the parietal lobes of the left hemisphere, with a more intense reduction from the anterior temporal lobe to the middle and inferior temporal gyri (**Figure 2C**).

Laboratory Examination

Beta-amyloid 1–42 (Aβ42) and phosphorylated tau protein (p-tau) in the patient's cerebrospinal fluid (CSF) were quantified on days 11 after admission. The patient's CSF Aβ42 level (1,023 pg/ml) was within the normal range, whereas the CSF p-tau level (68.3 pg/mL) was slightly elevated (reference value of <50 pg/ml) (30).

Outpatient Follow-Up

At her last visit to the hospital (3 years after hospitalization scrutiny), she had developed marked aphasia with phonological mishearing and sentence comprehension disorder. She still understood the written word better than the spoken word, but her understanding of the written word was also greatly declined, due in part to her progressive semantic comprehension disorder. The effort of speech production was not increased, and prosodic articulation was intact. Although she could produce a meaningful speech, she talked about the same content with similar phrasing and only superficial. Behavioral disorders did not worsen, except for obsession with handwashing. She continued to do well physically, and her neurological examinations were unchanged.

DISCUSSION

Herein, we presented a case of svPPA with impaired verbal sound discrimination. Although spared repetition ability is one of the supported diagnostic features of typical svPPA (1), our patient sometimes made errors in repetition tasks. However, the errors tended to occur with short words rather than sentences, and she understood written words better than spoken words. These symptoms were not likely to be a repetition disorder because of impaired verbal short-term memory. Thus, we performed a detailed assessment of auditory functions, verbal sound discrimination/recognition, and neuroradiological analyses. The results revealed that her temporal auditory acuity and accuracy of phoneme recognition were decreased, and the gray matter volumes in the left STG, PT, and bilateral SMG were significantly smaller than that in our disease control patients with typical svPPA.

Several studies have reported that most of the patients with PPA complicated with impaired verbal sound recognition eventually demonstrate apraxia of speech, suggesting nfvPPA (6–8, 10–12, 31–37). In addition, some of them demonstrated behavioral disorders and were considered to have frontotemporal dementia (6–8, 10, 32, 38). Among the patients with PPA complicated with impaired verbal sound recognition, none had svPPA and only one lvPPA was reported (9), which was diagnosed as Alzheimer's disease by ^{11}C-labeled Pittsburgh Compound-B [(11)C-PIB]-positron emission tomography. Thus, the presented case is the first case of svPPA with impaired verbal sound discrimination. Furthermore, the patient received sufficient clinical and neurophysiological assessments for auditory functions, which have been performed in limited studies. To confirm impairment of auditory verbal discrimination, systematic auditory examinations including auditory brainstem responses, pure-tone audiometry, and verbal sound discrimination/recognition are necessary. Only eight patients who were reported previously and our patient performed all these examinations (**Supplementary Table 3**) (6–9, 32, 34–36). In addition, temporal acuity, one of the causes of deficient verbal sound recognition (23, 24, 39), should be assessed by click counting and fusion tests.

There are two language processing pathways as follows: The dorsal (articulatory–phonological) pathway and the ventral (lexical–semantic) pathway (40). A recent model of the dorsal articulatory–phonological pathway proposes the existence of auditory–phonological representations of speech supported by the superior temporal cortex (41, 42). Johnson et al. (14) reported impaired auditory phonemic discrimination in lvPPA by assessing the discrimination of phonemes differing on a single acoustic characteristic and revealed that the impairment was positively correlated with the gray matter volume in the left angular gyrus through VBM on brain MRI. Hardy et al. (15) reported that patients with nfvPPA and svPPA have phonetic spectral processing deficit, which was "an analogous deficit has been demonstrated previously to affect a range of non-verbal sounds in both nfvPPA and svPPA," and the deficit was associated with the gray matter volume in the left SMG. In addition, the case of lvPPA with pure word deafness (9) had cortical thinning in bilateral Heschl's gyri, PT, and superior temporal sulcus (STS), compared with healthy controls. The case of nfvPPA with auditory agnosia had hypoperfusion mainly in the left superior temporal and inferior frontal gyri (12). A recent study using activation likelihood estimation meta-analysis of 23 fMRI experiments identified significant activation likelihoods in the left mid-posterior STS with phonetic and phonological processes (43).

These studies have suggested the regions important for verbal sound discrimination are the STS, STG, and PT among the auditory-association cortices. In our patient, the results of the neuroradiological analyses using VBM and ROI-based analyses of MRI demonstrated markedly smaller gray matter volumes in the left STG, PT, and bilateral SMG than in those of typical svPPA. These findings indicated that dysfunction of these regions affects phonemic processes in the present case.

Our patient with svPPA exhibited impairment of verbal sound discrimination. We searched for case reports in PubMed, Web of Science, and Japanese academic journals. The search included the keywords "word deafness," "auditory agnosia," and "cortical deafness." Then, we selected reports of patients with neurodegenerative diseases in which systematic auditory assessments, including pure-tone audiometry, verbal sound discrimination, and auditory brainstem responses, were performed. Eight patients fulfilled our criteria (**Supplementary Table 3**). Hypometabolic regions involved the

temporal lobes: bilateral in five patients, left in two patients, and right in 1 patient. Impaired verbal or non-verbal sound discrimination may be associated with lateralized temporal lobe dysfunction. The degree of dorsal pathway impairment may affect the severity of verbal and non-verbal sound discrimination deficits.

The most common cause of svPPA is frontotemporal lobar degeneration associated with TDP43 type C pathology (44). However, recent studies (44–46) have reported other types of pathological changes, such as Alzheimer's disease (AD). Patients with svPPA and AD pathology demonstrated a more widespread cerebral hypoperfusion than patients with svPPA and TDP43 pathology. Hypoperfusion areas encompass the inferior parietal lobule, posterior cingulate cortex, and precuneus, similar to patients with typical AD (47–49). Brain atrophy extended to the inferior parietal lobule, and increased p-tau levels in the CSF suggested AD pathology in the present case.

This study had a few limitations. First, we could not match the age of the present patient and those of individuals in the control group with svPPA in the VBM and ROI-based analysis. We could not recruit age-matched disease controls because our patient was older than patients with typical svPPA. Second, we could not fully investigate the perceptive function of non-verbal sounds because many factors such as auditory apperceptive processing and semantic processing affected her performance (50–52). In addition, age-matched control data for non-verbal sound discrimination tasks were unavailable.

This case provides further evidence that the extent of lesions involved in each patient with PPA affects the types of hearing impairment. A comprehensive hearing assessment is important for patients with PPA at the early stage of the disease, which may predict the extent of cerebral dysfunctions and related pathology.

DATA AVAILABILITY STATEMENT

The original contributions presented in the study are included in the article/**Supplementary Material**, further inquiries can be directed to the corresponding author/s.

ETHICS STATEMENT

Ethical review and approval was not required for the study on human participants in accordance with the Local Legislation and Institutional Requirements. The patients/participants provided their written informed consent to participate in this study. Written informed consent was obtained from the individual(s) for the publication of any potentially identifiable images or data included in this article.

AUTHOR CONTRIBUTIONS

NK acquired case data, designed the study and drafted the manuscript. AM, KK, YS, and EK acquired case data. NO designed some original tests. WN supervised the study. SK analyzed the data and supervised the study. KS supervised the study and helped to draft the manuscript. All authors contributed to the article and approved the submitted version.

FUNDING

This work was supported by Health Labor Sciences Research [Grants Nos. 20GB1002 and 20GC1008], Grant-in-Aid for Transformative Research Areas [Grant No. 20H05956], Grant-in-Aid for Scientific Research (B) [Grant No. 21H03779] to KS, and Grant-in-Aid for Early-Career Scientists [Grant No. 19K20381] to NK.

ACKNOWLEDGMENTS

The authors thank the patient and her family for their participation in this study.

SUPPLEMENTARY MATERIAL

The Supplementary Material for this article can be found online at: https://www.frontiersin.org/articles/10.3389/fneur.2022.873735/full#supplementary-material

REFERENCES

1. Gorno-Tempini ML, Hillis AE, Weintraub S, Kertesz A, Mendez M, Cappa SF, et al. Classification of primary progressive aphasia and its variants. *Neurology.* (2011) 76:1006–14. doi: 10.1212/WNL.0b013e31821103e6
2. Mesulam MM, Wieneke C, Thompson C, Rogalski E, Weintraub S. Quantitative classification of primary progressive aphasia at early and mild impairment stages. *Brain.* (2012) 135:1537–53. doi: 10.1093/brain/aws080
3. Rogalski E, Cobia D, Harrison TM, Wieneke C, Weintraub S, Mesulam MM. Progression of language decline and cortical atrophy in subtypes of primary progressive aphasia. *Neurology.* (2011) 76:1804–10. doi: 10.1212/WNL.0b013e31821ccd3c
4. Tee BL, Gorno-Tempini ML. Primary progressive aphasia: a model for neurodegenerative disease. *Curr Opin Neurol.* (2019) 32:255–65. doi: 10.1097/WCO.0000000000000673
5. Ruksenaite J, Volkmer A, Jiang J, Johnson JC, Marshall CR, Warren JD, et al. Primary progressive aphasia: toward a pathophysiological synthesis. *Curr Neurol Neurosci Rep.* (2021) 21:7. doi: 10.1007/s11910-021-01097-z
6. Otsuki M, Soma Y, Sato M, Homma A, Tsuji S. Slowly progressive pure word deafness. *Eur Neurol.* (1998) 39:135–40. doi: 10.1159/000007923
7. Kaga K, Nakamura M, Takayama Y, Momose H, A. case of cortical deafness and anarthria. *Acta Otolaryngol.* (2004) 124:202–5. doi: 10.1080/00016480310015975
8. Iizuka O, Suzuki K, Endo K, Fujii T, Mori E. Pure word deafness and pure anarthria in a patient with frontotemporal dementia. *Eur J Neurol.* (2007) 14:473–5. doi: 10.1111/j.1468-1331.2007.01671.x
9. Kim SH, Suh MK, Seo SW, Chin J, Han SH, Na DL. Pure word deafness in a patient with early-onset Alzheimer's disease: an unusual presentation. *J Clin Neurol.* (2011) 7:227–30. doi: 10.3988/jcn.2011.7.4.227
10. Gibbons C, Oken B, Fried-Oken M. Augmented input reveals word deafness in a man with frontotemporal dementia. *Behav Neurol.* (2012) 25:151–4. doi: 10.1155/2012/264927
11. Kuramoto S, Hirano T, Uyama E, Tokisato K, Miura M, Watanabe S, et al. case of slowly progressive aphasia with auditory agnosia. *Clin Neurol.* (2002) 42:299–303. Available online at: https://www.neurology-jp.org/Journal/cgi-bin/journal.cgi

12. Watanabe H, Ikeda M, Mori E. Non-fluent/agrammatic variant of primary progressive aphasia with generalized auditory agnosia. *Front Neurol.* (2020) 11:e519. doi: 10.3389/fneur.2020.00519
13. Uttner I, Mottaghy FM, Schreiber H, Riecker A, Ludolph AC, Kassubek J. Primary progressive aphasia accompanied by environmental sound agnosia: a neuropsychological, MRI and PET study. *Psychiatry Res.* (2006) 146:191–7. doi: 10.1016/j.pscychresns.2005.12.003
14. Johnson JCS, Jiang J, Bond RL, Benhamou E, Requena-Komuro MC, Russell LL, et al. Impaired phonemic discrimination in logopenic variant primary progressive aphasia. *Ann Clin Transl Neurol.* (2020) 7:1252–7. doi: 10.1002/acn3.51101
15. Hardy CJD, Agustus JL, Marshall CR, Clark CN, Russell LL, Bond RL, et al. Behavioral and neuroanatomical correlates of auditory speech analysis in primary progressive aphasias. *Alzheimers Res Ther.* (2017) 9:53. doi: 10.1186/s13195-017-0278-2
16. Hardy CJD, Agustus JL, Marshall CR, Clark CN, Russell LL, Brotherhood EV, et al. Functional neuroanatomy of speech signal decoding in primary progressive aphasias. *Neurobiol Aging.* (2017) 56:190–201. doi: 10.1016/j.neurobiolaging.2017.04.026
17. Bozeat S, Lambon Ralph MA, Patterson K, Garrard P, Hodges JR. Non-verbal semantic impairment in semantic dementia. *Neuropsychologia.* (2000) 38:1207–15. doi: 10.1016/S0028-3932(00)00034-8
18. Garrard P, Carroll E. Lost in semantic space: a multi-modal, non-verbal assessment of feature knowledge in semantic dementia. *Brain.* (2006) 129:1152–63. doi: 10.1093/brain/awl069
19. Golden HL, Downey LE, Fletcher PD, Mahoney CJ, Schott JM, Mummery CJ, et al. Identification of environmental sounds and melodies in syndromes of anterior temporal lobe degeneration. *J Neurol Sci.* (2015) 352:94–8. doi: 10.1016/j.jns.2015.03.007
20. Fushimi T, Komori K, Ikeda M, Lambon Ralph MA, Patterson K. The association between semantic dementia and surface dyslexia in Japanese. *Neuropsychologia.* (2009) 47:1061–8. doi: 10.1016/j.neuropsychologia.2008.12.030
21. Tanabe H, Ikeda M, Nakagawa Y, Yamamoto H, Ikejiri Y. Gogi (word meaning) aphasia and semantic memory for words. *Higher Brain Function Res.* (1992) 12:153–67. doi: 10.2496/apr.12.153
22. Sasanuma S, Monoi H. The syndrome of Gogi (word meaning) aphasia. Selective impairment of kanji processing. *Neurology.* (1975) 25:627–32. doi: 10.1212/WNL.25.7.627
23. Albert ML, Bear D. Time to understand. A case study of word deafness with reference to the role of time in auditory comprehension. *Brain.* (1957) 97:373–84. doi: 10.1093/brain/97.1.373
24. Auerbach SH, Allard T, Naeser M, Alexander MP, Albert ML. Pure word deafness. Analysis of a case with bilateral lesions and a defect at the prephonemic level. *Brain.* (1982) 105:271–300. doi: 10.1093/brain/105.2.271
25. Japanese Audiological Society. The method of speech audiometry. *Audiology.* (2003) 46:622–37. Available online at: https://audiology-japan.jp/gakujutsu-shi/
26. Christian Gaser RD. CAT-A Computational Anatomy Toolbox for the Analysis of Structual MRI Data HBM. (2016). Available online at: http://www.neuro.uni-jena.de/hbm2016/GaserHBM2016.pdf
27. Lin PH, Chen HH, Chen NC, Chang WN, Huang CW, Chang YT, et al. Anatomical correlates of non-verbal perception in dementia patients. *Front Aging Neurosci.* (2016) 8:e207. doi: 10.3389/fnagi.2016.00207
28. Maffei C, Capasso R, Cazzolli G, Colosimo C. Dell'Acqua F, Piludu F, et al. Pure word deafness following left temporal damage: behavioral and neuroanatomical evidence from a new case. *Cortex.* (2017) 97:240–54. doi: 10.1016/j.cortex.2017.10.006
29. Kim K, Adams L, Keator LM, Sheppard SM, Breining BL, Rorden C, et al. Neural processing critical for distinguishing between speech sounds. *Brain Lang.* (2019) 197:104677. doi: 10.1016/j.bandl.2019.104677
30. Arai H, Yoshida H. [Performance evaluation of phosphorylated tau protein kit "Fainoscalar pTAU"] Rinsanka tau tanpaku kitto "feinosukara pTAU" no seinou hyouka (in Japanese). *J Clin Lab Instrum Reag.* (2013) 36:713–7. Available online at: http://www.labos.jp/
31. Kirshner HS, Webb WG, Kelly MP, Wells CE. Language disturbance. An initial symptom of cortical degenerations and dementia. *Arch Neurol.* (1984) 41:491–6. doi: 10.1001/archneur.1984.04050170037012
32. Lee YAE, Ishiai S, Watabiki S, Takahashi M. A case of neurodegenerative disease presenting with primary progressive hearing loss and logoclonia. *JPN J Neuropsychol.* (2001) 17:54–61. Available online at: http://www.neuropsychology.gr.jp/journal/index.html
33. Jörgens S, Biermann-Ruben K, Kurz MW, Flügel C, Daehli Kurz K, Antke C, et al. Word deafness as a cortical auditory processing deficit: a case report with MEG. *Neurocase.* (2008) 14:307–16. doi: 10.1080/13554790802363738
34. Ota S, Matsuda M, Baba T, Endo K, Iizuka O, Mori E, et al. case of progressive word deafness and foreign accent syndrome. *JPN J Neuropsychol.* (2016) 32:361–9. doi: 10.20584/neuropsychology.32.4_361
35. Satoh M, Takashima S, Ito N. [Auditory agnosia - commentary and case presentation] Tyoukaku Shitsunin - Kaisetsu to syourei teiji (in Japanese). *JPN J Geriatr Psychiatry.* (2017) 28:74–9.
36. Sato M. [Evaluation and rehabilitation of primary progressive aphasia. A case report of Apraxia of speech, pure word deafness and amusia] Genpatsusei shinkousei shitsugo no hyouka to rihabiritesyon (in Japanese). *J JPN Soc Dement Care.* (2018) 17:538–45. Available online at: http://www.chihoucare.org/
37. Utianski RL, Duffy JR, Clark HM, Machulda MM, Dickson DW, Whitwell JL, et al. Prominent auditory deficits in primary progressive aphasia: a case study. *Cortex.* (2019) 117:396–406. doi: 10.1016/j.cortex.2019.01.021
38. Boban M. Letter to IIzuka-pure word deafness and frontotemporal dementia. *Eur J Neurol.* (2007) 14:e3; author reply e4. doi: 10.1111/j.1468-1331.2007.01899.x
39. Tanaka Y, Yamadori A, Mori E. Pure word deafness following bilateral lesions - a psychophysical analysis. *Brain.* (1987) 110:381–403. doi: 10.1093/brain/110.2.381
40. Hickok G, Poeppel D. The cortical organization of speech processing. *Nat Rev Neurosci.* (2007) 8:393–402. doi: 10.1038/nrn2113
41. Hickok G. The architecture of speech production and the role of the phoneme in speech processing. *Lang Cogn Processes.* (2014) 29:2–20. doi: 10.1080/01690965.2013.834370
42. Henry ML, Wilson SM, Babiak MC, Mandelli ML, Beeson PM, Miller ZA, et al. Phonological processing in primary progressive aphasia. *J Cogn Neurosci.* (2016) 28:210–22. doi: 10.1162/jocn_a_00901
43. Turkeltaub PE, Coslett HB. Localization of sublexical speech perception components. *Brain Lang.* (2010) 114:1–15. doi: 10.1016/j.bandl.2010.03.008
44. Landin-Romero R, Tan R, Hodges JR, Kumfor F. An update on semantic dementia: genetics, imaging, and pathology. *Alzheimers Res Ther.* (2016) 8:52. doi: 10.1186/s13195-016-0219-5
45. Chow TW, Varpetian A, Moss T, Vinters HV, Marquez S, Miller C. Alzheimer's disease neuropathologic changes in semantic dementia. *Neurocase.* (2010) 16:15–22. doi: 10.1080/13554790903193174
46. Chare L, Hodges JR, Leyton CE, McGinley C, Tan RH, Kril JJ, et al. New criteria for frontotemporal dementia syndromes: clinical and pathological diagnostic implications. *J Neurol Neurosurg Psychiatry.* (2014) 85:865–70. doi: 10.1136/jnnp-2013-306948
47. Kawakatsu S, Shibuya Y, Yamasaki T, Watabe T, Hayashi H, Kobayai R. [Differential diagnosis of dementia on the basis of image and pathological diagnosis] Gazou to byouri shindan wo fumaeta ninthisyou no kanbetsu shindan (in Japanese). *JPN J Geriatr Psychiatry.* (2011) 22:28–35.
48. Takano Y, Kunitoki K, Tatewaki Y, Mutoh T, Totsune T, Shimomura H, et al. Posterior associative and cingulate cortex involvement of Brain single-photon emission computed tomography (SPECT) imaging in semantic dementia with probable Alzheimer's disease pathology: a case report. *Am J Case Rep.* (2018) 19:153–7. doi: 10.12659/AJCR.907799
49. Bera G, Migliaccio R, Michelin T, Lamari F, Ferrieux S, Nogues M, et al. Parietal involvement in the semantic variant of primary progressive aphasia with Alzheimer's disease cerebrospinal fluid profile. *J Alzheimers Dis.* (2018) 66:271–80. doi: 10.3233/JAD-180087

50. Hardy CJ, Marshall CR, Golden HL, Clark CN, Mummery CJ, Griffiths TD, et al. Hearing and dementia. *J Neurol.* (2016) 263:2339–54. doi: 10.1007/s00415-016-8208-y
51. Saygin AP, Dick F, Wilson SM, Dronkers NF, Bates E. Neural resources for processing language and environmental sounds: evidence from aphasia. *Brain.* (2003) 126:928–45. doi: 10.1093/brain/awg082
52. Engelien A, Tüscher O, Hermans W, Isenberg N, Eidelberg D, Frith C, et al. Functional neuroanatomy of non-verbal semantic sound processing in humans. *J Neural Transm.* (2006) 113:599–608. doi: 10.1007/s00702-005-0342-0

Conflict of Interest: The authors declare that the research was conducted in the absence of any commercial or financial relationships that could be construed as a potential conflict of interest.

Publisher's Note: All claims expressed in this article are solely those of the authors and do not necessarily represent those of their affiliated organizations, or those of the publisher, the editors and the reviewers. Any product that may be evaluated in this article, or claim that may be made by its manufacturer, is not guaranteed or endorsed by the publisher.

frontiers | Frontiers in Neurology

CASE REPORT
published: 16 June 2022
doi: 10.3389/fneur.2022.879009

Case Report: Alzheimer's Dementia Associated With Cerebrospinal Fluid Neurochondrin Autoantibodies

Niels Hansen[1]*, *Berend Malchow*[1], *Bianca Teegen*[2], *Jens Wiltfang*[1,3,4] and *Claudia Bartels*[1]

[1] Department of Psychiatry and Psychotherapy, University Medical Center Goettingen, Göttingen, Germany, [2] Euroimmun Laboratory, Lübeck, Germany, [3] German Center for Neurodegenerative Diseases (DZNE), Göttingen, Germany, [4] Department of Medical Sciences, Neurosciences and Signaling Group, Institute of Biomedicine (iBiMED), University of Aveiro, Aveiro, Portugal

Background: Neurochondrin autoimmunity is a rare disorder mainly associated with cerebellar and vestibular syndromes. Our report aims to enlarge its phenotypic spectrum to encompass major cognitive disorder with very late onset never before reported in conjunction with neurochondrin antibodies.

Methods: We describe the case of an 85-year-old woman who presented in our memory clinic. Retrospective analysis of patient records included cerebrospinal fluid (CSF) analysis, magnetic resonance imaging (MRI), and neuropsychological testing using the CERAD-plus.

Results: Because of her unknown onset of progressive cognitive dysfunction in conjunction with speech and language problems, we decided to take an extensive differential diagnostic approach including a search for neural autoantibodies potentially involved in cognitive impairment. Our patient presented serum and CSF neurochondrin autoantibodies. Further CSF analysis revealed elevated tau and ptau 181 protein as well as a reduced Aß42/40 ratio in CSF, thus matching a biomarker profile of Alzheimer's disease (AD). Neuropsychological tests revealed predominant and severe deficits in verbal and visual memory. Her MRI showed reduced parietal and cerebellar brain volume.

Discussion: Taken together, this case reveals the novelty of a patient with a CSF-based and typical clinical and imaging profile of AD. She is also likely to have neurochondrin autoimmunity, as we detected neurochondrin autoantibodies in her CSF; we therefore diagnosed AD dementia associated with neurochondrin antibodies. Our case expands the spectrum of neurochondrin autoimmunity to disorders involving major cognitive disorder such as AD dementia. Furthermore, we speculate that neurochondrin autoimmunity might have triggered an acceleration of AD symptoms as its onset was reported only after a short 6-month interval via a synergistic or negatively additive hybrid mechanism of action between neurodegeneration and autoimmunity.

Keywords: neurochondrin autoantibody, Alzheimer's disease, cerebrospinal fluid, autoimmunity, dementia

OPEN ACCESS

Edited by:
Lidia Sabater, Institut de Recerca Biomèdica August Pi i Sunyer (IDIBAPS), Spain

Reviewed by:
Panagiotis Alexopoulos, University of Patras, Greece
Lars Komorowski, Institute for Experimental Immunology, Germany

***Correspondence:**
Niels Hansen
niels.hansen@med.uni-goettingen.de

Specialty section:
This article was submitted to Dementia and Neurodegenerative Diseases, a section of the journal Frontiers in Neurology

Received: *28 February 2022*
Accepted: *03 May 2022*
Published: *16 June 2022*

Citation:
Hansen N, Malchow B, Teegen B, Wiltfang J and Bartels C (2022) Case Report: Alzheimer's Dementia Associated With Cerebrospinal Fluid Neurochondrin Autoantibodies. Front. Neurol. 13:879009. doi: 10.3389/fneur.2022.879009

INTRODUCTION

Neurochondrin is an intracellular, neuronal protein in the cytosol that is a target of antibodies associated with neuropsychiatric conditions such as cerebellar ataxia, brainstem signs, rhombencephalitis, psychosis (1), and hyperkinetic movements such as chorea (2). Other symptoms such as cognitive dysfunction including memory disturbances and behavioral symptoms have been reported in children as occurring in conjunction with neurochondrin autoantibodies (3). These reports are evidence of neurochondrin autoantibodies coinciding with cognitive dysfunction. However, to our knowledge, no patient with dementia and a typical CSF profile indicative of Alzheimer's disease (AD) has been shown to be associated with serum and CSF neurochondrin autoantibodies until now. Our case highlights neurochondrin IgG autoimmunity in a patient suffering from progressive AD dementia.

CASE REPORT

An 85-year-old woman, retired and living on her own, presented in our memory clinic complaining of a progressive loss of spatial and time orientation and memory probably for 6 month. Her son, who is also her guardian, also mentioned slight speech and language problems, noticing disrupted sentences in her spontaneous speech, and difficulty speaking caused by word-finding problems; she was also impaired in performing everyday tasks and showed signs of social squalidness. Our patient has two sons. She lived first with one of them in another city. However, as he had to look after for another needy member of his family, he had no time to take care of his mother. Her condition worsened slowly and finally she lived in squalid conditions, so that her other son (and actual guardian) took her to his home in another city where he looked after her. It was there that he noticed her worsening memory and language problems. Both sons have been reporting memory disturbances for about 6 months. However, when exactly her symptoms' first onset appeared is unknown, thus a slowly progressive and no abrupt decline is most probable. This patient had no prior mental health or neurological disorder. She had several comorbidities that were treated pharmacologically as indicated in the following in brackets: (1) diabetes mellitus type 2 (metformin 2000 mg/d, glimepirid mg/d), (2) arterial hypertension (olemsartan /amlodipine/ hydrochlorothiazide 40/ 5/ 12.5 mg/d, bisoprolol 10 mg /d), (3) dermatitis (methylprednisolone ointment two times daily), (4) paroxysmal atrial fibrillation (Apixaban 10 mg/d, digitoxin 0.07 mg/d, bisoprolol 10mg/d), (5) hypothyreosis (L-Thyroxin 50 µg/ d), (6) tinea pedis (ciclopirox crème), and a (7) presbyacusis. The patient underwent a comprehensive dementia assessment. Her psychopathological assessment confirmed deficits in orientation, concentration, and memory. Furthermore, she had a reduced awareness of her cognitive abilities. In her neurological examination, no neurological deficits were detected. Cognitive screening results were normal for the clock drawing test (CDT = 2), but cognitive impairment became already obvious in the Mini-Mental Status Test (MMST = 21). Neuropsychological assessment further revealed impairments in cognitive flexibility and severe deficits in verbal and visual memory, including

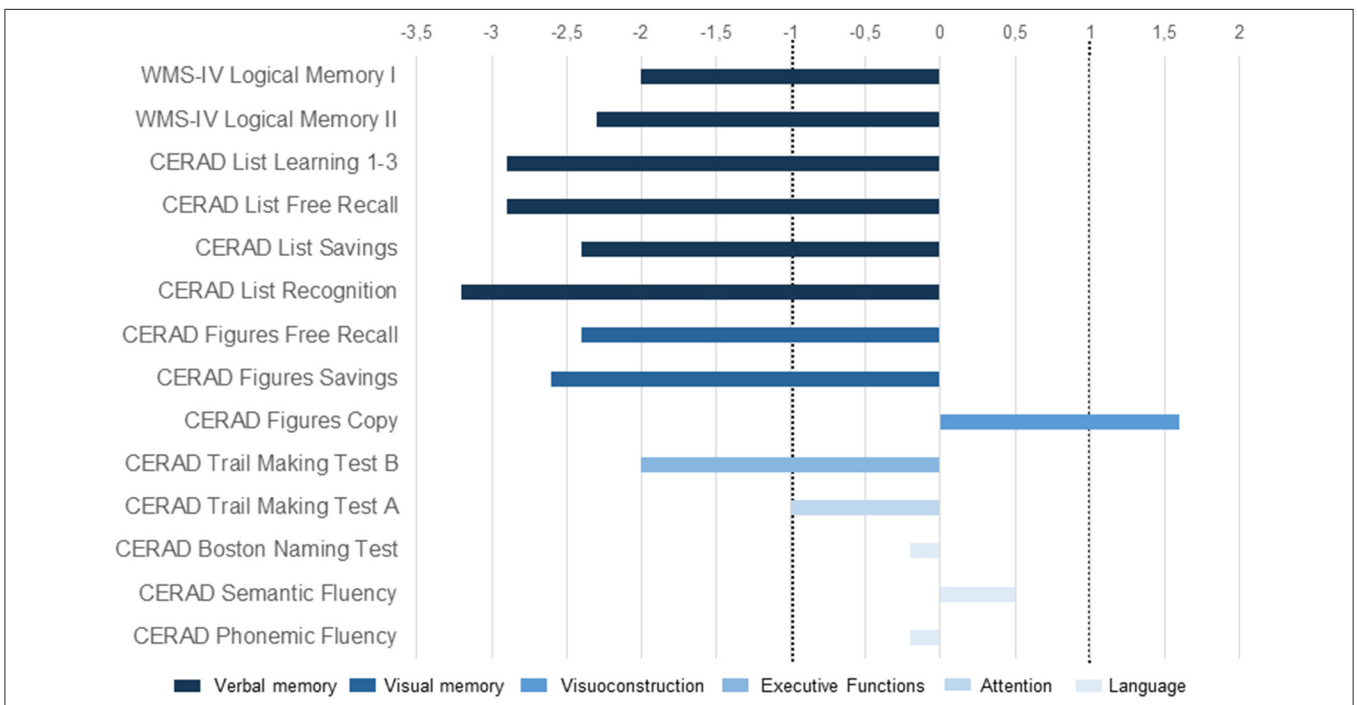

FIGURE 1 | Cognitive profile (clinical case with neurochondrin antibodies in association with AD dementia). Illustration of neuropsychological test results presented as z-scores. The area between dotted lines denotes the normal range. CERAD, Consortium to Establish a Registry for Alzheimer's Disease; WMS-IV, Wechsler Memory Scale–Fourth Edition.

immediate and delayed recall (**Figure 1**). Together with impaired activities of daily living, these findings were compatible with a diagnosis of mild dementia. MRI showed reduced parietal and cerebellar brain volume and microangiopathy, as well as a central necrosis in the corpora mammillaria. The unknown onset of symptoms with cognitive dysfunction accompanied by speech and language problems prompted us to perform an extensive differential diagnosis including a search for a wide spectrum of neural autoantibodies that could potentially be involved in the differential diagnosis of cognitive impairment such as neurochondrin autoantibodies. Neurochondrin autoantibodies have been reported to be associated with an encephalopathy and cognitive dysfunction (3). CSF analysis revealed neurochondrin autoantibodies in immunofluorescence testing (1:32). Furthermore, titin antibodies were detected in CSF via Euroline immunoblots. Both autoantibody types [neurochondrin (1:3,200) and titin] were also verified in blood samples. We found no specific intrathecal antibody synthesis of anti-neurochondrin antibodies in the central nervous system with an antibody specific index of 2.85 [cut off is higher than 4 for indirect immunohistochemistry due to non-linear quantification according to Reiber and Peter (4), **Table 1**]. Furthermore, we did not detect isolated oligoclonal bands in the CSF or an intrathecal IgG synthesis. However, a. Neurodegenerative markers were above normative levels in CSF (measured in the Neurochemistry Cerebrospinal Fluid Laboratory of the Neurology Department, University Medical Center Göttingen), i.e., tau protein and ptau 181 protein (**Table 1**) were above normative levels, and the ratio Aß42/40 was below normative levels (**Table 1**). Results of neurodegenerative CSF markers were confirmed by an external laboratory (Laboratory of Clinical Neurochemistry and Neurochemical Dementia Diagnostics, Department of Psychiatry and Psychotherapy, University Hospital Erlangen) (**Table 1**, second column). To assess brain damage, neurofilament phosphorylated heavy chain (pNfH) were determined in CSF at the Department of Neurology, University Hospital Ulm (**Table 1**). However, laboratory reference values adapted from the work of Steinacker et al. (5) from a cohort with amyotrophic lateral sclerosis indicated no levels above normative levels (**Table 1**). AD dementia is probable due to her typical hippocampal subtype of memory dysfunction together with biomarker-based AD (elevated ptau181, reduced Aß42/Aß40 ratio). Our patient 's normal Aß42 in the CSF fails to support the hypothesis of Alzheimer's disease. Nevertheless, the combination of a reduced Aß42/40 ratio and elevated ptau181 in the CSF argues for a biomarker-confirmed Alzheimer's disease concurring with the latest diagnostic criteria (6). However, as the coexistence of neurochondrin autoantibodies in her serum and CSF are relevant in our patient, we thus diagnosed an AD dementia associated with neurochondrin autoantibodies. A therapy with cholinesterase inhibitors rivastigmine at 4.6 mg per day has been started and is well tolerated so far. No adverse events were reported. 40 mg/d pipamperone was also applied to help her sleep. Immunotherapy with corticosteroids as an individual off label therapy was briefly discussed, but not considered as a therapeutic option, as AD is very likely caused by a biomarker profile and typical clinical syndrome entailing memory and orientation disturbances. The patient and her son accepted the diagnosis of AD with dignity. Potential neurochondrin autoimmunity was not mentioned as a separate diagnosis as it is not currently a diagnostic category for such a clinical presentation.

DISCUSSION

Our novel finding of neurochondrin autoantibodies in conjunction with AD dementia seems surprising at first glance, as neurochondrin autoimmunity has only been reported so far in association with vestibulocerebellar syndromes (1, 7–9) and movement disorders (2, 10) and only rarely with cognitive dysfunction in children (3). Neurochondrin is required during embryogenesis, as embryos lacking the neurochondrin gene die early during their embryogenesis (11). Furthermore, neurochondrin is involved in neuritic outgrowth and spatial learning processes (12)—evidence of the potential role of neurochondrin autoimmunity in cognitive processes such as in our patient. However, as neurochondrin is an intracellular protein, the autoantibodies are not believed to be pathogenic themselves; additional T-cell mechanisms might be the main pathomechanism of brain damage in our patient. More investigations employing flow cell cytometry should explore whether activated CD8+ T-cells can be detected as an indirect sign of an immune mechanism in such patients. It remains unclear but more likely that autoantibodies would develop in a patient with existing AD pathology, although it is also conceivable that an early manifestation of neurochondrin autoimmunity might trigger neurodegenerative processes leading to an AD pathology. Neurochondrin is located in structures also affected in AD, such as the hippocampus, indicating that neurodegenerative processes might be accelerated by neurochondrin autoantibodies, as they also target synaptic structures within the hippocampus, as shown by Shelly et al. (1). Neurochondrin IgG is often found in the hippocampus and in its subregions (like CA2 and CA3) as well as the dentate gyrus (1). As the hippocampus is the pivotal structure for forming memories, it is not surprising that our patient has memory dysfunction given the neurochondrin IgG deposition in her hippocampus. Furthermore, it is important to mention that neurochondrin (also known as norbin) interacts with glutamatergic signaling, as it interacts with mGluR5 receptors in mice (13). If we transfer such findings from mice to man, the interaction of neurochondrin IgG with mGluR5 receptors in the hippocampus would result in memory dysfunction caused by disrupted synaptic transmission within the hippocampus. We believe that this postulated mechanism may underly our patient's progressive severe memory deficits. From another perspective, the neurodegenerative and autoimmune mechanisms of action might not interact, but they might have a negative and synergistic impact on cognitive function. Neurochondrin autoimmunity might ultimately have accelerated the clinical manifestation of AD symptoms, or have led even to the appearance of clinical symptoms. Nevertheless, it has to be emphasized that the occurrence of neurochondrin autoantibodies in a patient with typical AD is surprising, in particular as neurochondrin

TABLE 1 | Clinical and laboratory parameters.

Demographic parameters	
Age y	85
Onset y	85
Psychopathology	
Disturbances of orientation	+
Disturbances of attention and memory	+
Formal thought disorders	–
Disturbances of affect	–
Disorders of drive and psychomotor activity	–
CSF	
Cell count (<5μg/L)	1
Lymphoctes in %	91
Monocytes in %	9
Lactat (mmol/l)	2.7
Total protein content (mg/L)	550
Albumin mg/L	318
IgG mg/L	29.1
IgA mg/ L	2.8
IgM mg/ L	1.6
Quotient Albumin %	8.1
Quotient IgG %	3.5
Quotient IgA %	1.7
Quotient IgM %	0.68
Neurochondrin Ab	1:32 ++
Titin Ab	++
Measles-AI	1.2
Rubella-AI	1.1
VZV-AI	1.1
HSV-AI	1.2
Tau protein (1:<450pg/ml, 2:<320 pg/ml)	1:1056, 2:1111
P Tau protein 181 (1:<61pg/ml, 2:<50 pg/ml)	1:198, 2:133.4
Aß42 (1:>450pg/ml, 2:>620pg/ml)	1:674, 2:861
Aß40	16850
Ratio Aß42/40 (1: x10: >0.5, 2: >0.05)	1:0.4, 2:0.04
pNfH (<560 pg/ml)	526
Intrathecal IgG synthesis	–
Isolated CSF oligoclonal bands	–
Antibody specific index (ASI) (< 4)	2.85
Blood	
Albumin g/L	39.2
IgG g/L	8.3
IgA g/L	1.6
IgM g/L	2.3
Neurochondrin Ab	1:3200 + + +
Titin Ab	++
CRP mg/l (≤5 mg/l)	3.0
Procalcitonin (≤0.07μg/L)	0.03
B-Leukocytes 10^ 3μl	6.09

Aß42, ß-amyloid 42; Aß40, ß-amyloid 40; CSF, cerebrospinal fluid; CRP, C reactive protein; IgA, immunoglobulin A; IgG, immunoglobulinG; IgM, immunoglobulin M; MRI, magnetic resonance imaging; P Tau Protein 181, phosphorylated tau protein 181; pNfH, neurofilament phosphorylated heavy chain; ratio Aß42/40, ratio ß-amyloid 42/ ß-amyloid 40; y, years; μg, microgram; g, gram; L, liter; mg, milligram; pg, picogram.
1: reference values and data from the Neurochemistry Cerebrospinal Fluid Laboratory of the Neurology Department, University Medical Center Göttingen. 2: reference values and data from the Laboratory of Clinical Neurochemistry and Neurochemical Dementia Diagnostics, Department of Psychiatry and Psychotherapy, University Hospital Erlangen. +, present; –, not present.

autoantibodies mostly have been reported up to now with other clinical features such as cerebellar ataxia (1, 9) or movement disorder (2). However, as proof of CSF neurochondrin autoantibodies accompanying clinical features of an intermittent anomic aphasia imply at least a coexisting autoimmune origin according to recent criteria (14), the neurochondrin autoantibodies are probably not merely incidental, despite clinical symptoms somewhat resembling those typical of AD. Nevertheless, we emphasize that the pathological significance of neurochondrin autoantibodies in the context of dementia and Alzheimer's disease is unclear because of the shortage of data. Furthermore, as no specific actual autoantibody-production in the CSF (such as an intrathecal IgG synthesis) was detected, neurochondrin autoimmunity's pathological significance is limited. However, as we had no access to left over biomaterial probes, no additional calculations were possible that might have highlighted the pathological significance of autoantibodies, as the determination of an elevated specific anti-neurochondrin antibody index would have done.

Taken together, our report demonstrates neurochondrin autoimmunity in a patient with an AD dementia, thereby expanding the extent of neurochondrin autoimmunity spectrum reported so far. The prognosis if neurochondrin autoimmunity at present is unclear, and no study data exists. The onset of AD might be accelerated by neurochondrin autoimmunity although the data is limited. Nevertheless, as there is no follow-up data on this patient, her prognosis over time course cannot be evaluated. Further research on neurochondrin autoimmunity in AD patients has considerable potential regarding the interaction between neurodegeneration and neural autoantibody-mediated immunity. The theoretical co-existence of neurochondrin autoantibodies in AD pathology might lead to two possible scenarios if a pathological significance of anti-neurochondrin autoantibodies is assumed: (1) worsening symptoms due to slowly progressing AD that is exacerbated by additional clinical features of neurochondrin autoimmunity and (2) the remission and relapse of some clinical features might reflect a potential time course of an autoantibody-related CNS disease. Because of the lack of data so far, it is unclear which condition our patient will suffer. Further studies will have to clarify whether neurochondrin antibodies themselves have pathogenic relevance for cognitive dysfunction, or if they co-exist with other neurological diseases such as ataxia or myelopathy (15).

DATA AVAILABILITY STATEMENT

The raw data supporting the conclusions of this article will be made available by the corresponding author, without undue reservation.

ETHICS STATEMENT

Ethical review and approval was not required for the retrospective case report on a human participant in accordance with the local legislation and institutional requirements. The patient provided written informed consent for publication of her data.

AUTHOR CONTRIBUTIONS

NH wrote the manuscript. BM, BT, JW, and CB revised the manuscript for important intellectual content. All authors contributed to the article and approved the submitted version.

FUNDING

Funding was received from the Open access fund of the University of Göttingen. JW was supported by an I.P. iBiMED (UIDB/04501/2020) at the University of Aveiro, Portugal.

REFERENCES

1. Shelly S, Kryzer TJ, Komorowski L, Miske R, Anderson MD, Flanagan EP, et al. *Neurochondrin neurological autoimmunityNeurol Neuroimmunol Neuroinflamm.* (2019) 6:e612. doi: 10.1212/NXI.0000000000000612
2. Rommel FR, Miske R, Stöcker,W, Arneth B, Neubauer BA, et al. Chorea minor associated with anti-neurochondrin autoantibodies. *Neuropediatrics.* (2017) 48:482–3. doi: 10.1055/s-0037-1606371
3. Schumacher M, Rommel FR, Arneth B, Renz H, Stöcker W, Windhorst A, et al. Encephalopathy associated with neurochondrin autoantibodies. *J Child Neurol.* (2019) 34:660–5. doi: 10.1177/0883073819849773
4. Reiber H, Peter JB. Cerebrospinal fluid analysis: disease-related data patterns and evaluation programs. *J Neurol Sci.* (2001) 184:101–22. doi: 10.1016/S0022-510X(00)00501-3
5. Steinacker P, Feneberg E, Weishaupt J, Brettschneider J, Tumani H, Andersen PM, et al. Neurofilaments in the diagnosis of motoneuron diseases: a prospective study on 455 patients. *J Neurol Neurosurg Psychiatry.* (2016) 87:12–20. doi: 10.1136/jnnp-2015-311387
6. Jack CR Jr, Bennett DA, Blennow K, Carrillo MC, Dunn B, Haeberlein SB, et al.; Contributors. NIA-AA Research Framework: Toward a biological definition of Alzheimer's disease. *Alzheimers Dement.* (2018) 14:535–62. doi: 10.1016/j.jalz.2018.02.018
7. Narayan RN, McKeon A, Fife TD. Autoimmune vestibulocerebellar syndromes. *Semin Neurol.* (2020) 40:97–115. doi: 10.1055/s-0039-3402061
8. Weihua Z, Haitao R, Fang F, Xunzhe Y, Jing W, Hongzhi G. Neurochondrin antibody serum positivity in three cases of autoimmune cerebellar. *Ataxia.Cerebellum.* (2019) 18:1137–42. doi: 10.1007/s12311-019-01048-y
9. Miske R, Gross CC, Scharf M, Golombeck KS, Hartwig M, Bhatia U, et al. Neurochondrin is a neuronal target antigen in autoimmune cerebellar degeneration. *Neurol Neuroimmunol Neuroinflamm.* (2016) 4:e307. doi: 10.1212/NXI.0000000000000307
10. Garza M, Piquet AL. Update in autoimmune movement disorders: newly described antigen targets in autoimmune and paraneoplastic cerebellar ataxia. *Front Neurol.* (2021) 12:683048. doi: 10.3389/fneur.2021.683048
11. Mochizuki R, Dateki M, Yanai K, Ishizuka Y, Amizuka N, Kawashima H, et al. Targeted disruption of the neurochondrin/norbin gene results in embryonic lethality. *Biochem Biophys Res Commun.* (2003) 310:1219–26. doi: 10.1016/j.bbrc.2003.09.153
12. Dateki M, Horii T, Kasuya Y, Mochizuki R, Nagao Y, Ishida J, et al. Neurochondrin negatively regulates CaMKII phosphorylation, and nervous system-specific gene disruption results in epileptic seizure. *J Biol Chem.* (2005) 280:20503–8. doi: 10.1074/jbc.M414033200
13. Wang H, Westin L, Nong Y, Birnbaum S, Bendor J, Brismar H, et al. Norbin is an endogenous regulator of metabotropic glutamate receptor 5 signaling. *Science.* (2009) 326:1554–7. doi: 10.1126/science.1178496
14. Hansen N, Lipp M, Vogelgsang J, Vukovich R, Zindler T, Luedecke D, et al. CAP (Cerebrospinal Fluid Analysis in Psychiatry) consortium. Autoantibody-associated psychiatric symptoms and syndromes in adults: a narrative review and proposed diagnostic approach. *Brain Behav Immun Health.* (2020) 9:100154. doi: 10.1016/j.bbih.2020.100154
15. Dominguez L, Collazo IVM, Sechi E, Bohm P, Chiriboga SL. Neurochondrin immunoglobulin G-associated myelopathy-ataxia syndrome. *J Neurol Sci.* (2022) 432:120058. doi: 10.1016/j.jns.2021.120058

Conflict of Interest: The authors declare that the research was conducted in the absence of any commercial or financial relationships that could be construed as a potential conflict of interest.

Publisher's Note: All claims expressed in this article are solely those of the authors and do not necessarily represent those of their affiliated organizations, or those of the publisher, the editors and the reviewers. Any product that may be evaluated in this article, or claim that may be made by its manufacturer, is not guaranteed or endorsed by the publisher.

frontiers | Frontiers in Neurology

CASE REPORT
published: 22 June 2022
doi: 10.3389/fneur.2022.909944

Case Report: Novel *CSF1R* Variant in a Patient With Behavioral Variant Frontotemporal Dementia Syndrome With Prodromal Repetitive Scratching Behavior

Adit Friedberg[1,2,3], *Eliana Marisa Ramos*[4], *Zhongan Yang*[5], *Luke W. Bonham*[1,6], *Jennifer S. Yokoyama*[1,2,3], *Peter A. Ljubenkov*[1], *Kyan Younes*[1], *Daniel H. Geschwind*[7,8,9] *and Bruce L. Miller*[1,2]*

[1] Department of Neurology, Memory and Aging Center, Weill Institute for Neurosciences, University of California, San Francisco, San Francisco, CA, United States, [2] Global Brain Health Institute, University of California, San Francisco, San Francisco, CA, United States, [3] Trinity College Dublin, Dublin, Ireland, [4] Department of Neurology, David Geffen School of Medicine, University of California, Los Angeles, Los Angeles, CA, United States, [5] Department of Psychiatry, David Geffen School of Medicine, University of California, Los Angeles, Los Angeles, CA, United States, [6] Department of Radiology and Biomedical Imaging, University of California, San Francisco, San Francisco, CA, United States, [7] Program in Neurogenetics, Department of Neurology, Center for Autism Research and Treatment, David Geffen School of Medicine, Semel Institute for Neuroscience and Human Behavior, University of California, Los Angeles, Los Angeles, CA, United States, [8] Department of Human Genetics, David Geffen School of Medicine, University of California, Los Angeles, Los Angeles, CA, United States, [9] Institute for Precision Health, University of California, Los Angeles, Los Angeles, CA, United States

OPEN ACCESS

Edited by:
Sudeshna Das, Massachusetts General Hospital, United States

Reviewed by:
Sergey Illarioshkin, Research Center of Neurology, Russia
Subasree Ramakrishnan, National Institute of Mental Health and Neurosciences (NIMHANS), India

***Correspondence:**
Bruce L. Miller
bruce.miller@ucsf.edu

Specialty section:
This article was submitted to Dementia and Neurodegenerative Diseases, a section of the journal Frontiers in Neurology

Received: *31 March 2022*
Accepted: *02 June 2022*
Published: *22 June 2022*

Citation:
Friedberg A, Ramos EM, Yang Z, Bonham LW, Yokoyama JS, Ljubenkov PA, Younes K, Geschwind DH and Miller BL (2022) Case Report: Novel CSF1R Variant in a Patient With Behavioral Variant Frontotemporal Dementia Syndrome With Prodromal Repetitive Scratching Behavior. Front. Neurol. 13:909944. doi: 10.3389/fneur.2022.909944

CSF1R-related leukoencephalopathy is an autosomal dominant neurodegenerative disease caused by mutations in the tyrosine kinase domain of the colony stimulating factor 1 receptor (CSF1R). Several studies have found that hematogenic stem cell transplantation is an effective disease modifying therapy however the literature regarding prodromal and early symptoms *CSF1R*-related leukoencephalopathy is limited. We describe a 63-year-old patient with 4 years of repetitive scratching and skin picking behavior followed by 10 years of progressive behavioral, cognitive, and motor decline in a pattern suggesting behavioral variant of frontotemporal dementia. Brain MRI demonstrated prominent frontal and parietal atrophy accompanied by underlying bilateral patchy white matter hyperintensities sparing the U fibers and cavum septum pellucidum. Whole-exome sequencing revealed a novel, predicted deleterious missense variant in a highly conserved amino acid in the tyrosine kinase domain of *CSF1R* (p.Gly872Arg). Given this evidence and the characteristic clinical and radiological findings this novel variant was classified as likely pathogenic according to the American College of Medical Genetics standard guidelines. Detailed description of the prodromal scratching and skin picking behavior and possible underlying mechanisms in this case furthers knowledge about early manifestations of *CSF1R*-related leukoencephalopathy with the hope that early detection and timely administration of disease modifying therapies becomes possible.

Keywords: *CSF1R*-related leukoencephalopathy, frontotemporal dementia, repetitive behaviors, early symptoms, scratching

INTRODUCTION

CSF1R-related leukoencephalopathy is an autosomal dominant neurodegenerative disease caused by mutations in the tyrosine kinase domain of the colony stimulating factor 1 receptor (*CSF1R*) (1). It accounts for ∼10% of adult-onset leukodystrophies in European cohorts (2). Clinically, *CSF1R*-related leukoencephalopathy presents with variable combinations of progressive cognitive decline, neuropsychiatric symptoms, pyramidal weakness and spasticity, parkinsonism, gait impairment and seizures. Often the pattern of behavioral and emotional change is similar to behavioral variant frontotemporal dementia (bvFTD) with apathy as a particularly prominent feature (1, 3). Disease onset is typically in the fourth or fifth decade of life and progression is relentless with mean disease duration till death of 6.8 years (4). Consistent radiological features on brain magnetic resonance imaging (MRI) include white matter hyperintensities (WMH) primarily involving the frontal and parietal lobes, with sparing of the U-fibers. Usually, these WMH are bilateral, initially patchy evolving to confluency with restricted diffusion in many cases. Thinning of the corpus callosum is characteristic. Gray matter atrophy is evident over the frontal and parietal lobes. A high incidence of a cavum septum pellucidum and cavum vergae was observed in several case series (5–7). Brain CT demonstrates calcifications distributed in the frontal white matter adjacent to the anterior horns of lateral ventricles and in the parietal subcortical white matter.

The *CSF1R* gene encodes a transmembrane tyrosine kinase receptor expressed in the brain, predominantly in microglia. Binding of CSF1R to its ligands (CSF1 and interleukin-34) leads to initiation of signal transductions, which contribute to development, maintenance, and activation of microglia (8). In zebrafish models, haploinsufficiency in CSF1R leads to reduced microglial density and in postmortem human brain tissue from patients with *CSF1R*-related leukoencephalopathy widespread microglia depletion is also evident (9). Moreover, homozygous mutations in *CSF1R* result in a congenital absence of microglia, abnormal brain development, and pediatric-onset leukoencephalopathy (10). *CSF1R*-related leukoencephalopathy is increasingly conceptualized as a neurodegenerative disease that occurs in large part due to microglial dysfunction—a primary microgliopathy (11). There are now more than 70 different pathogenic variants in *CSF1R*, most of which occur in the tyrosine kinase domain resulting in disruption of protein function (1).

There is emerging evidence that hematopoietic stem cell transplantation (HSCT) is a disease modifying therapy for *CSF1R*-related leukoencephalopathy that stabilizes disease progression, highlighting the clinical importance of early detection of individuals with pathogenic *CSF1R* variants (12–14). Nevertheless, detailed description of early/prodromal behavioral changes in *CSF1R*-related leukoencephalopathy is limited.

In this case study we report a patient with a novel likely pathogenic variant in *CSF1R* who presented with repetitive scratching behavior 4 years prior to the onset of progressive relentless behavioral, cognitive and motor decline accompanied by radiologic features highly consistent with *CSF1R*-related encephalopathy. Our goals are to enhance the field's knowledge about early phenotypic and genotypic features of *CSF1R*-related leukoencephalopathy and to further elucidate the heterogenous genetic causes of bvFTD clinical syndrome. We also discuss possible mechanisms underlying the scratching behavior.

METHODS

Clinical and genetic evaluation was performed at the University of California, San Francisco, Memory and Aging Center as part of a prospective research study: "Frontotemporal Dementia: Genes, Images, and Emotions" (15). For patient anonymity some details have been modified.

Whole-brain structural MRI images were acquired using a 3T (Magnetom Prisma) scanner manufactured by Siemens implementing previously published acquisition protocols (16).

Whole-exome sequencing (WES) was conducted to screen known genes associated with dementia and leukoencephalopathies. Whole-exome regions were captured with the SeqCap EZ Human Exome Kit v3 and sequenced on an Illumina HiSeq4000 at the UCLA Neuroscience Genomics Core (semel.ucla.edu/ungc). Sequence reads were mapped to the GRCh37/hg19 reference genome and variants joint-called according to the Genome Analysis Toolkit best practices recommendations (17). Series of filtering steps were applied to prioritize variants, and candidate variants were confirmed by Sanger sequencing. The hexanucleotide repeat of *C9orf72* was screened using both fluorescent and repeat-primed PCR, as previously described (18).

RESULTS

Case Description

L was a 63-year-old right-handed female who presented to evaluation in the memory clinic due to 10 years of progressive behavioral changes and cognitive decline. Her early developmental history was notable for mild reading and writing difficulties in elementary school. In her youth she suffered mild brain trauma, falling twice from her bike. With both events there was loss consciousness for a short duration and no residual symptoms. After high school L attended college, where she obtained a BA. She married in her twenties. Her baseline personality was described as delightful, kind and social. At the age of 45 she presented with an adult-onset epilepsy with generalized tonic-clonic seizures. The seizures were successfully controlled with valproic acid. At the age of 49 she developed a new behavior, repetitively scratching and picking the skin of her left torso and shoulder. She never explained to her family members the reason for the scratching and did not explicitly complain of pruritus. She did not report an increasing sense of tension prior to scratching or relief during or after the behavior. The scratching increased in frequency and severity. The behavior was not accompanied by any other perseverative, stereotyped or compulsive/ritualistic behaviors. She was examined by a dermatologist who found no causative skin lesion and defined her condition as "neurogenic itch." Four years later, at the age of 53 years she became socially withdrawn and less communicative. Her husband lost substantial

amounts of their money shopping but she took no action to protect herself. At the age of 55 years she could no longer manage her finances or run her own business. She was unable to operate her computer or other technological equipment. She asked her dentist to remove all her teeth and replace them with dentures, without expressing a reason for this request. At the age of 61 she started to purchase recklessly. She got into a physical fight with her husband and subsequently they divorced. L did not express concern about the divorce and seemed to show less empathy for others. She flew balloons in the neighborhood park for multiple hours a day. She also became hyperoral with preference to sweets. At the age of 63 when she presented to evaluation, the family noticed word finding difficulties. She gradually stopped talking but acknowledged people with eye contact and head movement. She undressed in front of her family and collected soda bottle caps. Her scratching behavior worsened, and she scratched her skin to the point of bleeding. Family history was taken for four generations and was unremarkable for either early onset dementia, psychiatric disease epilepsy or motor decline. Both of her parents lived into their eighties with no cognitive decline. Her paternal and maternal families originated from Western Europe. Neurological examination was remarkable for increased axial tone and rigidity and bradykinesia in her upper limbs more so on the right. In her mental status examination L seemed inattentive, abulic and stimulus bound. Her affect was flat. Verbal output was decreased with occasional Yes/No answers, and use of overlearned phrases such as "I don't think so." She could not follow instructions required for praxis examination. Her Mini-Mental State Examination score was 6/30. General physical examination was unremarkable except for minor excoriations over her torso secondary to scratching.

At the time of presentation, 14 years after the emergence of the scratching behavior, her complete blood count, renal and liver function tests were within normal limits suggesting that systemic causes of pruritus such as a solid or hematologic malignancy, cholestasis or renal insufficiency were not likely. Blood electrolyte levels, thyroid functions, coagulation tests, HBA1C, B12 levels, methylmalonic acid levels and very-long-chain fatty acid (VLCFA), were also all within normal limits.

Brain MRI demonstrated bilateral symmetrical global cortical atrophy (**Figure 1**). Atrophy was most pronounced in the frontal and parietal lobes, particularly in the medial frontal cortices. Profound thinning of the corpus callosum was evident. T2 FLAIR sequence showed bilateral patchy WMH involving frontal and parietal white matter, sparing the U fibers. Cavum septum pellucidum was noted. Diffusion weighted imaging did not show a pattern of restricted diffusion and T2* sequences did not demonstrate signal abnormalities consistent with calcifications.

The clinical syndrome met research criteria for probable bvFTD (19). The combination of gray matter atrophy and WMH led the neurologists to consider underlying neuropathological etiologies associated with white matter signal changes such as corticobasal degeneration and frontotemporal lobar degeneration (FTLD) TDP type A. The pattern of white matter involvement in the setting of protracted clinical course was suggestive of leukodystrophy as a primary etiology, particularly *CSF1R*-related leukoencephalopathy considering the characteristic brain MRI findings (20) and seizures. To promote the diagnostic process WES was performed to analyze a large panel of genes associated with dementia and leukoencephalopathies.

WES revealed a novel heterozygous missense variant c.2614G>A (p.Gly872Arg) in the *CSF1R* gene (**Figure 2**). This variant, not found in the Genome Aggregation Database (gnomAD) (21), was consistently predicted as damaging by multiple *in silico* tools [PolyPhen-2 (http://genetics.bwh.harvard.edu/pph2), SIFT (http://sift.jcvi.org) and CADD (http://cadd.gs.washington.edu)]. It lies in the tyrosine kinase domain, similarly to many other *CSF1R*-related leukoencephalopathy causing variants, in a highly conserved amino acid. Segregation analysis of this variant was not feasible due to unreachable relatives of the proband. Given these evidences and the characteristic clinical and radiologic findings (22), this variant was classified as likely pathogenic according to the American College of Medical Genetics standard guidelines (23).

At the time L presented to our care, HSCT was not yet considered a therapeutic option and was not offered. L passed away due to her neurogenerative disease and was not enrolled into an autopsy program.

DISCUSSION

We present a patient with a progressive behavioral cognitive and motor syndrome compatible with bvFTD which was preceded by adult onset generalized epilepsy and 4 years of repetitive scratching and skin picking behavior. The pattern of white and gray matter changes, the profound thinning of the corpus callosum and the occurrence of septum pellucidum cavum were all suggestive of *CSF1R*-related leukoencephalopathy (22). Genetic analysis revealed a novel likely pathogenic missense variant in the *CSF1R* gene. Since both parents were not affected clinically this may represent a *de novo* genetic variant. Other possibilities include incomplete penetrance or genetic mosaicism as was shown in other sporadic cases (1, 24).

Repetitive scratching and skin picking behavior have not yet been described in the literature as an early or prodromal symptom of *CSF1R*-related leukoencephalopathy. Delineating and highlighting such symptoms may contribute to early detection of patients with pathogenic *CSF1R* variants, allowing timely treatment with new disease modifying therapies.

We suggest several possible mechanisms underlying the scratching behavior in the context *CSF1R*-related encephalopathy which are not mutually exclusive and may act synergistically. Scratching is considered a self-grooming behavior aimed to protect the organism of potential external threats and is observed in multiple species. In humans excessive scratching and skin picking, in a pattern like the behavior observed in this case, is observed in skin picking disorder (SPD) (25). A diffuse tensor imaging study in skin picking disorder patients demonstrated reduced white matter integrity in tracts in proximity of the bilateral anterior cingulate cortex (ACC) implicating the importance of the ACC in regulation of this behavior (26). Interestingly L presented with severe

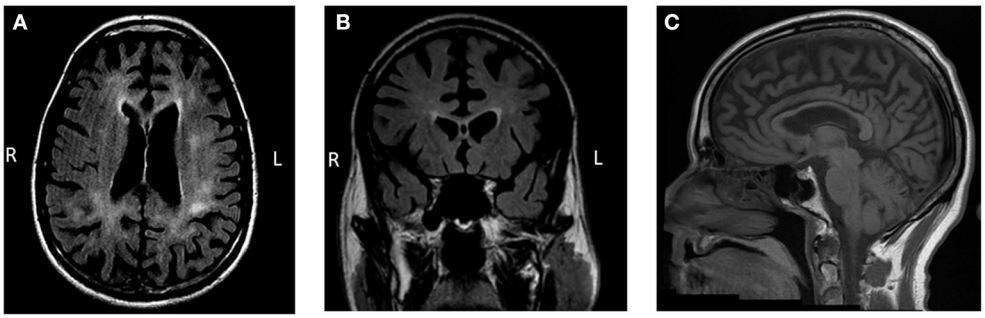

FIGURE 1 | Brain MRI findings. **(A,B)** Bilateral patchy and predominantly frontoparietal white matter hyperintensities with accompanying marked gray matter atrophy are observed on T2-weighted fluid-attenuated inversion recovery (FLAIR) imaging. Cavum septum pellucidum is also evident. **(C)** Thinning of the corpus callosum is observed on a T1-weighted sequence.

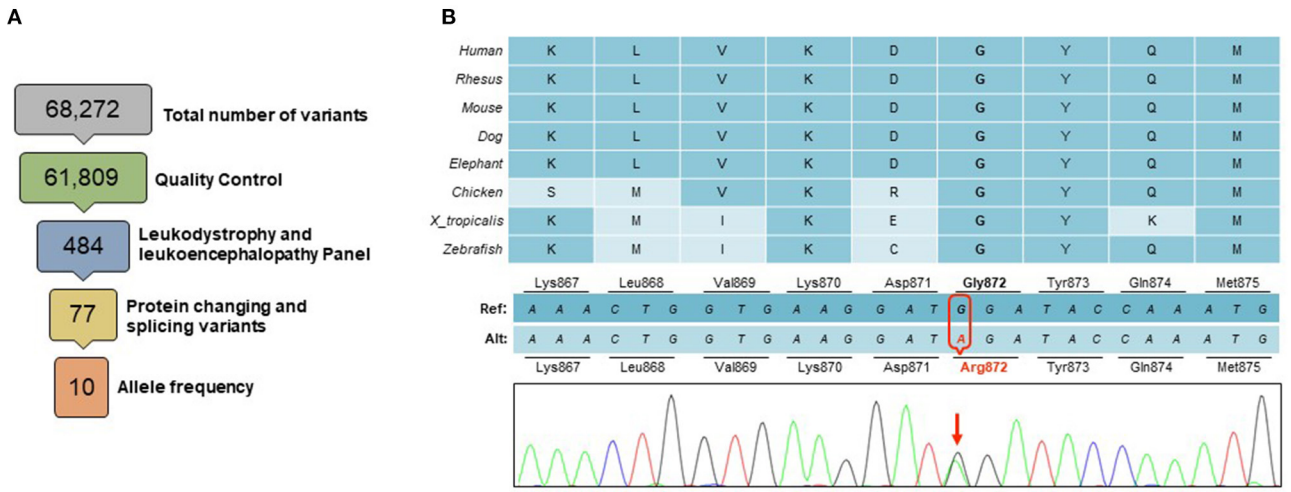

FIGURE 2 | Genetic findings. **(A)** A total of 68,272 variants were identified within the targeted exome. Variants of low quality were removed through quality control (GQ<20, RD<10, AF<0.25). Among a panel of 165 genes known to be associated with leukodystrophies and leukoencephalopathies, a total of 484 variants were identified, of which 77 were protein changing or splicing variants. Only 10 of these had an allele frequency <0.10 in gnomAD database, including a novel heterozygous missense variant in the *CSF1R* gene **(B)** This change in a highly conserved amino acid in the CSF1R tyrosine domain (p.Gly872Arg), was predicted to be deleterious by multiple *in silico* tools.

atrophy in the ACC bilaterally accompanied by adjacent white matter lesions (**Figure 1**). This pattern might indicate early regional involvement that accounted for the early onset of repetitive scratching and skin picking behavior. Moreover, a candidate animal model of skin picking disorder is the *Hoxb8* knockout mouse. Mice with mutations of the *Hoxb8* gene groom excessively, to the point of developing skin lesions (27). In this model *Hoxb8* is expressed in specific populations of microglia and neuronal cells (28). The *Hoxb8* gene is expressed in the orbital cortex, the anterior cingulate, the striatum, and the limbic system, structures implicated in repetitive and compulsive behaviors. Recent work in this mouse model suggested that the absence of proper maintenance of circuit modulation by *Hoxb8* expressing microglia results in the excessive grooming behavior (29). It is possible that early depletion of the *Hoxb8* expressing microglia population resulted in the predisposition to repetitive scratching behavior. Interestingly, in mouse models of FTD with progranulin deficiency, excessive grooming behaviors were present (30). This might imply converging neuroanatomical and/or underlying molecular mechanisms with scratching observed in *CSF1R*-related leukoencephalopathy. Lastly, in the previous decade CSF1R inhibitors were introduced in cancer treatment. Safety assessment of Emactuzumab, a monoclonal antibody that targets and inhibits CSF1R revealed that pruritus was a highly prevalent side effect affecting 56% of treated patients (31). Like other monoclonal antibodies Emactuzumab does not penetrate the blood brain barrier suggesting that CSF1R dysfunction in peripheral tissues might contribute to the scratching behavior.

Limitations

Definite causal evidence with regards to the pathogenicity of this variant was not obtained due to the unavailability of neuropathological data and unreachable family members for segregation analysis. However, building on the knowledge accumulated from multiple studies about the underlying biology and the clinical and radiological presentation of *CSF1R*-related encephalopathy there is high likelihood that this variant is disease causing. Future work is needed to establish definite causal relationship between this novel genetic variant and *CSF1R*-related encephalopathy and to delineate the pattern of early behavioral manifestations in this condition.

DATA AVAILABILITY STATEMENT

The datasets presented in this article are not readily available because of ethical and privacy restrictions. Requests to access the datasets should be directed to the corresponding author.

ETHICS STATEMENT

The studies involving human participants were reviewed and approved by University of California, San Francisco Human Research Protection Program Institutional Review Board. The patients/participants provided their written informed consent to participate in this study. Written informed consent was obtained from the individual(s) for the publication of any potentially identifiable images or data included in this article.

AUTHOR CONTRIBUTIONS

AF, ER, and BM conceptualized the study. AF conducted the literature review and wrote the manuscript. BM, KY, and PL examined the patient. ER, ZY, DG, LB, and JY were involved in genetic data generation, analysis, and interpretation. All authors reviewed and revised the final manuscript.

FUNDING

This work was supported by NIH grants P01 AG019724 and P30 AG062422, by grant 2021-A-023-FEL from the Larry L. Hillblom Foundation (AF), by the Global Brain Health Institute, Alzheimer's Association, and Alzheimer's Society Pilot Awards for Global Brain Health Leaders: GBHI ALZ UK-21-721419 (AF) and NIH-NIA grant R01 AG062588 (JY). Samples from the National Cell Repository for Alzheimer's Disease (NCRAD), which receives government support under a cooperative agreement grant (U24 AG021886) awarded by the National Institute on Aging (NIA), were used in this study.

ACKNOWLEDGMENTS

We thank L and her family for participating in dementia research. We also thank contributors who collected samples.

REFERENCES

1. Konno T, Kasanuki K, Ikeuchi T, Dickson DW, Wszolek ZK. CSF1R-related leukoencephalopathy: a major player in primary microgliopathies. *Neurology*. (2018) 91:1092–104. doi: 10.1212/WNL.0000000000006642
2. Lynch DS, Jaunmuktane Z, Sheerin UM, Phadke R, Brandner S, Milonas I, et al. Hereditary leukoencephalopathy with axonal spheroids: a spectrum of phenotypes from CNS vasculitis to Parkinsonism in an adult onset leukodystrophy series. *J Neurol Neurosurg Psychiatry*. (2016) 87:512–9. doi: 10.1136/jnnp-2015-310788
3. Ikeuchi T, Mezaki N, Miura T. Cognitive dysfunction and symptoms of movement disorders in adult-onset leukoencephalopathy with axonal spheroids and pigmented glia. *Parkinsonism Relat Disord.* (2018) 46(Suppl. 1):S39–41. doi: 10.1016/j.parkreldis.2017.08.018
4. Konno T, Yoshida K, Mizuno T, Kawarai T, Tada M, Nozaki H, et al. Clinical and genetic characterization of adult-onset leukoencephalopathy with axonal spheroids and pigmented glia associated with CSF1R mutation. *Eur J Neurol.* (2017) 24:37–45. doi: 10.1111/ene.13125
5. Konno T, Broderick DF, Mezaki N, Isami A, Kaneda D, Tashiro Y, et al. Diagnostic value of brain calcifications in adult-onset leukoencephalopathy with axonal spheroids and pigmented glia. *AJNR Am J Neuroradiol.* (2017) 38:77–83. doi: 10.3174/ajnr.A4938
6. Sundal C, Van Gerpen JA, Nicholson AM, Wider C, Shuster EA, Aasly J, et al. MRI characteristics and scoring in HDLS due to CSF1R gene mutations. *Neurology*. (2012) 79:566–74. doi: 10.1212/WNL.0b013e318263575a
7. Konno T, Tada M, Tada M, Koyama A, Nozaki H, Harigaya Y, et al. Haploinsufficiency of CSF-1R and clinicopathologic characterization in patients with HDLS. *Neurology*. (2014) 82:139–48. doi: 10.1212/WNL.0000000000000046
8. Chitu V, Gokhan S, Nandi S, Mehler MF, Stanley ER. Emerging roles for CSF-1 receptor and its ligands in the nervous system. *Trends Neurosci.* (2016) 39:378–93. doi: 10.1016/j.tins.2016.03.005
9. Oosterhof N, Kuil LE, van der Linde HC, Burm SM, Berdowski W, van Ijcken WFJ, et al. Colony-stimulating factor 1 receptor (CSF1R) regulates microglia density and distribution, but not microglia differentiation *in vivo*. *Cell Rep*. (2018) 24:1203–17.e6. doi: 10.1016/j.celrep.2018.06.113
10. Oosterhof N, Chang IJ, Karimiani EG, Kuil LE, Jensen DM, Daza R, et al. Homozygous mutations in CSF1R cause a pediatric-onset leukoencephalopathy and can result in congenital absence of microglia. *Am J Hum Genet.* (2019) 104:936–47. doi: 10.1016/j.ajhg.2019.03.010
11. Sirkis DW, Bonham LW, Yokoyama JS. The role of microglia in inherited white-matter disorders and connections to frontotemporal dementia. *Appl Clin Genet.* (2021) 14:195–207. doi: 10.2147/TACG.S245029
12. Eichler FS, Li J, Guo Y, Caruso PA, Bjonnes AC, Pan J, et al. CSF1R mosaicism in a family with hereditary diffuse leukoencephalopathy with spheroids. *Brain*. (2016) 139:1666–72. doi: 10.1093/brain/aww066
13. Gelfand JM, Greenfield AL, Barkovich M, Mendelsohn BA, Van Haren K, Hess CP, et al. Allogeneic HSCT for adult-onset leukoencephalopathy with spheroids and pigmented glia. *Brain.* (2020) 143:503–11. doi: 10.1093/brain/awz390
14. Tipton PW, Kenney-Jung D, Rush BK, Middlebrooks EH, Nascene D, Singh B, et al. Treatment of CSF1R-related leukoencephalopathy: breaking new ground. *Mov Disord*. (2021) 36:2901–9. doi: 10.1002/mds.28734
15. Rankin KP, Kramer JH, Miller BL. Patterns of cognitive and emotional empathy in frontotemporal lobar degeneration. *Cogn Behav Neurol.* (2005) 18:28–36. doi: 10.1097/01.wnn.0000152225.05377.ab
16. Illan-Gala I, Casaletto KB, Borrego-Ecija S, Arenaza-Urquijo EM, Wolf A, Cobigo Y, et al. Sex differences in the behavioral variant of frontotemporal dementia: A new window to executive and behavioral reserve. *Alzheimers Dement.* (2021) 17:1329–41. doi: 10.1002/alz.12299

17. McKenna A, Hanna M, Banks E, Sivachenko A, Cibulskis K, Kernytsky A, et al. The genome analysis toolkit: a mapreduce framework for analyzing next-generation DNA sequencing data. *Genome Res.* (2010) 20:1297–303. doi: 10.1101/gr.107524.110
18. DeJesus-Hernandez M, Mackenzie IR, Boeve BF, Boxer AL, Baker M, Rutherford NJ, et al. Expanded GGGGCC hexanucleotide repeat in noncoding region of C9ORF72 causes chromosome 9p-linked FTD and ALS. *Neuron.* (2011) 72:245–56. doi: 10.1016/j.neuron.2011.09.011
19. Rascovsky K, Hodges JR, Knopman D, Mendez MF, Kramer JH, Neuhaus J, et al. Sensitivity of revised diagnostic criteria for the behavioural variant of frontotemporal dementia. *Brain*. (2011) 134:2456–77. doi: 10.1093/brain/awr179
20. Resende LL, de Paiva ARB, Kok F, da Costa Leite C, Lucato LT. Adult leukodystrophies: a step-by-step diagnostic approach. *Radiographics.* (2019) 39:153–68. doi: 10.1148/rg.2019180081
21. Karczewski KJ, Francioli LC, Tiao G, Cummings BB, Alfoldi J, Wang Q, et al. The mutational constraint spectrum quantified from variation in 141,456 humans. *Nature.* (2020) 581:434–43. doi: 10.1038/s41586-020-2308-7
22. Konno T, Yoshida K, Mizuta I, Mizuno T, Kawarai T, Tada M, et al. Diagnostic criteria for adult-onset leukoencephalopathy with axonal spheroids and pigmented glia due to CSF1R mutation. *Eur J Neurol.* (2018) 25:142–7. doi: 10.1111/ene.13464
23. Richards S, Aziz N, Bale S, Bick D, Das S, Gastier-Foster J, et al. Standards and guidelines for the interpretation of sequence variants: a joint consensus recommendation of the American college of medical genetics and genomics and the association for molecular pathology. *Genet Med.* (2015) 17:405–24. doi: 10.1038/gim.2015.30
24. Saitoh BY, Yamasaki R, Hayashi S, Yoshimura S, Tateishi T, Ohyagi Y, et al. A case of hereditary diffuse leukoencephalopathy with axonal spheroids caused by a de novo mutation in CSF1R masquerading as primary progressive multiple sclerosis. *Mult Scler.* (2013) 19:1367–70. doi: 10.1177/1352458513489854
25. Grant JE, Odlaug BL, Chamberlain SR, Keuthen NJ, Lochner C, Stein DJ. Skin picking disorder. *Am J Psychiatry.* (2012) 169:1143–9. doi: 10.1176/appi.ajp.2012.12040508
26. Grant JE, Odlaug BL, Hampshire A, Schreiber LR, Chamberlain SR. White matter abnormalities in skin picking disorder: a diffusion tensor imaging study. *Neuropsychopharmacology.* (2013) 38:763–9. doi: 10.1038/npp.2012.241
27. Greer JM. Capecchi MR. Hoxb8 is required for normal grooming behavior in mice. *Neuron.* (2002) 33:23–34. doi: 10.1016/S0896-6273(01)00564-5
28. De S, Van Deren D, Peden E, Hockin M, Boulet A, Titen S, et al. Two distinct ontogenies confer heterogeneity to mouse brain microglia. *Development*. (2018) 145:dev175901. doi: 10.1242/dev.152306
29. Nagarajan N, Jones BW, West PJ, Marc RE, Capecchi MR. Corticostriatal circuit defects in Hoxb8 mutant mice. *Mol Psychiatry.* (2018) 23:1868–77. doi: 10.1038/mp.2017.180
30. Krabbe G, Minami SS, Etchegaray JI, Taneja P, Djukic B, Davalos D, et al. Microglial NFkappaB-TNFalpha hyperactivation induces obsessive-compulsive behavior in mouse models of progranulin-deficient frontotemporal dementia. *Proc Natl Acad Sci U S A.* (2017) 114:5029–34. doi: 10.1073/pnas.1700477114
31. Cassier PA, Italiano A, Gomez-Roca CA, Le Tourneau C, Toulmonde M, Cannarile MA, et al. CSF1R inhibition with emactuzumab in locally advanced diffuse-type tenosynovial giant cell tumours of the soft tissue: a dose-escalation and dose-expansion phase 1 study. *Lancet Oncol.* (2015) 16:949–56. doi: 10.1016/S1470-2045(15)00132-1

Conflict of Interest: The authors declare that the research was conducted in the absence of any commercial or financial relationships that could be construed as a potential conflict of interest.

Publisher's Note: All claims expressed in this article are solely those of the authors and do not necessarily represent those of their affiliated organizations, or those of the publisher, the editors and the reviewers. Any product that may be evaluated in this article, or claim that may be made by its manufacturer, is not guaranteed or endorsed by the publisher.

frontiers | Frontiers in Neurology

CASE REPORT
published: 29 June 2022
doi: 10.3389/fneur.2022.912592

Brain MRI Volumetry Analysis in an Indonesian Family of SCA 3 Patients: A Case-Based Study

Siti Aminah Sobana[1,2,3†], Fathul Huda[1,2,4*†], Robby Hermawan[5], Yunia Sribudiani[2,4], Tan Siauw Koan[5], Sofiati Dian[1], Paulus Anam Ong[1], Nushrotul Lailiyya Dahlan[1], Nastiti Utami[1], Iin Pusparini[1], Uni Gamayani[1], Norlinah Mohamed Ibrahim[6] and Tri Hanggono Achmad[2,4]*

[1] Department of Neurology, Faculty of Medicine, Dr. Hasan Sadikin Central General Hospital/Universitas Padjadjaran, Bandung, Indonesia, [2] Research Center of Medical Genetics, Faculty of Medicine, Universitas Padjadjaran, Bandung, Indonesia, [3] Doctoral Study Program, Faculty of Medicine, Universitas Padjadjaran, Bandung, Indonesia, [4] Department of Biomedical Sciences, Faculty of Medicine, Universitas Padjadjaran, Bandung, Indonesia, [5] Department of Radiology, Saint Borromeus Hospital, Bandung, Indonesia, [6] Department of Medicine, Faculty of Medicine, Universiti Kebangsaan Malaysia Medical Center, Kuala Lumpur, Malaysia

OPEN ACCESS

Edited by:
Bruce Miller, University of California, San Francisco, United States

Reviewed by:
Roberto Rodríguez-Labrada, Cuban Neuroscience Center, Cuba
Carlos Hernandez-Castillo, Dalhousie University, Canada
Carlos Henrique Ferreira Camargo, Federal University of Paraná, Brazil

***Correspondence:**
Fathul Huda
fathul@unpad.ac.id
Siti Aminah Sobana
aminah.dr@yahoo.co.id

† These authors have contributed equally to this work and share first authorship

Specialty section:
This article was submitted to Dementia and Neurodegenerative Diseases, a section of the journal Frontiers in Neurology

Received: *04 April 2022*
Accepted: *01 June 2022*
Published: *29 June 2022*

Citation:
Sobana SA, Huda F, Hermawan R, Sribudiani Y, Koan TS, Dian S, Ong PA, Dahlan NL, Utami N, Pusparini I, Gamayani U, Mohamed Ibrahim N and Achmad TH (2022) Brain MRI Volumetry Analysis in an Indonesian Family of SCA 3 Patients: A Case-Based Study. Front. Neurol. 13:912592. doi: 10.3389/fneur.2022.912592

Introduction: Spinocerebellar ataxia type-3 (SCA3) is an adult-onset autosomal dominant neurodegenerative disease. It is caused by expanding of CAG repeat in ATXN3 gene that later on would affect brain structures. This brain changes could be evaluated using brain MRI volumetric. However, findings across published brain volumetric studies have been inconsistent. Here, we report MRI brain volumetric analysis in a family of SCA 3 patients, which included pre-symptomatic and symptomatic patients.

Methodology: The study included affected and unaffected members from a large six-generation family of SCA 3, genetically confirmed using PolyQ/CAG repeat expansion analysis, Sanger sequencing, and PCR. Clinical evaluation was performed using Scale for the Assessment and Rating of Ataxia (SARA). Subjects' brains were scanned using 3.0-T MRI with a 3D T1 BRAVO sequence. Evaluations were performed by 2 independent neuroradiologists. An automated volumetric analysis was performed using FreeSurfer and CERES (for the cerebellum).

Result: We evaluated 7 subjects from this SCA3 family, including 3 subjects with SCA3 and 4 unaffected subjects. The volumetric evaluation revealed smaller brain volumes ($p < 0.05$) in the corpus callosum, cerebellar volume of lobules I-II, lobule IV, lobule VIIB and lobule IX; and in cerebellar gray matter volume of lobule IV, and VIIIA; in the pathologic/expanded CAG repeat group (SCA3).

Conclusion: Brain MRI volumetry of SCA3 subjects showed smaller brain volumes in multiple brain regions including the corpus callosum and gray matter volumes of several cerebellar lobules.

Keywords: SCA3, volumetry, brain, MRI, Indonesia

INTRODUCTION

Spinocerebellar ataxia type-3 (SCA3) is an autosomal dominant neurodegenerative disease characterized by progressive ataxia that usually starts in early to mid-adulthood decade resulting in early wheelchair dependence and immobilization. Although it is rare in the general population with a prevalence of 1–2/100,000 it is the most common subtype of spinocerebellar ataxias (SCA) worldwide (1, 2). SCA3 patients typically present with bilateral cerebellar syndrome, characterized by gait and limb ataxia, although non-ataxia symptoms are also quite common. The non-ataxia features of SCA3 are varied and include extrapyramidal manifestations such as dystonia, parkinsonism, tremor and spasticity (3, 4).

SCA3 is caused by CAG trinucleotide repeats which exceed 46 repeats in the ATXN3 gene located at the N-terminus of chromosome 14 (1, 2, 5–8). To date, there are no curative treatment or treatments that could halt the progression of SCA3. Current treatment is still aimed at symptomatic management using pharmacological therapies; while non-pharmacological management such as various forms of rehabilitation therapies are utilized to improve balance, mobility and speech. Promising disease-modifying therapies such anti-ATXN3 aggregation compounds, ATXN3 mRNA silencing therapies, autophagy stimulation, stem cell and gene therapies are still in the pipeline and or in Phase 2 clinical trials, and are still not available (1, 2, 6, 9).

Current evaluation of patients with SCA 3 include a detailed clinical assessment, coupled with the measurement of ataxia severity using validated instruments such as the Scale for the Assessment and Rating of Ataxia (SARA) (4, 10). Genetic analysis using Sanger sequencing methods for PolyQ/CAG repeat expansion is required for confirmatory diagnosis, and the detection of the number of CAG repeats. Magnetic resonance imaging (MRI) is part of the clinical workup, although there are no specific distinguishing or diagnostic features unique for SCA3, and typically shows cerebellar atrophy (7, 11–14). An MRI with 3.0-T magnetic field, which is already available in some of the developing countries, is perhaps necessary for a reliable spatial and contrast resolution for volumetric analysis (15, 16).

Recent publications have reported variable findings in the volumetry of various anatomical brain structures in patients with SCA3 (17–24). One recent study reported that patients with SCA 3 had decreased cerebellar and cerebral volumes, and also the basal ganglia, gray matter and the thalamus (18). Given the lack of reports on MRI brain volumetry in SCA3 from the South East Asia region, especially from Indonesia, we therefore conducted this study to evaluate the MRI brain volumetry in SCA 3 patients from a large Indonesian family and compared the findings to unaffected members. We also included volumetric analysis of other brain regions than previously reported.

Abbreviations: ATXN3, ataxin3 (could refer to gene or protein); CAG, trinucleotide repeat of CAG; CERES, Cerebellum Segmentation; MMSE, Mini-Mental State Examination; MoCA-Ina, Montreal Cognitive Assessment, Indonesian version; MRI, magnetic resonance imaging; PolyQ, polyglutamine; SARA, Scale for the Assessment and Rating of Ataxia; SCA, spinocerebellar ataxia.

METHODS

This was a cross-sectional, case-based study involving a large family with SCA 3 within the Garut Regency in Indonesia.

Ethics Statement

This study was reviewed and approved by the Research Ethics Committee of Universitas Padjadjaran no 032107017/2021. Written informed consent in accordance with the ethics committee and Declaration of Helsinki were obtained from all subjects.

Patient Recruitment

Subjects of this study were from a family with progressive hereditary ataxia who were genetically confirmed with ATXN3 gene mutation. This family has 208 members; of these, 34 members had already been clinically evaluated, and 16 of these members had been genetically screened for SCA repeats. Of these 16 subjects, seven consented to take part in this volumetric study (**Figures 1A,C**).

Clinical Assessment

Clinical assessment was measured using the Scale for Assessment and Rating of Ataxia (SARA). SARA consists of eight items, including tests of gait, stance, sitting, speech, finger-chase test, finger-nose test, fast alternating movements, and heel-shin test (4). According to criteria by Velazquez-Perez et al., an asymptomatic subject is a subject with SARA score of 0 and without any symptoms; those with SARA score of 0–2 and with ataxia symptoms are categorized as prodromal; while those with SARA score of 3 and above are included into ataxic group (10).

Genetic Evaluation

Genetic evaluation was done using blood sample with polyQ/CAG repeat expansion analysis according to Sanger sequencing. According to criteria by du Montcel et al., a person has SCA3 if the CAG repeat length is *expanded* $\geq$ 47; otherwise, the individual is considered an unaffected subject (8).

Brain MRI Protocols

Subjects' brain was scanned using 24 channel head coil in a 3.0-Tesla MRI scanner (Signa Pioneer; GE Healthcare, Chicago, United States). Scanning was done in the sagittal plane using isotropic 3D T1 BRAVO sequence (TR/TE 9 ms/3.5 ms, NEX 1, slice thickness 1 x 1 mm). This sequence is able to differentiate brain structure best suited for automatic identification by FreeSurfer and CERES (explained in following section). All brain MRI imaging and analysis were performed by (FH, RH) and two neuroradiology consultants (RH, TSK), who independently reviewed the images.

Image Capture

Captured MRI images were retrieved from DICOM images, using RadiANT ver 2020.2 (Medixant, Poznand, Polandia) (25) (**Figure 2**). Briefly, DICOM data were mounted to the software, then sagittal plane T1 BRAVO image sequences were loaded. Reconstruction method using multiplanar reformation

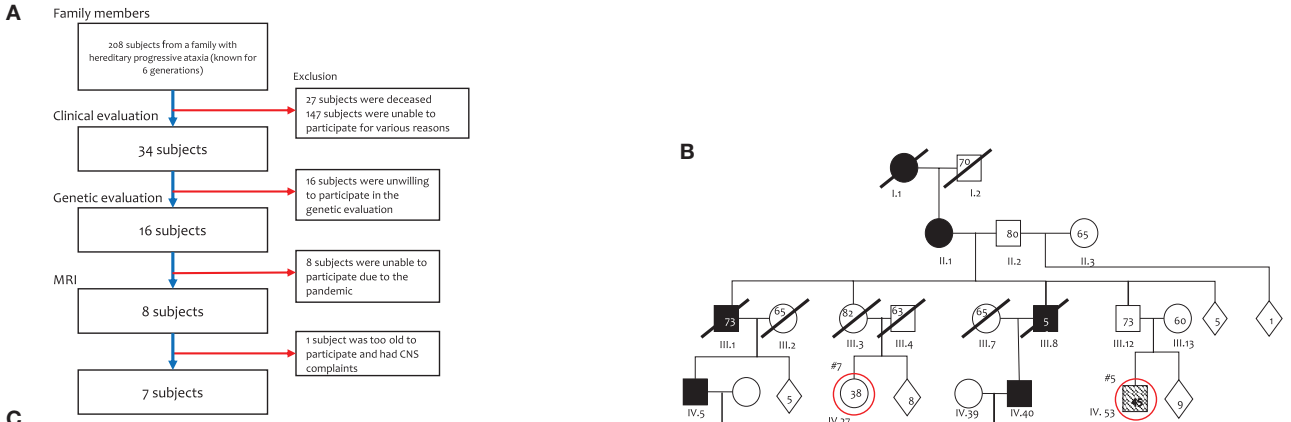

C

Subject	Gender	Age (years)	Onset age (years)	Duration (years)	CAG repeats			Clinical (SARA)	
					A1	A2	Category	Score	Category
1	f	35	22	13	8	68	*Expanded*	3	Ataxic
2	m	34	13	21	8	71	*Expanded*	14	Ataxic
3	m	18	15	3	8	73	*Expanded*	0 + symptoms	Prodromal
4	f	37	-	-	23	30	*Intermediate*	-	Not SCA
5	m	45	-	-	17	23	*Medium*	-	Not SCA
6	m	24	-	-	8	13	*Short*	-	Not SCA
7	f	38	-	-	9	13	*Short*	-	Not SCA

f: female; m: male; SARA: Scale for the Assessment and Rating of Ataxia

FIGURE 1 | Subject of this study. **(A)** Subject inclusion, **(B)** Family pedigree, and **(C)** Subject characteristics.

or reconstruction (MPR) were done, and Talairach line was set. Image capture of certain position was acquired.

Volumetric Calculation

Brain MRI images were analyzed automatically (except for cerebellum) using FreeSurfer ver 7.1.1, software from *Martinos Center of Biomedical Imaging*, and *Massachusetts General Hospital / Harvard University* (Boston, MA), *https://surfer.nmr.mgh.harvard.edu/*. Briefly, after installation of Freesurfer computer (Mac/Linux OS), designated T1 3D BRAVO images were loaded into the software. First, *-reconall* command was executed to get skull stripping, and brain mask feature applied to the image for volumetric evaluation. Volumetric evaluation was computed automatically which required ∼8–12 h per subject. The results were marked brain region, and inspected by two independent neuroradiology consultants. If the brain marking was not satisfactory, a tweak would be done, and automatic re-evaluation would be repeated from the beginning. And if after re-evaluation, brain marking was still not satisfactory, a second brain MRI scan was performed (26, 27).

For automatic cerebellar evaluation, CERES (*Cerebellum Segmentation*) ver 1.0 was used (developed by *Universidad Politecnica de Valencia and Université de Bordeaux* [*Informatica biomedica*-IBIME, Valencia, Spanyol], *https://www.volbrain.upv.es/*) (28). Briefly, DICOM image were converted to NIFTI format, then loaded to VolBrain server. CERES pipeline was selected, and evaluation gray matter volume, white matter volume, and cortical thickness of each cerebellar lobule was done automatically.

Volumetric Evaluation

Volumetric data calculated by FreeSurfer and CERES were processed and compared with the percentage intracranial volume that was provided by the volumetric analysis. Brain volumetry of the anatomical structures in this study was calculated as ratio of the individual subject's intracranial volume (ICV). The volume ratio is used since there is no standard or normal range for the volume of the various brain structures yet. In addition, the shape of the head and the volume of the human brain varies. Therefore, an objective standard is needed in the volumetric measurement of the brain. This can be achieved by measuring the ratio of volume relative to ICV. Since we use this ICV as the denominator in the volume calculation, so we name it percentage to ICV (%ICV), to be more precise.

Heat Map

In order to make the assessment easier, a heat-map color grading pattern was employed (**Tables 1A,B**). Briefly, the cells in the table are colored by conditional formatting using color scale feature, with green for the largest number gradating to yellow and red for the smallest number.

Statistical Analysis

Since the sample size is small, the non-parametric Mann-Whitney U test was used to compare two groups in terms of quantitative variables. Data were analyzed using SPSS ver 25.0 for Windows (IBM Corp. IBM SPSS Statistics fo Windows, Version 25.0 Armonk, NY: IBM Corp). Mann-Whitney U test

was employed for non-parametric. $P < 0.05$ is considered statistically significance.

RESULT

Our subjects came from a large six-generation family with 208 members with a history of progressive cerebellar syndrome, genetically confirmed as SCA3. Clinically affected family members were one person from the first generation; two members from the second generation, 10 members from the third generation, 54 people in the fourth generation, 89 people in the fifth generation and 11 people, thus far, in the sixth generation. The relevant pedigree in shown in (**Figures 1A,B**).

Out of those 208 members, only seven were willing to take part in this volumetric study (**Figure 1A**). Subjects 1–3 are SCA3 patients and siblings with Subject 4. They are descendants from a father (IV.40), paternal grandfather (III.8), great grandmother (II.1) and great-great grandmother (I.1), who had ataxia complaints. Subjects 5–7 are unaffected. Subject 5 had parents and grandparents with no ataxia complaints. Subject 6 is a descendant of a father (IV.5), paternal grandfather (III.1), great grandmother (II.1) and great-great grandmother (I.1), who had progressive ataxia complaints. The parents of Subject 7 had no ataxia complaint, despite a great grandmother (II.1) and great-great grandmother (I.1), who had ataxia complaints.

Genetic evaluation showed that subjects 1–3 were confirmed as SCA3 subjects (**Figure 1C**) as they had heterogeneous alleles, with one of the alleles having 68, 71 and 73 expanded CAG repeats, respectively. The other allele had 8 repeats in all three subjects. Subject 4 had an intermediate number of repeats with 23 and 30 CAG repeats. Subject 5 had medium number of CAG repeats (17 and 23), while Subjects 6 and 7 are included as short CAG repeats (13).

From a clinical point of view, according to criteria by Velazquez-Perez et al. (10), Subjects 1 and 2 are considered to have genetically confirmed SCA 3, while Subject 3 is considered prodromal. All other subjects were considered as unaffected. The clinical details of SCA 3 subjects and controls are shown in (**Figure 1C**).

The ages of subjects 1, 2 and 3 were 35, 34 and 18 years old, respectively and the onset of ataxia symptoms were at 22, 13 and 15 years of age, with disease duration of 13, 21, and 3 years, respectively. The clinical features of all three subjects are summarized in (**Figure 1C**). Subject 1, a female had gait ataxia and balance difficulties and muscle cramps, with mild cognitive impairment (MoCA-Ina: 22; MMSE: 24) and a SARA score of 3 (gait: 1; standing: 1; and heel-shin coordination: 1). Subject 2, male, is considered ataxic, complaining of walking and postural problems with a severe talking and mild/moderate coordination problems, with mild cognitive impairment (MoCA-Ina: 23) and a SARA score of 14 (gait: 4; standing: 2; talk: 3; finger chase: 1; nose-finger: 1; hand alternating movement: 1; and heel-shin: 2). Subject 3, male, is considered prodromal and, despite a normal motor condition, has had cognitive complaints from 15 years old (MoCA-Ina 22; MMSE: 21), and a SARA score of 0, plus numbness on his skin. All other

TABLE 1A | Brain MRI volumetry. **(A)** Cerebrum and brainstem.

Group	Subject No	Thalamus	Basal Ganglia	Ventricle	Brainstem	Hippo-campus	Amygdala	nucleus Accumbens	Diencephalon	Corpus Callosum	Cortical Volume	White Matter	Subcortical Gray Matter	Total Gray Matter Volume
SCA3	1	1.05%	1.42%	1.51%	1.51%	0.61%	0.19%	0.09%	0.54%	0.20%	32.93%	29.57%	4.02%	44.78%
	2	0.90%	1.26%	2.33%	1.26%	0.55%	0.21%	0.07%	0.48%	0.20%	29.90%	30.25%	3.59%	40.17%
	3	1.12%	1.58%	1.03%	1.46%	0.56%	0.22%	0.07%	0.57%	0.23%	36.34%	31.68%	4.22%	47.92%
Normal	4	1.06%	1.63%	1.32%	1.63%	0.61%	0.24%	0.08%	0.57%	0.24%	31.82%	31.67%	4.32%	44.13%
	5	0.99%	1.38%	0.97%	1.53%	0.55%	0.20%	0.07%	0.54%	0.23%	30.95%	32.41%	3.84%	42.46%
	6	0.99%	1.49%	1.33%	1.49%	0.50%	0.22%	0.08%	0.57%	0.24%	31.84%	30.94%	3.98%	42.73%
	7	1.07%	1.44%	0.88%	1.50%	0.51%	0.23%	0.09%	0.58%	0.25%	29.74%	31.99%	4.04%	41.33%
	p-value	0.571	0.314	0.114	0.114	0.314	0.114	0.429	0.114	**0.029***	0.200	0.114	0.429	0.314

*$p < 0.05$.

TABLE 1B | Cerebellum.

Group	Subject No	Lobule I-II	Lobule III	Lobule IV	Lobule V	Lobule VI	Lobule Crus I	Lobule Crus II	Lobule VIIB	Lobule VIIIA	Lobule VIIIB	Lobule IX	Lobule X	Total
Volume (%ICV)														
SCA3	1	0.01%	0.08%	0.32%	0.59%	1.30%	1.72%	1.39%	0.71%	0.80%	0.52%	0.48%	0.08%	8.99%
	2	0.01%	0.10%	0.26%	0.50%	1.11%	1.55%	1.13%	0.59%	0.79%	0.51%	0.44%	0.06%	7.98%
	3	0.01%	0.08%	0.33%	0.56%	1.16%	1.62%	1.07%	0.57%	0.90%	0.55%	0.45%	0.07%	8.42%
Normal	4	0.01%	0.09%	0.34%	0.58%	1.35%	2.03%	1.16%	0.78%	0.89%	0.60%	0.53%	0.09%	9.73%
	5	0.01%	0.09%	0.34%	0.55%	1.27%	1.80%	1.11%	0.58%	0.86%	0.62%	0.66%	0.09%	9.09%
	6	0.01%	0.08%	0.35%	0.58%	1.15%	1.45%	1.18%	0.62%	0.82%	0.56%	0.48%	0.07%	8.50%
	7	0.01%	0.10%	0.35%	0.59%	1.39%	2.03%	1.14%	0.66%	0.82%	0.68%	0.64%	0.07%	9.72%
	p-value	**0.029***	0.2	**0.029***	0.314	0.2	0.2	0.429	0.314	0.314	**0.029***	**0.029***	0.114	0.057
Gray Matter Volume (%ICV)														
SCA3	1	0.00%	0.06%	0.29%	0.54%	1.18%	1.50%	1.21%	0.63%	0.72%	0.45%	0.41%	0.07%	7.06%
	2	0.00%	0.08%	0.24%	0.44%	1.01%	1.36%	0.98%	0.53%	0.70%	0.45%	0.36%	0.05%	6.21%
	3	0.00%	0.07%	0.28%	0.46%	1.10%	1.58%	0.90%	0.63%	0.72%	0.48%	0.40%	0.07%	6.70%
Normal	4	0.00%	0.09%	0.35%	0.57%	1.33%	1.83%	1.14%	0.60%	0.89%	0.62%	0.63%	0.09%	8.15%
	5	0.00%	0.06%	0.29%	0.48%	1.04%	1.37%	0.91%	0.50%	0.78%	0.47%	0.36%	0.06%	6.34%
	6	0.00%	0.06%	0.32%	0.51%	1.05%	1.29%	1.05%	0.56%	0.73%	0.49%	0.41%	0.06%	6.53%
	7	0.01%	0.08%	0.30%	0.53%	1.26%	1.78%	0.98%	0.58%	0.72%	0.58%	0.53%	0.07%	7.44%
	p-value	0.314	0.571	**0.029***	0.2	0.314	0.429	0.429	0.2	**0.029***	0.057	0.2	0.571	0.314
Cortical Thickness (mm)														
SCA3	1	2.03	3.48	5.12	5.12	5.12	4.97	4.97	5.00	4.96	5.04	4.64	3.63	4.97
	2	3.56	3.96	5.21	5.11	5.12	5.11	5.02	4.94	4.87	5.04	4.43	3.47	4.98
	3	1.95	3.66	5.18	5.14	5.25	5.04	5.02	5.18	5.03	5.01	4.74	3.23	5.04
Normal	4	2.38	3.70	5.22	5.15	5.21	5.31	5.23	5.12	5.00	5.18	4.94	3.71	5.14
	5	2.28	3.55	5.13	5.01	5.15	5.02	4.84	5.03	4.87	5.04	4.52	3.22	4.94
	6	1.16	3.18	5.22	4.91	5.19	5.17	5.18	5.15	5.04	4.98	4.86	3.51	5.07
	7	2.52	3.30	5.07	5.17	5.17	5.10	4.83	4.96	4.93	4.97	4.54	3.63	4.97
	p-value	0.571	0.2	0.371	0.571	0.257	0.2	0.543	0.429	0.486	0.457	0.314	0.371	0.457

Volume is presented as a percentage of intracranial volume; cortical thickness is presented in mm.

*A heatmap color scale is used. *p < 0.05.*

red smallest — yellow intermediate — green largest

TABLE 1C | Cerebellar atrophy SCA3 subjects.

Subject No.	1	2	3	Function
Lobules I-II	v	v	v	Motor
Lobule III	v	-	v	Motor
Lobule IV	v	v	v	Motor
Lobule V	-	v	o	Motor
Lobule VI	-	v	o	Motor/cognitive
Crus I	-	o	o	Cognitive
Crus II	-	o	v	Cognitive
Lobule VIIB	-	o	v	Cognitive
Lobule VIIIA	v	v	-	Motor
Lobule VIIIB	v	v	v	Motor
Lobule IX	v	v	v	Cognitive
Lobule X	-	v	v	Cognitive

v = smaller volume than in normal subjects.
o = smaller volume than all but 1 normal subject.
- = approximately the same volume as in normal subjects.

subjects (4–7) had <47 CAG repeats, so they were considered unaffected subjects.

Qualitatively, we compared MRI brain images from SCA3 subjects (Subjects 1–3) and a unaffected subject (Subject 7) (**Figure 2**). Dilation of the lateral ventricle (red arrow) and fourth ventricle (green arrow) was observed in Subjects 1 and 2. We also observed smaller brainstem (yellow arrow) and cerebellar (orange arrowhead) volumes. In contrast, the quantitative MRI brain image of Subject 3 is presumably equal to that of a unaffected subject. This might be due to the duration of disease and young age.

Detailed brain volumetric results of subjects grouped by CAG repeats and clinical data can be found in (**Tables 1A,B**) Statistical analysis showed a statistical significance difference between SCA3 and unaffected subjects in volume of corpus callosum, and cerebellum (lobules I-II, lobule IV, lobule VIIB and lobule IX) and also in volume in gray matter of cerebellum (lobule IV, and VIIIA) but not in other measurements.

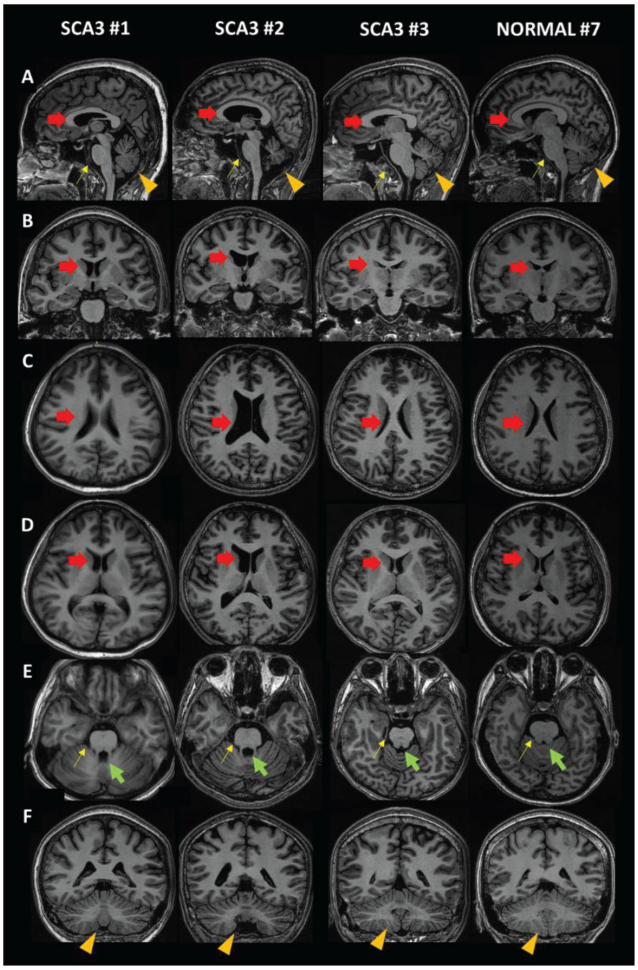

FIGURE 2 | MRI images of SCA3 patients compared to a normal subject. **(A)** Sagittal view. **(B,F)** Coronal view. **(C–E)** Axial view. Red arrow: lateral ventricle (dilated in SCA3); green arrow: fourth ventricle (dilated in SCA3); yellow arrow: brainstem (size reduced in SCA3); orange arrowhead: cerebellum (size reduced in SCA3).

DISCUSSION

SCA3 is a neurological disease which begins as early as the 2nd decade, characterized by progressive cerebellar syndrome and cerebellar atrophy. Brain atrophy occurs as a result of a toxic gain-of-function, mitochondrial bioenergetic problems, ion channel disturbance, RNA toxicity, repeat-associated non-AUG (RAN) translation, transcription problems, DNA damage, protein transport disturbance and altered ubiquitination processes in the brain. This leads to axonal damage and neuronal and glial death (2, 8). Cortical thinning in SCA3 patients has been associated with the death of Purkinje cells as the sole processing neuron in the cerebellum and damage to cortical glia (Bergmann's glia, stellate cells and basket cells), which contributes to progressive incoordination and ataxia (29, 30).

In this study, we were able to compare brain volumetric findings among members from the same family, who were clinically affected and had genetic confirmation of SCA 3 with unaffected subjects who did not carry SCA 3 genetic mutation. Expectedly, the cerebellar volume of the SCA3 subjects was lower than that of the unaffected subjects. There were however variations in the lobules affected among the three subjects affected by SCA 3. Motor and cognitive function are currently known to be controlled not only by the cerebrum but also by the cerebellum. According to the double motor and triple non-motor concept of cerebellar function, the cerebellar lobules are divided into two *motor* areas: (1) lobules I-VI and (2) lobule VIII, while the three non-motor areas are (1) lobule VI/crus I, (2) crus II/lobule VIIB, and (3) lobules IX/X (31–33).

In Subject 1, with an SCA3 duration of 13 years, there were lower brain volumes in almost all motor lobules with partial atrophy in the cognition lobules. Atrophy in the motor

TABLE 2 | Findings in this study compared to other studies.

	This study	**Wan et al.**	**Klaes et al.**	**Arruda et al.**	**de Rezende et al.**	**Guo et al.**	**Faber et al.**	**Hernandez-Castillo et al.**
Study	Indonesian population	Review of 12 studies	Review of 4 studies	Brazilian population	Brazilian population	Chinese population	Brazil, China, France, Germany, Netherland, Spain, UK, and US	Mexican Population
Number of subjects	3 SCA3 patients, 4 normal subjects	252 SCA3 patients, 250 normal subjects	246 SCA3 patients, 246 normal subjects	19 SCA3 patients, 19 normal subjects	49 SCA3 patients, 49 normal subjects	47 SCA3 patients, 49 normal subjects	210 SCA3 patients, 63 healthy subject	17 SCA3 patients, 17 healthy subject
Journal/year	-	*FNeu*: 2020	*Am J Neurorad*: 2016	*Cerebellum*: 2020	*Eur J Neu*: 2014	*Neurology*: 2020	Mov Dis: 2021	Cerebellum Ataxias: 2017
Brain region	**Cerebellum – Gray matter (lobule V, VIIIA) ↓ ***	Cerebellum ↓ (100%)	Cerebellum – hemisphere ↓ (100%) Dentate nucleus ↓(25%)	Cerebellum – cortex ↓	Cerebellum – cortex ↓	Cerebellum – cortex ↓	Cerebellum – volume ↓	Crus II, vermis IX, lobule I-IV – gray ↓
	Cerebellum (lobules I-II, IV, VIIIB, IX) ↓ *		Cerebellum – vermis ↓(75%)	Cerebellum – white matter↓	Cerebellum – white matter↓			
	Cerebellum – cortical thickness – ns		Cerebellum – peduncle ↓(50%)					
	Brainstem – ns	Brainstem ↓ (75%)	Brainstem ↓(100%) Midbrain ↓(50%) Pons ↓(75%) Medulla oblongata ↓(50%)	Brainstem ↓	Brainstem ↓		Midbrain ↓ Pons ↓ Medulla oblongata ↓	Pons ↓
	Ventricle – ns						Ventricle ↑	
	Cerebrum – white matter– ns	Cerebrum ↓ (67%)				Cerebrum – cortex ↓		Left lingual gyrus ↓
	Thalamus – ns	Thalamus ↓ (25%)		Thalamus – ns	Thalamus ↓		Thalamus ↓	
	Basal ganglia – ns	Basal ganglia ↓ (25%)		Pallidum – ns	Caudate nucleus, putamen, pallidum ↓		Caudate nucleus, pallidum ↓	
	Amygdala – ns	Limbic regions↓ (42%)						
	Nucleus accumbens – ns							
	Diencephalon – ns				Diencephalon ↓			
	Corpus callosum ↓*							
	Subcortical gray matter – ns			Subcortical & total gray matter				

*↓: Volume decrease; *: $p < 0.05$; ns, not significant; (%), percentage of patients showing the indicated change.*

regions was in accordance with the ataxia complaints; however, there were some discrepancies in the lobules that command cognition and the subject's cognitive condition. In Subject 2, the volumetric findings corresponded to the motor and cognitive conditions. In Subject 3, the cognitive findings were in accordance with the volumetric findings, although the motoric findings were not in accordance with the volumetric findings (**Table 1C**).

Based on recent publications, there have been different findings on volumetric differences in various brain anatomical structure of patients with SCA3 (17–24) (**Table 2**). Researchers from many regions reported their findings, however there were no report found on ASEAN populations. Wan et al. reviewed 12 publications with a total of 252 subjects and found atrophy in the cerebellum, brain stem, cerebrum, limbic system, basal ganglia and thalamus (19). Klaes et al. reviewed 4 volumetric studies with 246 subjects and found brain atrophy in the cerebellum and brainstem (20). Arruda et al. studied 19 SCA3 subjects in a Brazilian population and showed atrophy in the brainstem and cerebellum (18). Rezende et al. studied 43 SCA3 subjects in a Brazilian population and found vast atrophy in cortical and subcortical regions, including the cerebellum, thalamus, putamen, globus pallidum, diencephalon and brainstem (21). Guo et al. studied 47 SCA3 subjects in a Chinese population and showed progressive atrophy in cerebellar gray matter and several cerebrum regions (22). Faber et al. gathered 210 SCA3 subjects from 8 countries (Brazil, China, France, Germany, Netherland, Spain, UK, and US) and found atrophy in cerebellum, brainstem, thalamus, basal ganglia with dilation of ventricle (23). Hernandez-Castillo et al. studied 17 SCA3 patients from Mexican population and found atrophy in cerebellum, pons and left lingual gyrus (24). Overall there is an agreement that there is decreased cerebellar and cerebral volumes with various other affected regions and with varying degree. Hence, we evaluated MRI brain volumetry with more region than existing publication in SCA3 patients, moreover there are no study examining brain MRI of ASEAN and Indonesian origin. A more thorough evaluation with tractography and an analysis with all the related motor and cognitive brain regions is necessary to clarify the discrepancies observed.

Our patients had onset of disease in the second and third decades, which is relatively early compared to the average published mean age of onset which is in the fifth decade but still fell within the age range of second to sixth decade. Subject 3 was the youngest, with the shortest duration of disease, and therefore had unclear amount of brain atrophy, as age and duration of disease affect the degree of brain atrophy (8, 34–36).

LIMITATIONS OF STUDY

Being case-based and a pilot study, our study is limited by a small sample size, which was affected further by the COVID-19 pandemic during the study period. The COVID-19 pandemic hindered the ability of family members to participate and be examined, due to transportation limitations and isolation protocols from the regional government, in the efforts to prevent the spread of COVID-19 pandemic. A study with larger sample size would be necessary for a more generalizable conclusion.

Despite the limitations, we believe our study findings could contribute to the existing literature on brain volumetry and clinical details of SCA 3 patients, in the South East Asia region, given the paucity of data in this region. To our knowledge, this is the first volumetric evaluation of SCA3 patients conducted in Indonesia. Additionally, as we had also included more brain regions in our evaluation as compared to previous studies, we measured the thalamus, basal ganglia, ventricles, brainstem, amygdala, nucleus accumbens, diencephalon, corpus callosum, white matter, and subcortical gray matter, in addition to the measurement of cerebellar volume, cerebellar gray matter volume and cerebellar cortical thickness. Statistically significant differences were found in volume of corpus callosum, and cerebellum (lobules I-II, lobule IV, lobule VIIB and lobule IX) and also in volume in gray matter of cerebellum (lobule IV, and VIIIA) but not in other measurements.

In conclusion, our findings confirm previous findings that various brain regions are atrophied in SCA 3, and perhaps may involve other parts of the brain not previously reported. However, our findings remain preliminary and need to be verified further in larger studies. Brain MRI volumetric analysis could thus be an additional tool for non-invasive evaluation of patients with degenerative cerebellar ataxia in addition to the currently utilized clinical scales (20, 37).

DATA AVAILABILITY STATEMENT

The original contributions presented in the study are included in the article material, further inquiries can be directed to the corresponding authors.

ETHICS STATEMENT

The studies involving human participants were reviewed and approved by Universitas Padjadjaran, Research Ethic Committee. The patients/participants provided their written informed consent to participate in this study.

AUTHOR CONTRIBUTIONS

SS: study design, conceptualization, data collection, data analysis, manuscript revision, and funding. FH: study design, conceptualization, data collection, data analysis, manuscript drafting, and manuscript revision. TK: study design, data collection, and data analysis. RH: study design, data collection, data analysis, and manuscript drafting. YS: study design, conceptualization, data analysis, manuscript drafting, manuscript revision, and funding. SD, PO, and ND: data analysis

and manuscript revision. IP: study design, data collection, and manuscript revision. UG: study design, data analysis, and manuscript revision. NM: conceptualization and manuscript revision. TA: study design, conceptualization, manuscript revision, and funding. All authors contributed to the article and approved the submitted version.

FUNDING

This research was funded by National Research and Innovation Agency–Ministry of Education, Culture, Research and Technology of Indonesia, via Universitas Padjadjaran no 1207/UN6.3.1/PT.00/2021 for Tri Hanggono Achmad.

REFERENCES

1. Buijsen RaM, Toonen LJA, Gardiner SL, Van Roon-Mom WMC. Genetics, mechanisms, and therapeutic progress in polyglutamine spinocerebellar ataxias. *Neurotherapeutics.* (2019) 16:263–86. doi: 10.1007/s13311-018-00696-y
2. Klockgether T, Mariotti C, Paulson HL. Spinocerebellar ataxia. *Nat Rev Dis Primers.* (2019) 5:24. doi: 10.1038/s41572-019-0074-3
3. Jacobi H, Rakowicz M, Rola R, Fancellu R, Mariotti C, Charles P, et al. Inventory of non-ataxia signs (Inas): validation of a new clinical assessment instrument. *Cerebellum.* (2013) 12:418–28. doi: 10.1007/s12311-012-0421-3
4. Schmitz-Hubsch T, Du Montcel ST, Baliko L, Berciano J, Boesch S, Depondt C, et al. Scale for the assessment and rating of ataxia: development of a new clinical scale. *Neurology.* (2006) 66:1717–20. doi: 10.1212/01.wnl.0000219042.60538.92
5. Kazachkova N, Lima M. Towards a therapeutic intervention in polyglutamine ataxias: from models to clinical trials. *Front Clin Res-CNS Neurolog Disord.* (2015) 3:77–130. doi: 10.2174/9781608059263114030006
6. Matos CA, De Almeida LP, Nobrega C. Machado-joseph disease/spinocerebellar ataxia type 3: lessons from disease pathogenesis and clues into therapy. *J Neurochem.* (2019) 148:8–28. doi: 10.1111/jnc.14541
7. Rub U, Brunt ER, Deller T. New insights into the pathoanatomy of spinocerebellar ataxia type 3 (machado-joseph disease). *Curr Opin Neurol.* (2008) 21:111–6. doi: 10.1097/WCO.0b013e3282f7673d
8. Du Montcel ST, Durr A, Bauer P, Figueroa KP, Ichikawa Y, Brussino A, et al. Modulation of the age at onset in spinocerebellar ataxia by cag tracts in various genes. *Brain.* (2014) 137(Pt 9):2444–55. doi: 10.1093/brain/awu174
9. Da Silva JD, Teixeira-Castro A, Maciel P. From pathogenesis to novel therapeutics for spinocerebellar ataxia type 3: evading potholes on the way to translation. *Neurotherapeutics.* (2019) 16:1009–31. doi: 10.1007/s13311-019-00798-1
10. Velazquez-Perez LC, Rodriguez-Labrada R, Fernandez-Ruiz J. Spinocerebellar ataxia type 2: clinicogenetic aspects, mechanistic insights, and management approaches. *Front Neurol.* (2017) 8:472. doi: 10.3389/fneur.2017.00472
11. Seidel K, Den Dunnen WF, Schultz C, Paulson H, Frank S, De Vos RA, et al. Axonal inclusions in spinocerebellar ataxia type 3. *Acta Neuropathol.* (2010) 120:449–60. doi: 10.1007/s00401-010-0717-7
12. Seidel K, Siswanto S, Brunt ER, Den Dunnen W, Korf HW, Rub U. Brain pathology of spinocerebellar ataxias. *Acta Neuropathol.* (2012) 124:1–21. doi: 10.1007/s00401-012-1000-x
13. Mccord MR, Bigio EH, Kam KL, Fischer V, Obeidin F, White CL, et al. Spinocerebellar ataxia type 3: a case report and literature review. *J Neuropathol Exp Neurol.* (2020) 79:641–46. doi: 10.1093/jnen/nlaa033
14. Tada M, Nishizawa M, Onodera O. Redefining cerebellar ataxia in degenerative ataxias: lessons from recent research on cerebellar systems. *J Neurol Neurosurg Psychiatry.* (2015) 86:922–8. doi: 10.1136/jnnp-2013-307225
15. Chow N, Hwang KS, Hurtz S, Green AE, Sømme JH, Thompson PM, et al. Comparing 3t and 1.5t Mri for mapping hippocampal atrophy in the Alzheimer's disease neuroimaging initiative. *Am J Neuroradiol.* (2015) 36:653–60. doi: 10.3174/ajnr.A4228
16. Ladd ME, Bachert P, Meyerspeer M, Moser E, Nagel AM, Norris DG, et al. Pros and cons of ultra-high-field Mri/Mrs for human application. *Prog Nucl Magn Reson Spectrosc.* (2018) 109:1–50. doi: 10.1016/j.pnmrs.2018.06.001
17. Piccinin CC, Rezende TJR, De Paiva JLR, Moyses PC, Martinez ARM, Cendes F, et al. A 5-year longitudinal clinical and magnetic resonance imaging study in spinocerebellar ataxia type 3. *Mov Disord.* (2020) 35:1679–84. doi: 10.1002/mds.28113
18. Arruda WO, Meira AT, Ono SE, De Carvalho Neto A, Betting L, Raskin S, et al. Volumetric Mri changes in spinocerebellar ataxia (Sca3 and Sca10) patients. *Cerebellum.* (2020) 19:536–43. doi: 10.1007/s12311-020-01137-3
19. Wan N, Chen Z, Wan L, Tang B, Jiang H. Mr imaging of Sca3/Mjd. *Front Neurosci.* (2020) 14:749. doi: 10.3389/fnins.2020.00749
20. Klaes A, Reckziegel E, Franca MC Jr, Rezende TJ, Vedolin LM, Jardim LB, et al. Mr imaging in spinocerebellar ataxias: a systematic review AJNR. *Am J Neuroradiol.* (2016) 37:1405–12. doi: 10.3174/ajnr.A4760
21. De Rezende TJ, D'abreu A, Guimarães RP, Lopes TM, Lopes-Cendes I, Cendes F, et al. Cerebral cortex involvement in machado-joseph disease. *Eur J Neurol.* (2015) 22:277–83, e23–4. doi: 10.1111/ene.12559
22. Guo J, Chen H, Biswal BB, Guo X, Zhang H, Dai L, et al. Gray matter atrophy patterns within the cerebellum-neostriatum-cortical network in Sca3. *Neurology.* (2020) 95:e3036–44. doi: 10.1212/WNL.0000000000010986
23. Faber J, Schaprian T, Berkan K, Reetz K, Franca MC Jr, De Rezende TJR, et al. Regional brain and spinal cord volume loss in spinocerebellar ataxia type 3. *Mov Disord.* (2021) 36:2273–81. doi: 10.1002/mds.28610
24. Hernandez-Castillo CR, Diaz R, Campos-Romo A, Fernandez-Ruiz J. Neural correlates of ataxia severity in spinocerebellar ataxia type 3/machado-joseph disease. *Cerebellum Ataxias.* (2017) 4:7. doi: 10.1186/s40673-017-0065-7
25. Medixant. Radiant Dicom Viewer. 2020.2 ed2020. Available online at: https://www.radiantviewer.com
26. Reuter M, Schmansky NJ, Rosas HD, Fischl B. Within-subject template estimation for unbiased longitudinal image analysis. *Neuroimage.* (2012) 61:1402–18. doi: 10.1016/j.neuroimage.2012.02.084
27. Imaging MCFB. *Freesurfer. 711 ed: Harvard Medical School, Massachusetts General Hospital* (2021). Available online at: https://surfer.nmr.mgh.harvard.edu/
28. Manjon JV, Coupe P. Volbrain: an online Mri brain volumetry system. *Front Neuroinform.* (2016) 10:30. doi: 10.3389/fninf.2016.00030
29. Scherzed W, Brunt ER, Heinsen H, De Vos RA, Seidel K, Bürk K, et al. Pathoanatomy of cerebellar degeneration in spinocerebellar ataxia type 2 (Sca2) and type 3 (Sca3). *Cerebellum.* (2012) 11:749–60. doi: 10.1007/s12311-011-0340-8
30. Robinson KJ, Watchon M, Laird AS. Aberrant cerebellar circuitry in the spinocerebellar ataxias. *Front Neurosci.* (2020) 14:707. doi: 10.3389/fnins.2020.00707
31. Guell X, Schmahmann J. Cerebellar functional anatomy: a didactic summary based on human Fmri evidence. *The Cerebellum.* (2020) 19:1–5. doi: 10.1007/s12311-019-01083-9
32. Guell X, Gabrieli JDE, Schmahmann JD. Triple representation of language, working memory, social and emotion processing in the cerebellum: convergent evidence from task and seed-based resting-state fmri analyses in a single large cohort. *Neuroimage.* (2018) 172:437–49. doi: 10.1016/j.neuroimage.2018.01.082
33. Buckner RL, Krienen FM, Castellanos A, Diaz JC, Yeo BT. The organization of the human cerebellum estimated by intrinsic functional connectivity. *J Neurophysiol.* (2011) 106:2322–45. doi: 10.1152/jn.00339.2011
34. Paulson HL. The spinocerebellar ataxias. *J Neuroophthalmol.* (2009) 29:227–37. doi: 10.1097/WNO0b013e3181b416de
35. Mcloughlin HS, Moore LR, Paulson HL. Pathogenesis of Sca3 and Implications for other polyglutamine diseases. *Neurobiol Dis.* (2020) 134:104635. doi: 10.1016/j.nbd.2019.104635
36. Paulson HL, Shakkottai VG, Clark HB, Orr HT. Polyglutamine spinocerebellar ataxias - from genes to potential treatments. *Nat Rev Neurosci.* (2017) 18:613–26. doi: 10.1038/nrn.2017.92

37. Stefanescu MR, Dohnalek M, Maderwald S, Thürling M, Minnerop M, Beck A, et al. Structural and functional Mri abnormalities of cerebellar cortex and nuclei in Sca3, Sca6 and friedreich's ataxia. *Brain*. (2015) 138(Pt 5):1182–97. doi: 10.1093/brain/awv064

Conflict of Interest: The authors declare that the research was conducted in the absence of any commercial or financial relationships that could be construed as a potential conflict of interest.

Publisher's Note: All claims expressed in this article are solely those of the authors and do not necessarily represent those of their affiliated organizations, or those of the publisher, the editors and the reviewers. Any product that may be evaluated in this article, or claim that may be made by its manufacturer, is not guaranteed or endorsed by the publisher.

frontiers | Frontiers in Neurology

CASE REPORT
published: 13 July 2022
doi: 10.3389/fneur.2022.919280

Case Report: Dural Dissection With Ventral Spinal Fluid-Filled Collection in Superficial Siderosis: Insights Into the Pathology From Anterior-Approached Surgical Cases

Toshitaka Yoshii[1]*, *Takashi Hirai*[1], *Satoru Egawa*[1], *Motonori Hashimoto*[1], *Yu Matsukura*[1], *Hiroyuki Inose*[1], *Nobuo Sanjo*[2], *Takanori Yokota*[2] and *Atsushi Okawa*[1]

[1] Department of Orthopaedic and Spinal Surgery, Graduate School, Tokyo Medical and Dental University, Tokyo, Japan, [2] Department of Neurology, Tokyo Medical and Dental University, Tokyo, Japan

OPEN ACCESS

Edited by:
Bruce Miller,
University of California, San Francisco, United States

Reviewed by:
Luca Ricciardi,
Sapienza University of Rome, Italy
Ho-Sung Ryu,
Kyungpook National University Hospital, South Korea

***Correspondence:**
Toshitaka Yoshii
yoshii.orth@tmd.ac.jp

Specialty section:
This article was submitted to Dementia and Neurodegenerative Diseases, a section of the journal Frontiers in Neurology

Received: 13 April 2022
Accepted: 20 June 2022
Published: 13 July 2022

Citation:
Yoshii T, Hirai T, Egawa S, Hashimoto M, Matsukura Y, Inose H, Sanjo N, Yokota T and Okawa A (2022) Case Report: Dural Dissection With Ventral Spinal Fluid-Filled Collection in Superficial Siderosis: Insights Into the Pathology From Anterior-Approached Surgical Cases. Front. Neurol. 13:919280. doi: 10.3389/fneur.2022.919280

Superficial siderosis (SS) of the central nervous system is a rare disease caused by chronic and repeated hemorrhages in the subarachnoid space. Recently, attention has been paid on the association of SS and dural defect with ventral fluid-filled collection in the spinal canal (VFCC). The pathophysiology of hemosiderin deposition in patients with SS and dural defects is still unclear. However, previous studies have suggested the possible mechanism: cerebrospinal fluid (CSF) leaks into the epidural space through the ventral dural defect, and repetitive bleeding occurs from the epidural vessels that circulate back to the subarachnoid space through the dural defect, leading to hemosiderin deposition on the surface of the brain, the central nerves, and the spinal cord. Previously, the surgical closure of dural defect *via* the posterior approach has been reported to be effective in arresting the continued subarachnoid bleeding and disease progression. Herein, we describe SS cases whose dural defects were repaired *via* the anterior approach. From the direct anterior approach to the ventral dural defect findings, we confirmed that the outer fibrous dura layer is intact, and the defect is localized in the inner thin layer. From the findings of this study, our proposed theory is that dural tear at the inner dural layer causes "dural dissection," which is likely to occur between the outer fibrous layer and inner dural border cellular layer. Bleeding from the vessels between the inner and outer Line 39–40 dural layers seems to be the pathology of SS with dural defect.

Keywords: superficial siderosis, fluid-filled collection, anterior approach, dural closure, dural dissection, inner layer dural dissection in superficial siderosis 2

INTRODUCTION

Superficial siderosis (SS) of the central nervous system (CNS) is a rare disease caused by chronic and repeated hemorrhages in the subarachnoid space. The subsequent deposition of hemosiderin on the brain and spinal cord surfaces leads to the development of neurological disturbance (1, 2). Progressive cerebellar ataxia, sensorineural deafness, and dementia are clinical features of SS (2, 3). The causes of bleeding include prior intradural surgery, carcinoma, vascular malformation, nerve root avulsion, and dural abnormality (2–4).

Recently, attention has been paid on the association of SS and dural defect with ventral fluid-filled collection in the spinal canal (VFCC) (5–10). The pathophysiology of hemosiderin deposition in patients with SS and dural defects is still unclear. However, previous studies have suggested the possible mechanism: cerebrospinal fluid (CSF) leaks into the epidural space through the ventral dural defect, and repetitive bleeding occurs from the epidural vessels that infiltrate into the subarachnoid space through the dural defect, leading to hemosiderin deposition on the surface of the brain, central nerves, and the spinal cord (8, 11, 12). Therefore, dural closure is considered to stop the bleeding that enters to the subarachnoid space through the defect.

Previous pieces of literature have described the surgical closure of dural defect *via* the posterior approach is effective in arresting the continued subarachnoid bleeding and disease progression (5, 6, 11–14). Herein, we describe two SS cases whose dural defects were located at the C7-T1 level and were repaired *via* the anterior approach. This is the first report of cases implementing anterior-approached dural closures. We further describe a SS case who received dural closure *via* the traditional posterior approach. From these cases, we obtained important anatomical and histological findings: The outer fibrous dura layer is intact, and the defect is localized in the inner thin layer. The SS pathology from the findings of these cases is further discussed in this study.

ANTERIOR-APPROACHED DURAL CLOSURE

Written informed consent was obtained from the patients.

Case 1: A 51-year-old male (Case 1) presented with a 5-year history of hearing loss, ataxia, unsteady gait, diplopia, and slurred speech. The patient also had dull headache. The symptoms' onset was gradual, and the clinical course was slowly progressive. The patient showed hyperactive tendon reflexes. The CSF examination showed an increased red blood cell (RBC) count (>1,000) and low pressure (10-mm H_2O). Magnetic resonance imaging (MRI) showed a T2-weighted hypointensity in the superficial brain and along the spinal cord due to hemosiderin deposition (**Figures 1A,B**). Sagittal MRI image showed VFCC from C5 to T7 in the spinal canal (**Figure 1B**). A fast imaging employing steady-state acquisition (FIESTA) image demonstrated that a dural defect was suspected at the C7-T1 level (**Figure 1C**) and was confirmed by dynamic computed tomography (CT) myelography. No other abnormalities causing SS were found.

A C7 corpectomy was performed through standard left-anterior approach, and then the posterior longitudinal ligament (PLL) was resected. The T1's posterior vertebral edge was further undercut to make an appropriate space for the dural suture. The epidural space was completely exposed with approximately a 20-mm width, which revealed that the surface of outer dura mater is completely intact. Then, the dura (outer dura) was cut with a 20-mm longitudinal length, which revealed a 5-mm-long defect in the dura mater's inner layer (**Figure 1D**). A bleeding clot was recognized at the inter-layer between the inner and outer dural layers. The inner dural defect was closed using a 7-0 nylon suture (**Figure 1E**) and sealed with a fibrin glue. The inter-layer cavity was filled with mixture of muscle fragments and a fibrin glue, and then the outer layer was sutured using a 5-0 nylon. The superficial layer of the dura was histologically examined using hematoxylin-eosin staining, showing rich collagen fibers with hemosiderin deposition (**Figure 1F**). The spine was fused using a cage and a plate (**Figure 1G**). There were no perioperative adverse events. Post-operative MRI showed the dural defect was repaired (**Figure 1H**). Post-operatively, his headache was improved. The patient's neurological symptoms were stabilized, although a drastic improvement in the clinical manifestation was not observed. The patient was satisfied with the surgical treatment.

Case 2: A 69-year-old female presented with a 16-year history of hearing loss, progressive gait difficulties, diplopia, and dysarthria. The symptoms were gradually progressive. The patient had a history of severe headache at the age of 27 years old. The headache continued for more than 1 year but was spontaneously resolved. The CSF examination showed an increased RBC count (>1,000). A T2-weighted MRI revealed hypointensity in the superficial brain and along the spinal cord, suggestive of hemosiderin deposition (**Figures 2A,B**). VFCC was observed from C3 to T2 on the sagittal images (**Figure 2B**). A dural defect was detected at the C7-T1 level on the axial FIESTA image (**Figure 2C**) and dynamic CT myelography. The imaging studies did not show any other findings causing SS.

After C7 corpectomy and partial corpectomy of T1 were performed, the PLL was resected. Similarly, the outer layer of dura was completely intact. Then, the outer dura layer's center was cut longitudinally, which revealed a 4-mm-long defect in the dura mater's inner layer (**Figure 2D**). Since the inner dural layer was extremely thin and fragile, the defect was repaired using a free fat graft (**Figure 2E**). The fat graft was placed at the defect and was sutured with the surrounding inner dura mater. Then, a fibrin glue was used for sealing. The inter-layer cavity was filled with mixture of muscle fragments and a fibrin glue, and then the outer layer was sutured using a 5-0 nylon. The histology of the superficial layer demonstrated that rich collagen fibers were oriented in a longitudinal direction (**Figure 2F**). The spine was fused using a cage and a plate (**Figure 2G**), and post-operative MRI showed the dural defect was repaired (**Figure 2H**). Post-operatively, the patient's neurological symptoms did not deteriorate.

POSTERIOR-APPROACHED DURAL CLOSURE

Written informed consent was obtained from the patient. A 79-year-old male (Case 3) presented with a 24-year history of hearing loss, gait difficulties, and unilateral motor palsy in the left upper limb. The symptoms' onset was gradually progressive. The patient had not experienced obvious symptoms related to CSF hypovolemia. The CSF examination showed an increased RBC count (>1,000).

A T2-weighted MRI indicated hemosiderin deposition on the superficial brain and the spinal cord

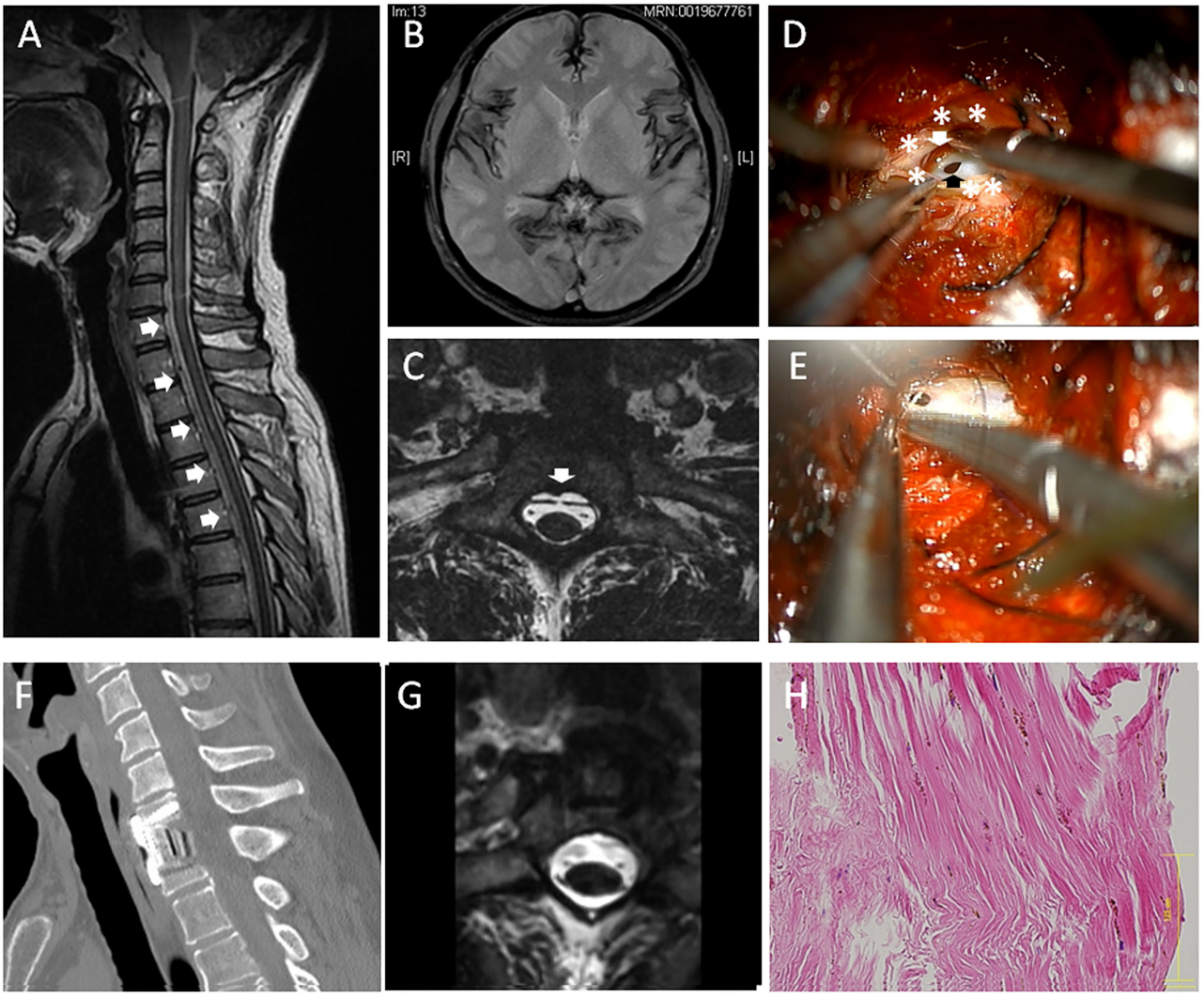

FIGURE 1 | A 51-year-old male (case 1). **(A)** Sagittal magnetic resonance imaging (MRI) showed ventral fluid-filled collection in the spinal canal (VFCC) (white arrows) from C5 to T7. **(B)** Brain MRI showed a T2-weighted hypointensity in the superficial brain. **(C)** A fast imaging employing steady-state acquisition (FIESTA) image demonstrated a dural defect at the C7-T1 level (the white arrow). **(D)** An intraoperative picture of anterior approach (case 1): After the outer dura layer (white asterisks) was cut longitudinally, we found a dural defect (the black arrow) in the dura mater's inner layer. A bleeding clot was recognized between the inner and outer dural layers (the white arrow). **(E)** The dural defect was sutured using a 7-0 nylon. **(F)** The spine was reconstructed using a cage and a plate. **(G)** Post-operative MRI showed the dural defect was successfully repaired. **(H)** The outer layer of the dura was histologically examined using hematoxylin-eosin (HE) staining, showing rich collagen fibers with hemosiderin deposition. The bar: 125 μm.

(**Figures 3A,B**). VFCC was observed from C7 to T7 on the sagittal images (**Figure 3B**). A dural defect was detected at the T2 level on the axial FIESTA image (**Figure 3C**). There were no other findings, which could cause SS.

A posterior laminectomy was performed from T1 to T2. The dura mater was incised at the left posterolateral, site and the spinal cord was gently retracted after the dentate ligament was resected. A 6-mm vertical dural defect was identified anteriorly on the paramedian left side at T1-2 level. We dissected the ventral epidural space and pushed the surface of dura (outer dura) from the anterolateral direction (**Figure 3D**). Then, we observed the intact outer dura through the dural defect, which was supposed to locate in the inner dura mater. We put mixture of muscle fragments and a fibrin glue into the inter-layer cavity through the dural defect, and sutured the ventral dural defect using a 7-0 nylon. Then, the posterolateral dura was closed and sealed with a glue. Similar to the anterior-approached cases, the histology of the superficial layer demonstrated rich collagen fibers oriented in a longitudinal direction (**Figure 3E**). Post-operatively, neurological symptoms did not deteriorate.

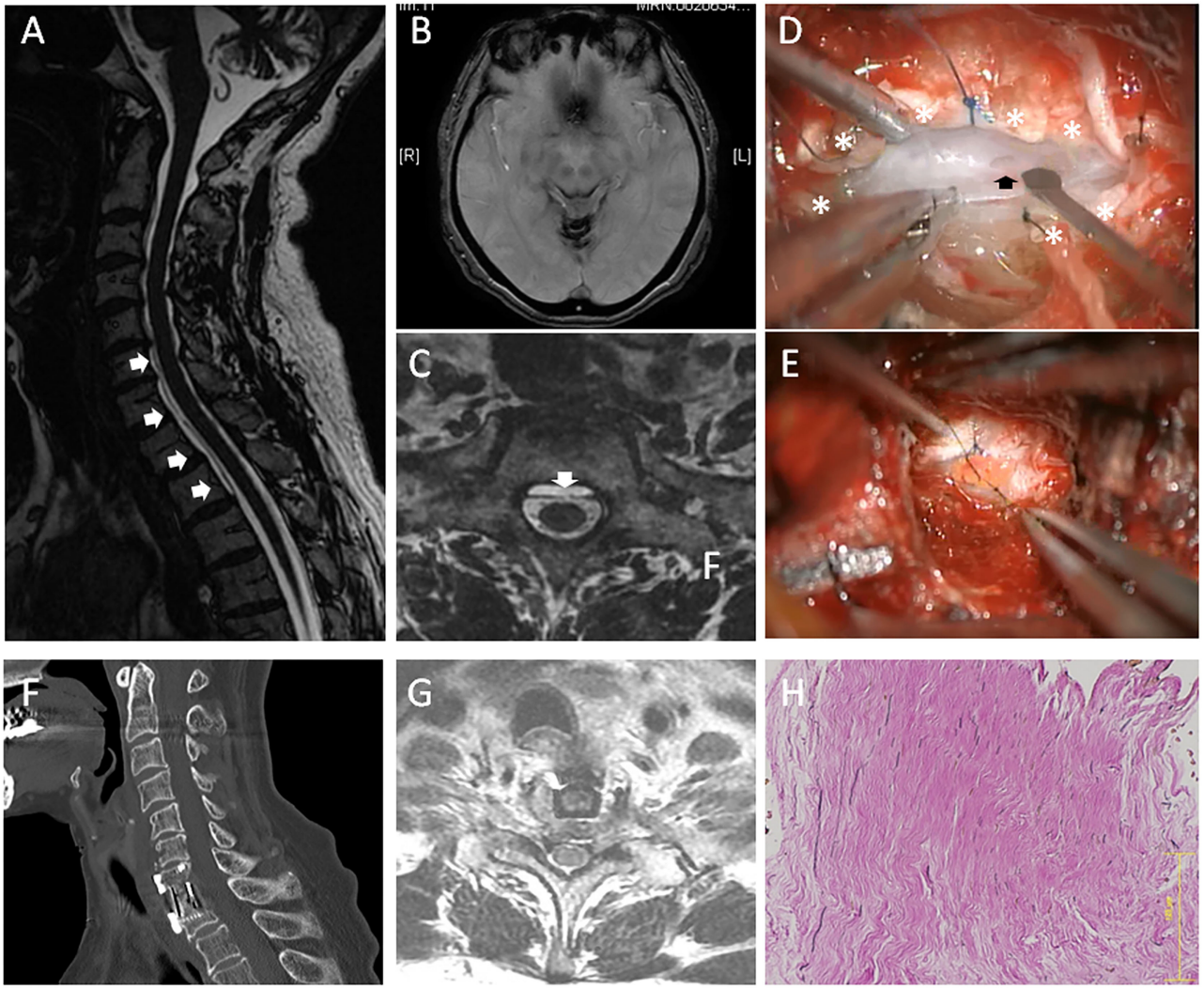

FIGURE 2 | A 69-year-old female (case 2). **(A)** Sagittal MRI showed VFCC from C3 to T2 in the spinal canal (white arrows). **(B)** Brain MRI showed a hemosiderin deposition in the superficial brain. **(C)** An axial FIESTA image demonstrated that a dural defect was located at the C7-T1 level (the white arrow). **(D)** An intraoperative picture of anterior approach (case 2): After the outer dura layer (white asterisks) was excised at the center, we found a dural defect (the black arrow) in the dura mater's inner layer. **(E)** Since the inner dural layer was extremely thin and fragile, the defect was repaired using a free fat graft. **(F)** The spine was fused using a cage and a plate. **(G)** Post-operative MRI showed the dural defect was repaired. **(H)** The histology of the outer layer (HE staining) demonstrated that rich collagen fibers were oriented in a longitudinal direction. The bar: 125 μm.

DISCUSSIONS

SS of the CNS is a rare condition. The clinical features include progressive cerebellar ataxia, dysarthria, sensorineural hearing loss, bladder disturbance, and myelopathy (1–3, 15). The pathology of SS is chronic and repetitive subarachnoid hemorrhaging and a resulting hemosiderin deposition around the brainstem, the cerebellum, and the spinal cord. Recurrent subarachnoid hemorrhaging leads to the overproduction of hemoglobin-degradation products (16): toxic and unbound ferric ions accumulate when the protective mechanisms are exhausted because of chronic and repetitive hemorrhaging. It is reported that the neuronal injury was caused by subsequent free radical damage, lipid peroxidation, and membrane dysfunction (16).

Recently, there have been increasing reports of SS cases accompanied with a ventral dural defect in the spinal canal (5–10). Several authors have reported on the effectiveness of surgical defect closure for this type of SS. The pathophysiology of hemosiderin deposition in patients with SS and dural defects is still unclear. However, many authors have suggested that CSF leaks into the "epidural" space through the ventral dural defect, and repetitive bleeding occurs from the "epidural" vessels that infiltrate back to the subarachnoid space through the dural defect, leading to hemosiderin deposition in the brain, the central

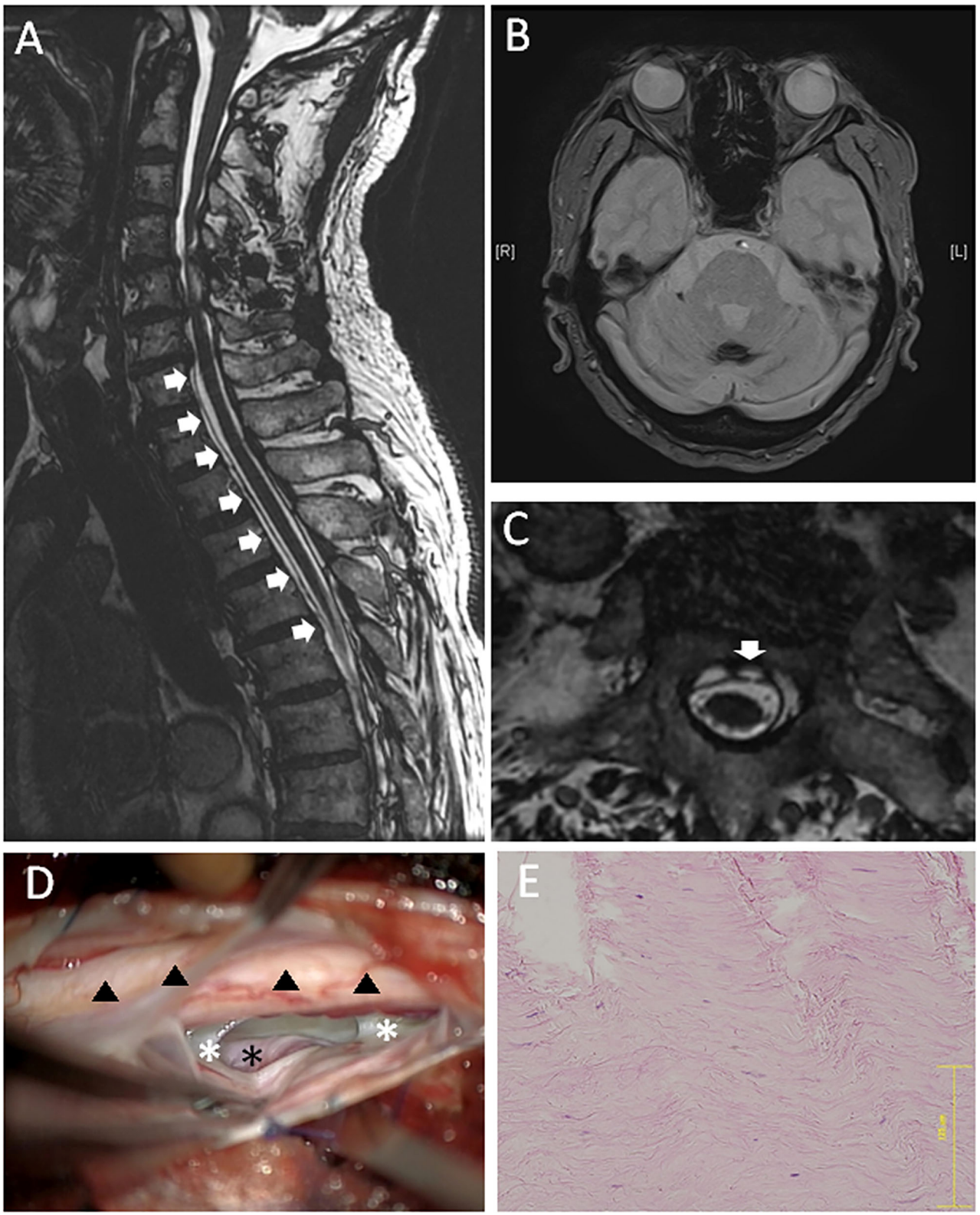

FIGURE 3 | A 79-year-old male (case 3). **(A)** Sagittal MRI showed VFCC from C7 to T7 in the spinal canal (white arrows). **(B)** Brain MRI showed a hemosiderin deposition at the sulcus. **(C)** An axial FIESTA image at the T2 level demonstrated a defect located at the left paramedian anterior dura (the white arrow). **(D)** An

(Continued)

FIGURE 3 | intraoperative picture of posterior approach: The left ventral epidural space was dissected, and the surface of dura (outer dura: white asterisks) was pushed up from the anterolateral direction. The intact outer dura was observed through the dural defect, which was supposed to locate in the inner dura mater (the black asterisk). Hemosiderin deposition was observed on the spinal cord (black triangles). **(E)** The histology of the outer layer (HE staining) demonstrated rich collagen fibers. The bar: 125 μm.

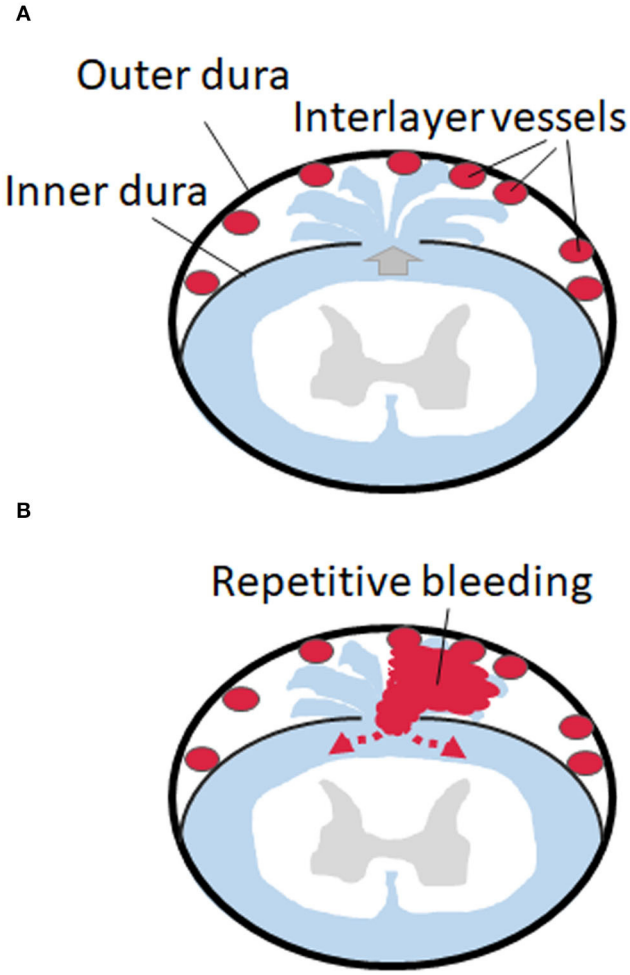

FIGURE 4 | Schemes of the dural dissection and bleeding form the dissected space. **(A)** Dural tear at the inner dural layer causes "dural dissection" between the outer fibrous thick layer and the inner thin layer. A CSF leak causes venous dilatation in the inter-layer space. **(B)** The receptive dynamic CSF flow into the dissected space causes the chronic bleeding from the rich-dilated vessels localized between the inner and outer layers, which circulate back to the subarachnoid space.

nerves, and the spinal cord (8, 10–12, 17). Therefore, dural closure can effectively stop not only the CSF leak but also the repetitive bleeding that enters to the subarachnoid space through the defect. Indeed, our study and others have reported that a surgical dural closure resulted in stopping of the CSF leak as well as bleeding and subsequent disease progression (5, 6, 8, 9, 14).

Surgical repair is generally performed *via* the posterior approach. After adequate levels of laminectomies are performed, the posterior dura is incised posteriorly, and the anterior dura is sutured while the spinal cord is gently retracted. When the defect is located at the anterior dura mater's center, this procedure is sometimes very difficult. Previous literature has shown that the defect is sometimes impossible to suture directly, and muscle fragments packing is performed instead (5, 14). Also, in cases with spinal cord herniation, surgeons sometimes prefer to expand the defect instead of a direct suture because of difficulty and risk of spinal cord injury (18). On the other hand, dural repair through an anterior approach can avoid spinal cord retraction, which can minimize the risk of neurological deterioration caused by surgery. If the dural defect is located at the C7-T1 level or above, surgeons can anatomically access the defect through an anterior approach and can easily make a direct suture without touching the spinal cord. Furthermore, we cannot sacrifice the C8 or T1 nerve root for spinal cord retraction. Therefore, anterior approach is more suitable for the C7-T1 level or above for safe surgery, especially in cases whose dural defect was located at the dura center. On the other hand, it is hard to anteriorly access the T2 level or below because the sternal bone anatomically disturbs the approach. A sternal splitting approach can make it possible but is associated with greater invasiveness. Therefore, if the defect is located at the T2 level or below, posterior approach is more preferable. Indeed, we selected anterior approach for Cases 1 and 2 (defects at C7-T1), but posterior approach for Case 3 (defect at T2).

We note that important findings were obtained from the anterior approach cases where we could observe the environment of the dural defect and CSF leak directly after removal of vertebrae and PLL. We observed that the dural defect was located at the dura's thin inner layer, while the thick outer layer was completely intact. As stated above, many authors have described that the bleeding occurs in the "epidural" space and infiltrates to the subarachnoid space *via* the small dural defect (8, 10, 11, 17, 19). Our findings refute these previous studies, reporting that the chronic repetitive bleeding occurs from the "epidural" vessels. Although a previous report has suggested the possibility of a "duplicate dura" in the cases of SS with VFCC (20) based on MRI images' findings, to our knowledge, no studies have proved the theory based on surgical and histological findings from anterior approach.

The dura's outermost portion was very thin membrane with less extracellular collagen, which is usually difficult to recognize during surgery. Except this thin membrane, there are two main layers of dura mater. The outer layer is the thickest portion, which is richly made up of extracellular collagen. This thick layer is called the "fibrous dura," which we usually recognized as the dura's superficial layer (outer dura). In the inner side of the fibrous dura, there is a thin layer called the dural border cellular layer (the DBC layer), characterized by relatively few

cell junctions, no extracellular collagen, and multiple enlarged extracellular spaces (21, 22). This has been suggested as the structurally weakest plane in the dura-arachnoid continuum. In our study's surgical findings, there existed a thick intact layer on the dura's outer side, and a defect was clearly detected in the inner thin layer in all these cases. The outer layer was histologically compatible to be a "fibrous dural layer" composed of rich collagen fibers. Thus, the thin inner layer is considered to be the weak DBC layer, which lacks cell junctions and extracellular collagen, where the dural defect was found. Since these DBC layers are composed of less vascularization, the defect may be difficult to repair spontaneously. Furthermore, the "epidural blood patch," which is a CSF leak treatment method by blood injection to the epidural space, is considered to have no effect for this dural defect, because the "epidural" injection does not reach the defect located in the inner dural layer.

Interestingly, it is known that rich vascular tissues exist in and around the fibrous dura layer (21, 22). Therefore, the pathology of an SS with spinal VFCC could be supposed as bleeding from the vessels located in the inter-dural layers (between the fibrous layer and the DBC layer) but not from "epidural" vessels. It is also known that a CSF leak can cause venous dilatation outside the arachnoid space. From the findings of this study, our proposed theory is that dural tear at the inner dural layer causes "dural dissection," which is likely to occur between the outer fibrous layer and the inner DBC layer. The receptive dynamic CSF flow into the dissected space causes the chronic bleeding from the rich-dilated vessels localized between the inner and outer layers (**Figures 4A,B**). Dynamic continuous CSF flow may disturb arrest of bleeding by removing clots over the vessels. Therefore, from the cases presented in this report, dural dissection and bleeding from the inter-layer vessels, rather than the bleeding from the epidural venous plexus, are considered the true pathology of the SS accompanied with VFCC.

CONCLUSION

From the direct approach to the ventral dural defect, we confirmed that the outer fibrous dura layer is intact, and the defect is localized in the inner thin layers. This finding suggests that dural dissection and bleeding from the space between the outer and inner dural layers seem to be the true pathology of SS with dural defect.

DATA AVAILABILITY STATEMENT

The raw data supporting the conclusions of this article will be made available by the authors, without undue reservation.

ETHICS STATEMENT

The studies involving human participants were reviewed and approved by the Tokyo Medical and Dental University Ethical Committee. The patients/participants provided their written informed consent to participate in this study. Written informed consent was obtained from the patients for the publication of any potentially identifiable images or data included in this article.

AUTHOR CONTRIBUTIONS

TYos, TH, SE, MH, YM, and HI designed the study, collected data, analyzed the data, interpreted the data for the work, drafted the work, critically revised it, and finally approved it. NS, TYok, and AO analyzed the results, drafted and critically revised the manuscript, and finally approved it. All authors agreed to be accountable for all the aspects of the work in ensuring that questions related to the accuracy or integrity of any part of the work are appropriately investigated and resolved.

REFERENCES

1. Fearnley JM, Stevens JM, Rudge P. Superficial siderosis of the central nervous system. *Brain.* (1995) 118(Pt 4):1051–66. doi: 10.1093/brain/118.4.1051
2. Kumar N, Cohen-Gadol AA, Wright RA, Miller GM, Piepgras DG, Ahlskog JE. Superficial siderosis. *Neurology.* (2006) 66:1144–52. doi: 10.1212/01.wnl.0000208510.76323.5b
3. Levy M, Turtzo C, Llinas RH. Superficial siderosis: a case report and review of the literature. *Nat Clin Pract Neurol.* (2007) 3:54–58. doi: 10.1038/ncpneuro0356
4. Miliaras G, Bostantjopoulou S, Argyropoulou M, Kyritsis A, Polyzoidis K. Superficial siderosis of the CNS: report of three cases and review of the literature. *Clin Neurol Neurosurg.* (2006) 108:499–502. doi: 10.1016/j.clineuro.2005.01.014
5. Kumar N, Lane JI, Piepgras DG. Superficial siderosis: sealing the defect. *Neurology.* (2009) 72:671–3. doi: 10.1212/01.wnl.0000342457.22536.af
6. Ikeda T, Noto D, Noguchi-Shinohara M, Ono K, Takahashi K, Ishida C, et al. CSF tau protein is a useful marker for effective treatment of superficial siderosis of the central nervous system: two case reports. *Clin Neurol Neurosurg.* (2010) 112:62–4. doi: 10.1016/j.clineuro.2009.08.020
7. Kumar N, Miller GM, Piepgras DG, Mokri B. A unifying hypothesis for a patient with superficial siderosis, low-pressure headache, intraspinal cyst, back pain, and prominent vascularity. *J Neurosurg.* (2010) 113:97–101. doi: 10.3171/2009.10.JNS091125
8. Cheng CY, Chen MH, Wang SJ, Lin KP. A proposed mechanism of superficial siderosis supported by surgical and neuroimaging findings. *Med Hypotheses.* (2011) 76:823–6. doi: 10.1016/j.mehy.2011.02.028
9. Kumar N. Beyond superficial siderosis: introducing "duropathies". *Neurology.* (2012) 78:1992–9. doi: 10.1212/WNL.0b013e318259e272
10. Kumar N. Diskogenic dural defect is the reason for the ventral location of the epidural spinal fluid collection seen in superficial siderosis. *Neurol Clin Pract.* (2021) 11:e508–15. doi: 10.1212/CPJ.0000000000001085
11. Takai K, Komori T, Niimura M, Taniguchi M. Superficial siderosis of the central nervous system associated with intraspinal hemorrhage from ventral thoracic epidural veins and a ventral spinal CSF leak: case report. *J Neurosurg Spine.* (2017) 26:751–3. doi: 10.3171/2016.11.SPINE16488
12. Takai K, Taniguchi M. Superficial siderosis of the central nervous system associated with ventral dural defects: bleeding from the epidural venous plexus. *J Neurol.* (2021) 268:1491–4. doi: 10.1007/s00415-020-10319-2
13. Shih P, Yang BP, Batjer HH, Liu JC. Surgical management of superficial siderosis. *Spine J.* (2009) 9:e16–9. doi: 10.1016/j.spinee.2009.03.004
14. Egawa S, Yoshii T, Sakaki K, Inose H, Kato T, Kawabata S, et al. Dural closure for the treatment of superficial siderosis. *J Neurosurg Spine.* (2013) 18:388–93. doi: 10.3171/2013.1.SPINE12649
15. Kale SU, Donaldson I, West RJ, Shehu A. Superficial siderosis of the meninges and its otolaryngologic connection: a series of five patients. *Otol Neurotol.* (2003) 24:90–5. doi: 10.1097/00129492-200301000-00019

16. Koeppen AH, Dickson AC, Chu RC, Thach RE. The pathogenesis of superficial siderosis of the central nervous system. *Ann Neurol.* (1993) 34:646–53. doi: 10.1002/ana.410340505
17. Wertz M, Cosnard G, Misson N, Ossemann M, Mormont E, Laloux P, et al. Superficial siderosis associated with multiple dural tears opening into a spinal epidural fluid collection. *Acta Neurol Belg.* (2011) 111:160–1.
18. Nakazawa H, Toyama Y, Satomi K, Fujimura Y, Hirabayashi K. Idiopathic spinal cord herniation. Report of two cases and review of the literature. *Spine.* (1993) 18:2138–41. doi: 10.1097/00007632-199310001-00036
19. Takai K, Komori T, Shin M, Niimura M, Taniguchi M. Superficial siderosis complicated by hydrocephalus: bleeding from the dura mater in the cerebrospinal fluid cavity after brain tumor surgery. *Acta Neurochir.* (2016) 158:1299–302. doi: 10.1007/s00701-016-2817-1
20. Hosokawa M, Murata KY, Hironishi M, Koh J, Nishioka K, Nakao N, et al. Superficial siderosis associated with duplicated dura mater detected by CISS reverse MRI. *J Neurol Sci.* (2018) 392:38–43. doi: 10.1016/j.jns.2018.07.001
21. Vandenabeele F, Creemers J, Lambrichts I. Ultrastructure of the human spinal arachnoid mater and dura mater. *J Anat.* (1996) 189(Pt 2):417–30.
22. Nagel SJ, Reddy CG, Frizon LA, Chardon MK, Holland M, Machado AG, et al. Spinal dura mater: biophysical characteristics relevant to medical device development. *J Med Eng Technol.* (2018) 42:128–39. doi: 10.1080/03091902.2018.1435745

Conflict of Interest: The authors declare that the research was conducted in the absence of any commercial or financial relationships that could be construed as a potential conflict of interest.

Publisher's Note: All claims expressed in this article are solely those of the authors and do not necessarily represent those of their affiliated organizations, or those of the publisher, the editors and the reviewers. Any product that may be evaluated in this article, or claim that may be made by its manufacturer, is not guaranteed or endorsed by the publisher.

frontiers | Frontiers in Neurology

TYPE Case Report
PUBLISHED 20 September 2022
DOI 10.3389/fneur.2022.963970

OPEN ACCESS

EDITED BY
Bruce Miller,
University of California, San Francisco, United States

REVIEWED BY
Per Östberg,
Karolinska Institutet (KI), Sweden
Cristina Polito,
Università degli Studi di Firenze, Italy

*CORRESPONDENCE
Xiaolu Wang
lucywxl@zju.edu.cn
Jiong Zhou
ze-zj@zju.edu.cn

SPECIALTY SECTION
This article was submitted to Dementia and Neurodegenerative Diseases, a section of the journal Frontiers in Neurology

RECEIVED 08 June 2022
ACCEPTED 23 August 2022
PUBLISHED 20 September 2022

CITATION
Huang B, Wang X, Jiang B, Kong L, Hou H and Zhou J (2022) Case Report: A neurolinguistic and neuroimaging study on a Chinese follow-up case with logopenic-variant of primary progressive aphasia.
Front. Neurol. 13:963970.
doi: 10.3389/fneur.2022.963970

Case Report: A neurolinguistic and neuroimaging study on a Chinese follow-up case with logopenic-variant of primary progressive aphasia

Binyao Huang[1], Xiaolu Wang[2]*, Biao Jiang[3], Linlin Kong[4], Haifeng Hou[5] and Jiong Zhou[4]*

[1]School of Foreign Languages, Zhejiang University of Finance and Economics, Hangzhou, China, [2]School of Foreign Languages, Zhejiang University City College, Hangzhou, China, [3]Department of Radiology, Second Affiliated Hospital, School of Medicine, Zhejiang University, Hangzhou, China, [4]Department of Neurology, Second Affiliated Hospital, School of Medicine, Zhejiang University, Hangzhou, China, [5]Department of Nuclear Medicine, Second Affiliated Hospital, School of Medicine, Zhejiang University, Hangzhou, China

Primary progressive aphasia (PPA), typically resulting from a neurodegenerative disease, is characterized by a progressive loss of specific language functions while other cognitive domains are relatively unaffected. The logopenic variant, characterized by impairments of word retrieval and sentence repetition along with preserved semantic, syntactic, and motor speech abilities, is the most recently described and remains less understood than other variants due to a comparatively small number of case studies and a lack of investigations with a thorough specification. In this article, we report a 2-year follow-up case study of a 74-year-old Chinese female patient with a logopenic variant of primary progressive aphasia, including its neurolinguistic study, magnetic resonance imaging (MRI), and 11C-Pittsburgh compound B-Positron emission tomography imaging analyses, as well as gene sequencing. This case confirms that, in addition to word-finding and sentence repetition difficulties, the logopenic variant may also present with mild auditory comprehension and naming deficits attributed to impaired access to lexical representations. The observation of clinical treatment suggests the efficacy of memantine hydrochloride tablet and rivastigmine transdermal patch in slowing down the cognitive deterioration of this patient. The description and exploration of this case may shed new insights into a better understanding of the Chinese logopenic variant of primary progressive aphasia.

KEYWORDS

Alzheimer's disease, primary progressive aphasia, logopenic-variant, neurolinguistics, neuroimaging

Introduction

Primary progressive aphasia (PPA) is a general term for a group of neurodegenerative diseases that primarily affect language processing. Three major variants can be classified based on their aphasia profile and atrophy pattern. The diagnostic criteria of PPA initially only comprised non-fluent/agrammatic variant PPA (navPPA) and semantic variant PPA (svPPA), whereas logopenic variant PPA (lvPPA) has been included only recently (1). Hence, the characterization of lvPPA remains incomplete and calls for a comprehensive description of lvPPA features. The in-depth study of lvPPA is furthermore essential because it contributes to expanding our understanding of the pathological process of Alzheimer's disease (AD), given that some studies have demonstrated a high proportion of underlying Alzheimer's pathology (2).

The concept of atypical forms of AD was recently proposed and precisely elaborated (3), including a posterior variant, a frontal variant, a logopenic variant, and a Down's syndrome variant. To our knowledge, few observations have been made regarding the neurolinguistic features of Chinese-speaking patients with lvPPA and the long-term structural changes of the brain accompanying the progressive course. Hence, patients with lvPPA from Chinese-speaking populations might exhibit some characteristics that should be explored in depth.

Patient consent

This case report and accompanying images were published with the written informed consent of the patient's guardian.

Description of the case

Reported here is the case of a Chinese right-handed female retired worker born in August 1948 who has been experiencing progressive language impairment in her native Han language since 2015. The patient has only 2 years of primary education and is virtually illiterate, unable to read or write. On 15 February 2019, the patient visited the memory clinic of our hospital for the first time, with complaints of speech difficulty for 4 years and mild memory loss for 2 years. According to the patient's family, she began having trouble finding words in 2015, which led to stumbling speech with progressive aggravation. In 2017, she started to show signs of memory loss, as evidenced by forgetting to take groceries after paying for them and pressing the button of the corresponding floor again after reaching the target floor by elevator. In 2018, she once went in the wrong direction when going out but never got lost. Her primary symptom in 2019 was word stumbling, which resulted in frequent pauses in her speaking. However, what she said can still be appropriately understood by others. The patient was in good general health except for a 10-year history of hypertension. Her physical examination was normal. Blood tests, such as routine blood examination, biochemistry, coagulation function, thyroid function, and screenings for human immunodeficiency virus (HIV), syphilis, and glycosylated hemoglobin, did not reveal significant abnormalities. The patient underwent brain magnetic resonance imaging (MRI; Simens, 1.5T) on the same day, and two neuroimaging specialists with more than 10 years of experience rated the scans. A mildly widened lateral sulcus was observed, with the left more pronounced than the right (Figure 1). Moreover, the bilateral lateral ventricular horns were slightly broad and blunt, which was evident in the coronal position. Lesions of white matter hyperintensities (WMH) on T2-weighted MRI were seen around the ventricles and under the frontoparietal cortex. The bilateral choroidal fissures were widened. Mild ventriculomegaly was detected on the left temporal horn of the lateral ventricle. The right hippocampal volume (HV) showed I-degree atrophy, while the left HV displayed II-degree atrophy.

On 21 February 2019, 11C-Pittsburgh compound B-Positron emission tomography imaging (PIB-PET) was performed, which presented a significant increase in amyloid β-protein (Aβ) in the cerebral cortex (Figure 2), including bilateral frontal (SUV_{mean} = 2.50), parietal (SUV_{mean} = 2.86), temporal (SUV_{mean} = 2.30), occipital (SUV_{mean} = 2.25) lobes, and cerebellar cortical (SUV_{mean} = 1.07).

The accumulation of amyloid is related to the evidence of AD, such as the deterioration in cognitive functioning, memory, fine motor movements, executive functioning, and visuospatial skills. Therefore, the patient was diagnosed with AD and began to receive treatment with memantine hydrochloride tablet and rivastigmine transdermal patch. The patient gradually reached the maximum daily dose (20 mg qd) of memantine hydrochloride tablet. The initial dose of rivastigmine transdermal patch was 4.5 mg qd, which was changed to 9.5 mg qd after 1 month.

On 5 August 2019, neurolinguistic and neuropsychological assessments were conducted and reported, including the Mini-Mental State Examination (MMSE) (4), the Clinical Dementia Rating (CDR) (5), the Neuropsychiatric Inventory (NPI) (6), and the Activities of Daily Life (ADL, the 20-item edition) (7) (Table 1). In addition, the patient was evaluated using the Aphasia Battery of Chinese modified by the First Affiliated Hospital of Peking University (ABC) (8). The results are shown in Table 2. The patient's MMSE score was 15 in 2019. She scored on the NPI of 0, CDR of 0.5, and ADL of 23. Moreover, the ABC test for language evaluation showed that her repetition and naming were deficient. Her poor performance in structure and visual space perception may be caused by her low level of education. The assessments also revealed her short-term memory impairment.

We analyzed the recordings of the patient's description of a cookie-theft chart during the first assessment in 2019. Among all errors, the most frequent occurrences are phonetic errors,

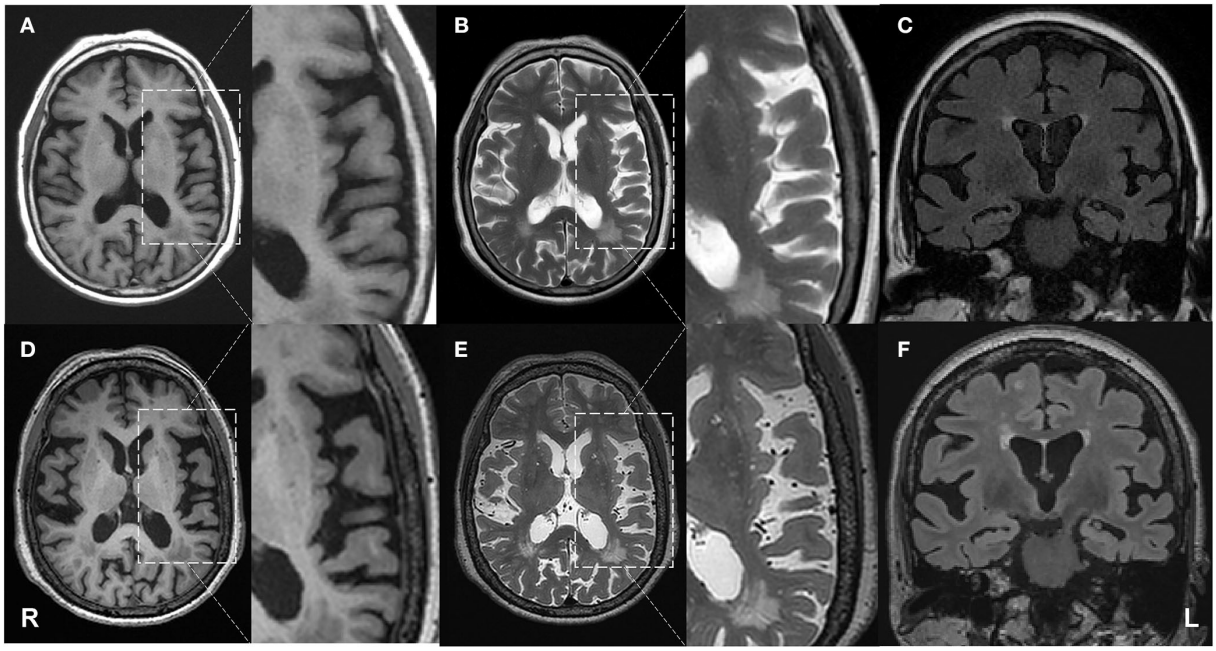

FIGURE 1
Progressive brain atrophy was detected by structural MRI. First row: MRI on 15 February 2019; second row: MRI on 25 April 2021. **(A,D)** axial T1 weighted images; **(B,E)** axial T2 weighted images; **(C,F)** coronal FLAIR images. The patient showed atrophy in the left temporal lobe compared with the baseline.

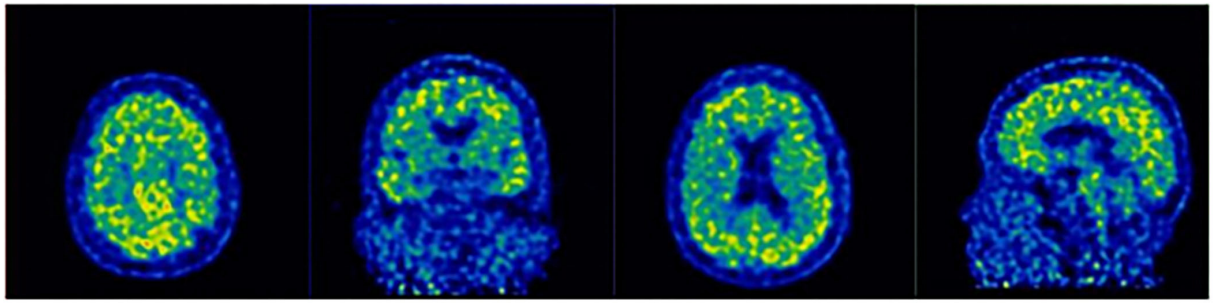

FIGURE 2
11C-Pittsburgh compound B-Positron emission tomography imaging (PIB-PET) revealed the accumulation of Aβ in the prefrontal cortex, temporal lobe, posterior cingulate cortex, and parietal-occipital junction cortex.

but semantic errors also occur occasionally. For example, this patient was able to correctly name "*deng zi*" in Chinese ("stool" in English), which proves her intact object knowledge. However, when she tried to describe the scene in the picture with the sentence "*zhe ge deng zi dao le*" ("This stool fell down"), she said, "*ze deng ze de dao le.*" Although the first part of her utterance "*ze deng ze de*" makes no sense in Chinese, the pronunciation sounds similar to the target "*zhe ge deng zi*," in which she retained most final vowels, so people could easily guess her meaning. Another example of phonological errors is that the patient mispronounced "*huo hua ma*" (which does not make sense in Chinese) instead of "*huo ha ma*" ("live toad") in a repetition task. When the patient described her condition and wanted to express the meaning that "the herbal medicine is burnt off," she said, "the herbal medicine has gone bad," which is a semantic error. All these errors were well-articulated without apraxia of speech.

She revisited the hospital for a follow-up consultation on 3 January 2020. Her relatives reported that the patient's speech was more fluent than before, and both word-finding difficulty and anxiety symptoms were improved. However, due to the impact of the coronavirus epidemic, the patient had not been actively seen since then.

10.3389/fneur.2022.963970

TABLE 1 Results of ADL evaluating at age 71 and 73.

Items	First evaluation score	Second evaluation score
Feeding	1	1
Dressing	1	1
Washing up	1	1
Transferring	1	1
Moving around the house	1	1
Toileting	1	1
Help with incontinence	1	1
Bathing	1	1
Using public transportation	2	2
Getting around outside	2	2
Cooking one's own meals	1	2
Taking medications	1	1
Light housework	1	1
Heavy housework	2	2
Doing laundry	1	1
Toenail clipping	1	1
Shopping	2	3
Using the telephone	2	3
Handling finances	2	3
Being alone at home	1	2
Total score	26	31

1: can do it by oneself without any difficulty.
2: can do it by oneself with some difficulties.
3: can do it with help.
4: cannot do it even with help.

TABLE 2 Results of ABC (Aphasia Battery of Chinese) evaluating at age 71 and 73.

Tasks	Items	First evaluation score	Second evaluation score
Oral expression	Amount of information	85 PR	80 PR
	Fluency	18/27	18/27
	Serial language	21/21	21/21
	Repetition	57/100	27/100
	Word naming	28/40	26/40
	Color naming	12/12	12/12
	Responsive naming	6/10	6/10
Auditory comprehension	True/False	44/60	44/60
	Auditory identification	73/90	72/90
	Oral instruction	31/80	39/80
Operation		18/30	17/30
Calculation		20/24	8/24
Structure and visual space perception		1/10	1/10

PR, percentage.

The patient was readmitted to our department on 8 April 2021. According to her relatives, she deteriorated so markedly in word-finding that she usually could only say the first half of one sentence. In addition, her memory function declined as the disease progressed, so she frequently forgot what she was supposed to pick up when trying to get something. Sometimes the patient failed to find the things right in front of her, such as her cell phone. She also lost her way when going out. These symptoms suggest that her visual perception may be impaired, and so is her visuospatial ability. Even though the patient still had a clear knowledge of her condition. For example, she knew that she was forgetful and always stayed at the stove when cooking.

Her symptoms were obviously alleviated. However, the medication efficacy diminished after 1 year. Thorough assessments further evidenced her worsened word-finding and salient repetition difficulty. The same experienced rater performed and reported the neurolinguistic and neuropsychological evaluations. The patient scored 13 on the MMSE assessment and had a score on the NPI of 1, CDR of 0.5, and ADL of 29. The second ABC evaluation revealed a significant deterioration in repetition and calculation. Apart from that, the scores for other tasks were roughly the same (Table 2).

On 25 April 2021, another MRI examination was performed at the hospital (Figure 1). Two neuroimaging specialists rated the patient's cortical atrophy. Compared with the MRI in 2019, the second one revealed a further widened left lateral sulcus and asymmetric atrophy of the temporal lobes, with the most significant widening in the posterior part of the left insula. There was an increase in focal hyperintensity on T2 weighted images in the subcortical white matter of bilateral frontal-parietal lobes and paraventricular white matter. Significant HV atrophy was detected, with III-degree atrophy on the left hippocampal and II-degree atrophy on the right. All the above features suggest left posterior cerebral atrophy. Her physical examination was the same as before. The whole exome sequencing (WES) was also performed on the patient. A novel splicing variant (c.1615 G>A, p.539 G>S) was reported. The mutation c.1615G>A was absent in the public database of gnomAD East Asia. It was predicted to be deleterious by silico software, including SIFT and PolyPhen-2. According to the American College of Medical Genetics and Genomics (ACMG) guidelines, this is classified as "variants of uncertain significance (VUS)" (PM2+PP2). The apolipoprotein

E (APOE) genotype was ε3ε3, and no causative gene for AD was detected.

Combined with the previously described and current diagnostic methods, the patient's presentation at the initial visit in 2019 met the diagnostic criteria for LVPPA. According to Gorno-Tempini's classification of PPA and its variants (9), establishing a clinical diagnosis involves a two-step process. Patients should first meet essential PPA criteria, which require a prominent, isolated language deficit during the initial phase of the disease. Based on Mesulam's guidelines (10), her most prominent clinical feature is difficulty with language, which is the primary cause of impaired daily living activities. Aphasia is the most remarkable deficit at symptom onset and for the initial phases of the disease. Therefore, all the inclusion criteria were answered positively. Meanwhile, her pattern of deficits could not be better accounted for by other non-degenerative nervous systems, nor could her cognitive disturbance be better accounted for by a psychiatric diagnosis. No significant initial episodic memory, visual memory, and visuoperceptual impairments or behavioral disturbance were observed. Hence, the exclusion criteria were answered negatively.

Therefore, the patient further meets the diagnostic criteria for lvPPA (9). For the clinical diagnosis of lvPPA, as the core features, both impaired single-word retrieval in spontaneous speech and naming and impaired repetition of sentences and phrases are present. Other features are also clearly present, such as speech (phonologic) errors in spontaneous speech and naming, spared single-word comprehension and object knowledge, and absence of frank agrammatism. Furthermore, the patient shows predominant left posterior perisylvian atrophy on MRI, meeting the imaging-supported diagnosis for lvPPA.

Discussion

We describe and explore the case from the following three aspects.

First, from the perspective of neurolinguistics and neuropsychological analysis, there is only a 2-point difference between the patient's scores on two MMSE assessments, indicating that her overall cognitive function was stable. The second NPI evaluation increased with a score of 1 for the "agitation/aggression" item, and the patient became more stubborn and difficult to get along with than before. Moreover, the second ADL rating was five points higher than the previous one. She is slightly degraded in her ability to shop, make phone calls, manage her money, cook meals, and be alone at home. Therefore, with the disease's progression, her personality disorder and executive function impairment were increasingly prominent, only second to language dysfunction.

In previous studies, it has been found that lvPPA is primarily distinguished by a word-finding difficulty in spontaneous speech and confrontation naming, related to a "word-on-the-tip-of-the-tongue" phenomenon, and by problems in the repetition and comprehension of sentences due to her deficits of short-term memory (11). In the first test, the patient's speech disorder was characterized by an intermediate state between fluent and non-fluent spontaneous speech, which was ascribed to a prominent impairment of word retrieval. However, the patient would immediately consent when the rater said the target words for her, indicating the relatively preserved input lexicon and object knowledge. Phonemic paraphasias accounted for most of her speech errors. There is no frank agrammatism. Her repetition impairment was evidenced by difficulty in repeating sentences of more than five Chinese characters. The error rate of repetition increased with the length of the sentence. The aforementioned symptoms fit the description of lvPPA from earlier investigations. The outcome of the second test was the same as the first, with the exception of her dramatically diminished calculation ability. Further analysis of the error types revealed that the patient could correctly answer all the addition calculation questions, indicating no problem with her memory and perception of the numbers. However, the patient completed the subsequent subtraction and multiplication calculations in an additive manner, which resulted in errors (e.g., 6–2 = 8, 6*7 = 13). She was unable to do division calculations. Another important phenomenon related to the calculation errors observed in this patient was that she repeatedly performed the first action she was instructed, regardless of the following different instructions from the rater. Sandson and Albert (12, 13) originally proposed three various forms of perseveration: recurrent, stuck-in set, and continuous. Each of them is linked to a specific neuroanatomical network and each is influenced by a different neurochemical profile. Recurrent perseveration is an unintentional, immediate, or delayed repetition of a previous response after an intervening stimulus, which is linked to left temporoparietal lesions (14) and to dysfunction in cholinergic systems, and caused by postactivation of normally inhibited memory traces (15). Furthermore, it is linked to working memory functions mediated by frontal regions (16, 17). In this case, recurrent perseveration is correlated with temporoparietal function impairment, consistent with the left posterior perisylvian atrophy found on MRI.

Sentence repetition was further aggravated, as shown by the difficulty in her repetition of sentences of more than four Chinese characters. When the patient experienced word-finding difficulty during the evaluating process, she could make correct judgments with the hints given by the rater, which indicated that the underlying language-related dysfunction in lvPPA may result from the impaired access to the input lexicon or from the actual damage to the output lexicon.

In agreement with previous research, these results have confirmed the extensive damage to the language network in this lvPPA case. Neurolinguistic assessments have shown severe repetition impairments (repetition 27/100), along with the

deficits of mild naming (word naming 26/40), and auditory comprehension (true/false questions 44/60), suggesting the possible presence of lesions in the left superior temporal gyrus and the left posterior inferior parietal lobe, as well as the bilateral fusiform gyrus (18).

Previous evidence suggests that 50–67% of the patients with lvPPA have probable Alzheimer's disease (19). In other words, AD might be the most common underlying pathology. Accordingly, lvPPA might be further divided into an expansive variant due to Alzheimer's disease (lvPPA due to AD, LDA) and a more localized variant not related to Alzheimer's pathology (lvPPA due to non-AD, LDNA). Previous research has demonstrated that cognitive impairments in LDA cases go even deeper into the language system (18). In addition, the effects of LDA extend beyond the language system, affecting syntactic processing and phoneme sequencing, thereby causing semantic representations to degrade further and even resulting in ideomotor apraxia. Pathologically, LDA involves predominant atrophy of the left temporal-parietal junction and a wider range of cerebral cortex than LDNA, including the inferior parietal lobe and the middle posterior temporal lobe in the left hemisphere.

As far as the current case is concerned, the patient should be classified as LDA because her positive PIB-PET result has indicated the presence of AD pathology. Her neurolinguistic and neuropsychological assessments have unveiled that the impairment of cortical function is not limited to her language function but extends to her short-term memory, calculation, visuospatial perception, and executive function. Furthermore, the recurrent perseveration exhibited by the patient in her execution of both verbal instructions and computational tasks suggests further impairment of the temporal-parietal lobe function. In line with the previous study (20), LvPPA may involve cortical regions beyond language areas, such as the parietal and frontal lobes.

According to epidemiological studies, patients with AD usually have an average annual decline of 4–5 points in the MMSE (21). However, the cognitive performance of this patient remained relatively stable. Her second MMSE score was two points lower than the first in 20 months, and the CDR assessments remained unchanged at 0.5 points. Two ADL evaluations differed by 6 points. It is clear from her slow rate of deterioration decline that the combination of rivastigmine transdermal patch and memantine hydrochloride tablet had been effective in maintaining her cognitive function. Schaeverbeke et al. investigated whether cholinergic alterations occur in PPA variants using N-[11 C]-Methylpiperidin-4-yl propionate (PMP)-PET, and found that only lvPPA cases, especially the cases show AD pathology, demonstrated decreases in Acetylcholinesterase (AChE) activity levels compared with controls. No differences were found in the navPPA or svPPA cases compared with controls (22). The cholinergic deficit in lvPPA in this study provides a potential rationale for the off-label use of AChE inhibitors in lvPPA due to AD pathology. This is also confirmed by the clinical efficacy of the current patient. Nevertheless, the patient still showed significant deterioration in repetition and calculation; thus, in-depth studies are needed to determine which specific mechanisms are involved.

Second, from the perspective of imaging analysis, different cortical atrophies and pathological changes are linked to different variants of PPA. With the imaging features of svPPA in the anterior and ventral temporal lobes and that of navPPA in the left inferior frontal and insula (23), it is crucial to identify abnormalities in the left temporoparietal junction area for the diagnosis of lvPPA. For the patient in this study, the analysis of MRI scans has shown the widened Sylvian fissures, suggesting the atrophy of the temporal lobe, which was more prominent on the left, as the initial detectable structural change in lvPPA. Furthermore, 20 months apart, the bilateral Sylvian fissure was further widened, with the most remarkable widening in the posterior part of the left insula. Significant hippocampal atrophy was also observed, suggesting that as the disease progresses, the temporal lobes and hippocampus could atrophy further bilaterally, and the atrophy is more pronounced on the left side.

Third, in addition to the above two aspects, WES identified the mutation of the MAPT gene. MAPT mutation is correlated with behavioral variant frontotemporal dementia, navPPA, svPPA, corticobasal degeneration, and progressive supernuclear palsy, while PGRN mutation may lead to lvPPA (24). According to our search of the relevant literature in the last decade, no case of MAPT mutation leading to lvPPA has been reported. This patient met the diagnostic criteria for clinical lvPPA and was found to have a progressive decline in short-term memory and visuospatial ability during follow-up, which does not support the diagnosis of frontotemporal dementia. The impact of the MAPT gene mutation on this patient is yet unknown. Further longitudinal and Tau-PET studies, even with pathological results, would be valuable.

Conclusion

This article reports a typical Chinese-speaking patient with LDA due to AD. The follow-up of clinical manifestations and neurolinguistic characteristics confirms that, in addition to the linguistic features, lvPPA may be accompanied by the involvement of multiple cognitive domains with the progression of the disease, providing insight into the pathological mechanisms of this disease. Moreover, this patient had a mutation in the MAPT gene. Despite the fact that we are yet unsure of the exact role that this mutation plays in the patient's condition, this case provides us with proof that there may be an association between the MAPT mutation and LDA. The patient was nearly illiterate and unable to write or read; therefore, part of the linguistic profile cannot be analyzed. Since

the evidence presented by one case is limited, further research is required to gather more thorough and convincing information.

Data availability statement

The datasets presented in this article are not readily available because of ethical and privacy restrictions. Requests to access the datasets should be directed to the corresponding authors.

Ethics statement

Written informed consent was obtained from the individual(s) and/or minor(s)' legal guardian/next of kin for the publication of any potentially identifiable images or data included in this article.

Author contributions

BH: interpreting the data, drafting the manuscript, and revising the content. XW: drafting the manuscript and revising the content. BJ: collecting and processing the magnetic resonance imaging data. LK: collecting the neurolinguistic and neuropsychological assessment data. HH: collecting and processing the radioactive imaging data. JZ: collecting, analyzing, interpreting clinical data, and taking responsibility for conducting research and final approval. All authors contributed to the article and approved the submitted version.

Conflict of interest

The authors declare that the research was conducted in the absence of any commercial or financial relationships that could be construed as a potential conflict of interest.

Publisher's note

All claims expressed in this article are solely those of the authors and do not necessarily represent those of their affiliated organizations, or those of the publisher, the editors and the reviewers. Any product that may be evaluated in this article, or claim that may be made by its manufacturer, is not guaranteed or endorsed by the publisher.

References

1. Gorno-Tempini ML, Dronkers NF, Rankin KP, Ogar JM, Phengrasamy L, Rosen HJ, et al. Cognition and anatomy in three variants of primary progressive aphasia. *Ann Neurol.* (2004) 55:335–46. doi: 10.1002/ana.10825

2. Leyton CE, Villemagne VL, Savage S, Pike KE, Ballard KJ, Piguet O, et al. Subtypes of progressive aphasia: application of the international consensus criteria and validation using beta-amyloid imaging. *Brain.* (2011) 134:3030–43. doi: 10.1093/brain/awr216

3. Dubois B, Feldman HH, Jacova C, Hampel H, Molinuevo JL, Blennow K, et al. Advancing research diagnostic criteria for Alzheimer's disease: the IWG-2 criteria. *Lancet Neurol.* (2014) 6:614–29. doi: 10.1016/S1474-4422(14)70090-0

4. Folstein MF, McHugh PR. 'Mini-mental state'. A practical method for grading the cognitive stat of patients for the clinician. *J Psychiatr Res.* (1975) 12:189–98. doi: 10.1016/0022-3956(75)90026-6

5. Hughes CP, Berg L, Danziger WL, Coben LA, Martin RL. A new clinical scale for the staging of dementia. *Br J Psychiatr.* (1982) 140:566–72. doi: 10.1192/bjp.140.6.566

6. Cummings JL, Mega M, Gray K, Rosenberg-Thompson S, Carusi DA, Gornbein J. The Neuropsychiatric Inventory: comprehensive assessment of psychopathology in dementia. *Neurology.* (1994) 12:2308–14. doi: 10.1212/WNL.44.12.2308

7. Dodge HH, Kadowaki T, Hayakawa T, Yamakawa M, Sekikawa A, Ueshima H. Cognitive impairment as a strong predictior of incident disability in specific ADL-IADL tasks among communitydwelling edlers. *Azuchi Study.* (2005) 45:222–30. doi: 10.1093/geront/45.2.222

8. Gao SR, Chu YF, Shi SQ, Peng Y, Dai SD, Wang YH, et al. standardization research of the Aphasia Battery of Chinese. *Chinese Mental Health J.* (1992) 6:125–8.

9. Gorno-Tempini ML, Hillis AE, Weintraub S, Kertesz A, Mendez M, Cappa SF, et al. Classification of primary progressive aphasia and its variants. *Neurology.* (2011) 76:1006–14. doi: 10.1212/WNL.0b013e31821103e6

10. Mesulam MM. Primary progressive aphasia. *Ann Neurol.* (2001) 49:425–32. doi: 10.1002/ana.91

11. Gorno-Tempini ML, Brambati SM, Ginex V, Ogar J, Dronkers NF, Marcone A, et al. The logopenic/phonological variant of primary progressive aphasia. *Neurology.* (2008) 71:1227–34. doi: 10.1212/01.wnl.0000320506.79811.da

12. Sandson J, Albert ML. Varieties of perseveration. *Neuropsychologia.* (1984) 22:715–32. doi: 10.1016/0028-3932(84)90098-8

13. Sandson J, Albert ML. Perseveration in behavioral neurology. *Neurology.* (1987) 37:1736–41. doi: 10.1212/WNL.37.11.1736

14. Vilkki J. Differential perseverations in verbal retrieval related to anterior and posterior left hemisphere lesions. *Brain Lang.* (1989) 36:543–54. doi: 10.1016/0093-934X(89)90085-0

15. Hudson AJ. Perseveration. *Brain.* (1968) 91:571–82. doi: 10.1093/brain/91.3.571

16. Paulesu E, Goldacre B, Scifo P, Cappa SF, Gilardi MC, Castiglioni I, et al. Functional heterogeneity of left inferior frontal cortex as revealed by fMRI. *Neuroreport.* (1997) 8:524–34. doi: 10.1097/00001756-199705260-00042

17. Smith EE, Jonides J. Storage and executive processes in the frontal lobes. *Science.* (1999) 283:1657–61. doi: 10.1126/science.283.5408.1657

18. Leyton CE, Hodges JR, Mclean CA, Catriona A, Kril JJ, Piguet O, et al. Is the logopenic-variant of primary progressive aphasia a unitary disorder? *Cortex.* (2015) 67:122–33. doi: 10.1016/j.cortex.2015.03.011

19. Bonner MF, Ash S, Grossman M. The new classification of primary progressive aphasia into semantic, logopenic, or nonfluent/agrammatic variants. *Curr Neurol Neurosci Rep.* (2010) 10:484–90. doi: 10.1007/s11910-010-0140-4

20. Teichmann M, Kas A, Boutet C, Ferrieux S, Nogues M, Samri D, et al. Deciphering logopenic primary progressive aphasia: a clinical, imaging and biomarker investigation. *Brain.* (2013) 136:3474–88. doi: 10.1093/brain/awt266

21. Dubois B, Hampel H, Feldman HH, Scheltens P, Aisene P, Andrieuf S, et al. Preclinical Alzheimer's disease: definition, natural history, and diagnostic criteria. *Alzheimer's Dement.* (2016) 12:292–323. doi: 10.1016/j.jalz.2016.02.002

22. Schaeverbeke J, Evenepoel C, Bruffaerts R, Van Laere K, Bormans G, Dries E, et al. Cholinergic depletion and basal forebrain volume in primary progressive aphasia *NeuroImage.* (2017) 13:271–9. doi: 10.1016/j.nicl.2016.11.027

23. Liu X, He F, Chen Z, Liu P, Peng G. A longitudinal study of a Chinese man presenting with non-fluent/agrammatic variant of primary progressive aphasia. *Front Neurol.* (2018) 9:75. doi: 10.3389/fneur.2018.00075

24. Pan X, Chen X. Clinic, neuropathology and molecular genetics of frontotemporal dementia: a mini-review. *Transl Neurodegener.* (2013) 2:1–9. doi: 10.1186/2047-9158-2-8

frontiers | Frontiers in Neurology

TYPE Case Report
PUBLISHED 23 September 2022
DOI 10.3389/fneur.2022.962684

OPEN ACCESS

EDITED BY
Bruce Miller,
University of California, San Francisco, United States

REVIEWED BY
Peng-Hu Wei,
Xuanwu Hospital, Capital Medical University, China
Preeti Sinha,
National Institute of Mental Health and Neurosciences (NIMHANS), India

*CORRESPONDENCE
Xuewei Xia
xxw7456@163.com
Zhiqi Mao
markmaoqi@163.com

SPECIALTY SECTION
This article was submitted to Dementia and Neurodegenerative Diseases, a section of the journal Frontiers in Neurology

RECEIVED 06 June 2022
ACCEPTED 18 July 2022
PUBLISHED 23 September 2022

CITATION
Liu Y, Tang C, Wei K, Liu D, Tang K, Chen M, Xia X and Mao Z (2022) Transcranial alternating current stimulation combined with sound stimulation improves the cognitive function of patients with Alzheimer's disease: A case report and literature review. *Front. Neurol.* 13:962684. doi: 10.3389/fneur.2022.962684

Transcranial alternating current stimulation combined with sound stimulation improves the cognitive function of patients with Alzheimer's disease: A case report and literature review

Yang Liu[1], Can Tang[1], Kailun Wei[1], Di Liu[2], Keke Tang[2], Meilian Chen[2], Xuewei Xia[1]* and Zhiqi Mao[3]*

[1]Department of Neurosurgery, Affiliated Hospital of Guilin Medical University, Guilin, China, [2]Guangzhou Kangzhi Digital Technology Co., Ltd., Guangzhou, China, [3]Department of Neurosurgery, Chinese PLA General Hospital, Beijing, China

Transcranial alternating current stimulation (tACS) is a relatively new non-invasive brain electrical stimulation method for the treatment of patients with Alzheimer's disease (AD), but it has poor offline effects. Therefore, we applied a new combined stimulation method to observe the offline effect on the cognitive function of patients with AD. Here, we describe the clinical results of a case in which tACS combined with sound stimulation was applied to treat moderate AD. The patient was a 73-year-old woman with a 2-year history of persistent cognitive deterioration despite the administration of Aricept and Sodium Oligomannate. Therefore, the patient received tACS combined with sound stimulation. Her cognitive scale scores improved after 15 sessions and continued to improve at 4 months of follow-up. Although the current report may provide a new alternative therapy for patients with AD, more clinical data are needed to support its efficacy.

Trial registration: Clinicaltrials.gov, NCT05251649.

KEYWORDS

Alzheimer's disease, cognition, transcranial alternating current stimulation, gamma rhythm, sound

Introduction

Alzheimer's disease (AD) is a severe neurodegenerative disease that has been among the top 10 causes of death worldwide and has caused a substantial economic burden on families (1). The characteristic performance of patients with AD is a gradual deterioration of cognition (2). However, existing drugs and some treatments have not achieved good results in improving cognition.

A relatively new non-invasive method for brain electrical stimulation is transcranial alternating current stimulation (tACS). It affects the manipulation and entrainment of intrinsic oscillations of the brain through the sinusoidal waveform current and regulates

the oscillatory activity of cortical regions (3, 4). tACS can interact with ongoing neuronal activity during cognitive processes, leading to changes in cognitive function (4, 5). tACS regulates higher-order cognitive processes, including memory (4, 6). It can be applied to the phase of coding and identification in learning and memory (7, 8). In addition, tACS is a safe form of stimulation and may have mild and transient side effects without serious adverse events (9). Therefore, tACS can be used to improve the cognition of patients with AD. Nevertheless, so far, tACS has only a temporary effect on cognitive improvement in patients with AD. However, the cognition of a patient with AD' gradually deteriorates as the disease worsens. Therefore, how to extend the offline effects of the treatment has become an urgent problem that needs to be solved.

Case report

Participant

Ms. Hu, aged 73, had a BMI of 24.2, normal blood pressure, primary school education, was a non-smoker and alcoholic (250 ml/day), and had undergone heart stent surgery. And she has no family history of AD. Diagnosed with AD for 2 years, taking Aricept (Donepezil Hydrochloride tablets) for 2 years and taking Sodium Oligomannate capsules for 1 year and still continuing, cognitive deterioration is still progressing. Moreover, the patient complained of a continuous rather than a sudden or volatile decline in memory to our hospital. Impaired ability to acquire and remember new information, as well as reason and process complex tasks, poor judgment, changes in personality or behavior, and occasional anxiety disrupted her daily activities. We assessed this patient on multiple psychometric scales at baseline, including: Alzheimer's Disease Assessment Scale-Cognitive subscale (ADAS-Cog) (10); Montreal Cognitive Assessment (MoCA) (11); Mini-Mental State Examination (MMSE) (12); Auditory Verbal Learning Test (AVLT); Clinical Dementia Rating (CDR) and Beck Anxiety Inventory (BAI). The scores are shown in Table 1.

TABLE 1 Raw score of all scales.

Scales	Sub-items	Baseline	Post-intervention	Follow-up
ADAS-Cog		17	14	10
	Word recall tasks	1	1	1
	Object and finger naming	1	1	1
	Execution of commands	0	0	0
	Structural exercises	3	3	1
	Imagery exercises	0	0	0
	Orienting power	5	4	5
	Word recognition tests	6	5	2
MoCA		12	14	16
MMSE		15	16	18
AVLT				
	Immediate recall	7	8	8
	Delayed recall (5 min/20 min)	0/0	1/0	2/2
	Recognition	10	16	16
BAI		4	6	4

Transcranial alternating current stimulation

The alternating current was non-invasively delivered using a transcranial electrical current stimulator (XPNS208-B, Suzhou Hypnos MD Co. Ltd., China). She received tACS with gamma frequency (40 Hz) and a peak-to-peak amplitude of 1.5 mA 15 times with 20-min sessions across 3 weeks (21 days). Two electrodes (4 × 6 cm) were placed in the dorsolateral prefrontal cortex and in the contralateral supraorbital area.

Sound stimulation

By placing two sponge earbuds in the ear and setting the sound stimulator to 40 Hz, 60 dB, and pure tone, the patient was able to hear clearly. The beginning of tACS coincided with the simultaneous activation of sound stimulation. The time of sound stimulation was set for 5-min stimulation, 5-min rest, 5-min stimulation, 1-min rest, and continued stimulation until tACS ended while turning off sound stimulation. tACS and sound stimulation started and ended at the same time (Figure 1).

Assessments

We measured the patient on several neuropsychological assessment scales. They included CDR, ADAS-Cog, MoCA, MMSE, AVLT, and BAI. All assessments were measured three times: baseline, after the intervention (the end of the treatment for 3 weeks), and follow-up (4 months after the intervention). As the main purpose of this treatment is to evaluate the cognitive effect of this double stimulation method on patients with AD, the main outcome is the change in the ADAS-Cog score, and the other scales are the secondary outcomes. After each treatment, this patient is questioned regarding any adverse reactions such as headaches, itchy skin, dizziness, flickering lights, tinnitus, fatigue, drowsiness, and acute mood changes.

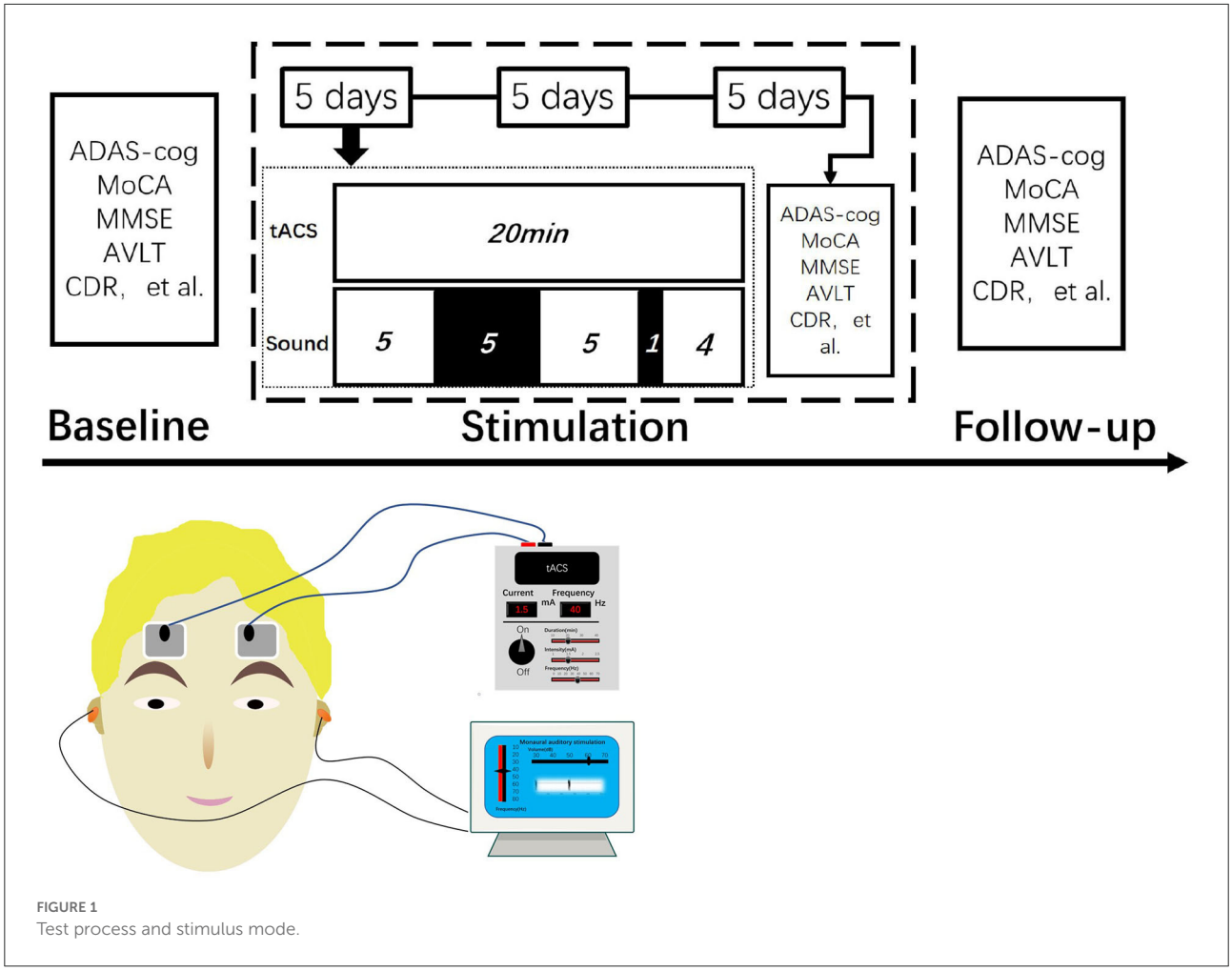

FIGURE 1
Test process and stimulus mode.

Outcome

After 15 days of treatment, the patient was re-evaluated with the scales. It was measured that the ADAS-Cog score dropped by three points, the MoCA score increased by two points, the MMSE score increased by one point, the AVLT score improved by one point for immediate recall, by one point for delayed recall (5 min), and by up to 6 points for recognition. We found that the ADAS-Cog score was decreased by seven points compared with the baseline in a 4-month follow-up, and the MoCA and MMSE scores both improved by two points compared with scores after the intervention, and the delayed recall of AVLT (5 and 20 min) was improved by two points compared with baseline (Figure 2, Table 1). Although the patient had self-reported anxiety symptoms, the BAI scale did not reveal anxiety.

Literature review

We searched the iterature from 2016.01 to 2022.05 in the Web of Science and PubMed databases. Based on Preferred Reporting Items for Systematic Evaluation and Meta-Analysis (PRISMA) guidelines, we performed a systematic evaluation of the available literature related to γ-tACS for the treatment of AD. A literature search was performed using the following terms in the search query. An initial search yielded 30 articles, and two additional studies were obtained in the primary literature reference. A screening for relevance was also performed. After excluding duplicates, reviews, animal experiments, and reports that did not meet the inclusion criteria, three reviewers screened the titles and abstracts of the papers to limit errors. Full-text articles were reviewed, and articles were manually reference checked to show additional references that were missed in the original search. Finally, we found seven articles with data relevant to our research. Considering the limited quantities of clinical trials where γ-tACS was applied to patients with AD, all case reports and small series were eligible. Cases were reported if they met the inclusion criteria. The extracted data included the following parameters: (1) references; (2) participants and design; (3) grouping; (4) electrode position; (5) frequency; (6) intensity; (7) duration; (8) follow-up; (9) assessment; and (10) outcome. Table 2 summarizes the seven studies included.

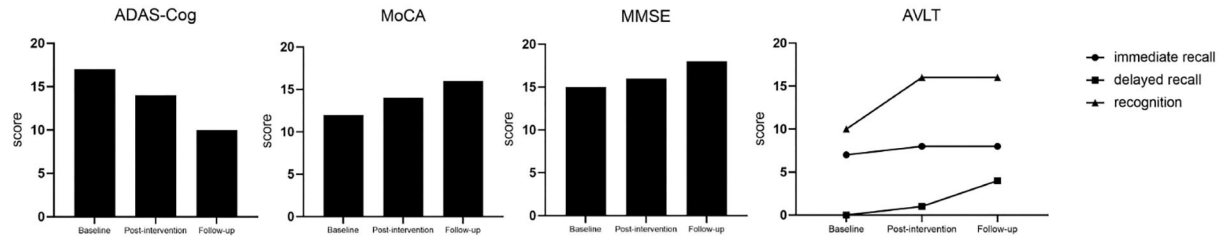

FIGURE 2
The changing trend of several cognitive scale scores. ADAS-Cog, Alzheimer's Disease Assessment Scale-Cognitive Scale; MoCA, Montreal Cognitive Assessment; MMSE, Mini-Mental State Examination; AVLT, Auditory Verbal Learning Test; CDR, Clinical Dementia Rating.

TABLE 2 Clinical trials of transcranial alternating current stimulation (tACS) for patients with Alzheimer's disease (AD) and stimulation parameters.

Reference	Participants and design	Grouping	Electrode position	Frequency	Intensity	Duration	Follow-up	Assessment	Outcome
Dhaynaut et al. (13)	4 AD	γ-tACS	Bitemporal lobes	40 Hz	2 mA	1 h, 4 w	-	ADAS-Cog, MMSE	No significant changes in overall cognition tests
Sprugnoli et al. (14)	15 AD	2 w/unilateral 2 w/bilateral 4 w/bilateral	Temporal lobes	40 Hz	4 mA	1 h, 2 w/4 w	-	ADAS-Cog, MMSE, MoCA CS 21, CFT (15)	No significant changes in overall cognition tests
Kim et al. (16)	20 MCI repeated-measures	γ-tACS; tDCS; sham-tACS	Prefrontal cortex	40 Hz	2 mA	30 min	-	Stroop test, TMT	The cognitive benefits of tACS superior tDCS
Benussi et al. (17)	20 MCI-AD cross-over study	γ-tACS; sham-tACS	Pz; right deltoid muscle	40 Hz	3 mA	1 h	-	RAVL FNAT	Memory improved
Bréchet et al. (18)	2 ADRD	γ-tACS	LAG	40 Hz	2 mA	20 min, 14 w	-	MoCA	Memory improved
Zhou et al. (19)	50 AD randomized, controlled	γ-tACS; sham-tACS	Bilateral temporal lobes	40 Hz	2 mA	20 min, 6 w	12 w	ADAS-cog, MMSE	Cognitive improvement but not sustained
Kehler et al. (20)	17 dementia	(γ-tACS/sham-tACS) + brain exercise	LDLPFC; contralateral supraorbital area	40 Hz	1.5 mA	30 min, 4 w	1 m	WMS-IV	Memory improved at post-intervention and follow-up.

ADAS-Cog, Alzheimer's Disease Cognitive Component Assessment; MMSE, Mini-Mental State Examination; MoCA, Montreal Cognitive Assessment; CS 21, Craft Story 21; CFT, Category Fluency Task; TMT, Trail-Making Test; RAVL, Rey auditory Verbal Learning Test; FNAT, face-name associations task; WMS-IV, Wechsler Memory Scale; ADRD, Alzheimer' s disease-related dementia; Pz, an area overlying the medial parietal cortex and the precuneus; LAG, left angular gyrus; LDLPFC, left dorsolateral prefrontal cortex.

Discussion

Although very few trials have been conducted on patients with AD, tACS has been shown to improve cognitive ability in healthy subjects (21), and its immediate effects on improved patient cognition are known based on existing trials. A single 60-min treatment with exposure to γ-tACS over Pz (an area overlying the medial parietal cortex and the precuneus) can improve memory function in patients with mild cognitive impairment due to Alzheimer's disease (MCI-AD) (17). There was a beneficial effect on cognition after intervention in two patients with Alzheimer's disease-related dementia (ADRD) for a 14-week long-term tACS (18). Patients with mild cognitive impairment (MCI) or dementia received 40 Hz tACS twice a day for 4 weeks, and their' memory improved after treatment and a 1-month follow-up (20). In a randomized controlled clinical trial of 50 patients with AD subjected to 40-Hz tACS (2 mA, 20 min) for 6 weeks, patients in the treatment group showed improvements in both the MMSE and ADAS-Cog scores after treatment. However, a downward trend toward both scale scores

was found in a 12-week follow-up compared to post-treatment (19). This is the largest clinical trial to date involving tACS in patients with AD. The ADAS-Cog and MMSE scores did not improve over the application of 40-Hz tACS (2 mA, 1 h) for 4 weeks compared with pre-treatment. However, after treatment, gamma spectral power on the electroencephalogram (EEG) increased, and the phosphorylated Tau showed a significant decrease following tACS. Most of the current trials reported the short-term efficacy of tACS for AD, but only two trials have patient follow-up data. However, cognitive improvements in patients with AD did not last in a follow-up.

However, we are more concerned about the offline effects of cognitive improvement in patients with AD. To our knowledge, this is the first treatment that combines electrical stimulation and sound stimulation to improve the cognition of patients with AD. The addition of 40-Hz sound stimulation to 40-Hz tACS alone distinguishes our trial from previous stimulation modalities reported in the literature. Our comparison of this treatment modality with previous studies showed surprising results in a follow-up despite the fact that there were no significant differences in cognitive scale improvements after treatment. Surprisingly, the effect was maintained 4 months after treatment. This may be due to electrical stimulation of the cerebral cortex, which causes the current to spread through the skull and activate a broad brain volume, activating multiple interconnected neural regions (22, 23). The effect of tACS can reach the deep structure of the brain (24). Sound stimulation can activate local neuronal populations that overlap with the extensive activation induced by surface electrical stimulation. Therefore, this coordinated activation of these two modalities can lead to enhanced modulation or paired plasticity within localized overlapping areas (25, 26). tACS increases auditory stimulus-evoked power and phase locking (27). Both stimuli were performed simultaneously, resulting in better treatment outcomes. As demonstrated by Conlon et al., a combination of electrical stimulation and sound stimulation effectively modified tinnitus, and the effect lasted for 12 months after treatment. Also, only two kinds of stimulation simultaneously produce the best effect (28).

We enrolled this patient with AD according to the NIA-AA label (29). Our findings are consistent with previous findings that tACS can improve patient cognition. This patient was assessed on the cognitive scales after treatment and showed an improvement compared to baseline. However, cognitive scales scores were better in a 4-month follow-up than in post-treatment. Patients with moderate AD can reduce the total ADAS-Cog score by 6–10 points per year without treatment. A 4-point improvement is usually used to determine the effectiveness of clinical anti-dementia therapy (10). In this treatment, the patient's ADAS-Cog can effectively reduce the score by seven points from baseline to follow-up, indicating that the tACS combined with sound stimulation improves the cognition of a patient with AD significantly, and there is an offline effect. Through the sub-scale analysis and summary of each scale, we found better improvements in recognition (ADAS-Cog word recognition test, AVLT recognition), visual perception, and attention. Recognition is an essential process of memory. Memory is the ability of humans to encode, store, and extract information, which plays an important role in daily life. Significantly, patients with AD have impaired memory that interferes with daily life. The AVLT scale, a measurement tool used to check episodic memory, also showed improved delayed recall score compared to the baseline after intervention and follow-up. In addition, the patient did not experience any adverse effects after each treatment. The patient and her family actively cooperated with each treatment. Although the patient said there was no significant change in cognition before and after the treatment, the patient's mood improved after the treatment and the tension in answering questions was relieved according to the statements by the patient's family members and the observation of a psychological evaluator.

The advantage of using tACS in this experiment is that its current can oscillate at a specific frequency and interact with the intrinsic oscillation of the brain. Selecting the stimulation frequency is significant for tACS to improve the cognition of patients with AD. We summarized the literature and found that most of the published trials for the treatment of patients with AD applied 40 Hz as the stimulation frequency of tACS. As gamma oscillations are closely related to cognitive function, they are impaired in multiple AD models (30). Approximately 40 Hz is the stimulation frequency used in this experiment because, in previous studies, it has been found that 40-Hz light flicker or 40-Hz tone flickering is applied to an animal or 40-Hz tACS is applied to a patient with AD can improve cognitive function and decrease amyloid and phosphorylated tau levels (13, 31, 32). The role of gamma frequency (35–48 Hz) in advanced cognitive processes (including attention, learning, and memory) has been studied (33, 34).

Gamma oscillations may play a more fundamental or universal role in the advanced cognitive function of the brain (35). During sensory processing or memory encoding, the power of gamma oscillation activity increases. A reduction in gamma oscillations is observed in the brain of patients with AD (36, 37). Therefore, the adjustment of the gamma band in patients with AD may help improve cognitive function (38).

Previously, in a mouse model of AD, the restoration of appropriate levels of interneuron-specific sodium channel proteins and parvalbumin (PV) cell-predominant sodium channel proteins was found to improve gamma oscillations and cognitive functions (e.g., spatial learning and memory retention) (39–41). The interneuron network is most sensitive to 40-Hz stimulation (42). After 1 h of light stimulation at 40 Hz, amyloid-β protein content in the visual cortex of mice can be reduced. Interestingly, 1 h of stimulation repeated for a week reduced not only amyloid levels in older mice but also neurotoxic plaque load as well as tau protein accumulation in the frontotemporal

dementia model and increased the activity of brain immune cells (i.e., microglia) (43). Memory performance in mouse models of AD can be improved by reducing amyloid protein loads and the spread of tau phosphorylation in the auditory cortex and the hippocampus using 40-Hz auditory stimulation at 1 h for 7 days (32). Sound stimulation can affect neuroelectric activity (44). In addition, when combining auditory and visual gamma stimulation, amyloid-β clearance was increased not only in the primary sensory cortex and the hippocampus but also in the medial prefrontal cortex and even throughout the neocortex (32). The most important complex pathophysiology of AD is the accumulation of amyloid-β and tau proteins. It can be seen that this method of combining multiple stimuli can better improve cognitive function.

Sensory stimulation with gamma frequency can improve synaptic function, enhance nerve protection factors, and reduce neuronal damage (45). Furthermore, this effect is well-expressed at a frequency of 40 Hz. Thus, the regulation of neuronal gamma activity using 40-Hz stimulation represents a novel non-invasive, non-pharmacological approach to patients with AD (38). The patient underwent tACS combined with sound stimulation treatments 15 times. During each treatment and follow-up, adverse reactions were evaluated. The patient had no headaches, itching, tinnitus, and other adverse reactions during the whole treatment period, and she was willing to receive treatment and actively cooperate with us during a follow-up. Therefore, safety, tolerability, and patient compliance with this treatment method can be confirmed. This preliminary study provides evidence to support the positive effects of tACS combined with sound stimulation on the cognition of patients with AD. Therefore, this combination therapy is expected to become a new method to improve cognition in patients with AD in the future. This case report also provides a new idea for treating patients with AD in the future. This trial paradigm has a good effect on improving the cognition of this patient with AD, but, in terms of stimulation frequency and duration, it continues to improve. Finding the best stimulation parameters is a question that we have explored and researched in the electrical stimulation therapy.

Being considered a novel treatment, it is unclear which mechanism improves cognition and has a sustained offline effect on patients with AD. Because only one patient with moderate AD received such treatment in this study, no general conclusions can be drawn. In addition, unfortunately, in order to study the effects of such stimulation modalities on brain network connectivity, this patient has undergone functional magnetic resonance imaging (MRI) measurements post- and pre-treatment, but studies of brain network connectivity require the combination of functional magnetic resonance imaging (fMRI) data from multiple patients, so the effect of this treatment on brain network connectivity could not be determined here. Additional patient data are currently being collected to confirm these results. Future studies will explore the detailed mechanisms underlying the effects of tACS combined with sound stimulation in patients with mild to moderate AD. The efficacy of tACS combined with sound stimulation is found in patients with moderate AD. As the patient with AD was able to self-manage (e.g., able to feed themselves, dress themselves, go up and down stairs alone, etc.) except for impaired cognitive function, the effect of this therapy on the functional and behavioral symptoms of patients with AD was not reported in this study. Although this patient had a 4-month follow-up, we would follow her for a longer period to explore the prolonged offline effects of tACS combined with sound stimulation.

We report a novel therapy that combines tACS with sound stimulation to improve cognition in patients with AD. This method produced a significant cognitive improvement in this patient, with no adverse effects.

Data availability statement

The original contributions presented in the study are included in the article/supplementary material, further inquiries can be directed to the corresponding author/s.

Ethics statement

The studies involving human participants were reviewed and approved by Chinese PLA General Hospital. The patients/participants provided their written informed consent to participate in this study. Written informed consent was obtained from the individual(s) for the publication of any potentially identifiable images or data included in this article.

Author contributions

Patients with AD were enrolled and treated by DL. Diagnosis of patients with AD was carried out by ZM. Data collection and analysis were carried out by KT and MC. The first draft of this manuscript was written by YL and KW. The experiment was designed by YL, XX, and ZM. The scale was evaluated by YL. English translation was done by CT. All authors contributed to the study conception and design, commented on previous versions of this manuscript, and read and approved the final manuscript.

Funding

This study was supported by grants from the China Brain Project (2021ZD0200407), the National Natural Science Foundation of China (No. 81871087), the Innovative Technique Project of Chinese PLA General Hospital (XJS-202103), and the National Clinical Research Center for Geriatric Diseases (No. NCRCG-PLAGH-2018006).

Conflict of interest

Authors DL, KT, and MC were employed by Guangzhou Kangzhi Digital Technology Co., Ltd.

The remaining authors declare that the research was conducted in the absence of any commercial or financial relationships that could be construed as a potential conflict of interest.

Publisher's note

References

1. 2021 Alzheimer's disease facts and figures. *Alzheimers Dement.* (2021) 17:327–406. doi: 10.1002/alz.12328

2. Reitz C, Brayne C, Mayeux R. Epidemiology of Alzheimer disease. *Nat Rev Neurol.* (2011) 7:137–52. doi: 10.1038/nrneurol.2011.2

3. Antal A, Paulus W. Transcranial alternating current stimulation (tACS). *Front Hum Neurosci.* (2013) 7:317. doi: 10.3389/fnhum.2013.00317

4. Tavakoli AV, Yun K. Transcranial alternating current stimulation (tACS) mechanisms and protocols. *Front Cell Neurosci.* (2017) 11:214. doi: 10.3389/fncel.2017.00214

5. Chang CH, Lane HY, Lin CH. Brain stimulation in Alzheimer's disease. *Front Psychiatry.* (2018) 9:201. doi: 10.3389/fpsyt.2018.00201

6. Herrmann CS, Rach S, Neuling T, Strüber D. Transcranial alternating current stimulation: a review of the underlying mechanisms and modulation of cognitive processes. *Front Hum Neurosci.* (2013) 7:279. doi: 10.3389/fnhum.2013.00279

7. Sandrini M, Brambilla M, Manenti R, Rosini S, Cohen LG, Cotelli M. Non-invasive stimulation of prefrontal cortex strengthens existing episodic memories and reduces forgetting in the elderly. *Front Aging Neurosci.* (2014) 6:289. doi: 10.3389/fnagi.2014.00289

8. Sandrini M, Manenti R, Brambilla M, Cobelli C, Cohen LG, Cotelli M. Older adults get episodic memory boosting from noninvasive stimulation of prefrontal cortex during learning. *Neurobiol Aging.* (2016) 39:210–6. doi: 10.1016/j.neurobiolaging.2015.12.010

9. Antal A, Alekseichuk I, Bikson M, Brockmöller J, Brunoni AR, Chen R, et al. Low intensity transcranial electric stimulation: safety, ethical, legal regulatory, and application guidelines. *Clin Neurophysiol.* (2017) 128:1774–809. doi: 10.1016/j.clinph.2017.06.001

10. Rosen WG, Mohs RC, Davis KL. A new rating scale for Alzheimer's disease. *Am J Psychiatry.* (1984) 141:1356–64. doi: 10.1176/ajp.141.11.1356

11. Nasreddine ZS, Phillips NA, Bédirian V, Charbonneau S, Whitehead V, Collin I, et al. The montreal cognitive assessment, MoCA: a brief screening tool for mild cognitive impairment. *J Am Geriatr Soc.* (2005) 53:695–9. doi: 10.1111/j.1532-5415.2005.53221.x

12. Cockrell JR, Folstein MF. Mini-mental state examination (MMSE). *Psychopharmacol Bull.* (1988) 24:689–92.

13. Dhaynaut M, Sprugnoli G, Cappon D, Macone J, Sanchez JS, Normandin MD, et al. Impact of 40 Hz transcranial alternating current stimulation on cerebral tau burden in patients with Alzheimer's disease: a case series. *J Alzheimers Dis.* (2022) 85:1667–76. doi: 10.3233/JAD-215072

14. Sprugnoli G, Munsch F, Cappon D, Paciorek R, Macone J, Connor A, et al. Impact of multisession 40Hz tACS on hippocampal perfusion in patients with Alzheimer's disease. *Alzheimers Res Ther.* (2021) 13:203. doi: 10.1186/s13195-021-00922-4

15. Morris JC, Heyman A, Mohs RC, Hughes JP, van Belle G, Fillenbaum G, et al. The consortium to establish a registry for Alzheimer's disease (CERAD). Part I Clinical and neuropsychological assessment of Alzheimer's disease. *Neurology.* (1989) 39:1159–65. doi: 10.1212/WNL.39.9.1159

16. Kim J, Kim H, Jeong H, Roh D, Kim DH. tACS as a promising therapeutic option for improving cognitive function in mild cognitive impairment: a direct comparison between tACS and tDCS. *J Psychiatr Res.* (2021) 141:248–56. doi: 10.1016/j.jpsychires.2021.07.012

17. Benussi A, Cantoni V, Cotelli MS, Cotelli M, Brattini C, Datta A, et al. Exposure to gamma tACS in Alzheimer's disease: a randomized, double-blind, sham-controlled, crossover, pilot study. *Brain Stimul.* (2021) 14:531–40. doi: 10.1016/j.brs.2021.03.007

18. Bréchet L, Yu W, Biagi MC, Ruffini G, Gagnon M, Manor B, et al. Patient-tailored, home-based non-invasive brain stimulation for memory deficits in dementia due to Alzheimer's disease. *Front Neurol.* (2021) 12:598135. doi: 10.3389/fneur.2021.598135

19. Zhou D, Li A, Li X, Zhuang W, Liang Y, Zheng CY, et al. Effects of 40 Hz transcranial alternating current stimulation (tACS) on cognitive functions of patients with Alzheimer's disease: a randomised, double-blind, sham-controlled clinical trial. *J Neurol Neurosurg Psychiatry.* (2022) 93:568–70. doi: 10.1136/jnnp-2021-326885

20. Kehler L, Francisco CO, Uehara MA, Moussavi Z. The effect of transcranial alternating current stimulation (tACS) on cognitive function in older adults with dementia. *Annu Int Conf IEEE Eng Med Biol Soc.* (2020) 2020:3649–53. doi: 10.1109/EMBC44109.2020.9175903

21. Gonzalez-Perez M, Wakui E, Thoma V, Nitsche MA, Rivolta D. Transcranial alternating current stimulation (tACS) at 40 Hz enhances face and object perception. *Neuropsychologia.* (2019) 135:107237. doi: 10.1016/j.neuropsychologia.2019.107237

22. Sathappan AV, Luber BM, Lisanby SH. The Dynamic Duo: Combining noninvasive brain stimulation with cognitive interventions. *Prog Neuropsychopharmacol Biol Psychiatry.* (2019) 89:347–60. doi: 10.1016/j.pnpbp.2018.10.006

23. Bikson M, Brunoni AR, Charvet LE, Clark VP, Cohen LG, Deng ZD, et al. Rigor and reproducibility in research with transcranial electrical stimulation: An NIMH-sponsored workshop. *Brain Stimul.* (2018) 11:465–80. doi: 10.1016/j.brs.2017.12.008

24. Krause MR, Vieira PG, Csorba BA, Pilly PK, Pack CC. Transcranial alternating current stimulation entrains single-neuron activity in the primate brain. *Proc Natl Acad Sci U S A.* (2019) 116:5747–55. doi: 10.1073/pnas.1815958116

25. Meyers EC, Kasliwal N, Solorzano BR, Lai E, Bendale G, Berry A, et al. Enhancing plasticity in central networks improves motor and sensory recovery after nerve damage. *Nat Commun.* (2019) 10:5782. doi: 10.1038/s41467-019-13695-0

26. Markewitz R, Engel S, Langguth B, Schecklmann M. Effects of acoustic paired associative stimulation on late auditory evoked potentials. *Brain Topogr.* (2019) 32:343–53. doi: 10.1007/s10548-018-00695-4

27. Jones KT, Johnson EL, Tauxe ZS, Rojas DC. Modulation of auditory gamma-band responses using transcranial electrical stimulation. *J Neurophysiol.* (2020) 123:2504–14. doi: 10.1152/jn.00003.2020

28. Conlon B, Langguth B, Hamilton C, Hughes S, Meade E, Connor CO, et al. Bimodal neuromodulation combining sound and tongue stimulation reduces tinnitus symptoms in a large randomized clinical study. *Sci Transl Med.* (2020) 12:2830. doi: 10.1126/scitranslmed.abb2830

29. Jack CR. Jr., Bennett DA, Blennow K, Carrillo MC, Dunn B, Haeberlein SB, et al. NIA-AA Research Framework: Toward a biological definition of Alzheimer's disease. *Alzheimers Dement.* (2018) 14:535–62. doi: 10.1016/j.jalz.2018.02.018

30. Driver JE, Racca C, Cunningham MO, Towers SK, Davies CH, Whittington MA, et al. Impairment of hippocampal gamma-frequency oscillations in vitro in mice overexpressing human amyloid precursor protein (APP). *Eur J Neurosci.* (2007) 26:1280–8. doi: 10.1111/j.1460-9568.2007.05705.x

31. Singer AC, Martorell AJ, Douglas JM, Abdurrob F, Attokaren MK, Tipton J, et al. Noninvasive 40-Hz light flicker to recruit microglia and reduce amyloid beta load. *Nat Protoc.* (2018) 13:1850–68. doi: 10.1038/s41596-018-0021-x

32. Martorell AJ, Paulson AL, Suk HJ, Abdurrob F, Drummond GT, Guan W, et al. Multi-sensory gamma stimulation ameliorates Alzheimer's-associated pathology and improves cognition. *Cell.* (2019) 177:256–71. doi: 10.1016/j.cell.2019.02.014

33. Yu Y, Jiang X, Fang X, Wang Y, Liu P, Ling J, et al. Transauricular vagal nerve stimulation at 40 Hz inhibitsn hippocampal P2X7R/NLRP3/caspase-1 signaling and improves spatial learning and memory in 6-month-old APP/PS1 mice. *Neuromodulation*. (2022) 13:11. doi: 10.1016/j.neurom.2022.03.011

34. Al Qasem W, Abubaker M, Kvašnák E. Working memory and transcranial-alternating current stimulation-state of the art: findings, missing, and challenges. *Front Psychol.* (2020) 13:822545. doi: 10.3389/fpsyg.2022.822545

35. Strüber D, Herrmann CS. Modulation of gamma oscillations as a possible therapeutic tool for neuropsychiatric diseases: a review and perspective. *Int J Psychophysiol.* (2020) 152:15–25. doi: 10.1016/j.ijpsycho.2020.03.003

36. Palop JJ, Mucke L. Network abnormalities and interneuron dysfunction in Alzheimer disease. *Nat Rev Neurosci.* (2016) 17:777–92. doi: 10.1038/nrn.2016.141

37. Herrmann CS, Demiralp T. Human EEG gamma oscillations in neuropsychiatric disorders. *Clin Neurophysiol.* (2005) 116:2719–33. doi: 10.1016/j.clinph.2005.07.007

38. McDermott B, Porter E, Hughes D, McGinley B, Lang M, O'Halloran M, et al. Gamma band neural stimulation in humans and the promise of a new modality to prevent and treat Alzheimer's disease. *J Alzheimers Dis.* (2018) 65:363–92. doi: 10.3233/JAD-180391

39. Martinez-Losa M, Tracy TE, Ma K, Verret L, Clemente-Perez A, Khan AS, et al. Nav1.1-overexpressing interneuron transplants restore brain rhythms and cognition in a mouse model of Alzheimer's disease. *Neuron.* (2018) 98:75–89. doi: 10.1016/j.neuron.2018.02.029

40. Verret L, Mann EO, Hang GB, Barth AM, Cobos I, Ho K, et al. Inhibitory interneuron deficit links altered network activity and cognitive dysfunction in Alzheimer model. *Cell.* (2012) 149:708–21. doi: 10.1016/j.cell.2012.02.046

41. Bero AW, Yan P, Roh JH, Cirrito JR, Stewart FR, Raichle ME, et al. Neuronal activity regulates the regional vulnerability to amyloid-β deposition. *Nat Neurosci.* (2011) 14:750–6. doi: 10.1038/nn.2801

42. Picton TW, John MS, Dimitrijevic A, Purcell D. Human auditory steady-state responses. *Int J Audiol.* (2003) 42:177–219. doi: 10.3109/14992020309101316

43. Iaccarino HF, Singer AC, Martorell AJ, Rudenko A, Gao F, Gillingham TZ, et al. Gamma frequency entrainment attenuates amyloid load and modifies microglia. *Nature.* (2016) 540:230–5. doi: 10.1038/nature20587

44. Becher AK, Höhne M, Axmacher N, Chaieb L, Elger CE, Fell J. Intracranial electroencephalography power and phase synchronization changes during monaural and binaural beat stimulation. *Eur J Neurosci.* (2015) 41:254–63. doi: 10.1111/ejn.12760

45. Adaikkan C, Middleton SJ, Marco A, Pao PC, Mathys H, Kim DN, et al. Gamma entrainment binds higher-order brain regions and offers neuroprotection. *Neuron.* (2019) 102:929–43. doi: 10.1016/j.neuron.2019.04.011

frontiers | Frontiers in Neurology

TYPE Case Report
PUBLISHED 29 September 2022
DOI 10.3389/fneur.2022.1006060

OPEN ACCESS

EDITED BY
Bruce Miller,
University of California, San Francisco, United States

REVIEWED BY
Rakesh Mishra,
Banaras Hindu University, India
Christopher Charles Glisson,
Michigan State University, United States

*CORRESPONDENCE
Per Kristian Eide
p.k.eide@medisin.uio.no;
peide@ous-hf.no

SPECIALTY SECTION
This article was submitted to Dementia and Neurodegenerative Diseases, a section of the journal Frontiers in Neurology

RECEIVED 28 July 2022
ACCEPTED 13 September 2022
PUBLISHED 29 September 2022

CITATION
Lashkarivand A and Eide PK (2022) The first report on brain sagging dementia caused by a cranial leak: A case report. *Front. Neurol.* 13:1006060. doi: 10.3389/fneur.2022.1006060

The first report on brain sagging dementia caused by a cranial leak: A case report

Aslan Lashkarivand[1,2] and Per Kristian Eide[1,2]*

[1]Department of Neurosurgery, Oslo University Hospital – Rikshospitalet, Oslo, Norway, [2]Institute of Clinical Medicine, Faculty of Medicine, University of Oslo, Oslo, Norway

Objective: Brain Sagging Dementia (BSD) is an increasingly recognized syndrome for which diagnostic criteria recently were proposed. There have been no reports on BSD caused by a cranial leak. Here we present the first report on a patient with BSD caused by a cranial leak.

Case description: A 60-year old male patient was admitted with a 2-year history of orthostatic headache and gradually progressive cognitive and behavioral changes. Traditional treatments for spontaneous intracranial hypotension, including repeated epidural blood patches, failed. Brain imaging showed severe brain sagging, and intracranial pressure monitoring demonstrated intracranial hypotension. No leakage site was found. His past medical history revealed an accident where a ski pole struck his head at age ten. Due to progressive clinical decline, surgery was pursued. A cranial defect with an accompanying cerebrospinal fluid leak site representing the trauma from his childhood was found and repaired. He also was in need of a ventriculoperitoneal shunt. Following surgery, he improved and recovered completely.

Discussion: This case report illustrates that a cranial leak may cause BSD, even with a "lucid interval" between trauma and symptom debut spanning many years. Moreover, this report validates well the recently proposed BSD diagnostic criteria.

KEYWORDS

cranial, CSF leak, brain, sagging, dementia, case report

Introduction

Brain sagging dementia (BSD) is a rare syndrome that results in behavioral and cognitive changes mimicking behavioral variant frontotemporal dementia (bvFTD) (1, 2). Spontaneous intracranial hypotension (SIH) caused by cerebrospinal fluid (CSF) leakage is thought to be the cause, however, no cranial leaks have been reported (3, 4). We present the first report on a patient fulfilling the recently proposed BSD diagnostic criteria (3), caused by a cranial CSF leakage.

Methods

The review was reported according to PRISMA guidelines and registered with the PROSPERO database CRD42020150709 (see Supplementary Table S1 and Supplementary Figure S1). The search was updated in May 2022 (see Supplementary material). The case report was reported according to CARE guidelines.

Case description

A 60-year-old Caucasian man was referred to our department in 2017 for a second opinion due to failed response to traditional SIH treatment. About 1 year earlier, he was admitted to the neurological department due to orthostatic headache and subtle cognitive changes recognized by his family members. Craniospinal magnetic resonance imaging (MRI) showed signs of SIH; however, no CSF leak was evident. Lumbar puncture showed a low opening pressure (near zero cmH_2O). Repeated attempts with lumbar epidural blood patch during the next few months had only partial and short-lived effects. Meanwhile, his condition gradually progressed. His past medical history was uneventful, except for a head injury at age ten when a ski pole struck his left temporal head region. He was discharged from hospital after 2 days with no great concern and no signs of skull fracture at X-ray. As an adolescent, he developed tension headaches (worst in supine position) that worsened during early adult life. In his 30 s, he was once hospitalized, diagnosed with migraine, and medicated for this until 2016. He then suffered a "new type of headache" that was worse in standing position (Figure 1). Thereafter, his condition progressed rapidly, manifesting a fulminant BSD (Table 1), with severe cognitive decline confirmed by neuropsychological assessment. He failed to perform at his job as a company director, and was on full sick leave.

During his stay in our department, imaging showed severe brain sagging with subsequent CSF flow obstruction through the cerebral aqueduct (Figure 2). A comprehensive search for CSF leakage was performed; dynamic computed tomography (CT) myelogram and repeated craniospinal MRI after administration of intrathecal gadobutrol (Gadovist, Bayer, GE), according to our department's protocol (5). However, no CSF leak was identified. Continuous intracranial pressure (ICP) monitoring revealed severe intracranial hypotension with ICP scores <— 10 mmHg (Figure 3). The mean wave amplitude (MWA) was within the normal range, suggesting no impaired intracranial compliance (6). The patient deteriorated further and developed severe antegrade amnesia, stereotyped and bizarre behavior, becoming socially and sexually inappropriate. At one point, he

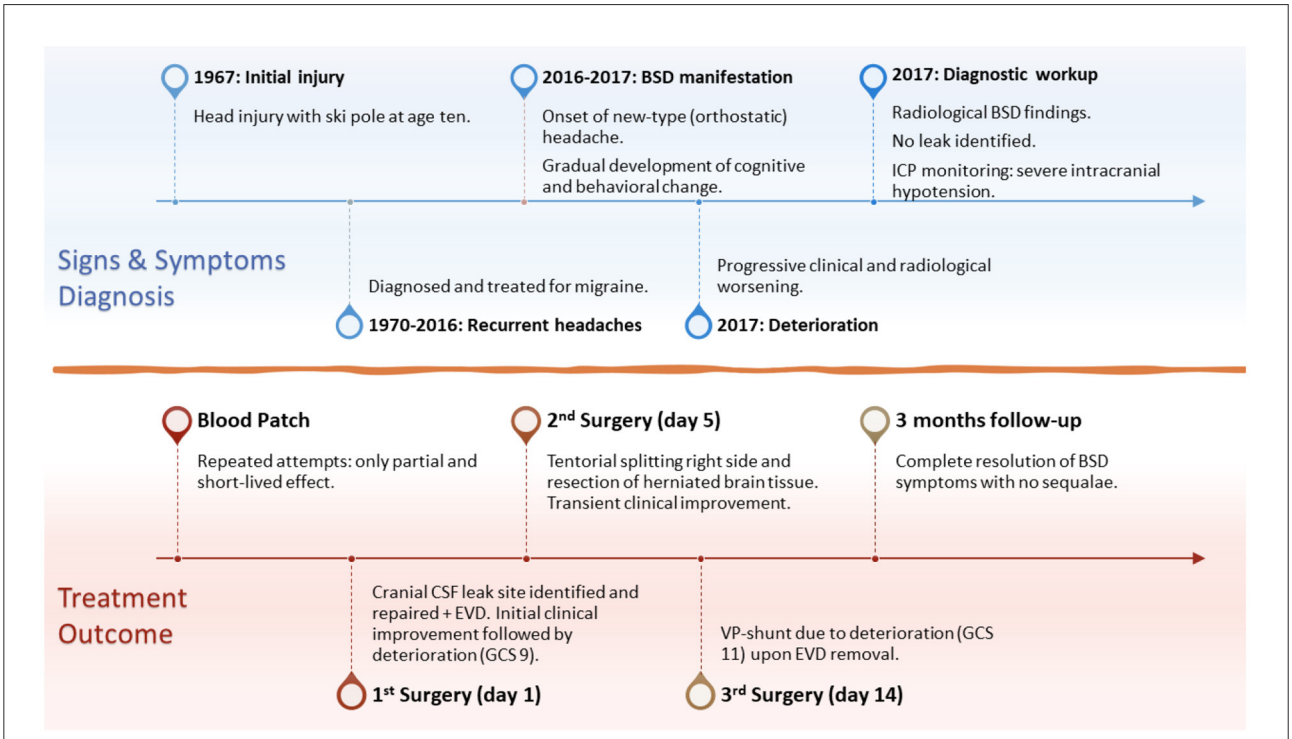

FIGURE 1
Timeline of the disease development and progression, signs and symptoms, diagnostic workup and findings, surgical treatment, and 3-months follow-up. BSD, brain sagging dementia; ICP, intracranial pressure; EVD, external ventricular drain; GCS, Glasgow Coma Scale; VP-shunt, ventriculoperitoneal shunt.

TABLE 1 Diagnostic criteria for brain sagging dementia (BSD) (3).

Absolute clinical and imaging criteria	Present	Absent
Signs and symptoms of bvFTD (1, 2)*	✓	
Absence of bvFTD imaging findings; frontotemporal atrophy†	✓	
Imaging findings of brain sagging	✓	
Insidious onset, and slowly progressing (>3/4 weeks)	✓	
No history of recent trauma or lumbar puncture	✓	
Symptom onset before 65 years of age	✓	
Symptoms cannot be explained by altered level of consciousness alone	✓	
At least one of the supporting clinical criteria (SIH) or 3 of the additional criteria	✓	
Supporting clinical criteria		
Orthostatic headache	✓	
Low lumbar puncture opening pressure	✓	
Improvement of symptoms after blood patch	✓	
Additional criteria		
Headache	✓	
Cerebellar signs and symptoms	✓	
Hypersomnolence	✓	
Choreiform movements		×
Pachymeningeal enhancement on imaging	✓	
Subdural effusion on imaging	✓	
Evidence of cerebrospinal fluid leak on myelogram		×

(1, 2) bvFTD, behavioral variant frontotemporal dementia; SIH, spontaneous intracranial hypotension.
*Signs and symptoms must meet the diagnostic criteria of bvFTD.
† Frontotemporal atrophy must be ruled out, while findings on PET and SPECT will not alter the diagnosis.
The International Classification of Headache Disorders, 3rd edition.

assaulted the nurse in his room, thus acquiring surveillance by a security guard. He lost insight, and his decision-making became seriously hampered. For instance, he insisted to divorce his wife. Mini-Mental exam score worsened in a matter of weeks from 26/30 to eventually a point where he could not cooperate for the test.

Due to his rapid clinical decline, a two-step cranial surgical approach was suggested, and his family consented. A cranial defect corresponding to his childhood head trauma was evident during the surgical exploration (Figure 2). The CSF leakage site was repaired, and an external ventricular drain was placed to overcome the supratentorial hydrocephalus induced by the brain sagging and subsequent CSF outflow obstruction. The splitting of the tentorium on the left side was also performed. The right tentorium was split in the second surgical step, and herniated brain tissue was resected. Despite a transient post-operative clinical improvement, his condition deteriorated. He became drowsy and showed clinical signs of herniation upon attempting to withdraw the drain. Therefore, he received a ventriculoperitoneal shunt with Codman-Hakim vale on a low setting (5 cmH_2O).

His condition improved remarkably after shunt surgery, and he was discharged shortly thereafter. At 3-months follow-up, he was in good shape, with no neurological deficits and no more headaches. He scored 30/30 on MMSE and showed a good quality of life on the Short Form Health Survey (SF-36). He was back in his position as company director. He had no recollection of the time around his stay and was deeply sorry for his bizarre behavior. There was no sign of relapse on the 5-years follow-up.

Discussion

The constellation of signs and symptoms of frontotemporal dementia caused by SIH, known as brain sagging dementia (BSD), has been increasingly recognized recently (7–9). The condition is twice as common in male patients and peaks in the sixth decade of life (3). Like in SIH, most patients present with some form of headache. In addition, BSD patients suffer from cognitive and behavioral changes that can potentially progress and severely impair their life.

Although a spinal CSF leakage is thought to be the etiology behind SIH and BSD, it is not radiologically evident in a significant number of patients (3, 4). In a recent review on BSD, a CSF leakage site was found in merely 13% of cases (3). Moreover, no cranial leak was reported in the two largest reviews on SIH and BSD (3, 4). Thus, this is the first report on a case of BSD caused by a cranial CSF leak.

This case report is remarkable for several reasons. First, it shows that a cranial cause of the leak must be explored thoroughly, particularly if no spinal leak is found. This is especially important as only the minority of leaks are successfully recognized in BSD patients (3). A thorough interview with the patient and their relatives may unveil details that can aid toward a potential CSF leakage site. In the current case, although no CSF leak was evident on radiological workup, the clinical picture, pathologically negative ICP, and past medical history with childhood cranial trauma with corresponding obscure radiological signs of old trauma in that area indicated surgical exploration.

Second, the complexity of this condition is well illustrated by the extended delay between the primary injury and fulminant disease with progressive signs and symptoms. Although the patient had some form of headache

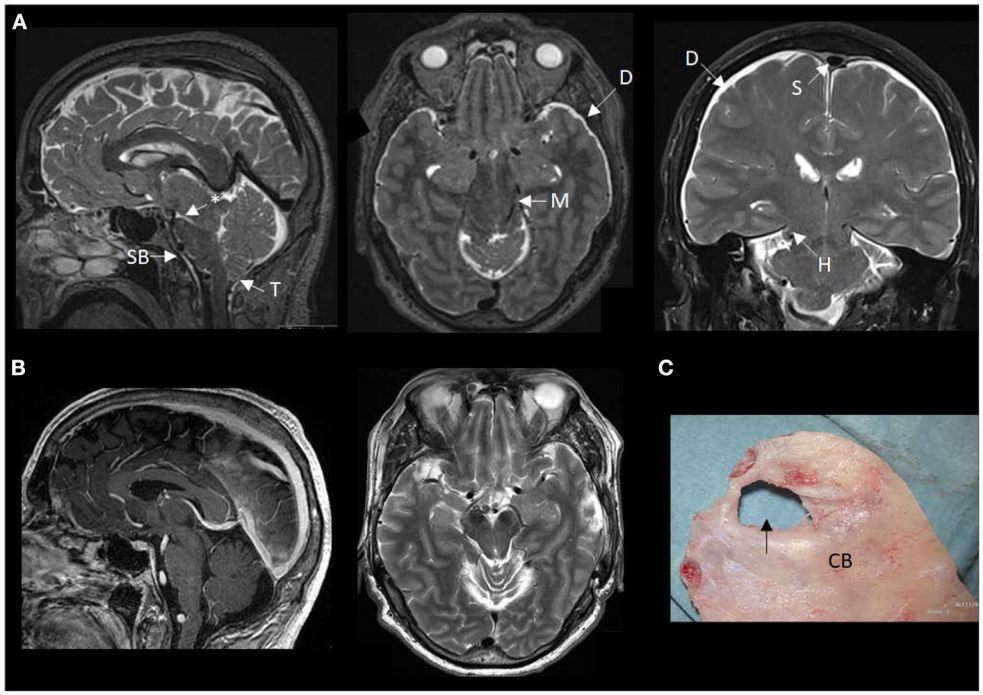

FIGURE 2
MRI findings of brain sagging dementia in this case. **(A)** The preoperative MRI in sagittal, axial and coronal planes show typical signs of intracranial hypotension, including sagging brainstem (SB) toward the clival bone, downward tonsillar (T) ectopy, smaller ponto-mesencephalic angle (indicated by an asterisk), enhancement of the dura (D), rounding of the cross-section of the dural venous sinus (S) indicative of dural venous engorgement, transtentorial herniation (H), and reduced space for the mesencephalon (M). **(B)** The postoperative MRI in sagittal and axial planes demonstrate reversal of the MRI signs of brain sagging. **(C)** The cranial bone (CB) with a defect (indicated by an arrow), as presented during surgical exploration.

throughout the years, his condition severely escalated during the last 2 years, with complete decompensation within months. Moreover, the fact that CSF shunting was his ultimate remedy shows the coping mechanism his CSF circulatory system had to withstand until absolute decompensation.

Although the exact mechanism behind this can only be speculated at this moment, it is presumably multifactorial, involving both the compensatory mechanism and cranial to spinal fluid shift concept that has been proposed in patients with SIH (10, 11). In our patient, we believe that the decompensation was preceded by CSF depletion, causing the brain sagging, responsible for patients' initial BSD signs and symptoms, as described in great detail in a narrative review that we recently published (3). Further progress resulted in CSF outflow obstruction at the cranio-cervical junction, impeding the CSF flow system (12). This may have instigated further escalation of the now "enclosed intracranial compartment" with profound hypovolemia and hypotension evident on ICP monitoring, ultimately resulting in patients' critical deterioration. This theory is supported by the fact that the patient developed severe supratentorial hydrocephalus following the surgical repair of the cranial leak that required a CSF diversion procedure. Although the so-called "rebound intracranial hypertension" following treatment of SIH is well described in the literature (13, 14), in our patient with a CSF outflow obstruction at the cerebral aqueduct, it would be detrimental if left untreated.

Finally, this report highlights the importance of recognizing and treating this potentially reversible form of early-onset dementia, regardless of the condition's etiology, severity, and duration. Being familiar with the diagnostic criteria for BSD may be helpful in this process.

Data availability statement

The raw data supporting the conclusions of this article will be made available by the authors, without undue reservation.

FIGURE 3
Intracranial pressure was measured from a Codman ICP sensor placed in the right frontal lobe. **(A)** The left window presents the trend plots of mean ICP (MeanP, light green) and mean ICP wave amplitude (MeanWave AMP, darker green). To the right is indicated the average values for the trend plots: Mean ICP – 8.7 mmHg, Mean Wave AMP (amplitude) 2.6 mmHg, Mean wave RT (Rise time) 0.22 s, Mean Wave RT Coeff (Rise time coefficient) 12.8 mmHg/s. Total 18,237 6-s windows were analyzed, wherein 13,157 were of acceptable quality for analysis (acceptance 72%). **(B)** The left window presents another trend plot of mean ICP (MeanP, light green) and of mean ICP wave amplitude (MeanWave AMP, darker green). To the right is indicated the average values for these trend plots: Mean ICP – 1.0 mmHg, Mean Wave AMP (amplitude) 3.0 mmHg, Mean wave RT (Rise time) 0.21 s, Mean Wave RT Coeff (Rise time coefficient) 16.0 mmHg/s. Total 20,001 6-s windows were analyzed, wherein 15,725 were of acceptable quality for analysis (acceptance 79%). **(C)** One 6-s time window is shown with five single pressure waves identified by their diastolic minimum and systolic maximum pressures. For this particular 6-s time window, parameters were: Mean ICP – 1.1 mmHg, Mean Wave AMP (amplitude) 3.4 mmHg, Mean wave RT (Rise time) 0.35 s, Mean Wave RT Coeff (Rise time coefficient) 9.5 mmHg/s. Image: Sensometrics RD Software (dPCom AS, Oslo, Norway).

Ethics statement

Ethical review and approval was not required for the study on human participants in accordance with the local legislation and institutional requirements. The patients/participants provided their written informed consent to participate in this study.

Author contributions

Conceptualization and design, data analysis, review and editing, and approval of the final manuscript: AL and PE. Writing—original draft: AL. Supervision, administration, and material requests: PE. Both authors contributed to the article and approved the submitted version.

Acknowledgments

The authors would like to thank Hilde Iren Flaatten, librarian at the Medical Library at Rikshospitalet—University of Oslo, for developing the search strategy and performing the database searches.

Conflict of interest

The authors declare that the research was conducted in the absence of any commercial or financial relationships that could be construed as a potential conflict of interest.

Publisher's note

All claims expressed in this article are solely those of the authors and do not necessarily represent those of their affiliated organizations, or those of the publisher, the editors and the reviewers. Any product that may be evaluated in this article, or claim that may be made by its manufacturer, is not guaranteed or endorsed by the publisher.

Supplementary material

The Supplementary Material for this article can be found online at: https://www.frontiersin.org/articles/10.3389/fneur.2022.1006060/full#supplementary-material

References

1. Neary D, Snowden JS, Gustafson L, Passant U, Stuss D, Black S, et al. Frontotemporal lobar degeneration: a consensus on clinical diagnostic criteria. *Neurology*. (1998) 51:1546–54. doi: 10.1212/WNL.51.6.1546

2. Rascovsky K, Hodges JR, Knopman D, Mendez MF, Kramer JH, Neuhaus J, et al. Sensitivity of revised diagnostic criteria for the behavioural variant of frontotemporal dementia. *Brain*. (2011) 134:2456–77. doi: 10.1093/brain/awr179

3. Lashkarivand A, Eide PK. Brain sagging dementia-diagnosis, treatment, and outcome: a review. *Neurology*. (2022) 98:798–805. doi: 10.1212/WNL.0000000000200511

4. D'Antona L, Jaime Merchan MA, Vassiliou A, Watkins LD, Davagnanam I, Toma AK, et al. Clinical presentation, investigation findings, and treatment outcomes of spontaneous intracranial hypotension syndrome: a systematic review and meta-analysis. *JAMA Neurol*. (2021) 78:329–37. doi: 10.1001/jamaneurol.2020.4799

5. Eide PK, Mariussen E, Uggerud H, Pripp AH, Lashkarivand A, Hassel B, et al. Clinical application of intrathecal gadobutrol for assessment of cerebrospinal fluid tracer clearance to blood. *JCI Insight*. (2021) 6:1–13. doi: 10.1172/jci.insight.147063

6. Eide PK. The correlation between pulsatile intracranial pressure and indices of intracranial pressure-volume reserve capacity: results from ventricular infusion testing. *J Neurosurg*. (2016) 125:1493–503. doi: 10.3171/2015.11.JNS151529

7. Wicklund MR, Mokri B, Drubach DA, Boeve BF, Parisi JE, Josephs KA. Frontotemporal brain sagging syndrome: an SIH-like presentation mimicking FTD. *Neurology*. (2011) 76:1377–82. doi: 10.1212/WNL.0b013e3182166e42

8. Vetrugno R, Mascalchi M, Chierichetti F, Gallassi R, Alessandria M, Guerrini L, et al. Hypoactive-hypoalert behavior ("psychic akinesia") in intracranial hypotension syndrome. *Neurology*. (2008) 71:1452–4. doi: 10.1212/01.wnl.0000327869.39403.82

9. Schievink WI, Maya MM, Barnard ZR, Moser FG, Jean-Pierre S, Waxman AD, et al. Behavioral variant frontotemporal dementia as a serious complication of spontaneous intracranial hypotension. *Operat. Neurosurgery*. (2018) 15:505–15. doi: 10.1093/ons/opy029

10. Häni L, Fung C, Jesse CM, Ulrich CT, Miesbach T, Cipriani DR, et al. Insights into the natural history of spontaneous intracranial hypotension from infusion testing. *Neurology*. (2020) 95:e247–e55. doi: 10.1212/WNL.0000000000009812

11. Goldberg J, Häni L, Jesse CM, Zubak I, Piechowiak EI, Gralla J, et al. Spontaneous Intracranial hypotension without CSF leakage-concept of a pathological cranial to spinal fluid shift. *Front Neurol*. (2021) 12:760081. doi: 10.3389/fneur.2021.760081

12. Eide PK, Valnes LM, Lindstrom EK, Mardal KA, Ringstad G. Direction and magnitude of cerebrospinal fluid flow vary substantially across central nervous system diseases. *Fluids Barriers CNS*. (2021) 18:16. doi: 10.1186/s12987-021-00251-6

13. Tsui H, Wu S, Kuo H, Chen C. Rebound intracranial hypertension after treatment of spontaneous intracranial hypotension. *Eur J Neurol*. (2006) 13:780–2. doi: 10.1111/j.1468-1331.2006.01369.x

14. Schievink WI, Maya MM, Jean-Pierre S, Moser FG, Nuño M, Pressman BD. Rebound high-pressure headache after treatment of spontaneous intracranial hypotension: MRV study. *Neurol Clin Pract*. (2019) 9:93–100. doi: 10.1212/CPJ.0000000000000550

frontiers | Frontiers in Neurology

TYPE Case Report
PUBLISHED 25 October 2022
DOI 10.3389/fneur.2022.1013213

OPEN ACCESS

EDITED BY
Bruce Miller,
University of California, San Francisco, United States

REVIEWED BY
Hao Chen,
The Affiliated Hospital of Xuzhou Medical University, China
Akihiro Shimotake,
Kyoto University, Japan

*CORRESPONDENCE
Yuming Xu
xuyuming@zzu.edu.cn
Jing Yang
yangjing9527@126.com
Song Tan
tansong@med.uestc.edu.cn

†These authors have contributed equally to this work and share first authorship

SPECIALTY SECTION
This article was submitted to Dementia and Neurodegenerative Diseases, a section of the journal Frontiers in Neurology

RECEIVED 06 August 2022
ACCEPTED 21 September 2022
PUBLISHED 25 October 2022

CITATION
Liu Y, Zeng L, Yuan Y, Wang Y, Chen K, Chen Y, Bai J, Xiao F, Xu Y, Yang J and Tan S (2022) Case report: Two siblings with neuronal intranuclear inclusion disease exhibiting distinct clinicoradiological findings. *Front. Neurol.* 13:1013213. doi: 10.3389/fneur.2022.1013213

Case report: Two siblings with neuronal intranuclear inclusion disease exhibiting distinct clinicoradiological findings

Yutao Liu[1,2,3†], Li Zeng[4†], Yanpeng Yuan[1,2,3], Yangyang Wang[1,2,3], Kai Chen[4], Yan Chen[5], Jiaying Bai[4], Feng Xiao[4], Yuming Xu[1,2,3*], Jing Yang[1,2,3*] and Song Tan[4,6*]

[1]Department of Neurology, The First Affiliated Hospital of Zhengzhou University, Zhengzhou University, Zhengzhou, China, [2]Key Laboratory of Cerebrovascular Disease of Henan Province, Zhengzhou University, Zhengzhou, China, [3]Henan Medical Key Laboratory of Neurogenetic and Neurodegenerative Disease, Zhengzhou, China, [4]Department of Neurology, Sichuan Provincial People's Hospital, University of Electronic Science and Technology of China, Chengdu, China, [5]Department of Neurology, The People's Hospital of Jianyang City, Jianyang, China, [6]Sichuan Provincial Key Laboratory for Human Disease Gene Study, Chengdu, China

Neuronal intranuclear inclusion disease (NIID) is a rare neurodegenerative disorder characterized by the presence of eosinophilic hyaline intranuclear inclusions. Owing to its widely varying clinical manifestations, NIID is frequently misdiagnosed or overlooked. However, a characteristic high-intensity corticomedullary junction signal on diffusion-weighted imaging (DWI) is often indicative of NIID. In this study, we described the case of two sisters with NIID who presented with distinct symptoms and imaging data. The younger sister showed symptoms similar to those of mitochondrial encephalopathy, with a reversible high-intensity signal from the cortex on T2 and DWI. The elder sister showed a characteristic high-signal "ribbon sign" in the corticomedullary junction on DWI. Skin biopsy confirmed that both had neuronal intranuclear inclusion. Two years later, the younger sister also developed the characteristic high-signal "ribbon sign" in the corticomedullary junction on DWI. This case study provides new insights into the complexity of NIID. The findings suggest that patients with this condition, including those belonging to the same family, may exhibit varying clinical and imaging features at different times.

KEYWORDS

neuronal intranuclear inclusion disease, mitochondrial encephalopathy, ribbon sign, *NOTCH2NLC* gene, siblings

Introduction

Neuronal intranuclear inclusion disease (NIID) is a gradually progressing neurodegenerative condition characterized by the presence of tissue-wide eosinophilic intranuclear hyaline inclusions in cells of the central and peripheral nervous systems (1). Given its varying clinical features and pathological findings, NIID is considered a heterogeneous disease, although a persistent, highly intense corticomedullary junction

on diffusion-weighted imaging (DWI) is generally considered to be a characteristic of this disease (2). Eosinophilic intranuclear inclusion bodies found in skin biopsy samples can also be indicative of NIID (3), and the disease can be confirmed by determining whether GGC repeats are present in the *NOTCH2NLC* gene (4, 5). In this study, we reported two siblings with adult-onset NIID and described their clinical, imaging, and pathological features. The imaging features in our initial patient's older sister provided important clues toward the younger's diagnosis. Two years later, the younger sister also began to exhibit typical hyper-intense signals in the corticomedullary junction on DWI. In particular, we demonstrated that the varying symptoms and imaging features we observed may present a challenge for accurate diagnosis. Our case is unique because none of the cases reported that the patient had typical MRI findings of mitochondrial encephalopathy in the early stage, and later had high signal in the corticomedullary junction following up for several years. This imaging change was discovered and reported for the first time by our group.

Case description

A 20-year-old woman (patient 1) visited our center after having experienced recurrent headache, blurred vision, and paroxysmal partial body numbness and weakness for 6 years. The patient's initial symptoms in 2016 consisted of right-side numbness from the calf to the upper limb and face that improved after 10 min and disappeared after 1 h. Several months later, the patient experienced blurring in her right visual field with a headache that disrupted sleep throughout the night. By the next morning, the patient's vision had cleared, while the severity of their headache had alleviated. Brain computed tomography (CT) and electroencephalography (EEG) showed normal results. In November 2019, the patient experienced another attack with paroxysmal right limb and face numbness and weakness accompanied by hemianopia, vomiting, and confusion, wherein the patient lost consciousness for 3 days. Later that month, the patient's electromyography (EMG) showed that motor and sensory nerve conduction velocities in her limbs were slower than normal. The F-wave conduction velocity was also slow. The motor unit potential time range of the detected muscles was normal, while the amplitude of the wave was high, risking neurogenic damage. Overall, obvious demyelination of peripheral nerves in four limbs was present. Brain magnetic resonance imaging (MRI) showed swelling of the gyri and shallow sulci in the left cerebral hemisphere, especially in the temporoparietal-occipital lobe, on T2, DWI, and T2 fluid-attenuated inversion recovery (FLAIR) sequence in November 2019 (Figures 1A1–A5,B1–B5,C1–C5); the signal was slightly higher in December 2019 (Figures 1A6–A10,C6–C10). Magnetic resonance spectroscopy (MRS) performed in December 2019 showed that a broad lactic acid peak was observed (Figure 1B6). Lactic acid exercise tests yielded elevated blood levels at baseline (3.5 mmol/L; reference: 0.5–2.2 mmol/L), after running for 15 min (8.3 mmol/L; three times higher than normal), and 10 min after completing the run (4.9 mmol/L; twice the normal level); hence, mitochondrial myopathy was suspected. The patient's liver and renal functions, electrolytes, trace element levels, myocardial enzymes, blood ammonia, thyroid function, tumor marker levels, hepatitis B test results, and HIV test results were normal. Antibody tests for autoimmune and paraneoplastic disorders were also negative on serum and cerebrospinal fluid analysis. Video EEG showed moderately abnormal, single-scattered sharp waves; additionally, sharp slow waves were observed in the frontal, parietal, and temporal areas on both sides. The patient was discharged after her symptoms improved. During the months after discharge, the patient experienced paroxysmal partial body numbness on three occasions, accompanied by difficulty speaking or by headache. As these symptoms all resolved within 5 min, the patient did not consult a physician. In August 2020, the patient returned to the hospital for re-examination, despite not experiencing any discomfort at the time. Physical examination revealed that the patient's memory had declined; cognitive screening tests showed that the patient's Mini-Mental State Examination (MMSE) score and Montreal Cognitive Assessment (MoCA) score were 24/30 and 20/30, respectively. Brain MRI showed no abnormalities in the sulci or gyri, and no diffusion limitation was found on DWI (Figures 1D1–D5,E1–E5,F1–F5). EMG showed symmetrical multiple peripheral nerve damage in the limbs as well as severe demyelination; the patient's muscles also exhibited neurogenic damage.

Given the chronic course of the central and peripheral nervous system defects, the patient's disease apparently began manifesting at approximately 20 years of age following poor exercise tolerance and fatigue experienced since childhood. Brain MRI showed laminar necrosis of the left temporo-occipital lobe, although the abnormality disappeared completely after 9 months. Given that the patient's aforementioned test data highly suggested mitochondrial encephalomyopathy, muscle biopsy and mitochondrial-related gene analysis were performed; however, both tests showed no abnormalities.

The patient's sister (patient 2) was 32 years old and had experienced symptom onset at 27 years of age; symptoms included recurrent headache with blurred vision and progressive contralateral limb numbness and weakness. At the onset of symptoms for 5 years before (in 2017), the patient's episodes occurred once in every 2–3 months and the symptoms improved significantly within 2–3 days. An EMG performed at West China Hospital in December 2017 showed peripheral neurogenic damage in the limbs with marked effects on sensory and motor nerve conduction. Brain MRI showed abnormal signals bilaterally in the frontotemporal cortex and corpus callosum. EEG results were mildly abnormal, with an increase in slow waves in each lead on both sides. The patient was

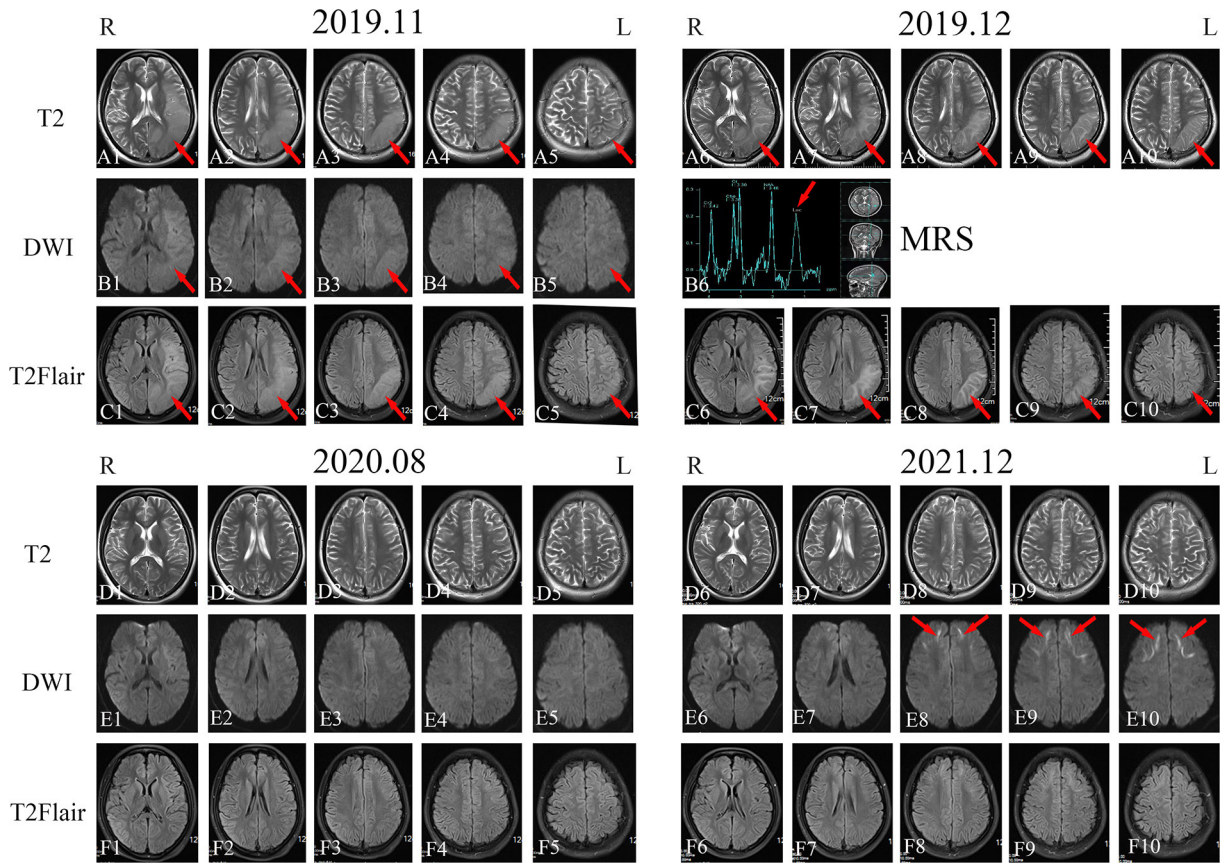

FIGURE 1
Imaging examination of patient 1. Head magnetic resonance imaging (MRI) in November 2019 showed high-signal intensity in the left temporal, parietal, and occipital lobes on T2-weighted imaging, diffusion-weighted imaging (DWI), and T2 fluid-attenuated inversion recovery (FLAIR) sequences [**(A1–A5)**, **(B1–B5)**, and **(C1–C5)**; red arrows]. MRI in December 2019 showed high-signal intensity in the left temporal, parietal, and occipital lobes on T2-weighted imaging, magnetic resonance spectroscopy, and T2 FLAIR sequences [**(A6–A10)**, **(B6)**, and **(C6–C10)**; red arrows]. Head MRI in August 2020 revealed that the high-intensity signal on the left temporal, parietal, and occipital lobes on T2-weighted imaging, DWI, and T2 FLAIR sequences had disappeared [**(D1–D5)**, **(E1–E5)**, and **(F1–F5)**]. Head MRI in December 2021 showed bilateral and relatively symmetrical ribbon signs with high-intensity signals along the corticomedullary junction of the frontotemporal-parietal lobes on DWI [**(D6–D10)**, **(E6–E10)**, and **(F6–F10)**; red arrows].

suspected to have NIID. On 27 November 2019, the patient experienced another headache as well as blurred vision in the right eye followed by vomiting and an inability to speak; these symptoms did not improve with anti-headache drugs. The patient subsequently performed second brain MRI on 5 December 2019, which showed extensive and slightly elongated T1 shadows, as well as a slightly elongated T2 signal shadow, bilaterally in the frontal, temporal, parietal, and occipital cortices and corpus callosum. Moreover, T2 FLAIR and DWI signals were high (Figures 2A1–A5,B1–B5,C1–C5). Lactic acid was within a normal range (1.6 mmol/L). The frequency of the patient's headache began to increase in March 2020, with several monthly attacks occurring. In August 2020, the patient's physical examination revealed that her memory and cognition had declined and that she exhibited signs of ataxia. On cognitive-screening testing, the patient's MMSE and MoCA scores were 27/30 and 21/30, respectively. Brain MRI showed symmetrical ribbon-like elongated T1 and slightly elongated T2 signals in the corticomedullary junction and corpus callosum of both cerebral hemispheres. T2 FLAIR showed a high signal, and the apparent diffusion coefficient slightly decreased; no enhancement was observed in the lesions (Figures 2D1–D5,E1–E5,F1–F5).

A review of patient 1's personal history revealed that she had exhibited poor performance in mathematics and sports (jump and long-running) since childhood; moreover, the patient was sensitive to pungent odors and coughed easily. The patient 1 (II-2)'s family history showed her mother (I-2) also had a long history of repeated severe headache and died at the age of 49 due to "headaches and disturbances in consciousness" without genetic testing. Her father (I-1) had no similar symptoms and was ruled out by genetic testing. Her old sister (patient 2, II-1) had symptoms that included recurrent headache with

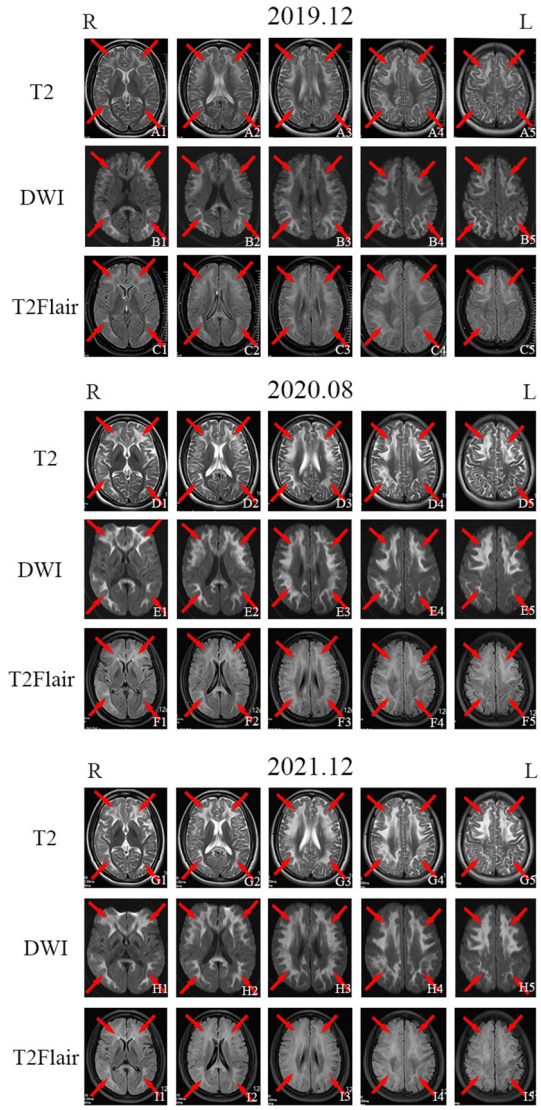

FIGURE 2
Imaging examination of patient 2. Head magnetic resonance imaging (MRI) in November 2019 showed bilateral and relatively symmetrical ribbon signs with high-intensity signals along the corticomedullary junction of the frontotemporal-parietal lobes and corpus callosum on T2-weighted imaging, diffusion-weighted imaging (DWI), and T2 fluid-attenuated inversion recovery (FLAIR) sequence [**(A1–A5)**, **(B1–B5)**, and **(C1–C5)**; red arrows]. Head MRI in August 2020 [**(D1–D5)**, **(E1–E5)**, and **(F1–F5)**; red arrows] and December 2021 [**(G1–G5)**, **(H1–H5)**, and **(I1–I5)**; red arrows] showed the same high signal along the corticomedullary junction of the frontotemporal-parietal lobes and corpus callosum on T2-weighted imaging, DWI, and T2 FLAIR sequences as were observed in November 2019.

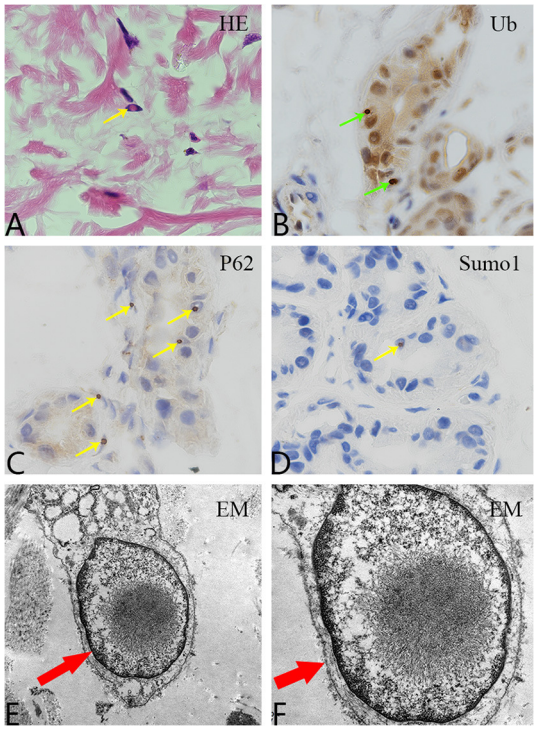

FIGURE 3
Pathological examination. **(A)** Hematoxylin and eosin staining shows eosinophilic inclusion bodies in some skin fibroblasts (100×, yellow arrow). **(B)** Anti-ubiquitin immunohistochemical staining. Inclusion bodies are visible in the nuclei of some skin sweat gland cells (100×, green arrow). **(C)** Anti-P62 immunohistochemical staining. Inclusion bodies are observed in the nuclei of some sweat gland cells (100×, yellow arrow). **(D)** Anti-SUMO1 immunohistochemical staining. Inclusion bodies are visible in the nuclei of some sweat gland cells (100×, yellow arrow). **(E,F)** Electron microscopy revealed a circular inclusion body structure in the nucleus of a sweat gland cell (15,000× and 30,000×, respectively; red arrows).

blurred vision and progressive contralateral limb numbness and weakness (Supplementary Figure 1).

Both sisters underwent skin biopsy. Light and electron microscopy showed eosinophilic, ubiquitin-positive, p62-positive, and SUMO-1-positive intranuclear inclusions in the adipocytes, fibroblasts, and sweat gland cells in both patients (Figures 3A–F). Both sisters were also tested for the *NOTCH2NLC* pathogenic gene of NIID; patients 1 and 2 had 70 and 66 GGC repeats, respectively (Figure 4), suggesting NIID. A genetic test for cerebral autosomal dominant arteriopathy with subcortical infarcts and leukoencephalopathy was negative, and subsequent genetic analysis of the fragile X chromosome mental retardation gene 1 showed normal GGC repeat numbers in both sisters, which ruled out fragile X-related tremor/ataxia syndrome. Given these clinical findings, both sisters were diagnosed with NIID.

Between her discharge in 2020 and the year after, patient 1 had another episode of right hemiparesis with a contralateral headache that was less severe than before. In December 2021, the patient returned to the hospital for re-examination; cognitive screening tests showed that her MMSE (27/30) and MoCA (25/30) scores were both higher than those in 2020. Brain

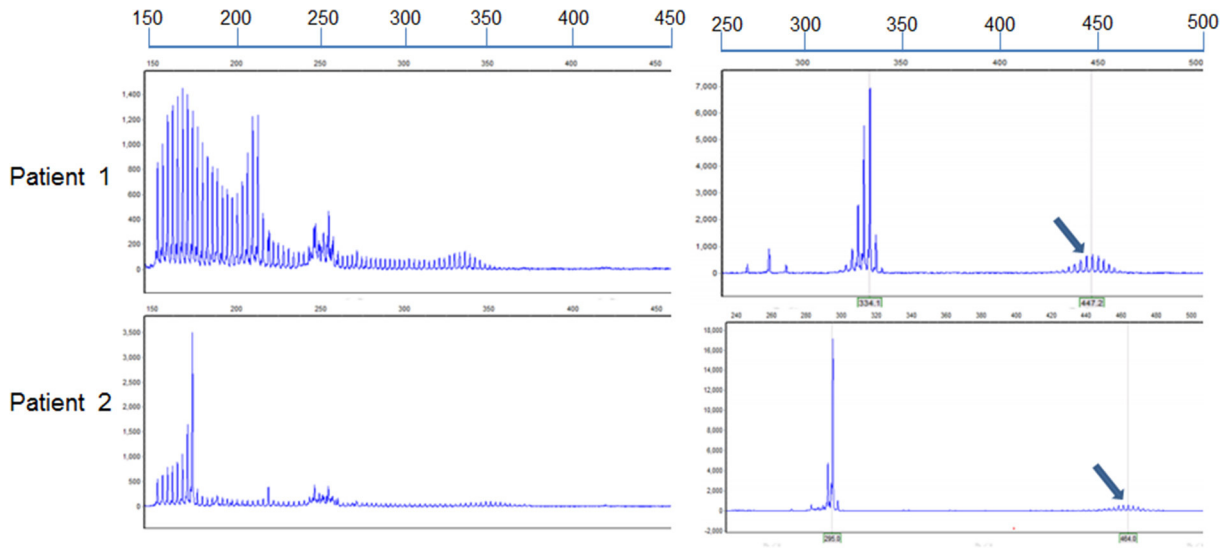

FIGURE 4
Identification of alleles with GGC repeat expansions in the two sisters. Repeat-primed PCR and fluorescence amplicon length analysis of both patients showed GGC repeat expansions. The number of repeats was determined by comparing the length of the highest signal peak of the expanded allele (arrows) to that of the human reference gene sequence as previously described (6). The formula to determine repeat size was (["length of the highest signal peak of the expanded allele" bp − 185 bp] / 3 bp + 13). The assumed length of the PCR product was 185 bp in accordance with the standardized GRCh38.p13 human genome, containing the reference (GGC)9(GGA)2(GGC)2 sequence ($n = 13$).

MRI in December 2021 showed bilateral corticomedullary junction white matter areas in the frontal lobes that were patchy with slightly elongated T1 and T2 signal shadows. T2 FLAIR showed a slightly elevated signal, while diffusion was limited on the DWI sequence (Figures 1D6–D10,E6–E10,F6–F10). Lactic acid levels in the blood were normal (2.2 mmol/L) at baseline. EMG showed that extensive peripheral nerve lesions and axonal myelin sheath damage were present, especially in the lower limbs.

Since October 2021, the frequency of patient 2's headache had increased to once a week with nausea and vomiting. On 30 November 2021, the patient's cognitive screening tests showed MMSE and MoCA scores of 27/30 and 22/30, respectively. Brain MRI in December 2021 revealed minimal change from August 2020 (Figures 2G1–G5,H1–H5,I1–I5). EMG showed symmetrical peripheral nerve damage (mainly demyelination) in the limbs, including both motor and sensory nerves.

Both patients' clinical features are shown in Supplementary Table 1.

Discussion

Neuronal intranuclear inclusion disease is a chronic progressive neurodegenerative disease characterized by transparent eosinophilic inclusions in the central and peripheral nervous systems and internal organs (2, 3). Brain images of patients with adult-onset NIID exhibit characteristic features (4); DWI shows a high-intensity signal at the corticomedullary junction known as the "ribbon sign" (2, 5). Histopathologically, adult-onset NIID is characterized by nuclear inclusions in skin cells, constituting the main diagnostic criterion for this condition (1, 7). GGC repeat expansion in the 5′UTR region of the human-specific *NOTCH2NLC* gene is the genetic underpinning of NIID (8, 9). While the number of GGC repeats normally does not exceed 40, patients with NIID typically present with a minimum of 60 repeats (6, 10). Some studies have also demonstrated that mitochondrial encephalomyopathy is a characteristic of NIID (11, 12). The presentations observed in our patients offer additional evidence regarding the clinical signs of this disease and help clarify the fact that mitochondrial diseases that lack accompanying pathological manifestations may be indicative of NIID.

The two patients in our study were sisters aged 14 and 27 years at the time of the onset of their diseases. Their symptoms indicated that they belonged to the limb-weakness subgroup of familial adult-onset NIID. According to previous studies, the main symptom of this disease is limb weakness in young people and memory loss in older individuals (13, 14). However, our patients developed cognitive impairment at a young age. Brain MRI analysis revealed reversible laminar necrosis of the cortex with no ribbon sign in patient 1, which is consistent with the imaging features of mitochondrial encephalomyopathy. In contrast, the DWI sequence of the head MRI of patient 2

showed the characteristic ribbon sign; these differences highlight the clinical heterogeneity of the disease. Even if the clinical manifestations of patients in the same family are similar, their imaging findings may be considerably different. The clinical manifestations, imaging features, and laboratory tests of patient 1 were highly indicative of mitochondrial encephalomyopathy; however, muscle pathology or genetic testing did not support this conclusion, thereby complicating the diagnosis. After performing a detailed evaluation of patient 2, we observed the characteristic ribbon sign on imaging that prompted further investigation of the possibility of NIID. Finally, skin biopsy and genetic testing confirmed the diagnosis of NIID in both sisters. Within 2 years of follow-up, patient 1 also began to exhibit typical hyper-intense signals in the corticomedullary junction on DWI; this indicated that the patients had different imaging features that changed over time. A DWI high signal at the junction of the cortex and medulla may be a typical manifestation of progression to the late stage of the disease. Different imaging manifestations characterize the early stage of the disease, such as those observed in mitochondrial encephalopathy in patient 1. Furthermore, a highly consistent ribbon sign tends to appear in the late stage. Moreover, in patient 1, the gyrus of the left cerebral hemisphere was swollen, and the sulci became shallow, which was obvious in the parietal-temporal-occipital lobe and similar to mitochondrial performance. However, the high signal in the corticomedullary junction area in the later stage began from the frontal lobe. Whether this typical imaging change also developed from front to back needs to be confirmed during follow-up visits. Patient 2 had a typical DWI high signal at the junction of the cortex and medulla more than 2 years after onset and continued to exhibit typical imaging manifestations until 5 years after the course of the disease. An imaging observation study that tracked a patient for 16 years found that the patient's initial T2 FLAIR images showed spatial high-intensity lesions in the subcortical white matter, while DWI showed no specific abnormalities (15). It took 16 years to develop leucoencephalopathy on T2 FLAIR images, and the high-intensity signal in the corticomedullary junction on DWI had gradually expanded after symptom onset. This is also an important reason why the disease is prone to oversight and misdiagnosis.

The number of GGC repeats is approximately 60 in patients with tremors, 80 in those with Parkinson's disease, 120 in those with cognitive impairment, and 200 in those with limb weakness. Patients 1 and 2 had 70 and 66 GGC repeats, respectively, but had symptoms of limb weakness and cognitive impairment; this ought to prompt additional exploration of the relationship between GGC repeats and clinical phenotypes. The correlation between the repetition times and clinical manifestations of other polynucleotide repeat diseases should also be considered. For example, ankylosing muscular dystrophy and ophthalmo-pharyngeal muscular dystrophy have similar relations with repetition times.

Conclusions

The two sisters presented with distinct clinical manifestations and imaging characteristics. By analyzing the images of patient 2, we were able to determine the diagnosis of patient 1. Overall, this case study provides new information regarding our understanding of NIID.

Data availability statement

The original contributions presented in the study are included in the article/Supplementary material, further inquiries can be directed to the corresponding author/s.

Ethics statement

Written informed consent was obtained from the individual(s) for the publication of any potentially identifiable images or data included in this article.

Author contributions

YL drafted and revised the manuscript and analyzed and interpreted the data. LZ performed skin biopsy, muscle pathology analysis, muscle pathology photography, and clinical evaluation. YY performed skin pathology analysis and photography. YW performed gene detections. KC performed a muscle biopsy. YC recommended patients, conducted partial examinations, and collected medical history. JB collected medical history and blood specimens. FX collected medical history. YX and JY performed a critical revision of the manuscript. ST collected family clinical data, performed the clinical evaluation and preliminary diagnosis, revised the manuscript, and supervised the study. All authors contributed to the article and approved the submitted version.

Funding

This study was supported by the Department of Science and Technology of Henan Province (Social Development, Grant No. 212102310825) to YL, the National Natural Science Foundation of China (Grant Nos. U1904207 and 91849115) and the National Key R&D Program of China (Grant No. 2017YFA0105003) to YX, the Provincial and Ministry of Health Construction

Committee of Henan Province (SB201902012), Henan Young and Middle-Aged Health Science and Technology Innovation Talent Training Project—Outstanding Young Talents to JY, the Sichuan Provincial People's Hospital (Grant No. 2017QN12), the Sichuan Provincial Science and Technology Department (Grant No. 2018JY0160) to YX, and the National Natural Science Foundation of China (Grant No. 81501026) to ST.

Conflict of interest

The authors declare that the research was conducted in the absence of any commercial or financial relationships that could be construed as a potential conflict of interest.

Publisher's note

Supplementary material

The Supplementary Material for this article can be found online at: https://www.frontiersin.org/articles/10.3389/fneur.2022.1013213/full#supplementary-material

References

1. Sone J, Mori K, Inagaki T, Katsumata R, Takagi S, Yokoi S, et al. Clinicopathological features of adult-onset neuronal intranuclear inclusion disease. *Brain*. (2016) 139(Pt 12):3170–86. doi: 10.1093/brain/aww249

2. Tokumaru AM, Saito Y, Murayma S. Diffusion-weighted imaging is key to diagnosing specific diseases. *Magn Reson Imaging Clin N Am*. (2021) 29:163–83. doi: 10.1016/j.mric.2021.02.001

3. Sone J, Tanaka F, Koike H, Inukai A, Katsuno M, Yoshida M,, et al. Skin biopsy is useful for the antemortem diagnosis of neuronal intranuclear inclusion disease. *Neurology*. (2011) 76:1372–6. doi: 10.1212/WNL.0b013e3182166e13

4. Sone J, Mitsuhashi S, Fujita A, Mizuguchi T, Hamanaka K, Mori K, et al. Long-read sequencing identifies GGC repeat expansions in NOTCH2NLC associated with neuronal intranuclear inclusion disease. *Nat Genet*. (2019) 51:1215–21. doi: 10.1038/s41588-019-0459-y

5. Ishiura H, Shibata S, Yoshimura J, Suzuki Y, Qu W, Doi K, et al. Noncoding CGG repeat expansions in neuronal intranuclear inclusion disease, oculopharyngodistal myopathy and an overlapping disease. *Nat Genet*. (2019) 51:1222–32. doi: 10.1038/s41588-019-0458-z

6. Westenberger A, Klein C. Essential phenotypes of NOTCH2NLC-related repeat expansion disorder. *Brain*. (2020) 143:5–8. doi: 10.1093/brain/awz404

7. Raza HK, Singh S, Rai P, Chansysouphanthong T, Amir A, Cui G, et al. Recent progress in neuronal intranuclear inclusion disease: a review of the literature. *Neurol Sci*. (2020) 41:1019–25. doi: 10.1007/s10072-019-04195-6

8. Chen Z, Yan Yau W, Jaunmuktane Z, Tucci A, Sivakumar P, Gagliano Taliun SA, et al. Neuronal intranuclear inclusion disease is genetically heterogeneous. *Ann Clin Transl Neurol*. (2020) 7:1716–25. doi: 10.1002/acn3.51151

9. Cao L, Yan Y, Zhao G. AUID- Oho. NOTCH2NLC-related repeat expansion disorders: an expanding group of neurodegenerative disorders. *Neurol Sci*. (2021) 42:4055–62. doi: 10.1007/s10072-021-05498-3

10. Sun QY, Xu Q, Tian Y, Hu ZM, Qin LX, Yang JX, et al. Expansion of GGC repeat in the human-specific NOTCH2NLC gene is associated with essential tremor. *Brain*. (2020) 143:222–33. doi: 10.1093/brain/awz372

11. Morimoto S, Hatsuta H, Komiya T, Kanemaru K, Tokumaru AM, Murayama S. Simultaneous skin-nerve-muscle biopsy and abnormal mitochondrial inclusions in intranuclear hyaline inclusion body disease. *J Neurol Sci*. (2017) 372:447–9. doi: 10.1016/j.jns.2016.10.042

12. Ishihara T, Okamoto T, Saida K, Saitoh Y, Oda S, Sano T, et al. Neuronal intranuclear inclusion disease presenting with an MELAS-like episode in chronic polyneuropathy. *Neurol Genet*. (2020) 6:e531. doi: 10.1212/NXG.0000000000000531

13. Huang XR, Tang BS, Jin P, Guo JF. AUID- Oho. The phenotypes and mechanisms of NOTCH2NLC-related GGC repeat expansion disorders: a comprehensive review. *Mol Neurobiol*. (2022) 59:523–34. doi: 10.1007/s12035-021-02616-2

14. Liang H, Wang B, Li Q, Deng J, Wang L, Wang H, et al. Clinical and pathological features in adult-onset NIID patients with cortical enhancement. *J Neurol*. (2020) 267:3187–98. doi: 10.1007/s00415-020-09945-7

15. Tamura A, Fujino Y, Sone J, Shiga K. Temporal changes in brain magnetic resonance imaging findings over 16 years in a patient with neuronal intranuclear inclusion disease. *Intern Med*. (2021) 60:2483–6. doi: 10.2169/internalmedicine.6371-20

frontiers | Frontiers in Neurology

TYPE Case Report
PUBLISHED 03 November 2022
DOI 10.3389/fneur.2022.993399

OPEN ACCESS

EDITED BY
Bruce Miller,
University of California, San Francisco, United States

REVIEWED BY
Fan Mei,
Peking University, China
Emilia J. Sitek,
Medical University of Gdansk, Poland

*CORRESPONDENCE
Pan Li
doc_panpan@163.com

SPECIALTY SECTION
This article was submitted to Dementia and Neurodegenerative Diseases, a section of the journal Frontiers in Neurology

RECEIVED 13 July 2022
ACCEPTED 04 October 2022
PUBLISHED 03 November 2022

CITATION
Li P, Y Y, Cai H, Zhang H and Zhou Y (2022) Case analysis of early-onset Alzheimer's disease associated with TBK1 p.Tyr235Phe gene mutation. *Front. Neurol.* 13:993399. doi: 10.3389/fneur.2022.993399

Case analysis of early-onset Alzheimer's disease associated with TBK1 p.Tyr235Phe gene mutation

Pan Li [1,2,3]*, Yuanyuan Y[1,2,3], Hao Cai[1,2,3], Huihong Zhang[1,2,3] and Yuying Zhou[1,2,3]

[1]Department of Neurology, Tianjin Huanhu Hospital, Tianjin, China, [2]Department of Neurology, Tianjin Huanhu Hospital Affiliated to Tianjin Medical University, Tianjin Huanhu Hospital Affiliated to Nankai University, Tianjin University Huanhu Hospital, Tianjin, China, [3]Tianjin Key Laboratory of Cerebral Vascular and Neurodegenerative Diseases, Tianjin Neurosurgery Institute, Tianjin Huanhu Hospital, Tianjin, China

TANK1-binding kinase 1 (TBK1) is mainly involved in the regulation of various cellular pathways through the autophagic lysosomal system, and the loss of function or hypofunction caused by TBK1 gene mutation mainly leads to frontotemporal lobar degeneration (FTLD), amyotrophic lateral sclerosis (ALS), and ALS-FTLD. Alzheimer's disease (AD) due to TBK1 gene mutation is extremely rare, and only one case has been reported in China so far. In this report, we described a patient with early-onset AD (EOAD) in whom a new probable pathogenic variant c.704A>T (p.Tyr235Phe) in the TBK1 gene was identified by a whole-genome sequencing analysis. It is suggested that FTLD gene mutation may exist in patients with clinical manifestations of AD.

KEYWORDS

TBK1 gene mutation, early-onset Alzheimer's disease, psychobehavioral abnormalities, neuroimaging, biomarkers

Introduction

TANK1-binding kinase 1 (TBK1) is a multifunctional kinase involved in the regulation of multiple cellular pathways, including immune response, inflammation, autophagy, cell proliferation, and insulin signaling (1). It has been demonstrated that TBK1 deficiency will promote serine/threonine-protein kinase 1 (RIPK1)-dependent apoptosis and synergize with genetic risk factors to promote neuroinflammation and lead to the onset of neurodegenerative disorders (2). It has been reported that loss of function (LoF) mutations in the TBK1 gene are the fourth common frontotemporal lobar degeneration (FTLD)-causing gene after repeat expansions in the chromosome 9 open reading frame 72 (C9ORF72), progranulin (GRN), and microtubule-associated protein tau (MAPT), and the second most common ALS-causing gene after C9ORF72 (3). Other rare phenotypes caused by TBK1, such as corticobasal degeneration (CBD) (4) or Alzheimer's disease (AD) (5), have been rarely reported. In this report, we described a case of a TBK1 c.704A>T (p.Tyr235Phe) carrier patient with episodic memory impairment as a prominent manifestation, accompanied by rapid onset of personality changes and behavioral abnormalities. The clinical, neuropsychological, and neuroimaging features and biological markers were consistent with a diagnosis of AD. Therefore, screening for mutations in other dementia-related genes is also needed in clinically diagnosed patients with AD.

Case report

Clinical history

The patient is a 53-year-old man and a university professor with a bachelor's degree, who visited our cognitive impairment clinic on 23 November 2020, mainly because of "progressive worsening of memory loss for more than 2 years. The patient was found to have reduced responsiveness during communication, was unable to remember things, and repeatedly asked questions about things he was told by his wife 2 years before the consultation. However, his normal work was not affected. One and a half year ago, the patient felt that his memory loss was deteriorating. He often forgot to give lessons to students and needed to record things to help himself remember. His ability to perform daily activities, such as teaching online, sending emails, managing money, and cooking, has declined. He was irritable and had sleep disturbances, which attracted the attention of his family and sent him to the hospital. He had no significant medical history, denying arterial hypertension, diabetes, coronary heart disease (CHD), cerebrovascular disease, and other chronic illnesses. Also, he had no history of infectious diseases such as hepatitis, tuberculosis, and malaria; history of trauma and blood transfusion; and history of food and drug allergy. According to his family, his uncle suffered from memory loss in his 50 s, which gradually progressed to be unable to recognize his family, accompanied by nocturnal sleep disturbances and abnormal behavioral symptoms, but he did not receive formal treatment until his death in his 60 s. The results of physical examination indicated a temperature of 36.5°C, a pulse of 74 times/min, a breathing rate of 19 times/min, blood pressure (BP) of 128/65 mmHg (1 mmHg = 0.133 kPa), no deformity in the thorax, and clear breath sounds in both lungs, with no dry and wet rales. The heart sounds were strong and rhythmic, and no pathological murmur was heard in the auscultation area of each valve. The abdomen was soft, with no pressure pain, and the liver and spleen were not palpable under the ribs. Both lower limbs were not swollen, and there was no deformity of the spinal limbs. Neurological examination showed no abnormalities except for a decrease in time and place orientation, calculation, and recent memory. The frontal lobe release signs of palm-grasping reflex, rooting reflex, and sucking reflex were all negative.

Auxiliary examinations

The routine blood, coagulation function, serum immune function, liver and kidney function, lipids, blood glucose, high sensitive C-reactive protein, homocysteine, thyroid function, folic acid, vitamin B12, ferritin, immune panel (hepatitis A, hepatitis B, hepatitis C, syphilis, and HIV), urine routine, and stool routine showed no significant abnormalities. The electrocardiogram showed normal sinus rhythm. The neuropsychological assessment showed a multidomain cognitive decline highlighted by delayed recall deficits, along with emotional irritability and sleep disturbances (Table 1). Brain magnetic resonance imaging (MRI) (November 23, 2020) showed atrophy of the bilateral temporoparietal and posterior cingulate gyrus, and widening of the ventricles, cisterna, brain fissures, and brain sulci (Figure 1). Automated brain tissue segmentation was performed by the Dr. Brain tool to extract multiparameter volumetric measurements from different brain regions (https://cloud.drbrain.net, registration number: 20212210359). The artificial intelligence brain structure imaging analysis showed decreased total white matter volume in the whole brain; decreased volume in the bilateral hippocampus, amygdala, left inferior parietal area, and left temporal pole; and thinning of cortical thickness in the bilateral inferior parietal gyrus, left superior parietal gyrus, left superior limbic gyrus, left precuneus, bilateral middle temporal gyrus, left olfactory area cortex, left posterior cingulate gyrus, and bilateral isthmus (Table 2). Multimodal molecular imaging of 18-fluoro-2-deoxy-D-glucose positron emission tomography (^{18}F-FDG PET-CT) results suggested the multiple hypometabolism in the bilateral parietal and combined temporoparietal areas, bilateral temporal lobes, and posterior cingulate gyrus (Figure 2). Cerebrospinal fluid (CSF) Aβ and tau were detected by the enzyme-linked immunosorbent assay (ELISA) (6, 7): beta-amyloid (1–42) (Aβ_{1-42}) was 191.15 pg/ml (normal values >651 pg/ml), beta-amyloid (1–40) (Aβ_{1-40}) was 7,945.40 pg/ml (normal values >7,000 pg/ml), Aβ_{1-42}/Aβ_{1-40} ratio was 0.024 (normal value > 0.05), total tau protein was 635.89 pg/ml (normal value ≤399 pg/ml), and phosphorylated tau181 (p-tau181) protein was 19.8 pg/ml (normal value ≤50 pg/ml). Combined with the medical history, clinical symptoms, and relevant examinations, mild cognitive impairment (MCI) due to AD (multidomain amnesia type) was considered according to the revised consensus for MCI diagnosis from the International Working Group (8).

Treatment and follow-up

Butylphthalide (0.6 g/day) was given orally. At 3 months, the patient's cognitive function and neuropsychiatric symptoms remained stable. At 6 months, immediate memory function began to be impaired and the activity of daily living function has worsened. At 9 months, the patient showed significant personality changes and behavioral abnormalities, manifested by stubbornness, repeated excessive shopping, confabulating, irritability, and disinhibition. At the same time, cognitive function (orientation and calculation) has declined more than before (Table 1). Molecular genetic screening was performed by whole-genome sequencing and repeat primer PCR: the patient carried a TBK1 c.704 A>T (p.Tyr235Phe) heterozygous mutation (Figure 3) with an APOE genotype of ε2/ε4. Further

TABLE 1 Neuropsychological scale outcomes for the first visit and follow-up.

Neuropsychological tests	First visit	3 months	6 months	9 months	12 months
MoCA [score/total score (prominent deficit subitems)]	18/30 (delayed recall, visuospatial orientation and executive function)	18/30 (delayed recall, visuospatial orientation and executive function)	17/30 (delayed recall, visuospatial orientation and executive function)	15/30 (delayed recall, visuospatial orientation and executive function)	16/30 (delayed recall, visuospatial orientation and executive function)
MMSE [score/total score (prominent deficit subitems)]	24/30 (delayed recall)	23/30 (delayed recall)	23/30 (delayed recall)	19/30 (delayed recall, orientation, and calculation)	21/30 (delayed recall, orientation, and calculation)
ADAS-cog (score/total scores)	Dec-70	Dec-70	14/70	14/70	16/70
Subitems scores:					
Word recall	6	6	6	6	6
Naming	0	0	0	0	0
Commands	0	0	1	1	0
Constructional praxis	1	1	1	1	1
Ideational praxis	1	1	1	1	2
Orientation	1	1	1	1	1
Word recognition	3	3	4	4	6
Remembering test instructions	0	0	0	0	0
Comprehension of spoken language	0	0	0	0	0
Word finding difficulty	0	0	0	0	0
Language	0	0	0	0	0
CDR [score/total score]	0.5/3	0.5/3	0.5/3	3-Jan	0.5/3
Immediate memory [score (abnormal value)]	14 (≤18)	14 (≤18)	7 (≤18)	5 (≤18)	8 (≤18)
Delayed recall [score (abnormal value)]	0 (≤6)	0 (≤6)	0 (≤6)	0 (≤6)	3 (≤6)
DST (the longest digit sequence recalled properly)					
Digits forwards [score/total score]					
Digits backwards [score/total score]	10-Jul	10-Jul	10-Jul	10-Jul	10-Aug
	8-May	8-May	8-Apr	8-Feb	8-Mar
Trail making test					
Part A [time in seconds/errors]	50 s/0	55 s/0	67 s/0	51 s/0	48 s/0
Part B [time in seconds/errors]	123 s/0	127 s/0	101 s/0	118 s/0	116 s/0
ADL [score/total score (prominent deficit subitems)]	24/80 (shopping and financial management)	22/80 (shopping and financial management)	24/80 (hopping, financial management and complicated housework)	25/80 (shopping, financial management and complicated housework)	25/80 (shopping, financial management and complicated housework)
NPI [score/total score (prominent deficit subitems)]	4/122 (sleep disturbance and irritability)	2/122 (sleep disturbance and irritability)	2/122 (sleep disturbance and irritability)	3/122 (Stubborn and irritability)	4/122 (Stubborn and irritability)
HAMD-17 [score/total score (prominent deficit subitems)]	9/55 (Sleep disturbances, reduced ability to work)	9/55(Sleep disturbances, reduced ability to work)	8/55 (Sleep disturbances, reduced ability to work)	9/55 (Sleep disturbances, reduced ability to work)	8/55 (Sleep disturbances, reduced ability to work)

MMSE, Mini-Mental State Examination; MoCA, Montreal Cognitive Assessment; ADAS-cog, Alzheimer's Disease Assessment Scale-Cognitive section; CDR, Clinical Dementia Rating; DST, Digital Span Test; ADL, Activity of Daily Life; NPI, Neuropsychiatric Inventory Questionnaire; HADM-17, The 17-items Hamilton Depression Rating Scale.

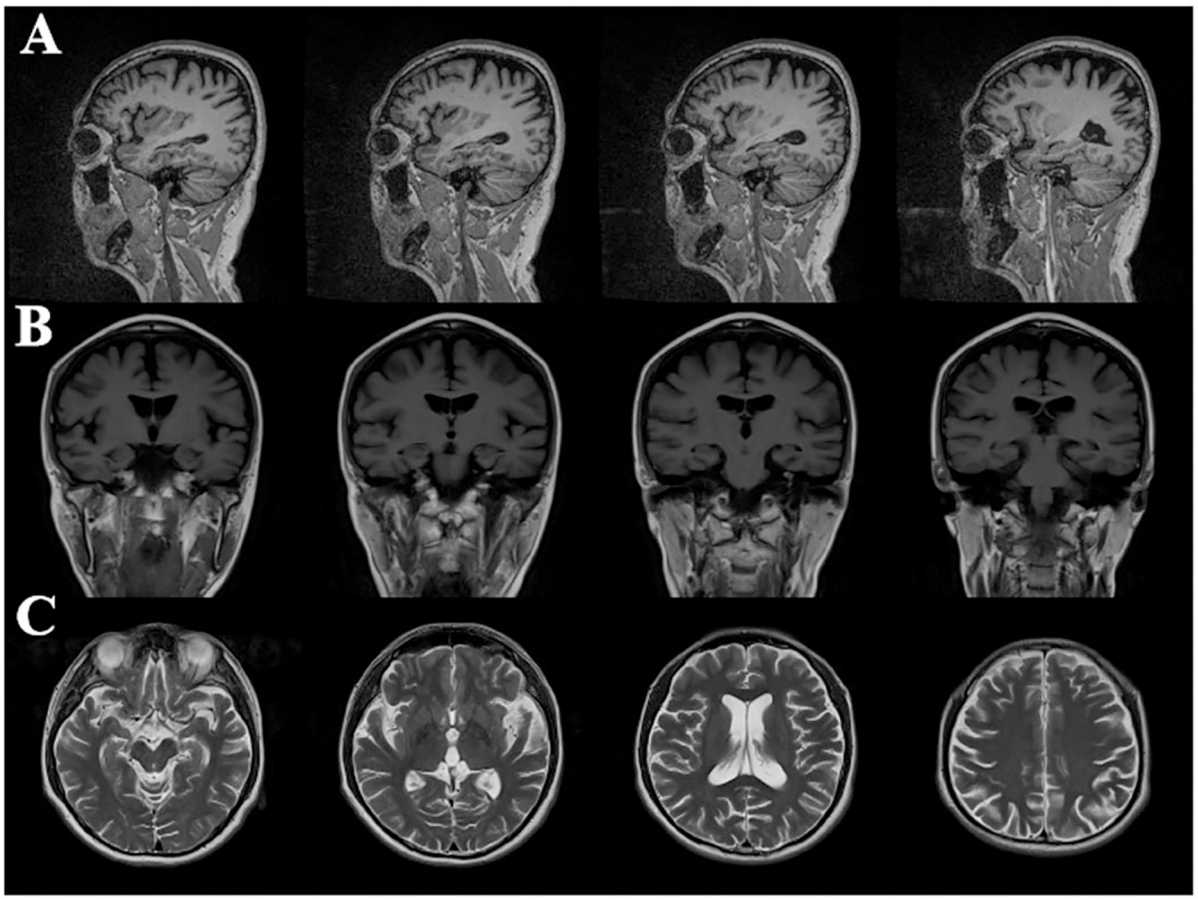

FIGURE 1
Cranial magnetic resonance imaging in patients with Alzheimer's disease: **(A)** sagittal image of T2 fluid attenuated inversion recovery (T2 FLAIR); **(B)** coronal image of T1-weighted image (T1WI); **(C)** cross-sectional sequences of T2-weighted image (T2WI); imaging results showed atrophy of bilateral temporal parietal lobe and posterior cingulate gyrus, and dilatation of ventricle, cistern, fissure, and sulci.

validation of the locus by Sanger sequencing was performed in the proband's family, and both his mother and daughter were wild type. Accordingly, the medication was adjusted to memantine and donepezil.

Discussion

Alzheimer's disease is a chronic progressive neurodegenerative disorder, and there is still a lack of effective and accurate diagnostic methods for early identification. AD is highly heterogeneous in terms of clinical manifestation and neuropathology, and the prominent manifestation of "episodic memory impairment" as a diagnosis of AD lacks high sensitivity and specificity for early diagnosis (9). On the contrary, even in the pathologically confirmed population with AD, FTLD-like phenotypes such as "neuropsychiatric abnormalities, personality and language disorders" and movement disorder phenotypes such as "myoclonus, epilepsy and spastic paraplegia" can also be manifested (10). Neuropathology remains the gold standard for AD diagnosis. In gross pathology, AD presents as diffuse brain atrophy, with typical AD dominated by hippocampal and medial temporal lobe atrophy, posterior variant AD by the temporal occipital lobe and posterior cingulate gyrus atrophy, frontal variant of AD (fvAD) by bilateral frontal lobe atrophy, and logopenic variant AD by left parietal–temporal lobe atrophy; however, these macroscopic features are a lack of specificity for AD diagnosis. In the microscopic pathology, in addition to typical pathological changes of extracellular amyloid plaque deposition and intracellular neurofibrillary tangles, AD also includes eosinophilic inclusions, hippocampal granular vacuolar degeneration, activated microglia, reactive astrocytes, amyloid vascular disease, and other pathological changes (9). Neurodegenerative diseases are characterized by the accumulation and deposition of misfolded proteins in the brain, most notably Aβ, tau, alpha-synuclein, and TAR DNA-binding protein 43 (TDP-43) (11), and may also be

TABLE 2 The structural MRI features based on artificial intelligence analysis.

	Structure	Volume (cm^3)	Ratio to intracranial volume (%)	Normal range (%)
The whole brain information	Gray matter	574.93	39.45%	35.94–47.91%
	White matter	460.03	31.57% ↓	31.62–41.96%
	Total cerebrospinal fluid	422.27	28.98%	11.78–30.24%
	Total intracranial space	1457.23	–	–
Hippocampus	Left hippocampus	1.93	0.13% ↓	0.16–0.24%
	Right hippocampus	2.48	0.17% ↓	0.18–0.27%
	Left Parahippocampus Gyrus	2.15	0.15%	0.15–0.22%
	Right Parahippocampus Gyrus	2.25	0.15%	0.15–0.22%
Amygdala	Left amygdala	0.58	0.04% ↓	0.05–0.07%
	Right amygdala	0.63	0.04% ↓	0.05–0.07%
	Structure	**Cortical thickness (mm)**	**Normal range (mm)**	
Cortical structure	Left inferior parietal gyrus	1.9 ↓	2.2–2.6	
	Left superior parietal gyrus	1.88 ↓	1.9–2.4	
	Left supramarginal gyrus	2.18 ↓	2.2–2.7	
	Left precuneus	1.99 ↓	2.1–2.6	
	Left middle temporal gyrus	2.42 ↓	2.5–3.1	
	Left entorhinal cortex	2.87 ↓	2.9–4.0	
	Left posterior cingutate	2.13 ↓	2.2–2.8	
	Left isthmus	1.98 ↓	2.0–2.7	
	Right inferior parietal gyrus	2.11 ↓	2.2–2.6	
	Right middle temporal gyrus	2.58 ↓	2.6–3.1	
	Right isthmus	1.95 ↓	2.0–2.7	

referred to as proteinopathies. Although the characteristic proteins differ across the disease spectrum, a growing number of studies confirm the prevalence of co-pathologies (12). Among the patients clinically diagnosed with AD, autopsy results showed that only 17.3–26.3% had AD pathology alone, 28.3–41.6% had Lewy body dementia, 13.9–49.2% had vascular dementia, and even 12.6% had no AD pathological changes (11, 13, 14). Conversely, some pathological alterations, such as tau protein and TDP-43 caused by FTLD-related pathogenic gene mutations of GRN, C9ORF72, and MAPT, can also be clinically manifested as a typical AD phenotype (15–17). The frequent occurrence of co-pathology will contribute to the heterogeneity of clinical symptoms, making the differential diagnosis challenging. In this study, we have identified a novel heterozygous mutation in FTLD- and ASL-related pathogenic genes in a patient with AD phenotype, Therefore, screening for mutations in TBK1 might be advisable in clinically diagnosed patients with AD.

An LoF mutation in the TBK1 gene was first identified in 2015 in a cohort study of patients with ALS, resulting in the degradation of mutant transcripts and reduced TBK1 protein. Subsequently, the same mutations were identified in the FTLD population (18). TBK1 LoF mutations are the third most frequent cause of clinical FTLD in the Belgian clinically based patient cohort, after C9ORF72 and GRN, and the second most common cause of clinical ALS after C9ORF72 (19). These findings reinforce that FTLD and ALS belong to the same disease continuum. TBK1 protein has four functional domains, including a serine/threonine kinase (S/TK) domain, which phosphorylates TBK1 substrates, a ubiquitin-like structural domain, and two coiled-coiled domains (CCD1 and CCD2). The CCD2 domain binds to optineurin and p62, the two key proteins involved in the autophagic pathway, and promotes substrate phosphorylation, thereby participating in neurodegenerative changes in ALS and FTLD (20). The correlation between the location of TBK1 LoF mutations and clinical phenotypes is still controversial. It has been reported that in patients with ALS and related dementia, TBK1 missense mutations are mostly located near the CCD2 domain and will affect its combination ability to optic nerve protein (18). Some studies have also proposed that missense mutations associated with FTLD and FTLD-ALS are always located in the S/TK or CDD2 domains (20). Genetic screening in this patient suggested a TBK1 c.704A>T (p.Tyr235Phe) heterozygous mutation, located in the S/TK structural domain, which is the first reported locus.

TBK1 mutation carriers mainly present with prominent psychological and behavioral abnormalities, such as apathy and disinhibition, and can also be accompanied by memory loss in the early stage of the disease. Some patients exhibit significant upper motor neuron symptoms and progressive

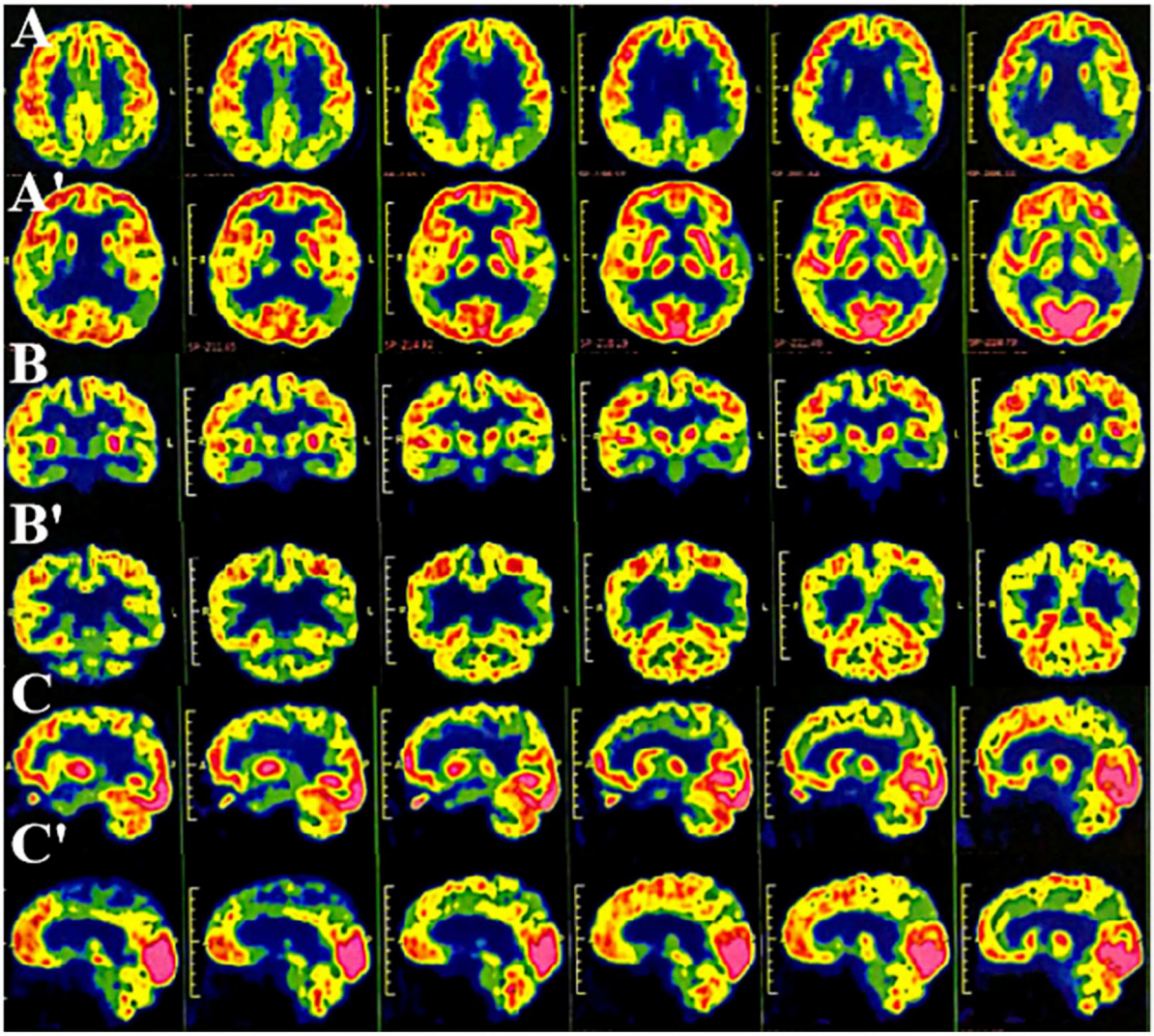

FIGURE 2
Multimode molecular imaging of 18-fluoro-2-deoxy-D-glucose positron emission tomography (^{18}F-FDG PET-CT) showed reduced multiple hypometabolism in the bilateral parietal and temporoparietal junction, bilateral temporal lobes (left), and posterior cingulate gyrus (**AA':** cross-sectional sequence; **BB':** coronal image; **CC':** sagittal image).

medullary paralysis. More than half of TBK1 LoF mutation or missense mutation carriers are clinically diagnosed with pure ALS, FTLD, and ALS-FTLD (21), and rarely patients present with other neurodegenerative disorders such as CBD (4), progressive supranuclear palsy (PSP) (21), progressive cerebellar ataxia (PCA) (21), and AD (5). A systematic screening of the coding sequence of TBK1 in a large cohort of 1,253 patients from eight European countries to investigate the frequency of TBK1 LoF mutations in the population with AD identified only 1 LoF mutation (p.Thr79del) in a patient clinically diagnosed with AD in a positive familial ALS cohort. It was the only reported case abroad at present (5). The patient was clinically diagnosed with sporadic EOAD at the age of 62 years, with the onset of first symptoms at 59 years old. The initial symptoms were visuospatial disorientation and recent memory deficits, and imaging suggested medial temporal lobe atrophy. The progressive cognitive decline was consistent with the characteristics of AD. With disease progression, frontal features became apparent, followed by bilateral parkinsonism at the late stages (5). A domestic research of gene mutations in a Han Chinese AD cohort showed a novel, heterozygous missense mutation at the TBK1 p.D534H locus with a typical AD phenotype of memory loss and disorientation (22). Although the common variant associated with reduced TBK1 expression may be more enriched in patients with EOAD than in controls, this requires further confirmation given the lack of association

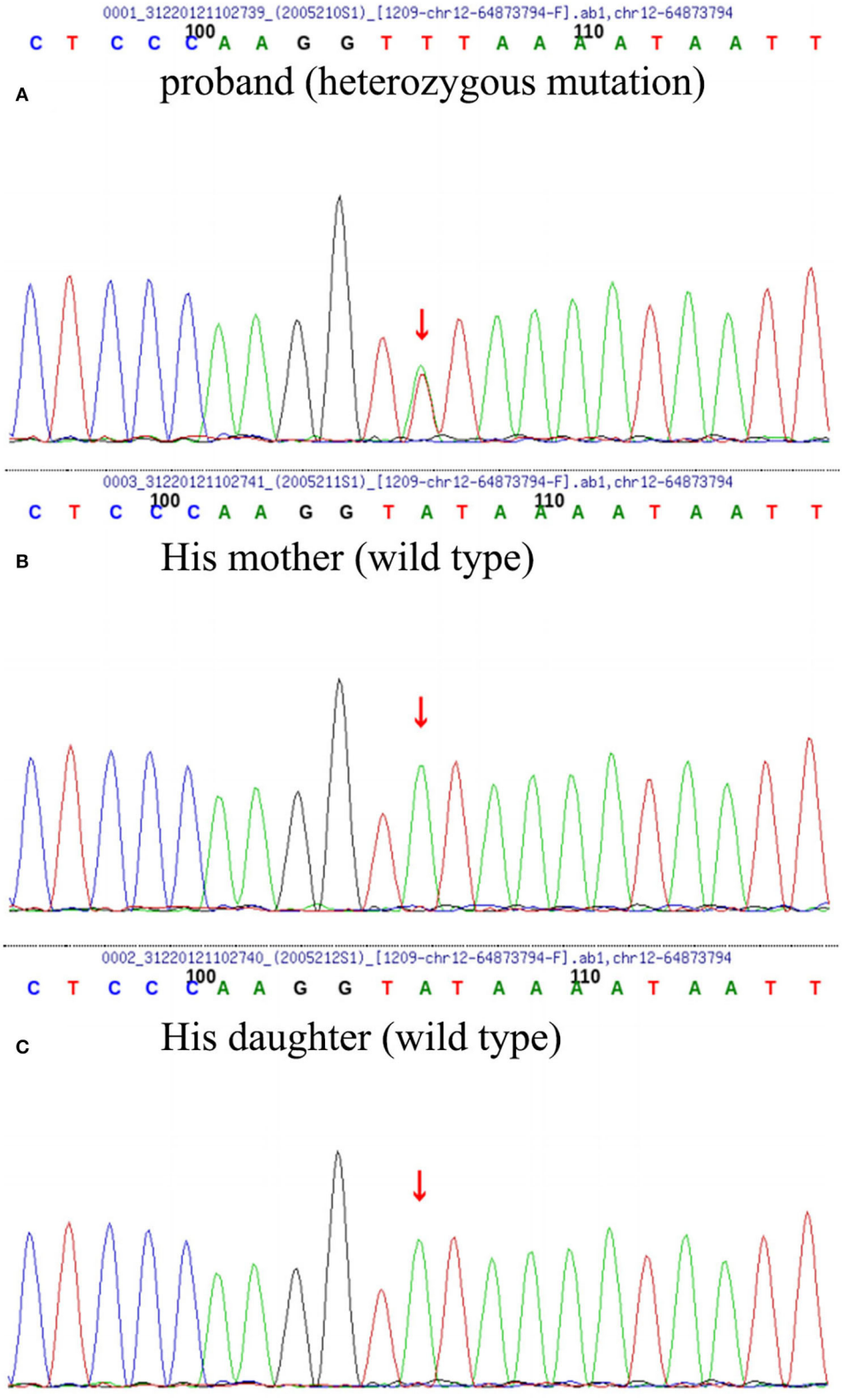

FIGURE 3
Whole-genome sequencing (WGS) and repeated primer PCR detection results of the patient **(A)**, his mother **(B)**, and daughter **(C)** the patient carried heterozygous missense mutation of *TBK1* c. 704A>T (p. Tyr235phe); however, his daughter and mother were wild type.

in late-onset AD, and further investigation of common variants affecting TBK1 expression is warranted (5).

In the present report, the patient was diagnosed with sporadic EOAD at 53 years old and had the onset of first symptoms at 51 years old. His clinical evaluation was considered to be in line with AD-type dementia due to the following supporting evidence: (1) recent memory decline was its early prominent manifestation, combined with visuospatial disorientation and other cognitive subdomains dysfunction; (2) multimodal imaging analysis of brain structure and PET-CT molecular imaging results suggested bilateral temporal lobe, parietal lobe and combined temporoparietal regions atrophy and hypometabolism, and multiple metabolic restrictive hypometabolism in the posterior cingulate gyrus; and (3) the decrease in $A\beta_{1-42}$ and $A\beta_{1-42}/A\beta_{1-40}$ ratio and the increase in total tau protein found in CSF. It is consistent with the diagnosis of typical AD according to clinical, neuropsychological, neuroimaging features and biological markers. However, during the follow-up, the patient soon developed behavioral abnormalities, such as disinhibition and stereotyped compulsive behavior, which could not exclude the modifying effect of TBK1 heterozygous mutation on the disease process and required to be tracked continuously. Actually, according to the new diagnostic criteria proposed by Ossenkoppele (23), the patient is clinically most reminiscent of fvAD. FvAD is a variant form of AD characterized by a milder and more restricted behavioral profile than in behavioral variant frontotemporal dementia, as well as the co-occurrence of memory dysfunction and high APOE ε4 prevalence; however, it shares most pathophysiological features with typical AD. It is worthy of further investigation that $A\beta_{1-42}/A\beta_{1-40}$ ratio and total tau protein level were altered in the CSF, whereas there was no change in the level of p-tau181. Numerous clinical studies have been presented that p-tau181 concentration is a promising new biomarker candidate for AD diagnosis and prognosis, and as the earliest reactive protein to $A\beta$ toxicity, the p-tau181 level can accurately predict the state of $A\beta$ deposition in the brain (24). However, an analysis obtained from the AD Neuroimaging Initiative (ADNI) suggested that nearly 20% of the study population showed $A\beta$ positive and p-tau181 negative phenotype (25). It is possible that there are multiple pathologies, other than β-amyloid plaques and neurofibrillary tangles, that synergistically contribute to brain damage in the patient (26).

In conclusion, our data report a case with a typical AD phenotype carrying TBK1 LoF variant with a biomarker-supported diagnosis of AD, which is the second case reported in China, and the phenotypic characteristics of the TBK1 c.704A>T (p.Tyr235Phe) heterozygous mutation are reported in the first case. Considering the development of frontal features in the course of the disease, this does not entirely exclude the possibility that this patient had co-existed FTLD with atypical clinical presentation due to early symptoms compatible with AD. This is consistent with the previous TBK1 LoF variation found in FTLD/ALS patients with a preliminary clinical diagnosis of AD. This study also suggests that FTLD gene mutations may also occur in clinically diagnosed patients with AD; hence, screening for mutations in other dementia genes in clinically diagnosed patients with AD may be desirable. The onset of the clinical pictures and the natural history is highly different in neurodegenerative diseases caused by TBK1 gene mutation. It is difficult to establish genotype–phenotype correlations because of the molecular complexity of TBK1 and pathological heterogeneity in carriers of TBK1 mutations. Thereby, further studies are needed to better understand the pathophysiology of TBK1, to provide comprehensive genetic counseling in affected families, and to improve prevention strategies as well as treatments.

Data availability statement

The datasets presented in this article are not readily available because of ethical and privacy restrictions. Requests to access the datasets should be directed to the corresponding author.

Ethics statement

The studies involving human participants were reviewed and approved by Tianjin Human Trial Committee and approved by Ethics Committee of Tianjin Huanhu Hospital. The patients/participants provided their written informed consent to participate in this study. Written informed consent was obtained from the individual(s) for the publication of any potentially identifiable images or data included in this article.

Author contributions

PL wrote the original manuscript and made modifications. HC and HZ performed the data collection. YZ and PL participated in clinical diagnosis. YY and HZ were responsible for patient care and scale assessment. All authors examined the results and authorized the final version of the manuscript.

Funding

This study was supported by Tianjin Municipal Health Commission Project (TJWJ2021MS029) and Tianjin Key Medical Discipline (Specialty) Construction Project (No. TJYXZDXK-052B). Both funds are chaired by PL.

Acknowledgments

We thank all our colleagues for their assistance and proposal throughout the research.

Conflict of interest

The authors declare that the research was conducted in the absence of any commercial or financial relationships that could be construed as a potential conflict of interest.

Publisher's note

All claims expressed in this article are solely those of the authors and do not necessarily represent those of their affiliated organizations, or those of the publisher, the editors and the reviewers. Any product that may be evaluated in this article, or claim that may be made by its manufacturer, is not guaranteed or endorsed by the publisher.

Supplementary material

The Supplementary Material for this article can be found online at: https://www.frontiersin.org/articles/10.3389/fneur.2022.993399/full#supplementary-material

References

1. Freischmidt A, Muller K, Ludolph AC, Weishaupt JH, Andersen PM. Association of mutations in TBK1 with sporadic and familial amyotrophic lateral sclerosis and frontotemporal dementia. *JAMA Neurol.* (2017) 74:110–3. doi: 10.1001/jamaneurol.2016.3712

2. Xu D, Jin T, Zhu H, Chen H, Ofengeim D, Zou C, et al. TBK1 suppresses RIPK1-driven apoptosis and inflammation during development and in aging. *Cell.* (2018) 174:1477–91. doi: 10.1016/j.cell.2018.07.041

3. Van Mossevelde S, van der Zee J, Gijselinck I, Engelborghs S, Sieben A, Van Langenhove T, et al. Clinical features of TBK1 carriers compared with C9ORF72, GRN and non-mutation carriers in a Belgian cohort. *Brain.* (2016) 139:452–67. doi: 10.1093/brain/awv358

4. van der Zee J, Gijselinck I, Van Mossevelde S, Perrone F, Dillen L, Heeman B, et al. TBK1 mutation spectrum in an extended European patient cohort with frontotemporal dementia and amyotrophic lateral sclerosis. *Hum Mutat.* (2017) 38:297–309. doi: 10.1002/humu.23161

5. Verheijen J, van der Zee J, Gijselinck I, Van den Bossche T, Dillen L, Heeman B, et al. Common and rare TBK1 variants in early-onset Alzheimer disease in a European cohort. *Neurobiol Aging.* (2018) 62:245e1–e7. doi: 10.1016/j.neurobiolaging.2017.10.012

6. Karikari TK, Pascoal TA, Ashton NJ, Janelidze S, Benedet AL, Rodriguez JL, et al. Blood phosphorylated tau 181 as a biomarker for Alzheimer's disease: a diagnostic performance and prediction modelling study using data from four prospective cohorts. *Lancet Neurol.* (2020) 19:422–33. doi: 10.1016/S1474-4422(20)30071-5

7. Palmqvist S, Janelidze S, Stomrud E, Zetterberg H, Karl J, Zink K, et al. Performance of fully automated plasma assays as screening tests for Alzheimer disease-related β-amyloid status. *JAMA Neurol.* (2019) 76:1060–9. doi: 10.1001/jamaneurol.2019.1632

8. Winblad B, Palmer K, Kivipelto M, Jelic V, Fratiglioni L, Wahlund LO, et al. Mild cognitive impairment—beyond controversies, towards a consensus: report of the international working group on mild cognitive impairment. *J Intern Med.* (2004) 256:240–6. doi: 10.1111/j.1365-2796.2004.01380.x

9. Shakir MN, Dugger BN. Advances in deep neuropathological phenotyping of Alzheimer disease: past, present, and future. *J Neuropathol Exp Neurol.* (2022) 81:2–15. doi: 10.1093/jnen/nlab122

10. Devanand DP, Lee S, Huey ED, Goldberg TE. Associations between neuropsychiatric symptoms and neuropathological diagnoses of Alzheimer disease and related dementias. *JAMA Psychiatry.* (2022) 79:359–67. doi: 10.1001/jamapsychiatry.2021.4363

11. Nag S, Yu L, Capuano AW, Wilson RS, Leurgans SE, Bennett DA, et al. Hippocampal sclerosis and TDP-43 pathology in aging and Alzheimer disease. *Ann Neurol.* (2015) 77:942–52. doi: 10.1002/ana.24388

12. Jellinger KA. Neuropathological aspects of Alzheimer disease, Parkinson disease and frontotemporal dementia. *Neurodegener Dis.* (2008) 5:118–21. doi: 10.1159/000113679

13. DeTure MA, Dickson DW. The neuropathological diagnosis of Alzheimer's disease. *Mol Neurodegener.* (2019) 14:32. doi: 10.1186/s13024-019-0333-5

14. Kovacs GG, Kovari V, Nagy Z. Frequency of different forms of dementia at the Department of Neuropathology of the Hungarian National Institute of Psychiatry and Neurology during a 3-year period. *Ideggyogy Sz.* (2008) 61:24–32.

15. Rademakers R, Dermaut B, Peeters K, Cruts M, Heutink P, Goate A, et al. Tau (MAPT) mutation Arg406Trp presenting clinically with Alzheimer disease does not share a common founder in Western Europe. *Hum Mutat.* (2003) 22:409–11. doi: 10.1002/humu.10269

16. Brouwers N, Nuytemans K, van der Zee J, Gijselinck I, Engelborghs S, Theuns J, et al. Alzheimer and Parkinson diagnoses in progranulin null mutation carriers in an extended founder family. *Arch Neurol.* (2007) 64:1436–46. doi: 10.1001/archneur.64.10.1436

17. Cacace R, Van Cauwenberghe C, Bettens K, Gijselinck I, van der Zee J, Engelborghs S, et al. C9ORF72 G4C2 repeat expansions in Alzheimer's disease and mild cognitive impairment. *Neurobiol Aging.* (2013) 34:1712e1–7. doi: 10.1016/j.neurobiolaging.2012.12.019

18. Freischmidt A, Wieland T, Richter B, Ruf W, Schaeffer V, Muller K, et al. Haploinsufficiency of TBK1 causes familial ALS and fronto-temporal dementia. *Nat Neurosci.* (2015) 18:631–6. doi: 10.1038/nn.4000

19. Gijselinck I, Van Mossevelde S, van der Zee J, Sieben A, Philtjens S, Heeman B, et al. Loss of TBK1 is a frequent cause of frontotemporal dementia in a Belgian cohort. *Neurology.* (2015) 85:2116–25. doi: 10.1212/WNL.0000000000002220

20. Le Ber I, De Septenville A, Millecamps S, Camuzat A, Caroppo P, Couratier P, et al. TBK1 mutation frequencies in French frontotemporal dementia and amyotrophic lateral sclerosis cohorts. *Neurobiol Aging.* (2015) 36:3116e5–e8. doi: 10.1016/j.neurobiolaging.2015.08.009

21. Van Mossevelde S, Engelborghs S, van der Zee J, Van Broeckhoven C. Genotype-phenotype links in frontotemporal lobar degeneration. *Nat Rev Neurol.* (2018) 14:363–78. doi: 10.1038/s41582-018-0009-8

22. Ma L, Zhang J, Shi Y, Wang W, Ren Z, Xia M, et al. Gene mutations in a Han Chinese Alzheimer's disease cohort. *Brain Behav.* (2019) 9:e01180. doi: 10.1002/brb3.1180

23. Ossenkoppele R, Singleton EH, Groot C, Dijkstra AA, Eikelboom WS, Seeley WW, et al. Research criteria for the behavioral variant of Alzheimer disease: a systematic review and meta-analysis. *JAMA Neurol.* (2022) 79:48–60. doi: 10.1001/jamaneurol.2021.4417

24. Palmqvist S, Tideman P, Cullen N, Zetterberg H, Blennow K., Dage JL, et al. Prediction of future Alzheimer's disease dementia using plasma phospho-tau combined with other accessible measures. *Nat Med.* (2021) 27:1034–42. doi: 10.1038/s41591-021-01348-z

25. Rauchmann BS, Schneider-Axmann T, Perneczky R. Alzheimer's Disease Neuroimaging Initiative (ADNI). Associations of longitudinal plasma p-tau181 and NfL with tau-PET, Aβ-PET and cognition. *J Neurol Neurosurg Psychiatry.* (2021) 92:1289–95. doi: 10.1136/jnnp-2020-325537

26. Jack CR, Bennett DA, Blennow K, Carrillo MC, Dunn B, Haeberlein SB, et al. NIA-AA research framework: toward a biological definition of Alzheimer's disease. *Alzheimers Dement.* (2018) 14:535–62. doi: 10.1016/j.jalz.2018.02.018

frontiers | Frontiers in Neurology

TYPE Case Report
PUBLISHED 15 November 2022
DOI 10.3389/fneur.2022.1049113

OPEN ACCESS

EDITED BY
Sonia Do Carmo,
McGill University, Canada

REVIEWED BY
Kazumasa Saigoh,
Kindai University Hospital, Japan
Neha Atulkumar Singh,
Mayo Clinic, United States

*CORRESPONDENCE
Masaru Mimura
mimura@a7.keio.jp

SPECIALTY SECTION
This article was submitted to Dementia and Neurodegenerative Diseases, a section of the journal Frontiers in Neurology

RECEIVED 20 September 2022
ACCEPTED 31 October 2022
PUBLISHED 15 November 2022

CITATION
Momota Y, Konishi M, Takahata K, Kishimoto T, Tezuka T, Bun S, Tabuchi H, Ito D and Mimura M (2022) Case report: Non-Alzheimer's disease tauopathy with logopenic variant primary progressive aphasia diagnosed using amyloid and tau PET. *Front. Neurol.* 13:1049113. doi: 10.3389/fneur.2022.1049113

Case report: Non-Alzheimer's disease tauopathy with logopenic variant primary progressive aphasia diagnosed using amyloid and tau PET

Yuki Momota[1], Mika Konishi[1], Keisuke Takahata[1,2], Taishiro Kishimoto[1,3], Toshiki Tezuka[4], Shogyoku Bun[1], Hajime Tabuchi[1], Daisuke Ito[5] and Masaru Mimura[1]*

[1]Department of Neuropsychiatry, Keio University School of Medicine, Tokyo, Japan, [2]Department of Functional Brain Imaging Research, National Institute of Radiological Sciences, National Institutes for Quantum and Radiological Science and Technology, Chiba, Japan, [3]Psychiatry Department, Donald and Barbara Zucker School of Medicine, New York, NY, United States, [4]Department of Neurology, Keio University School of Medicine, Tokyo, Japan, [5]Department of Physiology/Memory Center, Keio University School of Medicine, Tokyo, Japan

We report a patient with logopenic variant primary progressive aphasia (lv-PPA) who was diagnosed as having non-Alzheimer's disease (AD) tauopathy after multiple biophysical/biological examinations, including amyloid and ^{18}F-florzolotau tau positron emission tomography (PET), had been performed. A woman in her late 60s who had previously been diagnosed as having AD was referred to us for a further, detailed examination. She had been unaware of any symptoms at the time of AD diagnosis, but she subsequently became gradually aware of a speech impairment. She talked nearly completely and fluently, although she occasionally exhibited word-finding difficulty and made phonological errors during naming, word fluency testing, and sentence repetition; these findings met the criteria for the diagnosis of lv-PPA, which is known to be observed more commonly in AD than in other proteinopathies. Magnetic resonance imaging, single photon emission computed tomography, and plasma phosphorylated tau and plasma neurofilament light chain measurements showed an AD-like pattern. However, both ^{11}C-Pittsburgh compound-B and ^{18}F-florbetaben amyloid PET showed negative results, whereas ^{18}F-florzolotau tau PET yielded positive results, with radio signals predominantly in the left superior temporal gyrus, middle temporal gyrus, supramarginal gyrus, and frontal operculum. Whole-genome sequencing revealed no known dominantly inherited mutations in AD or frontotemporal lobar degeneration genes, including the genes encoding amyloid precursor protein, microtubule-associated protein tau, presenilin 1 and 2. To the best of our knowledge, this patient was a rare case of lv-PPA who was diagnosed as having non-AD tauopathy based on the results of multiple examinations, including whole-genome sequencing, plasma measurement, and amyloid and ^{18}F-florzolotau tau PET. This case underscores the clinicopathologically heterogeneous nature of this syndrome.

KEYWORDS

logopenic variant, primary progressive aphasia, tauopathy, Alzheimer's disease, frontotemporal lobar degeneration, positron emission tomography

Introduction

Primary progressive aphasia (PPA) is a neurodegenerative syndrome that is known to be associated with both Alzheimer's disease (AD) and frontotemporal lobar degeneration (FTLD), which is characterized by progressive language impairment as the most salient clinical feature and is commonly associated with a selective lesion in the perisylvian region of the left hemisphere (1, 2). Logopenic variant (lv-)PPA is a syndrome characterized by fluent speech and impaired sentence repetition and sentence comprehension, resembling vascular conduction aphasia (3); the most frequent cause is AD (4–6), while less than 20% of cases are found to have FTLD-tau (6, 7).

The clinical characteristics of AD-related proteinopathies are often similar, but they are concurrently heterogeneous in every patient, complicating diagnosis (8, 9). From this viewpoint, genetic and molecular biomarkers could provide better clues to the underlying pathology. Among the known genetic markers, presenilin 1 (*PSEN1*)/*PSEN2* and amyloid precursor protein (*APP*) variants can be observed in cases with lv-PPA, while chromosome 9 open reading frame 72 (*C9orf72)*, microtubule-associated protein tau (*MAPT*), and some progranulin (*GRN*) mutations have been reported in non-fluent/agrammatic variant (nfv-)PPA cases, and GRN/TAR DNA-binding protein of 43 kDa (TDP-43) has been reported in semantic variant (sv-)PPA cases (2). The plasma levels of phosphorylated tau (p-tau) 181 are elevated in AD (10), whereas the plasma levels of neurofilament light chain protein (NFL) are elevated in both AD and FTLD (11), although the levels are higher in FTLD (12). Positron emission tomography (PET), particularly tau PET, enables visual observation of the deposited causative proteins in a region-specific manner (13).

While the clinicopathological relationships in lv-PPA have remained somewhat unclear, recent studies have described the clinical characteristics of cases with atypical heterogeneous lv-PPA, as well as those of autopsy-confirmed cases of AD with lv-PPA, which have promoted a better understanding of the syndrome (5–7, 14–18). For example, approximately one-third of patients with lv-PPA may have cerebral microbleeds and superficial siderosis (16, 17); in rare instances, patients with lv-PPA may have GRN mutations (18).

Herein, we report a patient with lv-PPA who, despite an initial clinical diagnosis of AD, was suspected of having non-AD tauopathy. To the best of our knowledge, this patient represents an exceptional example of lv-PPA (19) in whom the pathological basis was difficult to predict even after multiple examinations including genome sequencing, plasma p-tau181 and NFL examinations, ^{11}C-Pittsburgh Compound-B (PiB) and ^{18}F-florbetaben (FBB) amyloid PET (20, 21), and ^{18}F-florzolotau, i.e., ^{18}F-PM-PBB3 (propanol modification of pyridinyl-butandienyl-benzothiazole 3) tau PET (22). We hope that this report provides further insight into the correlations among clinical symptoms, biomarkers, and brain imaging findings in proteinopathies, paving the way for early diagnosis and novel therapies for this disease entity.

Case report

A woman in her late 60s was referred to our hospital for a detailed examination of her language impairment. She was right-handed and had more than 16 years of education. Two years previous to her visit to our hospital, she had been referred to a dementia specialist after the Mini-Mental State Examination (MMSE) performed while she was hospitalized for hypertension revealed mild dementia-level scores. She was diagnosed as having AD, taking into consideration that fluorodeoxyglucose (FDG) PET demonstrated hypometabolism in her left medial temporal lobe, posterior cingulate gyrus, and precuneus; ^{11}C-Pittsburgh Compound-B (PiB) amyloid PET yielded a positive plausible result with marginal tracer accumulation in the white matter and partial accumulation in the parietal and lateral temporal lobes; the mean standard uptake value ratio (MSUVR) on PiB amyloid PET was 1.36, which was slightly lower than a previously reported cutoff value of 1.50 (23). She was unaware of any cognitive decline, including memory impairment, at the time of the diagnosis, but she subsequently became gradually aware of a language impairment. Another doctor was asked for a second opinion, and she was referred to our hospital based on a suspicion of primary progressive aphasia with a pathological basis of FTLD (or atypical AD).

Her chief complaint was stagnation of speech, especially when she was nervous. Her husband also told us that she sometimes mispronounced words while reading aloud. She had a professional career and had no remarkable problems at work. She was aware of an age-appropriate memory decline but had no obvious subjective memory complaints. Her past medical history included hypertension and coxarthrosis. She had no family history of dementia, stroke, or other neurodegenerative diseases.

Neurological findings

No obvious motor symptoms, pyramidal/extrapyramidal symptoms, or ataxia were observed. She looked cheerful, and she talked sociably and nearly completely and fluently without obvious apraxia of speech or paraphasia, although word-finding difficulty was occasionally observed during brief object naming and word fluency tasks. She was able to remember her daily events. Her episodic and semantic memory seemed to be well maintained.

TABLE 1 Neuropsychological test scores.

	Initial visit	One-year follow-up
Mini-mental state examination	23	22/30
Raven's colored progressive matrices	32	N/A/36
Rey-Osterrieth complex figure test		
(Copy)	36	N/A/36
(3-min delayed)	14	N/A/36
Logical memory		
(Immediate)	7	7/25
(Delayed)	3	3/25
Rey auditory verbal learning test		
Trial 1	2	N/A/15
Trial 2-3-4	4-5-3	N/A/15
Trial 5	4	N/A/15
Interference list B	3	N/A/15
Trial 6	3	N/A/15
Recognition	15	N/A/15
Word fluency		
(Category)	31	20
(Initial letter)	25	19

N/A represents tests that were not administered.

Neuropsychological test findings

Neuropsychological tests suggested mild to moderate impairment in language and verbal short-term memory (Table 1): her MMSE score (24) was 23/30; her Wechsler Memory Scale-Revised (WMS-R) Logical Memory score (25) was 7/25 for the immediate recall and 3/25 for the delayed recall; and her Rey-Osterrieth Complex Figure Test score (26, 27) was 36/36 for the copy and 14/36 for the 3-min delayed recall. An assessment using the Japanese Standard Language Test of Aphasia (28, 29) suggested marginal to mild overall language impairment, particularly in oral expressions, where word-finding difficulty and/or phonological errors were observed in naming and sentence repetition; the findings also suggested impaired auditory comprehension of not words, but sentences (e.g., Sequential Commands) (Supplementary Table 1). Similarly, in the sentence repetition task in the MMSE, she correctly repeated the first phrase and the first syllable of the subsequent phrase, but she could not continue thereafter. After receiving a clue for the first two syllables, she was able to continue the phrase correctly, although she failed to complete the last phrase, for which she substituted completely different words from those used in the original sentence.

An examination performed 1 year after her initial visit to our hospital showed a notable decline in the Word Fluency (3 min) score only (Category: 20, Initial letter: 19) (Table 1). In the sentence repetition task in the MMSE, she correctly repeated the first and the last phrases but omitted the two phrases in the middle. Three more tests were additionally performed at this time. On the Japanese version of the Alzheimer's Disease Assessment Scale-Cognitive subscale (ADAS-cog-J) (30), she scored 11.4/70 and exhibited phonological errors involving the replacement, omission or insertion of syllables [e.g., "*ki-me-tsu-ri*" instead of "*tsu-me-ki-ri*" (i.e., nail cutter), "*o-yu-bi*" for "*o-ya-yu-bi*" (i.e., thumb), "*ko-ya-yu-bi*" for "*ko-yu-bi*" (i.e., pinky); Supplementary Table 2]. On the Japanese Adult Reading Test (JART) (31), she scored 5/50 (equivalent to a predicted IQ of 81): three words with highly irregular readings (e.g., tobacco) were not scored after she answered using a gesture and/or explanation, 25 words were incorrect or partially correct, and 17 words were unanswered. Her Clinical Dementia Rating (CDR) score (32) was 0.5, and she was continuing to work as before without experiencing any remarkable problem. No obvious grammatical errors were observed in the above-mentioned assessments.

Clinical diagnosis

Based on the clinical findings, i.e., almost completely fluency speaking (except for slight language impairment in the form of word-finding difficulty and phonological errors), impairment in verbal short-term memory, absence of obvious cognitive decline in other domains including visual or episodic memory, and absence of motor and pyramidal/extrapyramidal symptoms, or ataxia, the most likely clinical diagnosis was lv-PPA with a questionable pathological basis of AD according to the criteria for lv-PPA (33).

Brain imaging

At the time of the patient's first visit to our hospital, visual assessments of magnetic resonance imaging (MRI) findings showed atrophy, particularly in the left temporal lobe and cerebellum; fluid-attenuated inversion recovery (FLAIR) imaging showed high signals in the white matter, suggesting old lacunar infarctions and/or chronic ischemic changes (Figure 1A). Single photon emission computed tomography (SPECT) showed left-predominant hypoperfusion in the parietal lobes and the left temporal lobe and mild hypoperfusion in both frontal lobes. A statistical analysis using 3D-stereotactic surface projections (3D-SSP) showed a mild decrease in blood flow in the posterior cingulate gyrus, the precuneus and the cerebellum (Figure 1B).

One year after the initial visit, visual assessments of MRI findings showed no remarkable changes, compared with the previous imaging findings. ^{18}F-florbetaben (FBB) amyloid PET (21) was negative, as judged by certified radiologists. However, ^{18}F-florzolotau tau PET (22) was positive, as judged by trained

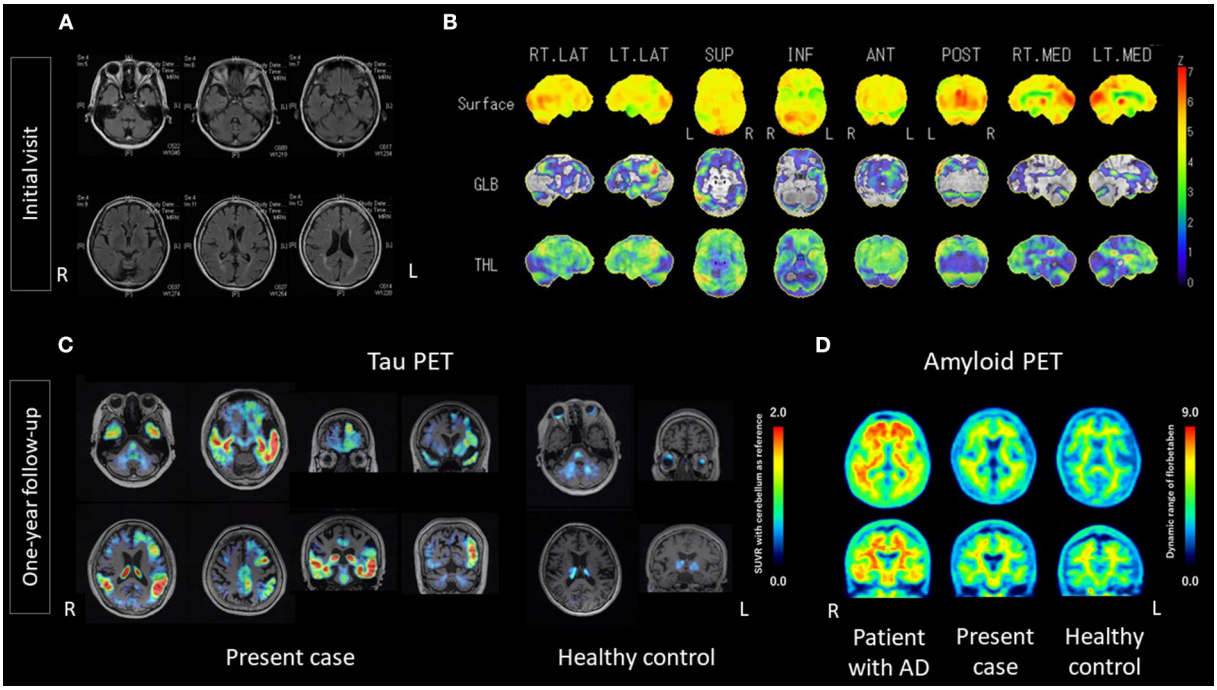

FIGURE 1
Results of MRI, 3D-SSP of SPECT, ^{18}F-florzolotau tau PET, and ^{18}F-florbetaben amyloid PET. **(A)** MRI at the initial visit showed mild atrophy of the cerebrum, with a left predominance, and of the cerebellum. Hyperintense signals in the white matter suggest old lacunar infarctions and/or chronic ischemic changes. **(B)** 3D-SSP of SPECT at the initial visit showed a mild decrease in blood flow in the posterior cingulate gyrus, precuneus and cerebellum. **(C)** ^{18}F-florzolotau tau PET at one-year follow-up showed intense radio signals predominantly in the left temporal lobe, particularly the superior temporal and middle temporal lobe, as well as the supramarginal gyrus, and marginal to mild signals in the frontal lobe. **(D)** ^{18}F-florbetaben amyloid PET at one-year follow-up did not show intense radio signals, compared with age/sex-matched controls. AD, Alzheimer's disease; ANT, anterior; GLB, global; INF, inferior; L; left; LT, left; MED, medial; POST, posterior; R, right; RT, right; SUP, superior; SUVR, standard uptake value ratio; THL, thalamus; 3D-SSP, Three-dimensional stereotactic surface projections.

neurologists and psychiatrists. The accumulations of ^{18}F-florzolotau were predominantly on the left side, particularly in the superior temporal gyrus, middle temporal gyrus, supramarginal gyrus, and frontal operculum (Figure 1C; see Supplementary Figure 1 for more details). Volume of interest (VOI) analyses using FreeSurfer 6.0 (http://surfer.nmr.mgh.harvard.edu/) from the Desikan-Killiany-Tourville atlas (34) demonstrated that the SUVRs in the present case were higher than those of healthy controls, with *z*-scores of 27.37, 10.95, 13.79, and 34.76 for the supramarginal, inferior-temporal, middle-temporal, and superior-temporal gyrus, respectively (Supplementary Table 3).

Positron emission tomography imaging acquisition, processing, and assessment were conducted as follows. ^{18}F-florbetaben amyloid PET images were acquired for 20 min using PET-CT (True Point Biograph 40/64; Siemens Japan K.K., Tokyo, Japan) at 90 min after the intravenous injection of 300 MBq ± 10% ^{18}F-florbetaben. The 20-min PET images were interpreted by two nuclear medicine experts who had completed a training program offered by the manufacturer (Piramal Imaging GmbH, Berlin, Germany). Following the NeuraCeq™ guidelines, amyloid-β positivity or negativity was determined based on assessments of tracer uptake in the gray matter in the following four brain regions: the lateral temporal lobes, the frontal lobes, the posterior cingulate cortex/precuneus, and the parietal lobes (http://www.accessdata.fda.gov/drugsatfda_docs/label/2014/204677s000lbl.pdf) (35). Amyloid-β negativity was established when the tracer uptake (i.e., signal intensity) in the gray matter was lower than that in the white matter in all four brain regions. ^{18}F-florzolotau tau PET images were acquired for 20 min using PET-CT (Biograph mCT flow, Siemens, Munich, Germany) at 90 min after the intravenous injection of 185MBq ± 10% ^{18}F-florzolotau. We used PMOD software (PMOD Technologies, Zürich, Switzerland) to process the 20-min PET images, and tau positivity or negativity was determined based on assessments of tracer uptake using SUVR with reference to the cerebellum. ^{18}F-FBB amyloid PET images with dynamic range are shown in Figure 1D.

Plasma measurements

One year after the initial visit to our hospital, the plasma p-tau181 and NFL levels were measured using the

commercial Quanterix® assay (Simoa® p-Tau181 Advantage Kit or Simoa® NF-light Kit) on an HD-1 analyzer or SR–X, in accordance with the respective manufacturer's instructions (Quanterix). The plasma level of p-tau181 was 2.99 pg/ml, while that of NFL was 22.71 pg/ml. These levels suggested an AD-like pattern when they were compared with preliminary cutoff values based on our in-lab data (2 pg/ml for p-tau181 and 35 pg/ml for NFL), although no universal cutoff values have been established (11).

Whole-genome sequencing

One year after the initial visit to our hospital, genomic DNA was extracted using the DNeasy Blood and Tissue kit (Qiagen). The extracted DNA was amplified by polymerase chain reaction (PCR) using primers designed specifically for target single nucleotide polymorphisms (SNP). Whole-genome sequencing revealed no known dominantly inherited mutations in the AD or FTLD genes, including *APP,* charged multivesicular body protein 2B (*CHMP2B*), *GRN, MAPT, PSEN1, PSEN2,* progranulin (*PGRN*), *TDP43,* and valosin-containing protein (*VCP*).

Discussion

Based on the clinical findings, particularly the negative results of amyloid PET and the positive results of tau PET, and the contradictory results of the plasma measurements, the present patient was considered to be a rare case of non-AD tauopathy with lv-PPA, with an underlying pathology that was difficult to predict.

Her language symptoms were considered typical of lv-PPA (4, 6), meeting all the features described in the widely accepted current criteria for the clinical diagnosis of lv-PPA (33): "impaired single-word retrieval in spontaneous speech and naming" and "impaired repetition of sentences and phrases" as the core features, and "speech (phonologic) errors in spontaneous speech and naming," "spared single-word comprehension and object knowledge," "spared motor speech," and "absence of frank agrammatism defined as the omission and/or substitution of grammatical morphemes with associated grammatical errors (36)" as non-core features.

The conspicuous tau PET tracer accumulations, which were predominantly in the left supramarginal/angular gyrus (Figure 1C), seemed to be consistent with the regional brain function and the manifested symptoms in the present case. In particular, tau PET tracer accumulations in the posterior temporal lobe and inferior parietal lobe (supramarginal/angular gyrus) may be the underlying neural basis for the "logopenic" status, which is explained by the dysfunction of the "phonological loop," a component of short-term memory that includes a store in which phonological memory traces are held over a period of a few seconds, and an articulatory rehearsal process that refreshes them (3). The impairment of the "phonological loop," which is generally well correlated with AD pathology (6, 14), seemed to have manifested in our patient as syllabic errors in naming and reading aloud, incomplete sentence repetition, and impaired auditory comprehension of sentences. For example, as also described in the Results section, she was able to repeat the first two or three words/morphemes in the sentence repetition task of the MMSE correctly, but she failed to complete subsequent parts because of simplifications or substitutions; in the SLTA, errors were observed in sentence-level auditory comprehension, despite spared word-level auditory comprehension and sentence-level reading comprehension; in the JART, she answered with gestures or a roundabout explanation for some kanji words with highly irregular readings, suggesting that she knew the meaning of the words, but could not find the proper words and/or phonological representation (i.e., how to read the words aloud). The same processes were assumed to account for most of the remaining unscored words. For these reasons, her predicted IQ of 81 (5/50 correct answers) was likely an underestimation caused by her verbal-predominant cognitive decline arising from disease-caused language impairment. Accordingly, the elements for a clinical diagnosis of lv-PPA based on the current diagnostic criteria (33) were applicable in this single case, even though the elements for an imaging-supported diagnosis or a diagnosis with a definite pathology were not present.

A decisive diagnosis based on the positive tau PET findings would be speculative, since ^{18}F-florzolotau does not discriminate among the subtypes of tau isoforms [i.e., 3-repeat (3R), 4-repeat (4R), and a mixture of 3- and 4-repeat (3R + 4R) isoforms]. Nevertheless, the diagnostic likelihood could be considered as follows. The most common and important differential diagnosis would be other 3R + 4R tauopathies, such as primary age-related tauopathy (PART), including senile dementia of the neurofibrillary tangle type (SD–NFT) without amyloid plaques; however, the clinical findings lacked the distinctive features of PART, namely, an obvious memory decline, a late onset (i.e., late-80s), and the characteristic limitation of tau lesions to the medial temporal lobe (37). In addition, the findings of tau PET imaging in the present case may not necessarily be PART-like, since the radio signals of ^{18}F-florzolotau were seen in the left superior and middle temporal gyrus, left supramarginal gyrus, and left frontal operculum, whereas those in the preclinical stage of AD or PART may expand from the medial temporal cortex, involving less-mature tau fibrils, to the other neocortical and limbic areas, along with the progression of the NFT stage (22). Four-repeat tauopathies such as corticobasal degeneration might be plausible, based on the asymmetric distribution patterns on tau PET imaging, despite not presenting with a typical corticobasal degeneration or progressive supranuclear palsy

pattern (22), since pyramidal/extrapyramidal symptoms can appear after cognitive decline (38). The absence of behavioral deficits due to frontal lobe dysfunction and characteristic brain atrophy on MRI such as knife-blade atrophy, suggests that Pick's disease is unlikely. Furthermore, ^{18}F-florzolotau distribution predominantly in the left supramarginal/angular gyrus is not consistent with three-repeat tauopathies (22).

In short, most of the biophysical and biological examinations (i.e., MRI, SPECT, FDG PET, and plasma p-tau and NFL measurements) showed an AD-like pattern consistent with the initial clinical diagnosis of AD. In contrast, amyloid PET using both ^{11}C-PiB and ^{18}F-FBB showed marginal-to-negative results. An ^{18}F-florzolotau tau PET and genome sequencing were informative, but the results were inconclusive. No known dominantly inherited mutations of AD or FTLD genes were identified. Notably, AD associated with the *APP* Osaka mutation E693Δ (39, 40) and the Arctic mutation E693G (41), which result in a markedly low amyloid PET retention, was ruled out because no known *APP* mutations were identified.

The above interpretations need to be understood in the context of the following issues. First, although ^{18}F-florzolotau shows improved selectivity for tau proteins, including autopsy-confirmed binding to tau proteins in FTLD-tau (22), and does not bind to monoamine oxidase (MAO)-A or MAO-B nor does it cross-react with amyloid-β (22), the possibility of nonspecific/off-target binding should still be considered. Since ^{18}F-florzolotau accumulates in the choroid plexus in healthy subjects, some type of off-target binding may exist in this region. Furthermore, in a recent report, the increased retention of ^{18}F-florzolotau was found in the basal ganglia of patients with multiple system atrophy, suggesting that cross-reaction with α-synuclein cannot be completely ruled out (42). Second, some potential assessments were not performed: although PET with ^{18}F-florzolotau can discriminate a wide range of tauopathies by the pattern of retention, a head-to-head comparison of ^{18}F-florzolotau with another tau PET tracer that hardly binds to 4R tau, such as ^{18}F-MK-6240 (43), or the dopamine transporter (DAT) imaging and/or ^{123}I-metaiodobenzylguanidine (MIBG) scintigraphy (44, 45), might be helpful for a differential diagnosis; it might be desirable to perform a forward digit span, as this task can be sensitive to impairments of the "phonological loop" (6). Third, positivity/negativity on the ^{18}F-FBB amyloid PET was determined based only on visual interpretations by certified radiologists. Although our judgmental standards agree with the established guidelines, a quantitative analysis would aid the interpretation and comparison of results. This issue should be pressed forward for future work, while quantitative measures such as the Centiloid (CL) scale, which may allow a direct comparison of results even across different PET tracers, scanning facilities, or analytical methods, are being standardized (46, 47). For the above reasons, long-term follow-up and pathological evaluations might lead to a more precise diagnosis and a better understanding of the clinicopathological basis.

To conclude, we have reported a patient with suspected non-AD tauopathy who presented with lv-PPA and had impairments in naming and sentence repetition as well as verbal short-term memory. Clinical examinations, including MRI, SPECT, FDG-PET, and plasma measurements, showed results compatible with a diagnosis of AD, whereas the amyloid PET yielded mainly negative results and the results of both tau PET and genome sequencing were inconclusive. Since an antemortem diagnosis of proteinopathies is often difficult, we consider the present case to be important from the viewpoint of obtaining a better understanding of proteinopathies, particularly for the collation of clinical symptoms and biological/biophysical findings.

Data availability statement

The original contributions presented in the study are included in the article/Supplementary material, further inquiries can be directed to the corresponding author/s.

Ethics statement

The studies involving human participants were reviewed and approved by Certified Review Board of Keio, Keio University School of Medicine. The patients/participants provided their written informed consent to participate in this study.

Author contributions

YM: conceptualization, resources, investigation, and writing—original draft preparation. MK, KT, TT, and SB: resources and writing—review and editing. TK: writing—review and editing. HT and DI: resources, project administration, and writing—review and editing. MM: resources, writing—review and editing, project administration, funding acquisition, and supervision. All authors contributed to the article and approved the submitted version.

Funding

This work was supported by the Japan Agency for Medical Research and Development under Grant Number JP17pc0101006 to MM.

Acknowledgments

^{18}F-florzolotau, the tau PET tracer used for this research, was provided by APRINOIA Therapeutics Inc. The authors would like to thank Dr. Jin Nakahara of the Department of Neurology, Dr. Masahiro Jinzaki of the Department of

Diagnostic Radiology, and Mr. Kiyotaka Nakajima and the staff of the Division of Nuclear Medicine and Department of Radiology for their help with the PET examinations and image processing at Keio University School of Medicine; they would also like to thank Dr. Kenji Tagai, Dr. Hitoshi Shimada, and Dr. Makoto Higuchi of the Department of Functional Brain Imaging Research, National Institute of Radiological Sciences, National Institutes for Quantum and Radiological Science and Technology, Chiba, Japan.

Conflict of interest

The authors declare that the research was conducted in the absence of any commercial or financial relationships that could be construed as a potential conflict of interest.

Publisher's note

Supplementary material

The Supplementary Material for this article can be found online at: https://www.frontiersin.org/articles/10.3389/fneur.2022.1049113/full#supplementary-material

References

1. Mesulam MM. Slowly progressive aphasia without dementia. *Ann Neurol.* (1982) 11:592–8. doi: 10.1002/ana.410110607

2. Ramos EM, Dokuru DR, Van Berlo V, Wojta K, Wang Q, Huang AY, et al. Genetic screen in a large series of patients with primary progressive aphasia. *Alzheimers Dement.* (2019) 15:553–60. doi: 10.1016/j.jalz.2018.10.009

3. Gorno-Tempini ML, Brambati SM, Ginex V, Ogar J, Dronkers NF, Marcone A, et al. The logopenic/phonological variant of primary progressive aphasia. *Neurology.* (2008) 71:1227–34. doi: 10.1212/01.wnl.0000320506.79811.da

4. Chare L, Hodges JR, Leyton CE, McGinley C, Tan RH, Kril JJ, et al. New criteria for frontotemporal dementia syndromes: clinical and pathological diagnostic implications. *J Neurol Neurosurg Psychiatry.* (2014) 85:866–71. doi: 10.1136/jnnp-2013-306948

5. Spinelli EG, Mandelli ML, Miller ZA, Santos-Santos MA, Wilson SM, Agosta F, et al. Typical and atypical pathology in primary progressive aphasia variants. *Ann Neurol.* (2017) 81:430–43. doi: 10.1002/ana.24885

6. Giannini LAA, Irwin DJ, Mcmillan CT, Ash S, Rascovsky K, Wolk DA, et al. Clinical marker for Alzheimer disease pathology in logopenic primary progressive aphasia. *Neurology.* (2017) 88:2276–84. doi: 10.1212/WNL.0000000000004034

7. Mesulam MM, Weintraub S, Rogalski EJ, Wieneke C, Geula C, Bigio EH. Asymmetry and heterogeneity of Alzheimer's and frontotemporal pathology in primary progressive aphasia. *Brain.* (2014) 137:1176–92. doi: 10.1093/brain/awu024

8. Josephs K, Tosakulwong N, Weigand S, Buciuc M, lowe V, Dickson D, et al. Relationship between 18 F-flortaucipir uptake and histologic lesion types in 4-repeat tauopathies. *J Nucl Med.* (2021) 63:931–5. doi: 10.2967/jnumed.121.262685

9. Shi Y, Zhang W, Yang Y, Murzin AG, Falcon B, Kotecha A, et al. Structure-based classification of tauopathies. *Nature.* (2021) 598:359–63. doi: 10.1038/s41586-021-03911-7

10. Karikari TK, Benedet AL, Ashton NJ, Lantero Rodriguez J, Snellman A, Suárez-Calvet M, et al. Diagnostic performance and prediction of clinical progression of plasma phospho-tau181 in the Alzheimer's disease neuroimaging initiative. *Mol Psychiatry.* (2021) 26:429–42. doi: 10.1038/s41380-020-00923-z

11. Chatterjee P, Pedrini S, Ashton NJ, Tegg M, Goozee K, Singh AK, et al. Diagnostic and prognostic plasma biomarkers for preclinical Alzheimer's disease. *Alzheimers Dement.* (2022) 18:1141–54. doi: 10.1002/alz.12447

12. Illán-Gala I, Lleo A, Karydas A, Staffaroni AM, Zetterberg H, Sivasankaran R, et al. Plasma tau and neurofilament light in frontotemporal lobar degeneration and Alzheimer disease. *Neurology.* (2021) 96:e671–83. doi: 10.1212/WNL.0000000000011226

13. Bejanin A, Schonhaut DR, La Joie R, Kramer JH, Baker SL, Sosa N, et al. Tau pathology and neurodegeneration contribute to cognitive impairment in Alzheimer's disease. *Brain.* (2017) 140:3286–300. doi: 10.1093/brain/awx243

14. Cousins KAQ, Bove J, Giannini LAA, Kinney NG, Balgenorth YR, Rascovsky K, et al. Longitudinal naming and repetition relates to AD pathology and burden in autopsy-confirmed primary progressive aphasia. *Alzheimers Dement Transl Res Clin Interv.* (2021) 7:1–10. doi: 10.1002/trc2.12188

15. Kawakatsu S, Kobayashi R, Hayashi H, Morioka D, Utsunomiya A, Kabasawa T, et al. Clinicopathological heterogeneity of Alzheimer's disease with pure Alzheimer's disease pathology: cases associated with dementia with Lewy bodies, very early-onset dementia, and primary progressive aphasia. *Neuropathology.* (2021) 41:427–49. doi: 10.1111/neup.12765

16. Whitwell JL, Jack CR, Duffy JR, Strand EA, Gunter JL, Senjem ML, et al. Microbleeds in the logopenic variant of primary progressive aphasia. *Alzheimers Dement.* (2014) 10:62–6. doi: 10.1016/j.jalz.2013.01.006

17. Buciuc M, Duffy JR, Machulda MM, Spychalla AJ, Gunter JL, Jack CR, et al. Association of amyloid angiopathy with microbleeds in logopenic progressive aphasia: an imaging-pathology study. *Eur J Neurol.* (2021) 28:670–5. doi: 10.1111/ene.14594

18. Basilico S, Ciricugno A, Gelosa G, Magnani FG, Mosca L, Popescu C, et al. Clinical characterization of atypical primary progressive aphasia in a 3-year longitudinal study: a case report. *Cogn Behav Neurol.* (2021) 34:233–44. doi: 10.1097/WNN.0000000000000273

19. Mesulam MM, Coventry CA, Rader BM, Kuang A, Sridhar J, Martersteck A, et al. Modularity and granularity across the language network-A primary progressive aphasia perspective. *Cortex.* (2021) 141:482–96. doi: 10.1016/j.cortex.2021.05.002

20. Klunk WE, Engler H, Nordberg A, Wang Y, Blomqvist G, Holt DP, et al. Imaging brain amyloid in Alzheimer's disease with pittsburgh compound-B. *Ann Neurol.* (2004) 55:306–19. doi: 10.1002/ana.20009

21. Sabri O, Sabbagh MN, Seibyl J, Barthel H, Akatsu H, Ouchi Y, et al. Florbetaben PET imaging to detect amyloid beta plaques in Alzheimer's disease: phase 3 study. *Alzheimers Dement.* (2015) 11:964–74. doi: 10.1016/j.jalz.2015.02.004

22. Tagai K, Ono M, Kubota M, Kitamura S, Takahata K, Seki C, et al. High-contrast *in vivo* imaging of tau pathologies in Alzheimer's and non-Alzheimer's disease tauopathies. *Neuron.* (2021) 109:42–58.e8. doi: 10.1016/j.neuron.2020.09.042

23. Klunk W, Cohen A, Bi W, Weissfeld L, Aizenstein H, McDade E, et al. O3-12-03: why we need two cutoffs for amyloid imaging: early versus Alzheimer's-like amyloid-positivity. *Alzheimers Dement.* (2012) 8(4S_Part_12):453–4. doi: 10.1016/j.jalz.2012.05.1208

24. Folstein MF, Folstein SE. McHugh PR. "Mini-mental state". *J Psychiatr Res.* (1975) 12:189–98. doi: 10.1016/0022-3956(75)90026-6

25. Wechsler D. *Wechsler Memory Scale-Revised*. New York, NY: Psychological Corporation (1987).

26. Rey A. L'examen psychologique dans les cas d'encéphalopathie traumatique. *Arch Psychol*. (1941) 28:21, 286–340.

27. Osterrieth P. Le test de copie d'une figure complexe. *Arch Psychol*. (1944) 30:206–356.

28. Hasegawa T, Kishi H, Shigeno K, Tanemura J, Kusunoki T, Kifune Y et al. A study on aphasia rating scale. A method for overall assessment of SLTA results. [Japanese]. *High Brain Funct Res*. (1984) 4:638—46. doi: 10.2496/apr.4.638

29. Hasegawa T, Kishi H, Shigeno K, Tanemura J, Kusunoki T. Three-dimensional structure in language tests of aphasia. *Folia Phoniatr Logop*. (1985) 37:246–58. doi: 10.1159/000265805

30. Rosen WG, Mohs RC, Davis KL. A new rating scale for Alzheimer's disease. *Am J Psychiatry*. (1984) 141:1356–64. doi: 10.1176/ajp.141.11.1356

31. Matsuoka K, Uno M, Kasai K, Koyama K, Kim Y. Estimation of premorbid IQ in individuals with Alzheimer's disease using Japanese ideographic script (Kanji) compound words: Japanese version of National Adult Reading Test. *Psychiatry Clin Neurosci*. (2006) 60:332–9. doi: 10.1111/j.1440-1819.2006.01510.x

32. Morris JC. The clinical dementia rating (CDR): current version and scoring rules. *Neurology*. (1993) 43:2412–4. doi: 10.1212/WNL.43.11.2412-a

33. Gorno-Tempini ML, Hillis AE, Weintraub S, Kertesz A, Mendez M, Cappa SF, et al. Classification of primary progressive aphasia and its variants. *Neurology*. (2011) 76:1006–14. doi: 10.1212/WNL.0b013e31821103e6

34. Klein A, Tourville J. 101 Labeled brain images and a consistent human cortical labeling protocol. *Front Neurosci*. (2012) 6:171. doi: 10.3389/fnins.2012.00171

35. Seibyl J, Catafau AM, Barthel H, Ishii K, Rowe CC, Leverenz JB, et al. Impact of training method on the robustness of the visual assessment of 18F-florbetaben PET scans: results from a phase-3 study. *J Nucl Med*. (2016) 57:900–6. doi: 10.2967/jnumed.115.161927

36. Graham NL, Leonard C, Tang-Wai DF, Black S, Chow TW, Scott CJM, et al. Lack of frank agrammatism in the nonfluent agrammatic variant of primary progressive aphasia. *Dement Geriatr Cogn Dis Extra*. (2016) 6:407–23. doi: 10.1159/000448944

37. Crary JF, Trojanowski JQ, Schneider JA, Abisambra JF, Abner EL, Alafuzoff I, et al. Primary age-related tauopathy (PART): a common pathology associated with human aging. *Acta Neuropathol*. (2014) 128:755–66. doi: 10.1007/s00401-014-1349-0

38. Murray R, Neumann M, Forman MS, Farmer J, Massimo L, Rice A, et al. Cognitive and motor assessment in autopsy-proven corticobasal degeneration. *Neurology*. (2007) 68:1274–83. doi: 10.1212/01.wnl.0000259519.78480.c3

39. Tomiyama T, Nagata T, Shimada H, Teraoka R, Fukushima A, Kanemitsu H, et al. A new amyloid β variant favoring oligomerization in Alzheimer's-type dementia. *Ann Neurol*. (2008) 63:377–87. doi: 10.1002/ana.21321

40. Tomiyama T, Shimada H. App osaka mutation in familial Alzheimer's disease—its discovery, phenotypes, and mechanism of recessive inheritance. *Int J Mol Sci*. (2020) 21:1413. doi: 10.3390/ijms21041413

41. Nilsberth C, Westlind-Danielsson A, Eckman CB, Condron MM, Axelman K, Forsell C, et al. The "Arctic" APP mutation (E693G) causes Alzheimer's disease by enhanced Aβ protofibril formation. *Nat Neurosci*. (2001) 4:887–93. doi: 10.1038/nn0901-887

42. Li L, Liu FT Li M, Lu JY, Sun YM, Liang X, et al. Clinical utility of 18F-APN-1607 tau PET imaging in patients with progressive supranuclear palsy. *Mov Disord*. (2021) 36:2314–23. doi: 10.1002/mds.28672

43. Levy JP, Bezgin G, Savard M, Pascoal TA, Finger E, Laforce R, et al. 18F-MK-6240 tau-PET in genetic frontotemporal dementia. *Brain*. (2021) 2021:1–26. doi: 10.1093/brain/awab392

44. Whitwell JL, Höglinger GU, Antonini A, Bordelon Y, Boxer AL, Colosimo C, et al. Radiological biomarkers for diagnosis in PSP: where are we and where do we need to be? *Mov Disord*. (2017) 32:955–71. doi: 10.1002/mds.27038

45. Orimo S, Suzuki M, Inaba A, Mizusawa H. 123I-MIBG myocardial scintigraphy for differentiating Parkinson's disease from other neurodegenerative parkinsonism: a systematic review and meta-analysis. *Park Relat Disord*. (2012) 18:494–500. doi: 10.1016/j.parkreldis.2012.01.009

46. Klunk WE, Koeppe RA, Price JC, Benzinger TL, Devous MD, Jagust WJ, et al. The centiloid project: standardizing quantitative amyloid plaque estimation by PET. *Alzheimers Dement*. (2015) 11:1–15.e4. doi: 10.1016/j.jalz.2014.07.003

47. Navitsky M, Joshi AD, Kennedy I, Klunk WE, Rowe CC, Wong DF, et al. Standardization of amyloid quantitation with florbetapir standardized uptake value ratios to the Centiloid scale. *Alzheimers Dement*. (2018) 14:1565–71. doi: 10.1016/j.jalz.2018.06.1353

frontiers | Frontiers in Neurology

TYPE Case Report
PUBLISHED 04 January 2023
DOI 10.3389/fneur.2022.1052341

OPEN ACCESS

EDITED BY
Giovanni Rizzo,
IRCCS Institute of Neurological Sciences of Bologna (ISNB), Italy

REVIEWED BY
Luke William Bonham,
University of California, San Francisco, United States
Nicola Ticozzi,
University of Milan, Italy

*CORRESPONDENCE
Ilaria Martinelli
martinelli.ilaria88@gmail.com

SPECIALTY SECTION
This article was submitted to Dementia and Neurodegenerative Diseases, a section of the journal Frontiers in Neurology

RECEIVED 23 September 2022
ACCEPTED 05 December 2022
PUBLISHED 04 January 2023

CITATION
Gianferrari G, Martinelli I, Simonini C, Zucchi E, Fini N, Carra S, Moglia C and Mandrioli J (2023) Case report: p.Glu134del *SOD1* mutation in two apparently unrelated ALS patients with mirrored phenotype.
Front. Neurol. 13:1052341.
doi: 10.3389/fneur.2022.1052341

Case report: p.Glu134del *SOD1* mutation in two apparently unrelated ALS patients with mirrored phenotype

Giulia Gianferrari[1], Ilaria Martinelli[2,3]*, Cecilia Simonini[1], Elisabetta Zucchi[2,4], Nicola Fini[2], Serena Carra[1], Cristina Moglia[5,6] and Jessica Mandrioli[1,2]

[1]Department of Biomedical, Metabolic and Neural Sciences, University of Modena and Reggio Emilia, Modena, Italy, [2]Department of Neurosciences, Azienda Ospedaliero-Universitaria di Modena, Modena, Italy, [3]Clinical and Experimental PhD Program, University of Modena and Reggio Emilia, Modena, Italy, [4]Neurosciences PhD Program, University of Modena and Reggio Emilia, Modena, Italy, [5]S.C Neurology 1U, Azienda Ospedaliero-Universitaria Città della Salute e della Scienza Torino, Torino, Italy, [6]"Rita Levi Montalcini" Department of Neuroscience, University of Turin, Torino, Italy

With upcoming personalized approaches based on genetics, it is important to report new mutations in amyotrophic lateral sclerosis (ALS) genes in order to understand their pathogenicity and possible patient responses to specific therapies. *SOD1* mutations are the second most frequent genetic cause of ALS in European populations. Here, we describe two seemingly unrelated Italian patients with ALS carrying the same *SOD1* heterozygous c.400_402 deletion (p.Glu134del). Both patients had spinal onset in their lower limbs, progressive muscular weakness with respiratory involvement, and sparing bulbar function. In addition to the clinical picture, we discuss the possible pathogenic role of this unfamiliar *SOD1* mutation.

KEYWORDS

ALS, genotype-phenotype correlation, p.Glu134del *SOD1*, case report, motor neuron diseases

Introduction

First identified by Rosen et al. (1), the *SOD1* gene has become significant in amyotrophic lateral sclerosis (ALS) genetics, representing the second most frequent gene involved in ALS European cohorts, after *C9ORF72* (2), and accounting for ∼18–20% of familial (fALS) and 1–2% of sporadic (sALS) cases (3). To date, more than 180 *SOD1* mutations have been associated with ALS (4).

Various mutations in *SOD1* differentially influence disease phenotypes across a broad spectrum of manifestations (4). In particular, data from the ALSoD database[1] show that ∼95% of *SOD1*-ALS patients have spinal onset in the lower limbs (5) with predominant lower motor neuron (LMN) involvement (6), a mean age of 48 years at onset, and no significant gender predominance. Increasing evidence from

1 ALSoD database: https://alsod.ac.uk/.

clinical cases and population studies has revealed that *SOD1*-ALS phenotypes can vary depending on the mutations (2, 7). Some of these, such as the A4V, H43R, L84V, G85R, N86S, and G93A mutations, are associated with an aggressive form of ALS with short survival rates; others, including G93C, D90A, and H46R, are associated with longer survival rates (7).

Although the predominant symptoms depend on LMN involvement, manifestations of upper motor neurons (UMN) may also be present, as reported in a systematic review by Connolly et al. (2). Additionally, the presence of pathological motor-evoked potentials (MEPs) with prolonged central conduction latencies has been described in patients with different *SOD1* mutations (8).

In recent decades, increasing literature data have revealed a great clinical variation in *SOD1*-ALS patients, encompassing extra-motor symptoms (4), and widening the one-to-one correspondence (2). Moreover, the demonstration of the pathogenic role of single variants is increasingly crucial because of the therapeutic intervention to prevent *SOD1* synthesis and accumulation (9, 10) by the intrathecally administered antisense oligonucleotide, Tofersen (10).

In this regard, the dysfunctional effect or evidence of familial segregation of a single *SOD1* variant could play a key role in pathogenicity validation and counseling in clinical practice (11).

Here, we describe the phenotypic and genotypic features of two seemingly unrelated Italian patients with ALS carrying a rare mutation in *SOD1*.

Case report

Case 1

A 61-year-old male presented with a 2-year history of progressive distal weakness of the lower limbs. His medical and social history were uninformative. He reported a family history of ALS (Figure 1B): his brother died at 59 years of age because of ALS, characterized by progressive weakness in the lower limbs with respiratory impairment leading to non-invasive ventilation (NIV) 5 years after onset. Neurological examination of the patient revealed moderate weakness in both lower limbs with hypotrophy, whereas the upper limb and bulbar function were initially spared. Widespread fasciculations involved all four limbs. Deep tendon reflexes were brisk in all limbs, more pronounced on the left side, and without spasticity. After an extensive diagnostic work-up, including neurophysiological studies that revealed active denervation and reinnervation potentials in three body regions, the diagnosis of ALS was established based on the revised El Escorial Criteria. Interestingly, MRI revealed UMN involvement as hypointensity along the bilateral motor cortex on T2-weighted images (Figures 1C, D), with a reduction in the fractional anisotropy (FA) values of the pyramidal bundle in tractography acquisitions.

Reduced amplitudes with normal latencies and central motor conduction times were observed in the lower limbs, as measured by transcranial MEPs.

Extensive neuropsychological testing revealed normal cognitive profiles. Respiratory function showed asymptomatic initial impairment [forced vital capacity (FVC):70%], and the revised ALS functional rating scale (ALSFRS-R) score was 41/48 (progression rate: 0.29 points/month). One year later, the weakness had spread to the upper limbs, and NIV was initiated to support respiratory function (Figure 1A). The patient remains alive 48 months after the onset of symptoms. He currently demonstrates weakness in four limbs with predominant LMN signs, respiratory impairment (FVC 25%) without bulbar involvement, and is undergoing treatment with intrathecal Tofersen (early access program).

Case 2

A 53-year-old male presented with an 8-month history of walking difficulties and upper-limb proximal weakness. His medical history included essential tremor (ET), bipolar disorder, asthma, and diverticular disease. Neurological examination showed mild proximal weakness in the upper limbs and mild weakness in the lower limbs, mainly on the right side, with hypotrophy of the intrinsic hand muscles and the right calf. Bulbar function was completely unaffected. Deep tendon reflexes were brisk in all limbs with bilateral Hoffman and Babinski signs. Spasticity was absent. No family history of ALS was reported (Figure 2B). Diagnostic tests led to an ALS diagnosis according to the revised El Escorial Criteria. Electrophysiological studies showed active denervation and reinnervation potentials in three body regions. Increased central motor conduction time with increased latency and reduced amplitude was observed in the right upper limb as measured by transcranial MEPs. MRI T2-weighted images showed hypointensity of the bilateral motor cortex and FLAIR hyperintensity of the left cortico-spinal bundle (Figure 2C). MRI tractography revealed reduced FA values in the cortico-spinal tract acquisitions. 18FDG-PET showed areas of hypermetabolism affecting both cerebellar hemispheres, with a prevalence in the right lobe (Figure 2D).

Respiratory symptoms emerged 11 months after onset, and NIV was initiated. The progression rate measured by ALSFRS-R revealed that monthly decline at diagnosis was slow (0.25 points/month); however, a subsequent acceleration (1.27 points/month) was present due to respiratory function decline (Figure 2A). The patient remains alive 20 months after the onset of symptoms. He currently demonstrates

10.3389/fneur.2022.1052341

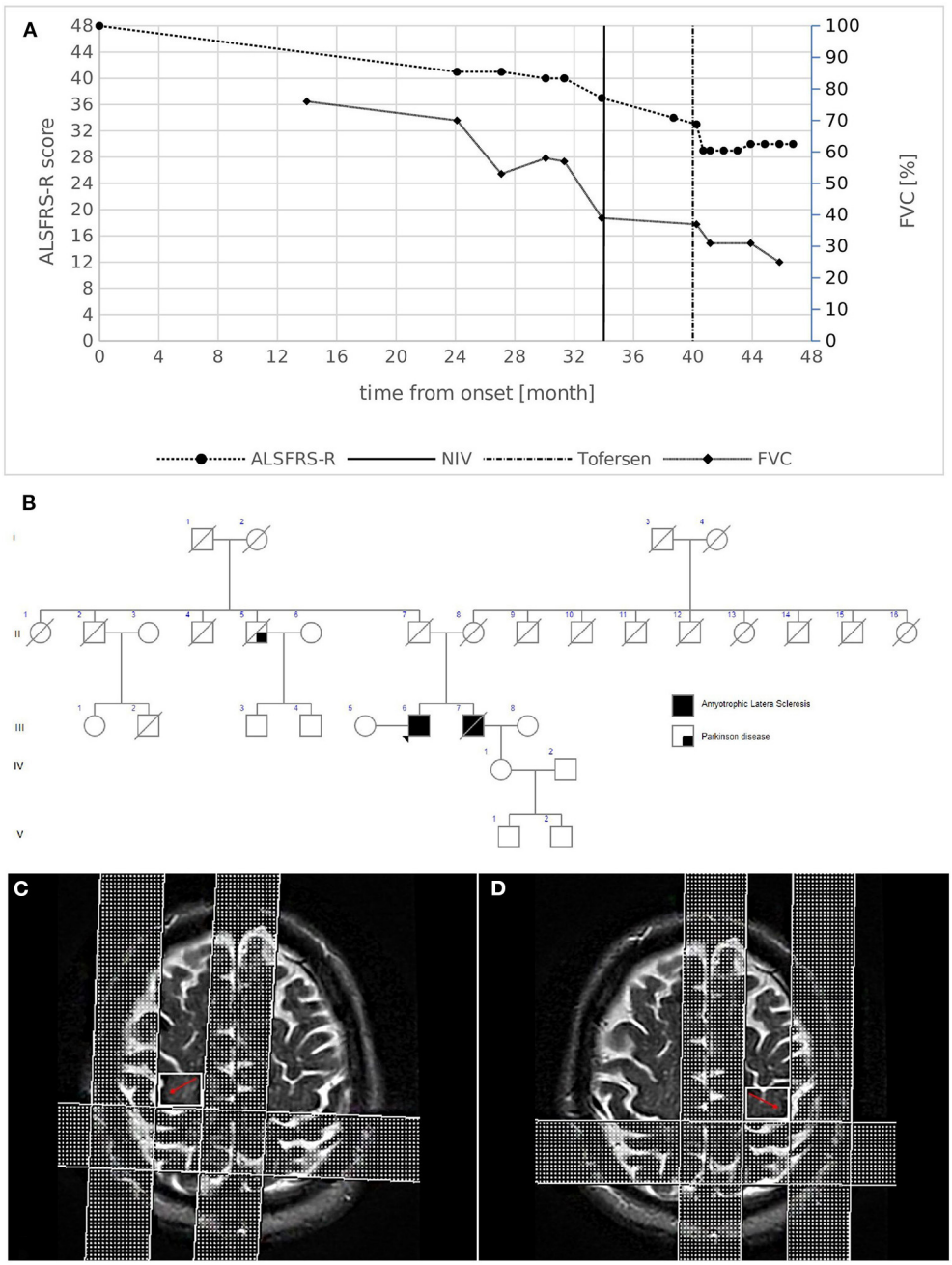

FIGURE 1
(A) Disease course of case 1. The graph shows ALSFRS-R total score (left) and FVC % (right) decline from disease onset. The bold vertical line represents the time when NIV was initiated, while the dashed vertical line represents the beginning of intrathecal Tofersen administration. **(B)** Family pedigree of case 1. Filled circle/square, affected individuals; open circle/square, unaffected individuals; arrow, proband; diagonal line, deceased individuals. The proband's mother died at 79 years of age from HCV infection complications and chronic COPD; the father died at 94 years of age after a hip fracture. A paternal uncle died at an advanced age because of Parkinson's disease. **(C,D)** Brain MRI images of case 1. MRI T2-weighted images revealing the hypointensity along the bilateral motor cortex (red arrows).

weakness in four limbs, respiratory impairment (FVC 45%), a predominant LMN phenotype without bulbar involvement, and is being treated with intrathecal Tofersen (early access program).

Methods

After sample processing (see Supplementary material), an NGS probe-based customized panel was performed (13),

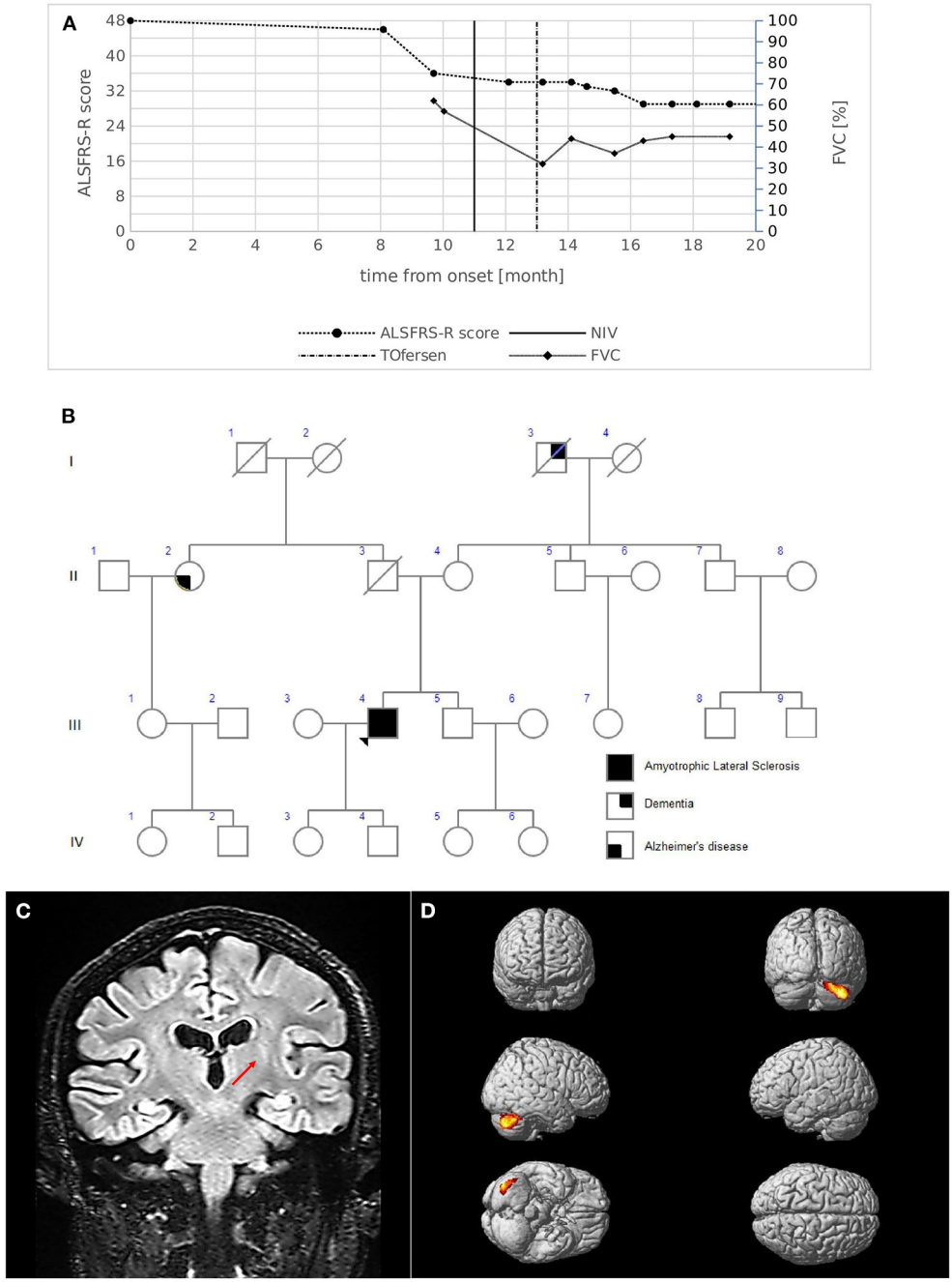

FIGURE 2
(A) Disease course of case 2. The graph shows ALSFRS-R total score (left) and FVC % (right) decline from the onset of symptoms. The bold vertical line represents the time when NIV was initiated, while the dashed vertical line represents the beginning of intrathecal Tofersen administration. **(B)** Family pedigree of case 2. Filled circle/square, affected individuals; open circle/square, unaffected individuals; arrow, proband; diagonal line, deceased individuals. The proband's father died at 56 years of age of colon cancer; the mother is still alive; a 51-year-old brother is alive and in good health and is currently undergoing psychological counseling to evaluate genetic testing. Maternal grandfather had dementia which started at an advanced age; a paternal aunt had Alzheimer's disease with onset at 75 years. **(C)** MRI coronal acquisition showing FLAIR hyperintensity of left cortico-spinal bundle; the red arrow indicates the peculiar involvement of the internal capsule segment. **(D)** ^{18}FDG-PET images Glass brain rendering of the comparison between subject 2 and 40 healthy controls (HC). The cluster showing a statistically significant relative hypermetabolism in subject 2 compared to HC is projected on the brain surface (height threshold $p < 0.001$; $p < 0.05$ FWE-corrected at cluster level). For ^{18}F-FDG-PET acquisition and elaboration details please refer to Canosa et al. (12) and Supplementary material.

revealing c.400_402 deletion in *SOD1* in both patients, resulting in heterozygous p.Glu134 deletion (Figure 3). The interpretation of this deletion was conducted in line with the ClinVar tools (see Supplementary material). Unfortunately, in the first case report, the proband's brother died without undergoing genetic testing, and a blood sample was not available.

Discussion

We describe a heterozygous deletion (c.400_402) in the *SOD1* gene rarely reported previously in two unrelated patients with and without a family history of ALS, which caused an *in-frame* 3-nucleotide deletion with loss of glutamic acid at position 134 (p.Glu134del) in the *SOD1* protein. This deletion is not present in population databases (ExAC no frequency)[2] and is classified as a Variant of Uncertain Significance (ClinVar[2]).

p.Glu134del of the *SOD1* gene translated into a polypeptide with one less amino acid than the wild-type: one glutamine instead of two would be present between positions 131 and 134, and previous experimental studies have shown that missense changes disrupt *SOD1* protein function (14, 15).

SOD1 variants with substantial metal binding and superoxide dismutase activities, called wild-type-like *SOD1* variants (15), are one of the two classes in which the variants of *SOD1* have been classified. They can primarily cause perturbation of the *SOD1* electrostatic loop (15) involving residues 133–144 (electrostatic ring) and adjacent residues 119–132 (electrostatic circuit). Similarly, the previously described p.Glu133 deletion, which is located in an alpha-helical segment in a loop element crucial for binding, is poorly tolerated and is associated with a higher propensity to aggregate (16). This leads to increased intermolecular interactions and fibril formation, aggregation, and loss of *SOD1* stability, which represent synergistic risk factors for ALS severity (15).

Moreover, considering the new nomenclature of *SOD1* variants, p.Glu134del could be comparable with the p.Glu133del mutation described by Hosler et al. (17) and Sabatelli et al. (18), in which TDP-43 abnormalities in fibroblasts derived from the patient were found (18).

Interestingly, the pathogenic effect of this mutation could be postulated by the discovery of the same mutation in two unrelated ALS cases and by the overlapping location and function at the sequence level, since both Glu residues are encoded by the same GAA codon (18).

The clinical picture related to p.Glu133 deletion consists of a lower motor neuron predominant phenotype, with disease onset at 55 years of age and a disease duration of 82 months (18).

In our cases, morphological MRI studies and tractography data were consistent with previous literature (19, 20). The peculiar metabolic alterations in cerebellar regions found in PET images for case 2 seem to be distinct from previous reports on *SOD1*-ALS (12, 21), which, compared to healthy controls, demonstrate relative hypermetabolism in the right precentral gyrus and paracentral lobule (12), or involvement of the precentral gyrus, superior, middle, and inferior frontal gyrus, anterior cingulate, and medial part of the superior gyrus (21).

Interestingly, case 2 reported a history of ET, which could contribute to cerebellar PET alterations, since previous studies found functional and structural abnormalities in several

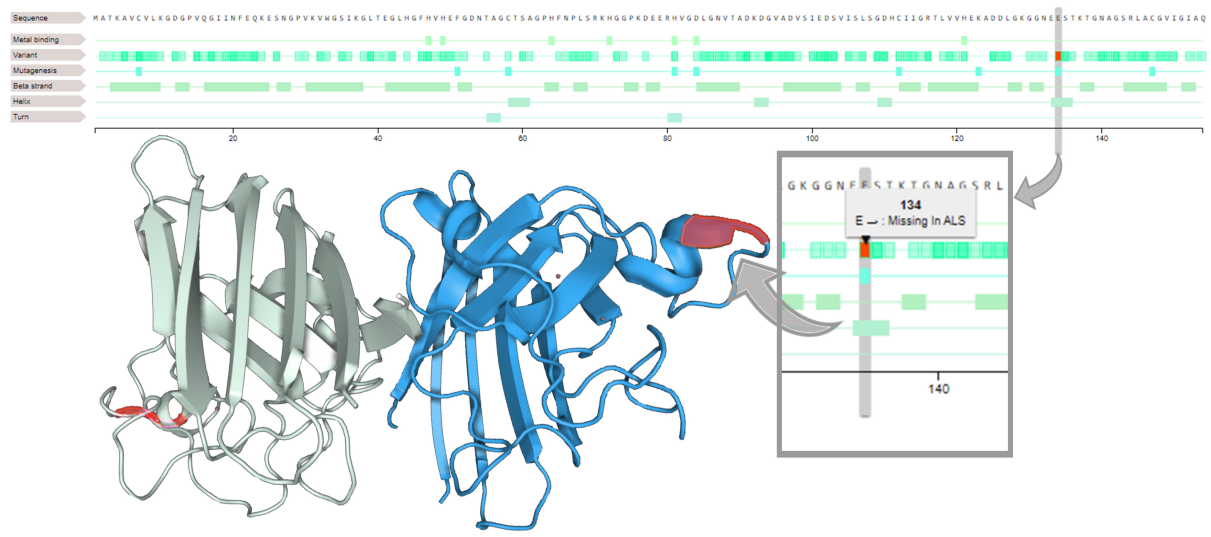

FIGURE 3
Loss of glutamic acid in position 134 (on the right). On the SOD1 3D structure (on the left), residues 133–144 form an electrostatic ring in an alpha helix segment, a loop element that is critical in the binding function of the protein.

parts of the anterior and posterior cerebellar lobules in ET (22). Additionally, in ALS literature, previous PET studies have detected hypermetabolism in various cerebellar regions (23) with different proposed biological explanations, such as microglial activation, loss of inhibition, or compensatory processes (24).

Interestingly, while both patients clinically presented with predominant LMN signs, they both had clinical signs and showed radiological and neurophysiological involvement of UMN, which is in line with recent studies suggesting widespread motor neuron involvement in *SOD1*-ALS (12).

Finally, with regard to the effect of ongoing treatment with Tofersen in the early access program[2], both patients experienced a slowdown in disease progression after starting the treatment as measured by ALSFRS-r, and a less rapid decline or stabilization of respiratory function, as recently reported in a phase III clinical trial (VALOR and OLE) (10). The patients were treated for 8 and 7 months, respectively, and the side effects reported were those associated with lumbar puncture, such as headache and procedural pain, consistent with the literature data (10).

Conclusions

We identified an *SOD1* p.Glu134 deletion in two seemingly unrelated Italian patients with an overlapping phenotype, characterized by a predominant LMN phenotype, with spinal onset in the lower limbs, and respiratory involvement.

The correlation between the p.Glu134del mutation and mirrored ALS phenotypes along with the molecular effects on *SOD1* stability suggest a possible pathogenic role of this mutation, becoming a possible target for *SOD1-specific* therapy. Signaling rare *SOD1* mutations and their corresponding phenotypes is gaining importance in this scientific era with the advent of personalized genetic-based approaches.

Data availability statement

The datasets presented in this article are not readily available because of ethical and privacy restrictions. Requests to access the datasets should be directed to the corresponding author.

Ethics statement

The studies involving human participants were reviewed and approved by Comitato Etico provinciale di Modena (number 124/08, September 2, 2008). The patients/participants provided their written informed consent to participate in this study. Written informed consent was obtained from the individual(s) for the publication of any potentially identifiable images or data included in this article.

Author contributions

JM and IM: conceptualization. JM, IM, GG, CS, and EZ: interpreting data. GG, IM, CS, EZ, NF, and CM: recruitment. GG, IM, JM, and SC: writing—original draft preparation. JM, SC, CM, IM, and EZ: writing—review and editing. JM: funding acquisition. All authors contributed to the article and approved the submitted version.

Funding

This work has been supported by Emilia Romagna Regional Health Authority for the project ERRALS (Emilia Romagna Register for ALS).

Acknowledgments

The authors are deeply grateful to Antonio Canosa from the ALS center of Turin for sharing the 18F-FDG-PET brain scans and elaboration.

Conflict of interest

The authors declare that the research was conducted in the absence of any commercial or financial relationships that could be construed as a potential conflict of interest.

Publisher's note

All claims expressed in this article are solely those of the authors and do not necessarily represent those of their affiliated organizations, or those of the publisher, the editors and the reviewers. Any product that may be evaluated in this article, or claim that may be made by its manufacturer, is not guaranteed or endorsed by the publisher.

Supplementary material

The Supplementary Material for this article can be found online at: https://www.frontiersin.org/articles/10.3389/fneur.2022.1052341/full#supplementary-material

2 https://www.biogen.com/en_us/access-programs.html

References

1. Rosen DR, Siddique T, Patterson D, Figlewicz DA, Sapp P, Hentati A, et al. Mutations in Cu/Zn superoxide dismutase gene are associated with familial amyotrophic lateral sclerosis. *Nature.* (1993) 362:59–62. doi: 10.1038/362059a0

2. Connolly O, le Gall L, McCluskey G, Donaghy CG, Duddy WJ, Duguez S. A systematic review of genotype–phenotype correlation across cohorts having causal mutations of different genes in ALS. *J Person Med.* (2020) 10:1–27. doi: 10.3390/jpm10030058

3. Zou ZY, Zhou ZR, Che CH, Liu CY, He RL, Huang HP. Genetic epidemiology of amyotrophic lateral sclerosis: a systematic review and meta-analysis. *J Neurol Neurosurg Psychiatry.* (2017) 88:540–9. doi: 10.1136/jnnp-2016-315018

4. Martinelli I, Zucchi E, Simonini C, Gianferrari G, Zamboni G, Pinti M, et al. The landscape of cognitive impairment in superoxide dismutase 1 - amyotrophic lateral sclerosis. *Neural Regen Res.* (In Press).

5. Mathis S, Goizet C, Soulages A, Vallat JM, le Masson G. Genetics of amyotrophic lateral sclerosis: a review. *J Neurol Sci.* (2019) 399:217–26. doi: 10.1016/j.jns.2019.02.030

6. Andersen PM, Al-Chalabi A. Clinical genetics of amyotrophic lateral sclerosis: what do we really know? *Nat Rev Neurol.* (2011) 7:603–15. doi: 10.1038/nrneurol.2011.150

7. Li HF, Wu ZY. Genotype-phenotype correlations of amyotrophic lateral sclerosis. *Transl Neurodegener.* (2016) 5:3. doi: 10.1186/s40035-016-0050-8

8. Stewart HG, Andersen PM, Eisen A, Weber M. Corticomotoneuronal dysfunction in ALS patients with different SOD1 mutations. *Clin Neurophysiol.* (2006) 117:1850–61. doi: 10.1016/j.clinph.2006.04.004

9. Mueller C, Berry JD, McKenna-Yasek DM, Gernoux G, Owegi MA, Pothier LM, et al. SOD1 suppression with adeno-associated virus and MicroRNA in familial ALS. *N Engl J Med.* (2020) 383:151–8. doi: 10.1056/NEJMoa2005056

10. Miller TM, Cudkowicz ME, Genge A, Shaw PJ, Sobue G, Bucelli RC, et al. Trial of antisense oligonucleotide Tofersen for *SOD1* ALS. *N Engl J Med.* (2022) 387:1099–110. doi: 10.1056/NEJMoa2204705

11. Ticozzi N, Tiloca C, Morelli C, Colombrita C, Poletti B, Doretti A, et al. Genetics of familial Amyotrophic lateral sclerosis. *Arch Ital Biol.* (2011) 149:65–82.

12. Canosa A, Calvo A, Moglia C, Vasta R, Palumbo F, Solero L, et al. Amyotrophic lateral sclerosis with SOD1 mutations shows distinct brain metabolic changes. *Eur J Nucl Med Mol Imaging.* (2022) 49:2242–50. doi: 10.1007/s00259-021-05668-7

13. Pensato V, Magri S, Bella ED, Tannorella P, Bersano E, Sorarù G, et al. Sorting rare ALS genetic variants by targeted re-sequencing panel in italian patients: OPTN, VCP, and SQSTM1 variants account for 3% of rare genetic forms. *J Clin Med.* (2020) 9:412. doi: 10.3390/jcm9020412

14. Prudencio M, Hart PJ, Borchelt DR, Andersen PM. Variation in aggregation propensities among ALS-associated variants of SOD1: correlation to human disease. *Hum Mol Genet.* (2009) 18:3217–26. doi: 10.1093/hmg/ddp260

15. Molnar KS, Karabacak NM, Johnson JL, Wang Q, Tiwari A, Hayward LJ, et al. A common property of amyotrophic lateral sclerosis-associated variants. Destabilization of the copper/zinc superoxide dismutase electrostatic loop. *J Biol Chem.* (2009) 284:30965–73. doi: 10.1074/jbc.M109.023945

16. Crown AM, Roberts BL, Crosby K, Brown H, Ayers JI, Hart PJ, et al. Experimental mutations in superoxide dismutase 1 provide insight into potential mechanisms involved in aberrant aggregation in familial amyotrophic lateral sclerosis. *G3 Genes Genomes Genet.* (2019) 9:719–28. doi: 10.1534/g3.118.200787

17. Hosler BA, Nicholson GA, Sapp PC, Chin W, Orrell RW, de Belleroche JS, et al. Three novel mutation and two variants in the gene for Cu/Zn superoxide dismutase in familial amyotrphic lateral sclerosis. *Neuromuscul Disord.* (1996) 6:361–6. doi: 10.1016/0960-8966(96)00353-7

18. Sabatelli M, Zollino M, Conte A, del Grande A, Marangi G, Lucchini M, et al. Primary fibroblasts cultures reveal TDP-43 abnormalities in amyotrophic lateral sclerosis patients with and without SOD1 mutations. *Neurobiol Aging.* (2015) 36:2005. e5–e13. doi: 10.1016/j.neurobiolaging.2015.02.009

19. Zejlon C, Nakhostin D, Winklhofer S, Pangalu A, Kulcsar Z, Lewandowski S, et al. Structural magnetic resonance imaging findings and histopathological correlations in motor neuron diseases-A systematic review and meta-analysis. *Front Neurol.* (2022) 13:947347. doi: 10.3389/fneur.2022.947347

20. Agosta F, Pagani E, Petrolini M, Caputo D, Perini M, Prelle A, et al. Assessment of white matter tract damage in patients with amyotrophic lateral sclerosis: a diffusion tensor MR imaging tractography study. *Am J Neuroradiol.* (2010) 31:1457–61. doi: 10.3174/ajnr.A2105

21. Tondo G, Iaccarino L, Cerami C, Vanoli GE, Presotto L, Masiello V, et al. 11C-PK11195 PET–based molecular study of microglia activation in SOD1 amyotrophic lateral sclerosis. *Ann Clin Transl Neurol.* (2020) 7:1513–23. doi: 10.1002/acn3.51112

22. Cerasa A, Quattrone A. Linking essential tremor to the cerebellum—neuroimaging evidence. *Cerebellum.* (2016) 15:263–75. doi: 10.1007/s12311-015-0739-8

23. Canosa A, Pagani M, Cistaro A, Montuschi A, Iazzolino B, Fania P, et al. 18F-FDG-PET correlates of cognitive impairment in ALS. *Neurology.* (2016) 86:44–9. doi: 10.1212/WNL.0000000000002242

24. Bede P, Chipika RH, Christidi F, Hengeveld JC, Karavasilis E, Argyropoulos GD, et al. Genotype-associated cerebellar profiles in ALS: Focal cerebellar pathology and cerebro-cerebellar connectivity alterations. *J Neurol Neurosurg Psychiatry.* (2021) 92:1197–205. doi: 10.1136/jnnp-2021-326854

frontiers | Frontiers in Neurology

TYPE Case Report
PUBLISHED 26 January 2023
DOI 10.3389/fneur.2023.1099077

OPEN ACCESS

EDITED BY
Bruce Miller,
University of California, San Francisco,
United States

REVIEWED BY
Marta Waliszewska-Prosół,
Wroclaw Medical University, Poland
Salvatore Iacono,
University of Palermo, Italy

*CORRESPONDENCE
Xinyu Zhou
✉ zhouxy0712@126.com
Kang Xie
✉ 760020220035@xzhmu.edu.cn

†These authors have contributed equally to this work

SPECIALTY SECTION
This article was submitted to Dementia and Neurodegenerative Diseases, a section of the journal Frontiers in Neurology

RECEIVED 15 November 2022
ACCEPTED 10 January 2023
PUBLISHED 26 January 2023

CITATION
Wu H, Huang H, Xu L, Ji N, Zhou X and Xie K (2023) Case report: Subacute combined degeneration of the spinal cord due to nitrous oxide abuse. *Front. Neurol.* 14:1099077. doi: 10.3389/fneur.2023.1099077

Case report: Subacute combined degeneration of the spinal cord due to nitrous oxide abuse

Huijuan Wu[1,2†], Huiqing Huang[3†], Liaoyang Xu[1†], Niu Ji[1], Xinyu Zhou[1,4*] and Kang Xie[1*]

[1]Department of Neurology, Affiliated Lianyungang Hospital of Xuzhou Medical University, Lianyungang, China, [2]Department of Neurology, Jinzhou Medical University, Jinzhou, China, [3]Department of Clinical Laboratory, Lianyungang Oriental Hospital, Lianyungang, Jiangsu, China, [4]Department of Neurology, Affiliated Hospital of Kangda College of Nanjing Medical University, Lianyungang, China

Background: Nitrous oxide (N_2O) is an increasingly popular recreational drug. N_2O irreversibly disturbs the metabolism of vitamin B_{12}, resulting in a functional deficiency. Vitamin B_{12} is vital for myelin synthesis and its deficiency primarily produces neurological complications. Inhaling N_2O is more common and neurological complications are more evident than before.

Case presentation: We report a young man who developed progressive limb numbness and unsteady walking after N_2O abuse. The dominant diagnosis was subacute combined degeneration of the spinal cord (SCD). The patient was admitted to the hospital and given adenosylcobalamin treatment, but his symptoms progressed significantly from before and he developed acute cognitive impairment. After methylprednisolone combined with vitamin B_{12} treatment, symptoms significantly improved.

Conclusion: Clinicians need to understand the presentation and treatment of SCD caused by N_2O abuse. When symptoms progress despite conventional vitamin B_{12} therapy, the combination of methylprednisolone and vitamin B_{12} may be considered.

KEYWORDS

nitrous oxide, subacute combined degeneration of the spinal cord, cognitive decline, vitamin B_{12}, methylprednisolone

Introduction

Nitrous oxide (N_2O), also called "laughing gas," is a colorless gas with a sweet taste and good stability. Its role as an inhaled anesthetic is primarily in dental and labor analgesia. Because laughing gas inhalation can produce euphoria, it is widely prevalent among young people who are blindly seeking excitement. Long-term abuse can cause severe neurological complications. In recent years, Smoking laughing gas has become increasingly popular, and as a result, neurological complications will be more evident than before. This case reports an adolescent patient with central and peripheral nervous system involvement and acute cognitive decline caused by long-term inhalation of N_2O. The patient's condition changes and treatment options are described in detail to improve clinicians' awareness of recreational N_2O abuse.

Case report

An 18-year-old man was admitted to the emergency center with progressive numbness in the limbs for 10 days. The patient developed numbness in both feet, which gradually progressed proximal end, with numbness in both lower limbs and hands, a sense of girdle in the front chest and abdomen, and a feeling of soreness in the back. After 3 days of admission, the patient's

condition progressed significantly compared with the previous. He presented with acute cognitive impairment and weakness in both lower extremities. Without support, he could not walk or stand.

The patient had a history of inhaling N_2O for 6 months (N_2O canned, 2 L/can, 2–8 L can be used at a time), 3–4 times/week. The last time he consumed about 10 L was significantly increased compared to the previous time.

Neurological examination

Clear consciousness, slow language, decreased calculation and orientation, recent memory decline (cannot recall what you ate for breakfast), blunt response and no abnormality were found in the examination of twelve pairs of cranial nerves. The muscle strength of both upper limbs was grade 4, and the muscle strength of both lower limbs was grade 3, the muscle tension was slightly increased, bilateral superficial paresthesias, the sense of position and vibration of both feet were weakened, needle-punching in both feet, inaccurate finger-nose test, unstable heel and knee shin, positive Romberg's sign, weakened tendon reflexes on both sides, involuntary stretch-like movements of both upper extremities, skin scratch test positive, no elicitation of bilateral Barthel's sign and no abnormal meningeal irritation sign.

Laboratory examination

Homocysteine 58.9 μmol/L (normal value 5–15 μmol/L), vitamin B_{12} (>1,144.0 pg/ml; normal value 200–900 pg/ml considered to be related to taking drugs before admission), folic acid 17.39 nmol/L (normal value is 7–45.1 nmol/L), and no abnormality was found in the rest.

Magnetic resonance imaging (MRI)

MRI of the spinal cord showed the diffuse high signal of the T2W1 sequence (Figure 1A) and the posterior cord of the spinal cord was mainly involved in the axial image, showing an "inverted V sign" (Figure 1B). There were no apparent abnormalities in the thoracic and lumbar spine. There was no obvious abnormality in the head MRI.

Electroneuromyography (EMG)

Peripheral nerve injury, the lower extremities became more significantly involved than the upper extremities.

The Mini-Mental State Examination Scale (MMSE) scored 18 points (5 points for orientation, 1 point for calculation, 5 points for memory, and 7 points for language ability).

Treatment was given with intramuscular Adenosylcobalamin (1.5 mg/day), and symptoms were further aggravation. The patient was given intramuscular injections of Adenosylcobalamin combined with Methylprednisolone intravenous infusion (500 mg/day for a 5-day course). Adenosylcobalamin (1.5 mg/day) was administered intramuscularly for 10 days. After 7 days of treatment, the patient's chest discomfort in the front, back soreness and numbness in limbs improved, and the orientation, calculation, and mental were improved. The patient was hospitalized for a total of 10 days. At the time of discharge, the muscle strength of his extremities was better than before. The muscle strength of his lower extremities was Grade 4, and that of his upper extremities was Grade 5. Oral medication and rehabilitation after discharge. After 1 month, the patient could walk independently. The Mini-Mental State Examination (MMSE) scored 27 points (8 points for orientation, 4 points for calculation, 6 points for memory, and 9 points for language ability). After 3 months of follow-up, the patient's limb numbness was significantly improved, and his daily life was not affected.

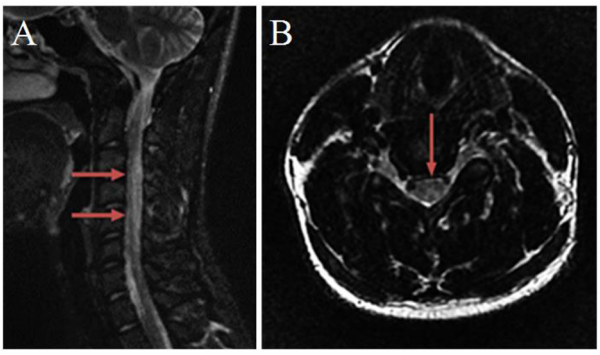

FIGURE 1
Magnetic resonance imaging of the cervical spinal cord. **(A)** T2-weighted sagittal image, from C2 to C7 spinal cord hyperintensity. **(B)** T2-weighted axial image, an "inverted V-sign" was shown.

Discussion

Neurological complications from N_2O inhalation have been rare before. In recent years, more N_2O abuse complications have been reported. Inhaling N_2O can create a relaxing feeling and is relatively easy to obtain. There are rich ways to buy it in the market and the price is low. More young people relax and indulge by inhaling large amounts of laughing gas. However, they are not aware of the possible side effects of inhaling. The extent of N_2O abuse is often difficult to quantify accurately, most people hide their history of N_2O use, so N_2O abuse is often severely underestimated.

To date, the poisoning mechanism of N_2O has not been fully elucidated. Methylcobalamin in vitamin B_{12} converts homocysteine to methionine, and S-adenosylmethionine, a metabolite of methionine, is irreplaceable for the formation and maintenance of myelin sheaths. Vitamin B_{12} deficiency leads to impaired myelin synthesis and methylation of myelin proteins (1), causing neural demyelination changes. N_2O interferes with the metabolic pathway of vitamin B_{12} by irreversibly oxidizing the cobalt element of vitamin B_{12}, leading to a decrease in vitamin B_{12} (2) and ultimately impaired myelin synthesis and neurological complications. N_2O interferes with the metabolism of intracellular vitamin B_{12}, while serology tests the level of extracellular vitamin B_{12}. In the early stages of the disease, in people with a normal diet or with self-supplementation of vitamin B_{12}, serum levels of Vit B12 may be normal, but the increase of homocysteine can indirectly reflect the lack of *in vivo* vitamin B_{12} functionality (3).

The patient has been inhaling laughing gas for 6 months, and the body does not have enough stored vitamin B_{12}. The patient once took vitamin B_{12} drugs orally, which increased the level of vitamin B_{12} in the blood. Therefore, the serum vitamin B_{12} test was beyond the normal range. And the last time, he inhaled a huge amount of N_2O, which caused N_2O toxicity.

The patient had decreased sense of position and vibration of the feet, involving the lamella and wedge tracts, and developed sensory ataxia. The patient's walking instability, inaccurate finger-nose test, and positive Romberg's sign suggest that the lesion involves the spinocerebellar tract. The diffusivity of N_2O is good, after inhalation, the partial pressure of oxygen in the alveoli can be reduced quickly, resulting in the reduction of oxygen delivered to the brain, resulting in brain hypoxia (4). The patient's muscle tone was slightly increased on admission, accompanied by involuntary stretch-like movements of both upper limbs, which may be related to the extrapyramidal symptoms of basal ganglia hypoxia after a large amount of N_2O inhalation. The previous literature reported generalized dystonia and involuntary movements for patients with N_2O abuse, which disappeared after vitamin B_{12} supplementation, suggesting that dyskinesia may be related to neurotoxicity (5).

The patient, in this case, has decreased calculation, spatial and temporal orientation and decreased memory, which is considered to be related to the cognitive dysfunction caused by N_2O inhalation. Dreyfus et al. (6) reported 2 cases of anesthesiologists with prolonged exposure to N_2O who experienced cognitive declines such as unresponsiveness, memory loss, and distraction. After stopping work and receiving professional treatment, the appeal symptoms were relieved. Shen et al. (7) described a patient with acute cognitive decline due to long-term inhalation of N_2O who recovered well after adequate vitamin B_{12} supplementation.

According to the patient's N_2O abuse history, clinical manifestations and signs, elevated homocysteine, MRI showed an inverted "V" sign, EMG showed limb nerve damage, N_2O abuse-induced SCD and acute cognitive impairment were diagnosed.

There is no specific treatment protocol for neurotoxicity due to N_2O abuse and it is mainly based on previous reports in the literature. In our case, the patient's clinical symptoms significantly progressed despite vitamin B_{12} supplementation. Hormones can alleviate spinal cord edema and also have neuroprotective effects, so we used hormones in combination with vitamin B_{12} to rapidly reverse the neurological damage caused by N_2O abuse. Previous studies have proposed that methylprednisolone decreases desynovial myelination and axonal damage (8). It also promotes the survival of neurons and supports myelin regeneration (9). Early rehabilitation is also essential for the recovery of nerve function and can vastly reduce the extent of nerve damage (10). When there is abnormal mental behavior, we should also pay attention to effective psychological counseling, give patients active psychological support treatment, encourage patients to stay away from N_2O, and develop healthy work and living habits.

Conclusion

In short, the clinical manifestations caused by long-term inhalation of N_2O are different. Clinicians should have sufficient knowledge of the clinical manifestations and treatment of N_2O toxicity. Clinically, when patients complain of neurological complications such as numbness of limbs, unstable walking, and weakness of limbs, especially in adolescents, clinicians should inquire whether they have a history of inhaling N_2O. The young patient with acute cognitive impairment should be associated with the possibility of N_2O poisoning. When symptoms progress despite treatment with vitamin B_{12} supplementation, a combination of methylprednisolone and vitamin B_{12} may be considered.

Data availability statement

The original contributions presented in the study are included in the article/supplementary material, further inquiries can be directed to the corresponding authors.

Author contributions

HW: data analysis, interpretation, and drafting of the manuscript. HH, LX, and NJ: critical revision of the manuscript. XZ: study concept and design and critical revision of the manuscript. KX: study concept and design and study supervision. All authors read and approved the final manuscript.

Acknowledgments

We thank the participant of the study.

Conflict of interest

The authors declare that the research was conducted in the absence of any commercial or financial relationships that could be construed as a potential conflict of interest.

Publisher's note

References

1. Zheng D, Ba F, Bi G, Guo Y, Gao Y, Li W. The sharp rise of neurological disorders associated with recreational nitrous oxide use in China: a single-center experience and a brief review of Chinese literature. *J Neurol.* (2020) 267:422–9. doi: 10.1007/s00415-019-09600-w

2. van Amsterdam J, Nabben T, van den Brink W. Recreational nitrous oxide use: Prevalence and risks. *Regul Toxicol Pharmacol.* (2015) 73:790–6. doi: 10.1016/j.yrtph.2015.10.017

3. Hathout L, El-Saden S. Nitrous oxide-induced $B1_2$ deficiency myelopathy: Perspectives on the clinical biochemistry of vitamin $B1_2$. *J Neurol Sci*. (2011) 301:1–8. doi: 10.1016/j.jns.2010.10.033

4. Brodsky JB, Cohen EN. Adverse effects of nitrous oxide. *Med Toxicol*. (1986) 1:362–74. doi: 10.1007/BF03259849

5. Chen HJ, Huang CS. Nitrous oxide-induced subacute combined degeneration presenting with dystonia and pseudoathetosis: a case report. *Acta Neurol Taiwan*. (2016) 25:50–5.

6. Dreyfus E, Tramoni E, Lehucher-Michel MP. Persistent cognitive functioning deficits in operating rooms: two cases. *Int Arch Occup Environ Health*. (2008) 82:125–30. doi: 10.1007/s00420-008-0302-8

7. Shen Q, Lu H, Wang H, Xu Y. Acute cognitive disorder as the initial manifestation of nitrous oxide abusing: a case report. *Neurol Sci*. (2021) 42:755–6. doi: 10.1007/s10072-019-04183-w

8. Yilmaz C, Karali K, Fodelianaki G, Gravanis A, Chavakis T, Charalampopoulos I, et al. Neurosteroids as regulators of neuroinflammation. *Front Neuroendocrinol*. (2019) 55:100788. doi: 10.1016/j.yfrne.2019.100788

9. Guennoun R. Progesterone in the brain: hormone, neurosteroid and neuroprotectant. *Int J Mol Sci*. (2020) 21:15. doi: 10.3390/ijms21155271

10. Chin J, Forzani B, Chowdhury N, Lombardo S, Rizzo JR, Ragucci M. Rehabilitation essential in the recovery of multifactorial subacute combined degeneration. *Ann Phys Rehabil Med*. (2015) 58:190–2. doi: 10.1016/j.rehab.2014.12.005

frontiers | Frontiers in Neurology

TYPE Case Report
PUBLISHED 10 February 2023
DOI 10.3389/fneur.2023.1117243

OPEN ACCESS

EDITED BY
Bruce Miller,
University of California, San Francisco,
United States

REVIEWED BY
Shunsuke Koga,
Mayo Clinic Florida, United States
Bo Cui,
Capital Medical University, China

*CORRESPONDENCE
Dongsheng Fan
✉ dsfan2010@aliyun.com

†These authors have contributed equally to this work

SPECIALTY SECTION
This article was submitted to Dementia and Neurodegenerative Diseases, a section of the journal Frontiers in Neurology

RECEIVED 06 December 2022
ACCEPTED 24 January 2023
PUBLISHED 10 February 2023

CITATION
Fu J, Zhao C, Hou G, Liu X, Zheng M, Zhang Y, Zhang S, Zheng D, Zhang Y, Huang X, Ye S and Fan D (2023) A case report of neuronal intranuclear inclusion disease with paroxysmal peripheral neuropathy-like onset lacking typical signs on diffusion-weighted imaging. *Front. Neurol.* 14:1117243. doi: 10.3389/fneur.2023.1117243

A case report of neuronal intranuclear inclusion disease with paroxysmal peripheral neuropathy-like onset lacking typical signs on diffusion-weighted imaging

Jiayu Fu[1,2†], Chen Zhao[1,2†], Guanghao Hou[1,2], Xiaoxuan Liu[1,2], Mei Zheng[1,2], Yingshuang Zhang[1,2], Shuo Zhang[1,2], Danfeng Zheng[3], Yixuan Zhang[1,2], Xiao Huang[1,2], Shan Ye[1,2] and Dongsheng Fan[1,2*]

[1]Department of Neurology, Peking University Third Hospital, Beijing, China, [2]Beijing Municipal Key Laboratory of Biomarker and Translational Research in Neurodegenerative Diseases, Beijing, China, [3]Department of Pathology, Peking University Third Hospital, Beijing, China

Background: Neuronal intranuclear inclusion disease (NIID) is a slowly progressive neurodegenerative disease characterized by eosinophilic hyaline intranuclear inclusions and the GGC repeats in the 5′-untranslated region of *NOTCH2NLC*. The prevalent presence of high-intensity signal along the corticomedullary junction on diffusion-weighted imaging (DWI) helps to recognize this heterogeneous disease despite of highly variable clinical manifestations. However, patients without the typical sign on DWI are often misdiagnosed. Besides, there are no reports of NIID patients presenting with paroxysmal peripheral neuropathy-like onset to date.

Case presentation: We present a patient with NIID who suffered recurrent transient numbness in arms for 17 months. Magnetic resonance imaging (MRI) showed diffuse, bilateral white matter lesions without typical subcortical DWI signals. Electrophysiological studies revealed mixed demyelinating and axonal sensorimotor polyneuropathies involving four extremities. After excluding differential diagnosis of peripheral neuropathy through body fluid tests and a sural nerve biopsy, NIID was confirmed by a skin biopsy and the genetic analysis of *NOTCH2NLC*.

Conclusion: This case innovatively demonstrates that NIID could manifest as paroxysmal peripheral neuropathy-like onset, and addresses the electrophysiological characteristics of NIID in depth. We broaden the clinical spectrum of NIID and provide new insights into its differential diagnosis from the perspective of peripheral neuropathy.

KEYWORDS

neuronal intranuclear inclusion disease, peripheral neuropathy, NOTCH2NLC gene, skin biopsy, neurodegenerative disease

Introduction

Neuronal intranuclear inclusion disease (NIID) is a rare neurodegenerative disease with a wide range of clinical manifestations, including dementia, movement disorder, muscle weakness, and autonomic dysfunction (1). Multiple organs are injured in NIID with the pathological presence of eosinophilic hyaline intranuclear inclusion bodies in cells of nervous system, visceral organs, and skin (2). Characteristic hyperintense areas in the corticomedullary junction on diffusion-weighted imaging (DWI) in brain magnetic resonance imaging (MRI) facilitates its

recognition (3). In recent years, diagnosis of NIID is confirmed by an abnormal GGC repeat expansion of the *NOTCH2NCL* gene or a positive skin biopsy with characteristic pathology (4). Whereas paroxysmal symptoms were reported in NIID, the episodes were restricted to encephalopathy with characteristic brain imaging findings (5). In this report, we present a case of NIID exhibiting paroxysmal peripheral neuropathy-like onset before the emergence of typical subcortical DWI signals. The patient's clinical manifestations are unique for NIID and the subclinical electrophysiological changes could be prevalent in the disease. His diagnosis was confirmed by a skin biopsy and genomic analysis.

Case presentation

A 60-year-old retired driver was admitted to our hospital because of recurrent transient numbness in his arms for 17 months in July 2022. The attacks, which lasted 10–30 min, initially occurred once or twice a month and involved the distal upper extremities from fingers to elbows. A year later the involved site spread to his face with similar numbness around the lips. However, the frequency and duration of the disturbance remained. During these attacks, the patient denied limb weakness, awareness impairment, epilepsy, headache, or other neurological defects. His daughter noticed a progressive cognitive decline manifested as recent amnesia and apathy which mildly limited activities of daily living. The insidious onset of his cognitive dysfunction was around a year ago when he began to forget the issues mentioned through phone calls. However, the patient could complete housework independently and had never lost his way so far. The patient had a history of macular degeneration for 30 years and was diagnosed with ischemic colitis when he was 59. His family had a hereditary history of essential tremor including the patient, his sister, father, and grandmother. His father was diagnosed with dementia of unknown etiology at the age of 60 and died of lung cancer in his eighties. No family history displayed neurodegenerative diseases or peripheral neuropathies. Neurologic examination demonstrated comprehensive cognitive decline including memory impairment, disorientation and attention disturbances, visuospatial dysfunction, language problem, and execution dysfunction. Miosis, static and postural tremors of hands, ataxia, reduced tendon reflexes, and bilateral hypoesthesia were noted without obvious muscle weakness or autonomic dysfunction. Mini-Mental State Examination and Frontal Assessment Battery were 19 and 8, respectively. The results of routine laboratory tests involving autoantibodies, biochemistry, and metabolism were within normal limits. The serum IgM level was elevated to 325 mg/dl with IgM-kappa–type M-protein identified by serum immune electrophoresis. However, no hematological cancer was identified through the biopsy of bone marrow. An increase of CYFRA21-1 (8.67 ng/ml) was noted and the patient was subsequently diagnosed with early-stage lung cancer through the related biopsy in the operation. Analysis of cerebrospinal fluid revealed increases in protein (126.5 mg/dl) and glucose (4 mmol/l) levels with a normal cell count. No abnormalities were found in either blood or cerebrospinal fluid autoantibody tests of peripheral neuropathy, including anti-ganglioside antibodies (GM1, GD1b, GQ1b), para-nodal antibodies (CNTN1, NF155, NF186, CASPR1), and paraneoplastic antibodies (Hu, Yo, Ri, CV2, Ma2, amphiphysin, GAD65). Brain MRI showed diffuse, bilateral white matter lesions without hyperintensity in the white matter adjacent to the cortex on DWI (Figures 1A, B). However, strokes or mitochondrial diseases were unsupported by negative findings in the magnetic resonance angiography and the magnetic resonance spectroscopy (Figures 1C, D). Brachial and lumbosacral plexus MRI showed extensive thickening in the nerve roots (Figures 1E, F). Electrophysiological studies revealed mixed demyelinating and axonal sensorimotor polyneuropathies, and the severity of those objective impairments in nerves were far beyond the clinical symptoms (Table 1). Motor and sensory nerve conduction velocity extensively decreased in the four extremities of the patient with relatively normal compound muscle action potentials (CMAP), while sensory nerve action potentials (SNAP) were absent in bilateral sural nerves. Prolonged latency of ulnar F-waves and tibial H-reflexes were noted. Neither pathological findings of a right sural nerve nor whole-exome sequencing suggested any hereditary peripheral neuropathies or inherited leukoencephalopathies. Therefore, we performed a skin biopsy and found eosinophilic inclusions positive for anti-p62 in the fibroblasts and sweat gland cells of the skin tissue (Figures 2A, B). Additionally, an expansion of 151 GGC repeated in the 5′-untranslated region of the *NOTCH2NLC* gene was detected by repeat-primed polymerase chain reaction (Figure 2C), further confirming the diagnosis of NIID.

Discussion

NIID is a heterogeneous disease entity with variable clinical manifestations involving cognitive, motor, sensory and autonomic systems (1). Similar to other neurodegenerative diseases, most symptoms of NIID progress chronically. Intriguingly, some patients have the paroxysmal phenotype of encephalitic episodes usually presented with disturbance of consciousness, stroke-like episodes, and generalized convulsions accompanied by autonomic dysfunction (5). However, no cases have yet been reported with paroxysmal sensory neuropathy-like onset symptoms to our knowledge. In this study, we reported such a NIID case with recurrent numbness attacks as the main complaint with extensively subclinical-impaired findings of electrophysiology and absent "cortical line sign" on DWI of MRI.

The sensory episodes in the present case were distinct from previously reported paroxysmal phenotype which usually involves diffused cortical lesions with unconsciousness, hemiplegia, aphasia, or epileptic seizures (6–9). Related hyperintensity, edematous areas, and perfusion alterations in the brain imaging have been reported to characterize those typical encephalitic attacks (3). Rather, our patient had very slight paresthesia in the upper extremities with atypical MRI findings of NIID which could not explain the symptom. Also, the distribution of the numbness is reminiscent of that in peripheral neuropathy and led us to decode the diagnosis from the electrophysiological studies.

This case provides a representative example of the mismatching feature between the subjective manifestation and objective examination in NIID, similar to other hereditary or neurodegenerative diseases (10, 11). Patients usually have very mild discomforts, which do not reconcile with the severity of their clinical examinations. Although electrophysiological tests revealed extensive lesions involving the lower extremities and the motor nerves, the patient has never complained of such discomfort throughout the course. Previous studies showed that 44.4–72.2% of NIID patients had clinically overt symptoms of peripheral neuropathy, while the overall reported incidence of NIID-related peripheral neuropathy

10.3389/fneur.2023.1117243

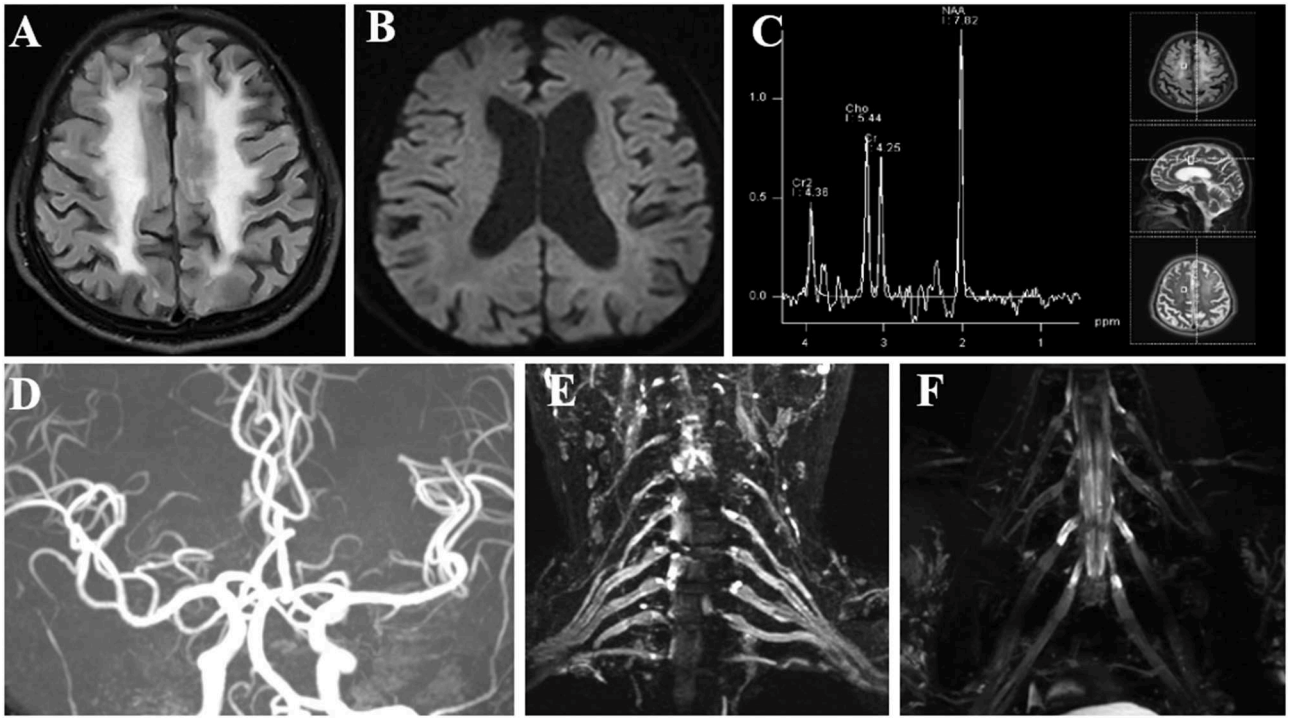

FIGURE 1
Imaging examinations of the patient. **(A)** FLAIR sequence shows diffuse, bilateral white matter lesions with hyperintensity. **(B)** DWI sequence shows no characteristic hyperintense areas in the corticomedullary junction. **(C)** MRS focused on the frontal lesion shows no lactate peak appearance. **(D)** MRA shows no significant intracranial aortic stenosis or occlusion changes. **(E, F)** Brachial and lumbosacral plexus MRI showed extensive thickening in the nerve roots. FLAIR, fluid-attenuated inversion recovery; DWI, diffusion-weighted image; MRS, magnetic resonance spectroscopy; MRA, magnetic resonance angiography; MRI, magnetic resonance imaging.

TABLE 1 Summary of electrophysiological data.

	Left			Right		
Motor	DML, ms	CMAP, mv	CV, m/s	DML, ms	CMAP, mv	CV, m/s
Median nerve	4.71 (<4.1)	6.5 (>4.0)	29.9 (>40)	5.02 (<4.1)	7.5 (>4.0)	35.4 (>40)
Ulnar nerve	8.54 (<3.2)	5.8 (>4.0)	35.9 (>40)	9.14 (<3.2)	7.2 (>4.0)	35.1 (>40)
Peroneal nerve	13.8 (<5.3)	3.7 (>2.0)	41.1 (>40)	14.7 (<5.3)	4.2 (>2.0)	3.67 (>40)
Tibial nerve	15.8 (<5.0)	7.1 (>4.0)	35.7 (>40)	17.9 (<5.0)	7.5 (>4.0)	31.2 (>40)
Sensory	DML, ms	SNAP, μv	CV, m/s	DML, ms	SNAP, μv	CV, m/s
Median nerve	2.71	9.8 (>5.0)	33.2 (>40)	2.95	10.3 (>5.0)	30.5 (>40)
Ulnar nerve	3.06	6.1 (>5.0)	32.7 (>40)	2.69	6.0 (>5.0)	35.3 (>40)
Sup peron. nerve	2.43	3.4 (>1.0)	45.3 (>40)	2.62	2.4 (>1.0)	47.4 (>40)
Sural nerve	/	/ (>1.0)	/ (>40)	/	/ (>1.0)	/ (>40)
Others	F-wave Lat, ms	F-wave Fre, %	H-reflex Lat, ms	F-wave Lat, ms	F-wave Fre, %	H-reflex Lat, ms
	38.4 (<33)	100 (>50)	40.9	37.8 (<33)	100 (>50)	40.8

DML, distal motor latency; CMAP, compound motor action potential; CV, conduction velocity; SNAP, sensory nerve action potential; Lat, latency; Fre, frequency. Reference values at relevant age in our laboratory were shown in brackets.

could be as high as 91.8% (1, 5, 12). This indicated the prevalent involvement of sub-clinical peripheral neuropathy in NIID, which is consistent with our patient. Overall, predominate demyelinating with mild axonal impairments are the primary electrophysiological pattern of NIID. The demyelinating impairments are homogeneous, extensive, and slight which presented with comprehensively decreased nerve conduction velocity and prolonged latency of F-waves and H-reflexes (13). This unique electrophysiological pattern provides subtle clues for differential diagnosis of NIID with other peripheral neuropathies from the functional perspective (14). The homogeneity of lesions with no conduction blocks or dispersions is distinguished from the immune-mediated neuropathy like chronic inflammatory demyelinating polyneuropathy (15). The relatively slight lesions are different from the ganglionopathy with

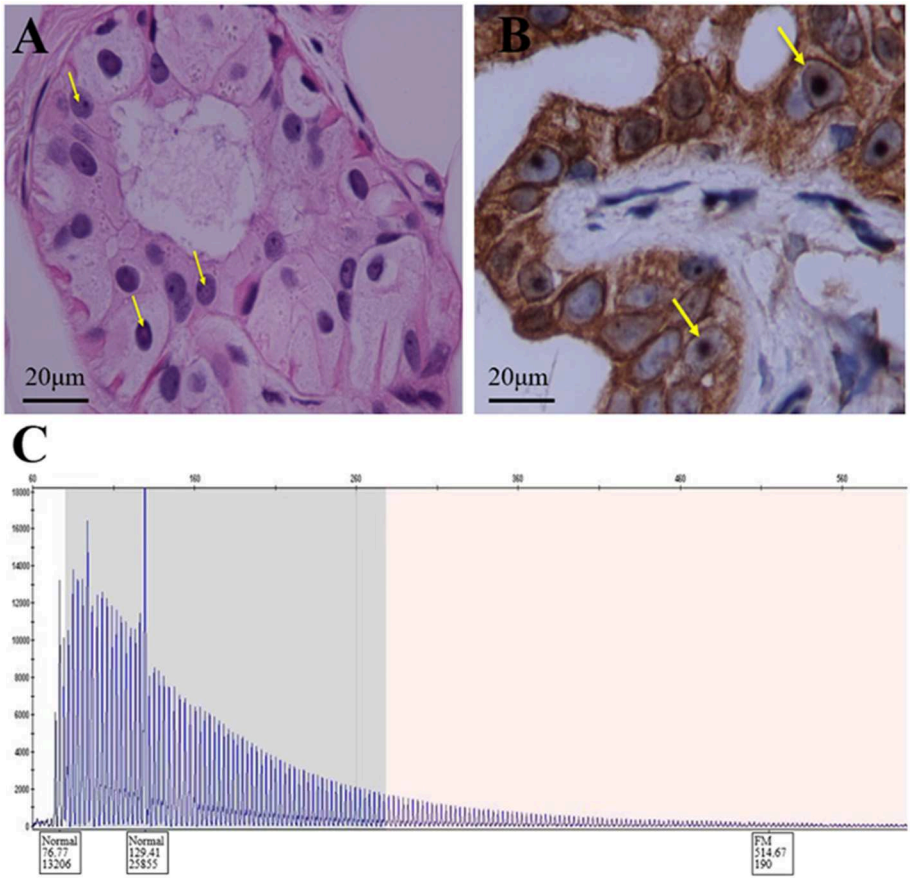

FIGURE 2
Histopathologic and genetic analyses of the patient. **(A)** Hematoxylin-eosin staining shows eosinophilic inclusion bodies in some sweat gland cells. Scale bars 20 μm. **(B)** Anti-P62 immunohistochemical staining. Visible inclusion bodies in the nucleus of some skin sweat gland cells. Scale bars 20 μm. **(C)** RP-PCR of the patient with a characteristic saw-tooth pattern for an expansion of 151 GGC repeated in the 5′-untranslated region of the NOTCH2NLC gene. RP-PCR, repeat-primed PCR.

paraneoplastic or other neurodegenerative etiologies (16). Although the extensive involvement of all extremities mimicking metabolic or toxic neuropathy, the minor lesions of axons are unsupported (17). Additionally, the plexus MRI and the sural nerve biopsy of our patient confirmed the representative lesions of NIID from the structural perspective. Further studies are needed to clarify the more susceptible role of the toxicity to Schwann cells than the neurons in the pathological mechanism of peripheral neuropathy in NIID (2).

The mechanisms of paroxysmal symptoms in NIID have not been fully understood yet. According to previous studies, we proposed three possible hypotheses for the recurrent sensory attacks in our patient. First, previous studies have identified the transient vasospasm and hypoperfusion in NIID leading to stroke-like episodes (7, 18). However, this was inconsistent with the negative MRI and MRA results of our patients. Further imaging of arterial spin labeling (ASL) and transcranial doppler (TCD) might help to identify the relevant impairments. Second, hypoxic encephalopathy with large areas of cytotoxic edema could cause epileptic seizures in NIID (19). However, absence of hyperintensity in DWI suggested no cytotoxic edema in our patient, and the clinical pattern of bilateral numbness with awareness remained and no auras was not common in the encephalitic attack. Indeed, electroencephalography (EEG) examinations are required to further confirm whether the patient has epilepsy or not, which we plan to conduct during the follow-up of our patient for more evidence. Third, as paroxysmal symptoms have been reported in patients with multiple sclerosis, the episodes could be mediated by ephaptic impulses and transmissions reflecting the impaired conductions of nerve fibers with partially demyelinated lesions (20–22). Although this seemed to be supported by the demyelination in both MRI and electrophysiological findings of our patient, further studies are needed to elucidate the pathophysiology of different paroxysmal symptoms in NIID.

Our patient showed a unique clinical symptom and uncommon MRI findings that made it difficult to diagnose him with NIID in the early stage. Initially, we focused on the diagnosis of peripheral neuropathy since the electrophysiological results were similar to those of Charcot–Marie–Tooth (CMT) disease (14). Besides, the positive serum immune electrophoresis indicated the diagnosis of neuropathy associated with IgM monoclonal gammopathy of undetermined significance (MGUS) (23). However, the pathological findings of the sural nerve were not supportive and the manifestation of tremors and cognitive impairment could not be explained. Thus, to further elucidate the case from the perspective of monism, we assume a likely diagnosis of NIID which was eventually confirmed by the skin biopsy and genetic analysis.

In summary, we should consider NIID as a differential diagnosis for the undetermined etiology of sensorimotor neuropathy even

lacking the characteristic brain MRI findings in the early stage. The present report demonstrates the electrophysiological characteristics of certain paroxysmal sensory deficits in NIID, which addresses the prevalence of sub-clinical peripheral nerve impairments and advances the clinical spectrum of NIID.

Data availability statement

The datasets presented in this article are not readily available because of ethical and privacy restrictions. Requests to access the datasets should be directed to the corresponding author.

Ethics statement

The studies involving human participants were reviewed and approved by the Institutional Ethics Committee of Peking University Third Hospital. The patients/participants provided their written informed consent to participate in this study. Written informed consent was obtained from the individual(s) for the publication of any potentially identifiable images or data included in this article.

Author contributions

JF and CZ: data collection and drafting the manuscript. GH, XL, and MZ: data evaluation and manuscript revision. YSZ and DZ: pathological test. SZ, YXZ, XH, and SY: data collection. DF: funding, data collection and evaluation, supervision, manuscript revision, and final approval. All authors contributed to the article and approved the submitted version.

Funding

This research was funded by the National Natural Science Foundation of China, grant numbers 81873784 and 82071426 and the Clinical Cohort Construction Program of Peking University Third Hospital, grant number BYSYDL2019002.

Conflict of interest

The authors declare that the research was conducted in the absence of any commercial or financial relationships that could be construed as a potential conflict of interest.

Publisher's note

All claims expressed in this article are solely those of the authors and do not necessarily represent those of their affiliated organizations, or those of the publisher, the editors and the reviewers. Any product that may be evaluated in this article, or claim that may be made by its manufacturer, is not guaranteed or endorsed by the publisher.

References

1. Sone J, Mori K, Inagaki T, Katsumata R, Takagi S, Yokoi S, et al. Clinicopathological features of adult-onset neuronal intranuclear inclusion disease. *Brain.* (2016) 139:3170–86. doi: 10.1093/brain/aww249

2. Park H, Yamanaka T, Toyama Y, Fujita A, Doi H, Nirasawa T, et al. Hornerin deposits in neuronal intranuclear inclusion disease: direct identification of proteins with compositionally biased regions in inclusions. *Acta Neuropathol Commun.* (2022) 10:28. doi: 10.1186/s40478-022-01333-8

3. Liang H, Wang B, Li Q, Deng J, Wang L, Wang H, et al. Clinical and pathological features in adult-onset NIID patients with cortical enhancement. *J Neurol.* (2020) 267:3187–98. doi: 10.1007/s00415-020-09945-7

4. Sone J, Mitsuhashi S, Fujita A, Mizuguchi T, Hamanaka K, Mori K, et al. Long-read sequencing identifies GGC repeat expansions in NOTCH2NLC associated with neuronal intranuclear inclusion disease. *Nat Genet.* (2019) 51:1215–21. doi: 10.1038/s41588-019-0459-y

5. Tian Y, Zhou L, Gao J, Jiao B, Zhang S, Xiao Q, et al. Clinical features of NOTCH2NLC-related neuronal intranuclear inclusion disease. *J Neurol Neurosurg Psychiatry.* (2022). doi: 10.1136/jnnp-2022-329772

6. Ishihara T, Okamoto T, Saida K, Saitoh Y, Oda S, Sano T, et al. Neuronal intranuclear inclusion disease presenting with an MELAS-like episode in chronic polyneuropathy. *Neurol Genet.* (2020) 6:e531. doi: 10.1212/NXG.0000000000000531

7. Fujita K, Osaki Y, Miyamoto R, Shimatani Y, Abe T, Sumikura H, et al. Neurologic attack and dynamic perfusion abnormality in neuronal intranuclear inclusion disease. *Neurol Clin Pract.* (2017) 7:e39–42. doi: 10.1212/CPJ.0000000000000389

8. Huang Y, Jin G, Zhan QL, Tian Y, Shen L. Adult-onset neuronal intranuclear inclusion disease, with both stroke-like onset and encephalitic attacks: a case report. *BMC Neurol.* (2021) 21:142. doi: 10.1186/s12883-021-02164-1

9. Xie F, Hu X, Liu P, Zhang D. A case report of neuronal intranuclear inclusion disease presenting with recurrent migraine-like attacks and cerebral edema: a mimicker of MELAS. *Front Neurol.* (2022) 13:837844. doi: 10.3389/fneur.2022.837844

10. Berciano J, García A, Gallardo E, Peeters K, Pelayo-Negro AL, Álvarez-Paradelo S, et al. Intermediate Charcot-Marie-Tooth disease: an electrophysiological reappraisal and systematic review. *J Neurol.* (2017) 264:1655–77. doi: 10.1007/s00415-017-8474-3

11. Szmulewicz DJ, Seiderer L, Halmagyi GM, Storey E, Roberts L. Neurophysiological evidence for generalized sensory neuronopathy in cerebellar ataxia with neuropathy and bilateral vestibular areflexia syndrome. *Muscle Nerve.* (2015) 51:600–3. doi: 10.1002/mus.24422

12. Wang Y, Wang B, Wang L, Yao S, Zhao J, Zhong S, et al. Diagnostic indicators for adult-onset neuronal intranuclear inclusion disease. *Clin Neuropathol.* (2020) 39:7–18. doi: 10.5414/NP301203

13. Hong D, Wang H, Zhu M, Peng Y, Huang P, Zheng Y, et al. Subclinical peripheral neuropathy is common in neuronal intranuclear inclusion disease with dominant encephalopathy. *Eur J Neurol.* (2022). doi: 10.1111/ene.15606

14. Vazquez Do Campo R. Electrodiagnostic Assessment of Polyneuropathy. *Neurol Clin.* (2021) 39:1015–34. doi: 10.1016/j.ncl.2021.06.012

15. Dyck PJB, Tracy JA. History, Diagnosis, and Management of Chronic Inflammatory Demyelinating Polyradiculoneuropathy. *Mayo Clin Proc.* (2018) 93:777–93. doi: 10.1016/j.mayocp.2018.03.026

16. Fargeot G, Echaniz-Laguna A. Sensory neuronopathies: new genes, new antibodies and new concepts. *J Neurol Neurosurg Psychiatry.* (2021). doi: 10.1136/jnnp-2020-325536

17. Gwathmey KG, Pearson KT. Diagnosis and management of sensory polyneuropathy. *BMJ.* (2019) 365:l1108. doi: 10.1136/bmj.l1108

18. Kikumoto M, Nezu T, Shiga Y, Motoda A, Toko M, Kurashige T, et al. Case of neuronal intranuclear inclusion disease with dynamic perfusion changes lacking typical signs on diffusion-weighted imaging. *Neurol Genet.* (2021) 7:e601. doi: 10.1212/NXG.0000000000000601

19. Shindo K, Tsuchiya M, Hata T, Ichinose Y, Koh K, Sone J, et al. Non-convulsive status epilepticus associated with neuronal intranuclear inclusion disease: A case report and literature review. *Epilepsy Behav Case Rep.* (2019) 11:103–6. doi: 10.1016/j.ebcr.2019.01.007

20. Zhang Y, Fan S, Han F, Xu Y. Paroxysmal symptoms as the first manifestation of multiple sclerosis mimicking a transient ischemic attack: a report of two cases. *Front Neurol.* (2017) 8:585. doi: 10.3389/fneur.2017.00585

21. Tüzün E, Akman-Demir G, Eraksoy M. Paroxysmal attacks in multiple sclerosis. *Mult Scler.* (2001) 7:402–4. doi: 10.1177/135245850100700609

22. Toru S, Yokota T, Tomimitsu H, Kanouchi T, Yamada M, Mizusawa H. Somatosensory-evoked cortical potential during attacks of paroxysmal dysesthesia in multiple sclerosis. *Eur J Neurol.* (2005) 12:233–4. doi: 10.1111/j.1468-1331.2004.00831.x

23. Leavell Y, Shin SC. Paraproteinemias and peripheral nerve disease. *Clin Geriatr Med.* (2021) 37:301–12. doi: 10.1016/j.cger.2021.01.004

frontiers | Frontiers in Neurology

TYPE Case Report
PUBLISHED 07 March 2023
DOI 10.3389/fneur.2023.1131888

OPEN ACCESS

EDITED BY
Bruce Miller,
University of California, San Francisco,
United States

REVIEWED BY
Luke William Bonham,
University of California, San Francisco,
United States
Chiara Reale,
IRCCS Carlo Besta Neurological Institute
Foundation, Italy
Sheng-Chiang Wang,
National Defense Medical Center, Taiwan

*CORRESPONDENCE
Hee Jin Kim
✉ evekhj@gmail.com

SPECIALTY SECTION
This article was submitted to
Dementia and Neurodegenerative Diseases,
a section of the journal
Frontiers in Neurology

RECEIVED 26 December 2022
ACCEPTED 14 February 2023
PUBLISHED 07 March 2023

CITATION
Chun MY, Heo NJ, Seo SW, Jang H, Suh Y-L, Jang J-H, Kim Y-E, Kim E-J, Moon SY, Jung N-Y, Lee SM and Kim HJ (2023) Case report: Cerebrotendinous xanthomatosis with a novel mutation in the *CYP27A1* gene mimicking behavioral variant frontotemporal dementia. *Front. Neurol.* 14:1131888. doi: 10.3389/fneur.2023.1131888

Case report: Cerebrotendinous xanthomatosis with a novel mutation in the *CYP27A1* gene mimicking behavioral variant frontotemporal dementia

Min Young Chun[1,2,3], Nam Jin Heo[1], Sang Won Seo[1,4,5,6], Hyemin Jang[1,5,6], Yeon-Lim Suh[7], Ja-Hyun Jang[8], Young-Eun Kim[9], Eun-Joo Kim[10], So Young Moon[11], Na-Yeon Jung[12], Sun Min Lee[11] and Hee Jin Kim[1,4,5,6]*

[1]Department of Neurology, Samsung Medical Center, Sungkyunkwan University School of Medicine, Seoul, Republic of Korea, [2]Department of Neurology, Yonsei University College of Medicine, Seoul, Republic of Korea, [3]Department of Neurology, Yongin Severance Hospital, Yonsei University Health System, Yongin, Republic of Korea, [4]Department of Health Sciences and Technology, SAIHST, Sungkyunkwan University, Seoul, Republic of Korea, [5]Department of Digital Health, SAIHST, Sungkyunkwan University, Seoul, Republic of Korea, [6]Alzheimer's Disease Convergence Research Center, Samsung Medical Center, Seoul, Republic of Korea, [7]Department of Pathology, Samsung Medical Center, Sungkyunkwan University School of Medicine, Seoul, Republic of Korea, [8]Department of Laboratory Medicine and Genetics, Samsung Medical Center, Sungkyunkwan University School of Medicine, Seoul, Republic of Korea, [9]Departments of Laboratory Medicine, Hanyang University College of Medicine, Seoul, Republic of Korea, [10]Department of Neurology, Pusan National University Hospital, Pusan National University School of Medicine and Medical Research Institute, Busan, Republic of Korea, [11]Department of Neurology, Ajou University School of Medicine, Suwon, Republic of Korea, [12]Department of Neurology, Pusan National University Yangsan Hospital, Research Institute for Convergence of Biomedical Science and Technology, Yangsan, Republic of Korea

Background: Cerebrotendinous xanthomatosis (CTX) is a rare autosomal recessive lipid storage disease caused by a mutation in the *CYP27A1* gene. Due to the disruption of bile acid synthesis leading to cholesterol and cholestanol accumulation, CTX manifests as premature cataracts, chronic diarrhea, and intellectual disability in childhood and adolescence. This report presents a case of CTX with an unusual phenotype of behavioral variant frontotemporal dementia (bvFTD) in middle age.

Case presentation: A 60-year-old woman presented with behavioral and personality changes. She showed disinhibition, such as hoarding and becoming aggressive over trifles; compulsive behavior, such as closing doors; apathy; and dietary change. The patient showed a progressive cognitive decline and relatively sparing memory and visuospatial function. She had hyperlipidemia but no family history of neurodegenerative disorders. Initial fluid-attenuated inversion recovery (FLAIR) images showed a high signal in the periventricular area, and brain spectroscopy showed hypoperfusion in the frontal and temporal lobes, mimicking bvFTD. However, on physical examination, xanthomas were found on both the dorsum of the hands and the Achilles tendons. Hyperactive deep tendon reflexes in the bilateral biceps, brachioradialis, and knee and positive Chaddock signs on both sides were observed. Four years later, FLAIR images showed symmetrical high signals in the bilateral dentate nuclei of the cerebellum. Her serum cholestanol (12.4 mg/L; normal value ≤6.0) and 7α,12α-dihydroxycholest-4-en-3-one (0.485 nmol/mL; normal value ≤0.100) levels were elevated. A novel likely pathogenic variant (c.1001T>A, p.Met334Lys) and a known pathogenic variant (c.1420C>T, p.Arg474Trp) of the *CYP27A1* gene were found in trans-location. The patient was diagnosed with CTX and prescribed chenodeoxycholic acid (750 mg/day).

Conclusions: This report discusses the case of a middle-aged CTX patient with an unusual phenotype of bvFTD. A novel likely pathogenic variant (c.1001T>A, p.Met334Lys) was identified in the *CYP27A1* gene. Early diagnosis is important because supplying chenodeoxycholic acid can prevent CTX progression.

KEYWORDS

behavioral variant frontotemporal dementia, cerebrotendinous xanthomatosis, *CYP27A1* gene mutation, novel likely pathogenic variant, case report

Introduction

Cerebrotendinous xanthomatosis (CTX, OMIM: 213700) is an autosomal recessive lipid storage disease caused by a mutation in the *CYP27A1* gene (chromosome 2q33-qter) (1). Mutations in the gene encoding the mitochondrial enzyme sterol 27-hydroxylase (CYP27) can lead to decreased bile acid synthesis, increased cholestanol production, and sterol accumulation in multiple systems, including the nervous system, tendons, and eye lenses (2). It is a rare disease with an incidence of ∼5 per 100,000 people worldwide, and 10 cases have been reported in South Korea (3–10). This report discusses a case of CTX with an unusual phenotype of behavioral variant frontotemporal dementia (bvFTD).

Case description

A 60-year-old woman visited the Department of Neurology, Samsung Medical Center in South Korea because of progressive abnormal behavior, personality change, and cognitive decline over the past 4 years. At the age of 56, she showed disinhibition, such as hoarding plastic bottles or paper cups and becoming aggressive over trifles. She also showed compulsive behavior, such as closing doors; apathy; and dietary change. The patient showed a progressive cognitive decline and relatively sparing memory and visuospatial function. However, at the age of 58, she started to show memory impairment as she could not remember where she put her money. She also showed visuospatial dysfunction as she got lost in her neighborhood and could not find her car in a parking lot. At the age of 60, disinhibition and apathy worsened along with increased appetite. In addition, she complained of nonspecific dizziness and unstable gait. She had a history of hyperlipidemia and no family history of neurological diseases in her first- or second-degree relatives.

On neuropsychological tests, her Mini-Mental State Examination score was 22, her clinical dementia rating score was 1, and the detailed results revealed global cognitive impairment (Table 1). On neurological examination, she showed hyperactive deep tendon reflexes in the bilateral biceps, brachioradialis, and knee and positive Chaddock signs on both sides. Although no gross gait abnormalities or ataxia were observed, she showed bilateral sway on tandem gait. Upon physical examination, xanthomas were found in the bilateral dorsum of the hands and the Achilles tendons (Figures 1a, b). A skin biopsy revealed diffuse infiltration of foamy macrophages in the dermis, and a tendon biopsy revealed numerous lipid crystal clefts and a small number of foamy macrophages (Figures 1c, d).

Brain spectroscopy performed at 56 years of age showed hypoperfusion in the bilateral frontal and right temporal lobes (Figure 2a). A brain magnetic resonance imaging (MRI) performed during the same period showed slight periventricular white matter changes on T2 FLAIR images, but no other specific abnormalities were observed (Figure 2b). An ^{18}F-flutemetamol PET scan was interpreted as negative for amyloid. Her clinical phenotype and spectroscopy findings corresponded to probable bvFTD based on Rascovsky criteria for bvFTD (12).

However, follow-up T2 FLAIR images, performed at the age of 60 years, demonstrated progression of periventricular white matter changes and newly developed symmetrical hyperintense lesions in the dentate nucleus of the cerebellum (Figure 2c). Although no evidence of peripheral neuropathy was found in the nerve conduction study (NCS), her posterior tibial somatosensory evoked potential (SSEP) and visual evoked potential tests (VEP) were abnormal. Bone mineral osteodensitometry revealed the presence of osteoporosis. Ophthalmic examination revealed age-related macular degeneration with no cataracts or retinal invasion.

CTX was suspected based on xanthomas and follow-up brain MRI findings; thus, serum cholestanol and related gene tests were performed. Serum cholestanol (12.4 mg/L; normal value ≤6.0) and 7α,12α-dihydroxycholest-4-en-3-one (0.485 nmol/mL; normal value ≤0.100) levels were elevated. The serum levels of very-long-chain fatty acids for X-linked adrenoleukodystrophy and arylsulfatase A for metachromatic leukodystrophy were within the normal range. In genetic analysis with whole exome sequencing, a likely pathogenic variant (LPV) (NM_00784.4:c.1001T>A, p.Met334Lys) and a pathogenic variant (PV, NM_000784.4: c.1420C>T, p.Arg474Trp) were found in the *CYP27A1* gene, which was confirmed to be translocated via genetic testing of her daughter and son, who carried each variant as heterozygous. The c.1001T>A (p.Met334Lys) had not been reported previously and the c.1420C>T (p.Arg474Trp) has been observed in several CTX patients and classified as pathogenic in ClinVar. (ClinVar accession number as VCV000004259.12) (13–18). The patient was finally diagnosed with CTX and was prescribed with chenodeoxycholic acid (750 mg/day). Eight months after the treatment, her disinhibition symptoms decreased. In neuropsychological tests, she showed improvements in visuospatial function, memory, frontal/executive function, general cognition, and global severity scales (Table 1).

TABLE 1 The neuropsychological test results.

Age	60 years old (before treatment)		61 years old (after treatment)	
Domain (highest possible score)	Raw score	z-score	Raw score	z-score
Attention				
Digit span forward (9)	6	0.04	6	0.04
Digit span backward (8)	3	−0.93	3	−0.93
Language				
Korean version of the Boston naming Test (60)	37*	−2.05	35*	−2.39
Visuospatial function				
Rey-Osterrieth Complex Figure Test (36)	23.5*	−2.93	27*	−1.81
Memory				
Seoul verbal learning test				
Immediate recall (1st, 2nd, 3rd free recall trials: 12 + 12 + 12 = 36)	12*	−1.97	19	−0.39
Delayed recall (12)	1*	−2.52	3*	−1.65
Recognition score (24)	13*	−4.32	19*	−1.11
Rey-Osterrieth complex figure test				
Immediate recall (36)	0*	−2.43	5*	−1.65
Delayed recall (36)	4*	−1.89	3*	−2.05
Recognition score (24)	17*	−1.61	10	0.04
Frontal/executive function				
Controlled oral word association test				
Semantic, animal (20)	6*	−2.43	9*	−1.68
Semantic, supermarket (20)	5*	−2.33	11*	−1.23
Phonemic, sum of scores from 3 alphabets (45)	8*	−1.90	3*	−2.47
Stroop test				
Word reading (112)	111		17	
Color reading (112)	52*	−2.06	73	−0.82
General cognition				
Mini-mental state examination (30)	22*	−3.69	26*	−1.23
Global severity scales				
Clinical dementia rating (sum of boxes)	1 (6)		0.5 (4)	
Global deterioration scale	5		4	
Neuropsychiatric inventory	38/144		9/144	

*Below −1.0 standard deviation of age- and education-matched norms derived from the Seoul Neuropsychological Screening Battery (11). The source for all tests is the Seoul Neuropsychological Screening Battery (11).

Discussion

This report discusses the case of a middle-aged CTX patient with an unusual phenotype of bvFTD, confirmed by a novel likely pathogenic and a known pathogenic variant, as compound heterozygous variants, (c.[1001T>A];[1420C>T], p.[Met334Lys];[Arg474Trp]) in the *CYP27A1* gene with elevated serum cholestanol and 7α,12α-dihydroxycholest-4-en-3-one levels.

Our CTX case is unique in that disease onset occurred during middle age and that the patient showed an unusual bvFTD phenotype. CTX is usually found in adolescence or early adulthood and is characterized by premature bilateral cataracts, chronic diarrhea in childhood, premature atherosclerosis, tendon xanthoma, and progressive neurological dysfunction (cerebellar and pyramidal signs, intellectual disability, peripheral neuropathy, and seizures) (19). However, our patient had no such premature symptoms and showed slow progressive abnormal behavior during late middle age. Her slowly progressive symptoms of disinhibition, apathy, compulsive behavior, and dietary changes and her frontotemporal hypoperfusion met the clinical criteria for probable bvFTD (12). There have been two rare case reports of CTX presenting with frontal dysfunction in adults.

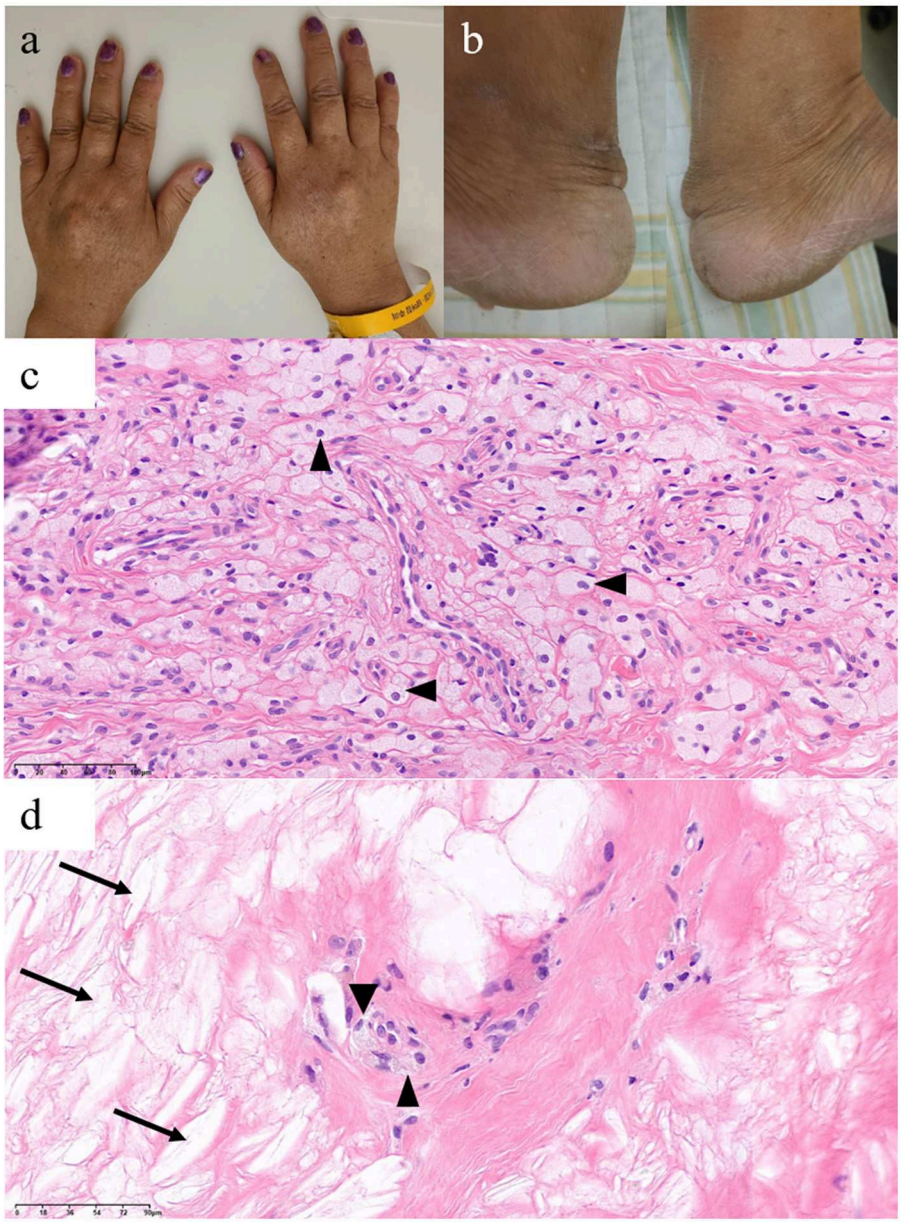

FIGURE 1
Xanthomas findings of this patient with cerebrotendinous xanthomatosis. Xanthomas on bilateral **(a)** dorsum of the hands and **(b)** Achilles tendons. Histological findings of the dorsum of the hand **(c)** and Achilles tendon **(d)** xanthomas show foamy macrophages (arrowheads) and lipid crystal clefts (arrows).

A 44-year-old woman with the FTD phenotype was reported in Japan (20). This patient had increased serum levels of cholestanol with a heterozygous mutation in the *CYP27A1* gene. Another 53-year-old man with the FTD phenotype of CTX was reported in the United States. This patient was compound heterozygous for two mutations in *CYP27A1* (NM_000784.3 (CYP27A1): a missense mutation of 1016C > T on one allele and a 1435C > G mutation on the other allele) (21). The two previously reported cases, along with our case, suggest that the middle-age-onset bvFTD phenotype might be a subtype of CTX.

The FTD phenotype of CTX can be explained by diffuse white matter pathology and neuronal loss, shown as symmetric high-intensity on brain MR T2-weighted images in the periventricular cerebral white matter as well as diffuse atrophy. White matter pathology may result from the disproportionate incorporation of cholesterol into the glial cell membrane and alterations in myelin lipid composition (22, 23). Also, intracerebral lipid deposition associated with xanthomas and local inflammatory responses can damage myelinated axons, gray matter formation, neuronal cell bodies, and neuronal integrity (19, 24), leading to neuronal loss and deterioration in behavior and cognition.

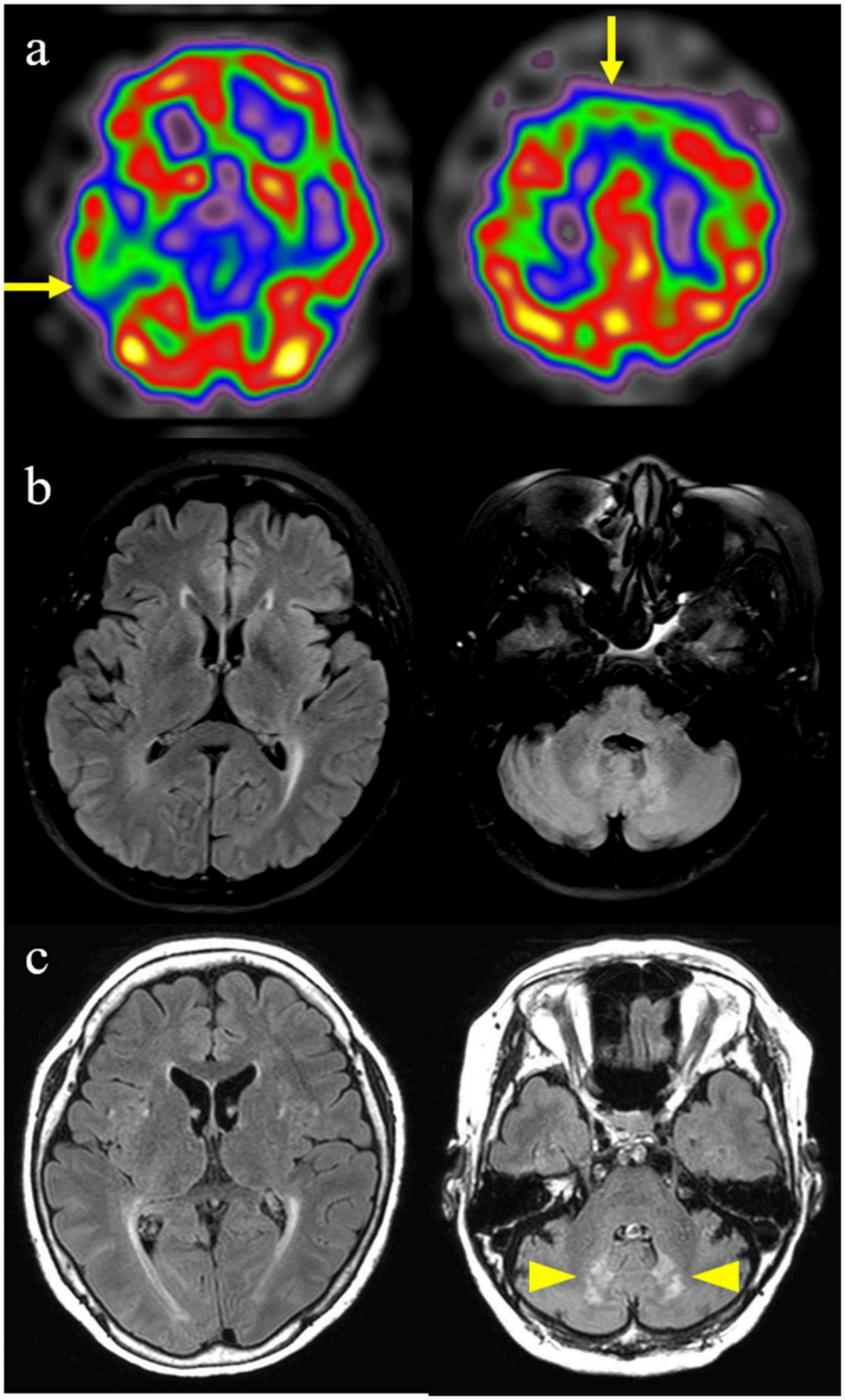

FIGURE 2
Brain imaging findings of this patient with cerebrotendinous xanthomatosis. **(a)** Brain spectroscopy shows hypoperfusion in bilateral frontal and right temporal lobes (arrows). **(b)** Initial fluid-attenuated inversion recovery image shows slight periventricular white matter changes. **(c)** Follow-up fluid-attenuated inversion recovery image performed 4 years later shows the progression of periventricular white matter changes and newly developed symmetrical hyperintense lesions in the dentate nucleus of the cerebellum (arrowheads).

Several differential diagnoses should be considered when assessing patients with xanthomas and symmetric lesions in the dentate nuclei of the cerebellum. Tendonous xanthomas need to be differentiated from other hereditary diseases, such as familial hypercholesterolemia and sitosterolemia (1). Familial hypercholesterolemia, the most common cause of tendon

xanthomas, is an autosomal dominant disorder that leads to increased low-density lipoprotein cholesterol levels, but with normal cholestanol levels (25). While familial hypercholesterolemia usually manifests as intertriginous xanthomas in children, sitosterolemia and CTX manifest as tendonous xanthomas in adults (1, 26). Sitosterolemia can be differentiated from CTX by the absence of neurological symptoms and premature cataracts (27). Furthermore, hyperintensities of dentate nuclei on MRI should be differentiated from other diseases, including metronidazole toxicity, lead poisoning, maple syrup urine disease, and progressive multifocal leukoencephalopathy caused by the JC virus (28). These disorders manifest as acute encephalopathy rather than the insidious onset seen in CTX. Thus, if progressive bvFTD symptoms appear in adults with xanthoma or a characteristic appearance of dentate in MRI, the possibility of CTX should be considered; the serum cholestanol and 7α,12α-dihydroxycholest-4-en-3-one levels should be further evaluated, and mutations in the *CYP27A1* gene (1) should be searched for.

In addition, the patient showed abnormalities in SSEP and VEP, which supports the diagnosis of CTX (1, 29–31). Our patient was also revealed to have osteoporosis and ocular abnormalities, which are widely described as common manifestations in CTX patients (1, 32, 33).

Our patient was confirmed to have CTX based on biochemical and genetic tests. Biochemical tests showed increased levels of cholestanol and 7α,12α-dihydroxycholest-4-en-3-one, which is a highly sensitive metabolic biomarker of CTX (34). Genetic tests identified an LPV (c.1001T>A, p.Met334Lys) and a PV (c.1420C>T, p.Arg474Trp) in the *CYP27A1* gene in trans. The variant c.1420C>T (p.Arg474Trp) has been found in several CTX patients as homozygous or compound heterozygous (13–18) and classified as pathogenic in ClinVar (accession number: VCV000004259.12). Although c.1001T>A (p.Met334Lys) has not been reported as a cause of CTX, we suggest the variant is likely pathogenic based on the following evidence: (i) The p.Met334Lys is located in a chemical substrate binding site in the P450 domain, which is a critical and well-established functional domain. In particular, the region from the 330th to the 345th amino acid is clustered by the binding site without any known benign variant (PM1). (ii) The p.Met334Lys is absent in the population database (gnomAD, https://gnomad.broadinstitute.org/, accessed on 27, Jan.2023) (PM2). (iii) The p.Met334Lys was located in *trans* with the PV, c.1420C>T (PM3), and the patient's phenotype and biochemical test results were highly specific for CTX (PP4). Therefore, we classified the variant as likely pathogenic with three moderate evidences of pathogenicity.

In conclusion, CTX is an underdiagnosed disease, and the phenotype is often incomplete. Progressive dementia can be the only neuropsychiatric sign associated with CTX (21). Early recognition and intervention of CTX are important because treatment with chenodeoxycholic acid reverses metabolic abnormalities and prevents or ameliorates nervous system dysfunction. Therefore, we suggest that the diagnosis of CTX should be considered in patients with progressive dementia and xanthoma, even in the absence of premature CTX symptoms.

Data availability statement

The datasets presented in this article are not readily available because of ethical and privacy restrictions. Requests to access the datasets should be directed to the corresponding author.

Ethics statement

The studies involving human participants were reviewed and approved by Institutional review board of Samsung Medical Center. The patients/participants provided their written informed consent to participate in this study. Written informed consent was obtained from the participant/patient(s) for the publication of this case report.

Author contributions

MC interpreted the patient data regarding cerebrotendinous xanthomatosis disease and was a major contributor to the writing of the manuscript. E-JK, SM, N-YJ, and SL collected data and helped to draft the manuscript. NH, SS, and HJ reviewed the patient data and manuscript. Y-LS performed a pathological examination of the skin. J-HJ and Y-EK performed the genetic analysis of the patient and the next of kin and interpreted the results. HK supervised and reviewed the manuscript. All authors contributed to the article and approved the submitted version.

Funding

This research was supported by the "National Institute of Health" research project (project No. 2021-ER1003-01 and 2021-ER1004-01); the National Research Foundation of Korea (NRF) grant funded by the Korea government (MSIT) (NRF-2022R1A2C2092346); and the MSIT (Ministry of Science and ICT), Korea, for the design of the study and interpretation of data and the ICT Creative Consilience program (IITP-2023-2020-0-01821) supervised by the IITP (Institute for Information & communications Technology Planning & Evaluation) for the collection and analysis of data.

Conflict of interest

The authors declare that the research was conducted in the absence of any commercial or financial relationships that could be construed as a potential conflict of interest.

Publisher's note

All claims expressed in this article are solely those of the authors and do not necessarily represent those of their affiliated organizations, or those of the publisher, the editors and the reviewers. Any product that may be evaluated in this article, or claim that may be made by its manufacturer, is not guaranteed or endorsed by the publisher.

References

1. Nie S, Chen G, Cao X, Zhang Y. Cerebrotendinous xanthomatosis: a comprehensive review of pathogenesis, clinical manifestations, diagnosis, and management. *Orphanet J Rare Dis.* (2014) 9:179. doi: 10.1186/s13023-014-0179-4

2. Bjorkhem I, Fausa O, Hopen G, Oftebro H, Pedersen JI, Skrede S, et al. Role of the 26-hydroxylase in the biosynthesis of bile acids in the normal state and in cerebrotendinous xanthomatosis. An *in vivo* study. *J Clin Invest.* (1983) 71:142–8. doi: 10.1172/JCI110742

3. Kim JS, Lee SS, Lee KW, Lee SB, Myung HJ, Chi JG, et al. Cerebrotendinous xanthomatosis–A case report of two siblings. *Seoul J Med.* (1988) 29:83–9.

4. Lee SJ, Lew M, Kim SJ. A Case of preeumect Cerebrotedinous Xanthomatosis. *J Korean Ophthalmol Soc.* (1988) 29:775–82.

5. Lee WK, Yoon BJ. A case of cerebrotendinous xanthomatosis. *J Korean Ophthalmol Soc.* (1988) 29:783–8.

6. Park CI, Kim YC, Shin JC, Kim YW, Lim KB. A case of cerebrotendinous xanthomatosis. *Ann Rehabil Med.* (1998) 22:460–4.

7. Jung SJ, Kim HT. A case of cerebrotendinous xanthomatosis. *J Korean Neurol Assoc.* (2000) 18:94–7.

8. Lee SW, Choi EH, Ahan SK. A case of cerebrotendinous xanthomatosis. *Korean J Dermatol.* (2002) 40:1261–3.

9. Suh S, Kim HK, Park HD, Ki CS, Kim MY, Jin SM, et al. Three siblings with cerebrotendinous xanthomatosis: a novel mutation in the CYP27A1 gene. *Eur J Med Genet.* (2012) 55:71–4. doi: 10.1016/j.ejmg.2011.08.003

10. Yoo S, Kim S, Bae DW, Park IS, Kim JS, Lee KS, et al. Cerebrotendinous xanthomatosis with spinal cord syndrome. *J Korean Neurol Assoc.* (2014) 32:215–7.

11. Kang Y, Na DL, Hahn SJIHBR. *Seoul Neuropsychological Screening Battery*. Incheon: Human Brain Research & Consulting Co.

12. Rascovsky, K., Hodges, J. R., Knopman, D., Mendez, M. F., Kramer, J. H., Neuhaus, J., et al.L. (2011). Sensitivity of revised diagnostic criteria for the behavioural variant of frontotemporal dementia. *Brain* 134, 2456–2477. doi: 10.1093/brain/awr179

13. Kim KS, Kubota S, Kuriyama M, Fujiyama J, Bjorkhem I, Eggertsen G, et al. Identification of new mutations in sterol 27-hydroxylase gene in Japanese patients with cerebrotendinous xanthomatosis (CTX). *J Lipid Res.* (1994) 35:1031–9. doi: 10.1016/S0022-2275(20)40096-3

14. Wakamatsu N, Hayashi M, Kawai H, Kondo H, Gotoda Y, Nishida Y, et al. Mutations producing premature termination of translation and an amino acid substitution in the sterol 27-hydroxylase gene cause cerebrotendinous xanthomatosis associated with parkinsonism. *J Neurol Neurosurg Psychiatry.* (1999) 67:195–8. doi: 10.1136/jnnp.67.2.195

15. Rystedt E, Olin M, Seyama Y, Buchmann M, Berstad A, Eggertsen G, et al. Cerebrotendinous xanthomatosis: molecular characterization of two Scandinavian sisters. *J Intern Med.* (2002) 252:259–64. doi: 10.1046/j.1365-2796.2002.01033.x

16. Wang Z, Yuan Y, Zhang W, Zhang Y, Feng L. Cerebrotendinous xanthomatosis with a compound heterozygote mutation and severe polyneuropathy. *Neuropathology.* (2007) 27:62–6. doi: 10.1111/j.1440-1789.2006.00739.x

17. Koyama S, Kawanami T, Tanji H, Arawaka S, Wada M, Saito N, et al. A case of cerebrotendinous xanthomatosis presenting with epilepsy as an initial symptom with a novel V413D mutation in the CYP27A1 gene. *Clin Neurol Neurosurg.* (2012) 114:1021–3. doi: 10.1016/j.clineuro.2012.01.032

18. Sekijima Y, Koyama S, Yoshinaga T, Koinuma M, Inaba Y. Nationwide survey on cerebrotendinous xanthomatosis in Japan. *J Hum Genet.* (2018) 63:271–80. doi: 10.1038/s10038-017-0389-4

19. Verrips A, Hoefsloot LH, Steenbergen GC, Theelen JP, Wevers RA, Gabreels FJ, et al. Clinical and molecular genetic characteristics of patients with cerebrotendinous xanthomatosis. *Brain 123 (Pt 5).* (2000) 908–19. doi: 10.1093/brain/123.5.908

20. Sugama S, Kimura A, Chen W, Kubota S, Seyama Y, Taira N, et al. Frontal lobe dementia with abnormal cholesterol metabolism and heterozygous mutation in sterol 27-hydroxylase gene (CYP27). *J Inherit Metab Dis.* (2001) 24:379–92. doi: 10.1023/A:1010564920930

21. Guyant-Marechal L, Verrips A, Girard C, Wevers RA, Zijlstra F, Sistermans E, et al. Unusual cerebrotendinous xanthomatosis with fronto-temporal dementia phenotype. *Am J Med Genet A 139A.* (2005) 114–7. doi: 10.1002/ajmg.a.30797

22. Vanrietvelde F, Lemmerling M, Mespreuve M, Crevits L, Reuck De, Kunnen J, et al. MRI of the brain in cerebrotendinous xanthomatosis (van Bogaert-Scherer-Epstein disease). *Eur Radiol.* (2000) 10:576–8. doi: 10.1007/s003300050964

23. Chang CC, Lui CC, Wang JJ, Huang SH, Lu CH, Chen C, et al. Multi-parametric neuroimaging evaluation of cerebrotendinous xanthomatosis and its correlation with neuropsychological presentations. *BMC Neurol.* (2010) 10:59. doi: 10.1186/1471-2377-10-59

24. Fraidakis MJ. Psychiatric manifestations in cerebrotendinous xanthomatosis. *Transl Psychiatry.* (2013) 3:e302. doi: 10.1038/tp.2013.76

25. Koopal C, Visseren FL, Marais AD, Westerink J, Spiering W. Tendon xanthomas: not always familial hypercholesterolemia. *J Clin Lipidol.* (2016) 10:1262–5. doi: 10.1016/j.jacl.2016.05.005

26. Cruz Jr PD, East C, Bergstresser PR. Dermal, subcutaneous, and tendon xanthomas: diagnostic markers for specific lipoprotein disorders. *J Am Acad Dermatol.* (1988) 19:95–111. doi: 10.1016/S0190-9622(88)70157-7

27. Kidambi S, Patel SB. Sitosterolaemia: pathophysiology, clinical presentation and laboratory diagnosis. *J Clin Pathol.* (2008) 61:588–94. doi: 10.1136/jcp.2007.049775

28. Bond KM, Brinjikji W, Eckel LJ, Kallmes DF, Mcdonald RJ, Carr CM, et al. Dentate update: imaging features of entities that affect the dentate nucleus. *AJNR Am J Neuroradiol.* (2017) 38:1467–74. doi: 10.3174/ajnr.A5138

29. Mondelli M, Rossi A, Scarpini C, Dotti MT, Federico A. Evoked potentials in cerebrotendinous xanthomatosis and effect induced by chenodeoxycholic acid. *Arch Neurol.* (1992) 49:469–75. doi: 10.1001/archneur.1992.00530290051011

30. Pilo-De-La-Fuente B, Jimenez-Escrig A, Lorenzo J, Pardo J, Arias M, Ares-Luque A, et al. Cerebrotendinous xanthomatosis in Spain: clinical, prognostic, and genetic survey. *Eur J Neurol.* (2011) 18:1203–11. doi: 10.1111/j.1468-1331.2011.03439.x

31. Ginanneschi F, Mignarri A, Mondelli M, Gallus G, Del Puppo M, Giorgi S, et al. Polyneuropathy in cerebrotendinous xanthomatosis and response to treatment with chenodeoxycholic acid. *J Neurol.* (2013) 260:268–74. doi: 10.1007/s00415-012-6630-3

32. Kuriyama M, Fujiyama J, Kubota R, Nakagawa M, Osame M. Osteoporosis and increased bone fractures in cerebrotendinous xanthomatosis. *Metabolism.* (1993) 42:1497–8. doi: 10.1016/0026-0495(93)90205-3

33. Federico A, Dotti MT. Cerebrotendinous xanthomatosis: clinical manifestations, diagnostic criteria, pathogenesis, and therapy. *J Child Neurol.* (2003) 18:633–8. doi: 10.1177/08830738030180091001

34. Hoflinger P, Hauser S, Yutuc E, Hengel H, Griffiths L, Radelfahr F, et al. Metabolic profiling in serum, cerebrospinal fluid, and brain of patients with cerebrotendinous xanthomatosis. *J Lipid Res.* (2021) 62:100078. doi: 10.1016/j.jlr.2021.100078

frontiers | Frontiers in Neurology

TYPE Case Report
PUBLISHED 20 March 2023
DOI 10.3389/fneur.2023.1134225

OPEN ACCESS

EDITED BY
Bruce Miller,
University of California, San Francisco,
United States

REVIEWED BY
Ignazio Cali,
Case Western Reserve University, United States
Maurizio Pocchiari,
Consultant, Rome, Italy

*CORRESPONDENCE
Ling Ling Rong
✉ lingling.rong@corewellhealth.com;
✉ linglingrong@yahoo.com

SPECIALTY SECTION
This article was submitted to
Dementia and Neurodegenerative Diseases,
a section of the journal
Frontiers in Neurology

RECEIVED 30 December 2022
ACCEPTED 23 February 2023
PUBLISHED 20 March 2023

CITATION
Rong LL, Lannen NJ, Tank EC, Feistel JL, Therasse CJ, Potluri A, Khan M and Min J (2023) Case report: Two clusters of Creutzfeldt–Jakob disease cases within 1 year in West Michigan. *Front. Neurol.* 14:1134225. doi: 10.3389/fneur.2023.1134225

Case report: Two clusters of Creutzfeldt–Jakob disease cases within 1 year in West Michigan

Ling Ling Rong[1]*, Nicholas J. Lannen[1], Evan C. Tank[1], Jessica L. Feistel[1], Christopher J. Therasse[2], Anvita Potluri[1], Muhib Khan[1] and Jiangyong Min[1]

[1]Department of Neurosciences, Corewell Health West, Michigan State University, Grand Rapids, MI, United States, [2]Department of Radiology, Corewell Health West, Michigan State University, Grand Rapids, MI, United States

Background: Creutzfeldt–Jakob disease (CJD) is a rare, rapidly progressive, and uniformly fatal neurodegenerative disease. The reported incidence of CJD is 1 to 2 per million people worldwide annually, with fewer than 1,000 cases in the United States per year. In this study, we report a unique case series on temporo-spatial clusters of CJD cases in West Michigan.

Methods: A total of five CJD cases consisting of two temporal clusters were seen from July 2021 to June 2022 at Corewell Health West hospitals. All patients had brain MRI, EEG, and CSF tests. Four patients underwent autopsies.

Results: All patients' MRIs showed characteristic CJD patterns. Four patients had positive CJD panels in CSF. One patient had typical CJD EEG findings. Four patients were confirmed as sporadic CJD by autopsy. All patients died within 3 months after CJD was suspected.

Discussion: All patients lived within a 90-mile radius of Grand Rapids, MI, and two lived in the same county. West Michigan has a population of 1.6 million people, and the four counties where five patients lived have a combined population of 395,104, indicating CJD's new case rate of 3.1 and 12.5 per million people, respectively. Corewell Health is one of the three major healthcare systems in West Michigan. The actual incidence of CJD in West Michigan is likely even higher. This dense temporal and spatial cluster of CJD cases poses a serious public health challenge and warrants urgent investigation.

KEYWORDS

Creutzfeldt-Jacob disease, cluster, rapidly progressive dementia, prion, real-time quaking-induced conversion, West Michigan

Introduction

Creutzfeldt–Jakob disease (CJD) is a transmissible, rapidly progressive neurological disease, caused by misfolded prion protein in the brain (1). The reported prevalence of CJD is 1 to 2 per million people worldwide annually and less than 1,000 cases in the United States per year (2–5)[1] CJD subtypes include sporadic, genetic, iatrogenic, and variant CJD with 85–90% of cases being sporadic (2, 6, 7). sCJD can further be divided into subtypes including MM/(MV)1, MM2, VV1, VV2, and MV2 based on disease-related prion protein features and prion protein genotype in the host at the methionine (M) and valine

1 https://case.edu/medicine/pathology/divisions/national-prion-disease-pathology-surveillance-center/human-prion-diseases

(V) polymorphic codon 129 (8–11)[1]. The clinical diagnostic criteria for probable sCJD are rapidly progressive dementia plus at least two of the following: myoclonus, visual or cerebellar signs, pyramidal/extrapyramidal signs, and akinetic mutism. Vertigo, headache, and neuropsychiatric symptoms can also present. Patients gradually lose mobility, speech, and progress into a comatose state (2, 6, 7, 12, 13). Despite extensive research since its initial description 100 years ago, CJD remains an incurable disease with a survival of 4–12 months from symptom onset in the vast majority of patients (2, 6, 7).

Over the past few decades, there have been increased reports on sCJD. Some studied regional or national geographical distribution or temporal occurrence, but their cases occurred during periods of 9 to 15 years (14–18). Few case series focused on cases with similar clinical presentation without patients' geographic information (19, 20), or on cases over 5 years in the same region (21).

Our case series includes two temporal clusters of CJD cases in one region. Within 1 year from July 2021 to June 2022, we observed five CJD cases at Corewell Health West Butterworth (BW) and Blodgett (BL) Hospitals in Grand Rapids, Michigan (MI). These two hospitals are 3 miles apart. All five cases had supportive brain magnetic resonance imaging (MRI), four of them had supportive cerebrospinal fluid (CSF) findings, and one case had a characteristic electroencephalogram (EEG) pattern. All patients died within 3 months after CJD was suspected. We report this dense temporo-spatial cluster of CJD cases to call for an urgent investigation by public health officials.

Case series

Patient 1: A 67-year-old white woman who worked as a clinic manager was admitted on 14 July 2021 to BW due to rapid neurological decline. Her initial symptom was severe insomnia starting in mid-January 2021. By February 2021, her symptoms progressed to vertigo, diplopia, and imbalance. By May 2021, she was not able to function at work due to cognitive impairment. Her family noticed intermittent "childlike" behavior. On admission, she was fully alert, awake, and oriented with normal cranial nerves. Montreal Cognitive Assessment (MoCA) testing revealed profound deficits with a corrected score of 17/30.

Patient 2: A 78-year-old white man who was a semi-retired funeral home director was admitted on 31 July 2021 to BW for rapidly progressive cognitive decline along with dysfunctional gait, abnormal speech, and intermittent body jerking. In early May 2021, he started to have intermittent hand weakness, paresthesia, and forgetfulness. Due to unsteadiness, he began using a cane in June 2021 but quickly progressed to a walker. Outpatient electromyography and nerve conduction velocity (EMG/NCV) studies were unrevealing. MRI brain reported a 3-mm subacute infarct in left caudate head and ventriculomegaly. In the same month, he developed expressive aphasia progressing to a paucity of speech. Over 2 weeks, he had a catastrophic decline with excessive daytime somnolence. He was unable to perform activities of daily living and developed alternating urinary incontinence and retention. On admission, he was somnolent but easily startled by auditory stimuli. He followed limited, one-step commands and moved all extremities but was oriented to self only.

Patient 3: A 77-year-old white man who was a semi-retired attorney was transferred to BL for continuous video EEG monitoring on 03 May 2022 from an outside hospital (OSH), which was 75 miles east of Grand Rapids. In mid-March 2022, he complained of "brain fog" after he started medication for his newly diagnosed hypertension. The dyscognia persisted despite discontinuation of the anti-hypertensive. He developed visual disturbance and reported seeing his own fingers abnormally elongated, and his legs were fat and bowed. He was able to provide a full history and had an intact neurological examination on admission at the OSH 6 days before transfer to our facility. Brain MRI at OSH reported subtle cortical restricted diffusion involving both posterior temporoparietal and occipital regions. Levetiracetam was initiated after a 1-h EEG captured intermittent delta slowing over the left frontal region without rhythmicity. CSF at OSH was unremarkable except pending the CJD panel. Upon transfer to BL, he was awake and alert but with limited orientation, verbal output, and impaired abstraction. His motor and sensory examinations were intact.

Patient 4: A 78-year-old white woman and homemaker presented to the local emergency department on 03 June 2022 for cognitive decline over several months, accelerating over a few weeks before presentation. Her brain MRI reported multiple infarcts in different territories concerning global hypoxic ischemia; the on-call tele-stroke physician requested transfer to BW for further evaluation as the MRI pattern suggested CJD rather than hypoxic ischemia. The patient's initial symptom was intermittent forgetfulness, which started in August 2021 and had worsened since late December 2021. In March 2022, she developed "pressure in head" and complained "I do not feel my brain work." The patient was diagnosed with anxiety and treated with anxiolytics without benefit. In late April 2022, gait abnormality and word-finding difficulties arose, and in May 2022, she developed auditory hallucinations. By June 2022, jerks in her upper extremities were noticed. Upon admission, she was oriented to person only and had impaired attention, reasoning, and verbal expression but had preserved motor strength and sensation.

Patient 5: A 64-year-old white woman who worked as a nurse was admitted to BL on 17 June 2022 for rapidly progressive cognitive decline. Her initial symptoms were "brain fog," dizziness, and fatigue, starting in January 2022. By late April 2022, she endorsed imbalance, diplopia, and multiple falls along with visual hallucinations, paranoia, and memory dysfunctions. On admission, she was awake, alert, oriented to self and could only recognize her close friends. Her cranial nerves were intact. She had mild proximal weakness in both bilateral upper and lower extremities. The vibratory sensation of bilateral lower extremities was impaired in a length-dependent distribution. She required stabilization on standing (Figure 1).

Laboratory testing and results

All five patients had initial or repeated 1.5 or 3 Tesla brain MRI with and without contrast (w/wo) at BW or BL, respectively, revealing restricted diffusion and corresponding hyperintense T2 FLAIR signal involving bilateral caudate nuclei and putamina in a symmetric pattern (patient 1); asymmetric diffusion restriction

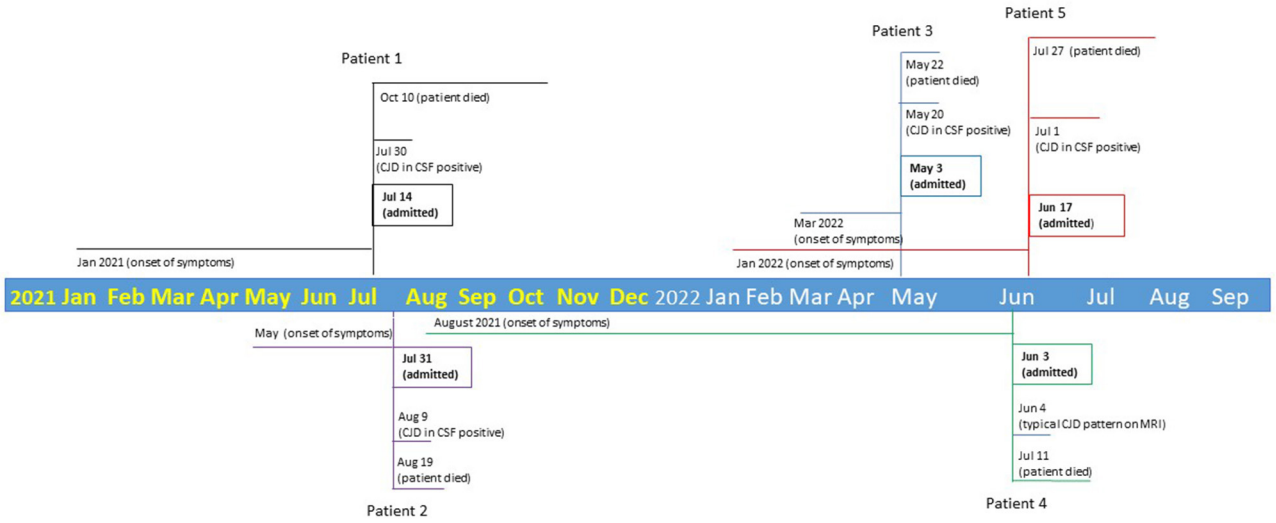

FIGURE 1
Timeline of two clusters of five CJD cases.

signals in the cerebral cortex of cingulum, left temporoparietal lobes, and caudate nucleus (patient 2); prominent multifocal diffusion restriction involving the bi-hemispheric cerebral cortex, more posteriorly and on the left compared to the right (patient 3); symmetric cortical diffusion restriction involving paramedian, lateral parietal cortices, temporal cortices, and to a lesser extent in the frontal lobe with involvement of left greater than the right (patient 4); restricted diffusion in the bilateral caudate nuclei (left > right) and the left mesial temporal lobe, including the amygdala, the hippocampus, and the forniceal column (patient 5) (Figure 2).

EEG was performed on all patients. The EEG of patient 3 showed periodic sharp wave complexes (PSWC), a characteristic CJD pattern. Other patients' EEGs were unremarkable (patient 5), had non-specific rare generalized periodic discharges with triphasic morphology (patients 1 and 4); moderate bitemporal slowing with a right predominance (patient 1); generalized rhythmic delta activity (patient 2) (Figure 3). Blood, CSF basic tests, and Mayo Clinic autoimmune encephalopathy panel in serum (ENS2) were negative. The autoimmune encephalopathy panel and paraneoplastic panel in CSF were all negative. All patients' CSF CJD panels from the National Prion Disease Pathology Surveillance Center (NPDPSC) reported >98% likelihood of prion disease except patient 4 whose CJD likelihood and 14-3-3 proteins were inconclusive, RT-QuIC was negative, and T-tau level was high (19937 pg/ml) (Table 1).

Treatment and final diagnosis

All patients (except patient 4) received empirical treatment: five doses of 1,000 mg methylprednisolone intravenously daily, followed by five rounds of plasma exchange (patient 1); one dose of 400 mg/kg intravenous immunoglobulin (IVIg) (patient 2); five doses of 400 mg/kg IVIg alone daily (patient 3); or with five doses of IV methylprednisolone daily (patient 5). Patients did not have any benefits from the aforementioned treatment. Patients died in October 2021, August 2021, May 2022, July 2022, and July 2022, respectively. Four patients underwent autopsy and genetic analysis (the family of patient 2 declined autopsy). No gene mutation was detected in any patient. Except for codon 129 polymorphism, no other polymorphism was found in any patient. The final diagnosis was as follows: patients 1 and 5 were sCJD-VV2, and patients 3 and 4 were sCJD-MM1 (Table 1).

Discussion

All patients in this case series had a rapid cognitive decline. Two patients also had visual disturbances (particularly patient 3 who presented with impaired visual perception at an early stage), and the illness progressed rapidly, possibly representing the Heidenhain variant of CJD (12, 22). On admission, the patients were 67, 78, 77, 78, and 64 years of age, and the durations from the time of symptoms onset to death were 8, 4, 3, 11, and 6 months, respectively. This is mostly consistent with sporadic CJD, which has reported a range of 55–75 years of peak onset age and a median survival duration of 4–12 months (2, 5, 7, 23). The durations from the time when positive CJD in CSF was reported (in patients 1, 2, 3, and 5) or from the time when brain MRI showed typical CJD patterns (patient 4) to death were 72, 10, 2, 26, and 43 days, respectively. All were shorter than the reported typical 4 to 6 months from diagnosis to death (5, 23).

Brain MRI, EEG, and advanced CSF studies are the most utilized diagnostic tests for CJD (7, 24–26). Brain MRI with diffusion-weighted imaging (DWI) has a sensitivity of 67–91% (27, 28) and a specificity of 97% for diagnosing sCJD (27). With increased awareness of sCJD, its diagnostic criteria, and improvement in MRI accessibility and scan quality, the sensitivity of MRI for CJD could reach 99% (28). Our five patients' brain MRI revealed typical sCJD patterns, that is hyperintensities in the cortical gray matter (cortical ribboning sign) and the deep nuclei (basal ganglia and thalamus). The cortical ribboning sign was proposed to be the biomarker in the prodromal phase of sCJD

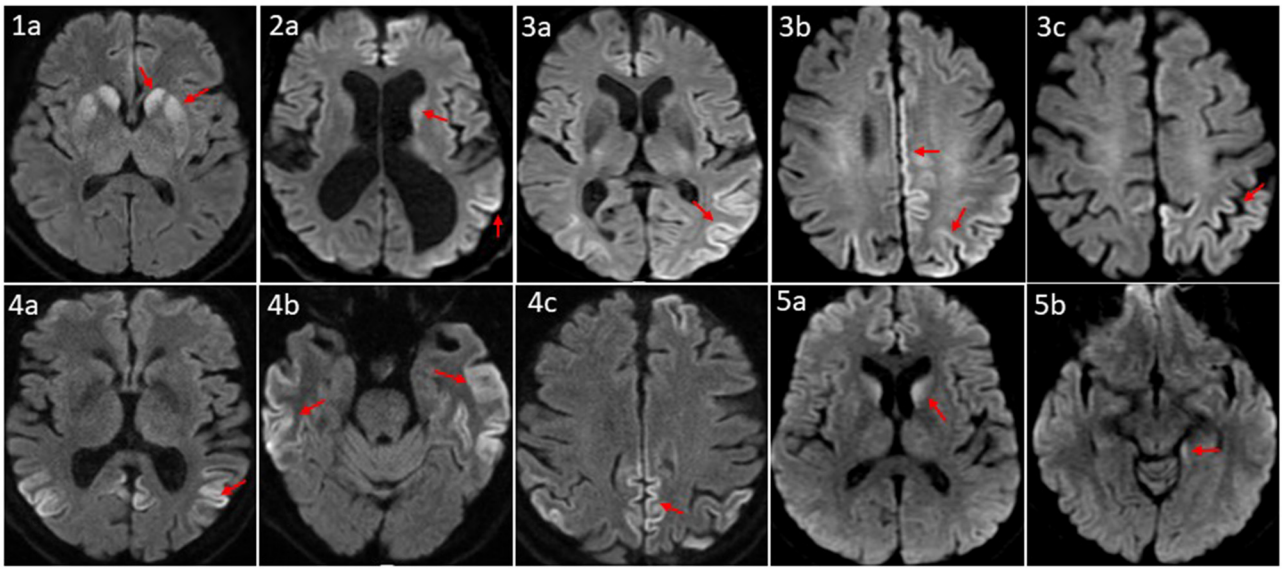

FIGURE 2
Axial MRI brain diffusion weighted images of five CID patients. **(1a)** Symmetric diffusion restriction in bilateral caudate nuclei and putamina. **(2a)** Subtle diffusion restriction involving the left caudate head, and left parletal cortex. **(3a–c)** Cortically based diffusion restriction involving the posterior left greater than right parietal lobes and paramedian left frontoparietal region. **(4a–c)** Intense cortically based restriction involving the paramedian and lateral parietal cortices, bilateral temporal cortices, and to a lesser extent the left greater that right frontal lobes. **(5a, b)** Relatively symmetric DWI within the caudate nuclei; subtle involvement of the posteromedial left hippocampus. Patient sequence was labeled from 1 to 5; red arrows point to sites of abnormal diffusion restriction.

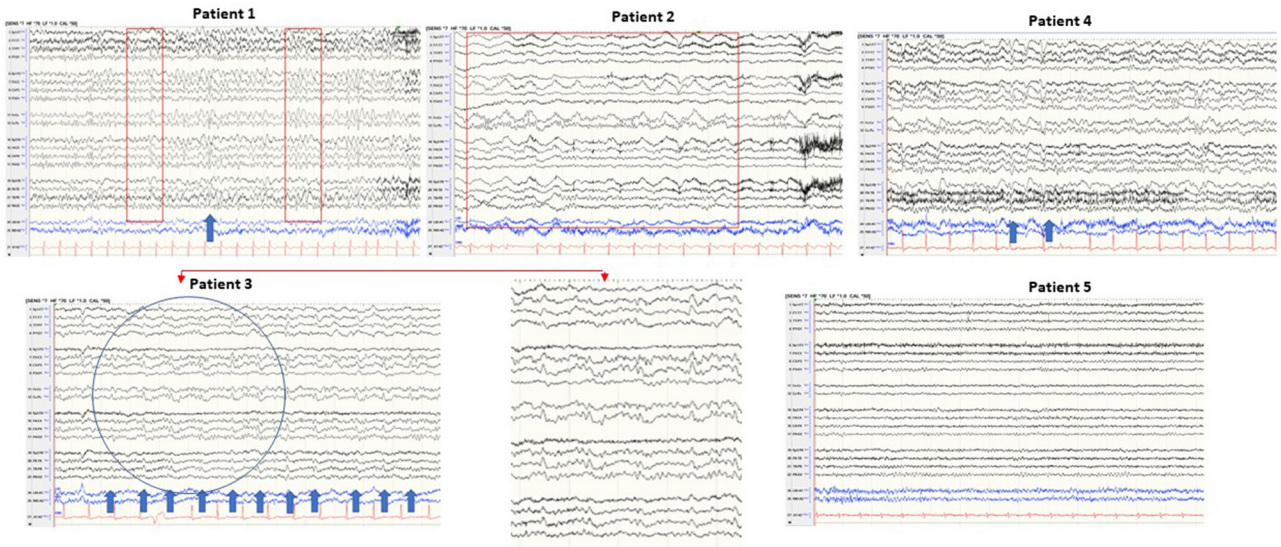

FIGURE 3
Typical samples of five patients in a standart anterior to posterior bipolar montage. Patient 1: background slowing and triphasic wave; patient 2: generalized rhythmic delta activity; patient 3: periodic sharp wave complexes (PSWC) at 1 Hz; patient 4: non-periodic triphasic wave; patient 5: normal EEG.

diagnosis (29, 30). The MRI of patient 1 demonstrated a symmetric pattern of bilateral DWI and T2 FLAIR correlated signal in caudate nuclei and putamina. MRIs of patients 2, 4, and 5 revealed asymmetric, cortically based DWI changes in the cingulate, the caudate nuclei, and the left temporoparietal cortex, and the MRI of patient 3 showed multifocal cortically based DWI pattern, more on the left. Park et al. found that being greater than 60 years of age and diffusion restriction in the caudate nucleus and putamen were independent prognostic factors of shorter survival duration in patients with sCJD (27) with median overall survival of 1.7 months compared to 14.2 months in the intermediate risk group. Radiographically, our five patients belong to the high-risk group.

RT-QuIC is a breakthrough technology for diagnosing CJD with specificity reaching 99–100% (31–33). Its sensitivity can

10.3389/fneur.2023.1134225

TABLE 1 Summary of patients' data, CSF CJD panel, and brain autopsy results.

Case	Age	Gender	Profession	Admission	Expired	CSF				Autopsy	Final diagnosis	129 Polymorphism
						CJD probability	RT-QuIC	T-tau protein (pg/ml)	14-3-3 GAMMA (AU/ml)			
1	67	Woman	Clinic Manager	Jul-2021	Oct-2021	>98%	Positive	>20,000	Positive	Yes	sCJD	VV2
2	78	Man	Funeral Home director	Jul-2021	Aug-2021	>98%	Positive	>20,000	Positive	No	NA	NA
3	77	Man	Semi-retired attorney	May-2022	May-2022	>98%	Positive	>20,000	72,061	Yes	sCJD	MM1
4	78	Woman	Homemaker	Jun-2022	Jul-2022	Inconclusive	Negative	19,937	Inconclusive	Yes	sCJD	MM1
5	64	Woman	Nurse	Jun-2022	Jul-2022	>98%	Positive	17,770	71,008	Yes	sCJD	VV2

increase from 77 to 96% after modified techniques (31). Patients' (1, 2, 3, and 5) CSF CJD panel reported a likelihood of CJD of more than 98%, positive RT-QuIC, high T-tau protein, and positive 14-3-3 protein (more than 71,000 Au/ml in patients 3 and 5, and no titer reported in patient 1 and 2). The CSF of patient 4 was inconclusive for CJD likelihood and 14-3-3 proteins. Her RT-QuIC was negative, but T-tau protein was 19,937 pg/ml. As per NPDPSC test report, the sensitivity of RT-QuIC is lower when specimens are discolored by blood. Shir et al. reported that elevated CSF 14-3-3 and T-tau proteins as well as clinical symptoms such as myoclonus and visual or cerebellar abnormalities are associated with shorter disease duration (7), which held true for patient 3.

EEG has a lower diagnostic value when compared to brain MRI and CJD panel in CSF. The reported sensitivity of EEG-specific abnormalities to diagnose probable sCJD ranged from 38.2 to 68.75% (34, 35). However, the characteristic EEG finding in CJD, periodic sharp wave complexes (PSWCs), has 86% specificity (36) and 95% positive predictive value (37). Our case series confirmed low sensitivity and high specificity of EEG for diagnosing CJD. Of the five patients, four patients showed EEG abnormality (80%) with 20% specific (patient 3 showed characteristic periodic sharp wave complexes PSWC at 1 Hz, bi-hemispheric with left predominance) and 60% non-specific abnormalities (patients 1, 2, and 5). Mundlamurri et al. reported that in the early stage of sCJD, patients' EEGs can be normal or non-specifically abnormal (35). In very early phases (1.67 months after onset and before the emergence of generalized PSWC) of sCJD, the predominant findings of EEG can be (1) lateralized periodic discharges (LPDs), (2) central sagittal sporadic epileptiform discharges (CSSEDs), and (3) focal epileptiform discharges (38). It is suggested that the early presence of the PSWC pattern has a prognostic value because these patients have significantly lower average survival time (39). The EEG of patient 3 captured PSWC on day 48 after the illness onset. He died 19 days after the EEG was done and 2 days after positive CJD in CSF was reported.

Brain biopsy or autopsy remains the gold standard for final diagnosis. Four patients underwent autopsy and genetic analysis. All four patients had sporadic CJD, of the two most common subtypes, sCJD-VV2 in Patients 1 and 5, and sCJD-MM1 in patients 3 and 4. Different subtypes have different clinical and neuropathological features, as well as survival times and test results (8, 40, 41). The sensitivity of RT-QuIC for detecting MM1 and VV2 is high (96.3%) but can be negative for MM2 and VV1 subtypes (33, 42). Younes et al. reported that MM1, MV1, and VV2 are related to short duration/fast progression, while MV2, VV1, and MM2 are associated with long duration/slow progression (43). Our case series revealed that patients 3 and 4 were sCJD-MM1 but with an 8-month difference in survival length; patients 1 and 5 were diagnosed with sCJD-VV2 with similar survival durations, 8 vs. 6 months. Patient 2 had a short survival duration; unfortunately, his family declined an autopsy.

Geographical clusters of sCJD have been reported, but most clusters contained cases distributed over many years (14, 17, 18, 44–48), and few were temporo-spatial clusters. A French cluster of three cases of CJD occurring in 1998 reported that two of the patients lived in the same village. Molecular and phenotypic analyses showed both patients were homozygous for methionine at the polymorphic codon 129 but one patient was MM1 while

another had mixed features of MM1 and MM2 both clinically and histo-pathologically (48). RT-QuIC was not yet invented. A Japanese cluster of three CJD cases occurred between 1988 and 1989 near Fukuoka city; no hospitalization time was mentioned in the report, nor were CSF studies or codon 129 polymorphism analyses done on these patients (49). A cluster of four cases in Burlington, Ontario, Canada, between April 1989 and April 1990 with two additional cases on further inquiry, and a cluster of seven cases in Nassau County, New York, between mid-June 1999 and mid-June 2000 (50, 51) were reported without genetic studies. Some clustering was found later to be an aggregation of genetic CJD cases (52, 53).

Our five cases in two clusters were seen within 1 year in Grand Rapids, Michigan. Cluster one included patients 1 and 2, seen within 1 month from July to August of 2021; cluster two included patients 3, 4, and 5, observed within 1 month between May and June of 2022. All patients lived within a 90-mile radius of Grand Rapids. No interpersonal connections were identified among them. All patients were white with differing professions (Table 1). None of them had a family history of Creutzfeldt–Jakob disease, or personal history of corneal transplants, craniotomy, administration of human growth hormone derived from pools of pituitary glands, or surgical procedure at the same facility. However, families of patients 1, 2, and 4 reported consuming venison. More intriguingly, families and relatives of these three patients reported additional (at least four) possible or probable CJD cases occurring between 2007 and 2022 in their friends or communities (unpublished data). One of the patients was a 63-year-old white woman and mayor, who lived 35 miles from patient 2, and died of CJD in March 2022. Thus, such a wave of dense temporo-spatial clustering of CJD in West Michigan is very unusual and alarming.

Our case series does not support that CJD incidence has no geographical differences (4, 54). West Michigan has 1.6 million people, and the combined population of four counties where five patients lived is 395,104 in 2022, which makes the CJD new case rate 3.1 and 12.5 per million people in West Michigan and combined four counties, respectively, which is higher than reported 1 to 2 per million people worldwide and 350–710 cases in the United States annually (2–5)[1]. Adding the cases reported by our three patients' families, the new case occurrence would be even higher. Michigan disease surveillance system (MDSS) reported 19 CJD cases by 31 December 2022 and only 12 cases in 2018, and this reflects a 58% increase[2] We do not have enough evidence to conclude that our two clusters are purely due to heightened awareness, more sensitive tests, and better ascertainment, nor could we be certain that they just simultaneously occurred (55). Our study has several limitations, including an observational study, a limited time period, not using the conventionally used solar year period, and a relatively small population and area in West Michigan. As such, this case series highlights only a possible trend. More research and evidence are certainly required to reach a conclusion. We have planned additional retrospective studies, which we expect will surmount these shortcomings. Epidemiological surveillance, research, development of new diagnostic technologies, and public health endeavors are critical (4, 56).

Conclusion

For five sCJD cases in two dense clusters within 1 year in Grand Rapids, MI is more than expected. Extensive screening in West Michigan may eventually arrive at a reliable incidence rate of CJD in this region. These two clusters along with additional cases reported by our patients' families warrant urgent investigation. Further research including epidemiological study regarding possible transmission events, common environmental factors that trigger CJD occurrence as well as continuous surveillance, and further improving diagnostic techniques are critical and necessary.

Data availability statement

The raw data supporting the conclusions of this article will be made available by the authors, without undue reservation.

Ethics statement

Ethical review and approval was not required for the study on human participants in accordance with the local legislation and institutional requirements. The patients/participants provided their written informed consent to participate in this study. Written informed consent was obtained from the individual(s) for the publication of any potentially identifiable images or data included in this article.

Author contributions

LR: writing the original draft, selecting MRI images, and finalizing the manuscript. NL, JF, AP, MK, and JM: reviewing and editing. ET: selecting EEG pictures, draft reviewing, and editing. CT: selecting MRI images. All authors contributed to the article and approved the submitted version.

Conflict of interest

The authors declare that the research was conducted in the absence of any commercial or financial relationships that could be construed as a potential conflict of interest.

Publisher's note

All claims expressed in this article are solely those of the authors and do not necessarily represent those of their affiliated organizations, or those of the publisher, the editors and the reviewers. Any product that may be evaluated in this article, or claim that may be made by its manufacturer, is not guaranteed or endorsed by the publisher.

2 https://www.michigan.gov/mdhhs/-/media/Project/Websites/mdhhs/CDINFO/WSR/Current_WSR.pdf?rev=2219a79dac8f486fa870c4afcb339848&hash=F23C8EB5D0CCD5378F6A5AE8CF1CB954.

References

1. Prusiner SB. Prions. *Proc Natl Acad Sci USA*. (1998) 95:13363–83. doi: 10.1073/pnas.95.23.13363

2. Sitammagari K, Masood W. *Creutzfeldt Jakob Disease*. Treasure Island (FL): StatPearls Publishing. (2022).

3. Watson N, Brandel JP, Green A, Hermann P, Ladogana A, Lindsay T, et al. The importance of ongoing international surveillance for Creutzfeldt-Jakob disease. *Nat Rev Neurol.* (2021) 17:362–79. doi: 10.1038/s41582-021-00488-7

4. Kotkowski E, Cabot JH, Lacci JV, Payne DH, Cavazos JE, Romero RS, et al. Creutzfeldt-Jakob disease: In-hospital demographics report of national data in the United States from 2016 and review of a rapidly-progressive case. *Clin Neurol Neurosurg.* (2020) 197:106103. doi: 10.1016/j.clineuro.2020.106103

5. Uttley L, Carroll C, Wong R, Hilton DA, Stevenson M. Creutzfeldt-Jakob disease: a systematic review of global incidence, prevalence, infectivity, and incubation. *Lancet Infect Dis.* (2020) 20:e2–e10. doi: 10.1016/S1473-3099(19)30615-2

6. Centers for Disease Control and Prevention. *Clinical and Pathologic Characteristics | Creutzfeldt-Jakob Disease, Classic (CJD) | Prion Disease | CDC*. (2021).

7. Shir D, Lazar EB, Graff-Radford J, Aksamit A, Cutsforth-Gregory JK, Jones DT, et al. Analysis of clinical features, diagnostic tests, and biomarkers in patients with suspected Creutzfeldt-Jakob disease, 2014-2021. *JAMA Netw Open.* (2022) 5:e2225098. doi: 10.1001/jamanetworkopen.2022.25098

8. Bizzi A, Pascuzzo R, Blevins J, Moscatelli MEM, Grisoli M, Lodi R, et al. Subtype diagnosis of sporadic Creutzfeldt-Jakob disease with diffusion magnetic resonance imaging. *Ann Neurol.* (2021) 89:560–72. doi: 10.1002/ana.25983

9. Parchi P, Giese A, Capellari S, Brown P, Schulz-Schaeffer W, Windl O, et al. Classification of sporadic Creutzfeldt-Jakob disease based on molecular and phenotypic analysis of 300 subjects. *Ann Neurol.* (1999) 46:224–233. doi: 10.1002/1531-8249(199908)46:2<224::AID-ANA12>3.0.CO;2-W

10. Gelpi E, Baiardi S, Nos C, Dellavalle S, Aldecoa I, Ruiz-Garcia R, et al. Sporadic Creutzfeldt-Jakob disease VM1: phenotypic and molecular characterization of a novel subtype of human prion disease. *Acta Neuropathol Commun.* (2022) 10:114. doi: 10.1186/s40478-022-01415-7

11. Parchi P, Strammiello R, Notari S, Giese A, Langeveld JPM, Ladogana A, et al. Incidence and Spectrum of sporadic Creutzfeldt-Jakob disease variants with mixed phenotype and co-occurrence of PrPSc types: an updated classification. *Acta Neuropathol.* (2009) 118:659–71. doi: 10.1007/s00401-009-0585-1

12. Appleby BS, Appleby K, Crain BJ, Onyike CU, Wallin MT, Rabins PV. Characteristics of established and proposed sporadic Creutzfeldt-Jakob disease variants. *Arch neurol.* (2009) 66:208–15. doi: 10.1001/archneurol.2008.533

13. Krasnianski A, Kaune J, Jung K, Kretzschmar HA, Zerr I. First symptom and initial diagnosis in sporadic CJD patients in Germany. *J Neurol.* (2014) 261:1811–7. doi: 10.1007/s00415-014-7410-z

14. Xiao K, Pang MF, Zhao YQ, Gao LP, Wu YZ, Wang Y, et al. Difference of geographic distributions of the Chinese patients with prion diseases in the permanent resident places and referring places. *Prion.* (2022) 16:58–65. doi: 10.1080/19336896.2022.2080921

15. Puopolo M, Catelan D, Capellari S, Ladogana A, Sanguedolce A, Fedele A, et al. Spatial epidemiology of sporadic Creutzfeldt-Jakob disease in Apulia, Italy. *Neuroepidemiology.* (2020) 54:83–80. doi: 10.1159/000503234

16. Chamosa S, Tamayo I, Arteagoitia-Axpe JM, Juste RA, RodriguezMartinez AB, Zarraz-Imirizaldu JJ, et al. Geographical analysis of the sporadic Creutzfeldt-Jakob disease distribution in the autonomous community of the Basque Country for the period 1995-2008. *Eur Neurol.* (2014) 72:20–5. doi: 10.1159/000358298

17. Nakatani E, Nishimura T, Zhou B, Kaneda H, Teramukai S, Nagai Y, et al. Temporal and regional variations in sporadic Creutzfeldt-Jakob disease in Japan, 2001-2010. *Epidemiol Infec.* (2015) 143:1073–1078. doi: 10.1017/S0950268814001605

18. Klug GM, Wang H, Boyd A, Law M, Whyte S, Kaldor J, et al. Enhanced geographically restricted surveillance simulates sporadic Creutzfeldt-Jakob disease cluster. *Brain.* (2009) 132:493–501. doi: 10.1093/brain/awn303

19. Corriveau-Lecavalier N, Li W, Ramanan VK, Drubach D, Day GS, Jones DT. Three cases of Creutzfeldt-Jakob disease presenting with a predominant dysexecutive syndrome. *J Neurol.* (2022) 269:4222–8. doi: 10.1007/s00415-022-11045-7

20. Gomez-Mayordomo V, Kojovic M, Lopez-Valdes E, Alonso-Frech F, Horga A, Fernandez-Rodriguez R, et al. Functional neurological symptoms as initial presentation of Creutzfeldt-Jakob disease: case series. *J Neurol.* (2022) 270:1141–6. doi: 10.1007/s00415-022-11376-5

21. Bawa A, Zhang YH. Creutzfelft-Jakob Disease: A focused literature review and retrospective case series of five patients from a community hospital. *J Neurol. Exper. Neurosci.* (2022) 8:13–7. doi: 10.17756/jnen.2022-095

22. Kropp S, Schulz-Schaeffer WJ, Finkenstaedt M, Riedemann C, Windl O, Steinhoff BJ, et al. The Heidenhain variant of Creutzfeldt-Jakob disease. *Arch Neurol.* (1999) 56:55–61. doi: 10.1001/archneur.56.1.55

23. Staffaroni AM, Kramer AO, Casey M, Kang H, Rojas JC, Orru CD, et al. Association of blood and cerebrospinal fluid tau level and other biomarkers with survival time in sporadic Creutzfeldt-Jakob disease. *JAMA Neurol.* (2019) 76:969–77. doi: 10.1001/jamaneurol.2019.1071

24. Hermann P, Appleby B, Brandel JP, Caughey B, Collins S, Geschwind MD, et al. Biomarkers and diagnostic guidelines for sporadic Creutzfeldt-Jakob disease. *Lancet Neurol.* (2021) 20:235–46. doi: 10.1016/S1474-4422(20)30477-4

25. Zerr I. Laboratory diagnosis of Creutzfeldt-Jakob disease. *N Engl J Med*. (2022) 386:1345–1350. doi: 10.1056/NEJMra2119323

26. Schmitz M, Canaslan S, Espinosa JC, Fernandez-Borges N, Villar-Pique A, Zerr I. Validation of plasma and CSF neurofilament light chain as an early marker for sporadic Creutzfeldt-Jakob disease. *Mol Neurobiol.* (2022) 59:1–9. doi: 10.1007/s12035-022-02891-7

27. Park HY, Kim M, Suh CH, Kim SY, Shim WH, Kim SJ. Diagnostic value of diffusion -weighted brain magnetic resonance imaging in patients with sporadic Creutzfeldt-Jakob disease: a systematic review and meta-analysis. *Eur Radiol.* (2021) 31:9073–85. doi: 10.1007/s00330-021-08031-4

28. Jesuthasan A, Sequeira D, Hyare H, Odd H, Rudge P, Mok TH, et al. Assessing initial MRI reports for suspected CJD patients. *J Neurol.* (2022) 269:4452. doi: 10.1007/s00415-022-11087-x

29. Hamada Y, Deguchi K, Tachi K, Kita M, Nonaka W, Takata T, et al. Significance of cortical ribboning as a biomarker in the prodromal phase of sporadic Creutzfeldt-Jakob disease. *Intern Med.* (2022) 61:2667–2670. doi: 10.2169/internalmedicine.8354-21

30. Yasuda M, Sugiyama A, Hokkoku H, Suichi T, Ito K, Satoh K, et al. Propagation of diffusion-weighted MRI abnormalities in the preclinical stage of sporadic Creutzfeldt-Jakob disease. *Neurology.* (2022) 99:699–702. doi: 10.1212/WNL.0000000000201221

31. Orru CD, Groveman B, Hughson A, Zanusso G, Coulthart M, Caughey B. Rapid and sensitive RT-QuIC detection of human Creutzfeldt-Jakob disease using cerebrospinal fluid. *MBio.* (2015) 6:e02451–14. doi: 10.1128/mBio.02451-14

32. Hermann P, Laux M, Glatzel M, Matschke J, Knipper T, Goebel S, et al. Validation and utilization of amended diagnostic criteria in Creutzfeldt-Jakob disease surveillance. *Neurology.* (2018) 91:e331–8. doi: 10.1212/WNL.0000000000005860

33. Rhoads DD, Wrona A, Foutz A, Blevins J, Glisic K, Person M, et al. Diagnosis of prion diseases by RT-QuIC results in improved surveillance. *Neurology.* (2020) 95:e1017–26. doi: 10.1212/WNL.0000000000010086

34. Qi C, Zhang JT, Zhao W, Xing XW, Yu SY. Sporadic Creutzfeldt-Jakob disease: A retrospective analysis of 104 cases. *Eur Neurol.* (2020) 83:65–72. doi: 10.1159/000507189

35. Mundlamurri RC, Shah R, Adiga MS, Chatterjee A, Gautham B, Raghavendra K, et al. EEG observations in probable sporadic CJD. *Ann Indian Acad Neurol.* (2020) 23:760–766. doi: 10.4103/aian.AIAN_672_20

36. Steinhoff BJ, Racker S, Herrendorf G, Poser S, Grosche S, Zerr I, et al. Accuracy and reliability of periodic sharp wave complexes in Creutzfeldt-Jakob disease. *Arch Neurol.* (1996) 53:162–6. doi: 10.1001/archneur.1996.00550020074017

37. Wieser HG, Schindler K, Zumsteg D. EEG in Creutzfeldt-Jakob disease. *Clin Neurophysiol.* (2006) 117:935–51. doi: 10.1016/j.clinph.2005.12.007

38. Matsubayashi T, Akaza M, Hayashi Y, Hamaguchi T, Satoh K, Kosami K, et al. Specific electroencephalogram features in the very early phases of sporadic Creutzfeldt-Jakob disease. *J Neurol Sci.* (2022) 437:120265. doi: 10.1016/j.jns.2022.120265

39. Castelli A, Placidi F, Bonomi CG, Giuliano FD, Martorana A, Pizzicannella G, et al. Periodic sharp wave complexes identify a distinctive phenotype in Creutzfeldt-Jakob disease. *Clin Neurophysiol.* (2022) 143:124–32. doi: 10.1016/j.clinph.2022.08.025

40. Tanev KS, Yilma M. An unusually presenting case of sCJD-the VV1 subtype. *Clin Neurology and Neurosurg.* (2009) 111:282–291. doi: 10.1016/j.clineuro.2008.09.017

41. Cali I, Puoti G, Smucny J, Curtiss PM, Cracco L, Kitamoto T, et al. Co-existence of PrP^{D} types 1 and 2 in sporadic Creutzfeldt-Jakob disease of the VV subgroup: phenotypic and prion protein characteristics. *Sci Rep.* (2020) 10:1503. doi: 10.1038/s41598-020-58446-0

42. Carrasco A, Appleby BS, Cali I, Okhravi HR. Atypical case of VV1 Creutzfeldt-Jakob disease subtype: care report. *Front Neurol.* (2022) 13:875370. doi: 10.3389/fneur.2022.875370

43. Younes K, Rojas JC, Wolf A, Sheng-Yang GM, Paoletti M, Toller G, et al. Selective vulnerability to atrophy in sporadic Creutzfeldt-Jakob disease. *Ann Clin Transl Neurol.* (2021) 8:2283–1199. doi: 10.1002/acn3.51290

44. Linsell L, Cousens SN, Smith PG, Knight RSG, Zeidler M, Stewart G, et al. case-control study of sporadic Creutzfeldt-Jakob disease in the United Kingdom: analysis of clustering. *Neurology.* (2004) 63:2077–83. doi: 10.1212/01.WNL.0000145844.53251.BC

45. Collins S, Boyd A, Fletcher A, Kaldor J, Hill A, Farish S, et al. Creutzfeldt-Jakob disease cluster in an Australian rural city. *Ann Neurol.* (2002) 52:115–8. doi: 10.1002/ana.10224

46. D'Aignaux JH, Cousens SN, Delasnerie-Laupretre N, Brandel JP, Salomon D, Laplanche JL, et al. Analysis of the grographical distribution of sporadic Creutzfeldt-Jakob disease in France between 1992 and 1998. *Int J Epidemiol.* (2002) 31:490–5. doi: 10.1093/ije/31.2.490

47. Ruegger J, Stoeck K, Amsler L, Blaettler T, Zwahlen M, Aguzzi A, et al. case-control study of sporadic Creutzfeldt-Jakob disease in Switzerland: analysis of potential risk factors with regard to an increased CJD incidence in the years 2001-2004. *BMC Public Health.* (2009) 9:19. doi: 10.1186/1471-2458-9-18

48. Beaudry P, Parchi P, Peoc'h K, Desbordes P, Dartigues JF, Vital A, et al. A French cluster of Creutzfeldt-Jakob disease: 1 molecular analysis. *Eur J Neurol.* (2002) 9:457–62. doi: 10.1046/j.1468-1331.2002.00456.x

49. Arakawa K, Nagara H, Itoyama Y, Doh-ura K, Tomokane N, Tateishi J, et al. Clustering of three cases of Creutzfeldt-Jakob disease near Fukuoka city, Japan. *Acta Neurol Scand.* (1991) 84:445–7. doi: 10.1111/j.1600-0404.1991.tb04986.x

50. Nosal R, Kapoor A, Shanin R. Cluster of cases of Creutzfelft-Jakob disease—Ontario. *Can Dis Wkly Rep.* (1991) 17:12.

51. Adikari D, Farmer P. A cluster of Creutzfeldt-Jakob disease patients from Nassau county, New York, USA. *Ann Clin Lab Sci.* (2001) 31:211–2.

52. Golfdarb LG, Mitroya E, Brown P, Toh BH, Gaidsek DC. Mutation in codon 200 of scrpie amyloid protein gene in two clusters of Creutzfeldt-Jakob disease in Slovakia. *Lancet.* (1990) 336:514–5. doi: 10.1016/0140-6736(90)92073-Q

53. Miyakawa T, Iseki KIE, Kawanishi C, Sugiyama N, Onishi H, Yamada Y, et al. Japanese Creutzfeldt-Jakob disease patients exhibiting high incidence of the E200K PRNP mutation and located in the basin of a river. *Neurol Res.* (1998) 20:684–8. doi: 10.1080/01616412.1998.11740584

54. Shi Q, Gao C, Zhou W, Zhang BY, Chen JM, Tian C, et al. Surveillance for Creutzfeldt-Jakob disease in China from 2006 to 2007. *BMC Public Health.* (2008) 8:360. doi: 10.1186/1471-2458-8-360

55. Raubertas RF, Brown P, Cathala F, Brown I. The question of clustering of Creutzfeldt-Jakob disease. *Am J Epidemiol.* (1989) 129:146–54. doi: 10.1093/oxfordjournals.aje.a115103

56. Watson N, Hermann P, Ladogana A, Denouel A, Baiardi S, Colaizzo E, et al. Validation of revised international Creutzfeldt-Jakob disease surveillance network diagnostic criteria for sporadic Creutzfeldt-Jakob disease. *JAMA Netw Open.* (2022) 5:e2146319. doi: 10.1001/jamanetworkopen.2021.46319

frontiers | Frontiers in Neurology

TYPE Case Report
PUBLISHED 06 April 2023
DOI 10.3389/fneur.2023.1151130

OPEN ACCESS

EDITED BY
Bruce Miller,
University of California,
San Francisco,
United States

REVIEWED BY
Simone Baiardi,
University of Bologna,
Italy
Vivek Lal,
Post Graduate Institute of Medical Education and Research (PGIMER),
India

*CORRESPONDENCE
Xiaoyan Liu
✉ yy6sweet@zju.edu.cn
Qing Ke
✉ keqing2003@zju.edu.cn

†These authors have contributed equally to this work

SPECIALTY SECTION
This article was submitted to Dementia and Neurodegenerative Diseases, a section of the journal Frontiers in Neurology

RECEIVED 25 January 2023
ACCEPTED 17 March 2023
PUBLISHED 06 April 2023

CITATION
Liu X, Fan Z, Chen X, Zhang Y, He F, Ma X and Ke Q (2023) Case report: A longitudinal study of an unusual rapidly progressive dementia case.
Front. Neurol. 14:1151130.
doi: 10.3389/fneur.2023.1151130

Case report: A longitudinal study of an unusual rapidly progressive dementia case

Xiaoyan Liu[1]*†, Ziqi Fan[1†], Xuanyu Chen[1], Yanyan Zhang[1], Fangping He[1], Xiaohua Ma[2] and Qing Ke[1]*

[1]Department of Neurology, The First Affiliated Hospital, Zhejiang University School of Medicine, Hangzhou, China, [2]Department of Neurology, The Second Division of Xinjiang Production and Construction Corps, Korla Hospital, Xinjiang, China

It is daunting to determine the etiology of rapidly progressive dementia (RPD), which includes metabolic, neoplastic, infectious, autoimmune, neurodegenerative and other conditions. Herein, we illustrate an unusual case of a patient primarily exhibiting RPD, overlapping sleep dysfunction, psychosis and abnormal movement, which was finally defined as anti-IgLON5 disease, a novel and rare autoimmune encephalopathy. Furthermore, we longitudinally described his cognitive and psychological performance in detail, and determined that early initiation of immunotherapy in this patient did not result in a good outcome. These data highlight anti-IgLON5 disease as a possible differential diagnosis in patients with RPD.

KEYWORDS

autoimmune encephalopathy, IgLON5, immunotherapy, psychosis, rapidly progressive dementia

Introduction

Rapidly progressive dementia (RPD) is a complicated condition, that originates from various types of etiologies, including vascular, infectious, toxic, metabolic, autoimmune, iatrogenic, neurodegenerative and other conditions (1). Hence, it is quite challenging to determine the etiology of RPD quickly. A novel neurological disease, anti-IgLON5, characterized by antibodies against the neuronal cell-adhesion protein IgLON5 has been gradually described since 2014 (2). This disease has been pathologically determined to involve tau inclusions; it is clinically characterized by chronic sleep disorder, accompanied by gait instability, bulbar symptoms, and cognitive impairment (3). Nonetheless, the current understanding of this disease is incomplete, and very few cases have been reported worldwide (4). Herein, we report a case of a patient with anti-IgLON5 disease who exhibited prominent RPD. In particular, we longitudinally describe his cognitive and psychological performance as well as his clinical outcome in response to immunotherapy and symptomatic treatment.

Case report

A 74-year-old, right-handed male was admitted to our hospital with jaw and bilateral hand movements for 3 months and RPD for 1 month, coupled with intermittent visual hallucinations and raving. Especially, he exhibited multiple involuntary movements (jaw tremor, motor tremor of hands), his hands always groped about, and would fell backward when he was walking or

seated. Besides, he could not recognize his family or his location; sometimes he observed a snack moving around or a dead man in the room. He was sent to a local hospital and administered olanzapine 2.5 mg per night without marked improvement. Thus, he was transferred to our hospital. His past history was traced back to 5 years ago when he suffered from rectal carcinoma and received surgery and chemotherapy.

On admission, neurologic examination revealed prominent cognitive impairment and psychiatric symptoms. Specifically, he failed to complete the Mini-Mental State Examination (MMSE) and had a Neuropsychiatric Inventory (NPI) score of 50 (Table 1), which included hallucination, agitation, disinhibition, irritability, aberrant motor behavior and night-time behavior. The right dorsal interosseous muscle and thenar muscle were atrophic, the muscle strength of his four extremities was reduced but somewhat incompatibility, and the muscle tone was elevated; bilateral Babinski signs were negative, In addition, his hands groped about, and he fell back when sitting. The cranial nerves, sensory system and reflexes were intact.

His clinical features supported lesions located in the cerebral cortex and basal ganglia and a probable diagnosis of cerebellum and anterior horn. Considering his tumor history, lack of trauma or poisoning, extensive involvement of the nervous system and subacute onset, etiological diagnoses were narrowed to tumor/paraneoplastic syndrome, inflammation or infection. Thus, we created the following workup.

MR imaging suggested ischemia within the periventricular area and centrum semiovale but revealed no contrast-enhanced lesions (Figure 1). Hematological screening was unremarkable, including a routine blood test, biochemistry, tumor marker, folate, vitamin B12, and thyroid function, as well as screenings for HIV, syphilis, and hepatitis B. A routine cerebrospinal fluid (CSF) test indicated normal pressure, leukocytosis (0×106/L), glucose and chlorine but mildly elevated protein levels (0.60 g/l, normal range 0.15–0.45 g/L). In serum and CSF autoantibody screening, anti-NMDA receptor, AMPA receptor 1 or 2, GABA-B receptor, LGI1, CASPR2 and DPPX6 IgG antibodies were negative, but anti-IgLON5 IgG antibody (serum: ++, 1:100; CSF: ++, 1:3.2) was positive, as shown in Figure 2. Human leukocyte antigen (HLA) typing did not reveal the presence of the HLA-DQB1*0501 or HLA-DRB1*1001 allele. A video electroencephalogram revealed increased slow activities without epileptic discharge. Ambulatory polysomnography (PSG) was conducted from 10 pm to 7 am and revealed extended stage N1 and N2 time, as well as shortened N3 and REM time; however, sleep efficiency was normal at 85.9%. During sleep time, he experienced 6 obstructive sleep apneic events, with an apnea hypopnea index of 6.7/h, and all 6 apnea events occurred during NREM sleep. The longest and mean apnea times were 42 s and 28 s, respectively.

TABLE 1 Results of longitudinal cognitive and psychiatric evaluations.

MMSE item	First evaluating score	Second evaluating score	Third evaluating score	Fourth evaluating score
Time frame	On admission (before immunotherapy)	On the 9th day of immunotherapy	On the 22nd day of immunotherapy	3months after discharge
Orientation	Not completed	6/10	4/10	5/10
Registration		2/3	3/3	3/3
Attention and calculation		0/5	0/5	0/5
Recall		0/3	0/3	0/3
Language and praxis		4/9	5/9	4/9
Total MMSE score		12/30	12/30	12/30
NPI item				
Delusion	0	4*3, 3	0	0
Hallucination	4*3, 3	4*3, 3	0	0
Agitation	3*2, 3	4*3, 3	0	0
Depression/dysphoria	0	3*1, 1	3*2, 1	3*2, 1
Anxitey	0	4*2, 1	3*2, 1	3*2, 1
Euphoria	0	0	0	0
Apathy	0	0	0	0
Disinhibition	2*1, 2	0	0	0
Irritability	3*2, 3	4*3, 3	2*1, 2	2*1, 2
Aberrant motor behavior	4*3, 2	4*3, 2	4*2, 1	4*2, 1
Night-time behavior	4*3, 5	4*3, 5	3*2, 3	3*2, 3
Appetite/eating changes	0	0	0	0
Total NPI score	50	83	28	28
Total disruption score	18	21	8	8

The subscales of NPI were expressed in frequency * severity, disruption score.

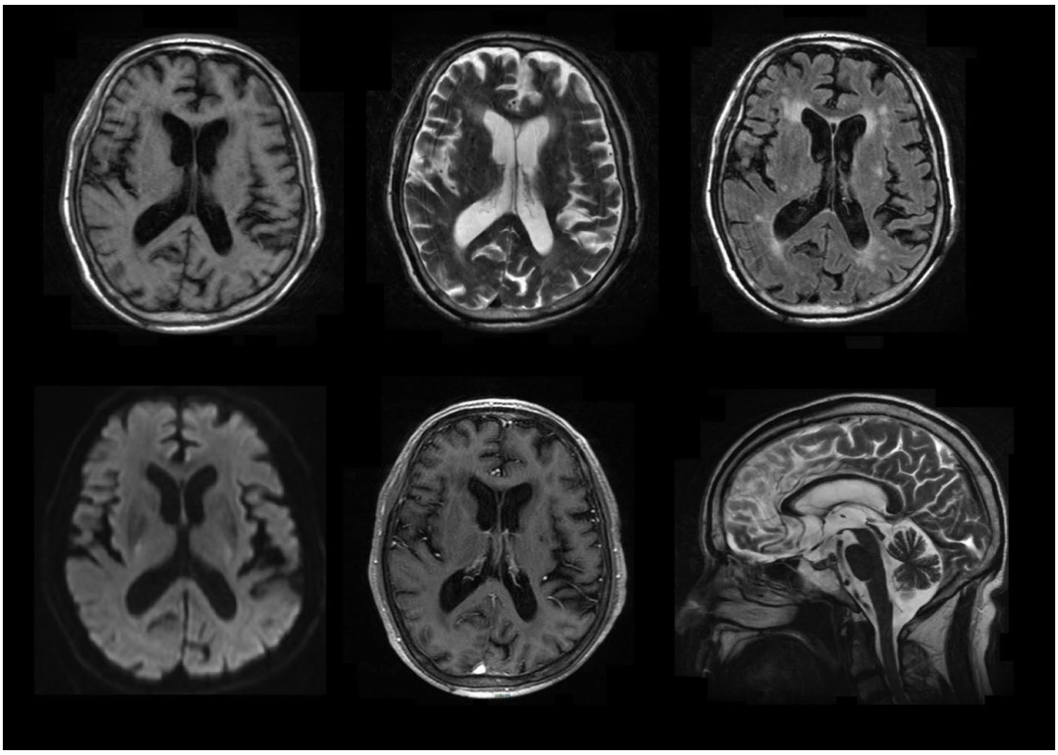

FIGURE 1
Selected brain MR images. It showed ischemia within the periventricular area and centrum semiovale but revealed no contrast-enhanced lesions.

Hypopnea occurred 34 times during NREM sleep and once during REM; the longest and mean hypopnea times were 172 s and 89.4 s, respectively. In addition, snoring occurred 438 times and accounted for 5% of his sleep time. His minimum SPO2 (64%) was recorded during NREM. However, no stridor was detected. Periodic leg movements occurred 50 and 51 times during NREM and wakefulness, respectively, with a mean power and duration of 17 dB and 1.7 s, respectively. Taken together, his PSG data suggested an aberrant sleep mode, characterized by disorganized sleep cycles, obstructive sleep apneic events, excessive snoring and increasing periodic leg movements. Nevertheless, PET-CT and electromyography data were unavailable because of his noncompliance. Therefore, he was confirmed to have anti-IgLON5 disease.

After hospitalization, he continued to take olanzapine 2.5 to 5 mg per night and was administered pramipexole and compound levodopa. When his diagnosis was confirmed, he was also treated with immunotherapy, including intravenous immunoglobulin (IVIG) 0.4 g/kg per day for 5 days, followed by intravenous methylprednisolone pulse therapy 500 mg per day for 5 days. Then, methylprednisolone was decreased to 80 mg per day, and mycophenolate mofetil 500 mg was administered twice a day. A follow-up evaluation was performed, as shown in Table 1. On the 9th day of immunotherapy, he was cooperative for MMSE evaluation, showing a total score of 12/30 and an improvement in orientation, immediate recall and naming and repetition function. However, his NPI score did not improve and indicated more severe delusion, agitation and irritability. Specifically, he accused his daughter and wife of attempting to kill him and intermittently shouted at and kicked them. On the 22nd day of immunotherapy, his MMSE score remained the same, but his NPI score decreased to 28; he mainly exhibited depression, anxiety, irritability, aberrant motor behavior and night-time behavior without hallucination, delusion or agitation. He was discharged home on the 26th day of immunotherapy and continued to take olanzapine, pramipexole, compound levodopa, mycophenolate mofetil and prednisolone orally 60 mg per day, with a decrease of 10 mg per month. At this time, his muscle atrophy and weakness remained at the same level, and abnormal movement had disappeared. Follow-up contacts at 3 and 6 months after discharge did not show further improvement, and follow-up contact at 12 months showed a final outcome of death due to cerebral hemorrhage. A schematic diagram of the clinical characterization and management of this male is shown in Figure 3.

Assays for CSF and serum autoantibody IgG were performed using cell-based indirect immune-fluorescence tests employing BIOCHIPs (EUROIMMUN AG, Luebeck, Germany) at EUROIMMUN Diagnostic Laboratory, China. Written informed consent for publication was obtained from the patient's legally authorized representative.

Discussion

Anti-IgLON5 disease is a rare and novel neurological disease. Fortunately, we adopted an up-to-date autoantibody screening method including a new item "anti-IgLON5 antibody" in this patient, especially when his sleep disruptions were unapparent. This finding is a humbling reminder that our clinicians should utilize new screening techniques and be aware of easily overlooked clinical signs.

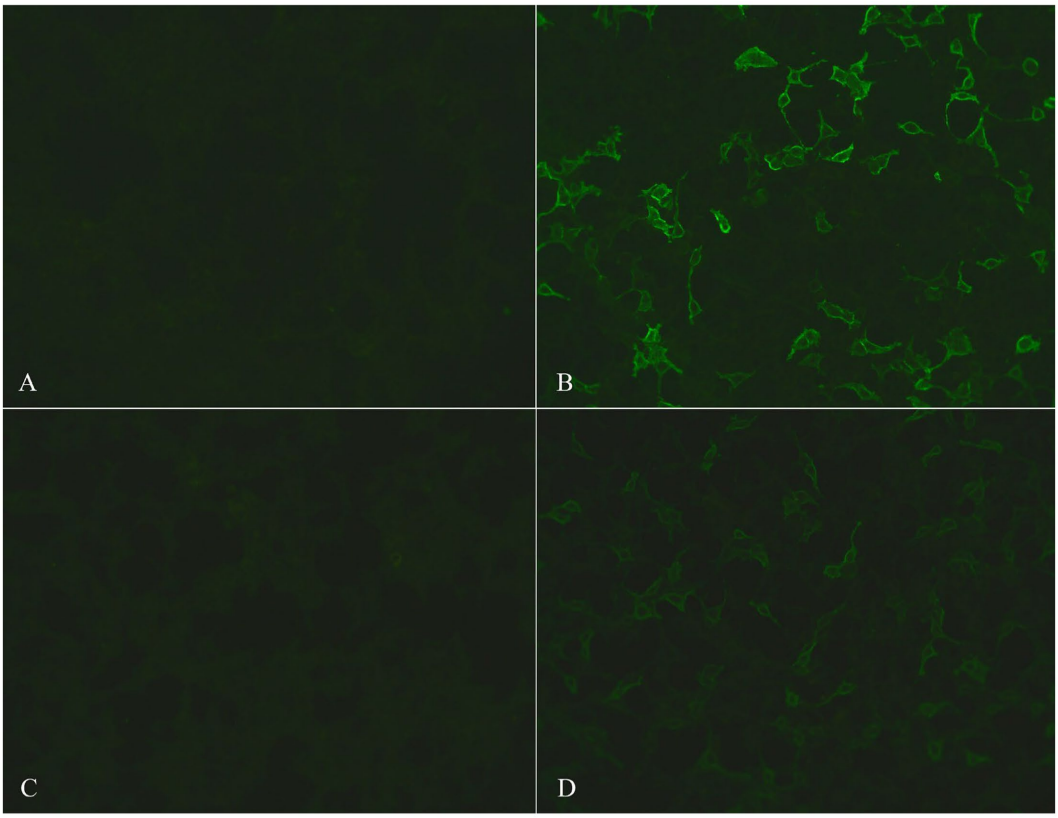

FIGURE 2
Photos of serum and CSF autoantibody screening. The photos of control-transfected cells in serum and CSF are shown in **(A)** and **(C)**, respectively; positive anti-IgLON5 antibodies in serum (++, 1:100) and CSF (++, 1:3.2) are shown in **(B)** and **(D)**, respectively.

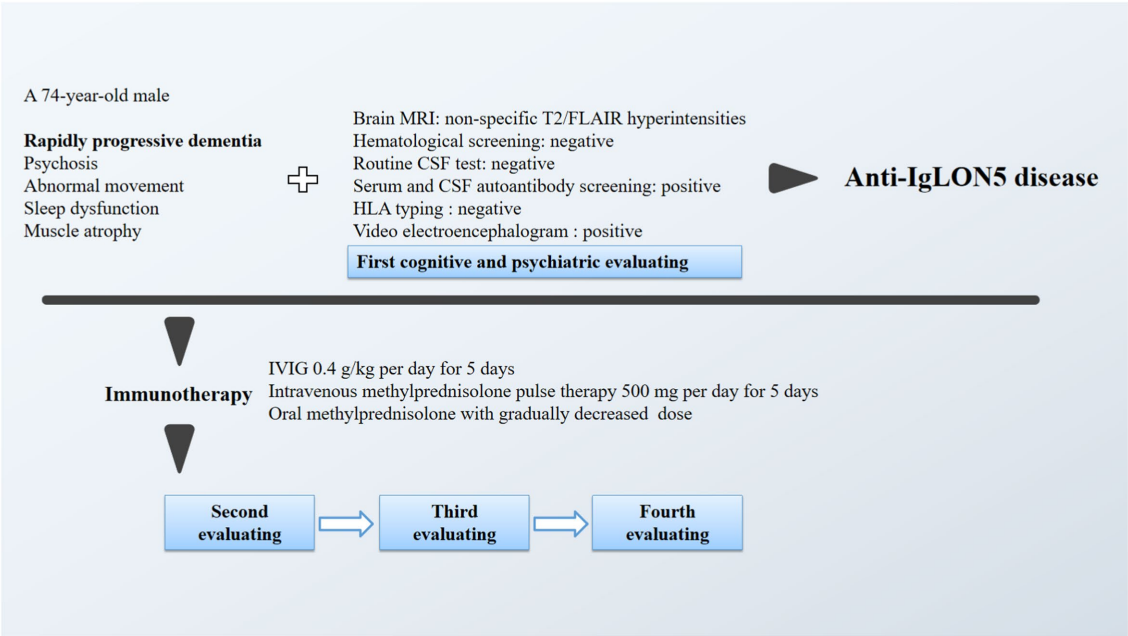

FIGURE 3
A schematic diagram of the clinical characterization and management of this male.

Here, we report a Chinese male with anti-IgLON5 disease who exhibited prominent RPD, overlapping sleep dysfunction, psychosis, abnormal movement, muscle atrophy and weakness. To our knowledge, RPD usually occurs over months, weeks or days. Given the established etiological categories of RPD, prion diseases are the leading causative factor; apart from neurodegenerative factors, autoimmune conditions are the second most common causative factor for nonprion RPD. In the literature, VGKC, Yo, Hu, Ma, CV2, GAD65 and other antibodies mediate autoimmune diseases (5). However, the current understanding of anti-IgLON5 disease is incomplete. To date, a few studies have examined this disease with RPD. Considering the rapid progression (< 3 months for memory deficits, which is considered rapid cognitive decline), a study reported this presentation in 3 patients with anti-IgLON5 disease and suggested that RPD was not a frequent clinical manifestation of this disease. Notably, patients in that study did not develop psychiatric symptoms (6). In addition, a recent study reported a female patient with anti-IgLON5 disease who presented with rapidly progressive cognitive decline, and she showed atypical inflammatory lesions on MRI, as well as HLA-DRB1*1001 and HLA-DQB1*0501 association (7). In contrast to other cases, our patient mostly exhibited rapid, extensive cognitive impairment that impacted orientation, execution, memory and language function. For example, he could state his name but could not identify his wife and daughter, state where he was or when it was, calculate 100 minus 7, or repeat what we said. Those issues occurred within 1 month; thus, these features were consistent with a diagnosis of RPD. Simultaneously, this man initially exhibited psychotic positive symptoms, including hallucination, agitation, disinhibition and irritability. In addition, the characteristics of PSG were evidenced by his sleep disruption. However, this male patient did not show HLA-DRB1*1001 and HLA-DQB1*0501 associations.

Furthermore, we longitudinally described his cognitive and psychological performance in detail and explored his response to immunotherapy and symptomatic treatment. With respect to immunotherapy options, IVIG combined with methylprednisolone and mycophenolate mofetil was administered to this patient. Notably, this therapy was associated with mild improvement in cognition at the initial stage, especially in the domains of orientation, registration and language function; as a consequence, he could somewhat communicate with others on the 9th day of immunotherapy. However, this performance did not further improve afterward, and prominent impairment of attention, calculation and recall function persisted. Moreover, his psychotic positive symptoms resolved and were replaced by psychotic negative symptoms, such as depression and anxiety. A longitudinal follow-up of his clinical course at 12 months revealed a poor outcome. This case indicated by this case, that immunotherapy combined with symptomatic treatment was partially effective for anti-IgLON5 disease at an early stage.

However, the exact mechanism of anti-IgLON5 antibody in this clinical manifestation, disease course and improved response remains unclear. Previous studies have indicated an intriguing association between tauopathy and anti-IgLON5 disease. Neuropathological features suggested noninflammatory pathology with tau hyperphosphorylation and accumulation in several brain regions, preferentially involving the hypothalamus, brainstem tegmentum and upper spinal cord (8), and appeared to support a chronic disease course. A possible explanation may lie in the membrane stabilization of IgLON5. The rapid disruption of IgLON5 may have induced corresponding tau hyperphosphorylation and accumulation; in turn, antibody-mediated effects repaired this disruption (9). HLA association might be a reason for disease recovery (8). Thus, we assume that the improved response may be associated with the opportunity to initiate this therapy; earlier treatment is better, especially before the formation of tauopathy.

Conclusion

We longitudinally described a patient with anti-IgLON5 disease, particularly his presentation of RPD and the curative effect. Our findings support the hypothesis that anti-IgLON5 antibody-mediated effects and HLA association modulate the disease course and its improved response, further promoting our understanding of the mechanisms underlying cognitive and psychological recovery. In addition, anti-IgLON5 disease should be considered a possible differential diagnosis in patients with RPD.

Data availability statement

The original contributions presented in the study are included in the article/supplementary material, further inquiries can be directed to the corresponding authors.

Ethics statement

Written informed consent was obtained from the patient' s legally authorized representative for the publication of this case report.

Author contributions

XL, ZF, and QK participated in the clinical treatment and writing of the study. XC, YZ, FH, and XM participated in the sample collection and analyses of the results. XL and QK gave the pivotal answers and guidance to the manuscript revision. All authors contributed to the article and approved the submitted version.

Funding

This work was supported by the National Natural Science Foundation of China (81801056).

Conflict of interest

The authors declare that the research was conducted in the absence of any commercial or financial relationships that could be construed as a potential conflict of interest.

Publisher's note

References

1. Geschwind MD, Haman A, Miller BL. Rapidly progressive dementia. *Neurol Clin*. (2007) 25:783–807, vii. doi: 10.1016/j.ncl.2007.04.001

2. Sabater L, Gaig C, Gelpi E, Bataller L, Lewerenz J, Torres-Vega E, et al. A novel non-rapid-eye movement and rapid-eye-movement parasomnia with sleep breathing disorder associated with antibodies to IgLON5: a case series, characterisation of the antigen, and post-mortem study. *Lancet Neurol*. (2014) 13:575–86. doi: 10.1016/S1474-4422(14)70051-1

3. Simabukuro MM, Sabater L, Adoni T, Cury RG, Haddad MS, Moreira CH, et al. Sleep disorder, chorea, and dementia associated with IgLON5 antibodies. *Neurol Neuroimmunol Neuroinflamm*. (2015) 2:e136. doi: 10.1212/NXI.0000000000000136

4. Graus F, Santamaria J. Understanding anti-IgLON5 disease. *Neurol Neuroimmunol Neuroinflamm*. (2017) 4:e393. doi: 10.1212/NXI.0000000000000393

5. Geschwind MD, Shu H, Haman A, Sejvar JJ, Miller BL. Rapidly progressive dementia. *Ann Neurol*. (2008) 64:97–108. doi: 10.1002/ana.21430

6. Escudero D, Guasp M, Ariño H, Gaig C, Martínez-Hernández E, Dalmau J, et al. Antibody-associated CNS syndromes without signs of inflammation in the elderly. *Neurology*. (2017) 89:1471–5. doi: 10.1212/WNL.0000000000004541

7. Montagna M, Amir R, De Volder I, Lammens M, Huyskens J, Willekens B. IgLON5-associated encephalitis with atypical brain magnetic resonance imaging and cerebrospinal fluid changes. *Front Neurol*. (2018) 9:329. doi: 10.3389/fneur.2018.00329

8. Gelpi E, Höftberger R, Graus F, Ling H, Holton JL, Dawson T, et al. Neuropathological criteria of anti-IgLON5-related tauopathy. *Acta Neuropathol*. (2016) 132:531–43. doi: 10.1007/s00401-016-1591-8

9. Hashimoto T, Yamada M, Maekawa S, Nakashima T, Miyata S. IgLON cell adhesion molecule Kilon is a crucial modulator for synapse number in hippocampal neurons. *Brain Res*. (2008) 1224:1–11. doi: 10.1016/j.brainres.2008.05.069

frontiers | Frontiers in Neurology

TYPE Case Report
PUBLISHED 28 April 2023
DOI 10.3389/fneur.2023.1170557

OPEN ACCESS

EDITED BY
Bruce Miller,
University of California, San Francisco, United States

REVIEWED BY
Anastasia Bougea,
National and Kapodistrian University of Athens, Greece
Celeste Panteghini,
IRCCS Carlo Besta Neurological Institute Foundation, Italy

*CORRESPONDENCE
Yilun Tao
✉ yltao21@163.com

†These authors have contributed equally to this work and share first authorship

RECEIVED 21 February 2023
ACCEPTED 04 April 2023
PUBLISHED 28 April 2023

CITATION
Tao Y, Zhao C, Han D, Wei Y, Wang L, Song W and Li X (2023) Typical pantothenate kinase-associated neurodegeneration caused by compound heterozygous mutations in *PANK2* gene in a Chinese patient: a case report and literature review.
Front. Neurol. 14:1170557.
doi: 10.3389/fneur.2023.1170557

Typical pantothenate kinase-associated neurodegeneration caused by compound heterozygous mutations in *PANK2* gene in a Chinese patient: a case report and literature review

Yilun Tao[1*†], Chen Zhao[2†], Dong Han[1†], Yiju Wei[3,4], Lihong Wang[2], Wenxia Song[5] and Xiaoze Li[1]

[1]Medical Genetic Center, Changzhi Maternal and Child Health Care Hospital, Changzhi, Shanxi, China, [2]Department of Pediatrics, Changzhi Maternal and Child Health Care Hospital, Changzhi, Shanxi, China, [3]School of Life Sciences, Shandong First Medical University and Shandong Academy of Medical Sciences, Jinan, Shandong, China, [4]Medical Science and Technology Innovation Center, Shandong First Medical University and Shandong Academy of Medical Sciences, Jinan, Shandong, China, [5]Obstetrics Department, Changzhi Maternal and Child Health Care Hospital, Changzhi, Shanxi, China

Pantothenate kinase-associated neurodegeneration (PKAN) is a rare genetic neurodegenerative disorder with brain iron accumulation characterized as dysarthria, spasticity, cognitive impairment, parkinsonism, and retinopathy. PKAN is caused by biallelic mutations in the mitochondrial pantothenate kinase 2 (*PANK2*) gene. Herein, we report a 4-year-old patient with PKAN from a Han Chinese family, who presented with developmental regression, progressive inability to walk, and limb tremors. Neuroimaging demonstrated "eye-of-the-tiger" sign. Whole exome sequencing (WES) identified compound heterozygous mutations of c.1213T>G (p.Tyr405Asp) and c.1502T>A (p.Ile501Asn) in *PANK2* gene. In addition, a review of all known *PANK2* variants observed in reported PKAN patients was conducted, to improve understanding of the genotype-phenotype associations that occur in PKAN patients.

KEYWORDS

***PANK2* gene, pantothenate kinase-associated neurodegeneration, whole exome sequencing, case report, review**

Introduction

Pantothenate kinase-associated neurodegeneration (PKAN, MIM 234200) is a rare autosomal recessive disorder characterized by progressive iron accumulation in the basal ganglia and other regions of the brain, resulting in extrapyramidal movements such as parkinsonism and dystonia (1). On brain magnetic resonance imaging (MRI), abnormalities are restricted to the globus pallidus and substantia nigra in most cases of PKAN, with almost 100% having an "eye of the tiger" sign (2, 3). PKAN incidence is extremely low, reaching ~1–3/1,00,00,000 globally (4, 5), but the accurate prevalence of PKAN is unclear, particularly in the Chinese population.

The disease was first described in 1922 by two German physicians, Hallervorden and Spatz (6). In 2001, the cause of PNAK was determined to be a homozygous or compound heterozygous mutation in *PANK2* gene (MIM 606157), which is located on chromosome 20p13 and encodes a pantothenate kinase (7). The enzyme localizes to the mitochondria and phosphorylates pantothenate to synthesize coenzyme A (CoA) (8). Impaired activity of this pantothenate kinase may lead to increased levels of cysteine and its intermediate products in the basal ganglia. And meanwhile, iron accumulates with an unexplained mechanism. Cysteine can be chelated with iron and rapidly oxidizes itself. The resulting free cysteine disturbs energy metabolism and has a toxic effect on cell membrane synthesis, which can eventually result in central nervous system dysfunction (9, 10).

According to the age at onset, rate of progression, and severity of motor symptoms, PKAN can be classified into two subtypes: typical and atypical (2, 3). In typical PKAN, symptoms present within the first decade of life and usually progress rapidly, with loss of ambulation ~10–15 years later. In the atypical form, patients have an onset in the second decade, with slower progression and variable clinical features. Patients may still ambulate decades after disease onset.

In this study, we described the clinical phenotypes, biochemical features, and genetic findings of a Chinese patient with PKAN who had compound heterozygous mutations c.1213T>G (p.Tyr405Asp) and c.1502T>A (p.Ile501Asn) of *PANK2*. Furthermore, we review the clinical and genetic features of reported PKAN patients, to help understand the genotype-phenotype relationship of PKAN.

Clinical report

The proband, a 4-year-old female, was the first-born child of healthy and non-consanguineous Chinese parents. No history of genetic diseases exists in her family. The mother had no history of teratogenic pathogens or drug exposure during gestation. The birth weight was 3,770 g (75th percentile), and the birth length was 51 cm (50th percentile) at week 41 of gestation. At 18 months of age, the subject could walk with some aid but exhibited poor balance. At 3 years and 11 months of age, she exhibited developmental regression and could not walk, with progressive tremors in both the upper limbs and choreoathetosis. She had superimposed choreiform movements, mainly involving the distal upper limbs, and displayed involuntary self-injurious behavior (Figure 1A). Meanwhile, she exhibited progressive backward language formation and mental, intellectual disability retardation; she could not speak even simple words such as "baba" and "mama." She seldom responded to language and was in a nearly semi-vegetative state. No feeding difficulties or dysphagia were found, and ophthalmological examination yielded normal results. Brain MRI at 4 years of age displayed a typical "eye-of-the-tiger" sign (Figure 1B). The child previously underwent rehabilitation therapy for several months; however, the effect was unsatisfactory. The couple underwent clinical genetic counseling and considered a prenatal diagnosis in a future pregnancy.

Materials and methods

Genetic analysis

A peripheral blood sample of the patient was collected. Genomic DNA was extracted using QIAamp DNA Mini Kit (Qiagen, China). DNA library preparation was performed following Illumina protocols, which included end repair, adapter ligation, and PCR enrichment. The amplified DNA was then captured using a Whole Exome Capture Kit (MyGenostics Inc., Beijing, China). Biotinylated capture probes were designed to tile all exons without repeating regions. The enriched libraries were sequenced for paired-end reads of 150 bp using Illumina HiSeq × Ten platforms.

After sequencing, the clean reads were aligned to the UCSC hg19 human reference genome using the Burrows-Wheeler Alignment tool. Duplicate reads were removed using Picard (http://broadinstitute.github.io/picard). Insertions, deletions, and SNP variants were detected and filtered using the Genome Analysis Toolkit. The identified variants were annotated using ANNOVAR and associated with the following databases: 1,000 Genomes, Exome Aggregation Consortium (ExAC), GnomAD Database, and Human Gene Mutation Database (HGMD). In addition, the identified variants were predicted using Amino acid substitutions were studied *in silico* to predict the pathogenic effect of the change using VarSome (https://varsome.com/), which utilizes multiple bioinformatic algorithms. Pathogenicity of the mutations was explored following the American College of Medical Genetics and Genomics guidelines (ACMG). Candidate variable sites were confirmed using Sanger sequencing of the patient and his parents. Target sequences were sequenced on an ABI 3730 genetic analyzer (Applied Biosystems, Foster City Carlsbad, CA, USA) and identified using Chromas 2.6.5 (Technelysium Pty Ltd, Australia).

Literature review

A literature search of PubMed, MEDLINE, and EMBASE databases for articles published on PKAN on August 1, 2022, was conducted. The following keywords were used in the literature search: "pantothenate kinase-associated neurodegeneration" or "*PANK2*." Pertinent articles found using the keywords and with definite molecular genetic features of PKAN were screened, and the clinical and genetic findings and prognosis conditions of patients were summarized.

Results

Whole exome sequencing (WES) data of the proband demonstrated two variants in *PANK2,* c.1213T>G (p.Tyr405Asp) and c.1502T>A (p.Ile501Asn) of transcript NM_153638.3, which were validated by Sanger sequencing (Figure 2A). The father was heterozygous for p.Ile501Asn and the mother was heterozygous for p.Tyr405Asp. Amino acid sequence alignment depicted that p.Tyr405Asp and p.Ile501Asn are highly conserved across different organisms, indicating that any non-synonymous change at positions 405 and 501 of PANK2 can be deleterious

10.3389/fneur.2023.1170557

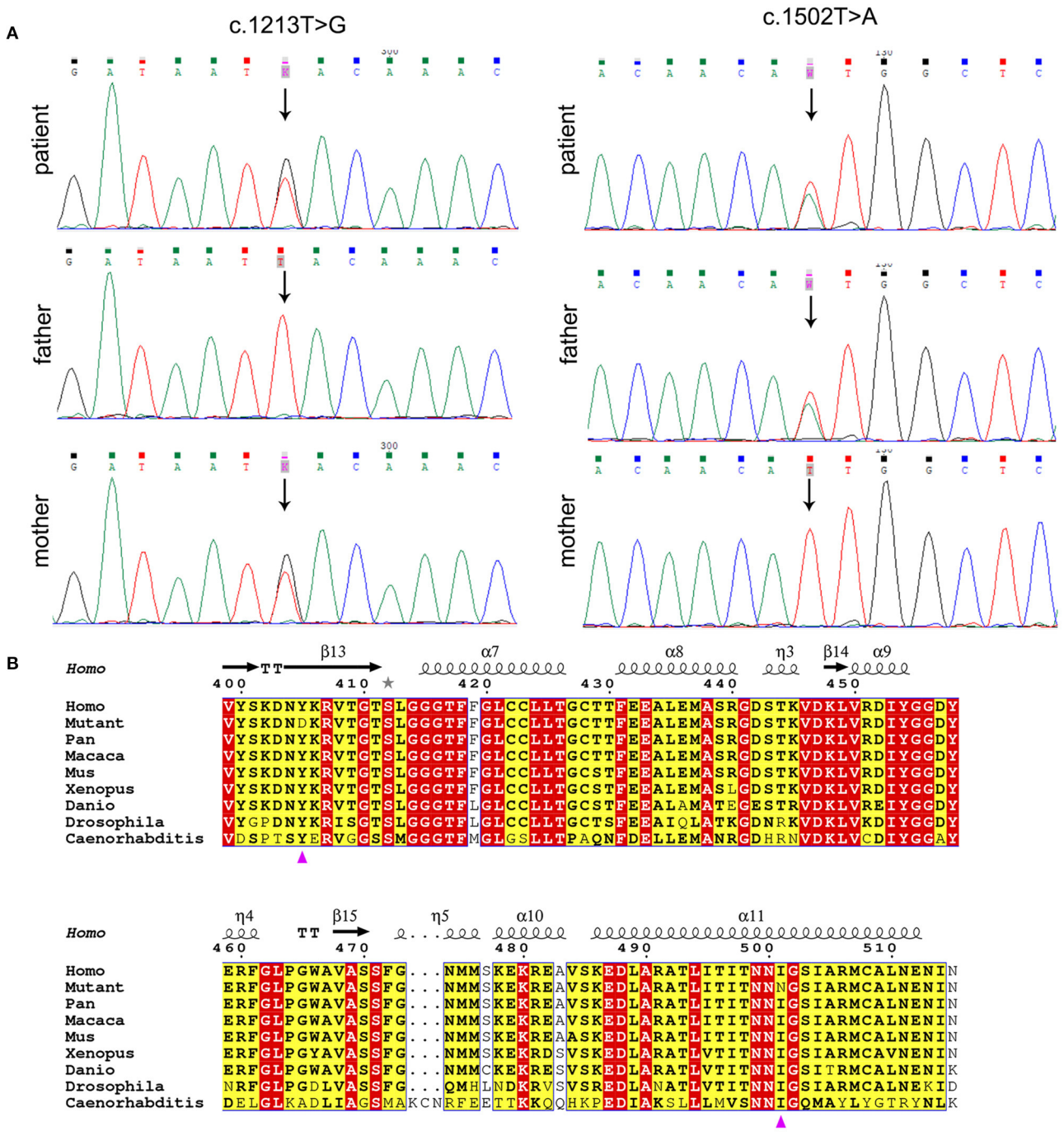

FIGURE 1
Clinical features and MRI examination of the proband. **(A)** Body scratches and bruise on the extremities by self-harm. **(B)** T2-weighted brain magnetic resonance image, showing the "eye-of-the-tiger" sign in the globus pallidus (arrow) at 4 years of age.

(Figure 2B). CADD values through VarSome were 26.7 for both two variants, also indicating the pathogenicity of both variants. According to ACMG classification, the two variants p.Tyr405Asp and p.Ile501Asn were predicted to be "likely pathogenic" (PP3_Strong+PM3+PM2_supporting) and "pathogenic" (PP3_Strong+PM3_strong+PM5+PM2_supporting). PAKN diagnosis in the proband was confirmed based on molecular genetics and available clinical findings.

Discussion

In this study, we report a case of typical PKAN in a patient who presented with developmental regression, dystonia, progressive inability to walk, limb tremors, cognitive impairment, and dysarthria. Two compound heterozygous variants in exons 3 (p.Tyr405Asp) and 5 (p.Ile501Asn) were identified. This novel genotype was found for the first time in this study, as far as

we know. Although p.Tyr405Asp was first reported in 2005 (3), no more cases have been reported, and this is the first report of this variant in China. Bioinformatic analysis revealed that the two variants were damaging, and the clinical presentation of the patient was compatible with PKAN. These findings indicate that p.Tyr405Asp and p.Ile501Asn variants are associated with PKAN pathogenesis. However, further functional studies are required to validate the pathogenicity of these variants.

The comprehensive clinical features and genetic analysis of 270 reported cases of PKAN (including the present case) are summarized in Supplementary Table 1. The majority of patients were Asian (96, 35.56%) or European (46, 17.04%). Among 266 patients with clear onset age, 167 cases (62.78%) showed the typical form, and 99 (37.21%), the atypical one. The mean age at presentation was 9.87 years (range 0.5–48). There is no sex-related difference in prevalence of PKAN, which were 52.34% (134/256) for males and 47.66% (122/256) for males, as well as in survival of PKAN ($p = 0.8355$). Most of the patients presented with dystonia (238/251, 94.82%), "eye-of-the-tiger" sign on MRI (246/258, 95.35%), gait disturbance (205/225, 91.11%), and dysarthria (174/198, 87.88%). Other common phenotypes included pyramidal signs (113/166, 68.07%), cognitive impairment (110/177, 62.14%), choreoathetosis (22/41, 53.66%), parkinsonism (68/127, 53.54%), ocular abnormalities (86/174, 49.43%), tremor (45/85, 52.94%), and developmental delay (25/72, 34.72%). In some patients (59/132, 44.70%), behavioral abnormalities developed, including psychosis, depression, hyperactivity, or obsessive-compulsive disorder. Only a few cases ($n = 8$) presented with seizures (11–16).

A total of 163 distinct *PANK2* variants were identified in these 270 patients (Supplementary Table 2), which were annotated based on transcript NM_153638.3. These 163 *PANK2* variants corresponded to 104 missenses, 31 frameshifts, 12 splice-sites, 11 non-senses and 5 large deletions. Variants were unevenly distributed throughout *PANK2* gene but were mainly concentrated in the exons (147/163, 90.18%), but particularly concentrated in exon 2 (27.61%), 3 (15.34%), and 4 (13.50%). One hundred and nine variants (66.87%) were observed only once or twice, indicating a high genetic heterogeneity among PKAN patients. The three most prevalent variants were p.Gly521Arg (5.91%), p.Asn404Ile (4.07%), and p.Thr528Met (3.88%), but have never been reported in the Chinese population. In addition, 114 out of 163 variants were absent in the Chinese population, and 40 variants were unique to the Chinese population. The six most prevalent variants in China, including p.Glu149Ter, p.Asp324Tyr,

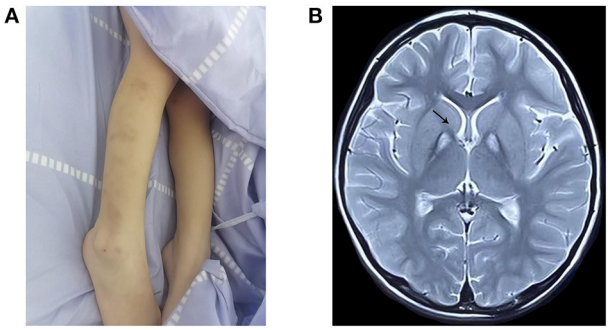

FIGURE 2
Molecular analysis of *PANK2* variants. **(A)** *PANK2* gene sequencing of the patient and his parents. The patient carried compound heterozygous PANK2 gene mutations of c.1213T>G and c.1502T>A; the father carried c.1502T>A, and the mother carried c.1213T>G. Arrow indicates the location of variants. **(B)** Multiple sequence alignment of PANK2 from different organisms. Residues are colored based on conservation. The white letters in red boxes represent the highest conservation-grade, black letters in yellow boxes represent the second-highest conservation grade, and no color indicates the least conserved grade. The variants p.Tyr405Asp and p.Ile501Asn are indicated by a purple triangle.

TABLE 1 Clinical features of PKAN patients.

Clinical feature	Frequency in reported affected individuals with pathogenic PANK2 variants			
	M/M[a]	N/N or M/N[a]	Total	This study
Eye-of-the-tiger	149/156 (95.51%)	97/102 (95.10%)	246/258 (95.35%)	+
Tremor	31/60 (51.67%)	14/25 (56.00%)	45/85 (52.94%)	+
Parkinsonism	40/81 (49.38%)	28/46 (60.87%)	68/127 (53.54%)	/
Developmental delay	14/46 (30.43%)	11/26 (42.31%)	25/72 (34.72%)	+
Pyramidal signs	59/95 (62.11%)	54/71 (76.06%)	113/166 (68.07%)	+
Choreoathetosis	12/23 (52.17%)	10/18 (55.56%)	22/41 (53.66%)	+
Dystonia	142/153 (92.81%)	96/98 (97.96%)	238/251 (94.82%)	+
Cognitive impairment	60/104 (57.69%)	50/73 (68.49%)	110/177 (62.14%)	+
Dysarthria	104/122 (85.25%)	70/76 (92.11%)	174/198 (87.88%)	+
Dysphagia	29/64 (45.31%)	24/34 (70.59%)	53/98 (54.08%)	-
Gait disturbance	123/135 (91.11%)	83/91 (91.21%)	205/225 (91.11%)	+
Abnormality of the ocular region	45/106 (42.45%)	42/69 (60.87%)	86/174 (49.43%)	–
Behavioral abnormality	43/95 (45.26%)	16/37 (43.24%)	59/132 (44.70%)	–

[a]M, missense allele; N, null allele, null alleles were defined as those containing non-sense, frameshift, or canonical splice site variants.

p.Asp378Gly, p.Asp452Gly, p.Ile501Thr and p.Phe519Leu, were only reported in Asia, including China, Korea, and Taiwan (4, 17–24). This finding indicates that the variants in *PANK2* are population-specific.

The genotypes of the 270 PKAN patients were found to be highly heterogeneous, with more than 45% of the patients presenting with a unique genotype, and 56.67% (153/270) with homozygous genotypes. A high amount of consanguineous marriages (45/115, 39.13%) may have contributed to the homogeneity. However, in China, only 29.41% (15/51) of the patients carried homozygous mutations, with a lower rate of consanguineous marriage (1/21, 4.76%).

In the current study, null *PANK2* alleles were defined as those containing non-sense, frameshift, and/or canonical splice site variants. Patients were divided into two groups with different genotypes: (i) M/M (missense/missense) (n = 161) and (ii) M/N (missense/null) or N/N (null/null) (n = 109). The age at onset was significantly earlier in "N/N" or "M/N" group than "M/M" group (median = 7.18 years vs. 11.24 years, p = 0.0003), and the ratio of typical early-onset patients in "N/N" or "M/N" group was larger than that in "M/M" group (80/107 vs. 87/159, 0.0009). Although there was no difference in survival of PKAN between patients with N/N or M/N and M/M genotypes (p = 0.4122), the death age was slight younger in those with null variants (median = 12.64 years vs. 14.80 years). Moreover, incidence of most phenotypes of the individuals with genotype "N/N" or "M/N" was larger compared with that of "M/M" group (Table 1). Taken together, these results indicate that patients with null variants might have a relatively poor survival. In this study, the proband carried compound heterozygous missense variants and was grouped in "M/M" genotype class. She appeared normal at birth, and there were no concerns about her development until over 3 years of age. The patient presented with the typical clinical manifestations of PKAN and a relatively poor prognosis. The patient also showed involuntary self-injurious behavior, which was not observed in any other PKAN patients, and poses challenges to the treatment and care of these patients.

In summary, a novel genotype of *PANK2*, c.1213T>G and c.1502T>A, was identified in this study. These findings provide further information regarding the genetic variants that cause PKAN. The review section describes all known *PANK2* variants, thus providing a basis for exploring genotype-phenotype correlations of PKAN.

Data availability statement

The original contributions presented in the study are publicly available. This data can be found here: NCBI, accession number SRR23634966.

Ethics statement

The studies involving human participants were reviewed and approved by Clinical Research Ethics Committee of Changzhi Maternal and Child Health Care Hospital. Written informed consent to participate in this study was provided by the participants' legal guardian/next of kin. Written informed consent was obtained from the individual(s), and minor(s)' legal guardian/next of kin, for the publication of any potentially identifiable images or data included in this article.

Author contributions

CZ and DH performed the experiment and patient follow-up. YT conceived and designed the experiment, conducted genetic data acquisition and interpretation, reviewed the published cases, and wrote the manuscript. CZ, LW, and XL performed in patient management. WS provided the clinical treatment guidance. YW analyzed the data and revised the manuscript. All authors have read and approved the final manuscript.

Acknowledgments

We are grateful to the patient and her families in our research. We express our gratitude to all the pediatricians who helped with this study.

Conflict of interest

The authors declare that the research was conducted in the absence of any commercial or financial relationships that could be construed as a potential conflict of interest.

Publisher's note

Supplementary material

The Supplementary Material for this article can be found online at: https://www.frontiersin.org/articles/10.3389/fneur.2023.1170557/full#supplementary-material

References

1. Gregory A, Polster BJ, Hayflick SJ. Clinical and genetic delineation of neurodegeneration with brain iron accumulation. *J Med Genet.* (2009) 46:73–80. doi: 10.1136/jmg.2008.061929

2. Hayflick SJ, Westaway SK, Levinson B, Zhou B, Johnson MA, Ching KHL, et al. Genetic, clinical, and radiographic delineation of Hallervorden-Spatz syndrome. *N Engl J Med.* (2003) 348:33–40. doi: 10.1056/NEJMoa020817

3. Pellecchia MT, Valente EM, Cif L, Salvi S, Albanese A, Scarano V, et al. The diverse phenotype and genotype of pantothenate kinase-associated neurodegeneration. *Neurology.* (2005) 64:1810–2. doi: 10.1212/01.WNL.0000161843.52641.EC

4. Mak CM, Sheng B, Lee HH, Lau K, Chan W, Lam C, et al. Young-onset parkinsonism in a Hong Kong Chinese man with adult-onset Hallervorden-Spatz syndrome. *Int J Neurosci.* (2011) 121:224–7. doi: 10.3109/00207454.2010.542843

5. Brezavar D, Bonnen PE. Incidence of PKAN determined by bioinformatic and population-based analysis of ~140,000 humans. *Mol Genet Metab.* (2019) 128:463–9. doi: 10.1016/j.ymgme.2019.09.002

6. Hallervorden J, Spatz H. Eigenartige erkrankung im extrapyramidalen system mit besonderer beteiligung des globus pallidus und der substantia nigra. *Zeitschrift Gesamte Neurol Psychiatr.* (1922) 79:254–302. doi: 10.1007/BF02878455

7. Zhou B, Westaway SK, Levinson B, Johnson MA, Gitschier J, Hayflick SJ. A novel pantothenate kinase gene (PANK2) is defective in Hallervorden-Spatz syndrome. *Nat Genet.* (2001) 28:345–9. doi: 10.1038/ng572

8. Alfonso-Pecchio A, Garcia M, Leonardi R, Jackowski S. Compartmentalization of mammalian pantothenate kinases. *PLoS ONE.* (2012) 7:e49509. doi: 10.1371/journal.pone.0049509

9. Tonekaboni SH, Mollamohammadi M. Neurodegeneration with brain iron accumulation: an overview. *Iran J child Neurol.* (2014) 8:1–8. doi: 10.22037/ijcn.v8i4.7574

10. Williams S, Gregory A, Hogarth P, Hayflick SJ, Gillingham MB. Metabolism and energy requirements in pantothenate kinase-associated neurodegeneration. *Mol Genet Metab.* (2013) 110:336–41. doi: 10.1016/j.ymgme.2013.06.017

11. Angural A, Singh I, Mahajan A, Pandoh P, Dhar MK, Kaul S, et al. A variation in PANK2 gene is causing Pantothenate kinase-associated Neurodegeneration in a family from Jammu and Kashmir - India. *Sci Rep.* (2017) 7:4834. doi: 10.1038/s41598-017-05388-9

12. Camargos ST, Gurgel-Giannetti J, Lees A, Hardy J, Singleton A, Cardoso F. Low prevalence of PANK2 mutations in Brazilian patients with early onset generalised dystonia and basal ganglia abnormalities on MRI. *J Neurol Neurosurg Psychiatry.* (2011) 82:1059–60. doi: 10.1136/jnnp.2009.200808

13. Dastsooz H, Nemati H, Fard MAF, Fardaei M, Faghihi MA. Novel mutations in PANK2 and PLA2G6 genes in patients with neurodegenerative disorders: two case reports. *BMC Med Genet.* (2017) 18:87. doi: 10.1186/s12881-017-0439-y

14. Li A, Paudel R, Johnson R, Courtney R, Lees AJ, Holton JL, et al. Pantothenate kinase-associated neurodegeneration is not a synucleinopathy. *Neuropathol Appl Neurobiol.* (2013) 39:121–31. doi: 10.1111/j.1365-2990.2012.01269.x

15. Dezfouli MA, Alavi A, Rohani M, Rezvani M, Nekuie T, Klotzle B, et al. PANK2 and C19orf12 mutations are common causes of neurodegeneration with brain iron accumulation. *Mov Disord.* (2013) 28:228–32. doi: 10.1002/mds.25271

16. Gatto E, Etcheverry JL, Converso DP, Bidinost C, Rosa A. Pantothenate kinase-associated neurodegeneration: novel mutations in the PANK2 gene in an Argentinean young woman. *Mov Disord.* (2010) 25:2262–64. doi: 10.1002/mds.23063

17. Wu YR, Chen C, Chao CY, Lyu RK, Lee-Chen GJ. Pantothenate kinase-associated neurodegeneration in two Taiwanese siblings: identification of a novel PANK2 gene mutation. *Mov Disord.* (2009) 24:940–1. doi: 10.1002/mds.22458

18. Lee JH, Park J, Ryu HS, Park H, Kim YE, Hong JY, et al. Clinical heterogeneity of atypical pantothenate kinase-associated neurodegeneration in Koreans. *J Mov Disord.* (2016) 9:20–7. doi: 10.14802/jmd.15058

19. Seo JH, Song SK, Lee PH. A novel PANK2 mutation in a patient with atypical pantothenate-kinase-associated neurodegeneration presenting with adult-onset parkinsonism. *J Clin Neurol.* (2009) 5:192–4. doi: 10.3988/jcn.2009.5.4.192

20. Zhang Y, Zhou D, Yang T. Novel PANK2 mutation in a Chinese boy with PANK2-associated neurodegeneration: a case report and review of Chinese cases. *Medicine.* (2019) 98:e14122. doi: 10.1097/MD.0000000000014122

21. Sakpichaisakul K, Saengow VE, Suwanpratheep P, Rongnoparat K, Panthan B, Trachoo O. Novel PANK2 mutation discovered among South East Asian children living in Thailand affected with pantothenate kinase associated neurodegeneration. *J Clin Neurosci.* (2019) 66:187–90. doi: 10.1016/j.jocn.2019.04.017

22. Ma LY, Wang L, Yang YM, Lu Y, Cheng FB, Wan XH. Novel gene mutations and clinical features in patients with pantothenate kinase-associated neurodegeneration. *Clin Genet.* (2015) 87:93–5. doi: 10.1111/cge.12341

23. Chang X, Zhang J, Jiang Y, Yao B, Wang J, Wu Y. Pilot trial on the efficacy and safety of pantethine in children with pantothenate kinase-associated neurodegeneration: a single-arm, open-label study. *Orphanet J Rare Dis.* (2020) 15:248. doi: 10.1186/s13023-020-01530-5

24. Guk HS, Koo DL, Nam H. Continuous positive airway pressure therapy in a patient with pantothenate-kinase-associated neurodegeneration. *J Clin Neurol.* (2019) 15:583–4. doi: 10.3988/jcn.2019.15.4.583

frontiers | Frontiers in Neurology

TYPE Case Report
PUBLISHED 25 May 2023
DOI 10.3389/fneur.2023.1190981

OPEN ACCESS

EDITED BY
Bruce Miller,
University of California, San Francisco,
United States

REVIEWED BY
Tomohiko Ishihara,
Niigata University, Japan
Akihiko Mitsutake,
The University of Tokyo Hospital, Japan

*CORRESPONDENCE
Qian Yang
✉ yangqian120@126.com
Xinfa Mao
✉ 2954935565@qq.com

RECEIVED 21 March 2023
ACCEPTED 10 May 2023
PUBLISHED 25 May 2023

CITATION
Zhu Y, Yang Q, Tian Y, Fan W and Mao X (2023) Rapidly progressive adult-onset neuronal intranuclear inclusion disease beginning with autonomic symptoms: a case report. *Front. Neurol.* 14:1190981. doi: 10.3389/fneur.2023.1190981

Rapidly progressive adult-onset neuronal intranuclear inclusion disease beginning with autonomic symptoms: a case report

Yi Zhu[1], Qian Yang[2]*, Yun Tian[3], Weibing Fan[2] and Xinfa Mao[2]*

[1]Department of Anesthesiology, Hunan Children's Hospital, Changsha, Hunan, China, [2]Department of Neurology, The Third Hospital of Changsha, Changsha, Hunan, China, [3]Department of Neurology, Xiangya Hospital, Central South University, Changsha, Hunan, China

Background: Neuronal intranuclear inclusion disease (NIID) is a rare neurodegenerative disease that can affect the nervous and other systems of the body. Its clinical manifestations are complex and easily misdiagnosed. Adult-onset NIID beginning with autonomic symptoms such as recurrent hypotension, profuse sweating, and syncope has not been reported.

Case presentation: An 81-year-old male was admitted to the hospital in June 2018 due to repeated episodes of hypotension, profuse sweating, pale complexion, and syncope for 3 years, and progressive dementia for 2 years. DWI was not possible due to the presence of metal residues in the body. Cutaneous histopathology revealed sweat gland cell nuclear inclusions and immunohistochemistry showed p62 nuclear immunoreactivity. Blood RP-PCR identified an abnormal GGC repeat expansion in the 5′UTR of the *NOTCH2NLC* gene. Accordingly, this case was diagnosed as adult-onset NIID in August 2018. The patient subsequently received vitamin C nutritional support, rehydration, and other vital signs maintenance treatments during hospitalization, but the above symptoms still recurred after discharge. With the development of the disease, lower extremity weakness, slow movement, dementia, repeated constipation, and vomiting appeared successively. In April 2019, he was hospitalized again for severe pneumonia, and died of multiple organ failure in June 2019.

Conclusion: The presented case exemplifies great clinical heterogeneity of NIID. Some patients may have neurological symptoms and other systemic symptoms simultaneously. This patient started with autonomic symptoms, including recurrent episodes of hypotension, profuse sweating, pallor, and syncope, which progressed rapidly. This case report provides new information for the diagnosis of NIID.

KEYWORDS

neuronal intranuclear inclusion disease, autonomic symptom, pathological change, case report, misdiagnose

Introduction

Neuronal intranuclear inclusion disease (NIID) is a rare chronic neurodegenerative disease that affects the central and peripheral nervous systems, as well as other organs throughout the body. Histopathological features of NIID include intranuclear inclusions found in the affected organs and tissues such as skin, internal organs, and skeletal muscle. Diffusion-weighted imaging (DWI) can reveal hyperintense lesions at the corticomedullary junction area. Further, genetic testing can reveal GGC trinucleotide repeat expansion in

the *NOTCH2NLC* gene. We present an atypical case of adult-onset NIID. The patient began to suffer from repeated hypotension, pallor, profuse sweating, and syncope, and was misdiagnosed many times. Finally, we made a diagnosis of NIID through skin biopsy and genetic testing. This report of a rare case of NIID with onset of autonomic symptoms will help to better understand the clinical features of this disease and make an early and accurate diagnosis.

Case presentation

An 81-year-old male was admitted to our hospital in June 2018 due to recurrent episodes of hypotension, profuse sweating, pale complexion, and syncope for 3 years and progressive dementia for 2 years. These symptoms beginning 2015 were not related to body posture. Blood pressure lower than 90/60 mmHg occurred several times during the episode, even undetectable in severe cases. Consciousness typically returned within 10 min. Pallor, profuse sweating, and hypotension usually fully recovered within 30 min. Before the episode, the patient had no limb movement disorder, dizziness, diplopia, slurred speech, palpitations, and chest pain. During the episode, the patient had no limb twitching, foaming at the mouth, and urinary and fecal incontinence, and multiple blood glucose test results were 6–16 mmol/L. About 1 year after the onset of autonomic symptoms, cognitive decline, weakness of limbs, unsteady walking, repeated vomiting, and intractable constipation gradually appeared.

Admission physical examination: blood pressure 120/80 mmHg, heart rate 80 beats/min, no obvious abnormalities in heart, lung, and abdomen. Neurological exam: decreased recent and remote memory, acalculia, and decreased spatiotemporal orientation. According to the Medical Research Council (MRC) scale, the patient's muscle strength was grade 5 in both upper limbs and grade 4 in both lower limbs. Muscle tone was normal in the four limbs, but the deep reflexes of the two lower limbs were symmetrically weakened. Negative pathological signs, positive Romberg's sign, and normal finger-nose and heel-knee-shin tests. Walking with the aid of a walker, the patient exhibited a wide-based gait. Mini-Mental State Examination score was 7. Head computed tomography (CT) scan on admission showed brain atrophy and white matter lesions (Figures 1A, B). Dynamic electrocardiogram revealed sinus rhythm, occasional atrial premature beats, incomplete paired beats, transient atrial tachycardia, and occasional ventricular premature beats. Echocardiography revealed thickened ventricular septum, decreased aortic elasticity, and decreased left ventricular diastolic function with an ejection fraction of 75%. Routine blood test: red blood cell count 3.53×10^{12}/L, hemoglobin 110 g/L, hematocrit 32.3%, albumin 30.40 g/L, low-density lipoprotein cholesterol 1.87 mmol/L, random blood glucose 12.48 mmol/L, and estimated glomerular filtration rate 71.12 mL/min/1.73 m^2. Cardiac enzymes, troponin, brain natriuretic peptide, electrolytes, coagulation tests, thyroid function, and β-hydroxybutyric acid were normal. Urinalysis revealed leukocyte count 178.90 μL. Stool routine examination was normal. DWI was not performed due to the presence of metal residues in the body. Skin biopsy indicated intranuclear inclusion bodies in eccrine sweat gland cells, fibroblasts, and adipocytes. p62 immunohistochemistry demonstrated nuclear immunoreactivity (Figure 2). Finally, genetic testing by repeat-primed polymerase chain reaction (RP-PCR) found that the patient had GGC repeats in the 5′UTR of the *NOTCH2NLC* gene (Figure 3). The patient was therefore diagnosed with adult-onset NIID.

During hospitalization, the patient was mainly given supportive care to maintain vital signs. Due to long-term malnutrition, the treatment plan included supplementing vitamin C and dextrose and sodium chloride injection, increasing oxygen supply though oxygen inhalation, and maintaining normal blood pressure and electrolyte balance. Since the onset of the disease, the patient manifested progressive aggravation of symptoms such as dementia and limb weakness, repeated vomiting, and intractable constipation, accompanied by recurrent episodes of autonomic symptoms such as pale complexion, excessive sweating, hypotension, and syncope.

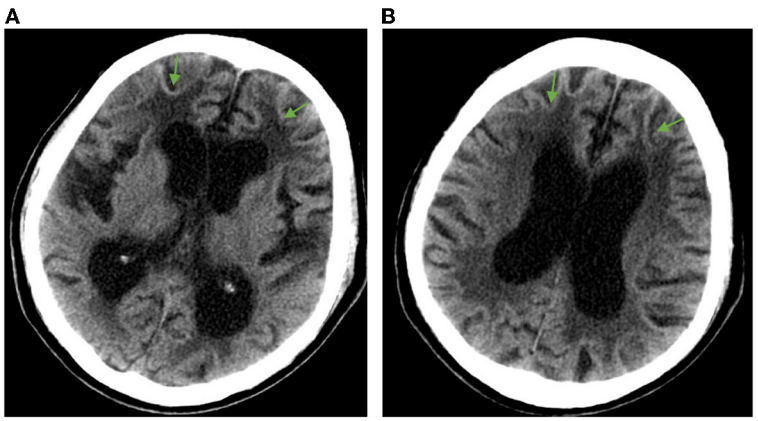

FIGURE 1
Head CT imaging showing brain atrophy and white matter lesions in the patient. **(A)** Enlargement of the anterior and posterior horns of the lateral ventricles and widening of the sulcus, with arrows showing white matter lesions around the anterior horns of the lateral ventricles. **(B)** Enlarged body of the lateral ventricle with arrows showing white matter lesions around the body of the lateral ventricle.

For some symptoms such as nausea and vomiting, the patient received symptomatic treatment. In 2019, the patient was already severely demented and bedridden. He was readmitted to our hospital in April with severe pneumonia. Eventually, he developed multi-organ failure and died in June 2019 at the age of 82.

Discussion

NIID is a rare slowly progressive neurodegenerative disease first described by Lindenberg and colleagues in 1968 (1). NIID is highly clinically heterogeneous and its pathological characteristics include the presence of eosinophilic hyaline intranuclear inclusions in the central and peripheral nervous systems and internal organs. Eosinophilic p62/ubiquitin-positive intranuclear inclusions in neurons and other somatic cells can be observed under light microscope, and dense membraneless filamentous substances can be seen under electron microscopy (2). Moreover, high signal intensity in the corticomedullary junction on DWI is characteristic of NIID (3). According to the age of onset, NIID can be classified into infantile, juvenile, and adult forms. Infantile and juvenile patients often present with ataxia or aberrant mental behavior as the first manifestation (4–7), while adult-onset patients usually begin with dementia or limb weakness as initial clinical symptoms. The adult form can be further divided into sporadic and familial subtypes. Sone *et al.*, summarized 38 sporadic adult-onset NIID cases, aged 51–76 years, with dementia onset as the main symptoms (94.7%), followed by limb tremor, ataxia, abnormal behavior, disturbance of consciousness, and encephalitis-like seizures (8, 9). Others reported NIID with Parkinson-like symptoms (10), abnormal emotional behavior (11), chronic headache (12), sensory disturbance (13), epileptic episodes (14), cardiomyopathy, constipation and gastroenteritis, bronchopneumonia and respiratory failure (15), and dysphagia (12). However, there were no reports of early autonomic symptoms such as hypotension, pallor, profuse sweating, and syncope in patients with NIID.

The patient we reported here initially presented with hypotension (<90/60 mmHg) and autonomic symptoms unrelated to postural changes. At the early stage of the onset, dynamic electrocardiograms showed no malignant arrhythmias such as cardiac arrest and conduction block, and cardiogenic syncope was ruled out. At the time, vasovagal syncope was considered. The patient had metal implants in his body that prevented an MRI of the head. At the same time, the patient's early symptoms were atypical, which brought great difficulties to clinical diagnosis. As the condition worsened, the patient subsequently developed dementia, weakness in both lower limbs, slow movement, repeated vomiting, and intractable constipation. The patient' symptoms and physical examination results suggested that the lesion may involve multiple systems and sites, such as autonomic nerves, peripheral nerves, cerebellum or extrapyramidal system, and cerebral cortex. After reviewing the literature, the patient was considered likely to have NIID. Subsequent dermatopathology and immunohistochemistry revealed p62-positive intranuclear inclusions in eccrine sweat gland cells, fibroblasts, and adipocytes (Figure 2) and genetic testing detected GGC repeat expansion (Figure 3), both confirming adult NIID diagnosis. Therefore, all symptoms of the patient can be reasonably explained.

NIID is genetically and phenotypically heterogeneous and can affect the nervous, circulatory, urinary, and digestive systems. In some patients, other systemic symptoms preceded neurologic symptoms, suggesting systemic heterogeneity in NIID (16). Current studies believe that NIID has multiple phenotypes, such as dementia, tremor, Parkinson-like, amyotrophic lateral sclerosis-like, oculopharyngodistal myopathy-like, and Charcot-Marie-Tooth-like phenotypes (17), which increase the difficulty of

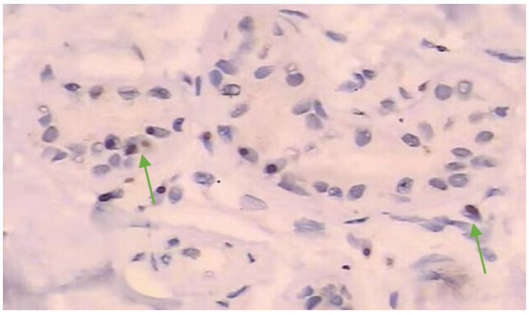

FIGURE 2
Histopathological examination of skin biopsy after admission showed round or nearly round inclusion bodies in the nucleus of sweat gland cells (magnification, ×200). Immunostaining displayed intranuclear inclusions with p62 (mouse antibody, 610833, BD Biosciences) immunoreactivity.

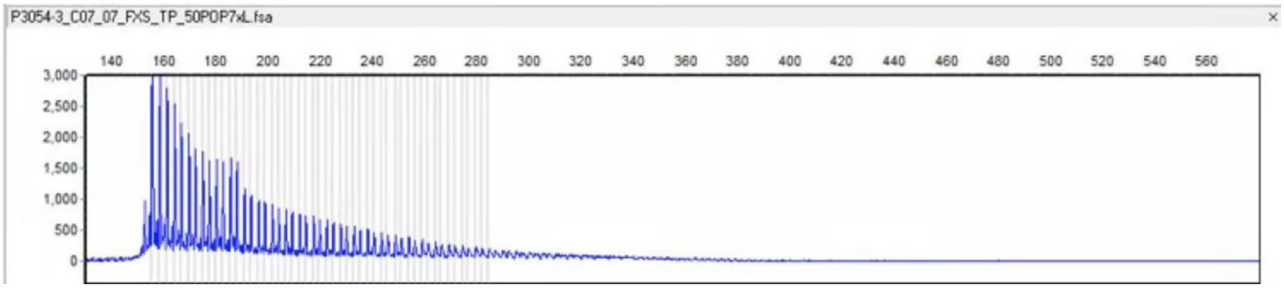

FIGURE 3
Genetic testing by RP-PCR revealed an aberrant GGC repeat expansion in the 5′UTR of the *NOTCH2NLC* gene.

diagnosis. In most patients with NIID, a hyperintense foci at the gray-white matter junction on DWI is an important diagnostic marker of NIID since it does not disappear throughout the course of the disease (8). Detection of ubiquitin-positive eosinophilic intranuclear inclusions in skin biopsies and GGC repeat expansion in the *NOTCH2NLC* gene can further aid in accurate diagnosis. At present, there are no proven treatments for NIID. Most NIID progress slowly. However, this patient progressed rapidly, became bedridden, and died five years later of severe pneumonia and multi-organ failure. The rare onset and rapid progression of the disease in this patient warrants further study.

Data availability statement

The original contributions presented in the study are included in the article/supplementary material, further inquiries can be directed to the corresponding authors.

Ethics statement

The studies involving human participants were reviewed and approved by Ethics Committee of Changsha Third Hospital. The patients/participants provided their written informed consent to participate in this study. Written informed consent was obtained from the individual(s) for the publication of any potentially identifiable images or data included in this article.

Author contributions

YZ and QY wrote the report. WF performed diagnostic testing. XM assisted in diagnosis. QY collected data and made diagnosis. YT confirmed pathological diagnosis. All authors contributed to the article and approved the submitted version.

Funding

This study was supported by the Project of Changsha Natural Fund (No. kq2202017).

Conflict of interest

The authors declare that the research was conducted in the absence of any commercial or financial relationships that could be construed as a potential conflict of interest.

Publisher's note

All claims expressed in this article are solely those of the authors and do not necessarily represent those of their affiliated organizations, or those of the publisher, the editors and the reviewers. Any product that may be evaluated in this article, or claim that may be made by its manufacturer, is not guaranteed or endorsed by the publisher.

References

1. Lindenberg R, Rubinstein LJ, Herman MM, Haydon GB. A light electron microscopy study of an unusual widespread nuclear inclusion body disease. A possible residuum of an old herpesvirus infection. *Acta Neuropathol.* (1968) 10:54–73. doi: 10.1007/bf00690510

2. Dickson DW, Wertkin A, Kress Y, Ksiezak-Reding H, Yen SH. Ubiquitin immunoreactive structures in normal human brains. Distribution and developmental aspects. *Lab Invest.* (1990) 63:87–99.

3. Aiba Y, Sakakibara R, Abe F, Higuchi T, Tokuyama W, Hiruta N, et al. Neuronal intranuclear inclusion disease with leukoencephalopathy and light motor-sensory and autonomic neuropathy diagnosed by skin biopsy. *J Neurol Sci.* (2016) 368:263–5. doi: 10.1016/j.jns.2016.07.042

4. Haltia M, Somer H, Palo J, Johnson WG. Neuronal intranuclear inclusion disease in identical twins. *Ann Neurol.* (1984) 15:316–21. doi: 10.1002/ana.410150403

5. Funata N, Maeda Y, Koike M, Yano Y, Kaseda M, Muro T, et al. Neuronal intranuclear hyaline inclusion disease: report of a case and review of the literature. *Clin Neuropathol.* (1990) 9:89–96.

6. Paviour DC, Revesz T, Holton JL, Evans A, Olsson JE, Lees AJ. Neuronal intranuclear inclusion disease: report on a case originally diagnosed as dopa-responsive dystonia with Lewy bodies. *Mov Disord.* (2005) 20:1345–9. doi: 10.1002/mds.20559

7. O'Sullivan JD, Hanagasi HA, Daniel SE, Tidswell P, Davies SW, Lees AJ, et al. Neuronal intranuclear inclusion disease and juvenile parkinsonism. *Mov Disord.* (2000) 15:990–5. doi: 10.1002/1531-8257(200009)15:5<990::aid-mds1035>3.0.co;2-i

8. Sone J, Mori K, Inagaki T, Katsumata R, Takagi S, Yokoi S, et al. Clinicopathological features of adult-onset neuronal intranuclear inclusion disease. *Brain.* (2016) 139:3170–86. doi: 10.1093/brain/aww249

9. Sone J, Mitsuhashi S, Fujita A, Mizuguchi T, Hamanaka K, Mori K, et al. Long-read sequencing identifies GGC repeat expansions in NOTCH2NLC associated with neuronal intranuclear inclusion disease. *Nat Genet.* (2019) 51:1215–21. doi: 10.1038/s41588-019-0459-y

10. Cupidi C, Dijkstra AA, Melhem S, Vernooij MW, Severijnen LA, Hukema RK, et al. Refining the spectrum of neuronal intranuclear inclusion disease: a case report. *J Neuropathol Exp Neurol.* (2019) 78:665–70. doi: 10.1093/jnen/nlz043

11. Han X, Han M, Liu N, Xu J, Zhang Y, Zhang Y, et al. Adult-onset neuronal intranuclear inclusion disease presenting with typical MRI changes. *Brain Behav.* (2019) 9:e01477. doi: 10.1002/brb3.1477

12. Nakamura M, Ueki S, Kubo M, Yagi H, Sasaki R, Okada Y, et al. Two cases of sporadic adult-onset neuronal intranuclear inclusion disease preceded by urinary disturbance for many years. *J Neurol Sci.* (2018) 392:89–93. doi: 10.1016/j.jns.2018.07.012

13. Yamanaka H, Hashimoto S, Suenaga T. Neuronal intranuclear inclusion disease with prolonged impaired consciousness and status epilepticus: a case report. *Rinsho Shinkeigaku.* (2019) 59:425–30. doi: 10.5692/clinicalneurol.cn-001264

14. Shindo K, Tsuchiya M, Hata T, Ichinose Y, Koh K, Sone J, et al. Non-convulsive status epilepticus associated with neuronal intranuclear inclusion disease: a case report and literature review. *Epilepsy Behav Case Rep.* (2019) 11:103–6. doi: 10.1016/j.ebcr.2019.01.007

15. Vermilion J, Johnson M, Srinivasan J, Mink JW. Neuronal intranuclear inclusion disease: longitudinal case report of motor and nonmotor symptoms. *J Child Neurol.* (2019) 34:801–5. doi: 10.1177/0883073819860566

16. Chen H, Lu L, Wang B, Cui G, Wang X, Wang Y, et al. Re-defining the clinicopathological spectrum of neuronal intranuclear inclusion disease. *Ann Clini Translat Neurol.* (2020) 7:19. doi: 10.1002/acn3.51189

17. Bao L, Zuo D, Li Q, Chen H, Cui G. Current advances in neuronal intranuclear inclusion disease. *J Neurol Sci.* (2023) 2:16. doi: 10.1007/s10072-023-06677-0

frontiers | Frontiers in Neurology

TYPE Case Report
PUBLISHED 02 June 2023
DOI 10.3389/fneur.2023.1184612

OPEN ACCESS

EDITED BY
Bruce Miller,
University of California, San Francisco, United States

REVIEWED BY
Chenhui Mao,
Peking Union Medical College Hospital (CAMS), China
Yun Tian,
Central South University, China
Yingying Luo,
Central South University, China

*CORRESPONDENCE
Julia Ting Bu
✉ J1bu@health.ucsd.edu

RECEIVED 12 March 2023
ACCEPTED 10 May 2023
PUBLISHED 02 June 2023

CITATION
Bu JT, Torres D, Robinson A, Malone C, Vera JC, Daghighi S, Dunn-Pirio A, Khoromi S, Nowell J, Léger GC, Ciacci JD, Goodwill VS, Estrella M, Coughlin DG, Guo Y and Farid N (2023) Case report: Neuronal intranuclear inclusion disease presenting with acute encephalopathy. *Front. Neurol.* 14:1184612. doi: 10.3389/fneur.2023.1184612

Case report: Neuronal intranuclear inclusion disease presenting with acute encephalopathy

Julia Ting Bu[1]*, Dolores Torres[1], Adam Robinson[2], Corey Malone[2], Juan Carlos Vera[3], Shadi Daghighi[4], Anastasie Dunn-Pirio[1], Suzan Khoromi[1], Justin Nowell[5], Gabriel C. Léger[1], Joseph D. Ciacci[2], Vanessa S. Goodwill[6], Melanie Estrella[2], David G. Coughlin[1], Yueyang Guo[2] and Nikdokht Farid[2]

[1]Department of Neurosciences, University of California, San Diego, La Jolla, CA, United States, [2]Department of Radiology, University of California, San Diego, La Jolla, CA, United States, [3]Sharp Rees-Stealy, Department of Radiology, San Diego, CA, United States, [4]Department of Radiology, State University of New York Upstate Medical University, Syracuse, NY, United States, [5]Sharp Rees-Stealy, Department of Neurology, San Diego, CA, United States, [6]Department of Pathology, University of California, San Diego, La Jolla, CA, United States

Neuronal intranuclear inclusion disease (NIID), a neurodegenerative disease previously thought to be rare, is increasingly recognized despite heterogeneous clinical presentations. NIID is pathologically characterized by ubiquitin and p-62 positive intranuclear eosinophilic inclusions that affect multiple organ systems, including the brain, skin, and other tissues. Although the diagnosis of NIID is challenging due to phenotypic heterogeneity, a greater understanding of the clinical and imaging presentations can improve accurate and early diagnosis. Here, we present three cases of pathologically proven adult-onset NIID, all presenting with episodes of acute encephalopathy with protracted workups and lengthy time between symptom onset and diagnosis. Case 1 highlights challenges in the diagnosis of NIID when MRI does not reveal classic abnormalities and provides a striking example of hyperperfusion in the setting of acute encephalopathy, as well as unique pathology with neuronal central chromatolysis, which has not been previously described. Case 2 highlights the progression of MRI findings associated with multiple NIID-related encephalopathic episodes over an extended time period, as well as the utility of skin biopsy for antemortem diagnosis.

KEYWORDS

neuronal intranuclear inclusion disease, magnetic resonance imaging, arterial spin labeling, chromatolysis, case report

Introduction

Neuronal intranuclear inclusion disease (NIID) is a genetic progressive leukoencephalopathy with multiple clinical presentations that make prompt diagnosis challenging in many cases (1). Clinical presentations have been classified in a variety of methods including age of onset (infantile-onset, juvenile-onset, and adult-onset subgroups), family history (sporadic or familial patterns), and affected areas of the nervous system (the central nervous system, peripheral nervous system, or autonomic nervous system predominant subtypes) (1). Adult-onset cases can be sub-grouped into dementia-dominant

and limb weakness-dominant phenotypes (2). Infantile-onset cases are marked by cerebellar findings of ataxia and dysarthria occurring before 5 years of age. Juvenile-onset cases are marked initially by behavior changes and then later the onset of pyramidal and cerebellar signs (3). Sporadic cases of NIID most commonly exhibit dementia, ataxia, autonomic dysfunction, and parkinsonism, whereas familial cases are more likely to be associated with muscle weakness, sensory disturbances, and juvenile onset (2). NIID is the second most common adult-onset genetic leukoencephalopathy, second to CADASIL (4). NIID is pathologically characterized by extensive intranuclear eosinophilic inclusions that are ubiquitin and p-62 positive on immunohistochemical staining affecting multiple organ systems including the brain and skin (1, 3, 5). Recently, a CGG repeat expansion in a non-coding region of *NOTCH2NLC* on chromosome 1 has been discovered (6) as a causative gene mutation leading to NIID.

One of the characteristic imaging features of NIID is the magnetic resonance (MR) imaging finding of hyperintense signal in the corticomedullary junction on diffusion-weighted imaging (DWI). A recent case report also noted high DWI in globus pallidus, suggesting that deep gray matter nuclei can also be affected (7). Other common MRI features include white matter changes, vermian T2 hyperintensities, and focal brain edema. Thus, the radiographic appearance of NIID has significant overlap with other leukoencephalopathies but also vascular, infectious, and toxic etiologies as well. Given the growing awareness of NIID and less invasive methods of identifying the pathognomonic inclusions through a skin biopsy, we reviewed three recent pathologically proven adult-onset dementia-predominant cases of NIID to illustrate the clinical and imaging heterogeneity of these cases along with novel imaging and pathological features. All cases presented with episodes of acute encephalopathy with periodic protracted hospitalizations and extensive workups, and all spanned several years between symptom onset and definitive diagnoses. Case 1 provides a striking example of ASL hyperperfusion in the setting of acute encephalopathy and also exhibits unique pathology with prominent neuronal central chromatolysis. Case 2 highlights the progression of MRI findings associated with multiple NIID-related encephalopathic episodes over an extended time period, as well as the utility of skin biopsy for antemortem diagnosis.

Case descriptions

Case 1

A 59-year-old Hispanic woman with a history of right MCA stroke 3 years prior complicated by localization-related epilepsy, as well as a history of systemic sclerosis, was admitted to the hospital for acute-onset encephalopathy and global aphasia. Before 15 days, she received her first COVID-19 vaccine (Moderna) followed by the seasonal influenza vaccine. At presentation, she was febrile to 101.2°F. MRI of the brain did not show acute changes. Continuous EEG showed diffuse slowing and epileptiform discharges over the right posterior quadrant without seizures. Empiric antibiotics and antiviral medications were started for presumed meningitis or encephalitis. After 4 days, she was found to have a right facial droop involving the forehead and right upper extremity hemiparesis. A repeat MRI was again negative for acute infarct. Lumbar puncture showed mildly increased protein at 55 mg/dL, <5 WBCs per mm^3, matching oligoclonal bands between the CSF and serum, and normal cytopathology and flow cytometry, but elevated CSF IL-6 to 67.6 pg/mL and soluble IL-2R cytokines to 29.2 pg/ml. An extensive laboratory workup was largely unremarkable for toxic, metabolic, and infectious etiologies (see Supplementary material). On hospital day 8, she underwent a repeat MRI brain demonstrating new left hemispheric gyral swelling and edema involving the occipital, parietal, temporal, and posterior frontal lobes with cortical/pial enhancement and marked hyperperfusion throughout that region (Figure 1). Empiric steroids were not administered given the concern of possibly provoking a scleroderma renal crisis, and she was treated with a course of intravenous immunoglobulin 2 mg/kg and antiepileptic medications. There was no clinical improvement and a repeat MRI on hospital day 12 found worsened left hemispheric gyral swelling and enhancement but decreased hyperperfusion. Clinically, there was a concern for possible adult-onset mitochondrial encephalopathy, lactic acidosis, and strokelike episodes (MELAS), and she was treated with intravenous arginine, alpha lipoic acid, taurine, levocarnitine, vitamin C, and coenzyme Q10. Ultimately, she underwent a brain biopsy on hospital day 13, which showed neuronal eosinophilic intranuclear inclusions, immunoreactive for ubiquitin, consistent with NIID (Figure 2). Additionally noted on biopsy was prominent neuronal central chromatolysis, where neurons appeared enlarged with Nissl substance pushed to the cytoplasmic periphery. A repeat MRI on hospital 14 showed persistent gyral swelling and edema but the resolution of enhancement and normalized perfusion. Repeat lumbar puncture on hospital day 22 was notable for normalized cytokines and protein. On day 25 in the hospital, she was speaking in three- to five-word sentences. Upon follow-up, 3 months after discharge, there was a significant improvement in her aphasia and encephalopathy with only minor residual deficits. A follow-up MRI 6 months after the acute episode revealed resolved cortical swelling with residual encephalomalacia and gliosis.

Case 2

A 60-year-old Asian female with hypertension presented after being found unconscious with unknown last known normal. She was noted to be encephalopathic with left-sided weakness and global aphasia. MRI brain showed elevated DWI restriction in the bilateral frontal lobes centered at the corticomedullary junction and confluent white matter T2 and FLAIR hyperintensity. LP CSF 14-3-3, PRP RT-QuIC, and West Nile Virus IgM were negative. Clinically, the patient gradually improved, and 2 years after the initial hospitalization, she was able to resume gardening and dancing, but the global aphasia persisted. She continued to have intermittent episodes of acute encephalopathy marked by confusion and aphasia requiring hospitalizations at years 4, 5, 6, and twice in year 7 after the initial presentation. Spinal fluid testing at years 4 and 6 post-initial hospitalization was notable for positive 14-3-3 protein with negative PRP RT-QuIC; T-tau 869 pg/mL; WBC <5/mm^3; and protein 40 mg/dL. Tests, such as CSF VDRL, coccidioides

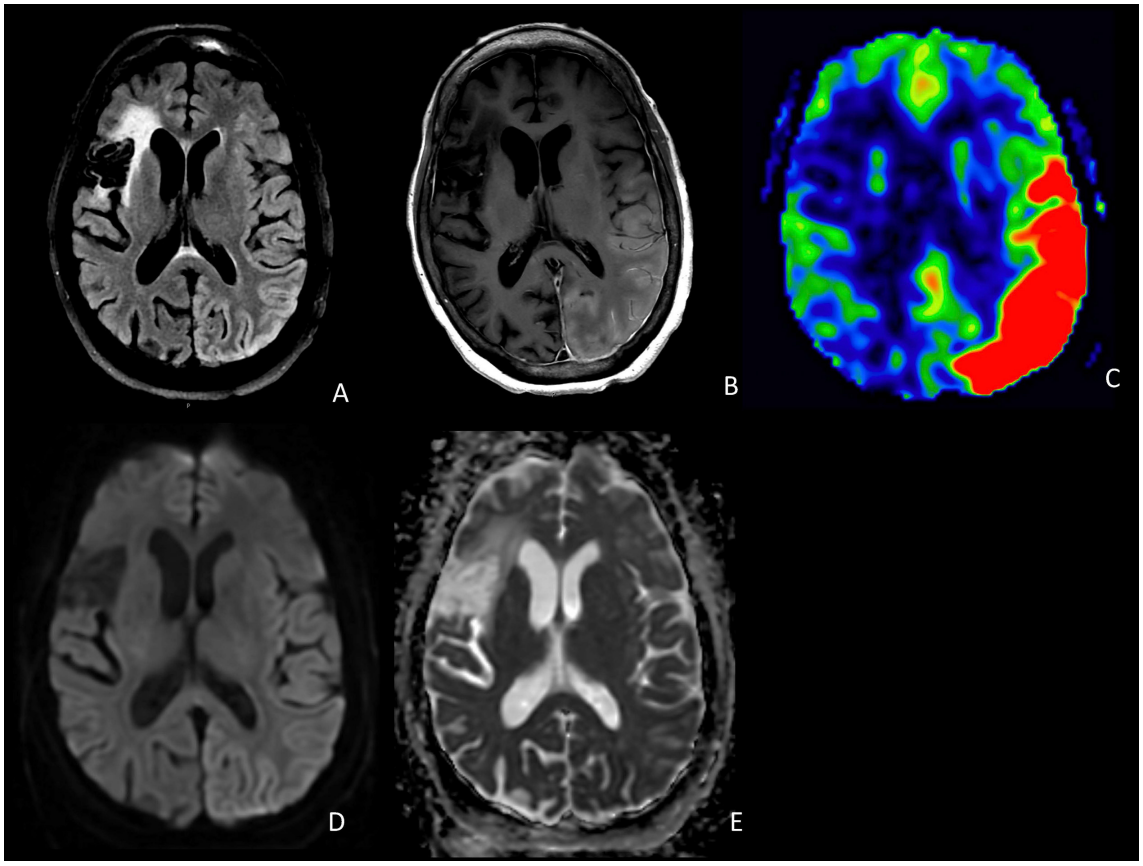

FIGURE 1
Axial FLAIR **(A)**, T1 post-contrast **(B)**, and ASL **(C)** demonstrate cortical edema, cortical and pial enhancement, and marked hyperperfusion involving the left temporal and occipital lobes. DWI **(D)** and ADC **(E)** show T2 shine-through but no definite restricted diffusion in the involved regions. Also noted is a chronic infarct in the right frontal lobe.

antibodies, cryptococcus antigen, HSV PCR, oligoclonal bands, flow cytometry, and paraneoplastic autoantibody panels, were all negative or normal. Repeat brain MRIs revealed progressively increasing symmetric DWI signal at the corticomedullary junction, extending posteriorly from the frontal lobes to involve the parietal and occipital lobes (Figure 3). Extensive genetic testing was unrevealing (see Supplementary material). Patient and family consistently declined brain biopsy; however, skin biopsy was obtained 7 years after the initial presentation which showed eosinophilic ubiquitin-positive intranuclear inclusions within the nuclei of eccrine sweat glands and adipocytes, consistent with NIID (Figure 2). The patient was discharged home with family support, and on a follow-up visit 2 months after admission, she was noted to be back to baseline with expressive aphasia, otherwise able to perform most of her activities of daily living and gardening.

Case 3

A 72-year-old Hispanic woman with ~8 years of progressive cognitive decline presented to the Emergency Department with confusion and lethargy. She was found to be febrile to 103.5°F, urinary retention, and with leukocytosis. In the preceding 5 years, she had multiple emergency room visits for episodes of confusion, dysarthria, headache, and fever thought to be secondary to urinary tract infections or TIAs and was noted by family to have had a progressive cognitive decline in between events. MR imaging demonstrated T2 hyperintensities with corresponding diffusion restriction raising concern for acute to subacute ischemia at several of these hospitalizations. At her fourth hospital admission, due to ongoing encephalopathy despite empiric antibiotics for the urinary tract infection, an expanded infectious workup was performed including a lumbar puncture. CSF studies were notable for neutrophilic pleocytosis (corrected WBC count 463 cells/mm^3), positive CSF HSV IgG, negative CSF cultures, and negative CSF autoimmune panel. She underwent treatment for presumed HSV encephalitis without clinical improvement. On hospital day 9, a repeat brain MRI demonstrated diffuse left hemispheric cortical enhancement. On hospital day 20, a follow-up brain MRI demonstrated worsening, predominantly left hemispheric, cortical enhancement, as well as gyral swelling and edema (Figure 4). A brain biopsy was performed which confirmed the diagnosis of NIID. Electron microscopy revealed scattered intranuclear inclusions, mostly filamentous (Figure 2). She subsequently underwent high-dose pulse steroid therapy (hospital days 22–26) and plasmapheresis (four pheresis treatments from hospital days 28–34) with clinical improvement,

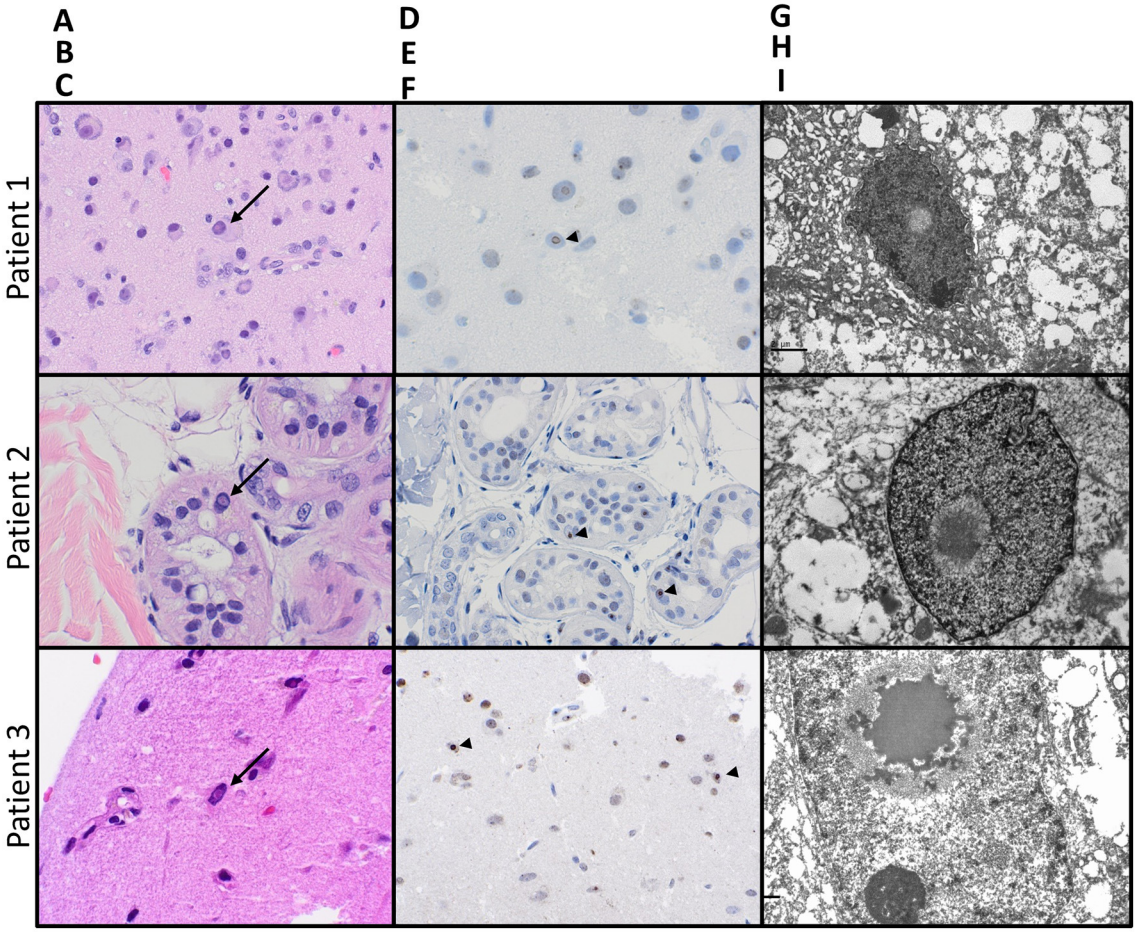

FIGURE 2
Pathologic features of NIID on biopsies from all three patients: Hematoxylin- and eosin-stained sections [**(A–C)**; 400x magnification] from biopsies on all three patients showed prominent intranuclear eosinophilic inclusions (arrows), seen within neurons also exhibiting central chromatolysis in the brain biopsy from patient 1, the eccrine glandular epithelium on the skin biopsy from patient 2, and neurons and glia on brain biopsy from patient 3. All intranuclear inclusions were immunoreactive for ubiquitin [**(D–F)**; arrowheads]. Electron microscopy on all three specimens confirmed the presence of intranuclear fibrillar inclusions **(G–I)**.

alert to surroundings but still with limited response. A brain MRI performed on hospital day 26 demonstrated resolving left hemispheric gyral swelling and edema and cortical enhancement. Post-hospitalization she remained minimally conversive. She was transitioned to hospice care and passed away shortly at age 72, ~8 years after her initial symptom onset.

Discussion

Neuronal intranuclear inclusion disease is marked by widely heterogeneous clinical presentations. However, among cases of adult-onset NIID, episodic attacks of acute encephalopathy appear to be an important diagnostic indicator. The cases in this series illustrate this presentation mimicking encephalitis in their CSF and imaging characteristics against a background of progressive dementia syndrome (1, 2). These patients had protracted periods of time that passed before definitive diagnoses could be made and underwent a number of procedures and treatments that potentially could have been avoided with more prompt recognition of their diagnosis. Two of the three cases had classical corticomedullary DWI restriction on brain MRI which is a helpful indicator, but the cases shown here also exhibit different changes that can occur during acute encephalopathic episodes including cortical swelling, contrast enhancement, and hyperperfusion. Spinal fluid sampling can show pleocytosis and inflammatory cytokine changes during and after encephalitic attacks. Case 1 is the first report of cytokine changes in NIID during an encephalitic attack. While it is not clear what provokes these attacks, the patient in case 1 had recently received COVID-19 and influenza vaccinations 2 weeks prior to presentation and immunological stress may be related to her presentation.

Case 2 also has a significant elevation in CSF 14-3-3 protein on testing, which likely reflects the acute neuronal injury caused by the encephalitic attack, as the more specific CSF PRP RT-QuiC test did not show indications of Creutzfeldt–Jakob disease. Elevations in 14-3-3 have been documented in other non-prion conditions such as acute neuronal injury (8) and Alzheimer's disease (9).

Case 3 also had a pleocytosis on presentation, and infectious encephalitis was initially on the differential. Previous publications

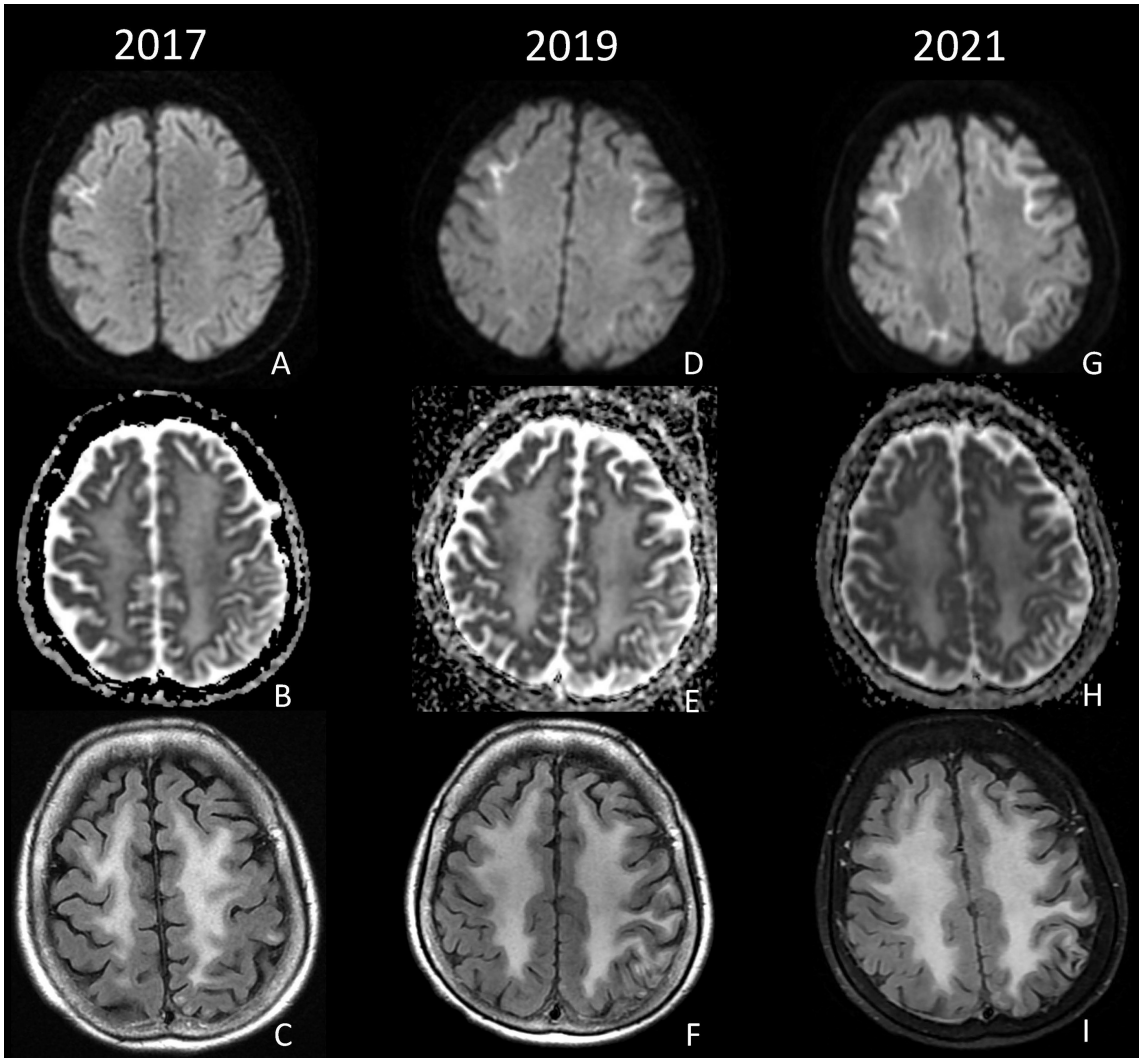

FIGURE 3
DWI, ADC, and FLAIR from 2017 **(A–C)**, 2019 **(D–F)**, and 2021 **(G–I)** demonstrate progressive diffusion restriction at the corticomedullary junction of the bilateral frontal and parietal lobes, as well as diffuse confluent white matter FLAIR hyperintensity.

have noted mild elevations in CSF protein and mild or no CSF pleocytosis in patients with NIID, even during encephalitic attacks (2, 5). Although no causative infectious agents were identified in case 3/s workup, we cannot fully exclude that she had a CNS infection that unmasked or worsened her underlying NIID and was the primary cause for her CSF pleocytosis, and it is less likely given that clinical improvement was noted after immunosuppressive treatment.

Previous cases of NIID demonstrating ASL hyperperfusion have been reported (10, 11). Interestingly, at least two cases of NIID with associated hypoperfusion have also been reported (12, 13). Pathologically, NIID is marked by eosinophilic inclusions in neurons, which are immunoreactive for ubiquitin or p62, and appear filamentous by electron microscopy. Interestingly, the biopsy from Case 1 also demonstrated prominent central chromatolysis, a histologic feature that may be seen in traumatic injuries or pellagra, but which has not been previously reported in NIID. It is now known that the pathognomonic intranuclear inclusions of NIID are present in peripheral tissues. Vascular smooth muscle cells have been shown to harbor the same eosinophilic inclusions that are present in other tissues in NIID, but the precise mechanism of the dynamic vascular changes that occur during encephalitic episodes is yet to be elucidated (14). Inclusions are also found in adipocytes, which raise the possibility of using skin biopsies to aid in diagnosing NIID in a less invasive fashion than a brain biopsy. This less invasive method was an important consideration for the family and patient in case 2 and was eventually implemented. It should be noted that similar intranuclear inclusions are also seen in adipocytes and other tissues in Fragile-X tremor ataxia syndrome (FXTAS), and in some situations, testing for a CGG repeat expansion in the FMR1 gene may be appropriate to rule out this condition which can cause a histological mimic (15). While the causative CGG repeat expansion in NOTCH2NLC and its association with NIID have been discovered, testing is not currently covered in most commercially available gene panels. It is likely that testing

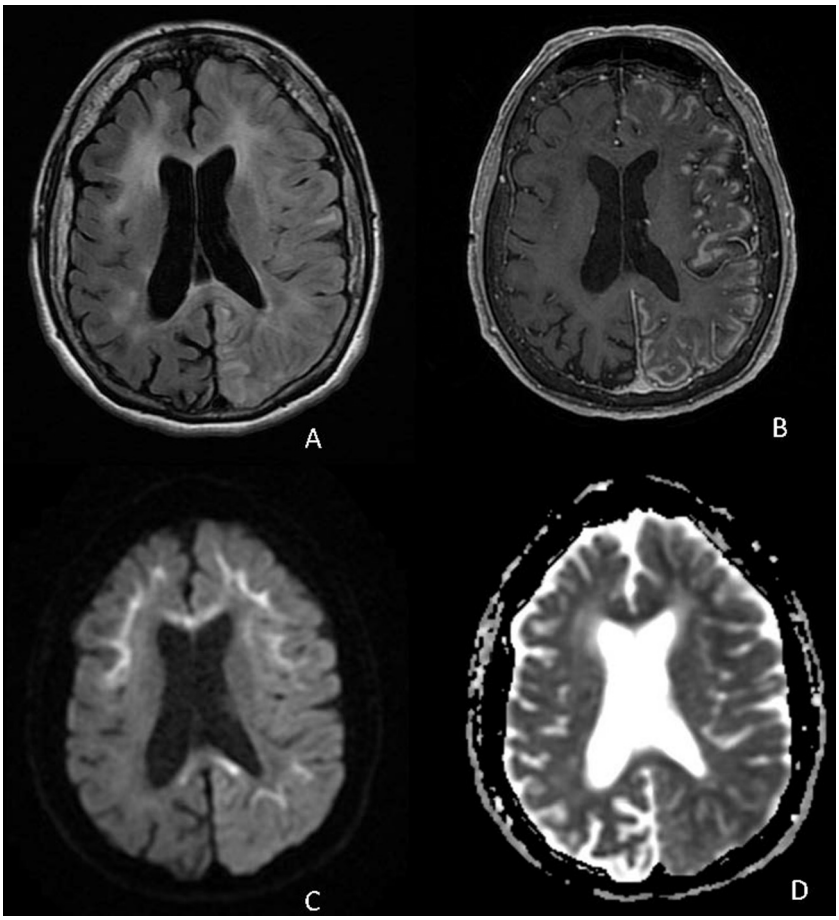

FIGURE 4
Axial FLAIR **(A)**, T1 post-contrast **(B)**, DWI **(C)**, and ADC **(D)** demonstrate diffuse cortical edema and patchy cortical enhancement throughout the left cerebral hemisphere on a background of corticomedullary diffusion restriction involving the bilateral frontal and left parietal lobes as well as diffusion restriction in the corpus callosum.

will be available in a more widespread fashion soon and will offer another method of diagnosing NIID without brain biopsy. It should be noted that NOTCH2NLC expansions are not universally associated with NIID as many non-Asian cases of NIID have been described that are NOTCH2NLC normal (16), and thus, a NOTCH2NLC mutation expansion may not be necessary to cause NIID, highlighting the importance of histopathology and corroborating clinical and radiological evidence.

Neuronal intranuclear inclusion disease remains an elusive diagnosis and should be considered in cases with atypical and recurrent episodes of acute encephalopathy, particularly when occurring on a background of progressive dementia. Furthermore, NIID should still be considered even in the absence of the more typical and well-described MRI finding of symmetric corticomedullary DWI hyperintensity, which may be more associated with the chronic phase of the disease. Given that less invasive methods of biopsy are now available, clinicians should have a low threshold to utilize skin biopsy in diagnosing this disease in the proper clinical context. Prognostic markers in this rare disease are generally lacking, as is guidance on the management during acute episodes of encephalopathy. However, increased awareness of this condition and its myriad clinical and imaging findings will promote a better understanding of the prevalence and phenotypic spectrum of this disease, which will aid in developing evidence-based guidance for its management.

Data availability statement

The original contributions presented in the study are included in the article/Supplementary material, further inquiries can be directed to the corresponding author.

Ethics statement

Written informed consent was obtained from the individual(s) for the publication of any potentially identifiable images or data included in this article.

Author contributions

JB and DT wrote the first draft of the manuscript. JB, DT, JN, and DC wrote sections of the manuscript. AR, VG, and NF

designed the figures. All authors contributed to the manuscript revision, read, and approved the submitted version.

Acknowledgments

We thank the patients and caregivers for agreeing to be part of this manuscript. We are also grateful to the care teams at the patients' respective hospitals.

Conflict of interest

The authors declare that the research was conducted in the absence of any commercial or financial relationships that could be construed as a potential conflict of interest.

Publisher's note

Supplementary material

The Supplementary Material for this article can be found online at: https://www.frontiersin.org/articles/10.3389/fneur.2023.1184612/full#supplementary-material

References

1. Lu X, Hong D. Neuronal intranuclear inclusion disease: Recognition and update. *J Neural Transm.* (2021) 128:295–303. doi: 10.1007/s00702-021-02313-3

2. Sone J, Mori K, Inagaki T, Katsumata R, Takagi S, Yokoi S, et al. Clinicopathological features of adult-onset neuronal intranuclear inclusion disease. *Brain.* (2016) 139:3170–86. doi: 10.1093/brain/aww249

3. Raza HK, Singh S, Rai P, Chansysouphanthong T, Amir A, Cui G, et al. Recent progress in neuronal intranuclear inclusion disease: A review of the literature. *Neurol Sci.* (2020) 41:1019–25. doi: 10.1007/s10072-019-04195-6

4. Wu C, Wang M, Wang X, Li W, Li S, Chen B, et al. The genetic and phenotypic spectra of adult genetic leukoencephalopathies in a cohort of 309 patients. *Brain.* (2022) 2022:awac426. doi: 10.1093/brain/awac426

5. Chen H, Lu L, Wang B, Cui G, Wang X, Wang Y, et al. Re-defining the clinicopathological spectrum of neuronal intranuclear inclusion disease. *Ann Clin Transl Neurol.* (2020) 7:1930. doi: 10.1002/acn3.51189

6. Ishiura H, Shibata S, Yoshimura J, Suzuki Y, Qu W, Doi K, et al. Noncoding CGG repeat expansions in neuronal intranuclear inclusion disease, oculopharyngodistal myopathy and an overlapping disease. *Nat Genet.* (2019) 51:1222–32. doi: 10.1038/s41588-019-0458-z

7. Guo X, Wang Z, Li F. Diffuse cortical injury and basal ganglia high signals on diffusion-weighted imaging in neuronal intranuclear inclusion disease. *J Am Med Assoc Neurol.* (2022) 79:1200–1. doi: 10.1001/jamaneurol.2022.2970

8. Satoh J, Kurohara K, Yukitake M, Kuroda Y. The 14-3-3 protein detectable in the cerebrospinal fluid of patients with prion-unrelated neurological diseases is expressed constitutively in neurons and glial cells in culture. *Eur Neurol.* (1999) 41:216–25. doi: 10.1159/000008054

9. Lu Y. Early increase of cerebrospinal fluid 14-3-3 protein in the Alzheimer's disease continuum. *Front Aging Neurosci.* (2022) 14:941927. doi: 10.3389/fnagi.2022.941927

10. Ishihara T, Okamoto T, Saida K, Saitoh Y, Oda S, Sano T, et al. Neuronal intranuclear inclusion disease presenting with an MELAS-like episode in chronic polyneuropathy. *Neurol Genet.* (2020) 6:531. doi: 10.1212/NXG.0000000000000531

11. Kikumoto M, Nezu T, Shiga Y, Motoda A, Toko M, Kurashige T, et al. Case of neuronal intranuclear inclusion disease with dynamic perfusion changes lacking typical signs on diffusion-weighted imaging. *Neurol Genet.* (2021) 7:e601. doi: 10.1212/NXG.0000000000000601

12. Kutsuna F, Tateishi Y, Yamashita K, Kanamoto T, Hirayama T, Shima T, et al. Perfusion abnormality in neuronal intranuclear inclusion disease with stroke-like episode: A case report. *Cereb Circ Cogn Behav.* (2022) 3:100127. doi: 10.1016/j.cccb.2022.100127

13. Fujita K, Osaki Y, Miyamoto R, Shimatani Y, Abe T, Sumikura H, et al. Neurologic attack and dynamic perfusion abnormality in neuronal intranuclear inclusion disease. *Neurol Clin Pract.* (2017) 7:e39–42. doi: 10.1212/CPJ.0000000000000389

14. Yadav N, Raja P, Shetty SS, Jitender S, Prasad C, Kamble NL, et al. Neuronal intranuclear inclusion disease: A rare etiology for rapidly progressive dementia. *Alzheimer Dis Assoc Disord.* (2019) 33:359–61. doi: 10.1097/WAD.0000000000000312

15. Toko M, Ohshita T, Kurashige T, Morino H, Kume K, Yamashita H, et al. FXTAS is difficult to differentiate from neuronal intranuclear inclusion disease through skin biopsy: A case report. *BMC Neurol.* (2021) 21:1–5. doi: 10.1186/s12883-021-02425-z

16. Chen Z, Yau W, Jaunmuktane Z, Tucci A, Sivakumar P, Taliun S, et al. Neuronal intranuclear inclusion disease is gentically heterogenous. *Ann Clin Transl Neurol.* (2020) 7:1716–25. doi: 10.1002/acn3.51151

frontiers | Frontiers in Neurology

TYPE Original Research
PUBLISHED 02 June 2023
DOI 10.3389/fneur.2023.1155387

OPEN ACCESS

EDITED BY
Bruce Miller,
University of California,
San Francisco, United States

REVIEWED BY
Renata Kochhann,
Hospital Moinhos de Vento, Brazil
Grigorios Nasios,
University of Ioannina, Greece

*CORRESPONDENCE
Beth K. Rush
✉ Rush.beth@mayo.edu

RECEIVED 31 January 2023
ACCEPTED 25 April 2023
PUBLISHED 02 June 2023

CITATION
Rush BK, Tipton PW, Strongosky A and Wszolek ZK (2023) Neuropsychological profile of CSF1R-related leukoencephalopathy. *Front. Neurol.* 14:1155387. doi: 10.3389/fneur.2023.1155387

Neuropsychological profile of CSF1R-related leukoencephalopathy

Beth K. Rush[1]*, Philip W. Tipton[2], Audrey Strongosky[2] and Zbigniew K. Wszolek[2]

[1]Department of Psychiatry and Psychology, Mayo Clinic, Jacksonville, FL, United States, [2]Department of Neurology, Mayo Clinic, Jacksonville, FL, United States

Introduction: The neuropsychological profile of CSF1R-related leukoencephalopathy (CRL) is undefined. This study defines the profile, contrasts it with that of other dementia syndromes, and highlights measures sensitive to cognitive impairment.

Methods: We administered a standardized battery of neuropsychological tests to five consecutive CRL cases.

Results: The neuropsychological profile of CRL reflects impaired general cognitive function, processing speed, executive function, speeded visual problem solving, verbal fluency, and self-reported depression and anxiety. Confrontation naming and memory are preserved. Within cognitive domains, certain measures more frequently identified impairment than others.

Discussion: CRL impairs general cognitive function, processing speed, executive function. Language and visual problem solving may be impaired if processing speed is required. Confrontation naming and memory are uniquely preserved, contrasting CRL to other dementia syndromes. Cognitive screens excluding processing speed and executive function may not detect CRL cognitive manifestations. Findings sharply define cognitive impairment of CRL and inform cognitive test selection.

KEYWORDS

CSF1R-related leukoencephalopathy, cognitive impairment, neuropsychology, cognitive profile, dementia

1. Introduction

Adult-onset leukoencephalopathy with spheroids and pigmented glia (ALSP) is a neurologic disease characterized by rapidly progressive cognitive and motor impairment. It is a rare disease with few known cases; it is frequently under-or mis-diagnosed (1). Symptoms typically emerge in the fourth decade of life and there is a great deal of phenotypic heterogeneity even among individuals sharing the same pathogenic variant. It is a middle age disease with short survival. Multiple genes have been implicated in ALSP with the most common being the colony stimulating factor 1 receptor (CSF1R) gene and ALSP associated with CSF1R mutations have been subsequently termed CSF1R-related leukoencephalopathy (CRL) (2).

CRL is a primary microgliopathy and preferentially effects cerebral white matter (3). Pathological hallmarks include neuroaxonal spheroids, and pigmented macrophages that decrease in abundance as white matter degeneration advances (4). MRI is a useful tool to

monitor disease progression and can demonstrate spread of white matter degeneration from focal to confluent distribution (5). MRI surveillance also demonstrates progressive cortical volume loss that often preferentially effects frontal and parietal lobes (6). The distribution of cortical atrophy influences individual phenotypes such that a patient may present very similarly to other primary neurodegenerative diseases, e.g., frontotemporal lobar degeneration (FTLD).

Cognitive impairment and dementia are well-recognized and referenced in descriptions of clinical phenotypes of CRL (7–9), with the most common description being that of "a frontal lobe syndrome" similar to behavioral variant frontal temporal dementia (bvFTD). There are no studies comparing the neuropsychological profile of CRL to those profiles of more common primary neurodegenerative diseases (e.g., FTLD clinical syndromes, Alzheimer's disease, and Lewy body disease). General cognitive screening measures have been used to capture this cognitive impairment (10) but no studies document the neuropsychological profile of CRL or provide empirical support for which tests may best detect clinical impairment. In a case series of 3 siblings with the same *CSF1R* variant, "memory and frontal deficits" were identified on clinical evaluation, but specific tests are not mentioned (11). In a single case report, a neuropsychological test battery is documented but there are no other empirical studies published using this test battery in CRL (10). As cognitive decline is implicit in disease progression, it is imperative that objective, standardized, valid, and reliable cognitive measures are used for initial and subsequent neuropsychological evaluations for documenting cognitive trajectory over time (2). Knowing which measures are sensitive and specific to the neuropsychological impairment of CRL is important for designing clinical trials and evaluating treatment outcomes.

Herein, we present results from the initial clinical neuropsychological evaluation of five consecutive patients with genetically confirmed CRL. Patients underwent a standardized neuropsychological test battery evaluating domains of general cognitive function, attention, executive function, memory, visual spatial skill, processing speed, and self-reported emotional function. Subsequently, we describe the neuropsychological profile of symptomatic CRL and propose a standardized testing battery for the assessment of patients with confirmed or suspected CRL.

2. Materials and methods

Five consecutive patients were referred to a single neuropsychologist (BKR) for clinical neuropsychological evaluation after initial neurology evaluation (WSZ, PWT) confirmed a diagnosis of symptomatic CRL. Disease duration was based on years since earliest reported neurological symptoms including cognitive symptoms, personality/behavior symptoms, and/or motor symptoms.

2.1. Standard protocol approvals, registrations, and patient consents

The study protocol associated with data reported here was approved by the Mayo Clinic Institutional Review Board (FWA# FWA00005001) on July 17, 2020. The study was approved, via expedited review, as a minimal risk study. Study approval confirmed that the research met requirements for research with human participants in accordance with The Code of Ethics of the World Medical Association and 45 CFR 46 of the U.S. Department of Health & Human Services, Office for Human Research Protections. Written informed consent for research was obtained from all participants (or guardians of participants) in the study.

2.2. Neuropsychological assessment

A standardized clinical neuropsychological test battery was administered to each patient. The test battery prospectively included measures of general cognitive function and measures within the following specific cognitive domains: attention, processing speed, executive function, language, visual processing skills, memory, and self-reported emotional distress. Clinically relevant cut-off scores are empirically supported, published, and universally accepted for the cognitive screening measures (MMSE, MOCA) and emotional distress screening measures (BDI-II, BAI) and are described below. For all other neuropsychological measure scores, Z-scores were calculated for each patient based on the closest possible age-matched normative reference population. For example, a 58-year-old person's score would be compared to a 60 year old normative score. Z-scores across tests within a cognitive domain were averaged for each patient and a radar chart was constructed to examine each patient's neuropsychological profile of impairment across cognitive domains. A mean radar chart across the 5 patients was also constructed. To examine rates of impairment on cognitive tests within a domain, scores falling 1.5 standard deviations below the mean of an age-adjusted normative reference population for each measure were considered "clinically impaired." For each test administered, the percentage of patients with an impaired score to examine whether specific cognitive tests with cognitive domains identified impairment.

2.2.1. General cognitive function

The Folstein Mini Mental Status Exam (MMSE) (12), the Montreal Cognitive Assessment (MOCA) (13) and the Mattis Dementia Rating Scale—2 (DRS-2) (14) were administered. Scores less than 25 on the MMSE, less than 26 on the MOCA, and less than 124 on the DRS-2 identified impairment.

2.2.2. Attention

The Attention subscale of the DRS-2 and the Digit Span subtest of the Wechsler Adult Intelligence Scale—IV (WAIS-IV) (15) assessed immediate attention, focused attention, and concentration.

2.2.3. Processing speed

Part A of the original Trail Making Test (TMT) (16) or the Trail Making test of the Delis Kaplan Executive Functioning System (D-KEFS) (17), and Word Reading and Color Naming trials of the Stroop Test (18) or the DKEFS Color Word test were administered.

2.2.4. Executive function

The Initiation and Conceptualization subtests of the DRS-2, Trail Making Test Part B or DKEFS Trails Condition 4, and the Color-Word trial of the Stroop or DKEFS Color Word test were administered.

2.2.5. Language

The Boston Naming Test (BNT) (19), Controlled Oral Word Association (20) or DKEFS Letter Fluency, and Semantic Fluence or DKEFS Semantic Fluency were administered.

2.2.6. Visual processing

The DRS-2 Construction subtest and WAIS-IV Block Design were administered.

2.2.7. Memory

DRS-2 Memory subtest, California Verbal Learning Test—2 (CVLT-2) (21) learning over Trials, and Logical Memory I and Logical Memory II of the Wechsler Memory Scale—4 (WMS-IV) (22) were administered.

2.2.8. Emotional distress

The Beck Depression Inventory—2 (BDI-II) (23) and the Beck Anxiety Inventory (BAI) (24) were administered. Scores >14 and >7 on the BDI-II and BAI, respectively, identified impairment.

2.3. Comparison of neuropsychologic features in CRL to other dementia syndromes

Ratings compare the neuropsychological profile of CRL defined in this study to the most common presenting cognitive impairments in clinical phenotypes of other well-recognized dementia syndromes. A rating of (+++) is given to a cognitive symptom that is commonly accepted as a primary or even pathognomonic feature to the cognitive phenotype. A rating of (++) is ascribed to a cognitive symptom present to a moderate degree in the cognitive phenotype. A rating of (+) is ascribed to a cognitive symptom present to some or a mild degree in the cognitive phenotype. Finally, a (−) is ascribed to a cognitive symptom not common or present at all in the cognitive phenotype.

3. Results

Patient descriptives are provided in Table 1. All 5 patients were Caucasian and right-hand dominant. Three patients identified as female and 2 as male, all between the ages of 37 and 51 years at the time of neuropsychological evaluation (mean: 42.2 years, standard deviaiton: 5.4 years). Patients ranged from 0.6 to 3.3 years of time between symptom onset and neuropsychological evaluation (mean: 2 years, standard deviation: 1 year). Raw test score descriptives for all neuropsychological measures administered are provided in Supplementary Table S1. For the General Cognitive Function domain, no patient's score on the MMSE was impaired using the established cut-off score of <25. A single patient was administered the MOCA and had an impaired score of 19. DRS Total scores were impaired for three of four patients that completed the DRS [mean: 123.2, standard deviation: 4.6, median: 121.5, range (120–130)]. Normative z-scores for measures within each cognitive domain are averaged and plotted in Figure 1. The mean plot of z-scores by cognitive domain reveals that tests of processing speed and executive function are disproportionately impaired in CRL. Figure 2 illustrates the percentage of impaired scores captured by each neuropsychological test within a cognitive domain. For the Attention domain, no patients obtained an impaired general attention score (DRS-2 Attention) but 2 of 5 patients were impaired on the WAIS-IV Digit Span (Figure 2A). For the Processing Speed domain (Figure 2B), all patients had impaired scores on color naming speed but only half of the patients had impaired scores on word reading speed. Four of 5 patients were impaired in simple visual sequencing speed (Trail Making Test Part A or Conditions 1, 2, 3, and 5 of the DKEFS Trail Making test). For the Executive Function domain (Figure 2C), 4 of 5 patients had impaired scores in speeded mental flexibility (Trail Making Test Part B or Condition 4 of the DKEFS Trail Making Test) and 3 of 4 patients had impaired scores on test of inhibitory control (Stroop Color Word Test, Color-Word Trial or Trial 3 of the DKEFS Color Word Test). General initiation was impaired in 3 of 4 patients (DRS Initiation). Abstract verbal reasoning and simple reasoning was not impaired in any patients. For the Language domain (Figure 2D), no patients earned impaired scores in confrontation naming (BNT) but 3 of 5 patients had impaired scores in letter fluency and in category fluency. For the Visual Processing domain (Figure 2E), 2 of 4 patients had impaired scores on untimed visual constructional skill exercises (DRS Construction), and 3 of 5 patients had impaired scores on speeded visual constructional problem solving (WAIS-IV Block Design). For the Memory domain (Figure 2F), no patients had impaired learning efficiency or delayed recall on a multiple trial word list learning test (CVLT2). General immediate memory was impaired in 1 of 4 patients (DRS-2 Memory subtest) and immediate story memory and delayed story recall were impaired in 1 of the 5 patients assessed (Logical Memory). Median BDI-II and BAI scores were clinically significant across patients. On the BDI-II, scores ranged from 7 to 28 (mean: 17.2, standard deviation: 9.9). On the BAI, scores ranged from 15 to 18 (mean: 16.5, standard deviation: 2.1). Suicidal ideation on the BDI-II was endorsed at the time of evaluation in one of the five patients. Table 2 presents

TABLE 1 Patient demographics.

	N (%)	Mean	SD	Median	Range
Total	5	–	–	–	–
Age at time of testing (years)	–	42.2	5.4	41	(37–51)
Formal education (years)	–	16.6	3.1	16	(12–20)
Disease duration at time of testing (years)	–	2	1	2.2	(0.6–3.3)
Female	3 (60)	–	–	–	–
Right-handed	5 (100)	–	–	–	–
Caucasian	5 (100)	–	–	–	–

the neuropsychological profile of CSF1R-related leukoencephalopathy in contrast to those of other dementia syndromes associated with primary neurodegenerative disease.

4. Discussion

A neuropsychological profile of CRL emerged from administering a standardized neuropsychological test battery to five consecutive patients referred for neuropsychological evaluation following confirmed diagnosis (Figure 1). Patients were impaired in general cognitive function to a degree that would suggest the presence of mild dementia. Processing speed and executive function were disproportionately impaired with additional cognitive inefficiencies observed in speeded visual processing and attention. In contrast, memory and language functions were relatively preserved. Patients self-reported clinically significant degrees of depression and anxiety symptoms. The emergent neuropsychological profile of CRL revealed reduced general cognitive function, slowed processing speed, impaired executive function, slowed word retrieval, slowed visual problem solving and self-reported symptoms of depression and anxiety. In contrast, reading, untimed naming, learning, and memory retention were relatively preserved. This finding is expected given that CRL preferentially affects white matter with cortical atrophy occurring as a later consequence of disease progression.

Within cognitive domains, some neuropsychological measures more frequently detected impairment relative to others. These differences further elucidate the specific neuropsychological profile of CRL and provide empirical support for test selection in describing cognitive manifestations of CRL. General cognitive function is impaired in CRL. Impairment was captured on the DRS-2 and MOCA, but not on the MMSE. The MMSE disproportionately emphasizes language and memory skills which are typically preserved in non-Alzheimer's dementia syndromes such as Parkinson's disease (PD). It has been previously shown that patients with PD may obtain normal MMSE scores despite scoring in the dementia range on other cognitive measures (25). In CRL, use of the MMSE may lead to false negative identification of cognitive impairment. Our results suggest that the DRS-2 Attention subtest may be less sensitive to impairment than a forward and backwards digit span task. In the evaluation of processing speed, measures of trail making and rates of word reading and color naming detect impairment frequently. Measures of mental flexibility and inhibitory control more commonly detected impairment than tests of abstract reasoning or simple reasoning. In the language domain, measures of speeded verbal fluency detected impairment, but a measure of untimed confrontation naming did not. In fact, there was no difference in the percentage of CRL patients impaired on letter fluency versus semantic fluency which is a pattern that emerges in other dementia syndromes (Table 2). This suggests that CRL patients may experience disturbances in language only to the degree that processing speed is inherent in the task. Alternatively, it is possible that impaired verbal fluency scores in CRL more likely related to impaired executive function than language function. Intersesting, disturbances in visual processing may only emerge when processing speed underlies performance as CRL patients were more frequently impaired on a speeded block assembly task than on untimed drawing tasks. In the memory domain, none of the neuropsychological measures frequently detected impairment in the cases. This contrasts to the prominent amnestic presentations observed in AD and MCI-Amnestic subtype cases and patterns of poor learning efficiency and memory retrieval observed in LBD, PSP, CBS, FTD, and depression cases. This suggests that memory measures may not need to be essential to neuropsychological test batteries designed to detect early cognitive impairment in CRL. More study is needed, with larger sample sizes and patients at varied stages of disease, to further inform which neuropsychological measures are most sensitive to the cognitive impact of CRL.

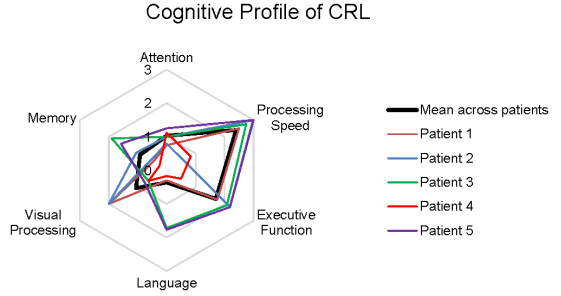

FIGURE 1
Radar plot of cognitive domain *Z*-scores for each patient and cohort mean. Concentric rings begin in the center at $z = 0.0$, with each expanding ring increasing by one standard deviation greater impairment to $z = -2.0$, and finally to $z = -3.0$. Colored lines represent individual patients. Thick black line represents mean across all patients.

Table 2 compares the neuropsychological features of CRL with dementia syndromes of other primary neurodegenerative diseases. The neuropsychological profile of CRL is distinct from AD dementia or prodromal AD, i.e., amnestic mild cognitive impairment, in that memory is not impaired. Further, confrontation naming is often impaired in early AD as a function of proliferating temporal lobe cognitive systems dysfunction but remains preserved in CRL. The neuropsychological profile of CRL is also distinct from that of LBD. Both CRL and LBD share frontal subcortical cognitive systems compromise resulting in cognitive slowing, reduced attention and concentration, and diminished executive function. However, the neuropsychological profile of CRL does not involve frontal subcortical memory dysfunction and parietal–temporal-occipital junction visual systems dysfunction that is present in LBD. There are many similarities between neuropsychological presentations of CRL and FTD but generalized cognitive slowing is more pronounced and unique to CRL. PSP may be more likely to adversely impact learning, retrieval, and memory retention compared to CRL whereas general cognitive function may be more impaired in CRL relative to PSP. CRL and CBS neuropsychological profiles may be quite similar. This is not entirely unexpected as prior studies have documented overlap between clinical presentations of CBS and ALSP with confirmed CSF1R mutation (11, 26). Further research on distinguishing CRL and CBS neuropsychological profiles in early stage, or even prodromal disease, could ultimately be useful particularly in cases for which neuropsychological manifestations precede motor presentations. Although cognitive and behavioral changes experienced in CRL have been associated with behavioral variant FTD, to date, there have been no such studies directly comparing the neuropsychological profiles and such a study could be helpful in future research. Finally, the neuropsychological profiles

of depression and CRL may be hard to distinguish as both involve impaired general cognitive function and prominent cognitive slowing. Our data suggest that learning, retrieval, and memory retention scores are more likely impaired in depression relative to CRL. Our data are the first to differentiate the neuropsychological profile of CRL from other primary neurodegenerative dementia syndromes and depression.

Patients with CRL reported mild depression symptoms and severe anxiety symptoms. Depression and anxiety are common in various forms of dementia and can even be observed in prodromal stages of dementia. For example, in a clinic-based sample of patients with Mild Cognitive Impairment, 40% of the sample reported significant depression (27). Rates of depression in atypical parkinsonian syndromes are more frequent and more severe than those reported in idiopathic PD (28). It is unknown if depression and anxiety are more prevalent in CRL than in other neurodegenerative conditions. From a methodological perspective, it is unclear whether self-report vs. informant-based neuropsychiatric symptom screening measures are most sensitive for screening neuropsychiatric symptoms in CRL. Prior work has suggested that the presence of diminished awareness, or anosognosia, accounts for variance in self-report accuracy when dementia patients must describe emotional distress relative to informant ratings (29). Prior descriptions of clinical symptoms in CRL have pointed out similarity to bvFTD but this study did not administer informant measures to evaluate frontal behavior and personality changes common in bvFTD and other associated frontal temporal lobar degeneration (FTLD) syndromes clinical syndromes. CRL symptom profiles on informant-based measures such as the Frontal Behavioral Inventory (FBI) (30) and the Neuropsychiatric Inventory—Questionnaire (NPI-Q) (31), which have been used in evaluating

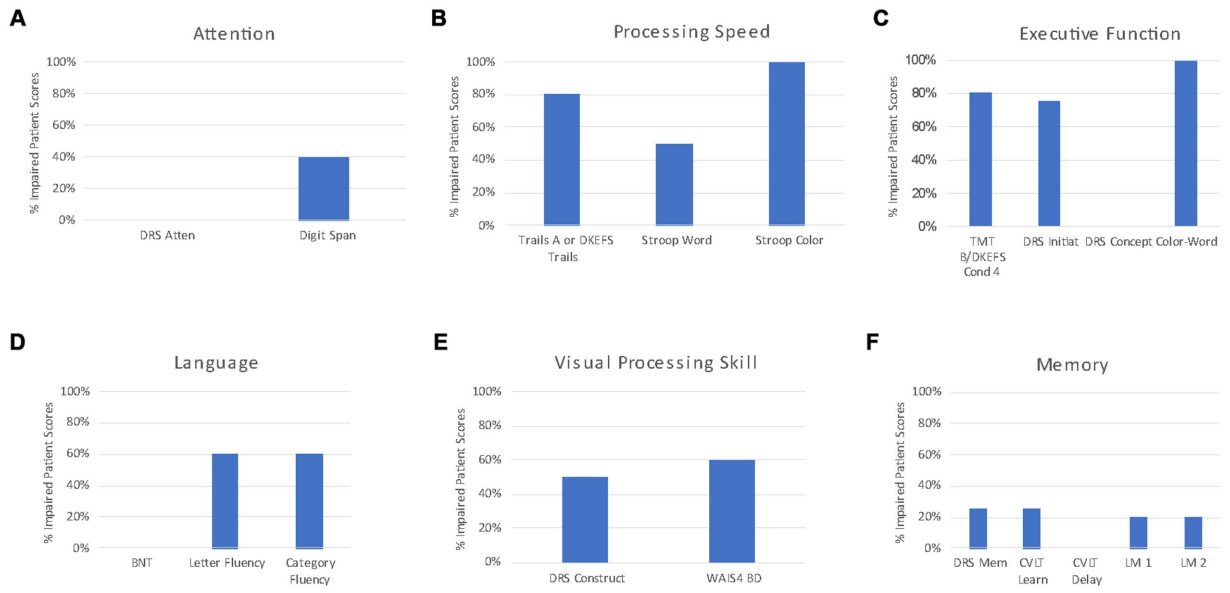

FIGURE 2
Bar graphs displaying percentage of impaired patient scores across tests within cognitive domains.

TABLE 2 Comparison of neuropsychologic features in CRL to other dementia syndromes.

	CRL	AD	LBD	FTD	PSP	CBS	Dep
General cognition	++	++	++	++	+	++	++
Attention	++	+	++	++	++	+	+
Processing speed	+++	+	+++	+	++	++	+++
Executive function	++	++	++	++	++	++	++
Naming	–	++	+	++	–	+	–
Verbal fluency	+++	++	++	+++	+	++	++
Visual processing	+	+	++	–	+	+	–
Learning/retrieval	–	+	++	++	+	+	++
Memory retention	–	+++	++	++	+	+	+
Emotional distress	+++	+	++	+	+	+	+++

CRL, CSF1R-related leukoencephalopathy; AD, Alzheimer's dementia; LBD, lewy body dementia; FTD, frontal temporal dementia; PSP, progressive supranuclear palsy; CBS, corticobasal degeneration syndrome; Dep, depression/psychiatric Illness.
(–), negligible or absent; (+), present to mild degree; (++), present to moderate degree; (+++), present to very significant degree.

other FTLD syndromes, may be particularly interesting in CRL. Further research is needed to document mood, personality and behavior symptoms in CRL, in contrast to other FTLD clinical syndromes. Such work can elaborate on identify disease-specific neuropsychiatric features to CRL.

CRL is rare and it is challenging to report meaningful data on a series of consecutive cases and draw conclusions from small sample sizes. Ideally, all patients in this study would have received the exact same neuropsychological tests to assess each cognitive domain. Based on the availability of normative reference samples for raw score interpretation, patients received different versions of tests evaluating the same component of a given cognitive domain. This study did not correlate neuropsychological test performance with brain imaging findings, e.g., degree of corpus callosal atrophy, extent of white matter involvement (32), or the presence and extent of brain calcifications. Future correlative studies will improve understanding of the neuropsychological profile of CRL at various stages of disease and may be helpful in diagnostic decision-making algorithms by which to pursue interventions, symptom management strategies, or clinical trials. For example, if cognitive and imaging findings are sufficiently impaired, patients, families and clinicians may not decide an intervention offers the same yield verus a situation for which cognitive and imaging findings suggest a more nascent stage of the disease process.

This study is the first to document neuropsychological findings from a comprehensive test battery with a consecutive series of patients with CRL. Processing speed and executive functions are prominently impaired, but studies with larger patient cohorts and serial neuropsychological assessments will shed light on any dynamics of the CRL neuropsychological profile, which may change with disease progression. Deeper understanding of the CRL neuropsychological profile will strengthen counseling of patients and families and may guide treatment decisions.

Data availability statement

The original contributions presented in the study are included in the article/Supplementary material, further inquiries can be directed to the corresponding author.

Ethics statement

The studies involving human participants were reviewed and approved by the study protocol associated with data reported here was approved by the Mayo Clinic Institutional Review Board (FWA# FWA00005001) on July 17, 2020. The study was approved, via expedited review, as a minimal risk study. Study approval confirmed that the research met requirements for research with human participants in accordance with the Code of Ethics of the World Medical Association and 45 CFR 46 of the U.S. Department of Health and Human Services, Office for Human Research Protections. Written informed consent for research was obtained from all participants (or guardians of participants) in the study. The patients/participants provided their written informed consent to participate in this study.

Author contributions

BR was the primary and corresponding author to this study. BR completed clinical evaluation of the patients, the data analyses, the primary preparation of the manuscript, and created supporting of tables and figures. PT was a co-author contributing to the clinical evaluation of the patients, data analyses, the creation of tables and figures, and preparing the manuscript. AS was a co-author and contributed to the clinical and research evaluation of the patients, assisted with data collection, and contributed to the analyses. ZW was a senior author contributing to the clinical and research evaluation of the patients, data analyses, and manuscript preparation. All authors contributed to the article and approved the submitted version.

Conflict of interest

The authors declare that the research was conducted in the absence of any commercial or financial relationships that could be construed as a potential conflict of interest.

Publisher's note

All claims expressed in this article are solely those of the authors and do not necessarily represent those of their affiliated organizations, or those of the publisher, the editors and the reviewers. Any product that may be evaluated in this article, or claim that may be made by its manufacturer, is not guaranteed or endorsed by the publisher.

Supplementary material

The Supplementary material for this article can be found online at: https://www.frontiersin.org/articles/10.3389/fneur.2023.1155387/full#supplementary-material

References

1. Wszolek ZK. First polish case of CSF1R-related leukoencephalopathy. *Neurol Neurochir Pol.* (2021) 55:239–40. doi: 10.5603/PJNNS.a2021.0022

2. Papapetropoulos S, Pontius A, Finger E, Karrenbauer V, Lynch DS, Brennan M, et al. Adult-onset leukoencephalopathy with axonal spheroids and pigmented glia: review of clinical manifestations as foundations for therapeutic development. *Front Neurol.* (2021) 12:788168. doi: 10.3389/fneur.2021.788168

3. Konno T, Yoshida K, Mizuta I, Mizuno T, Kawarai T, Tada M, et al. Diagnostic criteria for adult-onset leukoencephalopathy with axonal spheroids and pigmented glia due to CSF1R mutation. *Eur J Neurol.* (2018) 25:142–7. doi: 10.1111/ene.13464

4. Konno T, Yoshida K, Mizuno T, Kawarai T, Tada M, Nozaki H, et al. Clinical and genetic characterization of adult-onset leukoencephalopathy with axonal spheroids and pigmented glia associated with CSF1R mutation. *Eur J Neurol.* (2017) 24:37–45. doi: 10.1111/ene.13125

5. Ali S, Tipton PW, Koga S, Middlebrooks EH, Josephs KA, Strongosky A, et al. A novel CSF1R variant in a South Dakota family with CSF1R-related leukoencephalopathy. *Parkinsonism Relat Disord.* (2022) 102:51–3. doi: 10.1016/j.parkreldis.2022.07.016

6. Mickeviciute GC, Valiuskyte M, Platten M, Wszolek ZK, Andersen O, Karrenbauer VD, et al. Neuroimaging phenotypes of CSF1R-related leukoencephalopathy: systematic

review, meta-analysis, and imaging recommendations. *J Intern Med*. (2022) 291:269–82. doi: 10.1111/joim.13420

7. Tian WT, Zhan FX, Liu Q, Luan XH, Zhang C, Shang L, et al. Clinicopathologic characterization and abnormal autophagy of CSF1R-related leukoencephalopathy. *Transl Neurodegener*. (2019) 8:32. doi: 10.1186/s40035-019-0171-y

8. Rosenstein I, Andersen O, Victor D, Englund E, Granberg T, Hedberg-Oldfors C, et al. Four Swedish cases of CSF1R-related leukoencephalopathy: visualization of clinical phenotypes. *Acta Neurol Scand*. (2022) 145:599–609. doi: 10.1111/ane.13589

9. Chen J, Luo S, Li N, Li H, Han J, Ling L. A novel missense mutation of the CSF1R gene causes incurable CSF1R-related leukoencephalopathy: case report and review of literature. *Int J Gen Med*. (2020) 13:1613–20. doi: 10.2147/IJGM.S286421

10. Sohn EH, Lee J, Lee AY, Shin JH. A case of CSF1R-related leukoencephalopathy: serial neuroimaging and neuropsychological tests. *Neurocase*. (2021) 27:415–8. doi: 10.1080/13554794.2021.1981947

11. Robinson JL, Suh E, Wood EM, Lee EB, Coslett HB, Raible K, et al. Common neuropathological features underlie distinct clinical presentations in three siblings with hereditary diffuse leukoencephalopathy with spheroids caused by CSF1R p.Arg782His. *Acta Neuropathol Commun*. (2015) 3:42. doi: 10.1186/s40478-015-0219-x

12. Folstein MF, Folstein SF, McHugh PR. Mini-mental state: a practical method for grading the cognitive state of patients for the clinician. *J Psychiatry Res*. (1975) 12:189–98. doi: 10.1016/0022-3956(75)90026-6

13. Nasreddine ZS, Phillips NA, Bédirian V, Charbonneau S, Whitehead V, Collin I, et al. The Montreal cognitive assessment, MoCA: a brief screening tool for mild cognitive impairment. *J Am Geriatr Soc*. (2005) 53:695–9. doi: 10.1111/j.1532-5415.2005.53221.x

14. Jurica PJ, Leitten S, Mattis S. *Dementia rating scale-2: professional manual*. Lutz: Psychological Assessment Resources (2001).

15. Wechsler D. *Wechsler adult intelligence scale, fourth edition (WAIS-IV)*. Texas: Pearson (2008).

16. Reitan RM. Validity of the trail making test as an Indicator of organic brain damage. *Percept Motor Skills*. (1958) 8:271–6. doi: 10.2466/pms.1958.8.3.27

17. Delis D, Kaplan E, Kramer JH. *Delis-Kaplan executive function system (D-KEFS)*. San Antonio, TX: Psychological Corporation (2001).

18. Golden C. *Stroop color and word test: a manual for clinical and experimental uses*. Wood Dale, IL: Stoelting Company (1978).

19. Kaplan E, Goodglass H, Weintraub S. *The Boston naming test*. Philadelphia, PA: Lea & Febiger (1983).

20. Benton A, de Hamsher K. *Controlled oral word association test (COWAT)*. Iowa City, IA: AJA Associates (1983).

21. Delis DC, Kramer JH, Kaplan E, Ober BA. *California verbal learning test-second edition (CVLT-II)*. San Antonio, TX: Psychological Corporation (2000).

22. Wechsler D. *WMS-IV: Wechsler memory scale-fourth edition*. San Antonio, TX: Pearson (2009).

23. Beck AT, Steer A, Brown K. *Beck depression inventory–II (BDI-2)*. San Antonio, TX: Psychological Corporation (1996).

24. Beck A, Steer A. *Beck anxiety inventory manual*. San Antonio, TX: Psychological Corporation (1993).

25. Burdick DJ, Cholerton B, Watson GS, Siderowf A, Trojanowski JQ, Weintraub D, et al. People with Parkinson's disease and normal MMSE score have a broad range of cognitive performance. *Mov Disord*. (2014) 29:1258–64. doi: 10.1002/mds.25924

26. Guerreiro R, Kara E, Le Ber I, Bras J, Rohrer JD, Taipa R, et al. Genetic analysis of inherited Leukodystrophies: genotype-phenotype correlations in the CSF1R gene. *JAMA Neurol*. (2013) 70:875–82. doi: 10.1001/jamaneurol.2013.698

27. Ismail Z, Elbayoumi H, Fischer CE, Hogan DB, Millikin CP, Schweizer T, et al. Prevalence of depression in patients with mild cognitive impairment: a systematic review and Meta-analysis. *JAMA Psychiat*. (2017) 74:58–67. doi: 10.1001/jamapsychiatry.2016.3162

28. Almeida L, Ahmed B, Walz R, De Jesus S, Patterson A, Martinez-Ramirez D, et al. Depressive symptoms are frequent in atypical parkinsonian disorders. *Mov Disord Clin Pract*. (2017) 4:191–7. doi: 10.1002/mdc3.12382

29. Snow AL, Kunik ME, Molinari VA, Orengo CA, Doody R, Graham DP, et al. Accuracy of self-reported depression in persons with dementia. *J Am Geriatr Soc*. (2005) 53:389–96. doi: 10.1111/j.1532-5415.2005/53154-x

30. Kertesz A, Davidson W, Fox H. Frontal behavioral inventory: diagnostic criteria for frontal lobe dementia. *Can J Neurol Sci*. (1997) 24:29–36. doi: 10.1017/s0317167100021053

31. Kaufer DI, Cummings JL, Ketchel P, Smith V, MacMillan A, Shelley T, et al. Validation of the NPI-Q, a brief clinical form of the neuropsychiatric inventory. *J Neuropsychiatry Clin Neurosci*. (2000) 12:233–9. doi: 10.1176/jnp.12.2.233

32. Sundal C, Van Gerpen JA, Nicholson AM, Wider C, Shuster EA, Aasly J, et al. MRI characteristics and scoring in HDLS due to CSF1R gene mutations. *Neurology*. (2012) 79:566–74. doi: 10.1212/WNL.0b013e31826355an

frontiers | Frontiers in Neurology

TYPE Case Report
PUBLISHED 29 June 2023
DOI 10.3389/fneur.2023.878446

OPEN ACCESS

EDITED BY
Bruce Miller,
University of California, San Francisco,
United States

REVIEWED BY
Andrea Legati,
IRCCS Carlo Besta Neurological Institute Foundation, Italy
Daria Diodato,
Bambino Gesù Children's Hospital (IRCCS), Italy

*CORRESPONDENCE
Carmen Alaez-Verson
✉ calaez@inmegen.gob.mx

RECEIVED 18 February 2022
ACCEPTED 10 May 2023
PUBLISHED 29 June 2023

CITATION
Kazakova E, Téllez-Martínez JA, Flores-Lagunes L, Sosa-Ortiz AL, Carillo-Sánchez K, Molina-Garay C, González-Domínguez CA, Jimenez-Olivares M, Fernandez-Valverde F, Vargas-Cañas ES, Vázquez-Memije ME, Garcia-Latorre EA, Martínez-Duncker I and Alaez-Verson C (2023) Uterus *infantilis:* a novel phenotype associated with *AARS2* new genetic variants. A case report. *Front. Neurol.* 14:878446. doi: 10.3389/fneur.2023.878446

Uterus *infantilis:* a novel phenotype associated with *AARS2* new genetic variants. A case report

Ekaterina Kazakova[1], José Alberto Téllez-Martínez[2], Leonardo Flores-Lagunes[3], Ana Luisa Sosa-Ortiz[2], Karol Carillo-Sánchez[3], Carolina Molina-Garay[3], Carlos Alberto González-Domínguez[4], Marco Jimenez-Olivares[3], Francisca Fernandez-Valverde[5], Edwin Steven Vargas-Cañas[6], Martha Elisa Vázquez-Memije[1], Ethel Awilda Garcia-Latorre[7], Iván Martínez-Duncker[4] and Carmen Alaez-Verson[3]*

[1]Centro de Diagnóstico en Metabolismo Energético y Medicina Mitocondrial, Mexico City, Mexico, [2]Clínica de Cognición, Instituto Nacional de Neurología y Neurocirugía Manuel Velasco Suárez, Mexico City, Mexico, [3]Laboratorio de Diagnóstico Genómico, Instituto Nacional de Medicina Genómica, Mexico City, Mexico, [4]Laboratorio de Glicobiología Humana y Diagnóstico Molecular, Centro de Investigación en Dinámica Celular, Instituto de Investigación en Ciencias Básicas y Aplicadas, Universidad Autónoma del Estado de Morelos, Morelos, Mexico, [5]Laboratorio de Patología Experimental, Instituto Nacional de Neurología y Neurocirugía Manuel Velasco Suárez, Mexico City, Mexico, [6]Clínica de Nervio y Músculo, Instituto Nacional de Neurología y Neurocirugía Manuel Velasco Suárez, Mexico City, Mexico, [7]Escuela Nacional de Ciencias Biológicas, Instituto Politécnico Nacional, Mexico City, Mexico

Objectives: To report the first Mexican case with two novel *AARS2* mutations causing primary ovarian failure, uterus *infantilis,* and early-onset dementia secondary to leukoencephalopathy.

Methods: Detailed clinical, clinimetric, neuroimaging features, muscle biopsy with biochemical assays of the main oxidative phosphorylation complexes activities, and molecular studies were performed on samples from a Mexican female.

Results: We present a 41-year-old female patient with learning difficulties since childhood and primary amenorrhea who developed severe cognitive, motor, and behavioral impairment in early adulthood. Neuroimaging studies revealed frontal leukoencephalopathy with hypometabolism at the fronto-cerebellar cortex and caudate nucleus. Uterus *infantilis* was detected on ultrasound study. Clinical exome sequencing identified two novel variants, NM_020745:c.2864G>A (p.W955*) and NM_020745:c.1036C>A (p.P346T, p.P346Wfs*18), in *AARS2*. Histopathological and biochemical studies on muscle biopsy revealed mitochondrial disorder with cytochrome C oxidase (COX) deficiency.

Conclusions: Several adult-onset cases of leukoencephalopathy and ovarian failure associated with *AARS2* variants have been reported. To our best knowledge, none of them showed uterus *infantilis*. Here we enlarge the genetic and phenotypic spectrum of *AARS2*-related dementia with leukoencephalopathy and ovarian failure and contribute with detailed clinical, clinometric, neuroimaging, and molecular studies to disease and novel molecular variants characterization.

KEYWORDS

mitochondrial aminoacyl-tRNA synthetase, *AARS2*, adult-onset leukodystrophy, progressive leukoencephalopathy with ovarian failure, uterus *infantilis*, alanyl-transfer RNA synthetase 2 mutation-related leukodystrophy, early-onset dementia, AARS2 leukoencephalopathy

Background

The alanyl-tRNA synthetase 2 (*AARS2*, MIM#612035) is a 22 exons nuclear gene located on 6p21.1. It encodes the mitochondria-specific alanyl-tRNA synthetase enzyme, responsible for the aminoacylation between alanine and the tRNA during translation in the mitochondria. The AARS2 protein contains editing and aminoacylation domains. Deleterious variants in these sites affect the catalysis of aminoacylation (1).

Deficiency in aminoacyl-tRNA synthetases is known to contribute to mitochondrial diseases in association with a broad spectrum of clinical phenotypes (2, 3). *AARS2* pathogenic variants were first identified in infantile mitochondrial cardiomyopathy (4) and later found to cause an adult-onset autosomal recessive leukodystrophy, MIM#615889 (https://www.omim.org/) (5).

The classic presentation of alanyl-transfer RNA synthetase-2 mutation-related leukodystrophy (AARS2-L) is a childhood-to-adulthood onset neurologic deterioration primarily related to frontal and cerebellar dysfunction that manifests with ataxia, spasticity, cognitive decline, psychiatric disorders or executive dysfunction (6). MRI signal abnormalities are primarily found in frontal and parietal white matter and the corpus callosum. There is no established treatment for AARS2-L (5).

To our best knowledge, 27 index AARS2-L cases have been reported up to date (5, 7–14). Amazingly, most described cases are adult-onset with nearly invariable progression to severe disability and atrophy of the involved brain regions, often within a decade (5–7, 10).

Case presentation

Here we present the case of a 41-year-old female born to non-consanguineous Mexican parents. The patient has a family history of late-onset Alzheimer's disease (maternal grandmother), alcohol and drug abuse (father and elder brother), major depressive disorder, and a suicide attempt (mother). There is no further information on the father's family history.

The patient reports sexual abuse on one occasion at 13 years, with no medical or psychiatric attention. She has had a history of migraines since adolescence, treated with unspecified non-steroid anti-inflammatory drugs. The patient presented primary amenorrhea; therefore, a pelvic ultrasound was performed at 15 years, reporting uterus *infantilis* with atrophic endometrium. Menarche was hormonally induced at 15 years. The patient has never become pregnant.

From the age of 35 years, she is reported to have multiple sexual partners, and at 40, she began with a cognitive and behavioral impairment that resulted in a notable work-related dysfunction. The relative found her under deplorable hygienic conditions and crude self-care. However, she preserved partial functionality that allowed the completion of basic activities like bathing and feeding under supervision while losing the ability to carry out instrumented activities of daily life. At 41 years old, she was diagnosed with type I bipolar disorder and treated with quetiapine 100 mg/day and fluoxetine 20 mg/day, but no improvement was observed.

Since the deterioration progressed, at 41 years, she attended INNN and was evaluated by the Dementia Clinic. The most relevant clinical findings include: a puerile attitude, disorientation in space and time, emotional liability and pathological crying, inattention, altered speech (phonological paraphasias, substitutions, and perseverations), difficulty in understanding complex orders, perseverative behavior, increased psychomotricity due to anxiety, environmental dependence, and anosognosia.

On physical examination, cardiovascular alterations were absent, and pyramidal signs and frontoparietal dysfunction were present. Laboratory tests excluded infectious, toxic-metabolic, neoplasm, and endocrinologic etiologies. No alterations were detected in cerebrospinal fluid analysis, electroencephalographic studies, and karyotype. The brain magnetic resonance imaging (MRI) showed abnormal signals in the bilateral periventricular anterior white matter and the anterior part of the corpus callosum (Figures 1A–C). 18-F FDG PET/MRI showed frontal leukoencephalopathy with hypometabolism at the fronto-cerebellar cortex and caudate nucleus. The performance in cognitive tests and neuropsychiatric evaluation reports are shown in Supplementary Table 1 and Figures 1D–F.

At 46 years, due to the previous uterus *infantilis* report, an additional sonographic study on the pelvic region was performed. A Mindray Z6 computerized system and a multi-frequency convex transducer were used. The study revealed a diminished size uterus confirming the uterus *infantilis* (Figure 2).

Supportive treatment was initiated with citalopram 30 mg/24 h, quetiapine 200 mg/24 h, and gait rehabilitation. Some neuropsychiatric symptoms, mainly emotional lability, psychotic symptoms, and behavioral disturbances, were gradually improved. However, the patient continued rapidly deteriorating cognitive and motor aspects, and a complete loss of autonomy occurred at 43.

Genetic analysis

Clinical exome sequencing

DNA was extracted from peripheral blood. According to the manufacturer's protocol, library preparation was performed using the reagents provided in the Clinical Exome Sequencing panel kit, version 2 (Sophia Genetics SA, Saint Sulpice, Switzerland). The panel includes coding regions and intron/exon borders of 4,900 genes. Sequencing was performed on NextSeq Instrument (Illumina San Diego, CA). Sequencing data analysis and variant annotation were performed with the Sophia DDM® platform (Sophia Genetics SA, Saint Sulpice, Switzerland). Copy number variations were predicted from the sequencing data. Virtual panels were built, including the known genes associated with major neurocognitive disorders. Information from variant databases and international literature was used in the variant review process. Two novel variants were identified in the *AARS2* gene: NM_020745:c.1036C>A (p.P346T) and NM_020745:c.2864G>A (p.W955*).

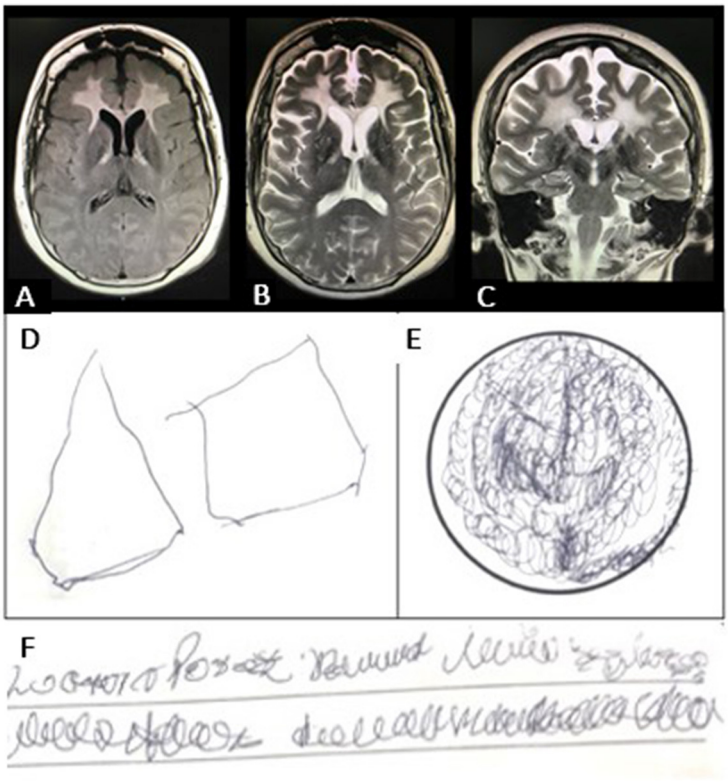

FIGURE 1
(A) Brain magnetic resonance imaging (MRI) shows abnormal signals in the bilateral periventricular anterior white matter and the anterior part of the corpus callosum. **(B)** Axial T2-weighted MRI shows abnormal signals in the frontal white matter and in the pyramidal tract at the internal capsule. There was no clear pattern of cortical atrophy, and the hippocampal volume was normal. **(C)** The diffusion-weighted image (DWI) shows patchy areas of restricted diffusion in the abnormal white matter. **(D)** Visuospatial ability performance in the Minimental Status Examination (MMSE) test showing visuospatial disintegration (no intersection, loss of some sides and angles); **(E)** Clock Drawing Test (CDT) with perseverative drawing; **(F)** Writing a sentence in the MMSE test showing dysgraphia.

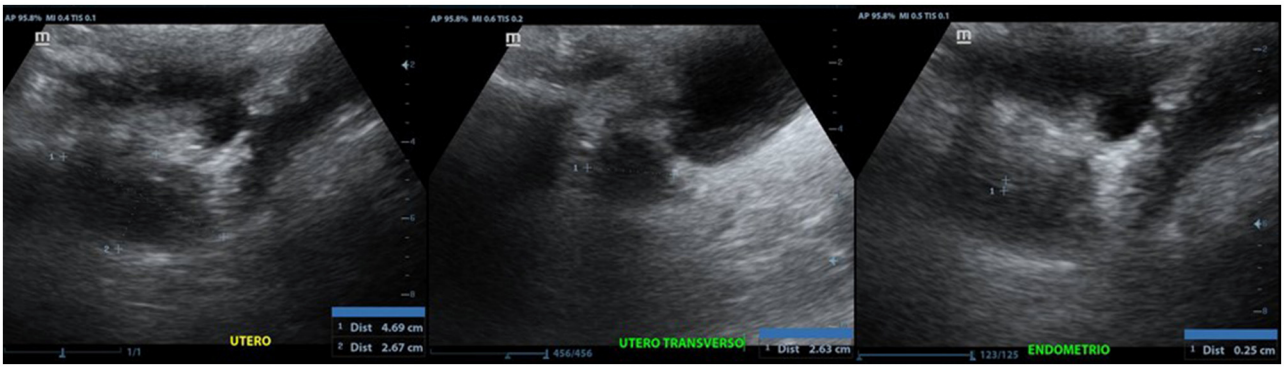

FIGURE 2
Anteverted uterus, with regular and poorly defined contours, with approximate dimensions of 4.6 x 2.6 x 2.6 cm in its longitudinal, transverse and anteroposterior axes, respectively.

Sanger sequencing confirmation

In order to confirm the identified variants, gDNA-polymerase chain reaction (PCR) products from the corresponding segments of the *AARS2* exons 6 and 22 were obtained. For exon 6 primers: F-AARS2-E6s 5′-CTGGATGTGGTTGGCTTTAGGG-3′ and R-AARS2-E6as 5′-CCAGTGTGTGCTCCCACCTC-3′ were used. For exon 22 F-AARS2-E22s 5′-CACTCTTGAGGGTACCTTG-3′ and R-AARS2-E22as 5′-CAGCCTCTAGTCCTCGC-3′ primers were used. Direct Sanger sequencing of PCR products was carried out. Electrophoretic analysis was performed on ABI Prism 3130xl genetic analyzer (Applied Biosystems, Foster City, CA). Both variants were confirmed by Sanger sequencing in the patient. The

variant c.2864G>A (p.W955*) was also identified in the patient's healthy mother (Figure 3A). No DNA from the father was available to complete the segregation analysis.

Variant classification

NM_020745:c.2864G>A is a nonsense variant in exon 22 that originates a premature stop codon p.W955*. This change is predicted to cause protein loss of 31 amino acids. The variant is absent from dbSNP, 1,000 Genomes Browser phase 3, ExAC, and gnomAD (exomes and genomes) databases. It is not listed in the ClinVar database nor the professional Human Gene Mutation Database (HGMD) (last accessed Nov 2022 for all databases). We classified p.W955* as pathogenic according to the American College of Medical Genetics (ACMG) criteria.

The variant NM_020745:c.1036C>A is a missense variant located in exon 6, that originates p.P346T amino acid substitution. Its population frequency is very low (frequency = 0.0000289) and has been identified in only one Latino individual, according to the gnomAD exomes database. It is absent from gnomAD genomes, 1,000 genomes, ExAC databases, and from a publicly available database that includes 480 exomes from Mexican Mestizo individuals (https://franklin.genoox.com/clinical-db/home). The variant is identified in the dbSNPs with rs1438347145. It does not have a clinical classification assigned in the ClinVar database and is not listed in the HGMD database (last accessed Nov 2022).

Amino acid alignment of the *AARS2* homologous gene is shown in Figure 4. The amino acid p.P346 is not highly conserved; only *Ptroglodytes* and *M. Mulatta* have proline in this position. The change from proline to threonine is not conservative (cyclic-no polar to aliphatic-polar). Predictions from *in silico* algorithm are conflicting: DANN, FATHMM-MKL, LIST-S2, M-CAP, MutationTaster, and SIFT predict as pathogenic while BayesDel_addAF, DEOGEN2, EIGEN, MVP, MutationAssessor and PrimateAI predict as benign.

However, the affected nucleotide (c.1036C) is conserved (PhiloP 2.745 and PhastCons 0.991). It is located five bases away from the canonical splicing site in the exon-intron border. The Mutation Taster algorithm predicts that this change would affect mRNA processing creating a new splicing donor site at position gDNA 6070 (score 0.86) that would affect the zinc-binding domain of the protein. The Human Splicing Finder program also predicts a possible alteration of the splicing (15).

Evaluation of possible alteration in splicing

Since variant c.1036C>A was predicted to affect mRNA processing, Sanger sequencing of cDNA-based PCR product of the coding sequence of *AARS2* was performed. The mRNA was obtained from the patient peripheral blood sample using RNeasy Mini Kit (QIAGEN N.V., Hilden, Germany). The primers used were: F-AARS2s 5′-ACACTGACCTCTTTTCCCCG-3′ and R-AARS2as5′-GCCCATGTCTCCTTGTGTCA-3′. The schematic representation and the results are shown in Figures 3B, C. Sanger sequencing revealed that the c.1036C>A variant causes both constitutive splicing harboring the p.P346T change and an alternative splicing caused by the activation of a cryptic donor splice site leading to deletion of seven nucleotides from exon 6, causing a frameshift and a premature stop codon (P346Wfs*18). These results confirm that the c.1036C>A originates leaky splicing.

Variant analysis for uterus *infantilis*

In order to establish if this feature would be related to pathogenic variants in known causative genes, virtual panels were built using the following Human Phenotype Ontology (HPO) terms: HP:0008684:Aplasia/hypoplasia of the uterus, HP:0000130:Abnormality of the uterus, HP0000013:Hypoplasia of the uterus and, HP0031105:Abnormal uterus morphology. No pathogenic o likely pathogenic variants in the sequenced genes were identified. The analyzed genes are listed in Supplementary material S1.

Muscle biopsy and mitochondrial respiratory chain findings

At 46 years of age, the patient underwent a left deltoid muscle biopsy. Muscle morphological studies revealed myopathic and neuronopathic changes with loss of COX activity in some fibers and blue fibers presence in Cytochrome C Oxidase/Succinate Dehydrogenase (COX/SDH) double-labeling method which suggests COX deficiency (Figure 5).

Biochemical evaluation of the mitochondrial respiratory chain function was performed by measuring citrate synthase, cytochrome c oxidase, and other mitochondrial enzyme activities in skeletal muscle homogenates, as previously described (16). A complex IV (COX) deficiency was confirmed. Decreased citrate synthase activity was detected, indicating a significant reduction of the mitochondrial content. The activity of other mitochondrial complexes (expressed as nmol/min per mg protein) was also reduced, but after correcting for citrate synthase activity, they were within the normal ranges (Supplementary Table 2).

Discussion

We report the first Mexican case of AARS2-L, a hereditary autosomal recessive metabolic dementia form with progressive leukoencephalopathy and ovarian failure. AARS2-L is an ultrarare disease with <40 cases described worldwide. The clinical onset usually occurs in the 3rd or 4th decade of life with signs and symptoms originating from fronto-cerebellar dysfunction, including cognitive, behavioral, and motor involvement (5, 17). Spasticity is the most consistent finding, and dystonia, dysarthria, or tremor may also be present (7, 10, 18). All adult-onset patients reported thus far, except two (13, 19), presented leukoencephalopathy. Typically, these patients advance to the point of no or limited interaction with the environment, non-ambulatory status, and in many cases, premature death within 5–10 years after the onset of the symptoms (7, 10, 18). The patient reported here had learning difficulties from childhood, and behavioral and cognitive disturbances began at a young age (apparently at 40 years), causing detriment of self-care and social and work impairment.

All female patients described so far presented primary or secondary ovarian failure except one (20). The ovarian failure in

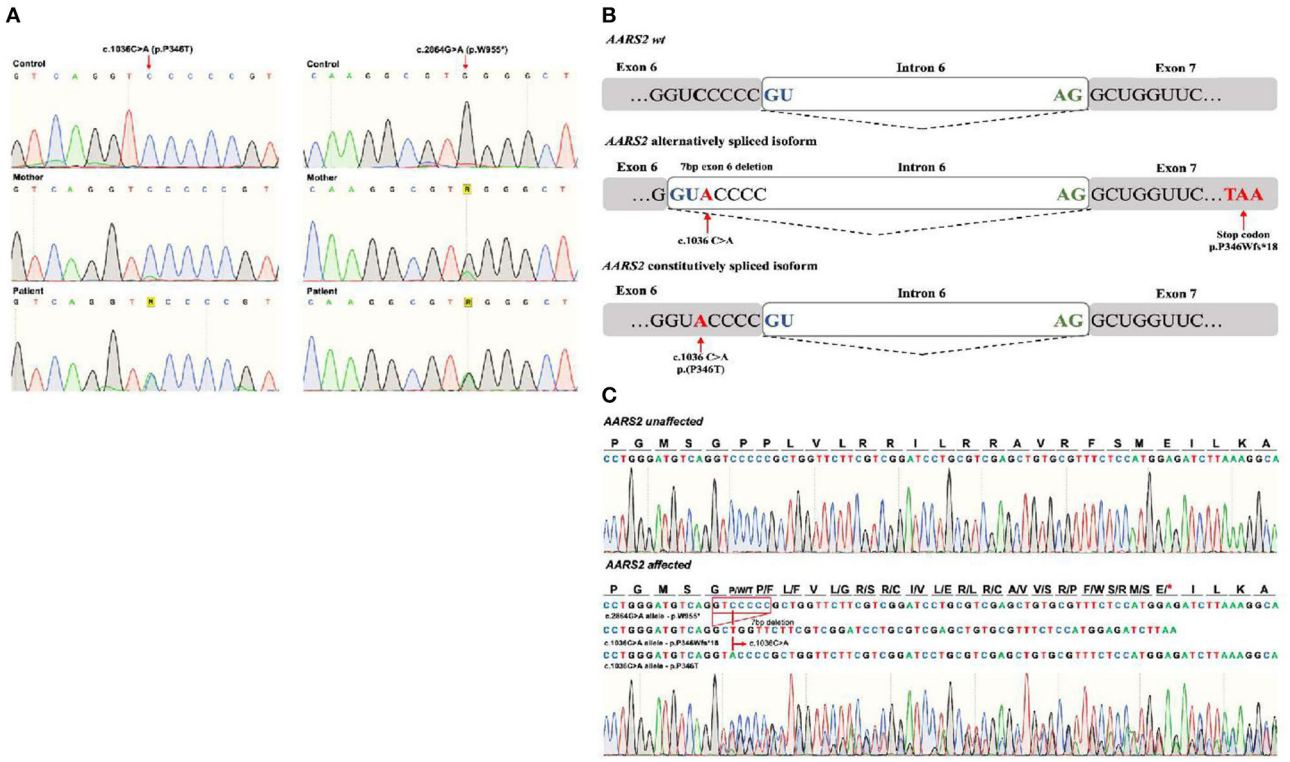

FIGURE 3
(A) Sanger sequencing of the *AARS2* in gDNA from the control, mother, and patient confirming the presence of both variants: NM_020745:c.1036C>A (p.P346T) and NM_020745:c.2864G>A (p.W955*) in the patient. The p. c.2864G>A * was identified in the mother. **(B)** Schematic representation of a wild type, and the alternative and constitutive splicing isoforms caused by the c.1036C>A variant. **(C)** Sanger sequencing showing the pathogenic alternative splicing caused by the c.1036C>A variant. Three PCR products were sequenced from a unique PCR band amplifying the *AARS2* transcript. The corresponding sequences are shown in the AARS2 affected" section of the figure: the first corresponds to the allele with the c.2864G>A, p.W955* variant that appears normal in the shown area. The second read showed a deletion of seven exon nucleotides that remove the c.1036C>A and causes a change in the reading frame with a premature stop codon as a predicted consequence (p.P346Wfs*18). The third read corresponds to the c.1036C>A constitutively spliced variant translating as a P346T aminoacid substitution without a change in the reading frame.

species	match	gene	aa	alignment
Human			346	I S D G I F P G M S G P P L V L R R I L R R A V
(p.P346T)	not conserved		346	I S D G I F P G M S G T P L V L R R I L R R A
P troglodytes	all identical	ENSPTRG00000018222	346	I S D G I F P G M S G P P L V L R R I L R R A
M mulatta	all identical	ENSMMUG00000014387	346	I S D G V F P G M S G P P L V L R R I L R R A
F catus	not conserved	ENSFCAG00000009773	48	I A D G V C P G M S G A P L V L R R I L R R A
M musculus	not conserved	ENSMUSG00000023938	341	I A D G V S P G M S G A P L V L R R I L R R A
G gallus	not conserved	ENSGALG00000010162	351	I T D G I Y P G L S G A E L V L R R
T rubripes	no homologue			
D rerio	not conserved	ENSDARG00000071240	376	I A D G V Y P G M A G A E L V L R R I L R R A
D melanogaster	not conserved	FBgn0027094	319	L A D G G T P D N T G R G Y V L R R I L R R A
C elegans	not conserved	F28H1.3	320	L S D G G R P D N S G R G Y V L R R I L R R G
X tropicalis	no homologue			

FIGURE 4
Amino acid alignment of the *AARS2* homologous proteins. The amino acid p.P346 is not conserved; only *Ptroglodytes* and *M. Mulatta* have proline in this position.

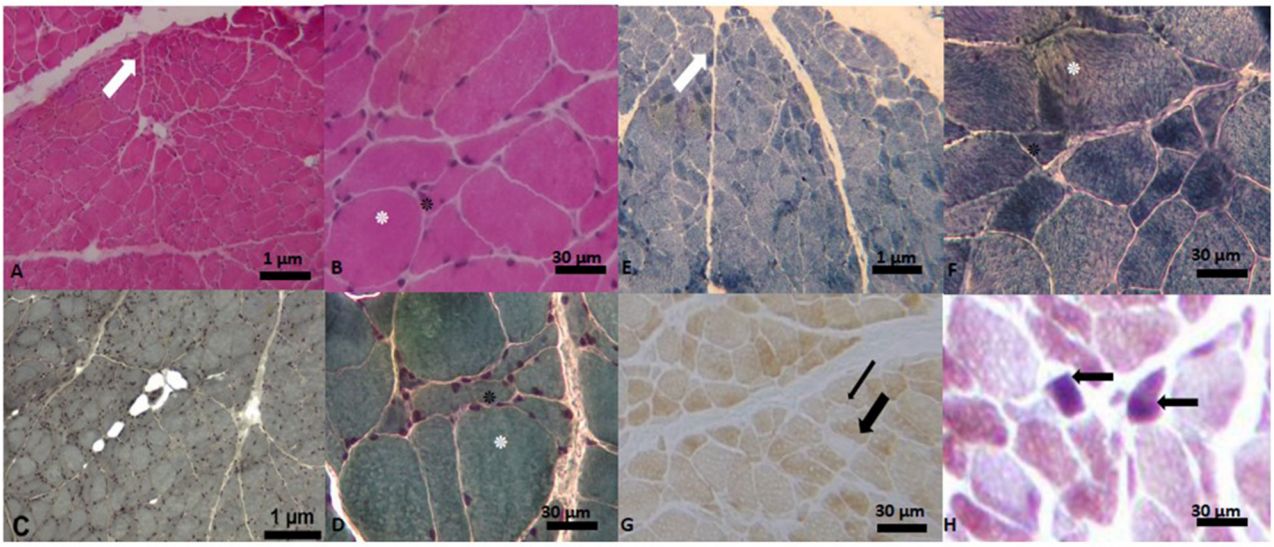

FIGURE 5
Muscle biopsy images. **(A)** Hematoxylin-Eosin Stain (H-E). Panoramic cross-sectional view of muscle with myopathic and angulated fascicles (marked with white arrow), difference in shape and size of the fiber, intra- and inter-fascicular connective tissue. In **(B)**, close-up of image **(A)** with the presence of the hypertrophic fiber (white asterisk), surrounded by angulated fibers (black asterisk). In **(C, D)** images (Gomori's Modified Trichrome Stain (T-G)) the same findings are observed as in **(A)**. In **(E)** panoramic view with the technique of Reduced Nicotinamide Adenine Dinucleotide-Tetrazolium Reductase (NADH-TR) with type I fibers of darker color and type II fibers of lighter color. In **(F)** close-up of the previous image, where a hypertrophic fiber is observed, surrounded by some angulated fibers. In **(G)**, view of a transverse section with cytochrome C oxidase (COX) showing pale (thin black arrow) and ghost (thick black arrow) fibers. In **(H)** Cytochrome C Oxidase/Succinate Dehydrogenase (COX/SDH) double-labeling method we observe two blue fibers.

our patient might be the cause of the primary amenorrhea. To our best knowledge, neither reproductive organs nor uterus *infantilis* malformations have been previously described in AARS-L. In our patient, uterus *infantilis* was confirmed by two independent pelvic ultrasound imaging studies.

Uterine hypoplasia is a major malformation due to incomplete morphogenesis. It has been reported in patients with syndromic ciliopathies (MIM#616258, #236700, #236680, #209900), Woodhouse–Sakati syndrome (MIM#241080), basal cell nevus syndrome (Gorlin syndrome) (MIM#109400), Turner syndrome and in Al-Awadi Raas-Rothschild syndrome (21).

Several genes have been related to the proper functioning of the female reproductive system, but challenges exist to prove causality for specific phenotypes (22). Alterations in *DHH, MCM8, MCM9, AMHR2, AMH, LMNA, DCAF17, NR5A1, STAG3,* and *PTPRF* genes have been associated with this malformation. However, in our patient, no pathogenic variants were identified in these genes, nor in other sequenced genes related to the phenotypes:HP0000130: Abnormality of the uterus; HP0031105:Abnormal uterus morphology; HP0008684: Aplasia/hypoplasia of the uterus, HP0000013: Hypoplasia of the uterus.

The *AARS2* gene is highly expressed in the uterus (mean Transcripts Per Million, TPM = 17.97), being overcome only by expression in the ovary (TPM = 20.42), cerebellum (TPM = 20.47) and cerebellar hemisphere (TPM = 21.97) (https://gtexportal.org/home/gene/AARS2). Therefore we might hypothesize that the uterus hypoplasia in this patient would be caused by *AARS2* pleiotropic effect. However, we can not completely rule out a causal pathogenic variant in genes not included in the clinical exome panel (Supplementary material S1).

A multidisciplinary diagnostic approach was performed, excluding the most common neurodegenerative diseases, like Alzheimer's, frontotemporal dementia, autoimmune encephalopathies, prion disease, infections, neoplasms, toxic-metabolic and vascular entities. The integration of clinical, laboratory, and neuroimaging findings, specifically the glycolytic uptake pattern on the F18-FDG PET and the white matter hyperintensities on the MRI, oriented to the diagnosis of leukoencephalopathy.

Massive parallel exome sequencing is a powerful diagnostic tool to identify the affected gene in diseases with high genetic and allelic heterogeneity, like leukoencephalopathies. This approach allows us to establish the etiologic diagnostic in our patient. Two novel deleterious variants in the *AARS2* gene are causing the disease: (NM_020745:c.2864G>A, p.W955*) and (NM_020745:c.1036C>A, P346T/P346Wfs*18) both of them confirmed by Sanger sequencing. According to HGMD professional database (last accessed Nov 2022), only 69 disease-causing variants have been identified so far; our results extended the mutational spectrum for this gene.

Loss of function of *AARS2* is a known disease mechanism; at least 25 pathogenic null variants have been reported across different exons, including the last one (exon 22) (https://my.qiagendigitalinsights.com/bbp/view/hgmd/pro/all.php). The variant NM_020745:c.2864G>A is a nonsense variant that originates a premature stop codon p.W955*, which causes the loss of 31 amino acids in the protein. Kamps et al. reported a patient with

severe cardiomyopathy, early onset brain disease and oxidative phosphorylation deficiency due to a compound heterozygous pathogenic variant in AARS2: p.R592W and p.Arg958* (HGMD ID: CM1822327) (23). The last variant is located in exon 22 and produces the loss of 28 aminoacids at the end of the protein, similar to p.W955* identified in the patient reported here, causing a 31 aminoacid loss.

The variant NM_020745:c.1036C>A was predicted to alter the normal splicing of the AARS2 transcript by *in silico* algorithms. cDNA-PCR Sanger sequencing analysis confirmed these predictions and demonstrated that the variant activated a cryptic splice site in exon 6 and produced leaky splicing. Two alternative isoforms were identified: one causing a loss-of-function protein due to seven nucleotide deletions that alter the reading frame originating a premature stop codon (p. P346Wfs*18), and the other coding a p.P346T amino acid substitution.

Loss-of-function variants in both alleles of AARS2 may be lethal due to the severe impairment in the mitochondrial protein translation process and mitochondrial functioning. Therefore we speculated that the p.P346T protein might retain some enzymatic activity. In support of that idea, none of the previously identified patients were homozygous or compounded heterozygous for loss-of-function variants, supporting that some residual AARS2 activity is needed to be compatible with life. Additionally, the constrain metrics for the *AARS2* gene in gnomAD database show a significant reduction in the number of loss of function variants observed in the population (55.3 expected vs. 35 observed; o/e = 0.63 (0.48–0.83) (https://gnomad.broadinstitute.org/gene/).

The clinical features presented by our patient support the diagnosis of AARS2-L with mitochondrial myopathic alterations. The mitochondrial abnormalities in histological studies may be very mild and even absent in genetically confirmed mitochondrial diseases, including AARS2-L (24). Muscle biopsies were not performed in all AARS2-L reported cases, but when available, the findings have included normal reports, ragged red fibers, and isolated COX deficiency (9, 24). In the patient we describe, the skeletal muscle biopsy showed COX-negative fibers suggesting a complex IV deficiency confirmed by the biochemical studies. COX is a multimeric enzyme composed of subunits encoded by both nuclear and mitochondrial genomes. Thus, pathogenic variants on the *AARS2* gene play a crucial role in mitochondrial translation and may affect mitochondrial protein synthesis and the functioning of the respiratory chain complexes (24). Ragged red fibers, generally associated with mitochondrial proliferation, were not detected. Still, in contrast, decreased citrate synthase activity, which indicates a reduction of the mitochondrial content, was found, probably related to the late clinical stage of this patient.

There are no specific treatments or disease modifiers for AARS2-L. The use of symptomatic therapy (antidepressants, antipsychotics), as in the case of the patient we present, can help to control some of the neuropsychiatric manifestations and relieve the burden of family/caregivers.

Conclusions

Inherited metabolic disorders are a rare etiology of early-onset dementias but should be considered in the diagnostic approach. The correlation with clinical findings and molecular biomarkers, including structural and functional neuroimaging and genetic analysis, allows us to establish the aetiologic diagnosis, which is particularly important in high heterogeneity phenotypic and genotypic diseases. In this work, we describe the first Mexican patient with the AARS2-L and characterize two novel variants of the *AARS2* gene. We might hypothesize that the uterus *infantilis* in this patient would be caused by the *AARS2* deficiency pleiotropic effect, but we cannot exclude other causative genes or etiology. This report contributes to enlarging the phenotypic and genetic spectrum of *AARS2* variants and widening the knowledge of early-onset dementias associated with leukoencephalopathy.

Author's note

In "Uterus Infantilis: a novel Phenotype Associated with AARS2 New Genetic Variants. A Case Report," we describe a Mexivcan patient showing two novel pathogenic variants in the *AARS2* gene and we enlarge the phenotype. *AARS2* encodes mitochondrial alanyl-tRNA synthetase, which is responsible for the aminoacylation between alanine and the tRNA during translation in the mitochondria. *AARS2* pathogenic variants were first identified in infantile mitochondrial cardiomyopathy in 2011 (4), and later found to cause adult-onset leukodystrophy, MIM#615889 (5). All adult-onset patients, less than two, present leukoencephalopathy (13, 19). All female patients, less than one (20) present ovarian failure, none has been described with uterus *infantilis*. With our paper, we inform the clinician about the detailed psychiatric involvement and describe the reproductive organs alteration possibly associated with *AARS2* related leukodystrophy. We describe two novel compound heterozygous pathogenic variants presenting with learning difficulties from childhood and primary amenorrhea, severe rapidly progressive cognitive, motor and behavioral impairment developed in early adulthood and uterus *infantilis*. Neuroimaging studies revealed frontal leukoencephalopathy with hypometabolism at the fronto-cerebellar cortex and caudate nucleus. Muscle biopsy and enzymatic activity of the respiratory chain, determined in a skeletal muscle biopsy sample, showed mitochondrial abnormalities pointing to the COX. We might speculate that the uterus hypoplasia presented by this patient is caused by a *AARS2* pleiotropic effect, but we cannot definitely exclude that other causative gene is involved. We think that the description of our case might help diagnose unsolved cases of early-onset dementia with leukodystrophy. We alert clinicians to consider inherited metabolic diseases as a possible cause of dementia.

Data availability statement

The datasets presented in this article are not readily available because of ethical and privacy restrictions. Requests to access the datasets should be directed to the corresponding author.

Ethics statement

The studies involving human participants were reviewed and approved by Instituto Nacional de Neurología Manuel Velasco Suarez Ethical Review Board for clinical studies. The patients/participants provided their written informed consent to participate in this study. Written informed consent was obtained from the participant/patient(s) for the publication of this case report.

Author contributions

EK conceived the study and design, analyzed the family history, (clinical, genetic, histopathological and biochemical) data of the patient, conceived the manuscript, wrote and drafted the manuscript, coordinated the collection and elaboration of blood samples data (genetic, histopathological, and biochemical), and contributed to the performing of the analysis of the molecular data. JT-M made the clinical diagnosis, recruited the patient, analyzed the clinical, neuropsychological, and imaging data of the patient, provided the images for Figure 1 and Table 1, conceived the manuscript, contributed to the writing of the case presentation and case presentation part of the discussion of the manuscript, read, and approved the manuscript. LF-L performed the clinical exome genetic analyses, contributed to genetic analysis (clinical exome sequencing, variant classification) part of the manuscript, read, and approved the manuscript. AS-O analyzed the clinical, neuropsychological, and imaging data of the patient, conceived the manuscript, provided patient's clinical data, coordinated the collection and elaboration of patient's data, supervised the study, contributed to the writing of the background, case presentation part of the discussion and conclusions the manuscript, drafted the manuscript, supervised the hole study project, read, and approved the manuscript. KC-S performed the clinical exome genetic analyses and contributed to genetic analysis (clinical exome sequencing, variant classification) part of the manuscript, read, and approved the manuscript. CM-G performed the clinical exome genetic analyses, contributed to genetic analysis (clinical exome sequencing, variant classification) part of the manuscript, contributed to genetic analysis part of the manuscript, read, and approved the manuscript. CG-D performed the segregation and mRNA studies, contributed to the evaluation of possible alteration in splicing part of the manuscript and related part of the discussion, read, and approved the manuscript. MJ-O performed the clinical exome genetic analyses and contributed to genetic analysis (clinical exome sequencing, variant classification) part of the manuscript. FF-V performed the histopathological studies, provided the histopathological images for Figure 5, contributed to histopathological studies interpretation, wrote the Muscle biopsy findings part of the manuscript, as well as to the related discussion of this findings in the manuscript, read, and approved the manuscript. EV-C performed the muscle biopsy and histopathological studies interpretation, revised the muscle biopsy findings part of the manuscript as well as the related discussion of this findings in the manuscript, read, and approved the manuscript. MV-M performed the enzymatic activity of the mitochondrial complexes of the respiratory chain, provided Table 2, wrote the mitochondrial respiratory chain findings part of the manuscript as well as the related discussion of this findings in the manuscript, read, and approved the manuscript. EG-L supervised the study, contributed to the writing of the background, discussion and conclusions parts of the manuscript, supervised the Ph.D. degree work, read, and approved the manuscript. IM-D performed the segregation and mRNA studies, provided the images for Figure 3, and wrote the evaluation of possible alteration in splicing part of the manuscript and related part of the discussion, read, and approved the manuscript. CA-V conceived the study and design, coordinated and supervised the performing of molecular studies (clinical exome sequencing), coordinated the performing of the Sanger sequencing and RNA studies, performed the analysis of the molecular genetic data (variant classification and analysis, variant analysis for uterus infantilis), contributed to the evaluation of possible alteration in splicing, wrote the manuscript, contributed to the editing the English version, contributed to the writing of the background, genetic analysis, discussion, and conclusions of the manuscript.

Funding

The research was conducted as part of the Ph.D. degree work of EK, who was receiving a Consejo Nacional de Ciencia y Technologia (CONACYT) scholarship number 860345. Molecular studies were performed with the resources of the Laboratorio de Diagnóstico Genómico, Instituto Nacional de Medicina Genómica and Laboratorio de Glicobiología Humana y Diagnóstico Molecular, Centro de Investigación en Dinámica Celular, Instituto de Investigación en Ciencias Básicas y Aplicadas, Universidad Autónoma del Estado de Morelos, Mexico.

Acknowledgments

The authors thank the patient and her family for participation in this study. We highly appreciate the advice on muscle biopsy results of Professor Edoardo Malfatti and on SDH-COX technique of Mr. Baptiste Periou from Centre de Référence de Maladies Neuromusculaires, UPEC - Paris Est University. A very special gratitude to Professor Jorge Pacheco Rosado for his guidance and advices.

Conflict of interest

The authors declare that the research was conducted in the absence of any commercial or financial relationships that could be construed as a potential conflict of interest.

Publisher's note

All claims expressed in this article are solely those of the authors and do not necessarily represent those of

their affiliated organizations, or those of the publisher, the editors and the reviewers. Any product that may be evaluated in this article, or claim that may be made by its manufacturer, is not guaranteed or endorsed by the publisher.

Supplementary material

The Supplementary Material for this article can be found online at: https://www.frontiersin.org/articles/10.3389/fneur.2023.878446/full#supplementary-material

References

1. Euro L, Konovalova S, Asin-Cayuela J, Tulinius M, Griffin H, Horvath R, et al. Structural modeling of tissue-specific mitochondrial alanyl-tRNA synthetase (AARS2) defects predicts differential effects on aminoacylation. *Front Genet.* (2015) 6:21. doi: 10.3389/fgene.2015.00021

2. Fuchs SA, Schene IF, Kok G, Jansen JM, Nikkels PGJ, van Gassen KLI, et al. Aminoacyl-tRNA synthetase deficiencies in search of common themes. *Genet Med.* (2019) 21:319–30. doi: 10.1038/s41436-018-0048-y

3. Konovalova S, Tyynismaa H. Mitochondrial aminoacyl- tRNA synthetases in human disease. *Mol Genet Metab.* (2013) 108:206. doi: 10.1016/j.ymgme.2013.01.010

4. Götz A, Tyynismaa H, Euro L, Ellonen P, Hyötyläinen T, Ojala T, et al. Exome sequencing identifies mitochondrial alanyl-tRNA synthetase mutations in infantile mitochondrial cardiomyopathy. *Am J Hum Genet.* (2011) 88:635–42. doi: 10.1016/j.ajhg.2011.04.006

5. Dallabona C, Diodato D, Kevelam SH, Haack TB, Wong LJ, Salomons GS, et al. Novel (ovario) leukodystrophy related to AARS2 mutations. *Neurology.* (2014) 82:2063–71. doi: 10.1212/WNL.0000000000000497

6. Fine AS, Nemeth CL, Kaufman ML, Fatemi A. Mitochondrial aminoacyl-tRNA synthetase disorders: an emerging group of developmental disorders of myelination. *J Neurodev Disord.* (2019) 11:29. doi: 10.1186/s11689-019-9292-y

7. Hamatani M, Jingami N, Tsurusaki Y, Shimada S, Shimojima K, Asada-Utsugi M, et al. The first Japanese case of leukodystrophy with ovarian failure arising from novel compound heterozygous AARS2 mutations. *J Hum Genet.* (2016) 61:899–902. doi: 10.1038/jhg.2016.64

8. Lee JM, Yang HJ, Kwon JH, Kim WJ, Kim SY, Lee EM, et al. Two Korean siblings with recently described ovarioleukodystrophy related to AARS2 mutations. *Eur J Neurol.* (2017) 24:e21–2. doi: 10.1111/ene.13245

9. Lynch DS, Zhang WJ, Lakshmanan R, Kinsella JA, Uzun GA, Karbay M, et al. Analysis of mutations in AARS2 in a series of CSF1R-negative patients with adult-onset leukoencephalopathy with axonal spheroids and pigmented glia. *JAMA Neurol.* (2016) 73:1433–9. doi: 10.1001/jamaneurol.2016.2229

10. Szpisjak L, Zsindely N, Engelhardt JI, Vecsei L, Kovacs GG, Klivenyi P, et al. Novel AARS2 gene mutation producing leukodystrophy: a case report. *J Hum Genet.* (2017) 62:329–33. doi: 10.1038/jhg.2016.126

11. Srivastava S, Butala A, Mahida S, Richter J, Mu W, Poretti A, et al. Expansion of the clinical spectrum associated with AARS2-related disorders. *Am J Med Genet A.* (2019) 179:1556–64. doi: 10.1002/ajmg.a.61188

12. Wang X, Wang Q, Tang H, Chen B, Dong X, Niu S, et al. Novel Alanyl-tRNA Synthetase 2 mutations in Leukodystrophies. *Front Neurol.* (2019) 10:1321. doi: 10.3389/fneur.2019.01321

13. Kuo ME, Antonellis A, Shakkottai VG. Alanyl-tRNA Synthetase 2 (AARS2)-related ataxia without leukoencephalopathy. *Cerebellum.* (2020) 19:154–60. doi: 10.1007/s12311-019-01080-y

14. Zhou Y, Chen B, Li L, Pan H, Liu B, Li T, et al. Novel alanyl-tRNA synthetase 2 (AARS2) homozygous mutation in a consanguineous Chinese family with premature ovarian insufficiency. *Fertil Steril.* (2019) 112:569–76.e2. doi: 10.1016/j.fertnstert.2019.05.005

15. Desmet FO, Hamroun D, Lalande M, Collod-Béroud G, Claustres M, Béroud C. Human Splicing Finder: an online bioinformatics tool to predict splicing signals. *Nucleic Acids Res.* 37:e67. doi: 10.1093/nar/gkp215

16. Vázquez-Memije ME, Cárdenas-Méndez MJ, Tolosa A, Hafidi ME. Respiratory chain complexes and membrane fatty acids composition in rat testis mitochondria throughout development and ageing. *Exp Gerontol.* (2005) 40:482–90. doi: 10.1016/j.exger.2005.03.006

17. Lakshmanan R, Adams ME, Lynch DS, Kinsella JA, Phadke R, Schott JM, et al. Redefining the phenotype of ALSP and AARS2 mutation-related leukodystrophy. *Neurol Genet.* (2017) 3:e135. doi: 10.1212/NXG.0000000000000135

18. Dong Q, Long L, Chang YY, Lin YJ, Liu M, Lu ZQ, et al. An adolescence-onset male leukoencephalopathy with remarkable cerebellar atrophy and novel compound heterozygous AARS2 gene mutations: a case report. *J Hum Genet.* (2018) 63:841–6. doi: 10.1038/s10038-018-0446-7

19. De Michele G, Galatolo D, Lieto M, Maione L, Cocozza S, Santorelli FM, et al. New AARS2 mutations in Two Siblings With Tremor, Downbeat Nystagmus, and Primary Amenorrhea: A Benign Phenotype Without Leukoencephalopathy. *Mov Disord Clin Pract.* (2020) 7:684–7. doi: 10.1002/mdc3.12991

20. Sun J, Quan C, Luo SS, Zhou L, Zhao CB. Leukodystrophy without ovarian failure caused by compound heterozygous Alanyl-tRNA synthetase 2 mutations. *Chin Med J (Engl).* (2017) 130:3021–2. doi: 10.4103/0366-6999.220300

21. Jacquinet A, Millar D, Lehman A. Etiologies of uterine malformations. *Am J Med GenetA.* (2016) 170:2141–72. doi: 10.1002/ajmg.a.37775

22. Volozonoka L, Miskova A, Kornejeva L, Kempa I, Bargatina V, Gailite LA, et al. systematic review and standardized clinical validity assessment of genes involved in female reproductive failure. *Reproduction.* (2022) 163:351–63. doi: 10.1530/REP-21-0486

23. Kamps R, Szklarczyk R, Theunissen TE, Hellebrekers DMEI, Sallevelt SCEH, Boesten IB, et al. Genetic defects in mtDNA-encoded protein translation cause pediatric, mitochondrial cardiomyopathy with early-onset brain disease. *Eur J Hum Genet.* (2018) 26:537–51. doi: 10.1038/s41431-017-0058-2

24. Tang Y, Qin Q, Xing Y, Guo D, Di L, Jia J, et al. AARS2 leukoencephalopathy: A new variant of mitochondrial encephalomyopathy. *Mol Genet Genomic Med.* (2019) 7:e00582. doi: 10.1002/mgg3.582

frontiers | Frontiers in Neurology

TYPE Case Report
PUBLISHED 18 July 2023
DOI 10.3389/fneur.2023.1227566

OPEN ACCESS

EDITED BY
Bruce Miller,
University of California, San Francisco,
United States

REVIEWED BY
Christopher William,
New York University, United States
Eva Bagyinszky,
Gachon University, Republic of Korea

*CORRESPONDENCE
Xiuli Shang
✉ lbz940943382@163.com

RECEIVED 24 May 2023
ACCEPTED 04 July 2023
PUBLISHED 18 July 2023

CITATION
Li B, Wang S, Han S, Hu N and Shang X (2023) Case report: Creutzfeldt-Jakob disease: a case that initiated with the onset of obsessive-compulsive state.
Front. Neurol. 14:1227566.
doi: 10.3389/fneur.2023.1227566

Case report: Creutzfeldt-Jakob disease: a case that initiated with the onset of obsessive-compulsive state

Baizhu Li, Shan Wang, Shiyu Han, Ning Hu and Xiuli Shang*

The First Affiliated Hospital of China Medical University, Shenyang, China

Background: Obsessive-compulsive disorder (OCD) is a common reason for patients to seek symptomatic treatment in psychiatric departments, which makes it challenging to consider underlying organic nervous system diseases. However, Creutzfeldt-Jakob disease (CJD) can present with atypical symptoms, sometimes even as initial symptoms, leading to misdiagnosis or missed diagnosis. Lumbar puncture and brain DWI are important diagnostic methods for CJD, and the detection of 1,433 protein can be performed to confirm the diagnosis.

Case presentation: We present the case of a 63-year-old woman who was initially diagnosed with obsessive-compulsive disorder in 2022. Despite seven months of symptomatic treatment, her symptoms did not improve. She also developed symptoms of altered consciousness, such as upper limb tremors and mutism. Based on brain DWI and positive results from the detection of 1,433 protein, she was ultimately diagnosed with CJD.

Conclusion: Creutzfeldt-Jakob disease (CJD) can manifest initially as obsessive-compulsive disorder (OCD) with atypical symptoms, making it prone to misdiagnosis. Therefore, it is crucial to conduct further investigations, including lumbar puncture and imaging, to exclude organic nervous system diseases before initiating symptomatic treatment for psychiatric disorders. This approach can facilitate early diagnosis of CJD and other potential organic neurological diseases.

KEYWORDS

obsessive-compulsive disorder, compulsive state, Creutzfeldt-Jakob disease, early diagnosis, case report, CJD

Introduction

Creutzfeldt-Jakob disease (CJD) is a progressive, degenerative, and ultimately fatal disease affecting the central nervous system. It is characterized by the abnormal accumulation of prion protein, leading to various neurological symptoms. The disease presents with progressive dementia, myoclonus (involuntary muscle jerks or twitches), and manifestations of cerebellar, pyramidal, and extrapyramidal dysfunction (1). It has been reported that psychiatric symptoms, including depression, can accompany Creutzfeldt-Jakob disease (CJD) and may even present as the initial signs of the disease. Alongside the neurological symptoms, individuals with CJD may experience changes in mood, behavior, and cognition, which can include depression. Therefore, it is important to consider psychiatric manifestations as potential indicators of CJD, especially when evaluating patients with unexplained psychiatric symptoms in conjunction with neurological abnormalities (2).

Recently, it has been observed that obsessive-compulsive disorder (OCD) can also serve as an early manifestation of Creutzfeldt-Jakob disease (CJD). In this report, we present a case where a patient was initially diagnosed with OCD by a psychiatrist but later diagnosed with CJD. The patient exhibited progressive dementia, myoclonus, immobility mutism, and other characteristic manifestations of CJD. The diagnosis of CJD was confirmed through additional investigations, including lumbar puncture and brain DWI examination. This case highlights the importance of considering CJD as a potential underlying cause when encountering patients with OCD symptoms accompanied by neurological deterioration (3). Compulsive behavior or psychological symptoms can indeed be part of the clinical manifestations of Creutzfeldt-Jakob disease (CJD). Recognizing these symptoms and utilizing additional diagnostic tools such as lumbar puncture and imaging can enhance our understanding of organic nervous system diseases in patients presenting with such mental states. These auxiliary means contribute to early diagnosis and prompt treatment, ultimately improving clinical outcomes. Early identification of CJD and other organic neurological conditions in individuals displaying compulsive behavior or psychological symptoms is crucial for appropriate management and support.

Patient and method

This article reports a patient who was initially diagnosed with obsessive-compulsive disorder but was finally diagnosed with Creutzfeldt-Jakob disease after 1 year of follow-up observation.

This is a retrospective study of the patient characteristics and treatment outcomes, ethical committee approval was not required for this study, written informed consent of all patients have been obtained.

Case

A 63-year-old woman developed stereotypical behavior in November 2022 without any apparent cause. She engaged in repetitive actions such as washing clothes for an entire day, repeatedly washing the same batch of clothes in the washing machine, or continuously wiping the floor or dust. She displayed heightened focus on personal and household hygiene, frequently washing her hands, while neglecting other household tasks and becoming lazier. However, her speech and self-care abilities remained normal.

On January 26, 2023, when she learned about her father's death in a car accident, her family noticed an increase in repetitive behaviors. These included repeatedly wiping parts of the floor and excessively washing her hands from morning till night. The symptoms worsened over the course of a week. Subsequently, she settled into a regular routine of compulsively washing her hands and wiping the floor. As a result, she was diagnosed with obsessive-compulsive disorder (OCD) at another hospital and received symptomatic medication for 2 weeks. However, the symptoms did not improve.

On March 7, 2023, she was admitted to the psychiatric department of my hospital, where she received a diagnosis of obsessive-compulsive disorder and underwent medication-based treatment. During the treatment, she frequently noticed her hand assuming a fixed position, such as being in a booth or elbow flexion, and experienced involuntary tremors in her left hand, although her muscle strength remained normal. The patient's ability to express herself through speech decreased, and she could only produce single words. She often did not answer phone calls, spent less time awake, experienced difficulty walking compared to before, had frequent trembling in her right hand, cried frequently, and exhibited significant mood fluctuations. However, the following tests and examinations did not reveal any notable abnormalities: rheumatic diseases, coagulation, blood routine, liver and kidney function, syphilis, brucella, AIDS, hepatitis C virus, hepatitis B virus, troponin, ion, erythrocyte sedimentation rate, thyroid function, procalcitonin, tumor markers, anticardiolipin antibodies, electrocardiogram, electroencephalogram, brain CT, MR plain scan +C, and related cervical, thoracic, and lumbar vertebrae MR. In addition to the above, I did a whole exome analysis on the patient, and did not find any genetic variant, which may be responsible for the disease.

After consultation with the neurology department on April 23, 2023, and ruling out the aforementioned symptoms, laboratory test results, and any obvious abnormalities in the examination results, dementia-related causes were excluded. When the patient's medical history and family genetic history were investigated, the patient's family members denied any relevant medical history or neurological symptoms within the family (Figure 1). Further examination of diffusion-weighted imaging (DWI) results revealed multiple abnormal diffusion-restricted signal changes in the brain with cortical and subcortical distribution, indicating a high possibility of infectious lesions and Creutzfeldt-Jakob disease (CJD) (Figure 2). A reexamination of the video electroencephalogram (VEEG) demonstrated the disappearance of the basic rhythm and the appearance of periodic triphasic waves in all leads. During monitoring, the patient exhibited increased muscle tension in the right upper limb with elbow flexion, and frequent rhythmic convulsions occurred in the distal upper limb. The EEG results showed widespread and severe abnormalities. The 1,433 protein test yielded a positive result, confirming the diagnosis of Creutzfeldt-Jakob disease. Following her discharge, the patient passed away in May 2023 during the follow-up period.

The temporal and occipital leads were predominant. A small amount of a waves (10–40μv, 8–9c/s), β waves (5–20μv, 18–24c/s) and δθ waves (10–100μv, 2–7c/s) were mixed. Open and closed eyes test: a wave was not suppressed. Response to flash stimulation: same as background figure. Sphenoid electrode: No seizure wave was observed. Clinical seizure: during the monitoring period, the patient's right upper limb muscle tension was increased in the elbow flexion position, and the distal end of both upper limbs frequently had rhythmic twitches. The corresponding electroencephalogram showed that the electromyogram showed motor unit potential, and the other leads were the same as the background map.

Video electroencephalogram results: extensive severe abnormal electroencephalogram.

10.3389/fneur.2023.1227566

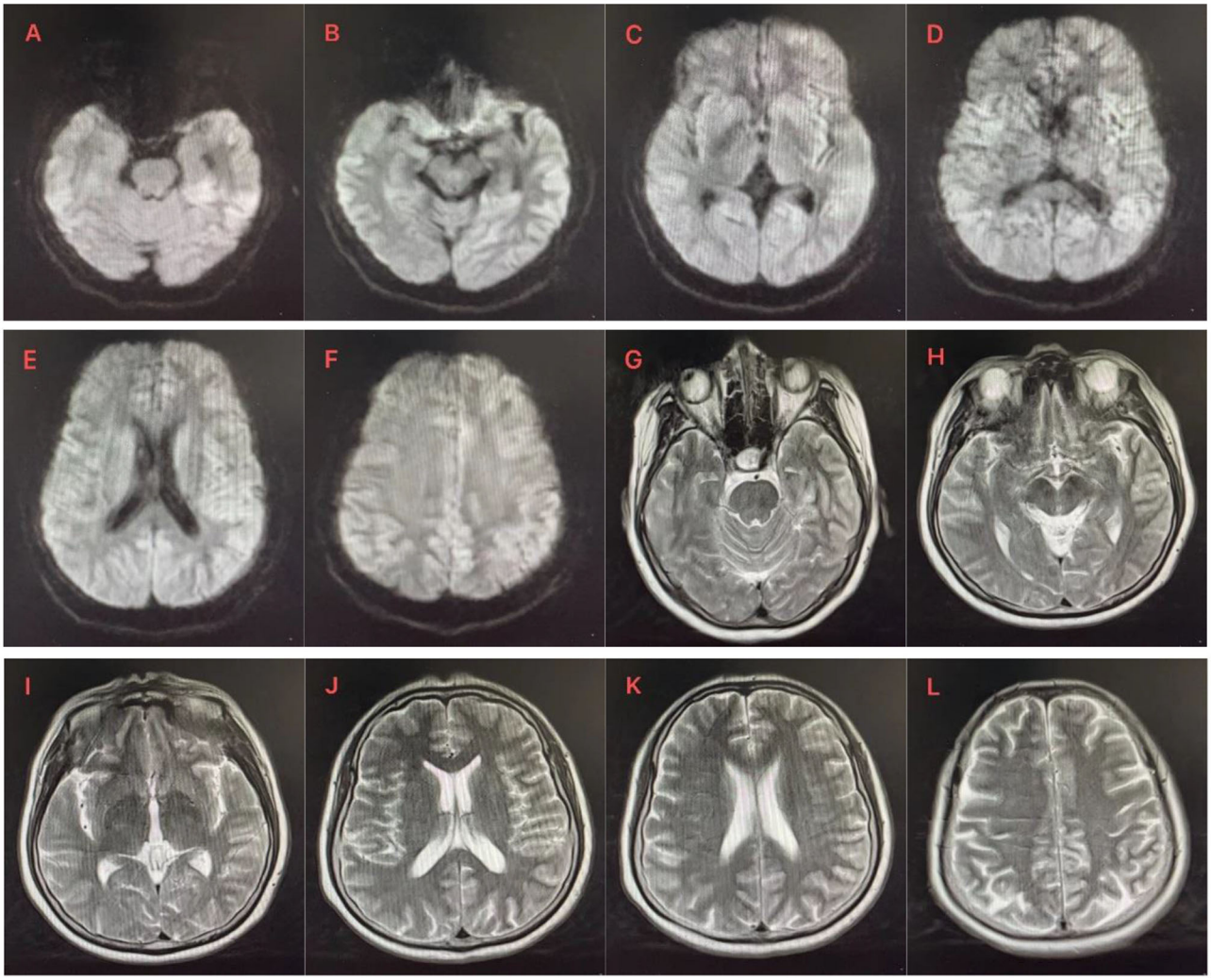

FIGURE 1
(A–F) DWI showed asymmetric cortical hyperintensity in the bilateral caudate nucleus, bilateral cingulate gyrus and frontoparietal, temporal and occipital gyrus, especially in the left. **(G–L)** Small patchy long T2 signal shadow was observed next to the posterior horn of the left lateral ventricle. There was no abnormal signal shadow in the remaining bilateral cerebral hemispheres, cerebellum, and brain stem, no abnormal morphological structure was found, the ventricular system was equal and symmetrical, the sulci cistern fissure was not significantly widened, and the midline structure was centered.

Discussion

Creutzfeldt-Jakob disease (CJD) is the most common prion disease in humans, with an annual incidence of approximately 1 case per million people (4). The typical onset age of CJD is between 45 and 75 years old, with an average age of onset at 60 years old (5, 6). Apart from dementia, the most common manifestations of CJD are pyramidal, extrapyramidal, and cerebral manifestations, and myoclonus. The typical manifestations of the disease, namely dementia, myoclonic convulsions, cranial MR, and EEG changes, may not be observed in 25% of patients, leading to difficulties in early diagnosis. There are three main categories of prion diseases (7), called sporadic, hereditary and acquired, of which 85% to 95% are sporadic (no family history or source of infection can be identified) and 5% are familial. In addition to typical symptoms, patients can also start with neuropsychiatric symptoms. Psychiatric symptoms, such as depression and personality changes, have been defined in one third of cases early in the illness (1), and are the initial symptoms in 10% of cases. Delusions and auditory hallucinations have been reported in patients with major depression for about 6 months, and ataxia and myoclonus have developed 7 months after the onset of these symptoms (1). It has also been shown that symptoms such as visual hallucinations are observed after depressive symptoms in 15% of patients with sporadic CJD (8, 9). Except for the difference in the first symptom, the onset time of the other symptoms was similar to that of this case, in which CJD first manifested as obsessive-compulsive disorder, repeatedly wiping the floor and ashes, and paying great attention to hygiene, which was extremely difficult to distinguish from obsessive-compulsive disorder patients in terms of clinical manifestations (10). There was no significant change in electroencephalogram and no response to symptomatic treatment. Within 6 months, the

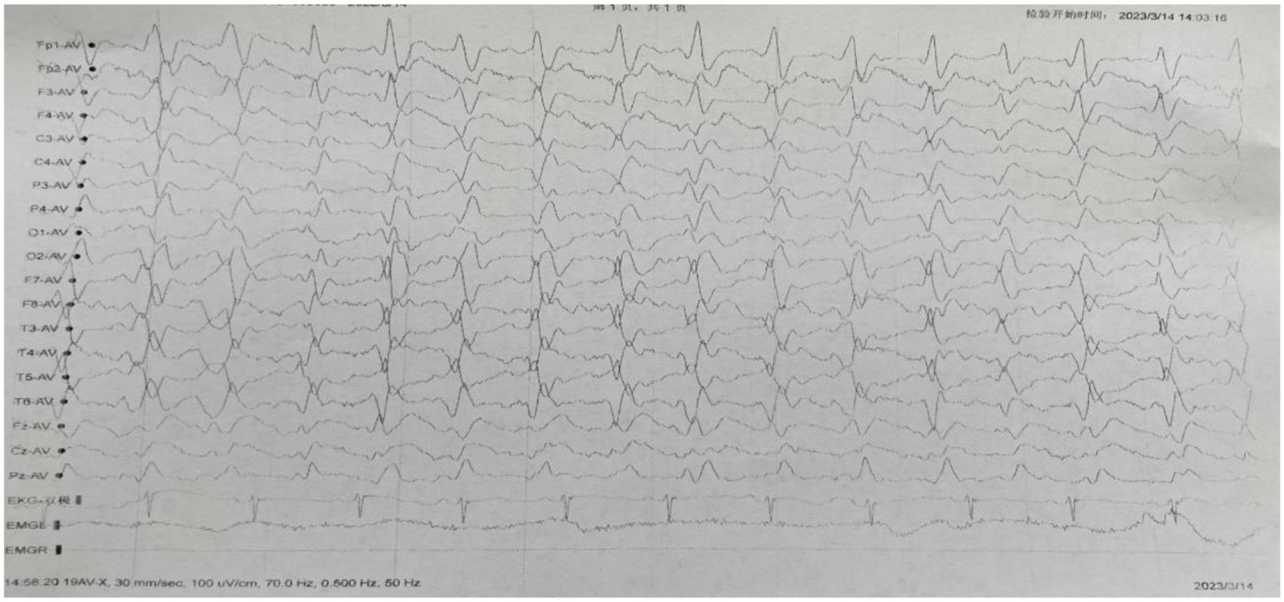

FIGURE 2
Electroencephalogram (EEG) showed that the basic rhythm disappeared, periodic three-phase waves appeared in all leads, with an inter-wave interval of 0.5–0.7s.

patient developed visual hallucinations, auditory hallucinations, myoclonus and other symptoms, which were consistent with the early symptoms of CJD patients. Moreover, the duration of clinical psychiatric symptoms of the disease is shorter (1) and the age of onset is later. Reexamination of electroencephalogram, brain DWI and positive delivery 1, 433 protein (11) supported the diagnosis of sporadic CJD.

These features on EEG are known to occur in the middle or late stages of CJD, but are not specific for CJD in the early stages. Therefore, the EEG of patients with suspected CJD should be reexamined many times. In this case, there was no obvious abnormality in the initial EEG, but periodic three-phase waves appeared in all leads of the EEG in the later stage, and the video EEG showed extensive and severe abnormal EEG. This is characteristic of sporadic CJD and can be observed in two thirds of CJD patients.

Brain MRI is an important examination for the diagnosis of CJD. MRI findings may be normal in 23% of patients with sporadic CJD (12). It has been reported that cranial DWI can be used even in the early stages of CJD, and it is an important modality for early diagnosis (13). In our patient, the first brain plain MR Scan showed no obvious abnormality in DWI, and then the brain DWI showed multiple abnormal diffusion limited signal changes in the brain, with cortical and subcortical distribution, considering infectious lesions and Creutzfeldt-Jakob disease.

In patients with CJD, CSF examination may be positive for 14–3-3 (14). The sensitivity and specificity of 14–3-3 for CJD were 94% and 84%, respectively (15). Therefore, a positive 14–3-3 result in CSF suggests a certain diagnosis in patients with sporadic CJD. In the present case, 14–3-3 was found in the patient's CSF.

Conclusion

In this report, we present a case of Creutzfeldt-Jakob disease (CJD) where the initial symptom was obsessive-compulsive disorder (OCD), and the patient was followed up for a period of 7 months. The challenging aspect of this case was that the patient's initial symptoms were purely psychiatric, making it difficult to differentiate them from common psychiatric disorders. By highlighting this case, we aim to raise awareness among clinicians about the importance of recognizing psychiatric symptoms, such as OCD, as potential early signs of CJD and other organic nervous system diseases. CJD should be considered as a differential diagnosis in patients who present with psychiatric symptoms, personality changes, and focal neurological symptoms. This case is particularly significant as it demonstrates that neurological symptoms can manifest after the onset of psychiatric symptoms in CJD.

Therefore, when evaluating patients with psychiatric symptoms, it is crucial to employ methods like lumbar puncture, imaging, and other diagnostic approaches to exclude organic nervous system diseases before initiating symptomatic treatment for psychiatric conditions. This approach can help avoid misdiagnosis of a progressive disease like CJD and differentiate it from other potentially treatable causes.

Data availability statement

The original contributions presented in the study are included in the article/Supplementary material, further inquiries can be directed to the corresponding author.

Ethics statement

Ethical review and approval was not required for the study on human participants in accordance with the local legislation and institutional requirements. The patients/participants provided their written informed consent to participate in this study. Written informed consent was obtained from the individual(s) for the publication of any potentially identifiable images or data included in this article.

Author contributions

BL wrote the manuscript. BL and XS revised the manuscript. All authors contributed to the follow-up, information collection, and approved the submitted version.

Acknowledgments

We would like to thank the participants and their families for their contributions to this work.

Conflict of interest

The authors declare that the research was conducted in the absence of any commercial or financial relationships that could be construed as a potential conflict of interest.

Publisher's note

All claims expressed in this article are solely those of the authors and do not necessarily represent those of their affiliated organizations, or those of the publisher, the editors and the reviewers. Any product that may be evaluated in this article, or claim that may be made by its manufacturer, is not guaranteed or endorsed by the publisher.

Supplementary material

The Supplementary Material for this article can be found online at: https://www.frontiersin.org/articles/10.3389/fneur.2023.1227566/full#supplementary-material

References

1. Dervaux A, Vicart S, Lopes F, Le Borgne MH. [Psychiatric manifestations of a new variant of Creutzfeldt-Jakob disease. *Apropos of a case] L'Encephale.* (2001) 27:194–7.

2. Gençer AG, Pelin Z, Küçükali C, Topçuoglu OB, Yilmaz N. Creutzfeldt-Jakob disease. *Psychogeriatrics.* (2011) 11:119–24. doi: 10.1111/j.1479-8301.2011.00361.x

3. Iwasaki Y. Creutzfeldt-Jakob disease. *Neuropathology.* (2017) 37:174–88. doi: 10.1111/neup.12355

4. Johnson RT. Prion diseases. *The Lancet Neurology.* (2005) 4:635–42. doi: 10.1016/S1474-4422(05)70192-7

5. Van Everbroeck B, Dobbeleir I, De Waele M, De Deyn P, Martin J-J, Cras P. Differential diagnosis of 201 possible Creutzfeldt-Jakob disease patients. *J Neurol.* (2004) 251:298–304. doi: 10.1007/s00415-004-0311-9

6. Glatzel M, Stoeck K, Seeger H, Lührs T, Aguzzi A. Human prion diseases: molecular and clinical aspects. *Arch Neurol.* (2005) 62:545–52. doi: 10.1001/archneur.62.4.545

7. Baldwin KJ, Correll CM. Prion disease. *Semin Neurol.* (2019) 39:428–39. doi: 10.1055/s-0039-1687841

8. Zeidler M, Johnstone EC, Bamber RW, Dickens CM, Fisher CJ, Francis AF, et al. New variant Creutzfeldt-Jakob disease: psychiatric features. *Lancet.* (1997) 350:908–10. doi: 10.1016/S0140-6736(97)03148-6

9. Brown P, Cathala F, Sadowsky D, Gajdusek DC. Creutzfeldt-Jakob disease in France: II. Clinical characteristics of 124 consecutive verified cases during the decade 1968-—1977. *Annal Neurol.* (1979) 6:430–7. doi: 10.1002/ana.410060510

10. Goodman WK, Grice DE, Lapidus KA, Coffey BJ. (2019). Obsessive-compulsive disorder. Nature reviews. *Disease Primers* 5:52. doi: 10.1038/s41572-019-0112-1

11. Chatzikonstantinou S, Kazis D, Karantali E, Knights M, McKenna J, Petridis F, et al. A meta-analysis on RT-QuIC for the diagnosis of sporadic CJD. *Acta Neurol Belg.* (2021) 121:341–9. doi: 10.1007/s13760-021-01596-3

12. Mizusawa H. Prion disease. *Rinsho Shinkeigaku.* (2010) 50:797–802. doi: 10.5692/clinicalneurol.50.797

13. Xia S, Ma GL. The value of MRI and MR DWI in diffuse lesion of the cerebral hemisphere. *Zhonghua yi xue za zhi.* (2011) 91:880–4.

14. Liu J, Cao S, Ding G, Wang B, Li Y, Zhao Y, et al. The role of 14-3-3 proteins in cell signalling pathways and virus infection. *J Cell Mol Med.* (2021) 25:4173–82. doi: 10.1111/jcmm.16490

15. Hermann P, Appleby B, Brandel J-P, Caughey B, Collins S, Geschwind MD, et al. Biomarkers and diagnostic guidelines for sporadic Creutzfeldt-Jakob disease. *The Lancet Neurol.* (2021) 20:235–46. doi: 10.1016/S1474-4422(20)30477-4

frontiers | Frontiers in Neurology

TYPE Case Report
PUBLISHED 23 August 2023
DOI 10.3389/fneur.2023.1160110

OPEN ACCESS

EDITED BY
Bruce Miller,
University of California, San Francisco,
United States

REVIEWED BY
Linda Gailite,
Riga Stradinš University, Latvia
Luke William Bonham,
University of California, San Francisco,
United States

*CORRESPONDENCE
Li-li Zeng
✉ llzeng@126.com
Hai-yan Zhou
✉ zhaiyan.com@163.com

RECEIVED 06 February 2023
ACCEPTED 16 June 2023
PUBLISHED 23 August 2023

CITATION
Lai Z-h, Liu X-y, Song Y-y, Zhou H-y and Zeng L-l (2023) Case report: Hereditary spastic paraplegia with a novel homozygous mutation in *ZFYVE26*. *Front. Neurol.* 14:1160110. doi: 10.3389/fneur.2023.1160110

Case report: Hereditary spastic paraplegia with a novel homozygous mutation in *ZFYVE26*

Ze-hua Lai[1,2], Xiao-ying Liu[1], Yuan-yue Song[1], Hai-yan Zhou[1]* and Li-li Zeng[1]*

[1]Department of Neurology and Institute of Neurology, Ruijin Hospital, Shanghai Jiao Tong University School of Medicine, Shanghai, China, [2]Department of Neurology, Yangpu Hospital, Tongji University School of Medicine, Shanghai, China

Hereditary spastic paraplegia (HSP) is a group of neurodegenerative diseases with genetic and clinical heterogeneity characterized by spasticity and weakness of the lower limbs. It includes four genetic inheritance forms: autosomal dominant inheritance (AD), autosomal recessive inheritance (AR), X-linked inheritance, and mitochondrial inheritance. To date, more than 82 gene loci have been found to cause HSP, and SPG15 (*ZFYVE26*) is one of the most common autosomal recessive hereditary spastic paraplegias (ARHSPs) with a thin corpus callosum (TCC), presents with early cognitive impairment and slowly progressive leg weakness. Here, we reported a homozygous pathogenic variant in *ZFYVE26*. A 19-year-old Chinese girl was admitted to our hospital presenting with a 2-year progressive bilateral leg spasticity and weakness; early cognitive impairment; corpus callosum dysplasia; chronic neurogenic injury of the medulla oblongata supplied muscles; and bilateral upper and lower limbs on electromyogram (EMG). Based on these clinical and electrophysiological features, HSP was suspected. Exome sequencing of the family was performed by high-throughput sequencing, and an analysis of the patient showed a *ZFYVE26* NM_015346: c.7111dupA p.(M2371Nfs*51) homozygous mutation. This case reported a new *ZFYVE26* pathogenic variant, which was different from the SPG15 gene mutation reported earlier.

KEYWORDS

hereditary spastic paraplegia, *ZFYVE26*, case report, novel homozygous mutation, SPG15

Introduction

Hereditary spastic paraplegia (HSP), also called spastic paraplegia (SPG), is a group of neurodegenerative diseases with genetic and clinical heterogeneity characterized by spasticity and weakness of the lower limbs (1), and the prevalence is ~1.8/100,000 (2). It includes four genetic inheritance forms, namely: autosomal dominant inheritance (AD), autosomal recessive inheritance (AR), X-linked inheritance, and mitochondrial inheritance (2). Until now, over 82 gene loci have been found to cause HSP (3–5). HSP patients may have either pure or complicated HSP, differing based on symptoms. Patients with pure HSP simply develop spasticity and weakness of the lower limbs (6), while patients with complicated HSP are often accompanied by other symptoms, such as early cognitive impairment, ataxia, visual disturbance, macular degeneration, dysarthria, and callosal agenesis (7).

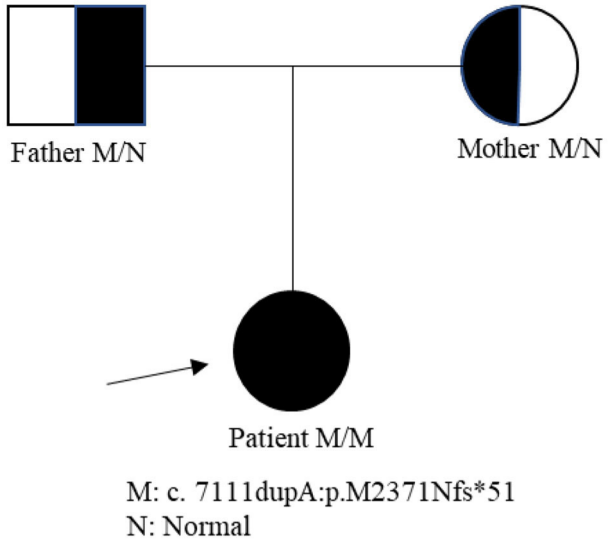

FIGURE 1
The patient's family tree of the novel mutation *ZFYVE26*.

SPG15 (Spastic Paraplegia type of 15, *ZFYVE26*) is one of the most common ARHSPs with thin corpus callosum (TCC) (8), and it presents with early cognitive impairment and slowly progressive leg weakness (9). *ZFYVE26* gene is localized at 14p24.1, and it encodes a zinc finger protein with an FYVE domain called "spastizin" (10). It forms a protein complex with Spatacsin (SPG11) and *KIAA0415* (SPG48), and participates in various cellular events such as membrane trafficking and signal transduction (10).

Here, we reported a homozygous mutation in *ZFYVE26*. A 19-year-old Chinese girl was admitted to our hospital presenting with a 2-year progressive bilateral leg spasticity and weakness, and early cognitive impairment; corpus callosum dysplasia and chronic neurogenic injury of the medulla oblongata supplied muscles; and bilateral upper and lower limbs on electromyogram (EMG). Based on these clinical features and the electrophysiological findings, HSP was suspected. Exome sequencing of the family was performed by high-throughput sequencing, and an analysis of the patient showed a c.7111dupA p.(M2371Nfs*51) (Exon 38) homozygous novel mutation in *ZFYVE26* gene. This case reported a new *ZFYVE26* pathogenic variant.

Case presentation

A 19-year-old girl was admitted to our hospital presenting with a 2-year progressive bilateral leg spasticity and weakness. Her medical history was not remarkable, and her family history was negative for genetic disease. Vital signs were in the normal ranges: body temperature, 36.7°C; respiratory rate, 22 breaths/min; pulse rate, 72 bpm; and blood pressure, 126/68 mm Hg. Neurological examinations revealed that the lower limbs' muscle strengths were of grades 3–5; hypermyotonia in her lower limbs, hyperreflexia in the knee and ankle reflexes, and bilateral Babinski signs (+), Chaddock signs (+), Gordon signs (+), and Oppenheim signs (+). Cranial nerve, the upper limb, and ataxia examination showed no abnormalities. She also had mild mental deficiency with a MoCA score of 22. Lab examinations, including metabolic, tumor marker, and immunity parameters, were all within normal ranges. Brain and cervical MRI revealed corpus callosum dysplasia and cervical disk herniation in C3/4 and C5/6. EMG reported that F wave latency for the ulnar nerve and the tibial nerve was normal; but EMG of the anterior tibial muscle showed fibrillations and positive sharp waves; and there were widened MUP time limit, increased wave amplitude, and increased polyphase wave during the light contraction in most muscles, and decreased recruitment phase during recontraction. These findings indicated that there was extensive chronic neurogenic electromyographic impairment; and anterior horn involvement was considered first (ball, cervix, and lumbar). The diagnosis of HSP was suspected. Biopsy of the right biceps muscle showed no obvious hyperplasia of connective tissue, no abnormalities in muscle bundle of the small vessel wall, and no inflammatory cells infiltration or abnormal deposits around blood vessels; and there was no muscle fiber atrophy, hypertrophy, necrosis, swirl or spiral change, no nuclei aggregation, and no vacuolar formation in muscle fiber. Therefore, neurogenic skeletal muscle injury was suspected. Second-generation gene sequencing test revealed that the patient carried a *ZFYVE26* NM_015346: c.7111dupA p.(M2371Nfs*51) homozygous mutation, which came from her heterozygous parents (Figure 1). Combined with clinical symptoms, a diagnosis of SPG15 was made. The patient was given 5 mg of baclofen twice a day. However, there was no significant improvement in her symptoms on discharge, but her symptoms were alleviated gradually in 3 months of follow-up.

Discussion

HSP, a kind of genetic neurodegenerative disease and clinical heterogeneity characterized by spasticity and weakness of the lower limbs, can be classified into two types, namely, the pure type (clinical manifestations include typical muscle spasms, hyperreflexia, clonus, gait disorder, and bladder dysfunction) (6) and the complicated type (besides the abovementioned symptoms, clinical manifestation includes early cognitive impairment, ataxia, visual disturbance, macular degeneration, dysarthria, and callosal agenesis) (11, 12).

The pathogenesis of HSP remains unknown, and the axonal degeneration caused by the various types of HSP has different molecular pathogenesis. There are four modes of mutation, namely, AD, AR, X-linked inheritance, and mitochondrial inheritance (13). To date, over 82 gene loci have been found to cause HSP (3). These genes are involved in many cellular events such as membrane trafficking, signal transduction, the morphology of the endoplasmic reticulum, microtubule dynamics and transport, mitochondrial function, lipid metabolism, and endosome/lysosome functions. The main pathological change of HSP is axonal degeneration, which may also be accompanied by other changes such as demyelination and loss of neurons. Axonal degeneration of the corticospinal tract

Abbreviations: HSP, Hereditary spastic paraplegia; AD, autosomal dominant inheritance; AR, autosomal recessive inheritance; TCC, thin corpus callosum; WMH, white matter hyperintensities; EMG, electromyogram; AP5, adaptor-related protein complex 5; ALR, autophagic lysosomal reformation.

TABLE 1 SPG15 gene loci mutation and clinical features.

Location	Mutation	References	Sex	Age	Age at onset	Lower limb weakness/ spasticity/ amyotrophy	Cognitive impairment/ Mental abnormality	Dysarthria	Axonal peripheral polyneuropathy	Babinski sign	Urinary problems/ Sphincter disturbances	Ataxia	Retinal degeneration/ Nystagmus	Clawfoot/ Strephenopodia	Sensory abnormalities decreased vibration sense; Superficial sensory; Deep sensory	Action tremor	Epilepsy	Hearing impairement	Upper limb weakness/ spasticity/ amyotrophy	MRI signs			
																				TCC	WMH	Cortical atrophy	Prominent cerebellar atrophy
Exon 2	c.43C > T p.Q15*	Goizet et al. (14)	NA	NA	NA	NA	NA	NA	NA	NA	NA	NA	NA	NA	NA	NA	NA	NA	NA	NA	NA	NA	NA
Intron 3-4	c.273 + 8G > A	Yoon et al. (15)	M	18	3	+/+/+	-/-	+	-	-	-/-	-	-/-	-/-	-/- /-	-	-	-	-/- /-	+	-	-	-
Exon 4	c.307G > T p.E103*	Goizet et al. (14)	F	41	7	+/+/-	+/+	+	+	+	+/-	-	+/+	-/-	-/- /-	-	-	-	-/- /-	+	+	-	-
Exon 5	c.427G > T p.E143*	Goizet et al. (14)	F	41	7	+/+/-	+/+	+	+	+	+/-	-	+/+	-/-	-/- /-	-	-	-	-/- /-	+	+	-	-
	c.592C > T p.R198*	Schüle et al. (16)	M	19	17	+/+/-	+/+	+	-	-	-/-	-	-/-	-/-	-/- /-	-	-	-	-/- /-	+	+	+	-
	c.728T > C p.L243P	Vantaggiato et al. (17)	NA	55	38	- /+/-	- /+	+	-	+	+/-	-	-/-	-/-	- /+/-	-	-	-	-/- /-	+	+	-	-
			NA	51	34	- /+/-	- /+	+	-	+	+/-	-	-/-	-/-	- /+/-	-	-	-	-/- /-	+	+	-	-
	c.836T > G		F	15	13	+/+/-	-/-	-	-	-	+/-	-	-/-	-/-	-/- /-	-	-	-	-/- /-	-	+	-	-
Exon 8	c.1240G > T p.E414*	Goizet et al. (14)	F	31	13	+/+/+	- /+	-	-	+	+/-	-	- /+	-/-	-/- /-	+	+	-	-/- /-	-	-	-	-

(Continued)

10.3389/fneur.2023.1160110

TABLE 1 (Continued)

Location	Mutation	References	Sex	Age	Age at onset	Lower limb weakness/ spasticity/ amyotrophy	Cognitive impairment/ Mental abnormality	Dysarthria	Axonal peripheral polyneuropathy	Babinski sign	Urinary problems/ Sphincter disturbances	Ataxia	Retinal degeneration/ Nystagmus	Clawfoot/ Strephenopodia	Sensory abnormalities decreased vibration sense; Superficial sensory; Deep sensory	Action tremor	Epilepsy	Hearing impairement	Upper limb weakness/ spasticity/ amyotrophy	MRI signs			
																				TCC	WMH	Cortical atrophy	Prominent cerebellar atrophy
Exon 10	c.1471C > T p.Q491*	Pensato et al. (18)	M	25	NA	+/+/-	-/-	-	-	-	-/-	-	-/-	-/-	-/- /-	-	-	-	-/- /-	-	-	-	-
	c.1477C > T p.Q493*	Hanein et al. (19)	F	20	14	+/+/-	-/-	-	-	-	-/-	-	-/-	+/-	-/- /-	-	-	-	-/- /-	-	-	+	+
			M	32	12	+/+/+	- /+	+	+	-	-/-	-	-/-	+/-	-/- /-	-	-	-	-/- /+	-	-	-	-
	c.1523T > A p.I508N	Vantaggiato et al. (17)	NA	46	20	+/+/+	- /+	+	+	+	-/-	-	-/-	+/-	- /+/+	-	-	-	- /+/+	+	+	+	-
			NA	47	22	+/+/+	- /+	+	+	+	-/-	+	-/-	+/-	- /+/+	-	-	-	- /+/+	+	+	-	-
	c.1630_1631 delTC p.S544Lfs* 824	Riazuddin et al. (20)	NA	NA	13	+/+/+	+/-	-	+	-	-/-	-	-/-	-/-	-/- /-	-	-	-	-/- /-	-	+	-	-
Exon 11	c.1730delA + c.1731C > T p.Asn577 IIefs*36	Pensato et al. (18)	NA	NA	NA	NA	NA	NA	NA	NA	NA	NA	NA	NA	NA	NA	NA	NA	NA	NA	NA	NA	NA
	c.1792delG p.D599 Tfs*163	Denora et al. (21)	F	33	21	+/+/-	-/-	-	-	+	-/-	-	+/-	-/-	-/- /-	-	-	+	-/- /-	-	-	-	-
	c.1844C > T p.S615F	Schüle et al. (16)	NA	NA	16	+/+/-	-/-	+	-	-	-/-	+	-/-	-/-	-/- /-	-	-	-	-/- /-	-	-	+	-
			NA	NA	1	+/+/-	- /+	+	+	-	-/-	+	-/-	-/-	-/- /-	-	-	-	-/- /-	-	-	-	-

(Continued)

10.3389/fneur.2023.1160110

TABLE 1 (Continued)

Location	Mutation	References	Sex	Age	Age at onset	Lower limb weakness/ spasticity/ amyotrophy	Cognitive impairment/ Mental abnormality	Dysarthria	Axonal peripheral polyneuropathy	Babinski sign	Urinary problems/ Sphincter disturbances	Ataxia	Retinal degeneration/ Nystagmus	Clawfoot/ Strephenopodia	Sensory abnormalities decreased vibration sense; Superficial sensory; Deep sensory	Action tremor	Epilepsy	Hearing impairement	Upper limb weakness/ spasticity/ amyotrophy	MRI signs			
																				TCC	WMH	Cortical atrophy	Prominent cerebellar atrophy
	c.1925C > T p.A642V	Schüle et al. (16)	NA	NA	1	+/+/-	-/+	-	-	-	-/-	-	-/-	-/-	-/-/-	-	-	-	-/-/-	-	-	-	-
	c.2049delT p.Phe 683Leufs*685	Hanein et al. (19)	F	28	11	+/+/+	-/+	+	+	-	-/-	-	-/-	+/-	-/-/-	-	-	-	-/-/-	-	-	-	-
			F	27	8	+/+/+	-/+	-	-	-	-/-	-	-/-	-/-	-/-/-	-	-	-	-/-/-	-	-	-	-
			F	9	8	+/+/-	-/+	-	-	-	-/-	-	-/-	-/-	-/-/-	-	-	-	-/-/-	-	-	-	-
	c.2074delC p.L692Sfs*52	Tunca et al. (22)	NA	NA	17	+/+/-	-/-	-	-	-	-/-	-	-/-	-/-	-/-/-	-	-	-	-/-/-	-	-	-	-
	c.2182C > T p.R728*	Goizet et al. (14)	M	17	12	+/+/-	+/+	-	-	-	-/-	-	-/-	-/-	-/-/-	+	-	-	+/+/-	+	+	-	-
	c.2196_2198 delTGT p.V733del	Karakaya et al. (23)	NA	NA	NA	NA	NA	NA	NA	NA	NA	NA	NA	NA	NA	NA	NA	NA	NA	NA	NA	NA	NA
Exon 12	c.2254C > T p.Glu752*	Pensato et al. (18)	NA	NA	NA	-/-/-	-/-	-	-	-	-/-	-	-/-	-/-	-/-/-	-	-	-	-/-/-	-	-	-	-
	c.2331_ 2332insA p.D778Rfs*15	Goizet et al. (14)	M	17	12	+/+/-	+/+	-	-	-	-/-	-	-/-	-/-	-/-/-	+	-	-	+/+/-	+	+	-	-
	c.2332 + 7delT	Schüle et al. (16)	NA	NA	22	+/+/-	-/-	-	+	-	-/-	-	-/-	-/-	-/-/-	-	-	-	-/-/-	-	-	-	-

(Continued)

10.3389/fneur.2023.1160110

TABLE 1 (Continued)

Location	Mutation	References	Sex	Age	Age at onset	Lower limb weakness/ spasticity/ amyotrophy	Cognitive impairment/ Mental abnormality	Dysarthria	Axonal peripheral polyneuropathy	Babinski sign	Urinary problems/ Sphincter disturbances	Ataxia	Retinal degeneration/ Nystagmus	Clawfoot/ Strephenopodia	Sensory abnormalities decreased vibration sense; Superficial sensory; Deep sensory	Action tremor	Epilepsy	Hearing impairement	Upper limb weakness/ spasticity/ amyotrophy	MRI signs			
																				TCC	WMH	Cortical atrophy	Prominent cerebellar atrophy
Exon 13	c.2338C > T p.R780*	Pyle et al. (24)	M	NA	32	+/+/-	-/-	-	+	-	-/-	+	-/-	-/-	-/- /-	-	-	-	-/- /-	-	-	+	-
	c.2450delT p.L817Cfs*12	Pyle et al. (24)	M	NA	32	+/+/-	-/-	-	+	-	-/-	+	-/-	-/-	-/- /-	-	-	-	-/- /-	-	-	+	-
Exon 14	c.2554-1 G > A	Renvoisé et al. (25)	F	26	15	+/+/-	+/+	+	-	-	-/-	-	-/-	-/-	-/- /-	+	-	-	-/- /-	+	+	-	-
	c.C2254T p.Q752*	Vinci et al. (26)	M	27	18	+/+/+	+/+	-	+	-	+/-	+	-/-	-/-	-/- /-	-	+	-	-/- /-	+	+	+	-
Exon 15	c.2615_2617 delGCTi nsTGAA p.R872 Lfs*17	Tunca et al. (22)	NA	NA	22	+/+/-	-/-	-	-	-	-/-	-	-/-	-/-	-/- /-	-	-	-	-/- /-	-	-	-	-
	c.2639T > C p.L880P	Kancheva et al. (27)	NA	NA	NA	NA	NA	NA	NA	NA	NA	NA	NA	NA	NA	NA	NA	NA	NA	NA	NA	NA	NA
	c.2826G > A p.M942I	Schüle et al. (16)	NA	NA	8	+/+/-	- /+	+	+	-	-/-	+	-/-	-/-	-/- /-	-	-	-	-/- /-	-	-	-	-
			NA	NA	3	+/+/-	- /+	-	-	-	-/-	-	-/-	-/-	-/- /-	-	-	-	-/- /-	+	-	-	-
			NA	NA	6	+/+/-	- /+	-	+	-	-/-	-	-/-	-/-	-/- /-	-	-	-	-/- /-	-	-	-	+

(Continued)

10.3389/fneur.2023.1160110

TABLE 1 (Continued)

Location	Mutation	References	Sex	Age	Age at onset	Lower limb weakness/ spasticity/ amyotrophy	Cognitive impairment/ Mental abnormality	Dysarthria	Axonal peripheral polyneuropathy	Babinski sign	Urinary problems/ Sphincter disturbances	Ataxia	Retinal degeneration/ Nystagmus	Clawfoot/ Strephenopodia	Sensory abnormalities decreased vibration sense; Superficial sensory; Deep sensory	Action tremor	Epilepsy	Hearing impairement	Upper limb weakness/ spasticity/ amyotrophy	MRI signs			
																				TCC	WMH	Cortical atrophy	Prominent cerebellar atrophy
Exon 20	p.Arg1209 fs*120	Hanein et al. (19)	M	38	12	+/+/-	+/-	+	+	-	-/-	-	+/-	-/-	-/- /-	-	-	+	-/- /-	+	+	+	+
			F	34	14	+/+/-	+/-	+	+	-	-/-	-	-/-	-/-	-/- /-	-	-	+	-/- /-	+	-	+	+
			M	21	9	+/+/-	+/-	+	+	-	-/-	-	+/+	-/-	-/- /-	-	-	+	-/- /-	+	+	-	-
			M	17	5	+/+/-	- /+	+	-	-	-/-	-	-/-	-/-	-/- /-	-	-	-	-/- /-	+	-	-	-
	c.3118T > A p.S1040T	Schüle et al. (16)	NA	NA	22	+/+/-	-/-	-	+	-	-/-	+	- /+	-/-	-/- /-	-	-	-	-/- /-	-	-	-	-
			NA	NA	11	+/+/-	- /+	-	-	-	-/-	-	- /+	-/-	-/- /-	+	-	-	-/- /-	+	-	+	-
			NA	NA	1	+/+/-	- /+	+	-	-	-/-	+	-/-	+/-	-/- /-	+	+	-	-/- /-	-	+	-	-
	c.3811delT p.S1271 Lfs44	Pashaei et al. (5)	F	20	5	+/+/-	+/-	-	-	-	+/-	-	-/-	-/-	-/- /-	-	-	-	-/- /-	+	+	-	-
Exon 21	c.3935C > A p.S1312*	Vantaggiato et al. (17)	NA	27	14	+/+/+	-/-	-	+	-	+/-	+	-/-	+/-	-/- /-	-	+	-	+/- /+	+	+	-	-
			NA	46	14	+/+/+	-/-	+	+	+	+/-	-	+/-	-/-	-/- /+	-	-	-	- /+/-	+	+	-	-
			NA	45	17	+/+/+	-/-	+	+	+	+/-	-	+/-	-/-	- /+/+	-	-	-	+/+/+	+	+	-	-

(Continued)

10.3389/fneur.2023.1160110

TABLE 1 (Continued)

Location	Mutation	References	Sex	Age	Age at onset	Lower limb weakness/ spasticity/ amyotrophy	Cognitive impairment/ Mental abnormality	Dysarthria	Axonal peripheral polyneuropathy	Babinski sign	Urinary problems/ Sphincter disturbances	Ataxia	Retinal degeneration/ Nystagmus	Clawfoot/ Strephenopodia	Sensory abnormalities decreased vibration sense; Superficial sensory; Deep sensory	Action tremor	Epilepsy	Hearing impairement	Upper limb weakness/ spasticity/ amyotrophy	MRI signs			
																				TCC	WMH	Cortical atrophy	Prominent cerebellar atrophy
	c.3417_3418 insTA p.Lys 1140*	Renvoisé et al. (25)	F	26	15	+/+/-	+/+	+	-	-	-/-	-	-/-	-/-	-/- /-	+	-	-	-/- /-	+	+	-	-
	c.4068_4069 delTG p.C1356*	Goizet et al. (14)	F	38	18	+/+/+	-/-	+	+	+	+/-	-	+/+	-/-	-/- /-	-	-	-	-/- /-	+	-	+	-
			M	34	18	+/+/+	-/-	+	+	+	+/-	-	+/+	-/-	-/- /-	-	-	-	-/- /-	+	-	+	-
	c.4132C > T p.Arg1378*	Pensato et al. (18)	M	22	NA	+/+/-	-/-	-	-	-	-/-	-	-/-	-/-	-/- /-	-	-	-	-/- /-	-	-	-	-
	c.4181G > A p.W1394*	Lazaridis et al. (28)	NA	NA	NA	NA	NA	NA	NA	NA	NA	NA	NA	NA	NA	NA	NA	NA	NA	NA	NA	NA	NA
	c.4401C > T p.P1467P	Schüle et al. (16)	NA	NA	20	+/+/-	-/-	+	-	-	-/-	+	- /+	-/-	-/- /-	-	-	-	-/- /-	-	-	-	-
	c. 4278 G > A	Dong et al. (29)	M	21	6	+/+/-	+/+	-	-	-	- /+	+	-/-	-/-	-/- /-	-	-	-	-/- /-	+	+	-	+
	c.4312C > T p.Arg1438*	Hanein et al. (19)	F	33	13	+/+/+	+/+	-	-	-	- /+	-	+/-	-/-	-/- /-	-	+	-	-/- /-	-	-	+	-
			M	32	14	+/+/+	+/+	+	-	-	- /+	-	+/-	-/-	-/- /-	-	-	-	-/- /-	-	-	-	-
			M	30	16	+/+/+	+/+	-	-	-	- /+	-	+/-	-/-	-/- /-	-	-	-	-/- /-	-	-	-	-

(Continued)

10.3389/fneur.2023.1160110

TABLE 1 (Continued)

Location	Mutation	References	Sex	Age	Age at onset	Lower limb weakness/ spasticity/ amyotrophy	Cognitive impairment/ Mental abnormality	Dysarthria	Axonal peripheral polyneuropathy	Babinski sign	Urinary problems/ Sphincter disturbances	Ataxia	Retinal degeneration/ Nystagmus	Clawfoot/ Strephenopodia	Sensory abnormalities decreased vibration sense; Superficial sensory; Deep sensory	Action tremor	Epilepsy	Hearing impairement	Upper limb weakness/ spasticity/ amyotrophy	MRI signs			
																				TCC	WMH	Cortical atrophy	Prominent cerebellar atrophy
			F	27	12	+/+/-	+/+	-	-	-	-/-	-	-/-	-/-	+/- /-	-	-	-	-/- /-	-	-	-	-
			M	27	12	+/+/-	+/-	-	-	-	-/-	-	-/-	-/-	+/- /-	-	-	-	-/- /-	-	-	-	-
			F	18	16	+/+/-	-/-	-	-	-	-/-	-	-/-	+/-	-/- /-	-	-	-	-/- /-	-	-	-	-
Exon 22	c.4539 delG p.K1514 Sfs*26	Koh et al. (30)	F	36	14	+/+/-	+/-	+	-	-	-/-	+	-/-	-/-	-/- /-	-	-	-	- /+/-	+	+	+	-
Exon 25	c.4804C > T p.Arg 1602Ter	Chakrabarty et al. (31)	F	24	4	+/+/-	-/-	-	-	-	-/-	-	-/-	-/-	-/- /-	-	-	-	-/- /-	-	-	-	-
Exon 26	c.5036delT p.L1679 Rfs*8	Goizet et al. (14)	M	23	4	+/+/-	+/+	+	-	+	-/-	-	-/-	-/-	-/- /-	-	-	-	-/- /-	+	+	-	-
	c.5203C > T p.Gln 1735*	Pensato et al. (18)	NA	NA	NA	NA	NA	NA	NA	NA	NA	NA	NA	NA	NA	NA	NA	NA	NA	NA	NA	NA	NA
	c.5215C > T p.Gln 1739*	Yoon et al. (15)	F	32	6	+/+/-	-/-	+	-	-	+/-	-	-/-	-/-	-/- /-	-	-	-	-/- /-	+	+	+	-

(Continued)

10.3389/fneur.2023.1160110

TABLE 1 (Continued)

Location	Mutation	References	Sex	Age	Age at onset	Lower limb weakness/ spasticity/ amyotrophy	Cognitive impairment/ Mental abnormality	Dysarthria	Axonal peripheral polyneuropathy	Babinski sign	Urinary problems/ Sphincter disturbances	Ataxia	Retinal degeneration/ Nystagmus	Clawfoot/ Strephenopodia	Sensory abnormalities decreased vibration sense; Superficial sensory; Deep sensory	Action tremor	Epilepsy	Hearing impairement	Upper limb weakness/ spasticity/ amyotrophy	MRI signs			
																				TCC	WMH	Cortical atrophy	Prominent cerebellar atrophy
Exon 28	c.5415delC p.R1806 Gfs*36	Hsu et al. (38)	F	31	9	+/+/-	+/-	-	-	+	+/-	-	-/-	-/-	-/- /-	-	-	-	-/- /-	+	+	-	-
	c.5422C > T p.Q1808*	Goizet et al. (14)	M	-	14	+/+/-	+/+	-	-	+	-/-	-	-/-	-/-	-/- /-	-	-	-	-/- /-	+	+	-	-
Intron 28-29	c.5485-1G > A	Hanein et al. (19)	F	31	12	+/+/+	+/+	-	+	-	-/-	-	-/-	+/+	+/- /-	-	-	-	-/- /-	-	-	-	-
			M	30	10	+/+/+	+/-	-	-	-	-/-	-	-/-	+/-	+/- /-	-	-	-	-/- /-	-	-	-	-
			F	25	10	+/+/+	-/-	-	-	-	-/-	-	-/-	-/-	+/- /-	-	-	-	-/- /-	-	-	-	-
			M	16	10	+/+/-	+/-	-	+	-	-/-	-	-/-	+/-	-/- /-	-	-	-	-/- /-	-	-	-	-
	c.5612G > A p.C1871Y	Schüle et al. (16)	NA	NA	16	+/+/-	-/-	+	-	-	-/-	+	-/-	-/-	-/- /-	-	-	-	-/- /-	-	-	+	-
			NA	NA	1	+/+/-	- /+	+	+	-	-/-	+	-/-	-/-	-/- /-	-	-	-	-/- /-	-	-	-	-
Intron 31-32	c.5791–6G > A r.5791_5792 ins5791–4_5791–1, p.A1931 PfxX1957X	Goizet et al. (14)	M	34	18	+/+/+	-/-	+	+	+	+/-	-	+/+	-/-	-/- /-	-	-	-	-/- /-	+	-	+	-

(Continued)

10.3389/fneur.2023.1160110

TABLE 1 (Continued)

			F	38	18	+/+/+	-/-	+	+	+	+/-	-	+/+	-/-	-/- /-	-	-	-	-/- /-	+	-	+	-
Exon 32	c.6011G > C p.S2004T	Goizet et al. (14)	M	29	16	+/+/-	+/-	-	-	+	-/-	-	-/-	-/-	-/- /-	-	-	-	-/- /-	+	+	+	+
			F	33	13	+/+/-	+/-	+	-	+	-/-	-	-/-	-/-	-/- /-	-	-	-	-/- /-	-	-	-	-
Exon 34	c.6296 dup p.Asn2100 Glufs*12	Mallaret et al. (32)	F	17	16	+/+/-	+/+	+	+	-	-/-	-	-/-	-/-	-/- /-	-	-	-	-/- /-	+	-	-	-
	c.6296_6297 insT p.L2099 Lfs*12	Goizet et al. (14)	F	30	14	+/+/+	+/+	+	-	+	-/-	-	-/-	-/-	-/- /-	-	-	-	+/+/-	-	-	-	-
Exon 35	c.6398_6401 delGGGA p.R2133 Asnfs*15	Özdemir et al. (33)	F	14	13	+/+/-	+/+	+	-	-	-/-	-	+/-	-/-	-/- /-	-	-	-	-/- /-	-	+	-	+
Exon 36	c.6702_6771del p.Trp2234 Cysfs*2238	Hanein et al. (19)	F	24	18	+/+/+	- /+	-	-	-	- /+	-	-/-	-/-	-/- /-	-	-	-	-/- /-	+	+	+	-
			F	23	19	+/+/+	- /+	-	-	-	-/-	-	-/-	-/-	+/- /-	+	-	-	+/+/-	+	+	-	-

(Continued)

10.3389/fneur.2023.1160110

TABLE 1 (Continued)

	c.6744_6746 delGAA p.2248 delLys	Pensato et al. (18)	M	25	NA	+/+/-	-/-	-	-	-	-/-	-	-/-	-/-	-/- /-	-	-	-	-/- /-	-	-	-	-
Exon 37	c.6787 delG p.D2263 Tfs*7	Jiao et al. (34)	M	24	16	+/+/-	-/-	+	-	-	-/-	-	-/-	-/-	-/- /-	-	-	-	-/- /-	+	+	-	-
	c.6940A > T p.K2314*	Denora et al. (21)	F	33	21	+/+/-	-/-	-	-	+	-/-	-	+/-	-/-	-/- /-	-	-	+	-/- /-	-	-	-	-
Exon 38	c.7111dupA p.M2371Nfs* 51	this case 2021	F	19	18	+/+/-	+/+	-	+	+	-/-	-	-/-	-/-	-/- /-	-	-	-	-/- /-	+	-	-	-
Intron 38-39	c.7128 + 1G > C	Schüle et al. (16)	M	19	17	+/+/-	+/+	+	-	-	-/-	-	-/-	-/-	-/- /-	-	-	-	-/- /-	+	+	+	-
Intron 38-39	c.7128 + 2T > A r.6987_ 7128del p.R2329R fsX2337	Goizet et al. (14)	F	31/13	13	+/+/+	- /+	-	-	+	+/-	-	- /+	-/-	-/- /-	+	+	-	-/- /-	-	-	-	-

F, female; M, male; + is positive, - is negative; TCC, Thin corpus callosum; WMH, White matter hyperintensities; NA, no data.

10.3389/fneur.2023.116

(most obvious in the thoracic spinal cord) and fasciculus gracilis fibrosis (most obvious in the cervical spinal cord) have also been detected in autopsy.

SPG15 (*ZFYVE26*) is a kind of early-onset complex ARHSP, which is characterized by typical atrophy of the corpus callosum, and its main clinical symptoms include urinary urgency and incontinence, visual impairment, retinal and macular degeneration, nystagmus, mood fluctuation, mental impairment, ataxia, spastic paraplegia, dysarthria, arcus plantaris, lower limb spasm, callosal agenesis, clonicity, fecal incontinence, bladder sphincter dysfunction, peripheral axon neurodegeneration, distal muscle atrophy, and lower limb muscle weakness (9). Most patients with SPG15 had the first symptoms in their adolescence, some born to consanguineous family even had language delay in infancy and gait disorder at the age of 11 years (5). Our patient presented with classical complicated type of HSP symptoms, including the paralysis of motor neurons in both lower limbs, mild mental impairment, and callosal agenesis. She had progressive bilateral leg spasticity and weakness at the age of 17 years but had no visual or hearing impairment. However, 19 disease-related genes caused HSP manifesting progressive spasticity of the lower limbs and TCC, including SPG1, SPG11, SPG15, SPG21, SPG30, SPG32, SPG35, SPG44, SPG44(65), SPG46, SPG47, SPG48, SPG49, SPG50, SPG52, SPG54, SPG56, SPG63, and SPG71. Furthermore, the onset of these SPGs occurs mainly in children and adolescents and is often accompanied by intellectual disability. While it is hard to distinguish them from clinical symptoms, gene testing is good at detecting specific genetic mutations. Second-generation gene sequencing test proved that this patient had a *ZFYVE26* NM_015346: c.7111dupA p.(M2371Nfs*51) homozygous mutation, and both her parents carried a *ZFYVE26* NM_015346: c.7111dupA p.(M2371Nfs*51) heterozygous variant. However, this gene loci mutation had not been reported earlier. Therefore, the patient was diagnosed with SPG15, which was composed of AR.

ZFYVE26/Spastizin mutations increase immature autophagosomes and lead to autophagy defects. A complex that is composed of *ZFYVE26*/Spastizin, SPG11/Spatacsin and AP5 (adaptor-related protein complex 5) is important in autophagic lysosomal reformation (ALR) (10). Although both *ZFYVE26* and SPG11 interact with RAB5A and RAB11, the two proteins regulating endosome trafficking and maturation, only *ZFYVE26* mutations affect RAB protein interactions and activation and make the fusion between autophagosomes and endosomes defective (10). The *ZFYVE26* c.7111dupA p.M2371Nfs*51 mutation identified in our patient is a novel mutation. This frameshift mutation possibly leads to the loss of some amino acid residues in the final protein product and causes loss of function. To date, there have been 62 mutations reported for SPG15 (Table 1) (5, 14–18, 21, 25, 26, 29, 31–38). There are 62.90% (39/62) missense mutations, 29.03% (18/62) deletion mutations, 3.23% (2/62) duplication mutations, and 8.06% (5/62) insertion mutations (Table 1). We searched published literature in PubMed and Web of Science databases and analyzed the clinical features of these 62 kinds of *ZFYVE26* mutations in 84 patients (Table 1). Most patients first had walking gait disorder at young age (13.75 ± 7.85 years), and some had language delay in infancy. The main clinical characteristics of the patients with these mutations include low limbs weakness (98.81%), spasticity (96.43%), and amyotrophy (30.95%); cognitive impairment (39.29%), mental abnormality (50%), dysarthria (46.43%), TCC (47.62%), and white matter hyperintensities (WMH) (39.29%) on MRI; axonal peripheral polyneuropathy (35.71%), Babinski sign positive (27.39%), urinary problems (21.43%), and sphincter (5.95%); and ataxia (17.86%), retinal degeneration (19.05%), nystagmus (14.29%), clawfoot (13.10%), strephenopodia (1.19%), sensory abnormalities, action tremor (9), epilepsy (10.71%), hearing impairment (5.95%), upper limbs weakness (7.14%), spasticity (10.71%), and amyotrophy (5.95%).

Options available for the treatment of spastic paraplegia are much less than its clinical and genetic types. Rehabilitation therapy and physical therapy are necessary for the maintenance of muscular strength and coordinated movement, and medications such as oral baclofen, intramuscular injections of botulinum toxin, or intrathecal injections of baclofen can relieve spasms. Although HSP has no impact on the lifespan of patients, it can cause serious disability. Genetic diagnosis and symptoms management are important. Early diagnosis and clinical intervention are also helpful to slow disease progression.

Conclusion

Here, we reported a new homozygous mutation of the *ZFYVE26* gene, c.7111dupA p.(M2371Nfs*51) (Exon 38). There have been no previous reports on this genetic locus mutation with HSP. Gene testing plays an important role in the diagnosis of HSP, and family genetic lineage reveals the source of the pathogenic gene. With the rapid improvement of gene testing technology, the number of known HSP disease-causing gene is increasing, which brings a challenge to the early diagnosis and clinical evolution.

Data availability statement

The raw data supporting the conclusions of this article will be made available by the authors, without undue reservation.

Ethics statement

Written informed consent was obtained from the participant/patient(s) for the publication of this case report.

Author contributions

Z-hL wrote this manuscript. X-yL and Y-yS collected clinical data and references. H-yZ and L-lZ guided the writing and revision of this manuscript. All authors contributed to the article and approved the submitted version.

Funding

The grant numbers and funding information: NSFC (82271313 to L-lZ), Shanghai Health Commission General Project (202240026 to L-lZ), and Clinical Research Plan of SHDC (SHDC2020CR2027B to L-lZ).

Acknowledgments

We thank Ruijin Hospital for providing a clinical platform, and the clinical work of all involved doctors and nurses. We also thank our patient and her family for their permission and support.

Conflict of interest

The authors declare that the research was conducted in the absence of any commercial or financial relationships that could be construed as a potential conflict of interest.

Publisher's note

All claims expressed in this article are solely those of the authors and do not necessarily represent those of their affiliated organizations, or those of the publisher, the editors and the reviewers. Any product that may be evaluated in this article, or claim that may be made by its manufacturer, is not guaranteed or endorsed by the publisher.

Supplementary material

The Supplementary Material for this article can be found online at: https://www.frontiersin.org/articles/10.3389/fneur.2023.1160110/full#supplementary-material

References

1. Berciano J, Gazulla J, Infante J. History of ataxias and paraplegias with an annotation on the first description of striatonigral degeneration. *Cerebellum.* (2021) 21:531–44. doi: 10.1007/s12311-021-01328-6

2. Murala S, Nagarajan E, Bollu PC. Hereditary spastic paraplegia. *Neurol Sci.* (2021) 42:883–94. doi: 10.1007/s10072-020-04981-7

3. Mackay-Sim A. Hereditary spastic paraplegia: from genes, cells and networks to novel pathways for drug discovery. *Brain Sci.* (2021) 11:403. doi: 10.3390/brainsci11030403

4. Parodi L, Fenu S, Stevanin G, Durr A. Hereditary spastic paraplegia: More than an upper motor neuron disease. *Rev Neurol.* (2017) 173:352–60. doi: 10.1016/j.neurol.2017.03.034

5. Pashaei M, Davarzani A, Hajati R, Zamani B, Nafissi S, Larti F, et al. Description of clinical features and genetic analysis of one ultra-rare (SPG64) and two common forms (SPG5A and SPG15) of hereditary spastic paraplegia families. *J Neurogenet.* (2021) 35:84–94. doi: 10.1080/01677063.2021.1895146

6. Harding AE. Hereditary "pure" spastic paraplegia: a clinical and genetic study of 22 families. *J Neurol Neurosurg Psychiatry.* (1981) 44:871–83. doi: 10.1136/jnnp.44.10.871

7. Nan H, Shiraku H, Mizuno T, Takiyama Y. A p.Arg499His mutation in SPAST is associated with infantile-onset complicated spastic paraplegia: a case report and review of the literature. *BMC Neurol.* (2021) 21:439. doi: 10.1186/s12883-021-02478-0

8. Ruano L, Melo C, Silva MC, Coutinho P. The global epidemiology of hereditary ataxia and spastic paraplegia: a systematic review of prevalence studies. *Neuroepidemiology.* (2014) 42:174–83. doi: 10.1159/000358801

9. Ebrahimi-Fakhari D, Alecu JE, Blackstone C. Spastic paraplegia 15. 2021 may 27. In: Adam MP, Ardinger HH, Pagon RA, Wallace SE, Bean LJH, Mirzaa G, et al., editors. *GeneReviews®*. Seattle, WA: University of Washington, Seattle (1993–2021).

10. Vantaggiato C, Panzeri E, Castelli M, Citterio A, Arnoldi A, Santorelli FM, et al. ZFYVE26/SPASTIZIN and SPG11/SPATACSIN mutations in hereditary spastic paraplegia types AR-SPG15 and AR-SPG11 have different effects on autophagy and endocytosis. *Autophagy.* (2019) 15:34–57. doi: 10.1080/15548627.2018.1507438

11. Lo Giudice T, Lombardi F, Santorelli FM, Kawarai T, Orlacchio A. Hereditary spastic paraplegia: clinical-genetic characteristics and evolving molecular mechanisms. *Expl Neurol.* (2014) 261:518–39. doi: 10.1016/j.expneurol.2014.06.011

12. Finsterer J, Löscher W, Quasthoff S, Wanschitz J, Auer-Grumbach M, Stevanin G. Hereditary spastic paraplegias with autosomal dominant, recessive, X-linked, or maternal trait of inheritance. *J Neurol Sci.* (2012) 318:1–18. doi: 10.1016/j.jns.2012.03.025

13. Peng F, Sun YM, Quan C, Wang J, Wu JJ. Two novel homozygous mutations of CAPN1 in Chinese patients with hereditary spastic paraplegia and literatures review. *Orphanet J Rare Dis.* (2019) 14:83. doi: 10.1186/s13023-019-1053-1

14. Goizet C, Boukhris A, Maltete D, Guyant-Maréchal L, Truchetto J, Mundwiller E, et al. SPG15 is the second most common cause of hereditary spastic paraplegia with thin corpus callosum. *Neurology.* (2009) 73:1111–9. doi: 10.1212/WNL.0b013e3181bacf59

15. Yoon G, Baskin B, Tarnopolsky M, Boycott KM, Geraghty MT, Sell E, et al. Autosomal recessive hereditary spastic paraplegia-clinical and genetic characteristics of a well-defined cohort. *Neurogenetics.* (2013) 14:181–8. doi: 10.1007/s10048-013-0366-9

16. Schüle R, Schlipf N, Synofzik M, Klebe S, Klimpe S, Hehr U, et al. Frequency and phenotype of SPG11 and SPG15 in complicated hereditary spastic paraplegia. *J Neurol Neurosurg Psychiatry.* (2009) 80:1402–4. doi: 10.1136/jnnp.2008.167528

17. Vantaggiato C, Crimella C, Airoldi G, Polishchuk R, Bonato S, Brighina E, et al. Defective autophagy in spastizin mutated patients with hereditary spastic paraparesis type 15. *Brain.* (2013) 136:3119–39. doi: 10.1093/brain/awt227

18. Pensato V, Castellotti B, Gellera C, Pareyson D, Ciano C, Nanetti L, et al. Overlapping phenotypes in complex spastic paraplegias SPG11, SPG15, SPG35 and SPG48. *Brain.* (2014) 137:1907–20. doi: 10.1093/brain/awu121

19. Hanein S, Martin E, Boukhris A, Byrne P, Goizet C, Hamri A, et al. Identification of the SPG15 gene, encoding spastizin, as a frequent cause of complicated autosomal-recessive spastic paraplegia, including Kjellin syndrome. *Am J Hum Genet.* (2008) 82:992–1002. doi: 10.1016/j.ajhg.2008.03.004

20. Riazuddin S, Hussain M, Razzaq A, Iqbal Z, Shahzad M, Polla DL, et al. Exome sequencing of Pakistani consanguineous families identifies 30 novel candidate genes for recessive intellectual disability. *Mol Psychiatry.* (2017) 22:1604–14. doi: 10.1038/mp.2016.109

21. Denora PS, Muglia M, Casali C, Truchetto J, Silvestri G, Messina D, et al. Spastic paraplegia with thinning of the corpus callosum and white matter abnormalities: further mutations and relative frequency in ZFYVE26/SPG15 in the Italian population. *J Neurol Sci.* (2009) 277:22–5. doi: 10.1016/j.jns.2008.09.039

22. Tunca C, Seker T, Akçimen F, Coskun C, Bayraktar E, Palvadeau R, et al. Revisiting the complex architecture of ALS in Turkey: Expanding genotypes, shared phenotypes, molecular networks, and a public variant database. *Hum Mutat.* (2020) 41:e7–e45. doi: 10.1002/humu.24055

23. Karakaya M, Storbeck M, Strathmann EA, Vedove AD, Hölker I, Altmueller J, et al. Targeted sequencing with expanded gene profile enables high diagnostic yield in non-5q-spinal muscular atrophies. *Hum Mutat.* (2018) 39:1284–1298. doi: 10.1002/humu.23560

24. Pyle A, Smertenko T, Bargiela D, Griffin H, Duff J, Appleton M, et al. Exome sequencing in undiagnosed inherited and sporadic ataxias. *Brain.* (2015) 138(Pt 2):276–83. doi: 10.1093/brain/awu348

25. Renvoisé B, Chang J, Singh R, Yonekawa S, FitzGibbon EJ, Mankodi A, et al. Lysosomal abnormalities in hereditary spastic paraplegia types SPG15 and SPG11. *Ann Clin Transl Neurol.* (2014) 1:379–89. doi: 10.1002/acn3.64

26. Vinci M, Fchera M, Antonino Musumeci S, Cali F, Aurelio Vitello G. Novel c.C2254T (p.Q752*) mutation in *ZFYVE26* (SPG15) gene in a patient with hereditary spastic paraparesis. *J Genet.* (2018) 97:1469–72. doi: 10.1007/s12041-018-1038-1

27. Kancheva D, Atkinson D, De Rijk P, Zimon M, Chamova T, Mitev V, et al. Novel mutations in genes causing hereditary spastic paraplegia and Charcot-Marie-Tooth neuropathy identified by an optimized protocol for homozygosity mapping based on whole-exome sequencing. *Genet Med.* (2016) 18:600–7. doi: 10.1038/gim.2015.139

28. Lazaridis KN, Schahl KA, Cousin MA, Babovic-Vuksanovic D, Riegert-Johnson DL, Gavrilova RH, et al. Outcome of whole exome sequencing for diagnostic odyssey cases of an individualized medicine clinic: The mayo clinic experience. *Mayo Clin Proc.* (2016) 91:297–307. doi: 10.1016/j.mayocp.2015.12.018

29. Dong Y, Li XY, Wang XL, Xu F, Wang ZJ, Song Y, et al. Genetic, clinical and neuroimaging profiles of sporadic and autosomal recessive hereditary spastic paraplegia cases in Chinese. *Neurosci Lett.* (2021) 761:136108. doi: 10.1016/j.neulet.2021.136108

30. Koh K, Tsuchiya M, Nagasaka T, Shindo K, Takiyama Y. Decreasing 123I-ioflupane SPECT accumulation and 123I-MIBG myocardial scintigraphy uptake in a patient with a novel homozygous mutation in the ZFYVE26 gene. *Neurol Sci.* (2019) 40:429–41. doi: 10.1007/s10072-018-3603-z

31. Chakrabarty S, Vijayakumar N, Radhakrishnan K, Satyamoorthy K. Spastizin mutation in hereditary spastic paraplegia with thin corpus callosum. *J Neurol.* (2016) 263:2130–2. doi: 10.1007/s00415-016-8258-1

32. Mallaret M, Lagha-Boukbiza O, Biskup S, Namer IJ, Rudolf G, Anheim M, et al. SPG15: a cause of juvenile atypical levodopa responsive parkinsonism. *J Neurol.* (2014) 261:435–7. doi: 10.1007/s00415-013-7216-4

33. Özdemir TR, Gençpinar P, Arican P, Öztekin Ö, Dündar NO, Özyilmaz B, et al. A case of spastic paraplegia-15 with a novel pathogenic variant in *ZFYVE26* gene. *Int J Neurosci.* (2019) 129:1198–202. doi: 10.1080/00207454.2019.1653293

34. Jiao B, Zhou Z, Hu Z, Du J, Liao X, Luo Y, et al. Homozygosity mapping and next generation sequencing for the genetic diagnosis of hereditary ataxia and spastic paraplegia in consanguineous families. *Parkinsonism Relat Disord.* (2020) 80:65–72. doi: 10.1016/j.parkreldis.2020.09.013

35. Pascual B, de Bot ST, Daniels MR, França MC Jr, Toro C, Riverol M, et al. "Ears of the Lynx" MRI Sign Is Associated with SPG11 and SPG15 Hereditary Spastic Paraplegia. *AJNR Am J Neuroradiol.* (2019) 40:199–203. doi: 10.3174/ajnr.A5935

36. Bibi F, Efthymiou S, Bourinaris T, Tariq A, Zafar F, Rana N, et al. Rare novel CYP2U1 and ZFYVE26 variants identified in two Pakistani families with spastic paraplegia. *J Neurol Sci.* (2020) 411:116669. doi: 10.1016/j.jns.2020.116669

37. Schicks J, Synofzik M, Pétursson H, Huttenlocher J, Reimold M, Schöls L, et al. Atypical juvenile parkinsonism in a consanguineous SPG15 family. *Mov Disord.* (2011) 26:564–6. doi: 10.1002/mds.23472

38. Hsu SL, Lu YJ, Tsai YS, Chao HC, Fuh JL, Liao YC, et al. Investigating ZFYVE26 mutations in a Taiwanese cohort with hereditary spastic paraplegia. *J Formos Med Assoc.* (2022) 121:126–33. doi: 10.1016/j.jfma.2021.02.005

Frontiers in Neurology

Explores neurological illness to improve patient care

The third most-cited clinical neurology journal explores the diagnosis, causes, treatment, and public health aspects of neurological illnesses. Its ultimate aim is to inform improvements in patient care.

Discover the latest Research Topics

See more →

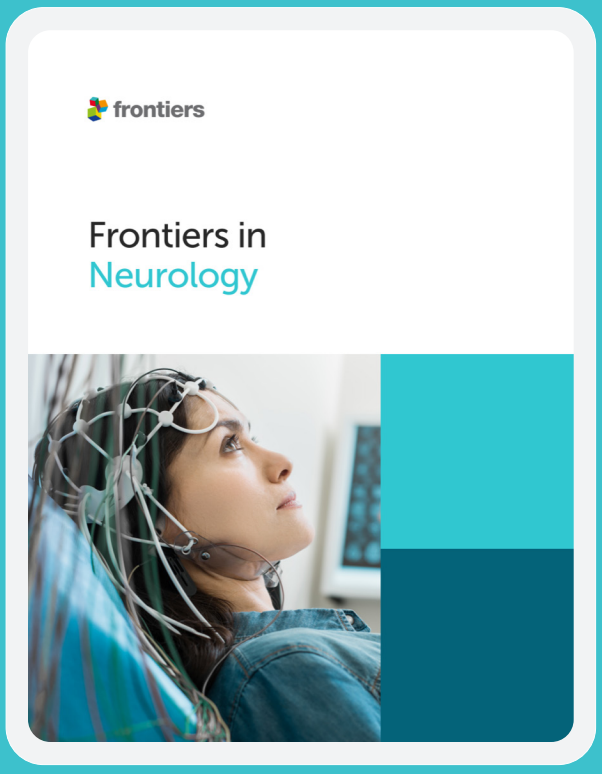

Frontiers

Avenue du Tribunal-Fédéral 34
1005 Lausanne, Switzerland
frontiersin.org

Contact us

+41 (0)21 510 17 00
frontiersin.org/about/contact